frontiers | Research Topics

Microorganisms in polar regions: Understanding their survival strategies for a sustainable future

Edited by
Prashant Kumar Singh, Shiv Mohan Singh and Trista J. Vick-Majors

Published in
Frontiers in Microbiology

ISSN 1664-8714
ISBN 978-2-8325-5111-0
DOI 10.3389/978-2-8325-5111-0

About Frontiers

Frontiers is more than just an open access publisher of scholarly articles: it is a pioneering approach to the world of academia, radically improving the way scholarly research is managed. The grand vision of Frontiers is a world where all people have an equal opportunity to seek, share and generate knowledge. Frontiers provides immediate and permanent online open access to all its publications, but this alone is not enough to realize our grand goals.

Frontiers journal series

The Frontiers journal series is a multi-tier and interdisciplinary set of open-access, online journals, promising a paradigm shift from the current review, selection and dissemination processes in academic publishing. All Frontiers journals are driven by researchers for researchers; therefore, they constitute a service to the scholarly community. At the same time, the *Frontiers journal series* operates on a revolutionary invention, the tiered publishing system, initially addressing specific communities of scholars, and gradually climbing up to broader public understanding, thus serving the interests of the lay society, too.

Dedication to quality

Each Frontiers article is a landmark of the highest quality, thanks to genuinely collaborative interactions between authors and review editors, who include some of the world's best academicians. Research must be certified by peers before entering a stream of knowledge that may eventually reach the public - and shape society; therefore, Frontiers only applies the most rigorous and unbiased reviews. Frontiers revolutionizes research publishing by freely delivering the most outstanding research, evaluated with no bias from both the academic and social point of view. By applying the most advanced information technologies, Frontiers is catapulting scholarly publishing into a new generation.

What are Frontiers Research Topics?

Frontiers Research Topics are very popular trademarks of the *Frontiers journals series*: they are collections of at least ten articles, all centered on a particular subject. With their unique mix of varied contributions from Original Research to Review Articles, Frontiers Research Topics unify the most influential researchers, the latest key findings and historical advances in a hot research area.

Find out more on how to host your own Frontiers Research Topic or contribute to one as an author by contacting the Frontiers editorial office: frontiersin.org/about/contact

Microorganisms in polar regions: Understanding their survival strategies for a sustainable future

Topic editors

Prashant Kumar Singh — Mizoram University, India

Shiv Mohan Singh — Banaras Hindu University, India

Trista J. Vick-Majors — Michigan Technological University, United States

Citation

Singh, P. K., Singh, S. M., Vick-Majors, T. J., eds. (2024). *Microorganisms in polar regions: Understanding their survival strategies for a sustainable future*. Lausanne: Frontiers Media SA. doi: 10.3389/978-2-8325-5111-0

Table of contents

frontiers | Frontiers in Microbiology

TYPE Editorial
PUBLISHED 24 June 2024
DOI 10.3389/fmicb.2024.1442926

OPEN ACCESS

EDITED AND REVIEWED BY
Andreas Teske,
University of North Carolina at Chapel Hill, United States

*CORRESPONDENCE
Trista J. Vick-Majors
✉ tjvickma@mtu.edu
Shiv Mohan Singh
✉ drshivmohansingh@gmail.com
Prashant Kumar Singh
✉ singhpk@pucollege.edu.in

RECEIVED 03 June 2024
ACCEPTED 10 June 2024
PUBLISHED 24 June 2024

CITATION
Vick-Majors TJ, Singh SM and Singh PK (2024) Editorial: Microorganisms in polar regions: understanding their survival strategies for a sustainable future.
Front. Microbiol. 15:1442926.
doi: 10.3389/fmicb.2024.1442926

Editorial: Microorganisms in polar regions: understanding their survival strategies for a sustainable future

Trista J. Vick-Majors[1]*, Shiv Mohan Singh[2]* and Prashant Kumar Singh[3]*

[1]Department of Biological Sciences, Michigan Technological University, Houghton, MI, United States, [2]Department of Botany, Banaras Hindu University, Varanasi, India, [3]Department of Biotechnology/Life Sciences, Pachhunga University College (A Constituent College of Mizoram University), Aizawl, Mizoram, India

KEYWORDS

psychrophile, Arctic, Antarctic, adaptation, biotechnology

Editorial on the Research Topic
Microorganisms in polar regions: understanding their survival strategies for a sustainable future

The Research Topic, *Microorganisms in Polar Regions: Understanding Their Survival Strategies for a Sustainable Future*, compiles contributions exploring aspects of polar microbiology ranging from specific adaptations to low-temperature environments to aspects of microbial community ecology in polar glaciers and aquatic environments. The Arctic and Antarctic are being transformed due to climate change, and ecosystem responses to environmental change are mediated by the metabolic activities of the microorganisms that inhabit them.

In the Research Topic, 11 articles focused on the unique adaptations and lifestyles of microbial life in the polar regions inform our understanding of their potential responses to changing environmental conditions, and some of the ways their adaptations can be harnessed for biotechnological development to support a sustainable future.

Dutta et al. investigated what drives the distribution of microbial ecological function along the coastal western Antarctica Peninsula. The authors subjected DNA samples collected as part of the Palmer Long Term Ecological Research project to metagenomic sequencing. They developed a pipeline for metagenomic data processing (iMAGine) that allowed them to uncover differences in microbial community functional potential across depth and regional profiles. Their data suggest metabolically flexible microorganisms are key to sustaining microbial community function under changing environmental conditions.

Vannier et al. examined metagenomes from Skaftárkatlar, two geothermally and volcanically influenced subglacial lakes beneath the Vatanjökull ice cap in Iceland. These environments are unique in blending geothermal and volcanic inputs with subglacial isolation (the ice cap is ~250 m thick). The authors found that chemolithoautotrophic metabolisms dominate the subglacial ecosystem and that enrichment cultures did not include the dominant organisms and metabolisms. This underscores the difficulty of working with these unique samples and the importance of conducting *in situ* investigations to understand microbial life in these environments.

Shaffer et al. demonstrated the utility of examining individual genomes by focusing on characterizing a red-pigmented, motile strain of the bacterium *Massilia frigida*. The organism was isolated from a microbial mat in the Don Juan Pond basin in Wright Valley, Antarctica. Don Juan Pond is a hypersaline environment, and they were able to identify not only metabolic pathways and genes related to salt and cold tolerance, but also to test the effect of UV-A radiation on the organism. The isolate produced prodigiosin, a bactericidal, nematocidal, and UV-protective compound, which may have implications for organismal interactions and resilience to UV exposure in microbial mats.

Prekrasna-Kviatkovska et al. focused on indirect effects of climate change in the rapidly changing central maritime region of the Antarctic. Moss banks in the region are capable of accumulating peat, but this process has been impacted by the southward expansion of Gentoo penguin colonies. The authors examined the effect of Gentoo penguin colonization pressure on the chemical composition of and microbial communities associated with moss banks. The results showed that penguin colonization was associated with phylum-level shifts in peat microbiota, and increases in peat pH and soluble nitrogen and phosphorus concentrations. Overall, the expansion of penguin colonies was associated with loss of acidiphilic microbiomes normally associated with moss banks.

Singh et al. examined cryoconite associated with the Hamtah Glacier, one of more than 50,000 glaciers located in India's Himalayas. Through the use of cultivation-dependent, cultivation-independent, and chemical methods, they assessed the diversity and functional potential of bacterial life and elemental composition in Hamtah cryoconite. The study revealed a diverse microbial community including organisms containing cold-active enzymes, which may be biotechnologically relevant.

In the review by Dopson et al., the focus was on eurypsychrophilic acidophiles which inhabit cold, acidic sites ranging from acid rock drainage that can be found in the South Shetland Islands, Antarctica, to sulfidic sediments of the Baltic Sea coastal region, and occur on extra-planetary bodies such as the Jovian moons. The work provided evolutionary, environmental, biotechnological, and exobiological perspectives on five characterized low-temperature adapted acidophiles whose capacities to impact the composition of metallic compounds make them biogeochemically and biotechnologically relevant.

Shrestha et al. examined the genome of the extremophilic bacterium, *Glaciimonas* sp. PAMC28666, which was originally isolated from Antarctic soil. In a laboratory-based experiment, they examined the survival of PAMC28666 in response to freezing and thawing. They revealed enhanced expression of *trehalose 6-phosphate synthase (otsA)* and *trehalose 6-phosphate phosphatase (otsB)* on shifting temperature from thawing to freezing. They also determined that the overexpression of *otsAB* led to enhanced production of trehalose, which may be important in cold adaptation.

Juchem et al. demonstrated the effect of prolonged exposure to dark conditions mimicking the seasonally fluctuating light conditions in Antarctica in benthic diatoms important in biogeochemical cycling and primary productivity. They isolated four distinct species of benthic diatoms, of which *Planothidium wetzelii* sp. nov. was newly described. After being subjected to a dark incubation period of 3 months, adaptive strategies were identified in the diatoms. They demonstrated chloroplast degradation and a decline in storage lipid content; however, no species exhibited a change in photosynthetic performance. They concluded that survival strategies manifested as biochemical cell biological changes allow benthic diatoms to survive the Antarctic night.

Ramasamy et al. reviewed the adaptive mechanisms of Antarctic marine bacteria to cope with climatic change at the mosphological, physiological, and molecular levels. They also addressed recent advances in "omics" techniques and machine learning approaches to generate molecular understanding of psychrophiles and bacterial diversity. Finally, the manuscript also described cold-adapted enzymes and compounds which may have commercial potential in biotechnology.

Liu et al. described current knowledge and recent advances related to enzymes derived from cold-adapted microorganisms. Their uses and the catalytic processes they are involved in were discussed, as were methods of molecular modification that may increase the utility of a given enzyme. Overall, the review set the stage for future research into the use of cold-adapted enzymes.

Xiao et al. isolated and identified a symbiotic bacterium, *Serratia myotis* L7-1, from an Antarctic fish, *Trematomus bernacchii*. On whole genome sequencing, they found that its genome encoded for carbohydrate-active enzymes (CAZymes), biosynthetic pathway genes, stress-responsive genes, antibiotic-resistant genes (ARGs), and a complete type IV secretion system. Based on sequencing results, they performed bioactivity-guided fractionation and identified *Serratia myotis* L7-1 as having antibacterial and antitumor activities.

This Research Topic of papers demonstrates the importance of polar microbes in both biotechnological and ecological contexts, and highlights work still to be done in understanding the diversity of microbial life in the polar regions. The research being conducted to uncover the biodiversity and understand the survival strategies of these microbes also sets the stage for biotechnological applications in the future, which may benefit from the unique adaptations of polar microbes. Together, the work in this Research Topic underscores the benefits of combining molecular information, machine learning techniques, and ecological data to futher our understanding of the microbiology of these unique and rapidly changing environments.

Author contributions

TV-M: Writing – original draft, Writing – review & editing. SS: Writing – original draft, Writing – review & editing. PS: Writing – original draft, Writing – review & editing, Project administration.

Funding

The author(s) declare financial support was received for the research, authorship, and/or publication of this article. PS thanks

the Department of Biotechnology (DBT), New Delhi, for a research grant (BT/PR47930/NER/95/1980/2023).

Conflict of interest

The authors declare that the research was conducted in the absence of any commercial or financial relationships that could be construed as a potential conflict of interest.

Publisher's note

frontiers | Frontiers in Microbiology

TYPE Original Research
PUBLISHED 13 January 2023
DOI 10.3389/fmicb.2022.1085063

OPEN ACCESS

EDITED BY
Prashant Kumar Singh,
Mizoram University,
India

REVIEWED BY
Kaushal Endra,
Pachhunga University College,
India
Pawan Kumar,
Agricultural Research Organization (ARO),
Israel

*CORRESPONDENCE
Liangbiao Chen
✉ lbchen@shou.edu.cn
Xi Yu
✉ xyu@shou.edu.cn

SPECIALTY SECTION
This article was submitted to Extreme Microbiology, a section of the journal Frontiers in Microbiology

RECEIVED 31 October 2022
ACCEPTED 14 December 2022
PUBLISHED 13 January 2023

CITATION
Xiao Y, Yan F, Cui Y, Du J, Hu G, Zhai W, Liu R, Zhang Z, Fang J, Chen L and Yu X (2023) A symbiotic bacterium of Antarctic fish reveals environmental adaptability mechanisms and biosynthetic potential towards antibacterial and cytotoxic activities.
Front. Microbiol. 13:1085063.
doi: 10.3389/fmicb.2022.1085063

A symbiotic bacterium of Antarctic fish reveals environmental adaptability mechanisms and biosynthetic potential towards antibacterial and cytotoxic activities

Yu Xiao[1], Fangfang Yan[1], Yukun Cui[1], Jiangtao Du[1], Guangzhao Hu[1], Wanying Zhai[2], Rulong Liu[1], Zhizhen Zhang[3], Jiasong Fang[1], Liangbiao Chen[2]* and Xi Yu[1]*

[1]Shanghai Engineering Research Center of Hadal Science and Technology, College of Marine Sciences, Shanghai Ocean University, Shanghai, China, [2]International Research Center for Marine Biosciences, Ministry of Science and Technology, Shanghai Ocean University, Shanghai, China, [3]Ocean College, Zhoushan Campus, Zhejiang University, Zhoushan, China

Antarctic microbes are important agents for evolutionary adaptation and natural resource of bioactive compounds, harboring the particular metabolic pathways to biosynthesize natural products. However, not much is known on symbiotic microbiomes of fish in the Antarctic zone. In the present study, the culture method and whole-genome sequencing were performed. Natural product analyses were carried out to determine the biosynthetic potential. We report the isolation and identification of a symbiotic bacterium *Serratia myotis* L7-1, that is highly adaptive and resides within Antarctic fish, *Trematomus bernacchii*. As revealed by genomic analyses, Antarctic strain *S. myotis* L7-1 possesses carbohydrate-active enzymes (CAZymes), biosynthetic gene clusters (BGCs), stress response genes, antibiotic resistant genes (ARGs), and a complete type IV secretion system which could facilitate competition and colonization in the extreme Antarctic environment. The identification of microbiome gene clusters indicates the biosynthetic potential of bioactive compounds. Based on bioactivity-guided fractionation, serranticin was purified and identified as the bioactive compound, showing significant antibacterial and antitumor activity. The serranticin gene cluster was identified and located on the chrome. Furthermore, the multidrug resistance and strong bacterial antagonism contribute competitive advantages in ecological niches. Our results highlight the existence of a symbiotic bacterium in Antarctic fish largely represented by bioactive natural products and the adaptability to survive in the fish living in Antarctic oceans.

KEYWORDS

Antarctic fish, symbiotic bacteria, *Serratia*, genome, bioactive metabolites

Introduction

The unique thermal and geographic isolation of the Antarctica continent creates some of the coldest and yet stable environmental conditions in the world's oceans (Tercero and Place, 2020; Giuliani et al., 2021). The high latitude Antarctic fishes, inhabiting the world's coldest environment, are ideal model organisms for decoding novel traits that may arise during the evolution in millions of years (Obrien, 2016). At present, the dominant species in Antarctic Ocean are the suborder Notothenioidei belonging to the Perciformes, including the *Trematomus bernacchii*, *Cottoperca gobio*, *Gymnodraco acuticeps*, etc. (Eastman, 2004). Given the ecological, morphological, and physiological diversification of the Antarctic fishes, one may anticipate that their symbiotic microbial communities have also evolved to accommodate the various trophic lifestyles of the hosts (Ward et al., 2009). Symbiotic bacteria have many roles in the host, most of which are correlated with host nutrition, immunity, development, and resistance against the cold environment (Sedláček et al., 2016; Song et al., 2016). The symbiotic microbiota contributes to the protective effects both through the direct influence *via* microbial metabolites and indirect effects of microbiota on the host immune system (Li et al., 2016). On the other hand, the symbionts develop extended survival capability to compete with other microbes and the external environment (Dixon, 2001).

An increasing number of studies have focused on the microbial potential to keep the functional genes and biosynthesize secondary metabolites as a reservoir (Xuan et al., 2015). Secondary metabolites are a major source of natural products, which act as an arsenal of antibiotics. These structurally unique natural products display potent biological activity, including antitumor, antimicrobial, antiviral, and antiparasitic activities, mediated by versatile biosynthetic gene clusters (Wang et al., 2020). Microbial natural products represent a huge and largely untapped resource of unique chemical structures that have been optimized by evolution and are produced for communication and in response to changes in microbial habitats, including environmental stresses (Gutierrez and Gonzalez, 2012). The close association between the symbiotic microbiota with these compounds could be important in bacterial antagonism under the high competition pressure. The attributes that characterize the fish symbiotic bacteria is still not well understood. Knowledge of bacterial species, associated with the potential production of bioactive compounds, is important to clarify the adaptation strategies of symbiotic microbiota in fish and benefit for extensive use in the pharmaceutical industry.

To understand microbial diversity and gene functions, multi-omics combined with taxonomic profiling and functional analyses has become one of the most effective approaches. A series of microbial metagenomic analysis from Antarctic zone were conducted for their ecological role and capabilities to influence the host. In the Antarctic fish gut microbiome, Proteobacteria, Actinobacteria and Firmicutes were the dominant phyla, and *Vibrio*, *Serratia*, *Aeromonas* were the dominant genera (Cormack and Fraile, 1990; Maccormack and Fraile, 1991; Ward et al., 2009; Sedláček et al., 2016; Song et al., 2016). However, only culture methods and 16S rRNA sequencing have been used in past studies to identify the composition of Antarctic fish symbiotic microbes. The lack of functional studies of symbiotic microbes hinders the understanding of microbial adaptation in the fish. In particular, natural product analyses of specific groups of animal symbiotic microbiota within such extreme environments is rarely performed.

Here we report the isolation and identification of *Serratia myotis* L7-1, a symbiotic bacterium of Antarctic fish, which showed high adaptation to the living environment. The detailed taxonomic analysis and genomic annotation of the sequenced symbiotic bacteria of a high-latitude benthic fish- *Trematomus bernacchii,* were provided. The functional analysis of the genome indicated the important roles of *S. myotis* L7-1 in microbial metabolism, antibiotic resistance, energy uptake, and health of the fish. The analyses of biosynthetic gene clusters and the bioactivity assay displayed that *S. myotis* has the capability of antibiotic production. Importantly, *S. myotis* L7-1 produced bioactive secondary metabolites to recruit weaponry during microbe-microbe communications, such as serranticin that effectively inhibits the growth of aquatic pathogens *Aeromonas hydrophila* and *Edwardsiella piscicida*, which may improve the competitiveness of *S. myotis* L7-1.

Materials and methods

Sample collection and preparation

Fish *T. bernacchii* (66.8 g) was collected by ice fishing from the Antarctic China Zhongshan Station (69°22′27″S, 76°22′20″E) in February 2020. After the morphological identification, the fish was characterized using DNA barcoding of cytochrome oxidase subunit I (COI). The fresh fish was sealed and stored in sterile plastic bags immediately at 4°C for subsequent experiments. The intact fish abdominal contents were aseptically dissected from the fish, and 2 ml were taken into a centrifuge tube to investigate the composition and function of symbiotic bacteria.

Symbiotic bacteria isolation

The fish abdominal contents were diluted with 3.4% NaCl to make dilutions. Each dilution (200 μl) was plated on the surface of the isolation medium. The media used for isolation were luria-bertani agar (LB), nutrient agar (NA), tryptose soya agar (TSA), reinforced clostridium medium (RCM), modified artificial seawater medium (MASM), potato dextrose agar (PDA), yeast malt glucose (YMG), minimal medium (MM; Supplementary Table S1), brain heart infusion agar (BHIA, Hopebio, Qingdao, China), 2216E agar (Acmec, Shanghai, China). The plates were incubated at 20°C for 3 days and bacterial growth were detected. The distinct colonies were picked up and purified *via* repeated streaking (at least three times) on the isolation

medium, which then were maintained in 50% glycerol and preserved at −80°C for further study.

16S rDNA cloning and sequencing for bacterial identification

Genomic DNA was extracted from bacteria cells using the Rapid Bacterial Genomic DNA Isolation Kit (Sangon, Shanghai, China) according to the manufacturer's instructions. The 16S rDNA genes were amplified by PCR using 27F (5'-AGAGTTTGATCCTGGCTCAG-3′) and 1492R (5'-GGTTACCTTGTTACGACTT-3′) primers. The amplified DNA sequences were analyzed by Azenta Life Science Co., Ltd. for 16S rDNA sequencing, and the 16S sequences were aligned and identified against existing sequences in the NCBI database using the BLAST program. Further, the nucleotide sequences of the isolates were aligned with closely related sequence using Mega software (Kumar et al., 2008) and a phylogenetic tree was constructed to show the relationship between the isolates and the reference strains.

DNA extraction and 16S rRNA deep sequencing

Genomic DNA was extracted using the E.Z.N.A.® soil DNA Kit (Omega Bio-tek, Norcross, GA, United States) based on the manufacturer's protocol. The hyper-variable regions V3-V4 of the 16S rRNA gene were amplified using a universal primer set 338F (5'-ACTCCTACGGGAGGCAGCAG-3′) and 806R (5'-GGACTACHVGGGTWTCTAAT-3′). Sequencing of the 16S amplification was performed by Majorbio Bio-Pharm Technology Co. Ltd. (Shanghai, China) on an Illumina MiSeq PE300 platform (Illumina, San Diego, United States) with two paired-end read cycles of 300 bases each. The raw 16S rRNA gene sequencing reads were demultiplexed, quality-filtered by fastp version 0.20.0 (Chen et al., 2018) and merged by FLASH version 1.2.7 (Magoč and Salzberg, 2011). Operational taxonomic units (OTUs) with 97% similarity cutoff (Stackebrandt and Goebel, 1994; Edgar, 2013) were clustered using UPARSE version 7.1 (Edgar, 2013), and chimeric sequences were identified and removed. The taxonomy of each OTU representative sequence was analyzed by RDP Classifier version 2.2 (Wang et al., 2007) against the 16S rRNA database using confidence threshold of 0.7.

Genomic DNA preparation and whole-genome sequencing

The Wizard® Genomic DNA Purification Kit (Promega) was used for genomic DNA extraction according to the manufacturer's protocol. We utilized the Nanopore (Oxford Nanopore) and Illumina HiSeq X Ten sequencing platforms to perform whole-genome shotgun sequencing. The sequencing service was provided by Majorbio Bio-Pharm Technology Co. Ltd. (Shanghai, China).

De novo genome assembly and genome annotation

The original image data was transferred into sequence data *via* base calling, which was defined as raw data or raw reads and saved as FASTQ file. A statistic of quality information was applied for quality trimming, by which the lower quality data was removed to form clean data. The reads were assembled into a contig using hierarchical genome assembly process (HGAP) and canu. The last circular step was checked and finished manually, generating a complete genome with seamless chromosomes and plasmids. Finally, error correction of the assembly results was performed using the Illumina reads. Glimmer (Delcher et al., 2007) was used for CDS prediction, tRNA-scan-SE (Chan and Lowe, 2019) was used for tRNA prediction and Barrnap was used for rRNA prediction. The predicted CDSs were annotated from NR, Swiss-Prot (Bairoch and Apweiler, 2000), Pfam (Finn et al., 2013), GO (Consortium G O, 2004), COG (Lars Juhl et al., 2008) and KEGG (Ogata et al., 1999) database using sequence alignment tools such as BLAST (Ye et al., 2006), Diamond (Neshich et al., 2005) and HMMER (Potter et al., 2018). Briefly, each set of query proteins were aligned with the databases, and annotations of best-matched subjects (e-value $<10^{-5}$) were obtained for gene annotation.

Mass culture of Strain *Serratia myotis* L7-1

Colonies of L7-1 were inoculated into 250 ml of sterile LB medium and then incubated at 20°C for 24 h on a rotary shaker (180 rpm) to produce seed broth. The seed broth (12 ml) was transferred into a 500 ml Erlenmeyer flask, containing fresh rice solid medium (rice 40 g, sterile seawater 60 ml). The flasks were in a state for cultivation at 20°C for 30 days. A total of 50 flasks were prepared for this study. The rice solid culture of L7-1 was extracted with ethyl acetate three times and evaporated dry by rotary evaporator to give a crude extract for subsequent analysis.

Extraction and isolation of compounds

The crude extract (16.7 g) was fractionated by a silica gel column eluting with mixed solvents of PET/EtOAc (2/1, 1/1, 1/2, 1/5, 1/10, v/v), and EtOAc/MeOH (5/1, 1/1, 1/5, v/v) to furnish eight fractions (Fr-1-Fr-8) based on the results of TLC analysis. Fr. 4 (3.4 g), was further purified by Octadecyl-functionalized silica gel column (ODS, Cosmosil 75C_{18}-Prep) with MeOH/H_2O (3,7,

1,1, 7:3, 1:0, v/v) to afford four subfractions (Fr. 4.1–4.4). Compound 1 (61 mg, t_R 20 min, MeOH/H_2O, 30/70) was purified from Fr. 4.3 by Agilent 1,260 HPLC using a column (Agilent Zorbax SB-C_{18}, 250 × 9.4 mm, 5 μm; flow rate: 1 ml/min; UV detection: 210 nm). HPLC and analytic grace solvents used for this study were purchased from Sinopharm Chemical Reagent Co. Ltd. (Shanghai, China).

Identification of compounds structures

Optical rotation was recorded on a RUDOLPH Autopol I Automatic polarimeter (Rudolph Research Analytical). NMR spectra were acquired on a Bruker 500 spectrometer or a JEOL 600 spectrometer using the standard programs and acquisition parameters and the chemical shifts were expressed in δ (ppm) relative to DMSO-d6 (δC 39.5 and δH 2.50).

Antibacterial assay of crude extracts

The indicator bacteria used in the bacteriostatic circle experiment were provided by Shanghai Rainbowfish Company, including *Chromobacterium violaceum* ATCC 12472, *Salmonella choleraesuis*, *Mycobacterium smegmatis* MC2155, *Escherichia coli* MG1655, *Enterococcus faecalis* FA2-2, *Staphylococcus aureus* ATCC25923. Cultures of six indicator bacteria (with an OD of approximately 0.5) were inoculated in LB medium in an amount of 100 μl. The sterilized circular filter paper sheets were attached to the LB. Dissolve 10 mg of the crude extract in 1 ml of methanol. Then 6 μl of the crude extracted metabolites and negative control (methanol) were dropped onto the circular filter paper sheet, after incubated at 37°C for 12 h. Antibacterial bioactivity was evaluated by measuring the area of the zones inhibition and calculating the inhibition rate, which was measured with Image J.

Antibacterial assay of serranticin

The antibacterial activities of serranticin inhibiting the growth of *C. violaceum*, *S. choleraesuis*, *M. smegmatis*, *E. coli*, *E. faecalis*, *S.aureus E. tarda,* and *A. hydrophila* were determined by the micro-broth dilution method (Xin et al., 2012). Gentamicin was used as a positive control and DMSO was used as a negative control.

Cell lines and culture

Human lung cancer NCI-H460, human breast carcinoma MCF-7 and MDA-MB-231 cell lines were obtained from the National Collection of Authenticated Cell Cultures (Shanghai, China). All cells were incubated at 37°C in a humidified incubator with 5% CO_2 incubator. Cells after the third generation were used for experiment.

Assay for anti-proliferation

The assay using 3-(4,5-dimethylthiazole-2-yl)-2,5-dip-. henyltetrazolium bromide (MTT) against the MDA-MB-231, NCI-H460, and MCF7 cell lines (Huang et al., 2008). Cells (3×10^3 per well for cancer cell lines) were seeded with 200 μl of medium in 96-well plates. we dissolved the test sample in dimethyl sulfoxide (DMSO) to final concentrations of 0.78, 1.56, 3.13, 6.25, 12.5, 25, 50, and 100 μM in each well in assays against the MDA-MB-231, NCI-H460 and MCF7 cell lines. The blank control treatment used an equivalent volume of DMSO.

Identification of the serranticin biosynthetic cluster

To find the gene cluster responsible for serranticin biosynthetic, we first download the whole genome sequence of *Serratia plymuthica* V4 (Accession number NZ_CP007439.1) and searched for the genome sequence of synthetic compound serratiochelin.

K-B agar diffusion assay for drug sensitivity

Drug sensitivity tests were performed on seven common clinical antibiotics *via* the K-B agar diffusion method. Cultures of *S. myotis* L7-1 (with an OD of approximately 0.5) were inoculated in LB medium in an amount of 100 μl. The sterilized circular filter paper sheets were attached to the LB. Then 6 μl of the antibiotics (1 mg/ml) and negative control (LB medium) were dropped onto the circular filter paper sheet, after incubated at 37°C for 18–24 h. Antibacterial assay was evaluated by measuring the diameter of the zone inhibition.

Results

Serratia bacteria are the core isolated symbionts of *Trematomus bernacchii*

The symbiotic microbiota is typically beneficial or neutral during the multi-species interactions (Moreau, 2020). To explore the role of symbionts, we designed and performed two assays to identify the composition of the fish symbiotic microbiota (Figure 1A). The bacteria enrichment samples of Antarctic fish *Trematomus bernacchii* were harvested. Symbiotic bacteria of *T. bernacchii* were isolated using the culture method (TB-I). A total of 47 distinct bacterial isolates were selected for 16S rDNA

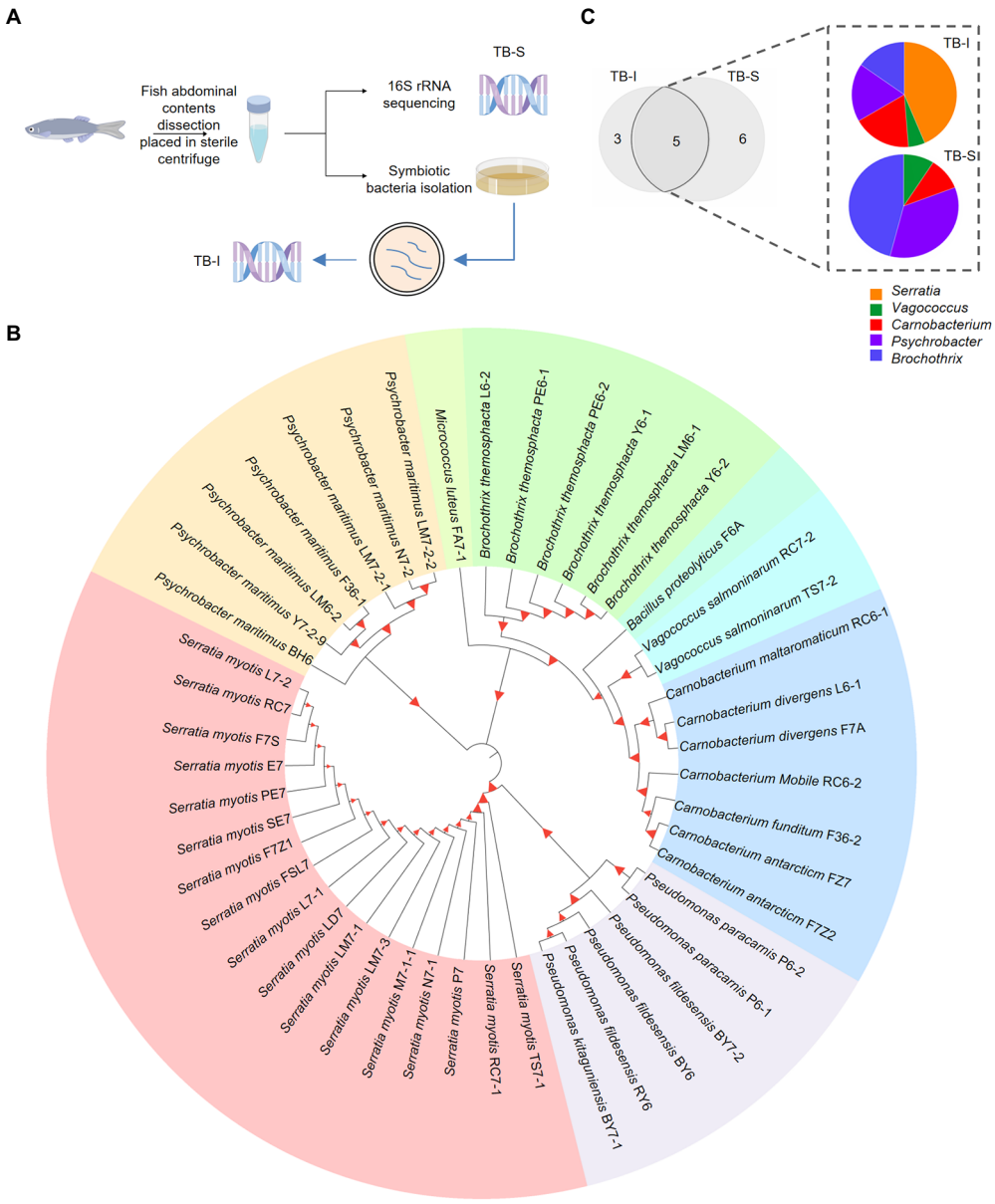

FIGURE 1
Isolation of the symbiotic *Serratia* bacteria of fish. **(A)** Workflow of the isolation and identification of symbiotic bacteria in *T. bernacchii* using *16S* rRNA sequencing and culture method (TB-I and TB-S). www.figdraw.com. **(B)** Phylogenetic tree showed the kinship and composition of 47 distinct bacterial strains isolated from *T. bernacchii*. Itol.embl.de. **(C)** Composition and relative abundance of the genera shared between the two methods. Origin 2022.

sequence identification (Figure 1B). Phylogenetic analysis revealed that a few taxa were predominated among these isolated strains, and the dominant bacterial species of *T. bernacchii* sample belonged to *Serratia*. Whether it was a nutrient-rich medium or a low-nutrient medium, *Serratia* was the abundant species (36.2%) and maintained growth under different nutrient conditions (Supplementary Figure S1A; Supplementary Tables S1, S2).

We also extracted DNA from *T. bernacchii* abdominal contents and deep sequencing of 16S rRNA (TB-S) revealed a total of 11 bacterial species (Supplementary Figure S1B). There were large differences in the bacterial compositions displayed by the two methods. Despite the differences in bacteria composition, the two methods shared five bacterial genera, *Serratia*, *Vagococcus*, *Carnobacterium*, *Psychrobacter*, and *Brochothrix* (Figure 1C). These 3 unique bacteria genera in TB-I included *Pseudomonas*, *Micrococcus*, and *Bacillus*. These 6 unique bacteria genera in TB-S included *norank-f-Bacillaceae*, *Photobacterium*, *Corynebacterium*, *Jeotgalicoccus*, *Aerococcus*, and *Paracoccus* (Figure 1C). Notably, the relative abundances of genus *Serratia* varied considerably among the shared bacterial

symbionts in the two compositions. *Serratia* (0.02%) was the least abundant bacteria in the 16S rRNA sequencing (TB-S). Whilst *Serratia* (43.6%) was the most abundant bacteria in the culture method (Figure 1C). Moreover, results of the different culture plates showed that *Serratia* species had the highest proportion among all the isolated strains from the various media. The growth assay determined that *Serratia* kept the highest growth viability in minimal nutrient media (MN; Supplementary Figure S2). The obtained results led us to assume that *Serratia* sp. was highly adaptive, and able to tolerate a range of nutrient conditions.

Serratia myotis L7-1 has the potential to biosynthesize bioactive compounds

A total of 17 strains of symbiotic bacteria were identified as *Serratia myotis* based on 16S rDNA sequence (Supplementary Table S2), with similarity between 99.50 to 99.86%. To determine the relationship between the 17 strains of *S. myotis*, we identified the homologous sequence between them using DNA star, with interspecific similarity between 99.40 to 100% (Supplementary Table S2). Based on the high similarity of sequences, *S. myotis* L7-1 was selected as a representative randomly for further studies (Figure 2A). The following description of *S. myotis* L7-1 was based on data reported previously. *S. myotis* is gram-stain-negative, facultative anaerobic, non-spore-forming, rod-shaped cells, 1–1.3 mm in length and 0.5–0.6 mm in diameter, and motile by subpolar flagella (García-Fraile et al., 2015). In our cultivation, *S. myotis* L7-1 colony morphology on LB agar medium was smooth, circular, convex and transparent, with a diameter of 1.5 to 2.0 mm after 48 h of growth at 20°C (Figure 2B). Optimal growth was observed at 25–31°C (Figure 2C; Supplementary Figure S3A), pH 6–9 (Figure 2D; Supplementary Figure S3B) and with 0–3% NaCl (Figure 2E; Supplementary Figure S3C). Type strain is 12 T (=CECT 8594^{T} = DSM 28726^{T}). 16S rDNA sequence accession number (GenBank) is KJ739884 (García-Fraile et al., 2015).

Chemical agents in the living environment of symbiotic microbiota exhibit a broad range of biological activities (Lu et al., 2016). Our next question was whether the natural products of *Serratia* sp. were of biological meaning as the antibiotics. To confirm their bioactivities, crude extracts from the isolates were tested for antimicrobial activity toward six bacterial species with the disk diffusion method. We found that the crude extract of *S. myotis* could consistently inhibit the growth of pathogenic bacteria (Figure 2F). Whereas, these of other isolated bacterial species from the same sample showed no significant antibacterial activity (Supplementary Figure S4). Next, we further investigated the effectiveness of *S. myotis* L7-1. The crude extract of *S. myotis* exhibited antibacterial activity against *Enterococcus faecalis*, *Mycobacterium smegmatis*, *Salmonella choleraesuis*, *Chromobacterium violaceum*, *Staphylococcus aureus* and *Escherichia coli* at 10 mg/ml, with inhibition rate of 71.8, 64.6, 66.9, 64.7, 63.0, 55.9% (Figure 2G), respectively. It seems that, *S. myotis* L7-1 could be a natural reservoir of bioactive secondary metabolites.

Serratia myotis L7-1 genome organization and genomic traits related to SMs production and adaptation

The whole genomic annotation was performed to decipher the functional genes of *S. myotis* in the Antarctic fish (Figure 3A). The sequences obtained from *S. myotis* L7-1 were assembled into one chromosome and four plasmids of size 5,503,952 bp (Chr 1; Figure 3B), 110,419 bp (pA; Supplementary Figure S5A), 49,145 bp (pB; Supplementary Figure S5B), 38,106 bp (pC; Supplementary Figure S5C), 3,223 bp (pD; Supplementary Figure S5D), with a GC content of 55.06%, and 5,272 genes with coding sequences. A total of 85 tRNA, 22 rRNA and 120 sRNA were detected. A total of 5,357 genes were predicted to display COG functional annotation, including 2,096 transport and metabolism genes, 2,550 cellular process and signal transduction genes, 526 information storage and processing genes, and 185 functionally unknown genes.

Functional classification of the microbial genes revealed the prevalence of genes for the metabolic system, including the putative biosynthetic gene clusters (BGCs) and carbohydrate-active enzymes (CAZymes). We identified a total of 285 BGCs associated genes and assigned secondary metabolic pathways using antiSMASH (Kai et al., 2017; Figure 3C). The results revealed the presence of 10 gene clusters encoding biosynthesis of secondary metabolites (SMs), including three non-ribosomal peptide-synthetase (NRPS; 37.5%), a hserlactone (5.3%), a NRPS-like (12.3%), a betalactone (7%), an arylpolyene, siderophore (15.8%), a thiopeptide (7%), a Ribosomally synthesized and post-translationally modified peptides-like (RiPP-like; 4.9%), and other (10.2%) gene clusters (Supplementary Figure S6). The percentage values mean the proportion of the related genes in the total BGCs genes. The abundant biosynthetic genes and related clusters indicated the important roles of versatile SMs production in *S. myotis* L7-1, as an untapped resource of undiscovered molecules. CAZymes analysis (Cantarel et al., 2009) identified 122 proteins belonging to the families of structurally-related catalytic and carbohydrate-binding modules (or functional domains) of enzymes that degrade, modify or create glycosidic bonds. Glycoside hydrolase (GH) family (47.5%) and glycosyl transferases (GTs; 35.2%) were the most abundant proteins in the CAZymes (Figure 3D).

Next, we showed *S. myotis* L7-1 harbored 85 genes associated with the "stress response" and linked to adaptation to extreme environments. Among these genes, universal stress genes (9.4%), multiple stress resistance genes (5.9%), dioxygenase genes (49.4%) and genes related to "oxidative stress" (9.4%), might assist the strain to cope with oxidative stress in seawater caused by the Antarctic environment. Cold shock protein genes (14.1%) and

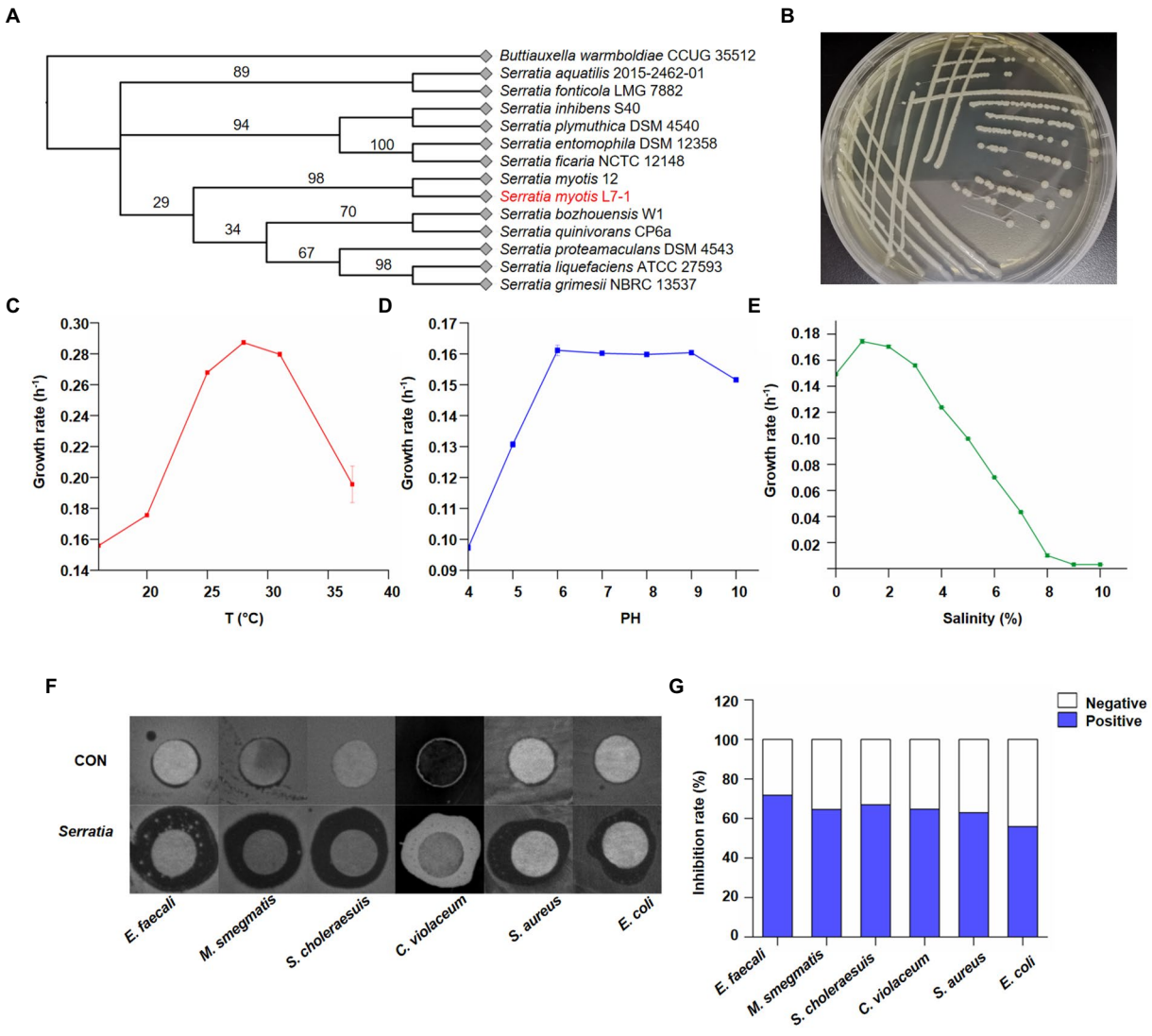

FIGURE 2
Identification of *Serratia myotis* as the core symbiotic bacteria. **(A)** Neighbor-joining tree based on nearly complete *16S* rDNA gene sequences of *Serratia myotis* L7-1 and close taxa of the genus *Serratia*. *Buttiauxella warmboldiae* CCUG 35512 was used as an outgroup. Itol.embl.de. **(B)** Macroscopic images showed the morphology of *S. myotis* L7-1 colony. **(C)** Growth rate of *S. myotis* L7-1 in different temperature (n=3). **(D)** Growth rate of *S. myotis* L7-1 in different PH values (n=3). **(E)** Growth rate of *S. myotis* L7-1 in different salinity (n=3). Origin 2022. **(F)** Zones of inhibition of the metabolites produced by *Serratia*. **(G)** *In-vitro* antimicrobial activity of the metabolites produced of the indicated *Serratia* strain. Origin 2022.

heat shock protein genes (11.8%) would facilitate the strain to survive in Antarctic temperatures (Figure 3E). Another interesting finding related with environmental adaptation was that several antibiotic-resistance genes (ARGs) and multiple antibiotic resistance mechanisms were predicted in the genome of *S. myotis* L7-1, by exploring the pan-genome analysis from the CARD database (Jia et al., 2016). The majority of ARGs contribute to encode the cephalosporin (5.9%), cephamycin (4.7%), carbapenem (4.3%), peptide antibiotic (4.1%), aminoglycoside antibiotic (3.4%), tetracycline antibiotic (12%), macrolide antibiotic (10.3%), fluoroquinolone antibiotic (10.1%), penam (7.1%) and others (38%; Figure 3F; details in Supplementary Table S3). Furthermore, antibiotic resistance mechanism included the reduced permeability to antibiotic (1.2%), antibiotic target replacement (0.9%), antibiotic efflux (70.9%), antibiotic target alteration (10%), antibiotic inactivation (7.1%), antibiotic target protection (6.8%), and antibiotic efflux, antibiotic target alteration (3.2%; Figure 3G). These results suggest that *S. myotis* had the ability to resist several antibiotics, and the ARGs possibly facilitated the competitiveness and colonization of bacteria in the extreme Antarctic environments.

Serratia myotis L7-1 exhibits the putative adaptability mechanisms *via* the comparative genomics

Serratia sp. are ubiquitous to different environments and show highly competitive fitness in versatile niches (Hover et al., 2016).

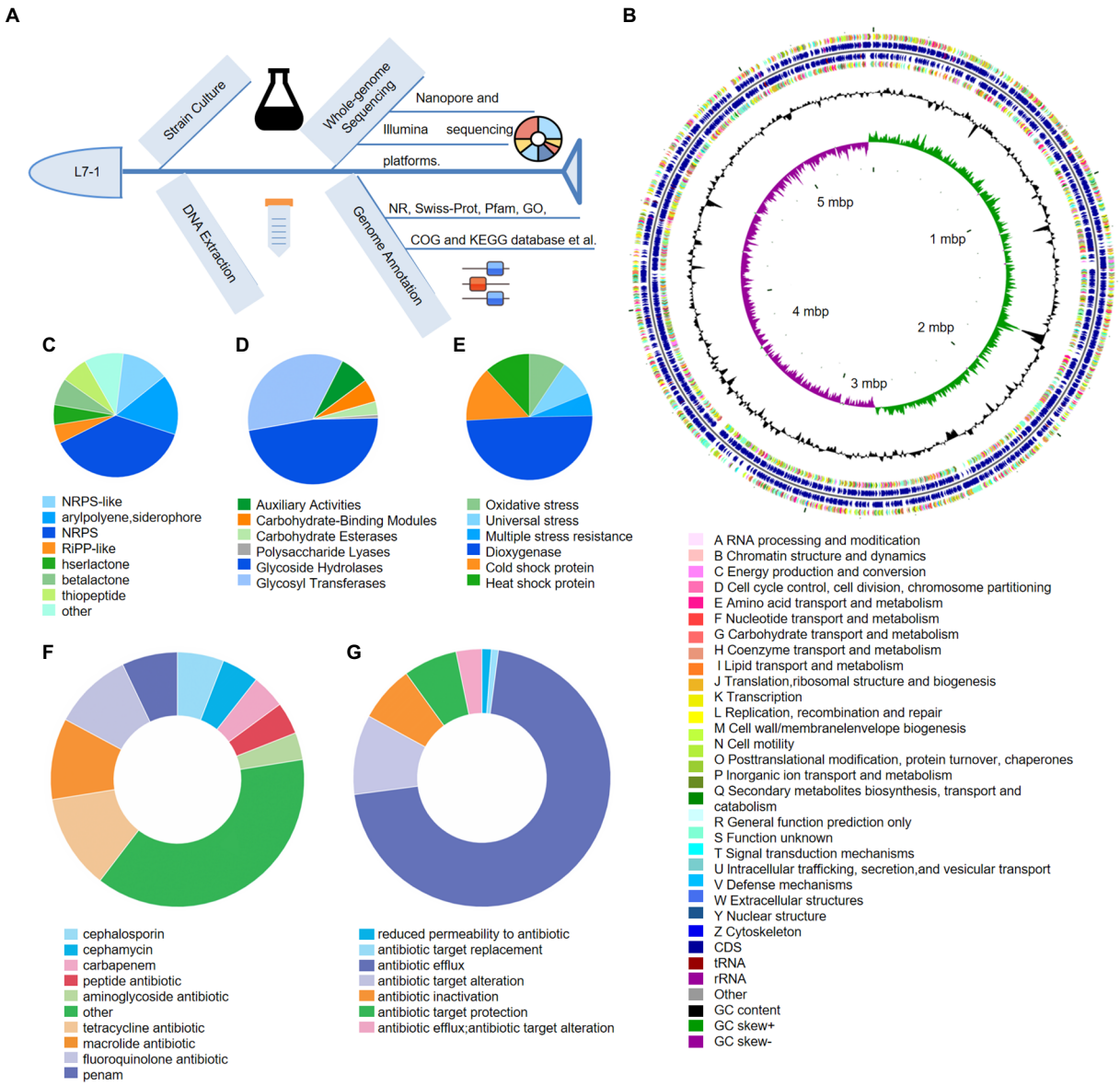

FIGURE 3
Genomic annotation and traits of *S. myotis* L7-1. **(A)** Workflow of the whole-genome sequencing of *S. myotis* L7-1 strain using Nanopore sequencing. **(B)** Circular map of chromosome of *S. myotis* L7-1. From outside to inside ring 1 and 4 depicts CDS in the positive strand and negative strand, different colors indicate different COG functional classifications. Ring 2 and 3 depicts CDS, tRNA and rRNA in the positive strand and negative strand. Ring 5 and 6 represents GC content and GC skew, respectively. cloud.majorbio.com. **(C)** Composition and relative abundance of secondary metabolic synthesis gene cluster genes of *S. myotis* L7-1. **(D)** Composition and relative abundance of CAZyme genes of *S. myotis* L7-1. **(E)** Composition and relative abundance of environmental adaptation genes of *S. myotis* L7-1. **(F)** Composition and relative abundance of antibiotic resistance genes of *S. myotis* L7-1. **(G)** Composition and relative abundance of antibiotic resistance mechanism of *S. myotis* L7-1. Origin 2022.

The available genomic data of symbiotic fish bacteria is limited. To decipher the highly adaptive features of *S. myotis*, we next compared *S. myotis* L7-1 genome with four closely related bacterial genomes, including *Serratia quinivorans* 13,188 isolated from soil (Ashelford et al., 2003), *Serratia grimesii* BXF1 isolated from the pinewood nematodes (Nascimento et al., 2018), *Serratia liquefaciens* ATCC 27592 isolated from the spacecraft assembly facilities (Schuerger et al., 2013), and *Serratia proteamaculans* 336x isolated from the rinds of cheeses (Zhang et al., 2018). A total of 118 BGCs genes and 109 CAZyme genes were common to the five *Serratia* genomes (Supplementary Figure S5E). The unique gene clusters associated with SMs production in *S. myotis* L7-1 included betalactone, RiPP-like, arylpolyene, and siderophore. The unique CAZymes included glycosyl transferases and polysaccharide lyases (Supplementary Figure S5F). A total of 2,479 KEGG genes and 2,087 COG genes were common to the five *Serratia* genomes (Figures 4A,B). These unique genes in *S. myotis* L7-1 include those encoded for trafficking proteins, membrane fusion proteins,

intracellular multiplication proteins, transport proteins, multiple enzymes and the others (Supplementary Tables S4, S5). Moreover, there was one notable feature that attracted our attention, the complete type IV secretion system with the particular plasmids.

L7-1 contained one chromosome and four plasmids, while other four reference bacterial genomes harbored one chromosome and no plasmids (Supplementary Figure S5). *S. myotis* L7-1 and all of the reference *Serratia* strains contained multiple secretion system genes, but only *S. myotis* L7-1 possessed a complete type IV secretion system (T4SS) located on the plasmids (Figure 4C). Many bacterial species deploy T4SSs to inject toxic effectors into target bacteria, thus inducing the death of rival cells (Rambow-Larsen and Weiss, 2004; Kutter et al., 2008; Juhas et al., 2010; Arslan-Aydogdu and Kimiran, 2018; Sgro et al., 2019). The type IV secretion system in *S. myotis* L7-1 included mainly type IV secretion system protein genes (virB1, 2, 4, 5, 6, 8, 9, 10, 11 and virD4) and a series of intracellular multiplication protein genes (icmB, E, G, J, K, L, O, P, T; Supplementary Table S4).

Purification and characterization of bioactive compounds *via* the bioactivity-guided fractionation

The versatile biosynthetic gene clusters and preliminary antimicrobial activity of the crude extract showed the great bioactive potential in *S. myotis* L7-1. To further determine the competitive roles of natural products, the bioactivity-guided fractionation assay against various pathogenic bacteria was conducted (Figure 5A). In total, 16.7 g of crude extract was obtained from a large-scale culture in rice solid medium. Bioactivity-guided purification and isolation strategy led to the

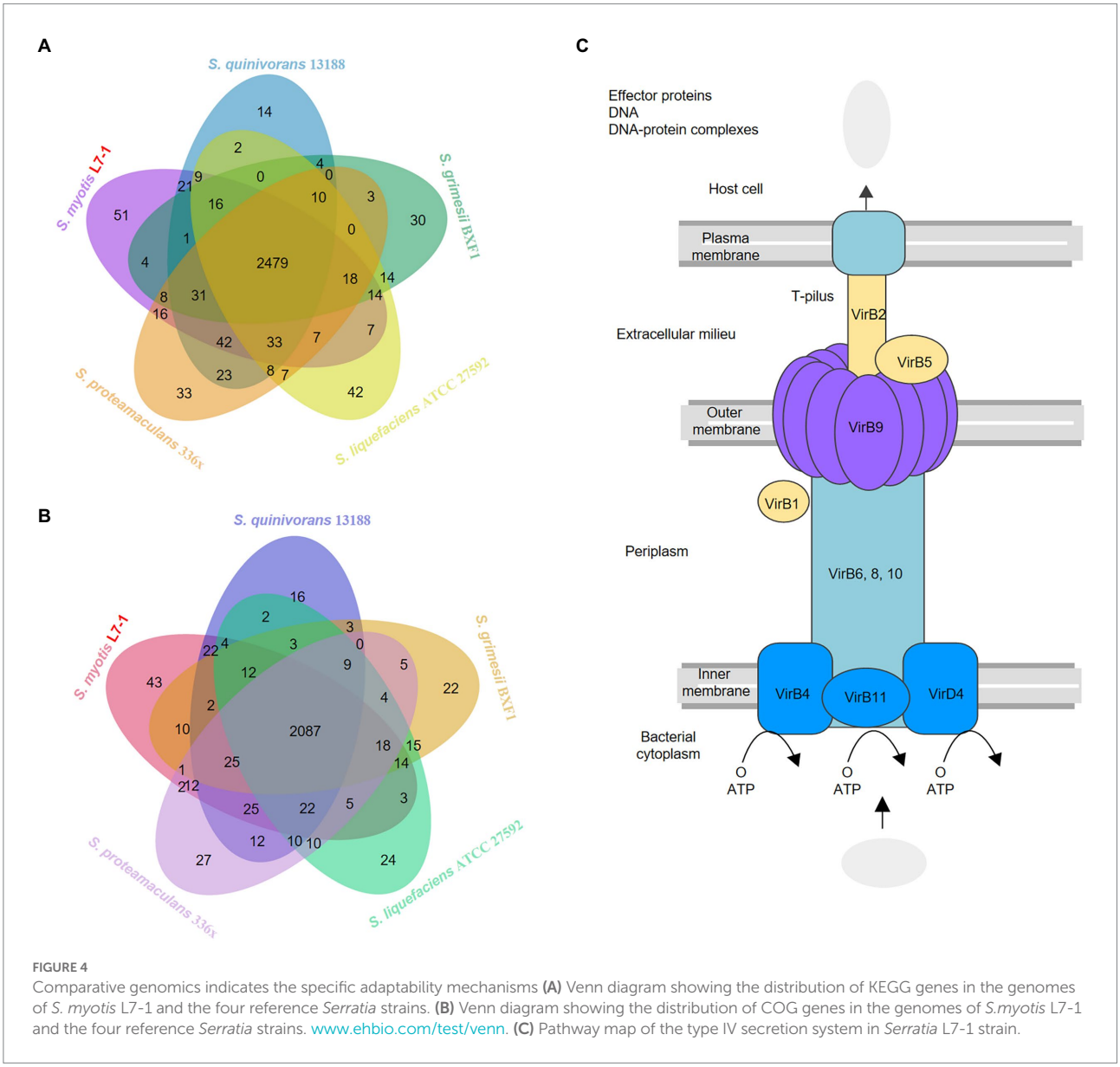

FIGURE 4
Comparative genomics indicates the specific adaptability mechanisms **(A)** Venn diagram showing the distribution of KEGG genes in the genomes of *S. myotis* L7-1 and the four reference *Serratia* strains. **(B)** Venn diagram showing the distribution of COG genes in the genomes of *S.myotis* L7-1 and the four reference *Serratia* strains. www.ehbio.com/test/venn. **(C)** Pathway map of the type IV secretion system in *Serratia* L7-1 strain.

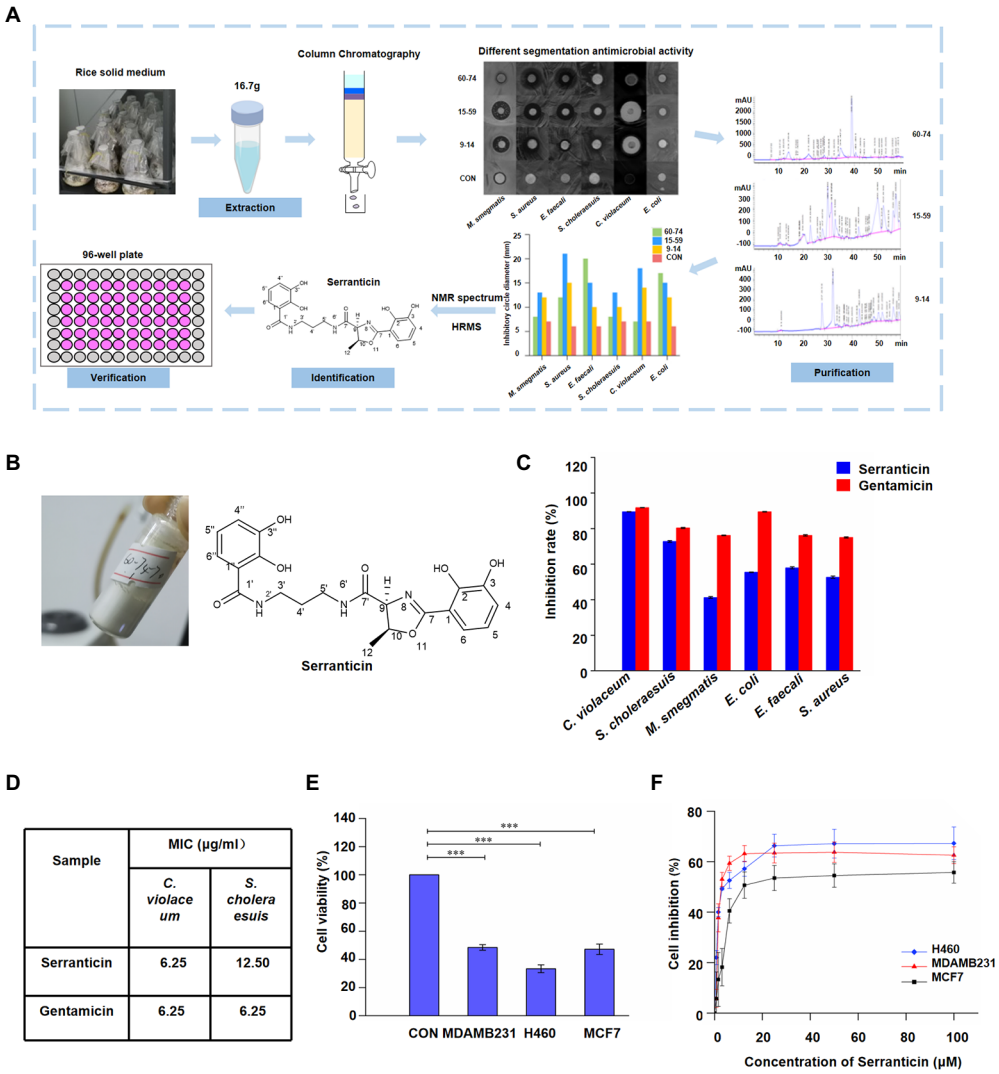

Sample	MIC (μg/ml)	
	C. violaceum	*S. choleraesuis*
Serranticin	6.25	12.50
Gentamicin	6.25	6.25

FIGURE 5
Purification and characterization of bioactive compound, serranticin. **(A)**, Workflow of the bioactivity-guided fractionation. **(B)**, Serranticin produced by *Serratia* L7-1 strain. ChemDraw 19.0 **(C)** *In-vitro* antimicrobial activity of the serranticin. Dates are the mean±s.d. The experiments were repeated tree times with similar results. *Blue squares* serranticin, *rad squares* Gentamicin. **(D)** The MIC values for inhibition of pathogenic bacteria of serranticin and the standard Gentamicin. Origin 2022. **(E)**, *In-vitro* cytotoxicity activity of the serranticin. Dates are the mean±s.d. The experiments were repeated tree times with similar results. Statistical significance of the test cell viability compared with the control group was determined using a two-tailed Student's t-test; the *p* values were as follows:<0.0001 MDAMB231, H460, and MCF7 cells. **(F)**, Inhibition of cell proliferation by serranticin against H460, MDAMB231 and MCF7 cells. Dates are the mean±s.d. The experiments were repeated tree times with similar results. *Blue diamond* H460, *rad triangle* MDAMB231, *black squares* MCF7. Origin 2022.

isolation of bioactive fraction, compound 1 (61 mg; Figure 5B). It is proved that compound 1 displayed significant anti-bacteria activity as a leading product, compared with that of the other compounds from *S. myotis* L7-1. The results demonstrated that bioactivity-guided fractionation was an attractive and effective approach for profiling and screening of bioactive compounds.

Compound 1 was isolated as a white powder with a UV absorption at 210 nm (Figure 5B) and a specific optical rotation value of $[\alpha]_D^{20}$–26.40° (*c* 1.05, acetone; Supplementary Table S6). Its molecular formula is $C_{21}H_{23}N_3O_7$ (429.15). Its ^{1}H NMR spectrum (600 MHz, in DMSO-d_6, Supplementary Figure S7A) showed the following signals: δ_H 2.23 (3H, d, *J* = 6.4 Hz, H-12), 3.28 (2H, m, H-4′), 3.97 (2H, m, H-5′), 4.08 (2H, m, H-3′), 5.24 (1H, d, *J* = 7.4 Hz, H-9), 5.64 (1H, m, H-10), 7.45 (1H, t, *J* = 8.0 Hz, H-5″), 7.52 (1H, t, *J* = 7.9 Hz, H-5), 7.68 (1H, dd, *J* = 7.9, 1.4 Hz, H-4), 7.75 (1H, dd, *J* = 7.9, 1.4 Hz, H-4″), 7.85 (1H, dd, *J* = 7.9, 1.4 Hz, H-6), 8.04 (1H, dd, *J* = 8.0, 1.4 Hz, H-6″), 9.09 (1H, t, *J* = 6.0, NH-2′), 9.58 (1H, t, *J* = 5.9 Hz, NH-6′), 10.00 (2H, s, OH-3, 3′), 12.52 (s, OH-2) and 13.54 (s, OH-2′). The ^{13}C NMR spectrum (150 MHz, in DMSO-d_6, Supplementary Figure S7B) showed 21 signals: δ_C 20.83 (q, C-12), 29.08 (t, C-4′), 36.74 (t, C-5′), 36.85 (t, C-3′), 73.88 (d, C-9), 78.97 (d, C-10), 110.49 (s, C-1), 115.09 (s, C-1″), 117.21 (d, C-6″), 118.01 (d, C-4), 118.08 (d, C-5″), 118.82 (d, C-5), 118.89 (d, C-4″), 119.58 (d, C-6), 145.91 (s, C-3), 146.42 (s, C-3″), 148.45 (s,

C-2), 149.92 (s, C-2″), 165.85 (s, C-7), 169.75 (s, C-1′), and 169.94 (s, C-7′). Based on its ^{1}H and ^{13}C NMR data, HRESIMS data, specific optical rotation value, and comparison with previous literature data (Kuo et al., 2011, 2012), compound 1 was proven to be identical to serranticin. The ^{1}H and ^{13}C NMR data of serranticin (1) were also summarized in Supplementary Table S7.

Serranticin shows significant antimicrobial activity and cytotoxicity

To further determine the bioactivity of serranticin in pharmaceutical potential, human pathogenic bacteria and tumor cells were chosen to conduct the antibiotic assay. Serranticin was tested against several bacterial strains, including *C. violaceum*, *S. choleraesuis*, *M. smegmatis*, *E. coli*, *E. faecalis*, and *S. aureus*. Gentamicin (an antibiotic against both Gram-positive and negative bacteria) was used as the positive control. The results showed that serranticin exhibited strong antibacterial activity against both *C. violaceum* and *S. choleraesuis* at 50 μg/ml, with inhibition rate of 89.5 and 72.8%, respectively (Figure 5C). In addition, serranticin also displayed moderate activity toward *M. smegmatis*, *E. coli*, *E. faecalis*, and *S. aureus* with inhibition rate of 41.2%，55.45%，57.9% and 52.6%, respectively. The antimicrobial activity was studied further to evaluate the minimum inhibitory concentration (MIC) against *C. violaceum* and *S. choleraesuis* by broth microdilution method. Serranticin showed excellent antimicrobial activities against *C. violaceum* and *S. choleraesuis* with MIC values of 6.25 and 12.50 μg/ml, while the MIC value of gentamicin were 6.25 and 6.25 μg/ml (Figure 5D). Serranticin approximately rivaled the antimicrobial activity of the positive control gentamicin.

Antitumor activities of serranticin were tested by the MTT method using the human breast carcinoma MDA-MB-231, MCF7 and human lung cancer NCI-H460 cell lines. Serranticin inhibited the growth of three tested cell lines significantly and the cell viability values at 100 μM were given below, 48.5% (MDA-MB-231), 33.4% (NCI-H460), and 47.2% (MCF7; Figure 5E), respectively. The half-inhibitory concentration (IC50) of serranticin on MDA-MB-231, NCI-H460 and MCF7 cell lines were determined to be 2.8, 3.8 and 12.1 μM (Figure 5F), respectively. The data indicated that serranticin showed strong inhibitory activity against human cancer cell lines, suggesting that it can be a potential candidate for pharmaceutical application.

Serratia myotis L7-1 confers protection for the colonization *via* metabolism

It seems that *S. myotis* L7-1 harbored the ARGs to resist several antibiotics. To further determine the multiple resistance of *S. myotis* L7-1, the drug sensitivity test was conducted. Using the Kirby-Bauerdisca (K-B) agar diffusion method (Figure 6A), we tested the drug susceptibility with common clinical antibiotics at 1 mg/ml, including ampicillin, spectinomycin, vancomycin, kanamycin, tetracyclines, gentamycin and amphotericin. LB medium was used as negative control. The results indicated that the activities of ampicillin, spectinomycin, amphotericin and vancomycin were equivalent to the negative control for *S. myotis* L7-1 in terms of inhibition, with no significant zone of inhibition shown (Figure 6B). The diameters of the inhibition circle were 13.3, 11.3 and 13.7 cm for kanamycin, tetracyclines and gentamycin. From these results, it is clear that *S. myotis* can tolerate ampicillin, spectinomycin, amphotericin and vancomycin, while it is sensitive to kanamycin, tetracyclines and gentamycin.

The BGCs analyses of *S. myotis* reveal the potential production of bioactive compounds. The preliminary antagonism assays indicated that *S. myotis* L7-1 inhibits the growth of bacteria pathogens (Figure 2F). Next, the bioactivity-guided fractionation against aquatic pathogen was conduct, presenting the excellent active agent, serranticin. The antimicrobial activity of serranticin was determined *in vitro* for against *Edwardsiella tarda* and *Aeromonas hydrophila*, the serious bacteria pathogens of fish. The results showed that serranticin was active against *E. tarda* and *A. hydrophila* at 50 μg/ml, with inhibition rate of 83.3 and 70.5% (Figure 6C). The MIC values of the serranticin were determined by the broth microdilution method. The results indicated that serranticin had strong anti-aquatic pathogenic bacteria activity in inhibiting the growth of *E. tarda* (MIC: 6.25 μg/ml), and *A. hydrophila* (MIC: 6.25 μg/ml; Figure 6D). Positive control gentamicin had anti-bacteria activity with an MIC value of 12.5 μg/ml against *E. tarda* and 12.5 μg/ml against *A. hydrophila*. Serranticin displayed even stronger antimicrobial activity than positive control gentamicin, that contributes to the development of probiotics and potential utility in fishery industry.

Discussion

The symbiotic microbiota have evolved environmental adaptation, and possess the potential production of abundant and novel natural products (Dou and Dong, 2019). However, there are still some issues that need to be resolved. For example, one overriding problem is how to find the core microbe to play the key roles in the environmental adaptation and the potential to be the industrial strains (Macintyre et al., 2014). Here, we showed the methods to discover the valuable strains from the huge nature resources, recruiting cultivable method and the genomic analyses (TB-S, TB-I). In our study, 58 cultivable bacteria have been isolated. The isolated strains from such extreme environment would offer excellent model organism to investigate the physiology of the symbionts and understand their ecological role in the host. However, it was still challenging to select the representative strain. Through the comparison of populations of TB-S and TB-I, *S. myotis* became the potential target genus among the isolated symbiotic bacteria as the prevalent genus with the high adaptability and bioactive potential. The intrinsic existence of *S. myotis* was also proved by the meta-genomic analyses of fish

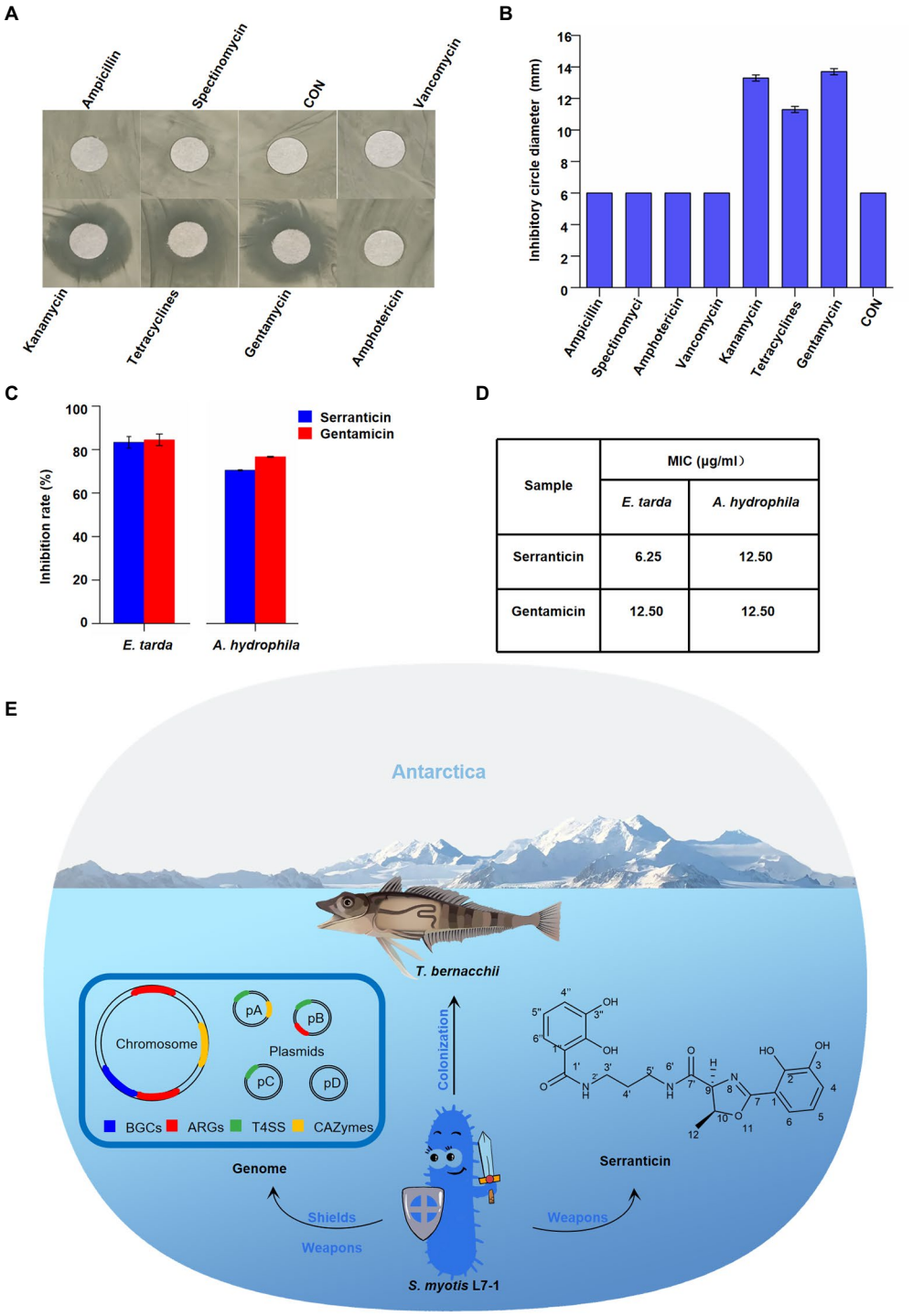

FIGURE 6
Effect of serranticin on bacteria antagonism. **(A)** Zone of inhibition of *S. myotis* L7-1 by antibiotics. **(B)** Antibiotic resistance activity of *S. myotis* L7-1. The diameter of circular filter paper sheets was 6mm. Dates are the mean±s.d. The experiments were repeated tree times with similar results. Origin 2022 **(C)**, *In-vitro* antimicrobial activity of the serranticin. Dates are the mean±s.d. The experiments were repeated tree times with similar results. *Blue squares* serranticin, *rad squares* Gentamicin. Origin 2022. **(D)** The MIC values for inhibition of aquatic pathogenic bacteria of serranticin and the standard Gentamicin. Origin 2022. **(E)** Diagram illustrating how *S. myotis* L7-1 from *T. bernacchii* helps hosts adapt to the extreme Antarctic environment and resist pathogenic bacteria through the unique genomic features and production of serranticin.

sample (data not shown). Although more research is needed, it seems to be an effective way to pick up the potential bacteria.

Serratia bacteria show versatile niche occupation abilities in plant, soil, water and animals, associated with a wide range of different hosts (Kalbe et al., 1996; Kamensky et al., 2003; Tsaplina et al., 2015; Zheng et al., 2021). It is still unclear what's the underlying causes in environmental adaptation of *Serratia* sp. (Nascimento et al., 2018). In our study, the general genome

features of *S. myotis* associated with the adaptation of extreme environment were characterized, like the genes related to cold adaptation (heat shock protein) and stress response. Furthermore, we speculate that the reservoir of antibiotic-resistance potential and multiple antibiotic resistance mechanisms facilitated *S. myotis* to survive in host under the selection pressure in adverse environment. Here, most of the ARGs located on the chromosome confers the intrinsic resistance of *S. myotis,* which is different from the other plasmid-carrying bacteria in an antibiotic-influenced environment (Luisa et al., 2018). However, most research on antibiotic-resistant bacteria (ARB) have focused on the mainland and offshore oceans, and its extent in polar regions has seldom been investigated (Na et al., 2021). It seems that it has been underestimated that Antarctic environment provides a natural reservoir for antibiotic resistance genes. Furthermore, the existence of type VI transporter system in plasmid of *S. myotis* was not found in the other four *Serratia* sp. T4SSs are used for the delivery of bacterial effector proteins across the membrane of eukaryotic target cells, contributing directly to the bacterial pathogenicity (Aguilar et al., 2010). The type IV secretion system may contribute to the evolvement of *S. myotis* as the toxin transporters in inter-bacterial antagonism and communication. Although more functional studies need to be tested, our genomic characterization could be a useful step in addressing the adaptation of symbionts in Antarctic fish in future.

Serratia bacteria show biosynthesized ability of a broad range of secondary metabolites (SMs; Soenens and Imperial, 2019). The ecological function of *Serratia* has been studied with multi-species by metabolome analyses (Clements et al., 2019). However, it remains open if SMs of *Serratia* from the Antarctic fish are involved in novel function. Our BGCs analyses indicated that *S. myotis* has the ability of abundant bioactive compounds production. We showed the purification and characterization of serranticin from *S. myotis*. The critical roles of antitumor activity and antibacterial activity, make serranticin tailored for the pharmaceutic and bio-control application. The structure of serranticin is analogous to siderophores, which are iron chelators in bacterial iron acquisition (Page, 2019). It appears that serranticin has never been reported in *S. myotis* in previous reports (Kuo et al., 2011). Compared with the sequence of biosynthetic cluster in the published data (Seyedsayamdost et al., 2012), two serranticin clusters of 21 kb and 12.3 kb, were assigned as src cluster in *S. myotis* (Supplementary Figure S8; Supplementary Tables S8, S9). The high homologous cluster sequence and the accepted role of this compound as siderophore give the hints of interpreting the role of serranticin in bacterial competition. Furthermore, serranticin inhibited the growth of *Aeromonas hydrophila* and *Edwardsiella piscicida*, which are harmful to the fish health. These results indicate that *Serratia* outcompete some fish pathogens. It is reasonable to suspect then that *S. myotis* can benefit from the production of serranticin and may even facilitate the host health. The obtained results led us to propose a hypothetical model. The strong activity in bacteria antagonism determines its ecological role as an active defense system in direct interactions with symbiotic microorganisms, while the antibiotic-resistance acts as a passive defense system in extreme environment (Figure 6E).

Our work emphasizes the discovery and importance of a symbiotic bacteria of fish from Antarctic, *S. myotis* L7-1. Host adaptability mechanism and its biosynthetic potential were investigated using the whole genomic sequencing and chemical characterization. Our study provides the first insights into the adaptative role of symbiotic microbiota in Antarctic fish from the extreme environment, that could pave the way for future research. Furthermore, Antarctic bacteria are hardly studied as potential sources of novel natural products for exploitation in medicine, agriculture, and food. Further detailed study on bioactive compounds could shed light on the discovery of novel natural products from the symbiotic microbiomes of fish.

Statistics and reproducibility

Unless specifically noted, each experiment was repeated three or more times independently. Data were collected from three biological and three technical replicates, unless otherwise noted. Data shown in column graphs or line chart represent mean ± the standard deviation (SD), as indicated in the figure legends. Statistical analysis was performed with Origin 2022.[1] Graph preparation was performed,[2] itol.embl.de and ChemDraw 19.0. More details were given in the figure legends and methods.

Data availability statement

The data presented in the study are deposited in the National Center for Biotechnology Information (NCBI, https://www.ncbi.nlm.nih.gov/) repository. The entire 16sRNA gene sequence dataset in this paper has been uploaded in the NCBI Sequence Read Archive (accession no. PRJNA852421). The whole-genome and the sequences of 4 plasmids have been deposited at the NCBI genome database under the accession numbers CP099707 (Chromosome), CP099708 (pL71A), CP099709 (pL71B), CP099710 (pL71C), and CP099711 (pL71D).

Author contributions

YX performed most of the experiments and analyzed the results. FY and YC participated in isolation of strains. JD and RL contributed to the genomic profiling assay. WZ collected the samples. ZZ analyzed the data about structure characterization. JF reviewed the manuscript. LC conceived the idea and supervised

1 www.ehbio.com/test/venn

2 www.figdraw.com

the project. XY designed, coordinated the study, provided all the infrastructure, supervised the project, and wrote the manuscript. All authors contributed to the article and approved the submitted version.

Funding

This work was supported by grants from National Natural Science Foundation of China 42006086 and 91951210, Shanghai sailing program 20YF1416900, Science and Technology Commission of Shanghai Municipality STCSM 20050501700, the National Key Research and Development Program of China (2018YFD0900601).

Acknowledgments

We would like to thank Jun Zou of Shanghai Ocean University, for providing the pathogenic bacteria strains used in this study. Correspondence and requests for materials should be addressed to XY.

Conflict of interest

The authors declare that the research was conducted in the absence of any commercial or financial relationships that could be construed as a potential conflict of interest.

Publisher's note

Supplementary material

The Supplementary material for this article can be found online at: https://www.frontiersin.org/articles/10.3389/fmicb.2022.1085063/full#supplementary-material

References

Aguilar, J., Zupan, J., Cameron, T. A., and Zambryski, P. C. (2010). Agrobacterium type IV secretion system and its substrates form helical arrays around the circumference of virulence-induced cells. *Proc. Natl. Acad. Sci. U. S. A.* 107, 3758–3763. doi: 10.1073/pnas.0914940107

Arslan-Aydogdu, E. Ö., and Kimiran, A. (2018). An investigation of virulence factors of legionella pneumophila environmental isolates. *Braz. J. Microbiol.* 49, 189–199. doi: 10.1016/j.bjm.2017.03.012

Ashelford, K. E., Day, M. J., and Fry, J. C. (2003). Elevated abundance of bacteriophage infecting bacteria in soil. *Appl. Environ. Microbiol.* 69, 285–289. doi: 10.1128/AEM.69.1.285-289.2003

Bairoch, A., and Apweiler, R. (2000). The SWISS-PROT protein sequence database and its supplement TrEMBL in 2000. *Nucleic Acids Res.* 28, 45–48. doi: 10.1093/nar/28.1.45

Cantarel, B. L., Coutinho, P. M., Rancurel, C., Bernard, T., and Lombard, V. (2009). The carbohydrate-active EnZymes database (CAZy): an expert resource for glycogenomics. *Nucleic Acids Res.* 37, D233–D238. doi: 10.1093/nar/gkn663

Chan, P. P., and Lowe, T. M. (2019). tRNAscan-SE: searching for tRNA genes in genomic sequences. *Methods Mol. Biol.* 1962, 1–14. doi: 10.1007/978-1-4939-9173-0_1

Chen, S., Zhou, Y., Chen, Y., and Jia, G. (2018). Fastp: an ultra-fast all-in-one FASTQ preprocessor. *Bioinformatics* 34, i884–i890. doi: 10.1093/bioinformatics/bty560

Clements, T., Ndlovu, T., Khan, S., and Khan, W. (2019). Biosurfactants produced by Serratia species: classification, biosynthesis, production and application. *Appl. Microbiol. Biotechnol.* 103, 589–602. doi: 10.1007/s00253-018-9520-5

Consortium G O (2004). The gene ontology (GO) database and informatics resource. *Nucleic Acids Res.* 32, 258D–2261D. doi: 10.1093/nar/gkh036

Cormack, W., and Fraile, E. R. (1990). Bacterial flora of newly caught Antarctic fish Notothenia neglecta. *Polar Biol.* 10, 413–417. doi: 10.1007/BF00233688

Delcher, A. L., Bratke, K. A., Powers, E. C., and Salzberg, S. L. (2007). Identifying bacterial genes and endosymbiont DNA with glimmer. *Bioinformatics* 23, 673–679. doi: 10.1093/bioinformatics/btm009

Dixon, R. A. (2001). Natural products and plant disease resistance. *Nat. Commun.* 411, 843–847. doi: 10.1038/35081178

Dou, X., and Dong, B. (2019). Origins and bioactivities of natural compounds derived from marine ascidians and their symbionts. *Mar. Drugs* 17:670. doi: 10.3390/md17120670

Eastman, J. T. (2004). The nature of the diversity of Antarctic fishes. *Polar Biol.* 28, 93–107. doi: 10.1007/s00300-004-0667-4

Edgar, R. C. (2013). UPARSE: highly accurate OTU sequences from microbial amplicon reads. *Nat. Methods* 10, 996–998. doi: 10.1038/nmeth.2604

Finn, R. D., Bateman, A., Clements, J., Coggill, P., Eberhardt, R. Y., Eddy, S. R., et al. (2013). Pfam: the protein families database. *Nucleic Acids Res.* 42, D222–D230. doi: 10.1093/nar/gkt1223

García-Fraile, P., Chudíčková, M., Benada, O., Pikula, J., and Kolařík, M. (2015). Serratia myotis sp. nov. and Serratia vespertilionis sp. nov., isolated from bats hibernating in caves. *Int. J. Syst. Evol. Microbiol.* 65, 90–94. doi: 10.1099/ijs.0.066407-0

Giuliani, M. E., Nardi, A., Carlo, M. D., Benedetti, M., and Regoli, F. (2021). Transcriptional and catalytic responsiveness of the Antarctic fish Trematomus bernacchii antioxidant system toward multiple stressors. *Antioxidants* 10:410. doi: 10.3390/antiox10030410

Gutierrez, R. M. P., and Gonzalez, A. M. N. (2012). Compounds derived from endophytes: a review of Phytochemistry and pharmacology. *Curr. Med. Chem.* 19, 2992–3030. doi: 10.2174/092986712800672111

Hover, T., Maya, T., Ron, S., Sandovsky, H., Shadkchan, Y., Kijner, N., et al. (2016). Mechanisms of bacterial (Serratia marcescens) attachment to, migration along, and killing of fungal hyphae. *Appl. Environ. Microbiol.* 82, 2585–2594. doi: 10.1128/AEM.04070-15

Huang, H. C., Liaw, C. C., Zhang, L. J., Ho, H. U., Kuo, L. M. Y., Shen, Y. C., et al. (2008). Triterpenoidal saponins from Hydrocotyle sibthorpioides. *Phytochemistry* 69, 1597–1603. doi: 10.1016/j.phytochem.2008.01.005

Jia, B., Raphenya, A. R., Alcock, B., Waglechner, N., and Mcarthur, A. G. (2016). CARD 2017: expansion and model-centric curation of the comprehensive antibiotic resistance database. *Nucleic Acids Res.* 45, D566–D573. doi: 10.1093/nar/gkw1004

Juhas, M., Crook, D. W., and Hood, D. W. (2010). Type IV secretion systems: tools of bacterial horizontal gene transfer and virulence. *Cell. Microbiol.* 10, 2377–2386. doi: 10.1111/j.1462-5822.2008.01187.x

Kai, B., Wolf, T., Chevrette, M. G., Lu, X., Schwalen, C. J., Kautsar, S. A., et al. (2017). antiSMASH 4.0—improvements in chemistry prediction and gene cluster boundary identification. *Nucleic Acids Res.* 45, W36–W41. doi:10.1093/nar/gkx319

Kalbe, C., Marten, P., and Berg, G. (1996). Strains of the genus Serratia as beneficial rhizobacteria of oilseed rape with antifungal properties. *Microbiol. Res.* 151, 433–439. doi: 10.1016/S0944-5013(96)80014-0

Kamensky, M., Ovadis, M., Chet, I., and Chernin, L. (2003). Soil-borne strain IC14 of Serratia plymuthica with multiple mechanisms of antifungal activity

provides biocontrol of Botrytis cinerea and Sclerotinia sclerotiorum diseases. *Soil Biol. Biochem.* 35, 323–331. doi: 10.1016/S0038-0717(02)00283-3

Kumar, S., Nei, M., Dudley, J., and Tamura, K. (2008). MEGA: a biologist-centric software for evolutionary analysis of DNA and protein sequences. *Brief. Bioinformatics* 9, 299–306. doi: 10.1093/bib/bbn017

Kuo, Y. H., Hsu, H. C., Chen, Y. C., Liang, T. W., Wang, S. L. J. J. O. A., and Chemistry, F. (2012). A novel compound with antioxidant activity produced by Serratia ureilytica TKU013. *Agric Food Chem* 60, 9043–9047. doi: 10.1021/jf302481n

Kuo, Y. H., Liang, T. W., Liu, K. C., Hsu, Y. W., Hsu, H. C., and Wang, S. L. (2011). Isolation and identification of a novel antioxidant with antitumour activity from Serratia ureilytica using squid pen as fermentation substrate. *Mar. Biotechnol.* 13, 451–461. doi: 10.1007/s10126-010-9316-9

Kutter, S., Buhrdorf, R., Haas, J., Schneider-Brachert, W., and Fischer, W. (2008). Protein subassemblies of the helicobacter pylori cag type IV secretion system revealed by localization and interaction studies. *J. Bacteriol.* 190, 2161–2171. doi: 10.1128/JB.01341-07

Lars Juhl, J., Philippe, J., Michael, K., Christian, V. M., Jean, M., Tobias, D., et al. (2008). eggNOG: automated construction and annotation of orthologous groups of genes. *Nucleic Acids Res.* 36, D250–D254. doi: 10.1093/nar/gkm796

Li, S. Y., Wang, P., Yuan, W., Su, Z. S., and Bullard, S. H. (2016). Endocidal regulation of secondary metabolites in the producing organisms. *Sci. Rep.* 6:29315. doi: 10.1038/srep29315

Lu, M., Hulcr, J., and Sun, J. H. (2016). The role of symbiotic microbes in insect invasions. *Annu. Rev. Ecol. Evol. Syst.* 47, 487–505. doi: 10.1146/annurev-ecolsys-121415-032050

Luisa, S. M., Pablo, V., Alejandro, C., and Rosario, M. E. (2018). The genomic basis of intrinsic and acquired antibiotic resistance in the genus Serratia. *Front. Microbiol.* 9:828. doi: 10.3389/fmicb.2018.00828

Maccormack, W. P., and Fraile, E. R. (1991). Bacterial flora of the digestive tract of specimens of Notothenia neglecta caught in Caleta Potter (south Shetland archipelago, Antarctica). *Rev. Argent. Microbiol.* 23, 160–165. PMID: 1815278

Macintyre, L., Zhang, T., Viegelmann, C., Martinez, I. J., Cheng, C., Dowdells, C., et al. (2014). Metabolomic tools for secondary metabolite discovery from marine microbial symbionts. *Mar. Drugs* 12, 3416–3448. doi: 10.3390/md12063416

Magoč, T., and Salzberg, S. L. (2011). FLASH: fast length adjustment of short reads to improve genome assemblies. *Bioinformatics* 27, 2957–2963. doi: 10.1093/bioinformatics/btr507

Moreau, C. S. (2020). Symbioses among ants and microbes. *Curr Opin Insect Sci* 39, 1–5. doi: 10.1016/j.cois.2020.01.002

Na, G., Zhang, W., Gao, H., Wang, C., Li, R., Zhao, F., et al. (2021). Occurrence and antibacterial resistance of culturable antibiotic-resistant bacteria in the Fildes peninsula. *Antarctica. Mar Pollut Bull* 162:111829. doi: 10.1016/j.marpolbul.2020.111829

Nascimento, F., Cláudia, V., Cock, P., Tavares, M., and Mota, M. (2018). From plants to nematodes: Serratia grimesii BXF1 genome reveals an adaptation to the modulation of multi-species interactions. *Microb Genom* 4, 1–13. doi: 10.1099/mgen.0.000178

Neshich, G., Borro, L. C., Higa, R. H., Kuser, P. R., Yamagishi, M. E. B., Franco, E. H., et al. (2005). The diamond STING server. *Nucleic Acids Res.* 33, W29–W35. doi: 10.1093/nar/gki397

Obrien, K. M. (2016). New lessons from an old fish: what Antarctic icefishes may reveal about the functions of oxygen-binding proteins. *Integr. Comp. Biol.* 56, 531–541. doi: 10.1093/icb/icw062

Ogata, H., Goto, S., Sato, K., Fujibuchi, W., Bono, H., and Kanehisa, M. (1999). KEGG: Kyoto encyclopedia of genes and genomes. *Nucleic Acids Res.* 27, 29–34. doi: 10.1093/nar/27.1.29

Page, M. G. P. (2019). The role of iron and Siderophores in infection, and the development of Siderophore antibiotics. *Clin. Infect. Dis.* 69, S529–S537. doi: 10.1093/cid/ciz825

Potter, S. C., Luciani, A., Eddy, S. R., Park, Y., Lopez, R., and Finn, R. D. (2018). HMMER web server: 2018 update. *Nucleic Acids Res.* 46, W200–W204. doi: 10.1093/nar/gky448

Rambow-Larsen, A. A., and Weiss, A. A. (2004). Temporal expression of pertussis toxin and Ptl secretion proteins by Bordetella pertussis. *J. Bacteriol.* 186, 43–50. doi: 10.1128/JB.186.1.43-50.2004

Schuerger, A. C., Ulrich, R., Berry, B. J., and Nicholson, W. L. (2013). Growth of Serratia liquefaciens under 7 mbar, 0°C, and CO2-enriched anoxic atmospheres. *Astrobiology* 13, 115–131. doi: 10.1089/ast.2011.0811

Sedláček, I., Staňková, E., and Švec, P. (2016). Composition of cultivable enteric bacteria from the intestine of Antarctic fish (family Nototheniidae). *Czech J Anim Sci* 61, 127–132. doi: 10.17221/8785-CJAS

Seyedsayamdost, M. R., Cleto, S., Carr, G., Vlamakis, H., Joao Vieira, M., Kolter, R., et al. (2012). Mixing and matching siderophore clusters: structure and biosynthesis of serratiochelins from Serratia sp. V4. *J. Am. Chem. Soc.* 134, 13550–13553. doi: 10.1021/ja304941d

Sgro, G. G., Oka, G. U., Souza, D. P., Cenens, W., Bayer-Santos, E., Matsuyama, B. Y., et al. (2019). Bacteria-killing type IV secretion systems. *Front. Microbiol.* 10:1078. doi: 10.3389/fmicb.2019.01078

Soenens, A., and Imperial, J. (2019). Biocontrol capabilities of the genus Serratia. *Phytochem. Rev.* 19, 577–587. doi: 10.1007/s11101-019-09657-5

Song, W., Li, L. Z., Huang, H. L., Jiang, K. J., Zhang, L. J., Chen, X. Z., et al. (2016). The gut microbial Community of Antarctic Fish Detected by 16S rRNA gene sequence analysis. *Biomed. Res. Int.* 2016, 3241529–3241527. doi: 10.1155/2016/3241529

Stackebrandt, E., and Goebel, B. M. (1994). Taxonomic note: a Place for DNA-DNA Reassociation and 16S rRNA sequence analysis in the present species definition in bacteriology. *Int. J. Syst. Bacteriol.* 44, 846–849. doi: 10.1099/00207713-44-4-846

Tercero, A. D., and Place, S. P. (2020). Characterizing gene copy number of heat shock protein gene families in the emerald Rockcod. *Trematomus bernacchii. Genes* 11:867. doi: 10.3390/genes11080867

Tsaplina, O., Bozhokina, E., Mardanova, A., and Khaitlina, S. (2015). Virulence factors contributing to invasive activities of Serratia grimesii and Serratia proteamaculans. *Arch. Microbiol.* 197, 481–488. doi: 10.1007/s00203-014-1079-7

Wang, Q., Garrity, G. M., Tiedje, J. M., and Cole, J. R. (2007). Naïve Bayesian classifier for rapid assignment of rRNA sequences into the new bacterial taxonomy. *Appl. Environ. Microbiol.* 73, 5261–5267. doi: 10.1128/AEM.00062-07

Wang, Y. N., Meng, L. H., and Wang, B. G. (2020). Progress in research on bioactive secondary metabolites from Deep-Sea derived microorganisms. *Mar. Drugs* 18:614. doi: 10.3390/md18120614

Ward, N. L., Steven, B., Penn, K., and Methé, B. A. (2009). Characterization of the intestinal microbiota of two Antarctic notothenioid fish species. *Extremophiles* 13, 679–685. doi: 10.1007/s00792-009-0252-4

Xin, W., Ye, X., Yu, S., Lian, X. Y., and Zhang, Z. (2012). New Capoamycin-type antibiotics and polyene acids from marine Streptomyces fradiae PTZ0025. *Mar. Drugs* 10, 2388–2402. doi: 10.3390/md10112388

Xuan, Z., Wei, W., and Tan, R. (2015). Symbionts, a promising source of bioactive natural products. *Sci. China Chem.* 58, 1097–1109. doi: 10.1007/s11426-015-5398-6

Ye, J., Mcginnis, S., and Madden, T. L. (2006). BLAST: improvements for better sequence analysis. *Nucleic Acids Res.* 34, W6–W9. doi: 10.1093/nar/gkl164

Zhang, Y. C., Kastman, E. K., Guasto, J. S., and Wolfe, B. E. (2018). Fungal networks shape dynamics of bacterial dispersal and community assembly in cheese rind microbiomes. *Nat. Commun.* 9:336. doi: 10.1038/s41467-017-02522-z

Zheng, Q., Meng, X., Cheng, M., Li, Y., and Chen, X. (2021). Cloning and characterization of a new Chitosanase from a Deep-Sea bacterium Serratia sp. *QD07. Front Microbiol* 12:619731. doi: 10.3389/fmicb.2021.619731

frontiers | Frontiers in Microbiology

TYPE Review
PUBLISHED 15 March 2023
DOI 10.3389/fmicb.2023.1149903

OPEN ACCESS

EDITED BY
Memory Tekere,
University of South Africa, South Africa

REVIEWED BY
Axel Schippers,
Federal Institute for Geosciences and Natural Resources, Germany
Grace Nkechinyere Ijoma,
University of South Africa, South Africa

*CORRESPONDENCE
Mark Dopson
✉ mark.dopson@lnu.se

SPECIALTY SECTION
This article was submitted to Extreme Microbiology, a section of the journal Frontiers in Microbiology

RECEIVED 23 January 2023
ACCEPTED 16 February 2023
PUBLISHED 15 March 2023

CITATION
Dopson M, González-Rosales C, Holmes DS and Mykytczuk N (2023) Eurypsychrophilic acidophiles: From (meta)genomes to low-temperature biotechnologies. *Front. Microbiol.* 14:1149903. doi: 10.3389/fmicb.2023.1149903

Eurypsychrophilic acidophiles: From (meta)genomes to low-temperature biotechnologies

Mark Dopson[1]*, Carolina González-Rosales[1,2], David S. Holmes[2,3] and Nadia Mykytczuk[4]

[1]Centre for Ecology and Evolution in Microbial Model Systems (EEMiS), Linnaeus University, Kalmar, Sweden, [2]Center for Bioinformatics and Genome Biology, Centro Ciencia & Vida, Fundación Ciencia & Vida, Santiago, Chile, [3]Facultad de Medicina y Ciencia, Universidad San Sebastian, Santiago, Chile, [4]Goodman School of Mines, Laurentian University, Sudbury, ON, Canada

Low temperature and acidic environments encompass natural milieus such as acid rock drainage in Antarctica and anthropogenic sites including drained sulfidic sediments in Scandinavia. The microorganisms inhabiting these environments include polyextremophiles that are both extreme acidophiles (defined as having an optimum growth pH <3), and eurypsychrophiles that grow at low temperatures down to approximately 4°C but have an optimum temperature for growth above 15°C. Eurypsychrophilic acidophiles have important roles in natural biogeochemical cycling on earth and potentially on other planetary bodies and moons along with biotechnological applications in, for instance, low-temperature metal dissolution from metal sulfides. Five low-temperature acidophiles are characterized, namely, *Acidithiobacillus ferriphilus*, *Acidithiobacillus ferrivorans*, *Acidithiobacillus ferrooxidans*, *"Ferrovum myxofaciens,"* and *Alicyclobacillus disulfidooxidans,* and their characteristics are reviewed. Our understanding of characterized and environmental eurypsychrophilic acidophiles has been accelerated by the application of "omics" techniques that have aided in revealing adaptations to low pH and temperature that can be synergistic, while other adaptations are potentially antagonistic. The lack of known acidophiles that exclusively grow below 15°C may be due to the antagonistic nature of adaptations in this polyextremophile. In conclusion, this review summarizes the knowledge of eurypsychrophilic acidophiles and places the information in evolutionary, environmental, biotechnological, and exobiology perspectives.

KEYWORDS

acidic (microbial) environments, astrobiology, bio-applications, polyextremophile, snowball earth, stenopsychrophile

Introduction

Natural acidic environments include weathered deposits of sulfidic minerals [reviewed in Hedrich and Schippers (2016)] such as in the Iberian pyrite belt where the acidity is generated underground and flows into the Río Tinto (Amils, 2016); volcanic hot pools in, e.g., Hell's Gate (Tikitere), New Zealand (Dunfield et al., 2007); and acid sulfate (AS) soils in Australia (Ling et al., 2015). The generation of anthropogenic acidic environments includes mining and processing of sulfidic ores for the generation of metals including "bioheaps" for copper recovery in the Atacama Desert, Chile (Petersen, 2016). While all the above

examples are from warm to hot environments, low-temperature acidic milieus also exist (Figure 1). These include acid rock drainage (ARD) of naturally exposed metal sulfides on, e.g., the South Shetland Islands, Antarctica (Dold et al., 2013); isostatic rebound of Baltic Sea coastal sulfidic sediments that once exposed to air become acid sulfate soils (AS soils) (Boman et al., 2010); and acid mine drainage (AMD) from metal sulfides mines in, e.g., Norway (Johnson et al., 2001).

Microorganisms that inhabit low pH environments are termed "acidophiles," and they have an optimum pH for growth of <5, while extreme acidophiles have an optimum pH of <3 (Johnson and Quatrini, 2016). Acidophilic bacteria obtain energy for growth *via* the oxidation of ferrous iron (Bonnefoy and Holmes, 2012), inorganic sulfur compounds (ISCs) (Dopson and Johnson, 2012), hydrogen (Hedrich and Johnson, 2013), and organic carbon (Johnson and Hallberg, 2009). Extreme acidophiles are found in all three domains of life (Aguilera et al., 2016; Dopson, 2016; Golyshina et al., 2016) although the most extreme are from the Archaea domain that can survive at negative pH values (Tyson et al., 2004). In addition, a large diversity of moderate acidophiles with growth ranges from pH 3 to 7.5, but with optima between pH 4 and 5 inhabit an array of environments including arctic tundra soils (Berestovskaya et al., 2002), *Sphagnum* peat bogs (Dedysh et al., 1998), and sulfidic deep sea sediments (Reysenbach et al., 2006). Characterized extreme acidophiles have growth temperatures ranging from approximately 4°C to >80°C. However, the most well-studied species-type strains have temperature optima ≥30°C including the model species, *Acidithiobacillus ferrooxidans* (Zhang et al., 2018; Moya-Beltrán et al., 2021). In contrast, fewer cold adapted species have been identified, and they are less well studied than their mesophilic and thermophilic counterparts.

Extremophilic microorganisms are used in a variety of biotechnological applications spanning the biomedical, pharmaceutical, industrial, environmental, and agricultural sectors (Raddadi et al., 2015; Banerjee et al., 2021; Verma, 2021). Applications of low-temperature microorganisms have seen numerous successes in the production of cold active proteases, lipases, and cellulases in food production, chemical synthesis, textile industry, pharmaceutical and molecular biology, bioremediation, and novel antimicrobials [reviewed in Cavicchioli et al. (2011) and Siddiqui (2015)]. Acidophiles in particular are exploited for their acid stable enzymes in food/animal feed processing (Sharma et al., 2016), in pharmaceutical delivery (Jensen et al., 2015), in microbial fuel cells (Sulonen et al., 2015; Ni et al., 2016), and in the production of novel biomaterials (Quehenberger et al., 2017). However, the most extensive exploitation of acidophiles is their use in "biomining" of metals such as copper and gold (Roberto and Schippers, 2022) where acidophiles catalyze the conversion of a solid metal sulfide to a soluble metal sulfate (Vera et al., 2022). The same microbes are also used for the remediation of environmentally damaging AMD that results from the extraction of metals (Nancucheo et al., 2017). However, as most biomining is carried out in warm countries and that pyrite/pyrrhotite oxidation is exothermic resulting in bioheaps reaching temperatures up to 90°C (Puhakka et al., 2007), investigation of low-temperature acidophiles in biotechnologies lags behind studies of mesophiles and thermophiles. Some mines and their corresponding impacted environments are located in the Polar Regions or high altitudes that are predominantly cold (e.g., Elberling et al., 2000). Further expansion of these biotechnologies requires a deeper understanding of low-temperature acidophiles.

Our interest in this review is in the particular niches occupied by extremely acidophilic prokaryotes that are also capable of growth at colder temperatures. To date, this only encompasses bacteria, as although cold-adapted archaea have been identified (Cavicchioli, 2006; Siddiqui et al., 2013), no low-temperature acidophilic Archaea have been described. It is unknown if this absence is due to sampling bias, and they remain to be discovered, or if they do not exist due to unidentified biological constraints. The fact that acidophiles are active at low temperatures has been known for many years since strains were isolated in the 1980s and the activities of these populations were observed in the environment down to 0°C (Langdahl and Ingvorsen, 1997).

Several terms have been formulated for low-temperature microorganisms including psychrotolerant and psychrotrophs with various definitions. A further term is "eurypsychrophiles" for microbes with a wide temperature tolerance that are able to grow at temperatures above and below 15°C but with a maximum growth temperature of 30°C (Bakermans and Nealson, 2004). In this review, we have used eurypsychrophiles but also included some strains with a maximum growth temperature slightly above Bakermans and Nealson (2004) cutoff. Although eurypsychrophilic acidophiles are still poorly understood, new data are emerging on this valuable and untapped niche with a range of potential biotechnological applications as well as their use as models for potential past or extant life on astrobiological targets.

Strategies to cope with acid and low temperature

To maintain a near pH neutral cytoplasm, acidophiles have a range of mechanisms defined as the "first and second lines of defense" (Vergara et al., 2020) similar to those found in neutrophilic microbes as well as several unique homeostasis strategies [reviewed in Slonczewski et al. (2009) and Zammit and Watkin (2016)]. Several studies have also investigated the evolution of acidophiles by the acquisition of genes coding for the first and second line of defense (Vergara et al., 2020; Boase et al., 2022; González-Rosales et al., 2022). The unique strategies include an inside positive membrane potential (i.e., reversed compared to neutrophiles) suggested to be generated by potassium or sodium ions that create an electrochemical barrier to proton influx (Buetti-Dinh et al., 2016; Neira et al., 2022). A second unique strategy is that acidophiles can have a rigid and impermeable membrane that is highly resistant to the influx of protons (van de Vossenberg et al., 1998). The membrane is also modified in acidophiles *via* membrane proteins with adaptations that impede proton permeability, such as a unique Omp40 porin protein in *At. ferrooxidans* (Guiliani and Jerez, 2000). Mechanisms of pH homeostasis that are shared with neutrophilic microorganisms include cytoplasmic buffering that in the short term can ameliorate acidification of the cytoplasm (Parro et al., 2007; Vergara et al., 2020). In addition, primary and secondary pumps exist that can remove excess cytoplasmic protons (González et al., 2014). Acidophiles also have the capacity to modify and repair DNA as a general response to damage (Parro et al., 2007),

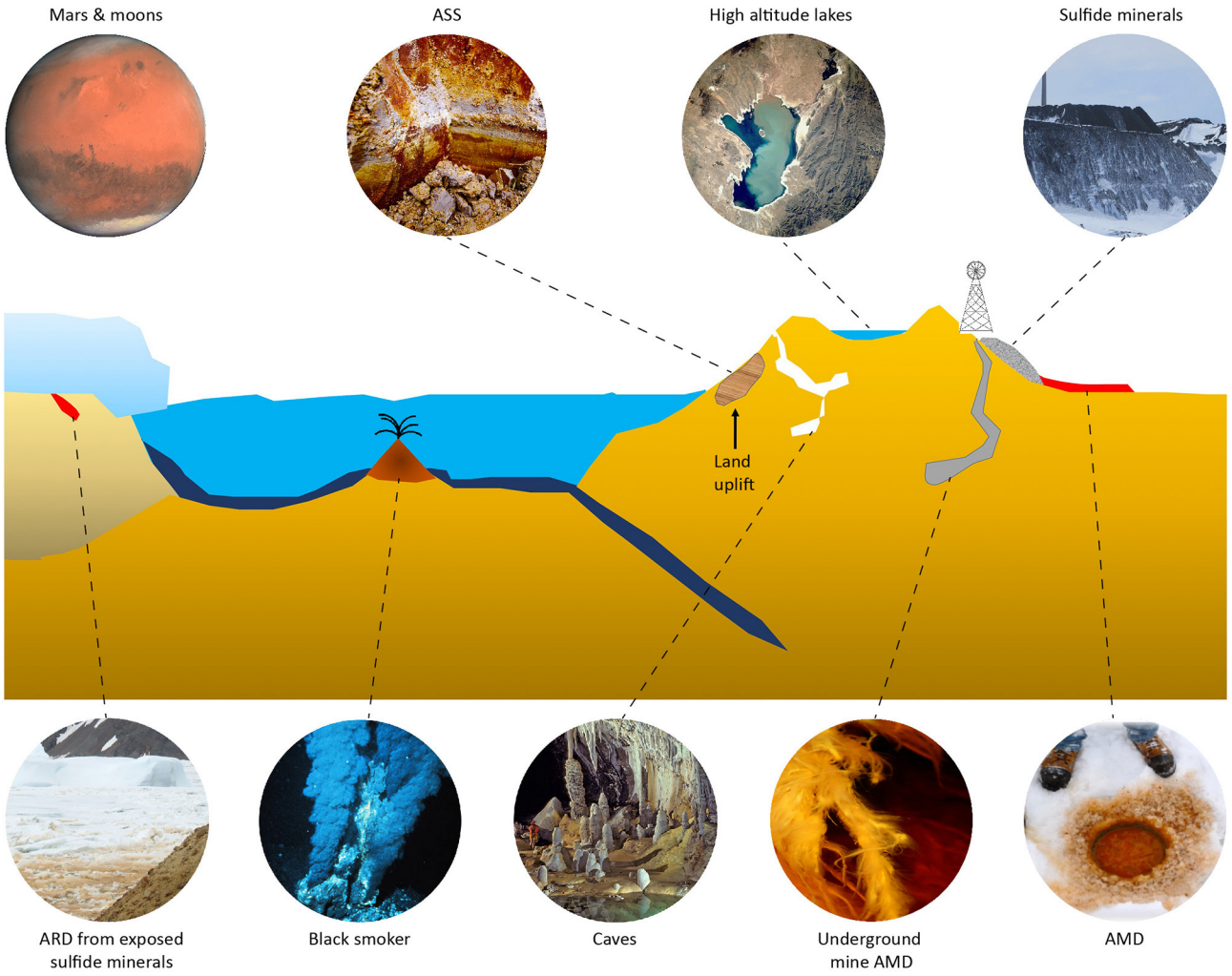

FIGURE 1
Acidic and low-temperature environments. Clockwise from top left: Mars and moons of Saturn and Jupiter (modified from Wikipedia CC BY-SA 3.0 IGO); boreal AS soil (ASS) created by land uplift (courtesy Eva Högfors-Rönnholm); high altitude lake (modified from Wikipedia public domain image); mining of metal sulfides at, e.g., high altitudes; AMD from under ice sulfide tailings seepage ponds; a low-temperature AMD stream in an underground mine; low-temperature caves (modified photograph by Dave Bunnell from Wikipedia CC BY-SA 2.5); black smokers releasing sulfides (modified from Wikipedia public domain image); and ARD from sulfide minerals, e.g., Antarctica (credit Ángeles Aguilera, Bernhard Dold, and Elena González-Toril), reproduced with permission.

and acidophiles may have a streamlined genome in response to their acidic growth pH (Cortez et al., 2022). Finally, the "*Fervidacidithiobacillus caldus*" (*ex-Acidithiobacillus caldus*) ferric uptake regulator (Fur) is important in acid resistance and shock by regulating genes involved in, e.g., key genes of certain cellular activities, such as iron transport, biofilm formation, and ISC metabolism (Chen et al., 2020).

Microbes that live at cold temperatures must deal with several biochemical and physiological challenges. These include reduced water activity, membrane fluidity (Bowman, 2008; Shivaji and Prakash, 2010), protein folding and activity (Feller, 2007; Collins et al., 2008; Metpally and Reddy, 2009), and enzyme reaction rates (Feller, 2007; Collins et al., 2008) along with increased osmotic pressure (Bowman, 2008) and risks of freezing (Kawahara, 2008) that are reviewed in Casanueva et al. (2010), De Maayer et al. (2014), and Dhaulaniya et al. (2019). Regarding eurypsychrophiles in general, reviews have highlighted key features of cold adaptation across a diversity of microorganisms (Margesin et al., 2008; Margesin and Miteva, 2011; Tribelli and Lopez, 2018). These can include increased enzyme flexibility through decreased core hydrophobicity, weaker interactions between subunits, fewer disulfide bridges, along with increased catalytic efficiency between the protein and substrate (Marx et al., 2007; Cavicchioli et al., 2011; Badieyan et al., 2012; Lian et al., 2015). Membranes of psychrophilic bacteria maintain their fluidity and phase through various mechanisms. These include increased amounts of unsaturated fatty acids, increased branched fatty acids, favoring higher *cis*/*trans* unsaturated fatty acid ratios, the synthesis of fatty acids with shorter acyl chain length, and larger or differently charged polar head groups (Los and Murata, 2004; Shivaji and Prakash, 2010; Králová, 2017). In both bacterial and archaeal membranes, the destabilization caused by membrane lipid alterations is commonly offset with an increase in pigments or carotenoids that provide added stability within the liquid-crystalline membrane state at

colder temperatures (Chattopadhyay et al., 1997). The response to cold shock also triggers adaptive mechanisms. These include the induction of cold shock proteins and increased expression of chaperones to assist with RNA stability, protein folding, and enzymatic activities, along with increased compatible solute synthesis and/or uptake, extracellular polysaccharide synthesis, or ice interacting proteins (Junge et al., 2006; Phadtare and Inouye, 2008; Jung et al., 2010, 2018; Galleguillos et al., 2018; Kumar et al., 2020).

Eurypsychrophilic acidophiles

Characterized eurypsychrophilic acidophiles

The characterized eurypsychrophilic acidophiles are from the Proteobacteria (*Acidithiobacillus ferrivorans*, *Acidithiobacillus ferriphilus*, *Acidithiobacillus ferrooxidans*, and "*Ferrovum myxofaciens*") and the Firmicutes (*Alicyclobacillus disulfidooxidans*; no genome sequence available) with their general characteristics summarized in Table 1 and their phylogenetic relationships represented in Figure 2.

The first eurypsychrophilic acidophile to be formally described was *At. ferrivorans* NO-37^T (Hallberg et al., 2010). The type strain was isolated from pH 2.7 to 3.7 AMD waters at an abandoned copper mine in Norway where temperatures are below freezing for approximately 7 months of the year (Johnson et al., 2001). *At. ferrivorans*^{T} is a Gram-negative facultative anaerobe that fixes carbon dioxide and nitrogen for growth with ferrous iron and ISCs as electron donors. *At. ferrivorans*^{T} grows at 4°C although its optimum growth temperature is 27°C to 32°C, and it has an optimum pH of 2.5 (growth range at least pH 1.9 to 3.4). Due to the type strain's growth at 32°C, it does not match the criterion used for eurypsychrophilic acidophiles (Bakermans and Nealson, 2004). Other isolates of *At. ferrivorans* comprise strains Peru6, OP14, and CF27 included in the analysis of the type strain (Hallberg et al., 2010), and a notable feature of strain CF27 is its formation of large amounts of extracellular polymeric substances during biofilm formation on mineral grains (Talla et al., 2014). *At. ferrivorans* SS3 was isolated from a sulfidic mineral mining site and is characterized as having a lower temperature optimum at 22°C and growing as low as 6°C using ferrous iron (Kupka et al., 2007) and ISCs (Kupka et al., 2009). Strain PQ33 that was isolated from an altitude of 4,621 m above sea level in Peru has a doubling time of 66.6 ± 5.1 h at pH 1.6 (Ccorahua-Santo et al., 2017). Strain YL15 was also isolated at altitude (4,600 m above sea level) from AMD at a copper mine in Tibet, China and grows on ferrous iron at both 6°C and 28°C (Peng et al., 2017). In addition, isolates PA-5, PA-8, and PA-20 were obtained from AMD in Balya, Turkey by culturing on ferrous iron containing plates (Aytar et al., 2015). Finally, *At. ferrivorans* ACH was isolated from the Aroma River in the Chilean Altiplano that has an average annual temperature of <5°C, grows on ferrous iron, ISCs, and pyrite as electron donors, and is able to attach to pyrite mineral at 4°C (Barahona et al., 2014).

Eleven strains of facultative anaerobic, ferrous iron and ISC oxidizing, autotrophic *At. ferriphilus* are characterized in the species description, and all are able to grow at 30°C (Falagan and Johnson, 2016). All of the strains were able to grow at 10°C (although some slowly) and three at 5°C including the type strain, classifying them as a eurypsychrophilic acidophiles. *At. ferriphilus* strains have been identified from, e.g., mine environments, while strains ST2 and KCT10 grew at salt concentrations similar to that of seawater.

A further eurypsychrophilic acidophile from the *Acidithiobacillus* genus is represented by two strains (PG05 and MC2.2) of *At. ferrooxidans* isolated from an old mine in southern Chile and King George Island, Antarctica, respectively (Muñoz-Villagrán et al., 2022). In addition, both strains, but especially PG05, have cellular electron dense areas indicative of polyphosphate granules that act in the response to stress conditions.

The fourth characterized eurypsychrophilic acidophile is the Betaproteobacteria "*F. myxofaciens*" (reclassified within the Gammaproteobacteria according to the GTDB database; Chaumeil et al., 2019). The proposed type strain, P3G, was cultured from AMD emanating from the Mynydd Parys, Wales (Johnson et al., 2014) where it dominated the streamer-type biofilms at this (Kay et al., 2013) and another mine site (Kimura et al., 2011). "*F. myxofaciens*" has a pH optimum of approximately 3.0, grows optimally at 30°C to 32°C, and exclusively uses ferrous iron and oxygen as electron donors and acceptors, respectively. "*F. myxofaciens*" P3G fixes both carbon dioxide and nitrogen to support the production of large amounts of extracellular polymeric substances that bind the cells together in streamer-like biofilms and to solid surfaces (Johnson et al., 2014).

A fifth eurypsychrophilic acidophile capable of not only sulfur oxidation but also heterotrophic metabolism is *Alb. disulfidooxidans* 51911^T (originally described as *Sulfobacillus disulfidooxidans*). This strain was isolated from wastewater sludge, has an optimal pH between 1.5 and 2.5, and a broad temperature range of 4°C to 40°C (Dufresne et al., 1996; Karavaiko et al., 2005).

Environmental strains and 16S *rRNA* gene sequences

Studies of mine tailings from Canadian arctic regions suggest microbial activity below 0°C (Meldrum et al., 2001; Elberling, 2005) with a potential explanation of solutes maintaining liquid water below 0°C or that local temperatures were higher due to exothermic reactions, especially if the cells were cocooned in biofilms. The microbial community in several low-temperature acidic environments has been characterized by traditional culturing and molecular 16S *rRNA* gene sequencing. In most cases, the identification of particular species did not always coincide with viability or activity measurements at cold temperatures. However, repeated observations indicate a diversity of eurypsychrophilic acidophiles in these environments. Some of the earliest reports of cold-tolerant acidophiles from AMD environments are reported as existing in Scandinavia and Canada, with their taxonomy determined to be *Thiobacillus ferrooxidans*-like or *At. ferrooxidans*-like (Ferroni et al., 1986; Ahonen and Tuovinen, 1989). Of these, *At. ferrivorans* strains D2, D6, and D7 were isolated from the Denison Uranium mines in Ontario, Canada (Ferroni et al., 1986; Berthelot et al., 1993). They were characterized as having a growth

TABLE 1 Selected characteristics of eurypsychrophilic acidophile species along with their genome availability.

Species	Strain	Selected growth characteristics	Temperature range	Genome state	Genome accession
At. ferrivorans	PQ33	Facultative anaerobe; fixes C and N; oxidizes Fe^{2+}, ISCs, and H_2; optimum pH 2.5;	5–24°C	Draft	CP021414.1 and CP021415.1
	SS3	Oxidizes Fe^{2+} and ISCs; grows at 6°C with optimum 22°C; growth optimum pH 1.9	5–30°C	Complete	CP002985.1
	YL15	Grown at pH of 2.0	6–28°C	Draft	MASQ01000000
	CF27	Notably forms large amount of extracellular polymeric substances during biofilm formation	<10–30°C	Complete	LT841305.1 and LT841306.1
	XJFY6S-08	Grown aerobically at pH 1.75	5–28°C	Complete	CP059488.1
	ACH	Oxidizes Fe^{2+}, ISCs, and FeS_2; attaches to mineral at 4°C	10–28°C	Draft	JAAZUD000000000
	NO-37	Fixes C and N; oxidizes Fe^{2+}, ISCs, and H_2; optimum of 27°C to 32°C; pH optimum pH 2.5 (range pH 1.9 to 3.4)	4–37°C	Draft	JAAOMR000000000
At. ferriphilus	M20	Facultative anaerobe; fixes C; oxidizes Fe^{2+} and ISCs; optimum temperature of 30°C and pH of 2.0	5–33°C	Draft	JAAZTY000000000
	Malay	Facultative anaerobe; fixes carbon; oxidizes Fe^{2+} and ISCs; optimum pH ~2.0; optimum temperature ~30°C	5–33°C	Draft	JAAOMQ000000000
	Riv13		10–33°C	Draft	JAAZUB000000000
	ST2	Grows in high salt concentrations	5–33°C	Draft	JAAZUC000000000
	SCUT-1	Oxidizes Fe^{2+}, ISCs, and FeS_2	22.1–30°C	Draft	NKQV00000000
At. ferrooxidans	PG05	Growth optima ≈20°C; contain polyphosphate granules	5–33°C	Draft	JAEQBE000000000
	MC2.2	Growth optima ≈20°C; contain polyphosphate granules	5–33°C	Draft	JAEQBG000000000
"*Ferrovum myxofaciens*"	P3G	Aerobe; fixes carbon and nitrogen; oxidizes Fe^{2+}; optimum pH 3.0 and temperature 32°C	4–36°C	Draft	JPOQ00000000
Alb. disulfidooxidans	SD-11	Mixotroph; oxidizes S^0 and FeS_2; optimum pH 1.5 range 0.5 to 6	4–40°C	—	Not available

At., *Acidithiobacillus*; *Alb.*, *Alicyclobacillus*; and ISCs, inorganic sulfur compounds.

10.3389/fmicb.2023.1149903

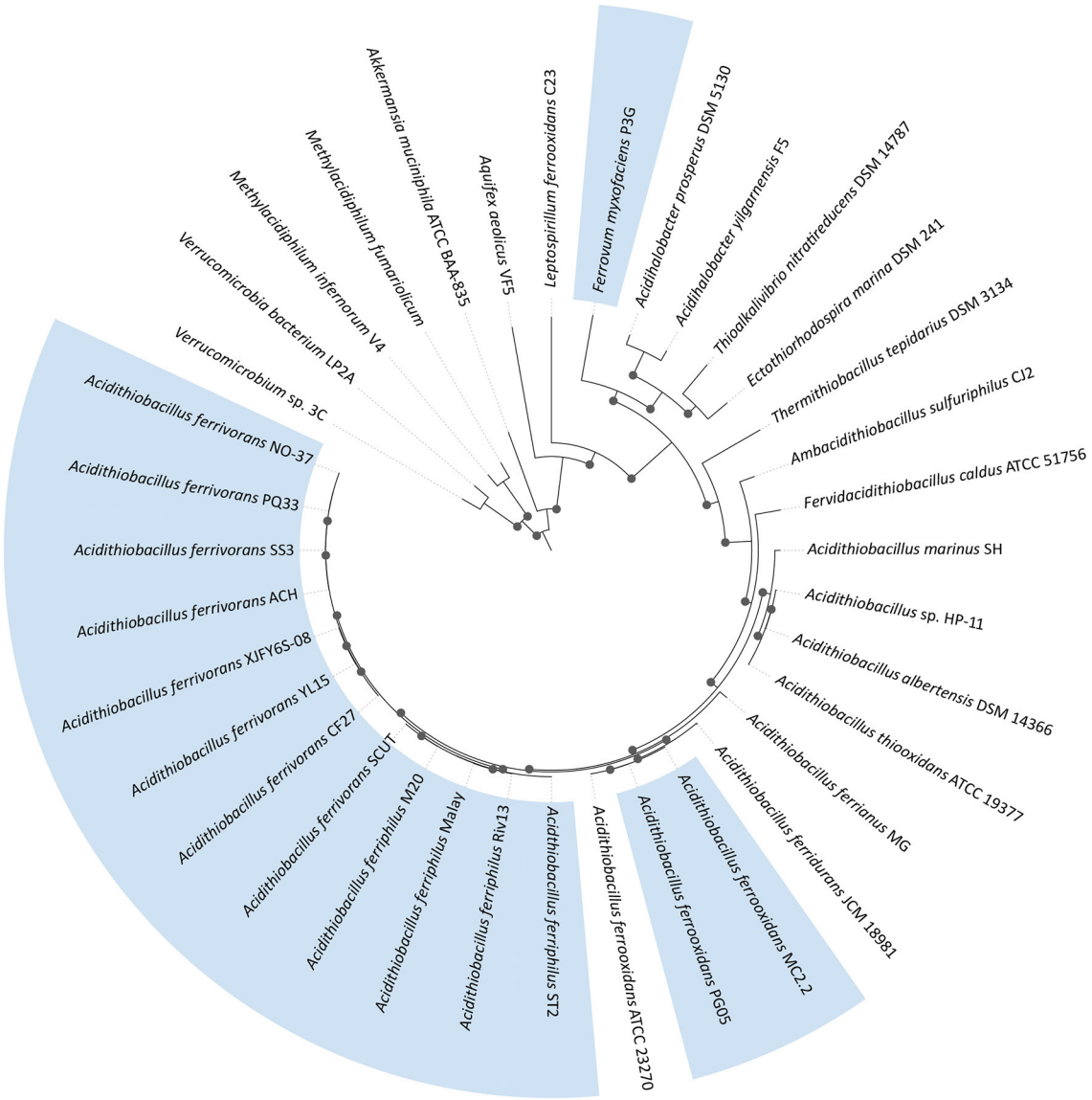

FIGURE 2
Maximum likelihood phylogenetic tree of eurypsychrophilic acidophiles (in blue) plus relatives. The tree was constructed using 31 conserved proteins (Ciccarelli et al., 2006) using 1,000 replicates. Bootstrap values of ≥60% are represented by black dots on the nodes. The phylogenomic tree was visualized with iTOL6 (Letunic and Bork, 2021).

temperature optimum of 25°C and growing as low as 2°C using ferrous iron (Leduc et al., 1993) with a growth range of at least pH 1.5 to 3.5 and an optimum of 2.1 (Mykytczuk et al., 2010b). These strains were also characterized for high metal tolerance that was maintained even when grown at colder temperatures with minimum inhibiting concentrations of 150 mM copper, 50 mM nickel, and 2.0 mM uranium (Leduc et al., 1997; Mykytczuk et al., 2011b).

In addition to the reports above, other studies used cultivation, molecular tools, and microscopy to observe diverse communities from cold and acidic environments. These include several descriptions of *At. ferrooxidans* and *At. ferrivorans* from Scandinavian mine sites (Kock and Schippers, 2008; Kupka et al., 2009); a 7.9 to 13.9°C acidic drainage system in Argentina containing a consortium including *At. ferrivorans* (Bernardelli et al., 2021); ice covered AMD ponds (Auld et al., 2017); *At. ferrivorans* and *Thiobacillus plumbophilus* from natural ARD in the South Shetland Islands, Antarctica (Dold et al., 2013); and mixed communities of chemolithotrophs plus chemoorganotrophs in mine waste sites, Ontario Canada (Asemaninejad et al., 2020). Many of these reports also include detection of other acidophiles including chemolithotrophs such as *Leptospirillum ferrooxidans* and *Ferrimicrobium* spp. from a coal mine in Svalbard, Norway (Garcia-Moyano et al., 2015) along with *L. ferrooxidans* and *Sulfobacillus* spp. from a tailings dump in Kristineberg, Sweden

(Kock and Schippers, 2008). Heterotrophic acidophiles were also detected in these systems including *Acidiphilium* and *Alicyclobacillus* spp. (Auld et al., 2017), *Acidisphaera* spp., and *Acidobacterium* spp. (Garcia-Moyano et al., 2015).

AS soils are generated when parent sulfidic sediments are exposed to air, and the reduced sediment is oxidized to release acidic, metal-laden solutions (Karimian et al., 2018). Boreal AS soils typically reach pH 3 to 5 and therefore contain a mixture of extreme and moderate acidophiles as well as a higher relative proportion of heterotrophic vs. autotrophic acidophiles compared to low organic carbon containing AMD (Högfors-Rönnholm et al., 2018). Samples taken from the oxidized layer in a Finnish AS soil contained many 16S *rRNA* gene sequences that aligned most closely to acidophiles found in AMD such as the ferrous iron and ISC-oxidizing *At. ferrooxidans*, the ferrous iron-oxidizing archaeon *Ferroplasma acidiphilum*, the acid-tolerant *Rhodanobacter* genus, and an uncultured *Acidimicrobiaceae* clone from an extremely acidic environment (Wu et al., 2013, 2015; Högfors-Rönnholm et al., 2018). However, if the parent sulfidic sediment is rapidly oxidized in the laboratory by active aeration, the pH level is decreased to 3, and sequences more similar to typical AMD environments are selected such as the low-temperature acidophile, *At. ferrivorans* (Wu et al., 2015). Finally, if metal sulfide-rich river sediment were to be dredged and the sediment is exposed to atmospheric oxygen, rapid oxidation occurs and representatives of the *Acidithiobacillus*, *Gallionella*, *Sulfuricurvum*, and *Sulfurimonas* genera become dominant (Johnson et al., 2022).

Growth substrates and oxidation rates

As noted in the characterization section above, both *At. ferrivorans* and "*F. myxofaciens*" can use ferrous iron as an electron donor (Hallberg et al., 2010; Johnson et al., 2014). In addition, ferrous iron appears to be *At. ferrivorans* SS3 preferred substrate as it is preferentially oxidized over ISCs (Liljeqvist et al., 2013). The rate constant for strain SS3 ferrous oxidation at 5°C is 0.0162–0.0104 h^{-1} dependent on the initial pH of the culture. As for other strains, the *At. ferrivorans* PQ33 ferrous oxidation rate is higher at 24°C compared to 5°C when it has a doubling time of 66.6 ± 5.1 h at pH 1.6 (Ccorahua-Santo et al., 2017). Eurypsychrophilic *At. ferrooxidans* strains oxidized ferrous iron and grew down to 5°C with doubling times between 12.8 and 14.1 h but had optimum growth rates at 20°C while still having a high growth rate at 37°C (Muñoz-Villagrán et al., 2022). Ferrous iron oxidation rates for "*F. myxofaciens*" peaked at 30°C, a value 12.5-fold higher than the corresponding rate at 5°C (Johnson et al., 2014). Ferrous iron is also a preferred substrate over ISCs for the *At. ferrivorans* D-strains (D2, D6, and D7; previously identified as *At. ferrooxidans*), and they have doubling rates of 253–306 ± 22 h when grown at 2°C and at pH 2.1 and 87–88 ± 1.5 h at 5°C (Leduc et al., 1993; Mykytczuk et al., 2011a). The combination of cold and sub- or supra-optimal pH increases these doubling rates, but are comparably longer than under pH stress alone (i.e., growth rates of 25–38 ± 3.3 h at pH 1.5 in ferrous iron media) (Mykytczuk et al., 2010a).

At. ferrivorans NO-37^T oxidizes sulfide, tetrathionate, thiosulfate, and elemental sulfur (Hallberg et al., 2010). ISC oxidation is most extensively investigated in *At. ferrivorans* SS3 with extended lag phases with tetrathionate as an electron donor at 5°C (Kupka et al., 2009). Temperature optima for tetrathionate and elemental sulfur were 25°C and 20°C, respectively. The *At. ferrivorans* D2, D6, and D7 strains also grow on various ISCs including sulfide, sulfite, thiosulfate, and elemental sulfur, but in all cases, they were grown at temperatures between 20°C and 25°C but not at lower temperatures (Berthelot et al., 1993; Leduc et al., 1993).

In the environment, dissimilatory ferric iron reduction is an important electron acceptor for the oxidation of organic and inorganic electron donors and is a driver in the iron cycle (Bird et al., 2011). Mesophilic and moderately thermophilic acidophiles carry out dissimilatory reduction of both soluble ferric iron and solid ferric minerals (Bridge and Johnson, 1998, 2000; Osorio et al., 2013; Malik and Hedrich, 2022), and a biotechnological process has been proposed that exploits this ability to extract, e.g., nickel from laterites (du Plessis et al., 2011; Hallberg et al., 2011). *At. ferrivorans* strains NO-37^T, Peru6, and CF27 anaerobically oxidize elemental sulfur as electron donors coupled to the reduction of ferric iron (Hallberg et al., 2011). In addition, *At. ferrivorans* SS3 coupled elemental sulfur to ferric iron reduction even in the presence of molecular oxygen (Kupka et al., 2009).

Alb. disulfidooxidans 51911^T metabolizes a wide range of organic carbon compounds including starch, glycogen, and glucose (Dufresne et al., 1996). Its ability to oxidize organic carbon, and in particular, organic acids places this species at a competitive advantage as it is able to reduce the concentration of these acids that are toxic to extreme acidophiles *via* acidification of the cytoplasm leading to cell death (Alexander et al., 1987).

Genomics and post genomics

Acidophiles have proven to be recalcitrant to analysis *via* traditional molecular biology tools, and only a few studies have succeeded such as the generation of *At. ferrooxidans* mutants (Jung et al., 2021); instead, acidophiles have been extensively studied by "omics" technologies. Consequently, there are approximately 600 finished or permanent draft acidophile genomes, 184 extreme acidophiles (optimum pH ≤3.0) genomes of which 15 are from eurypsychrophilic acidophiles (Neira et al., 2020). These studies allow the identification of genetic potential and RNA transcript-based gene activities of these populations.

Eurypsychrophilic acidophile genomes and post genomics

Several genomes of eurypsychrophilic acidophilic bacteria have been published (Table 1) including seven *At. ferrivorans* strains, namely, SS3 (Liljeqvist et al., 2011b), CF27 (Talla et al., 2013), PQ33 (Ccorahua-Santo et al., 2017), YL15 (Peng et al., 2017), ACH (Barahona et al., 2020), NO-37 (Moya-Beltrán et al., 2021), and XJFY6S-08 (Zhao et al., 2021). The *At. ferrivorans* SS3 genome codes for genes for carbon dioxide fixation *via* the Calvin-Benson-Bassham (CBB) cycle; nitrogen metabolism; ferrous iron oxidation; and ISC metabolism including the SOX oxidation complex (*soxYZ-hypB*) and a sulfur oxygenase:reductase *sor*

(Liljeqvist et al., 2011b). The *At. ferrivorans* SS3 ISC pathway was also identified by transcriptomics that revealed RNA transcripts for a thiosulfate quinone oxidoreductase (*doxDA*), heterodisulfide reductase (*hdr*) for elemental sulfur metabolism, and electron transport complexes for energy conservation (Christel et al., 2016a). The *At. ferrivorans* CF27 genome was also analyzed and found to code for an *iro* gene absent in *At. ferrooxidans* suggesting an alternative pathway for ferrous iron oxidation (Talla et al., 2013). Similar to strain SS3, genes involved in ISC oxidation were identified including sulfide oxidation (*sqr*), tetrathionate hydrolase (*tetH*), and sulfite oxidation (*sat* and *cytC*). The strain CF27 genome also contains genes encoding fucose biosynthesis (*fcl*) and glycosylation of surface layer glycoprotein that could explain the strains propensity to form gelatinous macroscopic biofilms (Talla et al., 2014). Finally for strain CF27, the genome harbors 51 genomic islands coding for genes associated with, e.g., chemotaxis, motility *via* flagella, and biofilm synthesis (Tran et al., 2017). Strain YL15 was isolated from an AMD environment, and its genome contains genes for metal resistance such as the *mer* operon for mercury, *arsRABCD* genes for arsenic, and *copB* plus *cusCBA* for copper (Peng et al., 2017). Microorganisms at high altitudes such as the alpine region from where strain YL15 was isolated are exposed to increased levels of ultraviolet radiation and the strain's genome coded for mycosporine-like amino acid production that combat this along with reactive oxygen scavenging systems that are generated by the radiation (Peng et al., 2017). In addition, the *At. ferrivorans* PQ33 genome harbors a genomic island containing a *rusB* gene (Ccorahua-Santo et al., 2017). Finally, strain *At. ferrivorans* XJFY6S-08, also from acid mine drainage, contains genes for metal assimilation plus resistance systems and DNA repair (Zhao et al., 2021), while strain ACH was analyzed for its ability to grow in high copper concentrations (up to 400 mM) and the corresponding resistance determinants included the *cop* and *cus* systems (Barahona et al., 2020).

The *At. ferriphilus* M20 and Riv13 genomes were sequenced during a large-scale characterization of the Acidithiobacillia class with the M20 strain containing genes coding for ferrous iron oxidation including *rus*, *cyc2*, and *petABC*; ISC metabolisms such as *sqr*, sulfur dioxygenase (*sdo*), *hdrABC*, *tetH*, and *doxDA*; and hydrogenases I-IV (Moya-Beltrán et al., 2021). *At. ferriphilus* SCUT-1 genome sequencing revealed genes involved in ferrous iron oxidation including a *rus* gene cluster (Fan et al., 2018). In addition, genes encoding ISC oxidation included *sqr*, *tetH*, *tqo*, *soxYZB* genes, and *hdrABC* that feed electrons to aa_3 and bo_3 electron acceptors. Finally, the *At. ferriphilus* Malay and ST2 genomes contain genes coding for ferrous iron and ISC metabolism (Moya-Beltrán et al., 2014).

The "*F. myxofaciens*" P3G genome also contains genes coding for the complete CBB cycle including carboxysome formation along with *nif* genes for the nitrogenase complex for carbon dioxide and nitrogen fixation, respectively (Moya-Beltrán et al., 2014). "*F. myxofaciens*" genes for ferrous iron oxidation are similar to the well-studied *At. ferrooxidans* system with an outer membrane *c*-type cytochrome connected with a chain of cytochromes with the exception of the cytochrome oxidase terminal electron acceptor that is absent (Quatrini et al., 2009). Obligate ferrous iron-oxidizing acidophile species also carry out "up-hill" electron transport to generate reducing power, and genes coding for the integral bc_1 complex were also identified (Moya-Beltrán et al., 2014). Finally, despite the type-strain being described as non-motile, genes coding for chemotaxis and flagella formation are present.

Low-temperature metagenomes and metatranscriptomes

Community DNA analysis of sulfide mineral mining environments suggests that the presence of eurypsychrophilic acidophiles and their metagenome-assembled genomes (MAGs) have been analyzed. Included in this section are community studies from acidic and low-temperature environments that match the criteria of ≤pH 3.1 and 15°C with the caveat that average environmental pH and temperatures are insufficient to prove the presence of eurypsychrophilic acidophiles.

Community DNA was extracted from a streamer-type biofilm in a 6°C to 10°C AMD stream in northern Sweden (Liljeqvist et al., 2015). Both the biofilm and planktonic cells were dominated by an *At. ferrivorans* strain along with other *Acidithiobacillus*, *Acidobacteria*-like, and *Gallionellaceae*-like populations. A comparison of the *At. ferrivorans* SS3 genome to the *At. ferrivorans*-like MAG identified metagenomic islands enriched with mobile elements and containing genes coding for metal resistance related to the high concentrations of metals in the AMD stream from where the *At. ferrivorans*-like strain was assembled (González et al., 2014).

A cold AMD stream (6.5°C and pH 2.65) was also sampled for community metagenomics from the Sherlovaya Gora mine, Eastern Siberia, Russia. The community was dominated by an uncultured ferrous iron and ISC-oxidizing *Candidatus* Gallionella acididurans species with lesser contributions from the genera *Thiobacillus, Acidobacterium, Acidisphaera,* and *Acidithiobacillus* (Kadnikov et al., 2016). Four additional Chinese AMD sites were analyzed by community "omics" with RNA transcripts suggesting *At. ferrivorans* populations were highly active in three of the four sites with a broad range of functions (Chen et al., 2015). For instance, RNA transcripts were detected for the majority of *At. ferrivorans* genes for ferrous iron and ISC oxidation along with nitrogen fixation. A further Chinese AMD study was used to assemble a 79% complete *Ferrovum* genome that had a relative abundance of >90% (Hua et al., 2015). RNA transcripts suggest this population to be fixing carbon dioxide but not nitrogen along with the highest number of RNA transcripts coding for oxidative phosphorylation.

A mine water treatment plant was analyzed by metagenomics from which a nearly complete genome of *Ferrovum* strain JA12 was assembled and suggested to be a second species alongside "*F. myxofaciens*" (Ullrich et al., 2016b). The JA12 genome was small (2.70 Mbp) but encoded *CBB cycle* genes for carbon dioxide fixation; assimilation of nitrogen from ammonium, nitrate, and urea; ferrous iron oxidation *via* a Cyc2-like protein; and both up- and downhill electron transport chains. JA12 adaptations to its environment include metal resistance genes such as *copA* and *arsC* (Ullrich et al., 2016b). Two further *Ferrovum* strains (Z-31 and PN-J185) were assembled from the same mine water treatment pilot

plant as JA12 in Nochten, Germany, with strain PN-J185 suggested to represent a third *Ferrovum* species (Ullrich et al., 2016a). Comparative genomics of the three strains together with the P3G type strain genome revealed distinctive metabolic profiles related to motility, chemotaxis, nitrogen fixation, and biofilm generation. An additional 8.1°C to 14.6°C AMD site in Cabin Branch, USA, is dominated by 16S *rRNA* gene amplicon sequences most closely related to "*F. myxofaciens*" and metagenome sequencing resulted in two nearly complete *Ferrovum* MAGs that also differed according to genes coding for motility and chemotaxis along with, e.g., nitrogen assimilation (Grettenberger et al., 2020). In addition to the *Ferrovum* MAGs, assembled genomes related to, e.g., the *Gallionella* and *Acidocella* genera along with a Thermoplasmata archaeon were identified.

Finally, metagenomes from a low-temperature boreal acid sulfate soil situated in Vasa, Finland showed that the metal sulfide oxidation of the parent reduced sediment was dominated by MAGs aligning with the acid-tolerant or moderately acidophilic iron-oxidizing *Gallionella* and sulfur-metabolizing *Sulfuricella* genera (Högfors-Rönnholm et al., 2022). In contrast to most (but not all) sequenced *Gallionella* genomes, the acid sulfate soil MAGs were suggested to also encode ISC oxidation.

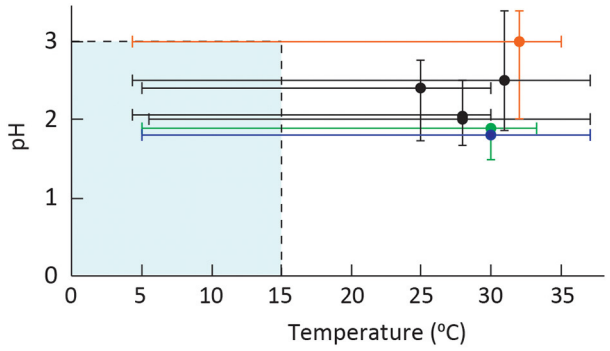

FIGURE 3
Plot of pH vs. temperature optima and ranges of characterized eurypsychrophilic acidophiles with the limits of low-temperature growth and extreme acidophiles are shaded in blue. The species are *A. ferrivorans* strains (all in black) from top to bottom NO-37, CF27, SS3, and ACH; *At. ferrooxidans* PG05 and MC2.2 represented as a single line (blue); "*F. myxofaciens*" P3G (orange); and *A. ferriphilus* M20 (green). The strains with an optimum pH of 2.5 were slightly adjusted for visual clarity.

Eurypsychrophilic acidophile adaptations

Microbial cells that can tolerate multiple physiochemical extremes are polyextremophiles, and they maintain cell homeostasis despite the pressures exerted on the cell (Figure 3). Low-temperature acidophiles exist in such environments where adaptation to both cold and acid stress can be different from the adaptation mechanisms commonly observed to either stress alone (Figure 4). While eurypsychrophiles are discussed in this study, there are no known stenopsychrophile acidophiles, and we hypothesize that the nature of some adaptations may have inhibited the evolution of acidophiles that exclusively grow below 15°C.

The adaptations to an acidophilic lifestyle identified in *At. ferrivorans* SS3 include a potassium transporting ATPase suggested to be involved in the inside positive (inversed) membrane potential and a P-type ATPase proton efflux pump that was not present in an *At. ferrivorans* MAG from a low-temperature AMD stream (González et al., 2014). In addition, the *At. ferrivorans* strain YL15 genome contains genes for the inversed membrane potential-related *kdp* potassium uptake system and a sodium:potassium antiporter; the membrane hopanoid squalene synthesis and associated genes *hpnAIJKNHM*; proton-consuming cytoplasmic buffering systems *adi* and *gadB*; and the acid resistance *clpXP* APT-dependent Clp protease genes (Peng et al., 2017). Furthermore, *At. ferrivorans* XJFY6S-08 contains *kdpDEABC* genes for the potassium uptake system; the *nhaA* sodium/proton antiporter; a *shc* squalene-hopene/tetraprenyl-beta-curcumene cyclase; *clpXPB* Clp protease; and proton-consuming *speA* arginine decarboxylase and *gadABC* glutamate decarboxylase (Zhao et al., 2021). Finally, a decreased proton permeability *via* an increased saturated fatty acid composition was most pronounced in *At. ferrivorans* growth at pH 1.5 (Mykytczuk et al., 2010a). *Ferrovum* strain JA12 adaptations to acidic pH include a Kef-type K^+ transport system and a K^+ transporter; *cfa* cyclopropane-fatty-acyl-phospholipid synthase membrane protein; cytoplasmic buffering systems including *adi* arginine decarboxylase, *panD* phosphatidylserine decarboxylase, and the *ureABCDEFGHJ* urease system; and spermidine synthase that inhibits proton influx *via* porins (Ullrich et al., 2016b). *Ferrovum* strain JA12 RNA transcripts in response to growth on ferrous iron showed maintenance of pH homeostasis including for the cyclopropane-fatty-acyl-phospholipid synthase, the Kef-type K^+ transport system, a K^+ transporter, and cytoplasmic buffering (Ullrich et al., 2018). In addition, "*Ferrovum*" strains P3G and Z-31 harbor the *kdpABCDE* K^+-transporting ATPase and the *nhaA* sodium/proton antiporter (Ullrich et al., 2016a). Finally and with the above-mentioned caveat regarding average environmental pH and temperatures, RNA transcripts assigned to the "*Ferrovum*" P3G MAG from an AMD site included the *kdpDE* signal transport system, a sodium:proton antiporter, and arginine decarboxylase (Hua et al., 2015). An additional AMD metagenome *Ca.* Gallionella acididurans MAG encoded the *kdpABC* K^+-transporting ATPase (Kadnikov et al., 2016), while a community analysis of Chinese low-grade copper tailings also assigned coding sequences to *kdpABC*, a voltage-gated potassium channel, and proton antiporters assigned to among other MAGs, *At. ferrivorans* (Zhang et al., 2016). Finally, community RNA transcript sequencing of the Finnish low-temperature boreal acid sulfate soil (Högfors-Rönnholm et al., 2022) revealed transcripts at the metal sulfide oxidation front coding for both "first line of defense" and "second line of defense" acid resistance systems including potassium transporters and components of the arginine-dependent acid resistance system (González-Rosales et al., 2022).

Low temperature adaptations identified in *At. ferrivorans* include production of the compatible solute trehalose (Liljeqvist et al., 2011b) that that has also been demonstrated to have a function in e.g., acidophile osmotic stress tolerance (Galleguillos et al., 2018). However, it was argued that the multiple trehalose

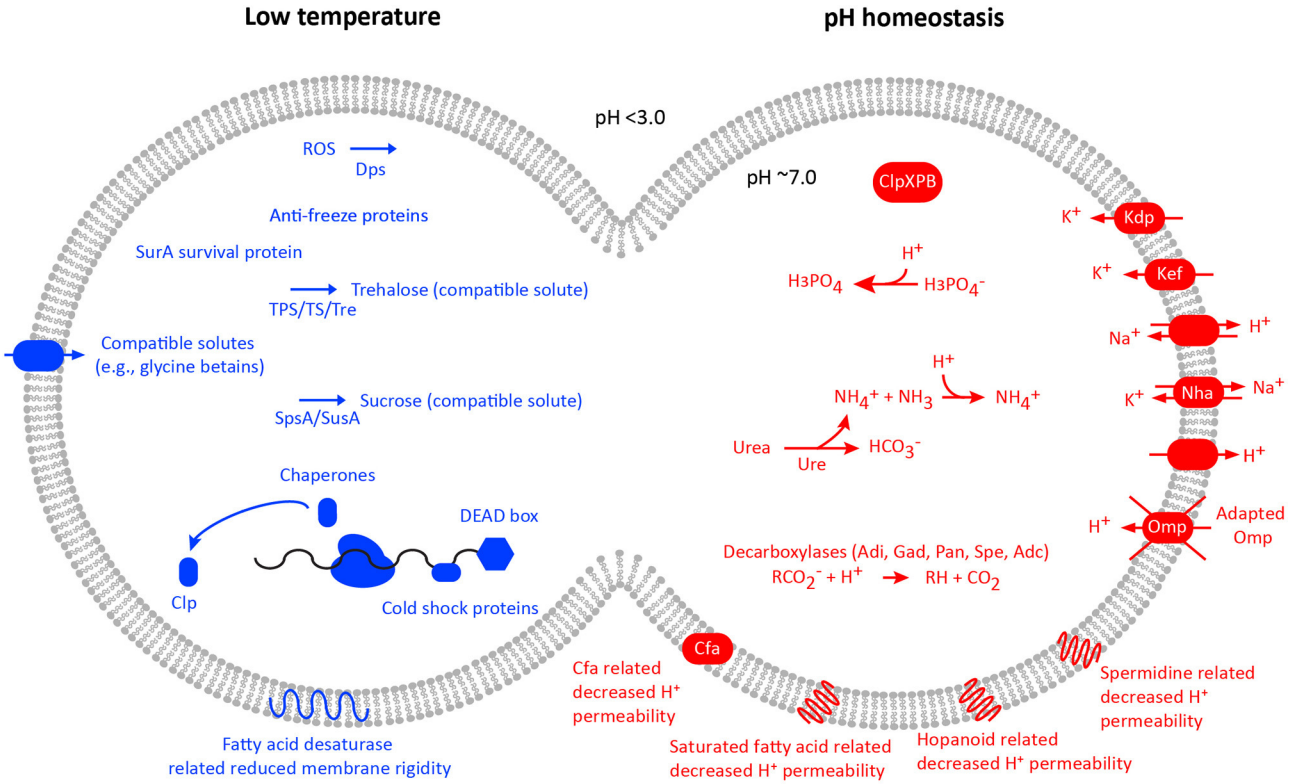

FIGURE 4
Acidophile and low-temperature adaptations for selected genomes based upon complete genomes and type strains of the available species. Data used during the preparation of the figure were drawn from the AciDB database of acidophilic organisms (Neira et al., 2020).

synthesis pathways in a *At. ferrivorans* MAG from a low-temperature AMD metagenome compared to mesophilic *Acidithiobacillus* spp. reflected its greater importance for growth at low temperatures (Liljeqvist et al., 2015). In addition, the AMD stream MAGs of the dominant populations contain further adaptations to the low temperature including cold-shock proteins and an anti-freeze protein (Liljeqvist et al., 2015). The *At. ferrivorans* CF27 genome also contains genes for adaptation to low temperatures including production of the compatible solutes trehalose and sucrose, cold shock proteins, chaperones, and membrane adaptations (Tran et al., 2017). Cold adaptation genes were also present in *At. ferrivorans* PQ33 including DEAD/H-box RNA helicases; fatty acid desaturases genes that increase membrane fluidity; trehalose synthase genes; and protein folding peptidyl-prolyl cis/trans isomerases (Ccorahua-Santo et al., 2017). Finally, *At. ferrivorans* XJFY6S-08 contains genes for low temperature such as chaperones, e.g., *groEL/ES* and trigger factor with peptidyl-prolyl cis/trans isomerase activity; five trehalose synthase pathways; and cold shock proteins (Zhao et al., 2021). However, the growth of *At. ferrivorans* SS3 at 8°C showed few RNA transcripts related to cold stress supporting its assignment as a eurypsychrophile (Christel et al., 2016b). In contrast, *At. ferrivorans* strain YL15 RNA transcript analysis identified systems for growth at low temperatures including membrane transport and energy metabolism along with *dps* gene transcripts for protection against oxidative stress (Peng et al., 2017). Proteomic comparisons of *At. ferrivorans* D6 strain to mesophilic strains of *At. ferrooxidans* grown near their lower temperature limits of 5°C and 15°C, respectively, revealed that both organisms shared increased levels of certain stress-related proteins (survival protein SurA, trigger factor, and antioxidant proteins) in response to colder temperatures (Mykytczuk et al., 2011a). However, the eurypsychrophilic strain D6 revealed upregulation of a significantly higher number of proteins related to membrane transport and pH homeostasis (e.g., ABC transporters and the MotA-TolQ-ExbB proton channel family protein) and membrane structure (e.g., PAP2 phosphatidic acid phosphatase, glycosyl transferase, and capsule polysaccharide export protein) compared to the mesophilic *At. ferrooxidans* (Mykytczuk et al., 2011a). Membrane adaptation in these eurypsychrophilic *At. ferrivorans* strains was notably different from mesophilic strains of *At. ferrooxidans* with an increase in desaturated fatty acids (16:1 w6c and 17:1 w8c) but a more rigid cytoplasmic membrane with a broader membrane phase transition temperature range in response to cold temperatures (Mykytczuk et al., 2010b). Finally, *At. ferrivorans* strain YL15 transcripts related to energy metabolism at colder temperatures also showed a 4 fold increase in rusticyanin production compared to growth at warmer temperatures. Similarly, Peng et al. (2017) observed increased expression of iron oxidation (*rusA* and *cycA1*) and sulfur oxidation genes (*hdrA*, *cyoC1*, and *doxDA*) of *At. ferrivorans* YL15 at 6°C compared to growth at 28°C. Both low temperature *At. ferrooxidans* strains PG05 and MC2.2 have draft genome sequences from which an analysis of the nine available *At. ferrooxidans* genomes showed, e.g., higher gene frequencies

for genes encoding cold tolerance compared to the type strain (Muñoz-Villagrán et al., 2022). These included genes for the compatible solute trehalose that has several functions including cold tolerance, a transporter for a further compatible solute glycine betaine, fatty acid desaturases, and hopanoid biosynthesis. In addition, genes coding for low-temperature-induced oxidative stress were particularly abundant in strain MC2.2.

Biotechnology

Eurypsychrophilic acidophiles have a niche for potential applications in biotechnology that differentiates them from applications under solely low temperature or acidic conditions. The clearest case for the application of eurypsychrophilic acidophiles is in metal dissolution and bioremediation of mining processes and wastewaters in boreal environments or at high altitudes. Other potential applications include targeting these populations for enzymes that can be used for other, non-mining applications.

Biomining and remediation

Bioheaps for nickel, zinc, cobalt, and copper recovery from a low-grade black schist ore in North-Eastern Finland have been in operation since 2008 at the Terrafame mine [originally Talvivaara Mining Company; (Riekkola-Vanhanen, 2010, 2013)]. Biomining of the metals was successful despite the average temperatures in winter ranging between zero to −20°C (with extreme lows of −30°C) as exergonic reactions during principally pyrrhotite oxidation resulted in the inner areas of the bioheap reaching 90°C (Halinen et al., 2012). Eurypsychrophilic acidophiles would have been important during bioheap initiation before the core had increased in temperature and in the niche temperature zone between the inner, hot bioheap and the extremely cold surface during the winter months. Early laboratory column studies of the black schist showed relatively high rates and yields at 5°C compared to 21°C (Puhakka et al., 2007). Molecular identification of the column microbial communities enriched at 5°C from mine site waters identified strains similar to *At. ferrooxidans* along with *At. thiooxidans* (Puhakka et al., 2007). However, at this time, strains now known to be *At. ferrivorans* were typically classified as *At. ferrooxidans,* and further work with the black schist ore suggested that *At. ferrooxidans* A7 is eurypsychrophilic (Dopson et al., 2007). Further laboratory tests of column bioleaching at 5°C vs. 30°C showed a small decrease in metal dissolution from pyrite, pyrite/arsenopyrite, and chalcopyrite concentrates when *At. ferrivorans* SS3 was used compared to *At. ferrooxidans*^{T} (Dopson et al., 2007). Chalcopyrite bioleaching was also investigated using a consortium enriched from AMD dominated by *Acidithiobacillus* spp. and *Sulfobacillus* spp. that outcompeted *At. ferrivorans* strain YL15 at 6°C (Peng et al., 2021). Finally, the accumulation of solid sulfur during chalcopyrite bioleaching was observed that was explained by decreased gene expression of genes coding for ISC oxidation in *At. ferrivorans* SS3 (Liljeqvist et al., 2013).

Another advantage of the activity of eurypsychrophilic acidophiles in bioheap applications, with for example *At. ferrivorans* strains, could be gained through their initiation of the oxidation process while limiting mineral passivation. In laboratory tests both in liquid media and on various sulfide tailings, the production of jarosite was greatly reduced at 5°C, decreasing the rate of mineral passivation and allowing Fe^{3+} concentrations to rise within the aqueous phase compared to higher incubation temperatures (Leduc et al., 1993; Mykytczuk et al., 2010b). In stirred bioreactor systems, it is unlikely that colder temperatures would be favorable or possible to achieve given the exothermic reactions; however, retaining ferric iron in solution could allow for the recycling of the oxidant. Recently, Peng et al. (2017) tested *At. ferrivorans* strain YL15 in chalcopyrite leaching in shake flasks at 6°C and observed no passivating layers on the mineral surface although corrosion was evident by scanning electron microscopy. Finally, all the tested *At. ferriphilus* strains catalyzed pyrite dissolution (Falagan and Johnson, 2016).

As detailed above, eurypsychrophilic acidophiles are often identified in low-temperature AMD environments (e.g., Escobar et al., 2010), and they can be exploited for the bioremediation of these contaminated waters. For example, room-temperature ferrous iron-oxidizing bioreactors were used to treat AMD that over time became dominated by a community including "*F. myxofaciens*" and *At. ferrivorans* (Jones and Johnson, 2016). Low temperature, passive systems such as wetlands, and active treatments to oxidize ferrous to ferric iron have also been studied [reviewed in Kaksonen et al. (2008)]. An example of low-temperature bioremediation is schwertmannite and jarosite production using "*F. myxofaciens*" EHS6 to remove iron- and sulfate from mine water at 14.5°C (Hedrich et al., 2011). A second example is the removal of ISCs from tailings water down to 5°C to 6°C with a mixed consortium dominated by *At. ferrivorans* (Liljeqvist et al., 2011a). Finally, coal desulfurization has been carried out with an *At. ferrivorans* strain (Aytar et al., 2013).

Conjecture on the survival of acidophilic eurypsychrophiles during snowball earth events

During its history, Earth is thought to have undergone several episodes of almost complete ice and snow-coverage that are known as Snowball Earth events (Kirschvink et al., 2000). Although mesophilic and thermophilic microorganisms could have survived such conditions in a limited number of warmer niches under the ice (e.g., thermal fields), psychrophiles potentially had an opportunity of surviving in a wider range of cold environments during these time periods. Of particular interest is the possibility that some acidophilic eurypsychrophiles might be especially adapted to survive cold temperatures by virtue of their ability to raise the temperature of their surroundings by catalyzing exothermic iron and sulfur oxidation reactions (Weast, 1978/79; Mraw and Naas, 1979). In addition, the presence of sulfuric acid lowers the freezing temperature of water (Gable et al., 1950) which could allow acidophiles to survive at sub-zero temperatures with the use of cellular cryoprotectants potentially enhancing that effect.

Analogs for life detection on planets and moons

Earth's extremophiles and their habitats are being investigated as analogs in the search for potentially habitable environments on exoplanets and moons (Martins et al., 2017; Merino et al., 2019; Carré et al., 2022). Mars, Enceladus (moon of Saturn), and Europa (moon of Jupiter) are candidates to harbor present or past life. Mars likely had a large water ocean in its earlier history, but it has subsequently dried out at least on its surface. As it dried out, lacustrine evaporates were created some of which are thought to have been acidic (Tosca et al., 2005). Eventually, the surface of Mars became hyperarid, extremely cold, and subjected to high levels of UV radiation. Today, water only remains in the subsurface cryosphere (Carr and Head, 2019) and under the south polar ice cap (Orosei et al., 2018).

Several sites around the world are being studied as analogs for ancient and modern Martian sites that could have harbored (or still do) acidophilic eurypsychrophiles (Fairén et al., 2010). These include acidic saline lakes in Western Australia (Benison and Bowen, 2006) and cold acidic lakes in the Altiplano of northern Chile that are also subjected to elevated levels of UV radiation because of the high altitude (Risacher et al., 2002; Demergasso et al., 2010). Terrestrial analog sites for potential life under ice or on the cold surface include Vostok ice in Antarctica (Price, 2000); arctic mineral assemblages in northern Greenland (Langdahl and Ingvorsen, 1997) and the Antarctic (Dold et al., 2013; Garcia-Lopez and Cid, 2017); and in sulfidic caves across the globe (Hose et al., 2000; Vlasceanu et al., 2000; Polyak and Provencio, 2001; Engel et al., 2004; Galdenzi et al., 2008; Jones et al., 2014; D'angeli et al., 2019). Metagenomic analyses of several cave and low-temperature environments revealed the presence of known extreme acidophiles (Langdahl and Ingvorsen, 1997; Vlasceanu et al., 2000) but none have been tested in the laboratory for low-temperature growth.

Both Enceladus and Europa are thought to contain water oceans under kilometers of ice (Carr et al., 1998; Collins and Goodman, 2007) that are kept liquid by ocean floor hydrothermal activity (Waite et al., 2017) or tidal forces (McKay et al., 2012). The ocean of Enceladus is thought to be alkaline (Glein et al., 2015) but there may be regions on the ocean floor that are more acidic such as are found close to terrestrial black smokers. The ocean of Europa may be acidic (Pasek and Greenberg, 2012) although this is controversial (Kargel et al., 2000; Russell et al., 2014). In either case, pH is likely to vary along strong geochemical gradients within the oceans on the icy moons displaying the potential for strongly alkaline to acidic habitats (McKay et al., 2012; Russell et al., 2014). Some of the terrestrial cold, acidic environments mentioned in the previous paragraph are being investigated as analogs for the oceans of Enceladus and Europa (Marion et al., 2003).

Moving forward

During the preparation of this manuscript, several environmental studies lacked the appropriate sample metadata that would have allowed the unequivocal identification of the environment as both acidic and cold. The importance of such data cannot be overly stressed. For example, in sulfidic cave studies where the air temperature deep inside the cave might be assumed to be cold, the actual temperature of the sample might be higher due to exothermic chemical and biological sulfide oxidation reactions. This potential creation of a "warm niche" that may promote the survival of co-habituating microorganisms (e.g., in biofilms in bioleaching heaps and environmental samples) with sulfide-oxidizing microbes is largely uninvestigated in laboratory simulations. A second lacuna in our knowledge that became evident was the lack of, e.g., RNA transcript-based support for the response to concurrent low temperature and acidic pH that should be a target for future studies.

Low-temperature and acidic environments have received less attention than their counterparts inhabiting higher temperatures, potentially as they are less easily accessed, e.g., at high altitudes or in Antarctica. Furthermore, although not covered in this review due to typically being inhabited by moderate acidophiles, arctic tundra environments are becoming more prominent in relation to thawing of permafrost due to climate change (Kwon et al., 2019). In consequence, this valuable niche remains untapped for, e.g., biotechnological applications plus understanding future climate and highlights the need for further investigation.

A notable gap in low-temperature acidophile microbiology is the lack of a true "stenopsychrophile" (i.e., growth at a narrow temperature range below 15°C). Potential environments to discover psychrophilic acidophiles are dark oligotrophic volcanic ecosystems, e.g., on Mount Erebus, Antarctica (Tebo et al., 2015) and Black Smokers (Han et al., 2018). Black Smokers are hydrothermal vents found on the ocean floor where spreading ridges occur as the result of either the moving apart of tectonic plates (Douville et al., 2002) or where tectonic plates are moving toward one another creating back-arc basins (Mottl et al., 2011; Reeves et al., 2011). The vents form when cold seawater is heated by underlying magma and re-emerges forming chimneys that spew out usually acidic (<pH 3.5) black fluid laden with sulfide mineral precipitates. However, the venting fluid can be extremely hot with temperatures reaching over 370°C (Von Damm, 1990) with significant differences in the chemical composition due to the nature of the underlying magma. For example, if the magma is hosted by basalt, the venting fluid is H_2S rich, H_2 poor, and less reducing, whereas if it is hosted by ultramafic rock, it tends to be H_2, Fe, and methane-rich and more reducing. These geological characteristics lead to variations in chimney composition and structure and the nature of surrounding sea-floor precipitates that, in turn, shape microbial community structure. Black smokers might seem like a poor place to search for eurypsychrophilic acidophiles, and indeed, thermophilic microbes abound in vent metagenome analyses. However, some vents are cool (<20°C), and since vents are surrounded by seawater of ~2°C, there are potentially habitats that could be occupied by eurypsychrophilic acidophiles (Adam et al., 2020). Metagenomic analyses have been carried out of several vent sites including the outside of chimneys with recorded temperatures of <20°C and in nearby seafloor precipitates (2°C). In these studies, populations have been detected that are phylogenetically related to known acidophile phylotypes. However, the phylogenies do not provide sufficient resolution to identify known eurypsychrophilic acidophiles at the species level. In addition, no laboratory work has been carried out to

experimentally determine if eurypsychrophiles exist on or close to venting chimneys (Nercessian et al., 2005; Flores et al., 2011; Ding et al., 2017; Hager et al., 2017) or if they are capable of growth at <15°C. These locations are especially interesting targets to search because the isolated nature of vent fields could promote allopatric speciation, potentially increasing the degree of microbial diversity.

Author contributions

MD conceived the study. All authors contributed to data collection, analysis, and manuscript preparation. All authors read and approved the final manuscript.

Funding

DH was supported by the Centro Ciencia & Vida, FB210008, Financiamiento Basal para Centros Científicos y Tecnológicos de Excelencia de ANID and Fondecyt 1181717. NM was supported by the Natural Sciences and Engineering Research Council grant no. 436206.

Conflict of interest

The authors declare that the research was conducted in the absence of any commercial or financial relationships that could be construed as a potential conflict of interest.

Publisher's note

References

Adam, N., Kriete, C., Garbe-Schönberg, D., Gonnella, G., Krause, S., Schippers, A., et al. (2020). Microbial community compositions and geochemistry of sediments with increasing distance to the hydrothermal vent outlet in the Kairei Field. *Geomicrobiol. J.* 37, 242–254. doi: 10.1080/01490451.2019.1694107

Aguilera, A., Olsson, S., and Puente-Sánchez, F. (2016). "Physiological and phylogenetic diversity of acidophilic eukaryotes," in *Acidophiles: Life in Extremely Acidic Environments,* eds. R. Quatrini and D.B. Johnson (UK: Caister Academic Press) 107–118. doi: 10.21775/9781910190333.07

Ahonen, L., and Tuovinen, O. H. (1989). Microbiological oxidation of ferrous iron at low temperatures. *Appl. Environ. Microbiol.* 55, 312–316. doi: 10.1128/aem.55.2.312-316.1989

Alexander, B., Leach, S., and Ingledew, W. J. (1987). The relationship between chemiosmotic parameters and sensitivity to anions and organic acids in the acidophile *Thiobacillus ferrooxidans*. *J. Gen. Microbiol.* 133, 1171–1179. doi: 10.1099/00221287-133-5-1171

Amils, R. (2016). Lessons learned from thirty years of geomicrobiological studies of Río Tinto. *Res. Microbiol.* 167, 539–545. doi: 10.1016/j.resmic.2016.06.001

Asemaninejad, A., Munford, K., Watmough, S., Campbell, D., Glasauer, S., Basiliko, N., et al. (2020). Structure of microbial communities in amended and unamended acid-generating mine wastes along gradients of soil amelioration and revegetation. *Appl. Soil Ecol.* 155, 103645. doi: 10.1016/j.apsoil.2020.103645

Auld, R. R., Mykytczuk, N. C. S., Leduc, L. G., and Merritt, T. J. S. (2017). Seasonal variation in an acid mine drainage microbial community. *Can. J. Microbiol.* 63, 137–152. doi: 10.1139/cjm-2016-0215

Aytar, P., Kay, C. M., Mutlu, M. B., and Cabuk, A. (2013). Coal desulfurization with *Acidithiobacillus ferrivorans*, from Balya acidic mine drainage. *Energy Fuels* 27, 3090–3098. doi: 10.1021/ef400360t

Aytar, P., Kay, C. M., Mutlu, M. B., Cabuk, A., and Johnson, D. B. (2015). Diversity of acidophilic prokaryotes at two acid mine drainage sites in Turkey. *Environ. Sci. Pollut. Res.* 22, 5995–6003. doi: 10.1007/s11356-014-3789-4

Badieyan, S., Bevan, D. R., and Zhang, C. (2012). Study and design of stability in GH5 cellulases. *Biotechnol. Bioeng.* 109, 31–44. doi: 10.1002/bit.23280

Bakermans, C., and Nealson, K. H. (2004). Relationship of critical temperature to macromolecular synthesis and growth yield in *Psychrobacter cryopegella*. *J. Bacteriol.* 186, 2340–2345. doi: 10.1128/JB.186.8.2340-2345.2004

Banerjee, A., Sarkar, S., Govil, T., Gonzalez-Faune, P., Cabrera-Barjas, G., Bandopadhyay, R., et al. (2021). Extremophilic exopolysaccharides: Biotechnologies and wastewater remediation. *Front. Microbiol.* 12, 721365. doi: 10.3389/fmicb.2021.721365

Barahona, S., Castro-Severyn, J., Dorador, C., Saavedra, C., and Remonsellez, F. (2020). Determinants of copper resistance in *Acidithiobacillus ferrivorans* ACH isolated from the Chilean altiplano. *Genes* 11, 844. doi: 10.3390/genes11080844

Barahona, S., Dorador, C., Zhang, R. Y., Aguilar, P., Sand, W., Vera, M., et al. (2014). Isolation and characterization of a novel *Acidithiobacillus ferrivorans* strain from the Chilean Altiplano: attachment and biofilm formation on pyrite at low temperature. *Res. Microbiol.* 165, 782–793. doi: 10.1016/j.resmic.2014.07.015

Benison, K. C., and Bowen, B. B. (2006). Acid saline lake systems give clues about past environments and the search for life on Mars. *Icarus* 183, 225–229. doi: 10.1016/j.icarus.2006.02.018

Berestovskaya, Y. Y., Vasil'eva, L. V., Chestnykh, O. V., and Zavarzin, G. A. (2002). Methanotrophs of the psychrophilic microbial community of the Russian Arctic Tundra. *Microbiology* 71, 460–466. doi: 10.1023/A:1019805929529

Bernardelli, C. E., Maza, S. N., Lecomte, K. L., Collo, G., Astini, R. A., and Donati, E. R. (2021). Acidophilic microorganisms enhancing geochemical dynamics in an acidic drainage system, Amarillo river in La Rioja, Argentina. *Chemosphere* 263, 128098. doi: 10.1016/j.chemosphere.2020.128098

Berthelot, D., Leduc, L. G., and Ferroni, G. D. (1993). Temperature studies of iron-oxidizing autotrophs and acidophilic heterotrophs isolated from uranium mines. *Can. J. Microbiol.* 39, 384–388. doi: 10.1139/m93-056

Bird, L. J., Bonnefoy, V., and Newman, D. K. (2011). Bioenergetic challenges of microbial iron metabolisms. *Trends Microbiol.* 19, 330–340. doi: 10.1016/j.tim.2011.05.001

Boase, K., González, C., Vergara, E., Neira, G., Holmes, D., and Watkin, E. (2022). Prediction and inferred evolution of acid tolerance genes in the biotechnologically important *Acidihalobacter* genus. *Front. Microbiol.* 13, 848410. doi: 10.3389/fmicb.2022.848410

Boman, A., Frojdo, S., Backlund, K., and Åström, M.E. (2010). Impact of isostatic land uplift and artificial drainage on oxidation of brackish-water sediments rich in metastable iron sulfide. *Geochim. Cosmochim. Acta* 74, 1268–1281. doi: 10.1016/j.gca.2009.11.026

Bonnefoy, V., and Holmes, D. S. (2012). Genomic insights into microbial oxidation and iron homeostasis in extremely acidic environments. *Environ. Microbiol.* 14, 1597–1611. doi: 10.1111/j.1462-2920.2011.02626.x

Bowman, J. P. (2008). "Genomic analysis of psychrophilic prokaryotes," in *Psychrophiles: From Biodiversity to Biotechnology,* eds. R. Margesin, F. Schinner, J.C. Marx and C. Gerday (Berlin-Heidelberg: Springer-Verlag) 265–285. doi: 10.1007/978-3-540-74335-4_16

Bridge, T. M., and Johnson, D.B. (1998). Reduction of soluble iron and reductive dissolution of ferric iron-containing minerals by moderately thermophilic iron-oxidizing bacteria. *Appl. Environ. Microbiol.* 64, 2181–2186. doi: 10.1128/AEM.64.6.2181-2186.1998

Bridge, T. M., and Johnson, D.B. (2000). Reductive dissolution of ferric iron minerals by *Acidiphilium* SJH. *Geomicrobiol. J.* 17, 193–206. doi: 10.1080/01490450050121161

Buetti-Dinh, A., Dethlefsen, O., Friedman, R., and Dopson, M. (2016). Transcriptomic analysis reveals how a lack of potassium ions increases *Sulfolobus acidocaldarius* sensitivity to pH changes. *Microbiology* 162, 1422–1434. doi: 10.1099/mic.0.000314

Carr, M., and Head, J. (2019). Mars: Formation and fate of a frozen Hesperian ocean. *Icarus* 319, 433–443. doi: 10.1016/j.icarus.2018.08.021

Carr, M. H., Belton, M. J. S., Chapman, C. R., Davies, M. E., Geissler, P., Greenberg, R., et al. (1998). Evidence for a subsurface ocean on Europa. *Nature* 391, 363–365. doi: 10.1038/34857

Carré, L., Zaccai, G., Delfosse, X., Girard, G., and Franzetti, B. (2022). Relevance of earth-bound extremophiles in the search for extraterrestrial life. *Astrobiology* 22, 322–367. doi: 10.1089/ast.2021.0033

Casanueva, A., Tuffin, M., Cary, C., and Cowan, D. A. (2010). Molecular adaptations to psychrophily: the impact of 'omic' technologies. *Trends Microbiol.* 18, 374–381. doi: 10.1016/j.tim.2010.05.002

Cavicchioli, R. (2006). Cold-adapted archaea. *Nat. Rev. Microbiol.* 4, 331–343. doi: 10.1038/nrmicro1390

Cavicchioli, R., Charlton, T., Ertan, H., Omar, S. M., Siddiqui, K. S., and Williams, T. J. (2011). Biotechnological uses of enzymes from psychrophiles. *Microbial. Biotechnol.* 4, 449–460. doi: 10.1111/j.1751-7915.2011.00258.x

Ccorahua-Santo, R., Eca, A., Abanto, M., Guerra, G., and Ramirez, P. (2017). Physiological and comparative genomic analysis of *Acidithiobacillus ferrivorans* PQ33 provides psychrotolerant fitness evidence for oxidation at low temperature. *Res. Microbiol.* 168, 482–492. doi: 10.1016/j.resmic.2017.01.007

Chattopadhyay, M. K., Jagannadham, M. V., Vairamani, M., and Shivaji, S. (1997). Carotenoid pigments of an Antarctic psychrotrophic bacterium *Micrococcus roseus*: Temperature dependent biosynthesis, structure, and interaction with synthetic membranes. *Biochem. Biophys. Res. Comm.* 239, 85–90. doi: 10.1006/bbrc.1997.7433

Chaumeil, P.-A., Mussig, A. J., Hugenholtz, P., and Parks, D. H. (2019). GTDB-Tk: a toolkit to classify genomes with the Genome Taxonomy Database. *Bioinformatics* 36, 1925–1927. doi: 10.1093/bioinformatics/btz848

Chen, L. X., Hu, M., Huang, L. N., Hua, Z. S., Kuang, J. L., Li, S. J., et al. (2015). Comparative metagenomic and metatranscriptomic analyses of microbial communities in acid mine drainage. *ISME J.* 9, 1579–1592. doi: 10.1038/ismej.2014.245

Chen, X. K., Li, X. Y., Ha, Y. F., Lin, J. Q., Liu, X. M., Pang, X., et al. (2020). Ferric uptake regulator provides a new strategy for acidophile adaptation to acidic ecosystems. *Appl. Environ. Microbiol.* 86, 220. doi: 10.1128/AEM.00268-20

Christel, S., Fridlund, J., Buetti-Dinh, A., Watkin, E. L., and Dopson, M. (2016a). RNA transcript sequencing reveals inorganic sulfur compound oxidation pathways in the acidophile *Acidithiobacillus ferrivorans*. *FEMS Microbiol. Letts.* 363, fnw057. doi: 10.1093/femsle/fnw057

Christel, S., Fridlund, J., Watkin, E. L., and Dopson, M. (2016b). *Acidithiobacillus ferrivorans* SS3 presents little RNA transcript response related to cold stress during growth at 8°C suggesting it is a eurypsychrophile. *Extremophiles* 20, 903–913. doi: 10.1007/s00792-016-0882-2

Ciccarelli, F. D., Doerks, T., Von Mering, C., Creevey, C. J., Snel, B., and Bork, P. (2006). Toward automatic reconstruction of a highly resolved Tree of Life. *Science* 311, 1283–1287. doi: 10.1126/science.1123061

Collins, G. C., and Goodman, J. C. (2007). Enceladus' south polar sea. *Icarus* 189, 72–82. doi: 10.1016/j.icarus.2007.01.010

Collins, T., Roulling, F., Piette, F., Marx, J.-C., Feller, G., Gerday, C., et al. (2008). "Fundamentals of cold-adapted enzymes," in *Psychrophiles: from Biodiversity to Biotechnology,* eds. R. Margesin, F. Schinner, J.-C. Marx and C. Gerday (Berlin: Springer-Verlag) 211–227. doi: 10.1007/978-3-540-74335-4_13

Cortez, D., Neira, G., González, C., Vergara, E., and Holmes, D. S. (2022). A large-scale genome-based survey of acidophilic bacteria suggests that genome streamlining is an adaption for life at low pH. *Front. Microbiol.* 13, 803241. doi: 10.3389/fmicb.2022.803241

D'angeli, I. M., Parise, M., Vattano, M., Madonia, G., Galdenzi, S., and De Waele, J. (2019). Sulfuric acid caves of Italy: A review. *Geomorphology* 333, 105–122. doi: 10.1016/j.geomorph.2019.02.025

De Maayer, P., Anderson, D., Cary, C., and Cowan, D. A. (2014). Some like it cold: understanding the survival strategies of psychrophiles. *EMBO Rep.* 15, 508–517. doi: 10.1002/embr.201338170

Dedysh, S. N., Panikov, N. S., and Tiedje, J. M. (1998). Acidophilic methanotrophic communities from Sphagnum peat bogs. *Appl. Environ. Microbiol.* 64, 922–929. doi: 10.1128/AEM.64.3.922-929.1998

Demergasso, C., Dorador, C., Meneses, D., Blamey, J., Cabrol, N., Escudero, L., et al. (2010). Prokaryotic diversity pattern in high-altitude ecosystems of the Chilean Altiplano. *J. Geophys. Res.* 115, 2008JG000836. doi: 10.1029/2008JG000836

Dhaulaniya, A. S., Balan, B., Kumar, M., Agrawal, P. K., and Singh, D. K. (2019). Cold survival strategies for bacteria, recent advancement and potential industrial applications. *Arch. Microbiol.* 201, 1–16. doi: 10.1007/s00203-018-1602-3

Ding, J., Zhang, Y., Wang, H., Jian, H., Leng, H., and Xiao, X. (2017). Microbial community structure of deep-sea hydrothermal vents on the ultraslow spreading Southwest Indian Ridge. *Front. Microbiol.* 8, 1012. doi: 10.3389/fmicb.2017.01012

Dold, B., Gonzalez-Toril, E., Aguilera, A., Lopez-Pamo, E., Cisternas, M. E., Bucchi, F., et al. (2013). Acid rock drainage and rock weathering in Antarctica: Important sources for iron cycling in the Southern Ocean. *Environ. Sci. Technol.* 47, 6129–6136. doi: 10.1021/es305141b

Dopson, M. (2016). "Physiological and phylogenetic diversity of acidophilic bacteria," in *Acidophiles: Life in Extremely Acidic Environments,* eds. R. Quatrini and D.B. Johnson (London, UK: Caister Academic Press) 79–92. doi: 10.21775/9781910190333.05

Dopson, M., Halinen, A. K., Rahunen, N., Ozkaya, B., Sahinkaya, E., Kaksonen, A. H., et al. (2007). Mineral and iron oxidation at low temperatures by pure and mixed cultures of acidophilic microorganisms. *Biotechnol. Bioengin.* 97, 1205–1215. doi: 10.1002/bit.21312

Dopson, M., and Johnson, D. B. (2012). Biodiversity, metabolism and applications of acidophilic sulfur-metabolizing micro-organisms. *Environ. Microbiol.* 14, 2620–2631. doi: 10.1111/j.1462-2920.2012.02749.x

Douville, E., Charlou, J. L., Oelkers, E. H., Bienvenu, P., Jove Colon, C. F., Donval, J. P., et al. (2002). The rainbow vent fluids (36°14′N, MAR): the influence of ultramafic rocks and phase separation on trace metal content in Mid-Atlantic Ridge hydrothermal fluids. *Chem. Geol.* 184, 37–48. doi: 10.1016/S0009-2541(01)00351-5

du Plessis, C. A., Slabbert, W., Hallberg, K. B., and Johnson, D. B. (2011). Ferredox: a biohydrometallurgical processing concept for limonitic nickel laterites. *Hydrometallurgy* 109, 221–229. doi: 10.1016/j.hydromet.2011.07.005

Dufresne, S., Bousquet, J., Boissinot, M., and Guay, R. (1996). *Sulfobacillus disulfidooxidans* sp. nov., a new acidophilic, disulfide-oxidizing, gram-positive, spore-forming bacterium. *Int. J. Syst. Bacteriol.* 46, 1056–1064. doi: 10.1099/00207713-46-4-1056

Dunfield, P. F., Yuryev, A., Senin, P., Smirnova, A. V., Stott, M. B., Hou, S., et al. (2007). Methane oxidation by an extremely acidophilic bacterium of the phylum Verrucomicrobia. *Nature* 450, 879–882. doi: 10.1038/nature06411

Elberling, B. (2005). Temperature and oxygen control on pyrite oxidation in frozen mine tailings. *Cold Regions Sci. Technol.* 41, 121–133. doi: 10.1016/j.coldregions.2004.09.004

Elberling, B., Schippers, A., and Sand, W. (2000). Bacterial and chemical oxidation of pyritic mine tailings at low temperatures. *J. Contam. Hydrol.* 41, 225–238. doi: 10.1016/S0169-7722(99)00085-6

Engel, A. S., Porter, M. L., Stern, L. A., Quinlan, S., and Bennett, P. C. (2004). Bacterial diversity and ecosystem function of filamentous microbial mats from aphotic (cave) sulfidic springs dominated by chemolithoautotrophic "Epsilonproteobacteria". *FEMS Microbiol. Ecol.* 51, 31–53. doi: 10.1016/j.femsec.2004.07.004

Escobar, B., Buccicardi, S., Morales, G., and Wiertz, J. (2010). Biooxidation of ferrous iron and sulphide at low temperatures: Implications on acid mine drainage and bioleaching of sulphide minerals. *Hydrometallurgy* 104, 454–458. doi: 10.1016/j.hydromet.2010.03.027

Fairén, A. G., Davila, A. F., Lim, D., Bramall, N., Bonaccorsi, R., Zavaleta, J., et al. (2010). Astrobiology through the ages of Mars: The study of terrestrial analogues to understand the habitability of Mars. *Astrobiology* 10, 821–843. doi: 10.1089/ast.2009.0440

Falagan, C., and Johnson, D. B. (2016). *Acidithiobacillus ferriphilus* sp. nov., a facultatively anaerobic iron- and sulfur-metabolizing extreme acidophile. *Int. J. Syst. Evol. Microbiol.* 66, 206–211. doi: 10.1099/ijsem.0.000698

Fan, W., Peng, Y., Meng, Y., Zhang, W., Zhu, N., Wang, J., et al. (2018). Transcriptomic analysis reveals reduced inorganic sulfur compound oxidation mechanism in *Acidithiobacillus ferriphilus*. *Microbiology* 87, 486–501. doi: 10.1134/S0026261718040070

Feller, G. (2007). Life at low temperatures: is disorder the driving force? *Extremophiles* 11, 211–216. doi: 10.1007/s00792-006-0050-1

Ferroni, G. D., Leduc, L. G., and Todd, M. (1986). Isolation and temperature characterization of psychrotrophic strains of *Thiobacillus ferrooxidans* from the environment of a uranium mine. *J. Gen. Appl. Microbiol.* 32, 169–175. doi: 10.2323/jgam.32.169

Flores, G. E., Campbell, J. H., Kirshtein, J. D., Meneghin, J., Podar, M., Steinberg, J. I., et al. (2011). Microbial community structure of hydrothermal deposits from geochemically different vent fields along the Mid-Atlantic Ridge. *Environ. Microbiol.* 13, 2158–2171. doi: 10.1111/j.1462-2920.2011.02463.x

Gable, C. M., Betz, H. F., and Maron, S. H. (1950). Phase equilibria of the system sulfur trioxide-water1. *J. Am. Chem. Soc.* 72, 1445–1448. doi: 10.1021/ja01160a005

Galdenzi, S., Cocchioni, M., Morichetti, L., Amici, V., and Scuri, S. (2008). Sulfidic ground-water chemistry in the Frasassi caves, Italy. *J. Cave Karst Stud.* 70, 94–107.

Galleguillos, P. A., Grail, B. M., Hallberg, K. B., Demergasso, C. S., and Johnson, D. B. (2018). Identification of trehalose as a compatible solute in different species of acidophilic bacteria. *J. Microbiol.* 56, 727–733. doi: 10.1007/s12275-018-8176-2

Garcia-Lopez, E., and Cid, C. (2017). Glaciers and ice sheets as analog environments of potentially habitable icy worlds. *Front. Microbiol.* 8, 1407. doi: 10.3389/fmicb.2017.01407

Garcia-Moyano, A., Austnes, A. E., Lanzen, A., Gonzalez-Toril, E., Aguilera, A., and Ovreas, L. (2015). Novel and unexpected microbial diversity in acid mine drainage in Svalbard (78 °N), revealed by culture-independent approaches. *Microorganisms* 3, 667–694. doi: 10.3390/microorganisms3040667

Glein, C. R., Baross, J. A., and Waite, J. H. (2015). The pH of Enceladus' ocean. *Geochim. Cosmochim. Acta* 162, 202–219. doi: 10.1016/j.gca.2015.04.017

Golyshina, O., Ferrer, M., and Golyshin, P. N. (2016). "Diversity and physiologies of acidophilic archaea," in *Acidophiles: Life in Extremely Acidic Environments,* eds. R. Quatrini and D.B. Johnson (London, UK: Caister Academic Press) 93–106. doi: 10.21775/9781910190333.06

González, C., Yanquepe, M., Cardenas, J. P., Valdes, J., Quatrini, R., Holmes, D. S., et al. (2014). Genetic variability of psychrotolerant *Acidithiobacillus ferrivorans* revealed by (meta)genomic analysis. *Res. Microbiol.* 165, 726–734. doi: 10.1016/j.resmic.2014.08.005

González-Rosales, C., Vergara, E., Dopson, M., Valdés, J. H., and Holmes, D. S. (2022). Integrative genomics sheds light on evolutionary forces shaping the Acidithiobacillia class acidophilic lifestyle. *Front. Microbiol.* 12, 822229. doi: 10.3389/fmicb.2021.822229

Grettenberger, C. L., Havig, J. R., and Hamilton, T. L. (2020). Metabolic diversity and co-occurrence of multiple *Ferrovum* species at an acid mine drainage site. *BMC Microbiol.* 20, 1–14. doi: 10.1186/s12866-020-01768-w

Guiliani, N., and Jerez, C. A. (2000). Molecular cloning, sequencing, and expression of *omp-40*, the gene coding for the major outer membrane protein from the acidophilic bacterium *Thiobacillus ferrooxidans*. *Appl. Environ. Microbiol.* 66, 2318–2324. doi: 10.1128/AEM.66.6.2318-2324.2000

Hager, K. W., Fullerton, H., Butterfield, D. A., and Moyer, C. L. (2017). Community structure of lithotrophically-driven hydrothermal microbial mats from the Mariana Arc and Back-Arc. *Front. Microbiol.* 8, 1578. doi: 10.3389/fmicb.2017.01578

Halinen, A.-K., Beecroft, N. J., Määttä, K., Nurmi, P., Laukkanen, K., Kaksonen, A. H., et al. (2012). Microbial community dynamics during a demonstration-scale bioheap leaching operation. *Hydrometallurgy* 126, 34–41. doi: 10.1016/j.hydromet.2012.05.001

Hallberg, K. B., Gonzalez-Toril, E., and Johnson, D. B. (2010). *Acidithiobacillus ferrivorans*, sp. nov.; facultatively anaerobic, psychrotolerant iron-, and sulfur-oxidizing acidophiles isolated from metal mine-impacted environments. *Extremophiles* 14, 9–19. doi: 10.1007/s00792-009-0282-y

Hallberg, K. B., Grail, B. M., Du Plessis, C., and Johnson, D. B. (2011). Reductive dissolution of ferric iron minerals: a new approach for bioprocessing nickel laterites. *Min. Engin.* 24, 620–624. doi: 10.1016/j.mineng.2010.09.005

Han, Y., Gonnella, G., Adam, N., Schippers, A., Burkhardt, L., Kurtz, S., et al. (2018). Hydrothermal chimneys host habitat-specific microbial communities: analogues for studying the possible impact of mining seafloor massive sulfide deposits. *Sci. Rep.* 8, 10386. doi: 10.1038/s41598-018-28613-5

Hedrich, S., and Johnson, D. B. (2013). Aerobic and anaerobic oxidation of hydrogen by acidophilic bacteria. *FEMS Microbiol. Lett.* 349, 40–45. doi: 10.1111/1574-6968.12290

Hedrich, S., Lunsdorf, H., Keeberg, R., Heide, G., Seifert, J., and Schlomann, M. (2011). Schwertmannite formation adjacent to bacterial cells in a mine water treatment plant and in pure cultures of *Ferrovum myxofaciens*. *Environ. Sci. Technol.* 45, 7685–7692. doi: 10.1021/es201564g

Hedrich, S., and Schippers, A. (2016). "Distribution of acidophilic microorganisms in natural and man-made acidic enviroments," in *Acidophiles: Life in extremely acidic environments,* eds. R. Quatrini and D.B. Johnson (Norfolk, UK: Caister Academic Press) 153–175. doi: 10.21775/9781910190333.10

Högfors-Rönnholm, E., Christel, S., Dalhem, K., Lillhonga, T., Engblom, S., Österholm, P., et al. (2018). Chemical and microbiological evaluation of novel chemical treatment methods for acid sulfate soils. *Sci. Tot. Environ.* 625, 39–49. doi: 10.1016/j.scitotenv.2017.12.287

Högfors-Rönnholm, E., Lundin, D., Brambilla, D., Christel, S., Lopez-Fernandez, M., Lillhonga, T., et al. (2022). *Gallionella* and *Sulfuricella* populations are dominant during the transition of boreal potential to actual acid sulfate soils. *Comms Earth Environ.* 3, 304. doi: 10.1038/s43247-022-00642-z

Hose, L. D., Palmer, A. N., Palmer, M. V., Northup, D. E., Boston, P. J., and Duchene, H. R. (2000). Microbiology and geochemistry in a hydrogen-sulphide-rich karst environment. *Chem. Geol.* 169, 399–423. doi: 10.1016/S0009-2541(00)00217-5

Hua, Z. S., Han, Y. J., Chen, L. X., Liu, J., Hu, M., Li, S. J., et al. (2015). Ecological roles of dominant and rare prokaryotes in acid mine drainage revealed by metagenomics and metatranscriptomics. *ISME J.* 9, 1280–1294. doi: 10.1038/ismej.2014.212

Jensen, S. M., Christensen, C. J., Petersen, J. M., Treusch, A. H., and Brandl, M. (2015). Liposomes containing lipids from *Sulfolobus islandicus* withstand intestinal bile salts: An approach for oral drug delivery? *Int. J. Pharmaceut* 493, 63–69. doi: 10.1016/j.ijpharm.2015.07.026

Johnson, A., Högfors-Rönnholm, E., Engblom, S., Österholm, P., Åström, M., and Dopson, M. (2022). Dredging and deposition of metal sulfide rich river sediments results in rapid conversion to acid sulfate soil materials. *Sci. Tot. Environ.* 813, 151864. doi: 10.1016/j.scitotenv.2021.151864

Johnson, D. B., and Hallberg, K. B. (2009). Carbon, iron and sulfur metabolism in acidophilic micro-organisms. *Adv. Microb. Physiol.* 54, 201–255. doi: 10.1016/S0065-2911(08)00003-9

Johnson, D. B., Hallberg, K. B., and Hedrich, S. (2014). Uncovering a microbial enigma: Isolation and characterization of the streamer-generating, iron-oxidizing, acidophilic bacterium "*Ferrovum myxofaciens*". *Appl. Environ. Microbiol.* 80, 672–680. doi: 10.1128/AEM.03230-13

Johnson, D. B., and Quatrini, R. (2016). "Acidophile microbiology in space and time," in *Acidophiles: Life in Extremely acidic environments,* eds. D.B. Johnson and R. Quatrini. (Norfolk, UK: Caister Academic Press) 3–16. doi: 10.21775/9781910190333.01

Johnson, D. B., Rolfe, S., Hallberg, K. B., and Iversen, E. (2001). Isolation and phylogenetic characterization of acidophilic microorganisms indigenous to acidic drainage waters at an abandoned Norwegian copper mine. *Environ. Microbiol.* 3, 630–637. doi: 10.1046/j.1462-2920.2001.00234.x

Jones, D. S., Schaperdoth, I., and Macalady, J. L. (2014). Metagenomic evidence for sulfide oxidation in extremely acidic cave biofilms. *Geomicrobiol. J.* 31, 194–204. doi: 10.1080/01490451.2013.834008

Jones, R. M., and Johnson, D. B. (2016). Iron kinetics and evolution of microbial populations in low-pH, ferrous iron-oxidizing bioreactors. *Environ. Sci. Technol.* 50, 8239–8245. doi: 10.1021/acs.est.6b02141

Jung, H., Inaba, Y., and Banta, S. (2021). Genetic engineering of the acidophilic chemolithoautotroph *Acidithiobacillus ferrooxidans*. *Trends Biotechnol.* 40, 677–692. doi: 10.1016/j.tibtech.2021.10.004

Jung, Y. H., Lee, Y. K., Lee, H. K., Lee, K., and Im, H. (2018). CspB of an arctic bacterium, *Polaribacter irgensii* KOPRI 22228, confers extraordinary freeze -tolerance. *Brazil J. Microbiol.* 49, 97–103. doi: 10.1016/j.bjm.2017.04.006

Jung, Y. H., Yi, J. Y., Jung, H., Lee, Y. K., Lee, H. K., Naicker, M. C., et al. (2010). Overexpression of cold shock protein A of *Psychromonas arctica* KOPRI 22215 confers cold-resistance. *Protein J.* 29, 136–142. doi: 10.1007/s10930-010-9233-9

Junge, K., Eicken, H., Swanson, B. D., and Deming, J. W. (2006). Bacterial incorporation of leucine into protein down to−20°C with evidence for potential activity in sub-eutectic saline ice formations. *Cryobiology* 52, 417–429. doi: 10.1016/j.cryobiol.2006.03.002

Kadnikov, V. V., Ivasenko, D. A., Beletskii, A. V., Mardanov, A. V., Danilova, E. V., Pimenov, N. V., et al. (2016). A novel uncultured bacterium of the family Gallionellaceae: Description and genome reconstruction based on metagenomic analysis of microbial community in acid mine drainage. *Microbiology* 85, 449–461. doi: 10.1134/S002626171604010X

Kaksonen, A. H., Dopson, M., Karnachuk, O. V., Tuovinen, O. H., and Puhakka, J. A. (2008). "Biological iron oxidation and sulfate reduction in the treatment of acid mine drainage at low temperatures," in *Psychrophiles: From Biodiversity to Biotechnology,* eds. R. Margesin, F. Schinner, J.-C. Marx and C. Gerday (Berlin: Springer-Verlag) 429–454. doi: 10.1007/978-3-540-74335-4_25

Karavaiko, G. I., Bogdanova, T. I., Tourova, T. P., Kondrat'eva, T. F., Tsaplina, I. A., Egorova, M. A., et al. (2005). Reclassification of '*Sulfobacillus thermosulfidooxidans* subsp. *thermotolerans*' strain K1 as *Alicyclobacillus tolerans* sp. nov. and *Sulfobacillus disulfidooxidans* Dufresne et al., 1996 as *Alicyclobacillus disulfidooxidans* comb. nov., and emended description of the genus Alicyclobacillus. *Int. J. Syst. Evol. Microbiol.* 55, 941–947. doi: 10.1099/ijs.0.63300-0

Kargel, J. S., Kaye, J. Z., Head, J. W., Marion, G. M., Sassen, R., Crowley, J. K., et al. (2000). Europa's crust and ocean: Origin, composition, and the prospects for life. *Icarus* 148, 226–265. doi: 10.1006/icar.2000.6471

Karimian, N., Johnston, S. G., and Burton, E. D. (2018). Iron and sulfur cycling in acid sulfate soil wetlands under dynamic redox conditions: A review. *Chemosphere* 197, 803–816. doi: 10.1016/j.chemosphere.2018.01.096

Kawahara, H. (2008). "Cryoprotectants and ice-binding proteins," in *Psychrophiles: From biodiversity to biotechnology,* eds. R. Margesin, F. Schinner, J.C. Marx and C. Gerday (Berlin: Springer) 229–246. doi: 10.1007/978-3-540-74335-4_14

Kay, C. M., Rowe, O. F., Rocchetti, L., Coupland, K., Hallberg, K. B., and Johnson, D. B. (2013). Evolution of microbial "streamer" growths in an acidic, metal-contaminated stream draining an abandoned underground copper mine. *Life* 3, 189–210. doi: 10.3390/life3010189

Kimura, S., Bryan, C. G., Hallberg, K. B., and Johnson, D. B. (2011). Biodiversity and geochemistry of an extremely acidic, low-temperature subterranean environment sustained by chemolithotrophy. *Environ. Microbiol.* 13, 2092–2104. doi: 10.1111/j.1462-2920.2011.02434.x

Kirschvink, J. L., Gaidos, E. J., Bertani, L. E., Beukes, N. J., Gutzmer, J., Maepa, L. N., et al. (2000). Paleoproterozoic snowball Earth: Extreme climatic and geochemical global change and its biological consequences. *Proc. Nat. Acad. Sci. USA* 97, 1400–1405. doi: 10.1073/pnas.97.4.1400

Kock, D., and Schippers, A. (2008). Quantitative microbial community analysis of three different sulfidic mine tailing dumps generating acid mine drainage. *Appl. Environ. Microbiol.* 74, 5211–5219. doi: 10.1128/AEM.00649-08

Králová, S. (2017). Role of fatty acids in cold adaptation of Antarctic psychrophilic *Flavobacterium* spp. *Syst. Appl. Microbiol.* 40, 329–333. doi: 10.1016/j.syapm.2017.06.001

Kumar, S., Suyal, D. C., Yadav, A., Shouche, Y., and Goel, R. (2020). Psychrophilic *Pseudomonas helmanticensis* proteome under simulated cold stress. *Cell Stress Chaperones* 25, 1025–1032. doi: 10.1007/s12192-020-01139-4

Kupka, D., Liljeqvist, M., Nurmi, P., Puhakka, J. A., Tuovinen, O. H., and Dopson, M. (2009). Oxidation of elemental sulfur, tetrathionate, and ferrous iron by the psychrotolerant *Acidithiobacillus* strain SS3. *Res. Microbiol.* 160, 767–774. doi: 10.1016/j.resmic.2009.08.022

Kupka, D., Rzhepishevska, O. I., Dopson, M., Lindstrom, E. B., Karnachuk, O. V., and Tuovinen, O. H. (2007). Bacterial oxidation of ferrous iron at low temperatures. *Biotechnol. Bioengin.* 97, 1470–1478. doi: 10.1002/bit.21371

Kwon, M. J., Jung, J. Y., Tripathi, B. M., Gockede, M., Lee, Y. K., and Kim, M. (2019). Dynamics of microbial communities and CO_2 and CH_4 fluxes in the tundra ecosystems of the changing Arctic. *J. Microbiol.* 57, 325–336. doi: 10.1007/s12275-019-8661-2

Langdahl, B. R., and Ingvorsen, K. (1997). Temperature characteristics of bacterial iron solubilisation and ^{14}C assimilation in naturally exposed sulfide ore material at Citronen Fjord, North Greenland (83°N). *FEMS Microbiol. Ecol.* 23, 275–283. doi: 10.1016/S0168-6496(97)00032-9

Leduc, L. G., Ferroni, G. D., and Trevors, J. T. (1997). Resistance to heavy metals in different strains of *Thiobacillus ferrooxidans*. *World J. Microbiol. Biotechnol.* 13, 453–455. doi: 10.1023/A:1018584402487

Leduc, L. G., Trevors, J. T., and Ferroni, G. D. (1993). Thermal characterization of different isolates of *Thiobacillus ferrooxidans*. *FEMS Microbiol. Lett.* 108, 189–194. doi: 10.1111/j.1574-6968.1993.tb06097.x

Letunic, I., and Bork, P. (2021). Interactive Tree Of Life (iTOL) v5: an online tool for phylogenetic tree display and annotation. *Nucleic. Acids Res.* 49, W293–w296. doi: 10.1093/nar/gkab301

Lian, K., Leiros, H.-K. S., and Moe, E. (2015). MutT from the fish pathogen *Aliivibrio salmonicida* is a cold-active nucleotide-pool sanitization enzyme with unexpectedly high thermostability. *FEBS Open Bio.* 5, 107–116. doi: 10.1016/j.fob.2015.01.006

Liljeqvist, M., Ossandon, F. J., González, C., Rajan, S., Stell, A., Valdes, J., et al. (2015). Metagenomic analysis reveals adaptations to a cold-adapted lifestyle in a low-temperature acid mine drainage stream. *FEMS Microb. Ecol.* 91, 1011. doi: 10.1093/femsec/fiv011

Liljeqvist, M., Rzhepishevska, O. I., and Dopson, M. (2013). Gene identification and substrate regulation provides insights into sulfur accumulation during bioleaching with the psychrotolerant acidophile *Acidithiobacillus ferrivorans*. *Appl. Environ. Microbiol.* 71, 951–957. doi: 10.1128/AEM.02989-12

Liljeqvist, M., Sundkvist, J.-E., Saleh, A., and Dopson, M. (2011a). Low temperature removal of inorganic sulfur compounds from mining process waters. *Biotechnol. Bioengin.* 108, 1251–1259. doi: 10.1002/bit.23057

Liljeqvist, M., Valdes, J., Holmes, D. S., and Dopson, M. (2011b). Draft genome of the psychrotolerant acidophile *Acidithiobacillus ferrivorans* SS3. *J. Bacteriol.* 193, 4304–4305. doi: 10.1128/JB.05373-11

Ling, Y.-C., Moreau, J., Berwick, L., Tulipani, S., Grice, K., and Bush, R. (2015). Distribution of iron- and sulfate-reducing bacteria across a coastal acid sulfate soil (CASS) environment: implications for passive bioremediation by tidal inundation. *Front. Microbiol.* 6, 624. doi: 10.3389/fmicb.2015.00624

Los, D. A., and Murata, N. (2004). Membrane fluidity and its roles in the perception of environmental signals. *Biochim. Biophys. Acta-Biomembr.* 1666, 142–157. doi: 10.1016/j.bbamem.2004.08.002

Malik, L., and Hedrich, S. (2022). Ferric iron reduction in extreme acidophiles. *Front. Microbiol.* 12, 818414. doi: 10.3389/fmicb.2021.818414

Margesin, R., and Miteva, V. (2011). Diversity and ecology of psychrophilic microorganisms. *Res. Microbiol.* 162, 346–361. doi: 10.1016/j.resmic.2010.12.004

Margesin, R., Schinner, F., Marx, J.C., and Gerday, C. (2008). *Psychrophiles. From Biodiversity to Biotechnology*. Berlin Heidelberg: Springer Verlag. doi: 10.1007/978-3-540-74335-4

Marion, G. M., Fritsen, C. H., Eicken, H., and Payne, M. C. (2003). The search for life on Europa: limiting environmental factors, potential habitats, and Earth analogues. *Astrobiology* 3, 785–811. doi: 10.1089/153110703322736105

Martins, Z., Cottin, H., Kotler, J. M., Carrasco, N., Cockell, C. S., De la Torre Noetzel, R., et al. (2017). Earth as a tool for astrobiology—A European perspective. *Space Sci. Rev.* 209, 43–81. doi: 10.1007/s11214-017-0369-1

Marx, J. C., Collins, T., D'amico, S., Feller, G., and Gerday, C. (2007). Cold-adapted enzymes from marine antarctic microorganisms. *Mar. Biotechnol.* 9, 293–304. doi: 10.1007/s10126-006-6103-8

McKay, C., Mykytczuk, N. C. S., and Whyte, L. G. (2012). "Life in Ice on Other Worlds," in *Polar Microbiology: Life in a Deepfreeze,* eds. R. Miller and L.G. Whyte. (Washington: ASM Press).

Meldrum, J. L., Jamieson, H. E., and Dyke, L. D. (2001). Oxidation of mine tailings from Rankin Inlet, Nunavut, at subzero temperatures. *Can. Geotechnol. J.* 38, 957–966. doi: 10.1139/t01-028

Merino, N., Aronson, H. S., Bojanova, D. P., Feyhl-Buska, J., Wong, M. L., Zhang, S., et al. (2019). Living at the extremes: Extremophiles and the limits of life in a planetary context. *Front. Microbiol.* 10, 780. doi: 10.3389/fmicb.2019.00780

Metpally, R. P. R., and Reddy, B. V. B. (2009). Comparative proteome analysis of psychrophilic versus mesophilic bacterial species: Insights into the molecular basis of cold adaptation of proteins. *BMC Genomics* 10, 1–10. doi: 10.1186/1471-2164-10-11

Mottl, M. J., Seewald, J. S., Wheat, C. G., Tivey, M. K., Michael, P. J., Proskurowski, G., et al. (2011). Chemistry of hot springs along the Eastern Lau Spreading Center. *Geochim. Cosmochim. Acta* 75, 1013–1038. doi: 10.1016/j.gca.2010.12.008

Moya-Beltrán, A., Beard, S., Rojas-Villalobos, C., Issotta, F., Gallardo, Y., Ulloa, R., et al. (2021). Genomic evolution of the class *Acidithiobacillia*: deep-branching Proteobacteria living in extreme acidic conditions. *ISME J.* 15, 3221–3238. doi: 10.1038/s41396-021-00995-x

Moya-Beltrán, A., Cárdenas, J. P., Covarrubias, P. C., Issotta, F., Ossandon, F. J., Grail, B. M., et al. (2014). Draft genome sequence of the nominated type strain of "*Ferrovum myxofaciens*," an acidophilic, iron-oxidizing Betaproteobacterium. *Genome Announc.* 2, 814. doi: 10.1128/genomeA.00834-14

Mraw, S. C., and Naas, D. F. (1979). The measurement of accurate heat capacities by differential scanning calorimetry Comparison of d.s.c. results on pyrite (100 to 800 K) with literature values from precision adiabatic calorimetry. *J. Chem. Thermodyn.* 11, 567–584. doi: 10.1016/0021-9614(79)90097-1

Muñoz-Villagrán, C., Grossolli-Gálvez, J., Acevedo-Arbunic, J., Valenzuela, X., Ferrer, A., Díez, B., et al. (2022). Characterization and genomic analysis of two novel psychrotolerant *Acidithiobacillus ferrooxidans* strains from polar and subpolar environments. *Front. Microbiol.* 13, 960324. doi: 10.3389/fmicb.2022.960324

Mykytczuk, N. C. S., Trevors, J. T., Ferroni, G. D., and Leduc, L. G. (2010a). Cytoplasmic membrane fluidity and fatty acid composition of *Acidithiobacillus ferrooxidans* in response to pH stress. *Extremophiles* 14, 427–441. doi: 10.1007/s00792-010-0319-2

Mykytczuk, N. C. S., Trevors, J. T., Ferroni, G. D., and Leduc, L. G. (2011b). Cytoplasmic membrane response to copper and nickel in *Acidithiobacillus ferrooxidans*. *Microbiol. Res.* 166, 186–206. doi: 10.1016/j.micres.2010.03.004

Mykytczuk, N. C. S., Trevors, J. T., Foote, S. J., Leduc, L. G., Ferroni, G. D., and Twine, S. M. (2011a). Proteomic insights into cold adaptation of psychrotrophic and mesophilic *Acidithiobacillus ferrooxidans* strains. *Antonie van Leeuwen* 100, 259–277. doi: 10.1007/s10482-011-9584-z

Mykytczuk, N. C. S., Trevors, J. T., Twine, S. M., Ferroni, G. D., and Leduc, L. G. (2010b). Membrane fluidity and fatty acid comparisons in psychrotrophic and mesophilic strains of *Acidithiobacillus ferrooxidans* under cold growth temperatures. *Arch. Microbiol.* 192, 1005–1018. doi: 10.1007/s00203-010-0629-x

Nancucheo, I., Bitencourt, J., a,.P., Sahoo, P. K., Alves, J. O., Siqueira, J. O., et al. (2017). Recent developments for remediating acidic mine waters using sulfidogenic bacteria. *Biomed Res Int.* 2017, 7256582. doi: 10.1155/2017/7256582

Neira, G., Cortez, D., Jil, J., and Holmes, D. S. (2020). AciDB 1.0: a database of acidophilic organisms, their genomic information and associated metadata. *Bioinformatics* 36, 4970–4971. doi: 10.1093/bioinformatics/btaa638

Neira, G., Vergara, E., and Holmes, D. S. (2022). Genome-guided prediction of acid resistance mechanisms in acidophilic methanotrophs of phylogenetically deep-rooted Verrucomicrobia isolated from geothermal environments. *Front. Microbiol.* 13, 900531. doi: 10.3389/fmicb.2022.900531

Nercessian, O., Fouquet, Y., Pierre, C., Prieur, D., and Jeanthon, C. (2005). Diversity of Bacteria and Archaea associated with a carbonate-rich metalliferous sediment sample from the Rainbow vent field on the Mid-Atlantic Ridge. *Environ. Microbiol.* 7, 698–714. doi: 10.1111/j.1462-2920.2005.00744.x

Ni, G., Christel, S., Roman, P., Wong, Z. L., Bijmans, M. F., and Dopson, M. (2016). Electricity generation from an inorganic sulfur compound containing mining wastewater by acidophilic microorganisms. *Res. Microbiol.* 167, 568–575. doi: 10.1016/j.resmic.2016.04.010

Orosei, R., Lauro, S. E., Pettinelli, E., Cicchetti, A., Coradini, M., Cosciotti, B., et al. (2018). Radar evidence of subglacial liquid water on Mars. *Science* 361, 490–493. doi: 10.1126/science.aar7268

Osorio, H., Mangold, S., Denis, Y., Nancucheo, I., Johnson, D. B., Bonnefoy, V., et al. (2013). Anaerobic sulfur metabolism coupled to dissimilatory iron reduction in the extremophile *Acidithiobacillus ferrooxidans*. *Appl. Environ. Microbiol.* 79, 2172–2181. doi: 10.1128/AEM.03057-12

Parro, V., Moreno-Paz, M., and González-Toril, E. (2007). Analysis of environmental transcriptomes by DNA microarrays. *Environ. Microbiol.* 9, 453–464. doi: 10.1111/j.1462-2920.2006.01162.x

Pasek, M. A., and Greenberg, R. (2012). Acidification of Europa's subsurface ocean as a consequence of oxidant delivery. *Astrobiology* 12, 151–159. doi: 10.1089/ast.2011.0666

Peng, T., Liao, W., Wang, J., Miao, J., Peng, Y., Gu, G., et al. (2021). Bioleaching and electrochemical behavior of chalcopyrite by a mixed culture at low temperature. *Front. Microbiol.* 12, 663757. doi: 10.3389/fmicb.2021.663757

Peng, T. J., Ma, L. Y., Feng, X., Tao, J. M., Nan, M. H., Liu, Y. D., et al. (2017). Genomic and transcriptomic analyses reveal adaptation mechanisms of an *Acidithiobacillus ferrivorans* strain YL15 to alpine acid mine drainage. *PLoS ONE* 12, e0178008. doi: 10.1371/journal.pone.0178008

Petersen, J. (2016). Heap leaching as a key technology for recovery of values from low-grade ores – A brief overview. *Hydrometallurgy* 165, 206–212. doi: 10.1016/j.hydromet.2015.09.001

Phadtare, S., and Inouye, M. (2008). "Cold-shock protein," in Psychrophiles: from Biodiversity to Biotechnology, eds. R. Margesin, F. Schinner, J.-C. Marx and C. Gerday (Berlin: Springer-Verlag) 191–209. doi: 10.1007/978-3-540-74335-4_12

Polyak, V., and Provencio, P. (2001). By-product materials related to H_2S-H_2SO_4 influenced speleogenesis of Carlsbad, Lechuguilla, and other caves of the Guadalupe mountains, New Mexico. *J. Cave Karst Stud.* 63, 23–32.

Price, P. B. (2000). A habitat for psychrophiles in deep Antarctic ice. *Proc. Nat. Acad. Sci. USA* 97, 1247–1251. doi: 10.1073/pnas.97.3.1247

Puhakka, J. A., Kaksonen, A. H., and Riekkola-Vanhanen, M. (2007). "Heap leaching of black schist," in *Biomining,* eds. D.E. Rawlings and D.B. Johnson (Berlin: Springer-Verlag) 139–151. doi: 10.1007/978-3-540-34911-2_7

Quatrini, R., Appia-Ayme, C., Denis, Y., Jedlicki, E., Holmes, D., and Bonnefoy, V. (2009). Extending the models for iron and sulfur oxidation in the extreme acidophile *Acidithiobacillus ferrooxidans*. *BMC Gen.* 10, 394. doi: 10.1186/1471-2164-10-394

Quehenberger, J., Shen, L., Albers, S. V., Siebers, B., and Spadiut, O. (2017). *Sulfolobus* - A potential key organism in future biotechnology. *Front. Microbiol.* 8, 2474. doi: 10.3389/fmicb.2017.02474

Raddadi, N., Cherif, A., Daffonchio, D., Neifar, M., and Fava, F. (2015). Biotechnological applications of extremophiles, extremozymes and extremolytes. *Appl. Microbiol. Biotechnol.* 99, 7907–7913. doi: 10.1007/s00253-015-6874-9

Reeves, E. P., Seewald, J. S., Saccocia, P., Bach, W., Craddock, P. R., Shanks, W. C., et al. (2011). Geochemistry of hydrothermal fluids from the PACMANUS, Northeast Pual and Vienna Woods hydrothermal fields, Manus Basin, Papua New Guinea. *Geoch. Cosmochim. Acta* 75, 1088–1123. doi: 10.1016/j.gca.2010.11.008

Reysenbach, A. L., Liu, Y., Banta, A. B., Beveridge, T. J., Kirshtein, J. D., Schouten, S., et al. (2006). A ubiquitous thermoacidophilic archaeon from deep-sea hydrothermal vents. *Nature* 442, 444–447. doi: 10.1038/nature04921

Riekkola-Vanhanen, M. (2010). Talvivaara Sotkamo Mine – Bioleaching of polymetallic nickel ore in subarctic climate. *Nova Biotechnol.* 10, 7–14. doi: 10.36547/nbc.1058

Riekkola-Vanhanen, M. (2013). Talvivaara mining company – From a project to a mine. *Min. Engin.* 48, 2–9. doi: 10.1016/j.mineng.2013.04.018

Risacher, F., Alonso, H., and Salazar, C. (2002). Hydrochemistry of two adjacent acid saline lakes in the Andes of northern Chile. *Chem. Geol.* 187, 39–57. doi: 10.1016/S0009-2541(02)00021-9

Roberto, F. F., and Schippers, A. (2022). Progress in bioleaching: part B, applications of microbial processes by the minerals industries. *Appl. Microbiol. Biotechnol.* 106, 5913–5928. doi: 10.1007/s00253-022-12085-9

Russell, M. J., Barge, L. M., Bhartia, R., Bocanegra, D., Bracher, P. J., Branscomb, E., et al. (2014). The drive to life on wet and icy worlds. *Astrobiology* 14, 308–343. doi: 10.1089/ast.2013.1110

Sharma, M., Chaurasia, P. K., Yadav, A., Yadav, R. S. S., Yadava, S., and Yadav, K. D. S. (2016). Purification and characterization of a thermally stable yellow laccase from *Daedalea flavida* MTCC-145 with higher catalytic performance towards selective synthesis of substituted benzaldehydes. *Russ. J. Bioorg. Chem.* 42, 59–68. doi: 10.1134/S1068162016010143

Shivaji, S., and Prakash, J. S. S. (2010). How do bacteria sense and respond to low temperature? *Arch. Microbiol.* 192, 85–95. doi: 10.1007/s00203-009-0539-y

Siddiqui, K. S. (2015). Some like it hot, some like it cold: Temperature dependent biotechnological applications and improvements in extremophilic enzymes. *Biotechnol. Adv.* 33, 1912–1922. doi: 10.1016/j.biotechadv.2015.11.001

Siddiqui, K. S., Williams, T. J., Wilkins, D., Yau, S., Allen, M. A., Brown, M. V., et al. (2013). Psychrophiles. *Ann. Rev. Earth Planet Sci.* 41, 87–115. doi: 10.1146/annurev-earth-040610-133514

Slonczewski, J. L., Fujisawa, M., Dopson, M., and Krulwich, T. A. (2009). Cytoplasmic pH measurement and homeostasis in bacteria and archaea. *Adv. Microb. Physiol.* 55, 1–79. doi: 10.1016/S0065-2911(09)05501-5

Sulonen, M. L., Kokko, M. E., Lakaniemi, A. M., and Puhakka, J. A. (2015). Electricity generation from tetrathionate in microbial fuel cells by acidophiles. *J. Hazard Mater.* 284, 182–189. doi: 10.1016/j.jhazmat.2014.10.045

Talla, E., Hedrich, S., Ji, B. Y., Johnson, D. B., and Bonnefoy, V. (2013). Genome analysis of the psychrotolerant acidophile *Acidithiobacillus ferrivorans* CF27. *Adv. Mat. Res.* 825, 145–148. doi: 10.4028/www.scientific.net/AMR.825.145

Talla, E., Hedrich, S., Mangenot, S., Ji, B. Y., Johnson, D. B., Barbe, V., et al. (2014). Insights into the pathways of iron- and sulfur-oxidation, and biofilm formation from the chemolithotrophic acidophile *Acidithiobacillus ferrivorans* CF27. *Res. Microbiol.* 165, 753–760. doi: 10.1016/j.resmic.2014.08.002

Tebo, B. M., Davis, R. E., Anitori, R. P., Connell, L. B., Schiffman, P., and Staudigel, H. (2015). Microbial communities in dark oligotrophic volcanic ice cave ecosystems of Mt. Erebus, Antarctica. *Front. Microbiol.* 6, 179–179. doi: 10.3389/fmicb.2015.00179

Tosca, N. J., Mclennan, S. M., Clark, B. C., Grotzinger, J. P., Hurowitz, J. A., Knoll, A. H., et al. (2005). Geochemical modeling of evaporation processes on Mars: Insight from the sedimentary record at Meridiani Planum. *Earth Planet Sci. Lett.* 240, 122–148. doi: 10.1016/j.epsl.2005.09.042

Tran, T. T. T., Mangenot, S., Magdelenat, G., Payen, E., Rouy, Z., Belahbib, H., et al. (2017). Comparative genome analysis provides insights into both the lifestyle of *Acidithiobacillus ferrivorans* strain CF27 and the chimeric nature of the iron-oxidizing Acidithiobacilli genomes. *Front. Microbiol.* 8, 1009. doi: 10.3389/fmicb.2017.01009

Tribelli, P. M., and Lopez, N. I. (2018). Reporting key features in cold-adapted bacteria. *Life* 8, 8. doi: 10.3390/life8010008

Tyson, G. W., Chapman, J., Hugenholtz, P., Allen, E. E., Ram, R. J., and Richardson, P. M. (2004). Community structure and metabolism through reconstruction of microbial genomes from the environment. *Nature* 428, 37–43. doi: 10.1038/nature02340

Ullrich, S. R., González, C., Poehlein, A., Tischler, J. S., Daniel, R., Schlömann, M., et al. (2016a). Gene loss and horizontal gene transfer contributed to the genome evolution of the extreme acidophile "*Ferrovum*". *Front. Microbiol.* 7, 00797. doi: 10.3389/fmicb.2016.00797

Ullrich, S. R., Poehlein, A., Levican, G., Muhling, M., and Schlomann, M. (2018). Iron targeted transcriptome study draws attention to novel redox protein candidates involved in ferrous iron oxidation in "*Ferrovum*" sp. JA12. *Res. Microbiol.* 169, 618–627. doi: 10.1016/j.resmic.2018.05.009

Ullrich, S. R., Poehlein, A., Tischler, J. S., Gonzalez, C., Ossandon, F. J., Daniel, R., et al. (2016b). Genome analysis of the biotechnologically relevant acidophilic iron oxidising strain JA12 indicates phylogenetic and metabolic diversity within the novel genus "*Ferrovum*". *PLoS ONE* 11, e0146832. doi: 10.1371/journal.pone.0146832

van de Vossenberg, J. L. C. M., Driessen, A. J. M., Zillig, W., and Konings, W. N. (1998). Bioenergetics and cytoplasmic membrane stability of the extremely acidophilic, thermophilic archaeon *Picrophilus oshimae*. *Extremophiles* 2, 67–74. doi: 10.1007/s007920050044

Vera, M., Schippers, A., Hedrich, S., and Sand, W. (2022). Progress in bioleaching: fundamentals and mechanisms of microbial metal sulfide oxidation – part A. *Appl. Microbiol. Biotechnol.* 106, 6933–6952. doi: 10.1007/s00253-022-12168-7

Vergara, E., Neira, G., González, C., Cortez, D., Dopson, M., and Holmes, D. S. (2020). Evolution of predicted acid resistance mechanisms in the extremely acidophilic *Leptospirillum* genus. *Genes* 11, 389. doi: 10.3390/genes11040389

Verma, D. (2021). Extremophilic prokaryotic endoxylanases: diversity, applicability, and molecular Insights. *Front. Microbiol.* 12, 728475. doi: 10.3389/fmicb.2021.728475

Vlasceanu, L., Sarbu, S. M., Engel, A. S., and Kinkle, B. K. (2000). Acidic cave-wall biofilms loacated in the Frasissi Gorge, Italy. *Geomicrobiol. J.* 17, 125–139. doi: 10.1080/01490450050023809

Von Damm, K. L. (1990). Seafloor hydrothermal activity: Black smoker chemistry and chimneys. *Ann. Rev. Earth Planet Sci.* 18, 173–204. doi: 10.1146/annurev.ea.18.050190.001133

Waite, J. H., Glein, C. R., Perryman, R. S., Teolis, B. D., Magee, B. A., Miller, G., et al. (2017). Cassini finds molecular hydrogen in the Enceladus plume: Evidence for hydrothermal processes. *Science* 356, 155–159. doi: 10.1126/science.aai8703

Weast, R.C. (1978/79). *CRC Handbook of Chemistry and Physics.* West Palm Beach, U.S.A.: CRC Press.

Wu, X., Sten, P., Engblom, E., Nowak, P., Österholm, P., and Dopson, M. (2015). Impact of mitigation strategies on microbial community from an Ostrobothnian acid sulfate soil. *Sci. Tot. Environ.* 526, 215–221. doi: 10.1016/j.scitotenv.2015.04.049

Wu, X., Wong, Z. L., Sten, P., Engblom, S., Österholm, P., and Dopson, M. (2013). Microbial community potentially responsible for acid and metal release from an Ostrobothnian acid sulfate soil. *FEMS Microbiol. Ecol.* 84, 555–563. doi: 10.1111/1574-6941.12084

Zammit, C. M., and Watkin, E. L. J. (2016). "Adaptation to extreme acidity and osmotic stress," in *Acidophiles: life in extremely acidic environments,* eds. R. Quatrini and D.B. Johnson (UK: Caister Academic Press) 49–62. doi: 10.21775/9781910190333.03

Zhang, S., Yan, L., Xing, W. J., Chen, P., Zhang, Y., and Wang, W. D. (2018). *Acidithiobacillus ferrooxidans* and its potential application. *Extremophiles* 22, 563–579. doi: 10.1007/s00792-018-1024-9

Zhang, X., Niu, J., Liang, Y., Liu, X., and Yin, H. (2016). Metagenome-scale analysis yields insights into the structure and function of microbial communities in a copper bioleaching heap. *BMC Genetics* 17, 21. doi: 10.1186/s12863-016-0330-4

Zhao, D., Yang, J., Liu, T., Lu, D., Zhang, S., Yan, L., et al. (2021). Complete genome sequence analysis of *Acidithiobacillus ferrivorans* XJFY6S-08 reveals environmental adaptation to alpine acid mine drainage. *Curr. Microbiol.* 78, 1488–1498. doi: 10.1007/s00284-021-02423-x

frontiers | Frontiers in Microbiology

TYPE Original Research
PUBLISHED 30 March 2023
DOI 10.3389/fmicb.2023.1122184

OPEN ACCESS

EDITED BY
Prashant Kumar Singh,
Mizoram University, India

REVIEWED BY
Marek Stibal,
Charles University, Czechia
Naveen Chandra Joshi,
Amity University, Noida, India

*CORRESPONDENCE
Pauline Vannier
✉ pauline.vannier@matis.is
Viggó Þór Marteinsson
✉ viggo.marteinsson@matis.is

†These authors have contributed equally to this work and share first authorship

SPECIALTY SECTION
This article was submitted to Extreme Microbiology, a section of the journal Frontiers in Microbiology

RECEIVED 12 December 2022
ACCEPTED 13 March 2023
PUBLISHED 30 March 2023

CITATION
Vannier P, Farrant GK, Klonowski A, Gaidos E, Thorsteinsson T and Marteinsson VÞ (2023) Metagenomic analyses of a microbial assemblage in a subglacial lake beneath the Vatnajökull ice cap, Iceland. *Front. Microbiol.* 14:1122184. doi: 10.3389/fmicb.2023.1122184

Metagenomic analyses of a microbial assemblage in a subglacial lake beneath the Vatnajökull ice cap, Iceland

Pauline Vannier[1*†], Gregory K. Farrant[1†], Alexandra Klonowski[1], Eric Gaidos[2], Thorsteinn Thorsteinsson[3] and Viggó Þór Marteinsson[1,4*]

[1]MATIS, Department of Research and Innovation, Reykjavík, Iceland, [2]Department of Earth Sciences, University of Hawai'i at Mānoa, Honolulu, HI, United States, [3]Icelandic Meteorological Office, Reykjavík, Iceland, [4]Faculty of Food Science and Nutrition, University of Iceland, Reykjavík, Iceland

Skaftárkatlar are two subglacial lakes located beneath the Vatnajökull ice cap in Iceland associated with geothermal and volcanic activity. Previous studies of these lakes with ribosomal gene (16S rDNA) tag sequencing revealed a limited diversity of bacteria adapted to cold, dark, and nutrient-poor waters. In this study, we present analyses of metagenomes from the lake which give new insights into its microbial ecology. Analyses of the 16S rDNA genes in the metagenomes confirmed the existence of a low-diversity core microbial assemblage in the lake and insights into the potential metabolisms of the dominant members. Seven taxonomic genera, *Sulfuricurvum*, *Sulfurospirillum*, *Acetobacterium*, *Pelobacter/Geobacter*, *Saccharibacteria, Caldisericum,* and an unclassified member of Prolixibacteraceae, comprised more than 98% of the rDNA reads in the library. Functional characterisation of the lake metagenomes revealed complete metabolic pathways for sulphur cycling, nitrogen metabolism, carbon fixation *via* the reverse Krebs cycle, and acetogenesis. These results show that chemolithoautotrophy constitutes the main metabolism in this subglacial ecosystem. This assemblage and its metabolisms are not reflected in enrichment cultures, demonstrating the importance of *in situ* investigations of this environment.

KEYWORDS

subglacial lakes, Iceland, microbial assemblage, metagenome, metabolism

1. Introduction

Subglacial lakes can form where water collects at hydrostatic stable points beneath an ice sheet, when geothermal heat, pressure-induced freezing point depression, and/or high salinity prevent complete freezing (Livingstone et al., 2022). These lakes are relatively isolated ecosystems that can host life despite low temperatures, low nutrient abundance, and the absence of sunlight as an energy source. Terrestrial subglacial lakes are considered accessible if imperfect, analogues to ice-covered environments in the past and present Solar system: the ice-covered oceans of "Snowball" Earth (Kirschvink et al., 2000), lakes beneath

the south polar cap of Mars (Lauro et al., 2020) and oceans in some of the icy satellites of Jupiter and Saturn (Kivelson et al., 2000, 2002; Thomas et al., 2016). Studies of these systems complement research on other lakes with comparatively thin (metres) ice covers, e.g., the Dry Valleys lakes (Chinn, 1993) and epishelf lakes of Antarctica (Davies et al., 2017), where sufficient photosynthetic active radiation can reach the water column and support phototrophic communities (Howard-Williams et al., 1998).

There are more than 700 reported subglacial lakes in Antarctica (Livingstone et al., 2022), three in Iceland under the Vatnajökull glacier (Bjornsson, 2003), two in Greenland (Palmer et al., 2013), and one recently discovered in the Canadian Arctic (Rutishauser et al., 2018). The biological exploration of some of these lakes has begun, namely Lake Vostok (Karl et al., 1999; Priscu et al., 1999; Christner et al., 2001; Bulat, 2016; Gura and Rogers, 2020), Subglacial Lake Whillans (Tulaczyk et al., 2014), Subglacial Lake Mercer in Antarctica (Priscu et al., 2021), and all three Icelandic lakes (Gaidos et al., 2004, 2009; Marteinsson et al., 2013). In the cases of Antarctica and Iceland, the data unambiguously point to the presence of active assemblages of bacterial taxa which are distinct from the distribution in the overlying ice or surrounding glaciated terrain (Gaidos et al., 2004, 2009; Marteinsson et al., 2013; Achberger et al., 2016).

The three main Icelandic lakes, called Grímsvötn, Western, and Eastern Skaftárkatlar lakes, are distinguished by their location on active volcanoes and are maintained by geothermal melting at the base of the 250–300-m thick Vatnajökull ice cap. The chemistry of the approximately 100-m-deep water columns of these lakes is substantially influenced by volcanic gases and hydrothermal fluids, maintaining an anoxic and highly sulphidic environment (Agustsdottir and Brantley, 1994; Johannesson et al., 2007). Mixing of anoxic lake water with oxygenated glacial meltwater creates chemical disequilibrium that can serve as an energy source for chemolithotrophic microorganisms (Gaidos et al., 2004, 2009; Marteinsson et al., 2013). Previous investigations have used molecular tag-based methods to identify the dominant microbial taxa in the water column of the Skaftárkatlar lakes and link chemical reactions of the inorganic substrates thought present in the lakes with potential metabolisms of these taxa, e.g., acetogenesis, sulphide oxidation, sulphate reduction, iron reduction, and hydrogen oxidation by members of *Acetobacterium*, *Geobacter*, *Sulfuricurvum*, *Sulfurospirillum,* and *Desulfosporosinus* (Gaidos et al., 2009; Marteinsson et al., 2013). In Subglacial Lake Whillans, the chemoautotrophic microbial taxa, distinct from that taxa of the Icelandic subglacial lakes, use reduced nitrogen, iron or sulphur compounds as energy sources (Christner et al., 2014).

Here, we performed a metagenomic analysis on four water column samples collected from the Eastern Skaftárkatlar lake in 2007, as well as on enrichment cultures from the same samples (Marteinsson et al., 2013). Our study aimed to: (1) confirm the previously reported microbial community structure, (2) investigate the metabolic strategies of the microorganisms in the lake, and (3) analyse potential pathways within microbes grown in enrichment cultures under different conditions. Compared to the previous study done on the same water samples but only with a 16S rRNA sequencing approach, we adopted a metagenomic approach as a more informative, less biassed method to gain further understanding of the microbial diversity and community structure but also and most importantly of the functional capabilities both at the taxon and community level occurring in such a specific environment. Our analyses show unambiguously that the microbial communities of this Icelandic subglacial lake are dominated by seven taxonomic genera: *Sulfuricurvum*, *Sulfurospirillum*, *Acetobacterium*, *Pelobacter/Geobacter*, *Saccharibacteria, Caldisericum,* and an unclassified Prolixibacteraceae. Chemolithoautotrophy is the main metabolism of these communities and is adapted to their environment with oxidation/reduction of sulphur, nitrogen metabolism, carbon fixation *via* the reverse Krebs cycle, and acetogenesis.

2. Materials and methods

2.1. Environmental samples

Water column samples were collected from the East Skaftárkatlar lake, in June 2007 as described by Marteinsson et al. (2013). Two boreholes A and B were drilled through the overlying 280-m-thick ice sheet with a sterilising hot water drill (Thorsteinsson et al., 2008). Each collected sample was about 1 L and the results of chemical analyses of the samples (Marteinsson et al., 2013) are reported in **Supplementary Table 1**. As B_1 and B_4 samples appeared chemically homogeneous (**Supplementary Table 1**), a pool of the B_1 to B_4 samples was created, B_{mix}, to increase total DNA yield.

2.2. Enrichment samples

The E_{mix} sample consists of biomass pooled from enrichment cultures that showed growth as previously described (Marteinsson et al., 2013). Media were designed to cultivate chemolithotrophs and chemo-organotrophs at 4, 60, and 80°C. Briefly, different enrichment media were used and inoculated with 1% of water lake samples under anaerobic conditions. Sample of 0.22 μm micron-filtered lake water was used as a medium for enrichment cultures labelled "WN_2," "WO_2," "C-J," and "A-J" for respectively "Water N_2," "Water O_2," "Enrichment C-jökull" (meaning glacier in Icelandic), and "Enrichment A-jökull." A supplement yeast extract solution (0.01%), vitamin solution, Balch element solution (Balch et al., 1979), S^0, and resazurin were added to WN_2 and WO_2 enrichment cultures. WO_2 was used aerobically whereas WN_2 was incubated with pure N_2 and supplemented with 0.025% final wt v^{-1} $Na_2S.9H_2O$. A volume of sterile water was supplemented with 1X of yeast-acetate medium (Gaidos et al., 2009) and used as media for C-J and A-J. C-J was incubated with 80/20% H_2/CO_2 and 0.025% final wt. v^{-1} $Na_2S.9H_2O$ whereas A-J was incubated aerobically. Finally, enrichment cultures were done aerobically with 162 Thermus medium (Degryse et al., 1978) and Reasoner's 2A (R_2A) medium (Reasoner and Geldreich, 1985) whereas Thermotoga and Yeast Peptone Sulphur (YPS) media were used anaerobically with pure N_2 (Marteinsson et al., 1997, 2001). Pellets of cells from these enrichments were obtained by centrifugation at 8,000 rpm for 25 min and used for DNA extraction.

2.3. DNA extraction and sequencing

DNA was extracted from filtered water samples and enrichment cultures as previously described (Gaidos et al., 2009). Three different DNA samples were sequenced: A_3, B_{mix}, and E_{mix} (**Table 1**). The DNA was sent to the Marine Biological Laboratory at the Woods Hole Institute for sequencing on an Illumina HiSeq (Illumina, Inc., CA, USA) as part of the Census of Deep Life of the Deep Carbon Observatory. DNA was sheared using a Covaris S2 sonicator (Covaris, Woburn, MA, USA) and libraries were constructed with the Nugen Ovation Ultralow Library protocol (NuGEN Technologies, San Carlos, CA, USA). Expected insert size of 175 bp enabled overlapping reads. Amplified libraries were visualised on an Agilent DNA1000 chip (Agilent, Santa Clara, CA, USA) or Caliper HiSens Bioanalyzer assay (Perkin Elmer, Waltham MA, USA), pooled at equimolar concentrations and size selected using a Sage PippinPrep 2% cassette (Sage Science, Beverly, MA, USA). The library pool was quantified using a Kapa Biosystems qPCR library quantification kit (Kapa Biosystems, Wilmington, MA, USA), then sequenced on the HiSeq1000 (Illumina) in a 2 × 108 bp paired-end sequencing run using dedicated read indexing. The samples were then demultiplexed (barcode-based sorting of sequences from different samples) with CASAVA (v.1.8.2; Illumina) while removing the Illumina adaptors. Reads were then merged using FLASH v1.2.11 (Magoč and Salzberg, 2011) with default parameters. Short reads and low-quality bases were then removed using the clc_quality_trim command in CLC (v4.4.0.122465; options used: minlength 90, badfraction 0, i.e., no low-quality nucleotides allowed; CLC Bio, Aarhus, Denmark).

TABLE 1 Sample information from East Skaftárkatlar lake.

Sample name	Sample type	Depth (metres)	DNA concentration (ng/μl)
A_3	Water	379	56
B_1	Water	284	15
B_2	Water	336	31
B_3	Water	377	22
B_4	Water	388	68
B_{mix}	DNA pool of B_1, B_2, B_3, and B_4	–	136
E_3	Enrichment culture at 4°C	–	246
E_{60}	Enrichment culture at 60°C	–	269
E_{80}	Enrichment culture at 80°C	–	158
E_{mix}	DNA pool of E_3, E_{60}, and E_{80}	–	673

The bold font was to highlight the samples that were analyzed in this article.

2.4. Biodiversity analysis based on rDNA $_{mi}$TAGs

Reads corresponding to rDNA genes, a.k.a. $_{mi}$TAGs for metagenome Illumina tags (Logares et al., 2014), were extracted from the metagenomes using Hidden Markov Models (HMM) in Meta-RNA (Huang et al., 2009). The reads were assembled on Geneious (R10, Biomatters, Auckland, New Zealand) with conservative settings ("Fastest," <1% mismatch, otherwise default parameters) to avoid chimeric assembly. Using iterative mappings of the rest of the reads with Geneious (Biomatters), the contigs were manually extended and assembled-when the coverage was sufficient- into complete ribosomal operons containing the 16S, 23S, and 5S rDNA genes and homogeneous coverage, allowing more reliable taxonomic assignments than with partial or single genes. These assembled rDNA genes were then annotated using either BLASTN+ against public databases NT and SILVA (Camacho et al., 2009; Quast et al., 2012) or the online RDP classifier (Wang et al., 2007). Most contigs get a significant assignment (>98% 16S identity) with the notable exception among the dominant taxa of *Caldisericum* sp. (96% identity against the closest 16S barcode and only 83% identity against the closest genome of *Caldisericum exile*). The rDNA genes were then aligned and trimmed to about 1,819; 3,731, and 115 bp (for 16S, 23S, and 5S, respectively) and used as references to recruit the ribosomal fraction of the raw metagenomic reads with high stringency (≥50% alignment coverage and ≥98% identity). From this point, we assumed that each assemblage represents a distinct taxon. To better reflect the actual community structure, read counts per taxon were then normalised based on actual gene length and the number of copies of the operon in each taxon. The estimation of the copy number of each ribosomal operon was obtained from ribosomal RNA operon copy number database (rrnDB) (Stoddard et al., 2014) by rounding the average number of rDNA operon copies at the taxonomic level retained for each operon (see **Table 2**).

Additionally, binning experiments based on nucleotide composition, GC%, and differential coverage in A_3, B_{mix}, and E_{mix} [CONCOCT (Alneberg et al., 2014)] were tried and failed at properly separating some closely related taxa, partly due to an overall low sequencing depth and lack of variation in the taxonomic profile of available samples.

2.5. Microbial metagenome, functional potential

With regards to their comparable community composition shown through the rDNA $_{mi}$TAG analyses (see section "Results" and **Figure 1**), the raw metagenomes A_3 and B_{mix} were co-assembled *de novo* to improve the functional analyses. At first, default configurations of IDBA-UD (Peng et al., 2012) and SPAdes (Bankevich et al., 2012) were run to generate reliable contigs. The resulting contigs were then assembled into "supercontigs" using Geneious (Biomatters; default "Fastest" with 2% mismatch allowed). These "supercontigs" and the other unassembled original contigs were used for the functional exploration of the water column metagenome. MetaGeneMark (Zhu et al., 2010) was used online with default parameters to detect open reading frames (ORFs) even truncated at the edge of contigs. Function and taxonomy were then assigned to these genes by amino-acid alignment against the Kyoto Encyclopedia of Genes and Genomes database (KEGG, FTP Release 12-02-2018)

TABLE 2 Genetic materials of East Skaftárkatlar lake and associated analyses used in this study (*A_3-B_{mix} co-assembly).

	Sample name	A_3	B_{mix}		E_{mix}
De novo Illumina sequencing, merging, and cleaning	Amount of DNA (ng)	56	136		673
	Number of pair-end reads (x2)	35,404,237	30,780,977		32,362,167
	Number of merged base-pairs	5,262,627,789	4,552,871,144		4,320,910,461
	Average length (bp)	157.05	155.85		151.59
rDNA read extraction and assembly	Number of rDNA reads	209,089	175,427		80,189
	Number of rDNA sequences	16S: 27 – 23S: 26 – 5S: 26			
		A_3	B_{mix}	A_3-B_{mix}*	E_{mix}
2-steps metagenome assembly	Number of contigs	61,052	47,708	64,905	44,111
	Number of base pairs	60,396,455	68,986,232	83,643,503	66,501,590
	Minimum length (bp)	80	78	80	79
	Maximum length (bp)	247,938	357,766	279,868	1,472,397
	Average length (bp)	989.26	1,446.01	1,288.71	1,507.60
	N50	2,502	6,373	5,182	5,533
	N90	348	413	377	424
ORFs detection	Number of ORFs	95,010	99,688	124,531	97,036
	Minimum length (bp)	57	57	57	57
	Maximum length (bp)	10,023	12,087	12,756	11,385
	Average length (bp)	526.29	594.54	570.19	608.75

(Kanehisa and Goto, 2000; Kanehisa et al., 2015) using DIAMOND (with 60% identity cut-off) (Buchfink et al., 2015) and their abundance in the metagenome was estimated by recruiting the raw metagenomics reads using BLASTN (Camacho et al., 2009). The results were manually checked and when 80% of the genes involved in a pathway were detected, the pathways were considered as present. Errors in the taxonomic assignments of the ORFs are generally caused by low taxonomic resolution or the absence of close relatives in the reference dataset and may result on genes being assigned to close relatives of the represented diversity. These were reduced by collapsing branches of the trees using TaxonomyCollapsor.[1] This algorithm sorts the leaves on the phylogenetic trees according to decreasing abundance (as read counts) and flags as significant those for which the cumulated abundance contains 95% of the total abundance. Leaves that do not reach the significance criteria are then reassigned by order of priority to their closest significant relative of the same rank or at a higher taxonomical level.

3. Results

3.1. Metagenome sequence yield

DNA was extracted and sequenced from samples collected from the bottom of the lake (sample A_3), from a mixture of four water column samples collected at different depths (sample B_{mix}), and from enrichments grown under various culture conditions (sample E_{mix}) (**Tables 1**, **2**). The metagenomes A_3 and B_{mix} allow us to investigate the microbial community of the lake water column whereas E_{mix} permits to identify the growing organisms that might be rare in the environment but can be enriched under laboratory conditions. The sequencing of all the DNA available for A_3, B_{mix}, and E_{mix} resulted in 30–35 $\times$ 10^6 overlapping paired reads per sample with respectively an average merged length of 157.05 bp (σ = 15.65 bp), 155.85 bp (σ = 19.84 bp), and 151.59 bp (σ = 18.96 bp) (**Table 2**).

3.2. Diversity and community structure based on ribosomal DNA sequences

Hidden Markov Models were used to identify 209,089, 175,427, and 80,189 rDNA reads in the A_3, B_{mix}, and E_{mix} libraries, respectively (**Table 2**). Conservative *de novo* assembly and manual improvements of these assemblies yielded 25 distinct high-quality full-length rDNA operons (each consisting of 5S, 16S, and 23S genes and intergenic regions) and 4 partial operons (missing all or part of a rDNA gene) (**Table 3** and **Supplementary Table 2**). The libraries sequenced from the natural samples A_3 and B_{mix} both contain seven taxa with relative read abundance >1%, namely *Acetobacterium* sp., *Sulfuricurvum* sp., *Sulfurospirillum* sp., *Geobacter* sp./*Pelobacter* sp., *Caldisericum* sp., *Saccharibacteria* sp., and an unclassified Prolixibacteraceae. Together, those taxa recruit 98.0 to 99.2% of the total rDNA reads in A_3 and B_{mix}, respectively. Based on 16S-rDNA $_{mi}$TAGs, Shannon's α-diversity is 1.18 and 1.83 for A_3 and B_{mix}, respectively, while evenness is 0.14 and 0.33, respectively. While the A_3 metagenome is dominated by *Sulfuricurvum* sp. (74% of the 16S reads), followed by *Acetobacterium* (16%), B_{mix} seems to be more evenly distributed,

1 https://github.com/gfarrant/astrolakes

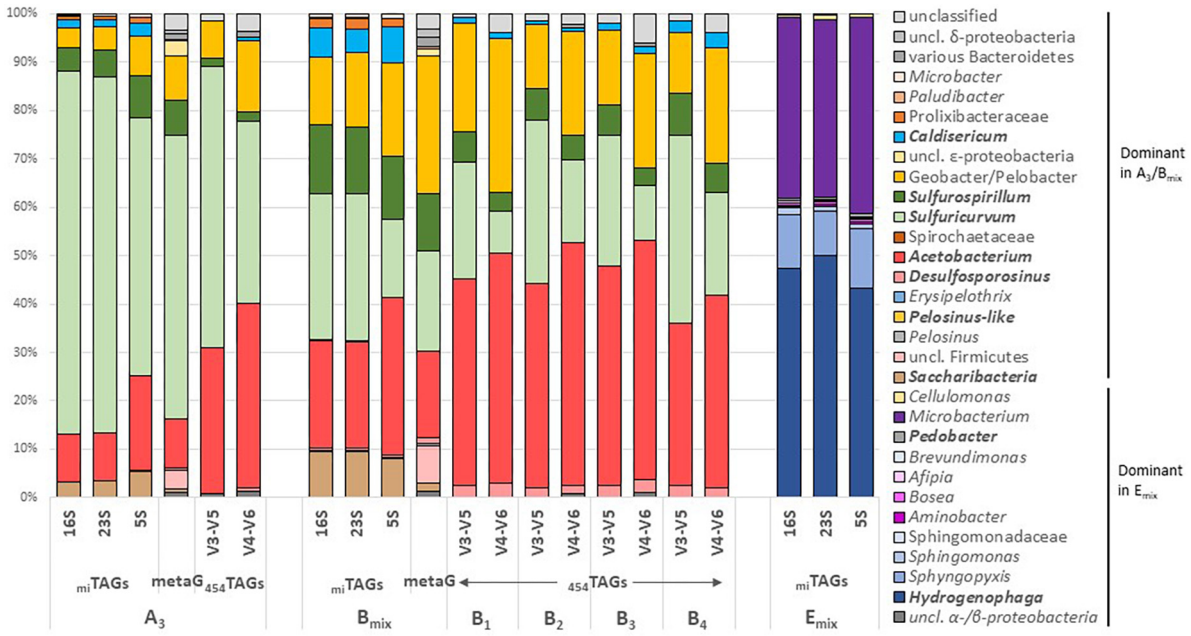

FIGURE 1
Community structure of metagenomes A_3, B_{mix}, and E_{mix} from East Skaftárkatlar lake based on metagenome extracted rDNA $_{mi}$TAGs. Assignments were performed using BLASTN against SILVA 128 (Quast et al., 2012; Yilmaz et al., 2013).

consisting of *Sulfuricurvum* (30%), *Acetobacterium* sp. (22%), *Sulfurospirillum* (14%) and *Geobacter* sp./*Pelobacter* sp. (13%). The community structure observed for the three samples based on 16S-, 23S-, and 5S-rDNA $_{mi}$TAGs [metagenome Illumina tags (Logares et al., 2014)] was compared to that observed in samples A_3 and B_{1-4} obtained by Marteinsson et al. (2013) using 16S rDNA pyrosequencing (**Figure 1**).

Unlike these first four taxa, which are relatively close to their cultivated relatives (over 97% identity), the lower abundance taxa *Caldisericum* sp. candidate (1.7% of 16S-rDNA $_{mi}$TAGs in A_3, 6.0% in B_{mix}) and *Saccharibacteria* sp. (3.3% in A_3, 9.5% in B_{mix}) are more distant from their closest relatives in public databases. The *Caldisericum* sp. candidate 16S and 23S assembled contigs show an alignment identity of 83% with publicly available *C. exile* AZM16c01 (Mori et al., 2009). *Saccharibacteria* sp. rDNA contigs show 94% identity (16S and 23S) with the genome of Candidatus *Saccharibacteria* bacterium GW2011_GWC2_44_17 (Brown et al., 2015), which belongs to the recently described phylum Saccharibacteria (Ferrari et al., 2014). Other taxa were also found belonging to the Prolixibacteraceae family or the *Microbacter* genus and to *Paludibacter*, *Desulfosporosinus*, *Brevundimonas,* and *Pelosinus* in A_3. Taxa related to members of *Desulfosporosinus*, *Paludibacter*, and *Pelosinus* were also detected in B_{mix} as well as *Erysipelothrix* and *Hydrogenophaga*. In contrast, about 97% of the $_{mi}$TAGs in E_{mix} were recruited by four full-length ribosomal operons assigned to *Hydrogenophaga* sp. (49%), *Microbacterium* sp. (36%), *Sphingopyxis* sp. (10%), and *Sphingomonas* sp. (1.2%) (**Figure 1** and **Table 3**).

A dozen different short (about 100 bp) fragments of 16S rDNA genes that showed identity >95% to various archaeal lineages (*Crenarchaeota*, *Euryarchaeota,* and *Thaumarchaeota*) were assembled from A_3 and E_{mix}. The corresponding reads originally accounted for about 7% of the raw 16S reads extracted from metagenomes A_3 and E_{mix}. The full-length 16S rDNA gene of Euryarchaeota *Candidatus Methanoplasma termitum* MpT1 (CP010070) was used as a reference to recruit the corresponding reads in A_3 (**Supplementary Figure 1**). Recruited reads do not homogeneously cover the reference gene, instead, all the reads match two overlapping segments of the reference 16S located between positions 850–957 and 891–1,000. Hence, no full-length 16S rDNA belonging to Archaea was detected in the metagenome and those fragments were considered artefacts and discarded from the rDNA pool used for community structure evaluation.

3.3. Metabolic profiling of the subglacial East Skaftárkatlar lake microbiome

The conservative co-assembly of A_3 and B_{mix} resulted in 64,905 contigs (assembly contiguity statistics: N50 = 5,182 bp, N90 = 377 bp) (**Table 2**). The online MetaGeneMark algorithm detected 124,531 ORFs in these contigs to which we assigned functions and analysed further. Using a 60% amino acid identity cut-off, we identified 58,203 ORFs (47%) having a significant hit against genes from the KEGG (Kanehisa et al., 2015). Those taxa that dominated the miTAGs analyses (*Acetobacterium*, *Sulfuricurvum*, *Sulfurospirillum*, and *Geobacter/Pelobacter)* also dominated these identified ORFs (**Figure 2**).

3.3.1. Carbon fixation

Nearly complete pathways for the reductive citric acid cycle and acetogenesis (Wood-Ljungdahl cycle), both allowing fixation of CO_2 or HCO_3^-, were identified (**Figure 2**). *Sulfuricurvum*, *Sulfurospirillum,* and *Geobacter/Pelobacter* taxa were found to have

TABLE 3 rDNA contig assembly results.

Complete taxonomy	Assignment	Copy number	16S identity	23S identity	5S identity	Origin
Bacteria; Epsilonproteobacteria; Campylobacterales; Helicobacteraceae; *Sulfuricurvum kujiense*	*Sulfuricurvum kujiense*	3	99%	97%	99%	N
Bacteria; Firmicutes; Clostridia; Clostridiales; Eubacteriaceae; *Acetobacterium woodii*	*Acetobacterium woodii*	5	n.d.	96%	99%	N
Bacteria; Deltaproteobacteria; Desulfuromonadales; Desulfuromonadaceae; *Geobacter* Bacteria; Deltaproteobacteria; Desulfuromonadales; Desulfuromonadaceae; *Pelobacter*	*Geobacter*/*Pelobacter* sp.	4	98%	96%	99%	N
Bacteria; Epsilonproteobacteria; Campylobacterales; Campylobacteraceae; *Sulfurospirillum*	*Sulfurospirillum* sp.	2	98%	98%	94%	N
Bacteria; Epsilonproteobacteria; Campylobacterales; Campylobacteraceae; *Sulfurospirillum*	*Sulfurospirillum* sp. TAX2	2	n.d.	97%	95%	N
Bacteria; unclassified Bacteria; Bacteria candidate phyla; Candidatus Saccharibacteria	Unclassified Saccharibacteria	1	99% (94%)	91%	96%	N
Bacteria; Caldiserica; Caldisericia; Caldisericales; Caldisericaceae; *Caldisericum*	*Caldisericum* sp.	1	96% (83%)	<78%	*No hit*	N
Bacteria; Bacteroidetes; Bacteroidia; Bacteroidales; Prolixibacteraceae	Unclassified Prolixibacteraceae	2	98% (89%)	85%	94%	N
Bacteria; Bacteroidetes; Bacteroidia; Bacteroidales; Porphyromonadaceae; *Microbacter*	*Microbacter* sp.	3	97% (95%)	88%	92%	N
Bacteria; Bacteroidetes; Bacteroidia; Bacteroidales; Paludibacteraceae; *Paludibacter*	*Paludibacter* sp.	3	99% (96%)	88%	98%	N
Bacteria; Firmicutes; Clostridia; Clostridiales; Peptococcaceae; *Desulfosporosinus*	*Desulfosporosinus* sp.	11	97%+5 var.	91%+2 var.	93%	N
Bacteria; Spirochaetes; Spirochaetia; Spirochaetales; Spirochaetaceae	Unclassified Spirochaetaceae	2	96%	83%	85%	N
Bacteria; Firmicutes; Erysipelotrichia; Erysipelotrichales; Erysipelotrichaceae; *Erysipelothrix*	*Erysipelothrix* sp.	5	99% (91%)	89%	88%	N
Bacteria; Firmicutes; Negativicutes; Selenomonadales; Sporomusaceae; *Pelosinus* sp.	*Pelosinus* sp. TAX1	12	95%	88%	85%	N
Bacteria; Firmicutes; Negativicutes; Selenomonadales; Sporomusaceae; *Pelosinus* sp.	*Pelosinus* sp. TAX2	12	98%	95%	93%	N
Bacteria; Betaproteobacteria; Burkholderiales; Comamonadaceae; *Hydrogenophaga*	*Hydrogenophaga* sp.	1	99%	99%	97%	E
Bacteria; Actinobacteria; Micrococcales; Microbacteriaceae; *Microbacterium*	*Microbacterium* sp.	2	100%	100%	100%	E
Bacteria; Alphaproteobacteria; Sphingomonadales; Sphingomonadaceae; *Sphingopyxis bauzanensis*	*Sphingopyxis bauzanensis*	1	99%	n.d.	n.d.	E
Bacteria; Alphaproteobacteria; Sphingomonadales; Sphingomonadaceae; *Sphingopyxis fribergensis*	*Sphingopyxis fribergensis*	1	99%	99%	100%	E
Bacteria; Alphaproteobacteria; Sphingomonadales; Sphingomonadaceae; *Sphingomonas*	*Sphingomonas* sp.	2	98%	94%	96%	E
Bacteria; Alphaproteobacteria; Sphingomonadales; Sphingomonadaceae	Unclassified Sphingomonadaceae	2	98%*	n.d.	n.d.	E
Bacteria; Actinobacteria; Micrococcales; Cellulomonadaceae; *Cellulomonas*	*Cellulomonas* sp.	2	98%	96%	97%	E
Bacteria; Alphaproteobacteria; Rhizobiales; Phyllobacteriaceae; *Aminobacter*	*Aminobacter* sp.	3	100%	100%	100%	E
Bacteria; Bacteroidetes; Bacteroidia; Sphingobacteriales; Sphingobacteriaceae; *Pedobacter*	*Pedobacter* sp.	1	99%	92%	99%	E
Bacteria; Alphaproteobacteria; Rhizobiales; Bradyrhizobiaceae; *Bosea*	*Bosea* sp.	2	99%	98%	100%	E
Bacteria; Alphaproteobacteria; Rhizobiales; Bradyrhizobiaceae; *Afipia*	*Afipia* sp.	1	96%	98%	100%	E
Bacteria; Alphaproteobacteria; Caulobacterales; Caulobacteraceae; *Brevundimonas*	*Brevundimonas* sp.	2	100%	96%	98%	E
Bacteria; Deltaproteobacteria; Desulfuromonadales; Desulfuromonadaceae; *Geobacter*	*Geobacter* sp.	2	95–97%	94%*	n.d.	E
Bacteria; Firmicutes; Bacilli; Bacillales; Staphylococcaceae; *Staphylococcus pasteuri*	*Staphylococcus pasteuri*	5	100%	99%	100%	C

Assignment and taxonomy are based on SILVA and/or NCBI's NT. Origin: N, natural sample A_3/B_{mix}; E, E_{mix}; C, contamination. Unless stated otherwise, the contigs fully cover the ribosomal gene. *Gene fragment, (xx%) best hit on a genome, when very different, n.d.: not detected. The number of copies of each operon was estimated from the closest relatives at rrndb.umms.med.umich.edu.

10.3389/fmicb.2023.1122184

10.3389/fmicb.2023.1122184

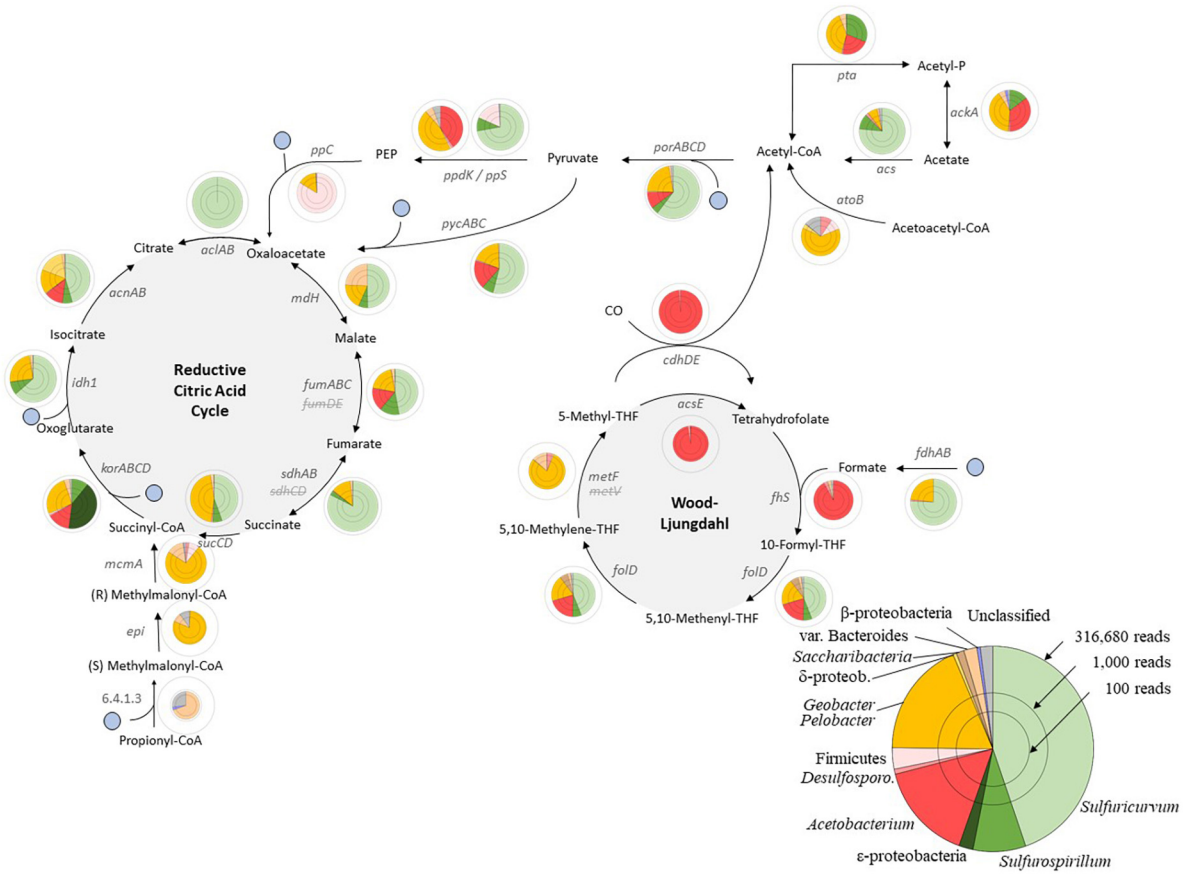

FIGURE 2
Carbon fixation in East Skaftárkatlar lake and global functional gene recruitment profile. Circular diagrams represent the abundance and taxonomic assignment of the associated reads, with the radius representing the log(nb of reads). CO_2/HCO_3^-.

most of the genes involved in the reductive citric acid cycle. The genes coding for subunits of fumarate hydratase (*fumD* and *fumE*) and succinate dehydrogenase (*sdhC* and *sdhD*) were not detected.

3.3.2. Sulphur metabolism

Complete pathways for assimilatory sulphate reduction and dissimilatory reduction of sulphur species were detected with notable taxonomic specificity (Figure 3B). The genes coding for sulphate adenylyltransferase (*sat*), adenylylsulphate reductase (*aprAB*), and dissimilatory sulphite reductase (*dsrABC*) were identified and belong mainly to *Desulfosporosinus* and *Acetobacterium*. These enzymes take sulphate to adenosine-5-phosphosulfate (APS), APS to sulphite, and sulphite to sulphide for dissimilatory reduction of sulphate. Thiosulfate might be oxidised to sulphate by *Sulfuricurvum via* the thiosulfate sulfurtransferase (TST).

This sequence of genes does not appear in *Sulfurospirillum* and instead the presence of a polysulphide reductase chain A *(phsA),* or a homologue of *phsA,* suggests that reduction of sulphur species for energy conservation only includes reduction of elemental sulphur or thiosulphate to sulphate in this taxon. Genes coding for assimilatory sulphate reduction such as sulphate adenylyltransferases subunits 1 and 2 (*cysDN)*, adenylylsulphate kinase (*cysC)*, phosphoadenosine phosphosulphate reductase (*cysH*), and sulphite reductase (ferredoxin) (*sir*) were indeed assigned preferentially to *Sulfurospirillum*.

Moreover, the main enzymes involved in sulphur-disproportionation were not detected in the co-assembly metagenome. In that pathway, thiosulphate, sulphite, or elemental sulphur can serve as both electron or acceptor donors and are converted into sulphate and hydrogen sulphide.

3.3.3. Nitrogen metabolism

Some of the genes involved in nitrogen metabolism were detected in the metagenome (Figure 3B). No taxon has a complete assimilatory nitrate reduction pathway. The genes coding for the ferredoxin-nitrate reductase (*narB*) and the catalytic subunit of the assimilatory nitrate reductase (*nasA*) were detected but not the genes coding for the NADPH nitrate reductase (NR) or the assimilatory nitrate reductase electron transfer (*nasB*). Likewise, the gene coding for the ferredoxin-nitrite reductase (*nirA*) was detected but not the gene coding for the assimilatory nitrite reductase (*nit*-6). The detected genes are mainly taxonomically related to *Sulfuricurvum*. Some of the genes involved in dissimilatory nitrate reduction were found: *napA* but not *napB* from the cluster of genes coding the NapAB protein and *narG*, *narH* but not *narI* from the

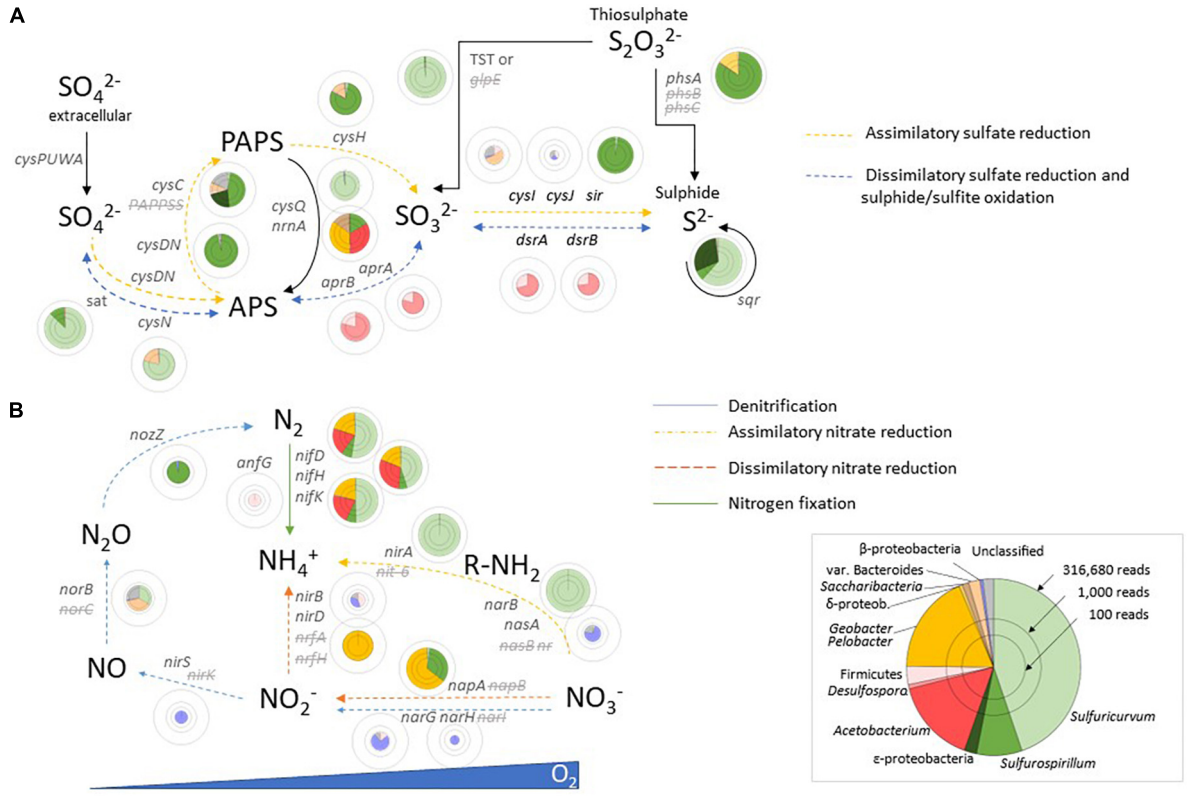

FIGURE 3
Sulphur metabolism **(A)** and nitrogen metabolism **(B)** in East Skaftárkatlar lake. APS, adenosine-5-phosphosulfate; PAPS, 3-phospho adenosine-5-phosphosulfate; PEP, phosphoenolpyruvate.

NarGHI cluster. Nitrite can then be reduced to ammonia with the nitrite reductase coded by the *nirB* and *nirD* genes found in our metagenomes. Genes involved in dissimilatory nitrate reduction seem to be related mainly to *Geobacter/Pedobacter*. Nitrogen fixation seems to be widespread in the Skaftárkatlar biome as all the genes coding for the dinitrogenase (*nifD*, *nifK*, *nifH*, and *anfG*), a molybdenum-iron protein reducing dinitrogen to ammonia, were detected, and were assigned to *Sulfurospirillum*, *Sulfuricurvum*, *Acetobacterium*, and *Geobacter/Pelobacter*.

3.3.4. Hydrogen

Potential utilisation of dihydrogen was investigated, revealing the presence of genes coding for the quinone-reactive Ni/Fe-hydrogenase small (*hydA*) and large subunit (*hydB*) and assigned to *Sulfuricurvum* and *Sulfurospirillum*. The genes coding for the different NADP-reducing hydrogenase subunits (*hndB, hndC*, and *hndD*) were identified to belong to *Acetobacterium*. The presence of these genes supports the use of H_2 as an electron donor in these taxa.

3.3.5. Other metabolisms

Gene coding for arsenate reductase with disulphide as an acceptor was found (*arsC*) and assigned to *Sulfuricurvum* and *Sulfurospirillum*. Sulphide oxidation can be tied to the reduction of arsenate to arsenide by arsenate respiration. This ability was described for *Sulfurospirillum* (Stolz et al., 1999). Genes involved in anaerobic fumaric respiration such as fumarate reductase, flavoprotein subunit (*frdA*), and iron-sulphur subunit (*fdrB*) were identified and assigned to *Sulfuricurvum*, *Sulfurospirillum,* and *Geobacter/Pelobacter*. Only the *cooS* gene from the gene cluster coding for enzymes allowing anaerobic carboxydotrophy was detected and affiliated to *Acetobacterium*. Genes coding for enzymes involved in the dissimilatory reduction of Fe^{3+} were not detected.

4. Discussion

This study presents the first analysis of metagenomes originating from volcanic subglacial lake: one sample collected from the bottom of the lake (A_3), a second from four pooled water column samples collected from different depths in the lake (B_{mix}), and a third from combined enrichments, i.e., growth under conditions that attempted to mimic those in the subglacial lake (E_{mix}). The metagenomic analysis of the collected samples enabled a reconstruction of the potential metabolic pathways existing in the lake and a more robust description of the microbial community structure than before. Environmental metagenome analysis such as these have been shown to be more quantitative for microbial community studies, compared to amplicon-tag-based studies, due

to the absence of Polymerase Chain Reaction (PCR) amplification bias (Parada et al., 2016; Brumfield et al., 2020).

This study not only confirms a previous study of the lake using 16S rRNA tag sequencing and Fluorescence *In Situ* Hybridisation (FISH) (Marteinsson et al., 2013) but also provides more robust evidence that only a few bacterial taxa dominate the microbial community in the lake water column (*Sulfuricurvum*, *Acetobacterium*, *Geobacter*/*Pelobacter,* and *Sulfurospirillum*). Metagenomic analyses in this study also confirm the presence of lower abundance taxa (e.g., *Caldisericum* and *Desulfosporosinus*) and reveal new additional lineages (*Saccharibacteria* and *Pelosinus)* which had not been observed by the previous amplicon-based studies. The relatively low microbial diversity (∼20 taxa) represented in the metagenome of this ecosystem resulted in high sampling depth and allowed assemblage of full-length 16S, 23S, and often also 5S sequences for most of the taxa. Full-length sequences permitted a more precise taxonomic assignment of the most abundant community members as well as 14 minor taxa with relative abundance ranging from 0.05 to 1%. Many of these taxa are closely related to psychrotolerant strains, including a member of *Brevundimonas*, a taxon detected in the Arctic (Trivedi et al., 2018) and Antarctic (González-Toril et al., 2009) and which is known to be resistant to cold temperatures (Dartnell et al., 2010) and the genus *Pedobacter,* also found in Arctic environments (Zhou et al., 2012; Peter and Sommaruga, 2016; Trivedi et al., 2018).

In a broader context, this study has confirmed previous results (Marteinsson et al., 2013) that the community in the East Skaftárkatlar lake is substantially different from that of other subglacial lakes such as Subglacial Lake Whillans in Antarctica. The former is dominated by Betaproteobacteria such as *Polaromonas*, *Sideroxydans* or *Thiobacillus*, Bacteroidetes, and Actinobacteria (Achberger et al., 2016) while the East Skaftárkatlar lake is dominated by Epsilonbacteria: *Sulfuricurvum* and *Sulfurospirillum,* and Firmicutes: *Acetobacterium*. East Skaftárkatlar could be significantly influenced by hydrothermal activity emanating from the underlying lake bed and thus can host, among others, sulphur oxidisers or reducers (Johannesson et al., 2007). Furthermore, the lake is a mix of glacial melt (containing oxygen) as well as sulphide from disproportionation of dissolved volcanic SO_2 that supports a sulphur cycle. Then, *Sulfurospirillum deleyianum* is known to be able to oxidise sulphide with nitrate, producing ammonium and intracellular elemental sulphur (Eisenmann et al., 1995). This ability is also known in *Sulfuricurvum* species, the most abundant member of the microbial community in the sample collected at the bottom of the lake 75% (A_3) compared to 30% in the water column samples (B_{mix}). The relative abundance of *Sulfuricurvum* correlates with the sulphate concentration, which was about five times higher in A_3 than in the other pooled sample B_{mix} (4.71 ppm in A_3 *vs.* from 0.29 to 1.43 ppm in B_1 to B_4, **Supplementary Table 1**). Compared to A_3, a higher diversity was observed in B_{mix} (Shannon's α-diversity of 1.18 and 1.83, respectively, data not shown) including three additional taxa: Peptococcaceae, Bacteroidetes, and *Caldisericum* spp. which might indicate that growth and metabolism are faster than the mixing time of the water column across any vertical or lateral chemical gradients in the lake. The higher diversity could also be a result of the fact that B_{mix} is derived from a mixture of samples.

Despite many different enrichment conditions, none of the dominant taxa found in the water column samples were enriched under the conditions of our incubations. The absence of culturable members of the main diversity is not unexpected as uncultivated phyla frequently dominate diverse environments (Lloyd et al., 2018). Interestingly, the dominant taxa found in E_{mix}, *Microbacterium*, *Hydrogenophaga,* and *Sphingopyxis* were only marginally detectable in the metagenome (<10 raw rDNA reads) of the two environmental samples A_3 and B_{mix} (**Figure 1**) and not detected in the rRNA tag sequences of Marteinsson et al. (2013).

Remarkably, no evidence of members of Archaea in the lake was detected in the previous 16S rRNA amplicon-tag sequencing study (Marteinsson et al., 2013). This includes all known chemolithotrophic methanogens, which could potentially compete with homoacetogens for H_2. In this metagenome sequencing-based study, which is not affected by PCR bias, we identified a significant number of archaea-like sequences in A_3 (data not shown). Nevertheless, a detailed analysis of those reads shows that they are not randomly distributed over a complete reference archaeal 16S rDNA gene (**Supplementary Figure 1**) and are instead localised to two overlapping regions. The absence of flanking sequence to these clusters and their exclusive location indicates that those reads do not originate from a complete gene. Therefore, we are not able to detect the presence of archaea in the lake with our metagenomic approach. The DNA extraction method used might also be a bias with an incomplete lysis of recalcitrant archaeal cells as it was noted in previous subsurface communities (Webster et al., 2003).

Since light is absent in the lake, chemoautotrophy must be responsible for the microbial growth as primary producers such as in subglacial lakes Vostok or Whillans (Rogers et al., 2013; Vick-Majors et al., 2016). The metabolic pathways detected in a combination of A_3 and B_{mix} for carbon fixation are shown in **Figure 2**. *Acetobacterium* sp. contains most of the genes involved in the Wood–Ljungdahl homoacetogenesis pathway. This pathway uses H_2 as an electron donor and CO_2 both as an electron acceptor and carbon source to generate acetyl-CoA. Acetogenesis seems to be an important energy source in this ecosystem and supports the previous findings that the lakes contain taxon with homoacetogens as the closest relatives (Gaidos et al., 2004, 2009; Marteinsson et al., 2013). The closest cultured relative to *Acetobacterium* is *Acetobacterium woodii*, a strain using the Wood–Ljungdahl (reverse acetyl-CoA) pathway and H_2 to fix CO_2 into acetate and maintain a sodium ion gradient for ATP synthesis (Poehlein et al., 2012). Prokaryotes living close to the thermodynamic limit, like methanogens and acetogens, use the reductive acetyl-coA pathway for both CO_2 fixation and energy conservation (Ragsdale and Pierce, 2008; Thauer et al., 2008). We propose that environmental factors such as low temperature and high H_2 concentration in this ecosystem favour acetogens over methanogens (Nozhevnikova et al., 1994). The absence of methanogens in this unique ecosystem could also potentially be explained by the presence of bacteria such as Sulphate Reducing Bacteria (SRB) that out-compete methanogens for hydrogen or produced acetate in the lake, with lower K_s values for H_2 and acetate (Kristjansson et al., 1982; Schönheit et al., 1982).

Complete pathways for assimilatory sulphur reduction into sulphide were detected and mainly assigned to *Sulfurospirillum* sp. whereas the dissimilatory reduction of sulphur in sulphide was assigned mainly to *Acetobacterium* sp. (**Figure 3A**). This

difference might be the result of *Sulfurospirillum* only performing assimilatory sulphate reduction (i.e., to produce organosulphur compounds) and *Acetobacterium* the dissimilatory one to conserve energy. *Sulfuricurvum* was described as a sulphur oxidiser (Han et al., 2012) and not as a sulphate reducer which can explain why assimilatory genes were mainly assigned to *Sulfurospirillum*. Moreover, the reason why *Sulfurospirillum* has *phsA* gene and not standard dissimilatory genes might be explained by the low sulphate concentration in the lake making sulphate reduction difficult. Sulphide production might be energetically unfavourable against the background of high sulphide in the lake (around 1 mM). Thus sulphur-cycling species might take sulphur only to sulphite and then cycle it back to sulphate or sulphur under microaerobic conditions. *Sulfuricurvum* sp. and *Sulfurospirillum* sp. also play a role in activating sulphur with a polysulphide reductase. These results emphasise the central role of sulphur species as sources of electrons (S^{2-}, SO_4^{2-}, and $S_2O_3^{2-}$) for chemolithoautotrophy in the lake and, as expected, in the metabolism of amino acids. Respiratory sulphate reduction is a common process in environments with a high sulphate concentration whereas in sulphate-depleted anoxic environments, acetogenesis is favoured over sulphate reduction (Laanbroek et al., 1982; Muyzer and Stams, 2008; Stams and Plugge, 2009).

No complete nitrogen metabolic pathways were found in the co-assembly metagenome except for nitrogen fixation. The genes involved in the nitrogen fixation pathway were detected and belong mainly to *Sulfuricurvum* sp. The genus *Sulfuricurvum* sp. has not been reported as being diazotrophic but its sequenced representative *Sulfuricurvum kujiense* YK-1^T also possesses the necessary genes (Kodama and Watanabe, 2004; Han et al., 2012). The dissimilatory nitrate reduction to ammonium, which is an important reaction of the reductive branch of the nitrogen cycle (Simon and Klotz, 2013), is mainly taxonomically affiliated with *Geobacter/Pedobacter* genus. Whereas nitrification is an important chemoautotrophic pathway of new organic carbon production in Subglacial Lake Whillans (Christner et al., 2014), none of the genes involved in this pathway were found in our metagenomes. The presence of *nir* (NADH-dependent) but absence of *nrf* (periplasmic) genes might imply that assimilatory reduction but not respiratory reduction (for energy conservation) might be occurring in this oligotrophic environment.

The study of microbial communities inhabiting subglacial lakes is of importance as such ecosystems remain underexplored. Only four subglacial lakes were sampled for microbial analyses at the time this paper was written (Gaidos et al., 2004, 2009; Christner et al., 2014; Priscu et al., 2021). The results in our research support the former hypothesis that was based on a taxonomy study, but it also gives insight into the metabolic pathways. The ecosystem in this subglacial lake appears to have a chemolithoautotrophic foundation with sulphur and carbon cycling that is fuelled by H_2, CO_2, and sulphur species originating from the geothermal activity and by O_2 from melted ice. By identifying the potential metabolic pathways to specific taxa in the microbial assemblage, we have gained insight into the ecology of microbiomes in the water column of such an extreme environment. However, we should assume that other ecological niches may exist, e.g., on the bottom of the lake, in the lake sediments, or at the ice/lake interface, and these remain undiscovered. Moreover, nearly half of the sequence reads in our metagenomic library were not assigned and are a source for future advances. Also, new targeted sampling with larger volume is needed e.g., samples collected close to potential geothermal vents at the bottom of the lake might reveal thermophiles belonging to both the Bacteria and Archaea by sequencing and cultivation strategies. Even if analysed samples were collected in 2007, the results of this study might still correlate with the current situation of the lake as the latter has experienced similar conditions and has undergone continuous filling and draining (called jökulhlaup) since records have been kept.

Finally, due to recent Arctic warming, ice caps are thinning, notably in Iceland (Gudmundsson et al., 2008). Despite their isolation from the surface, these lakes are influenced by the dynamics and melting of glaciers, which are changing with climate change (Livingstone et al., 2022). The existence of subglacial lakes is thus threatened in the long run. The complete exploration of the microbial diversity of this ecosystem needs to happen quickly to monitor such future changes.

Data availability statement

The data presented in this study are deposited in NCBI Sequences Read Archive repository under the accession number: SRP011365 (https://www.ncbi.nlm.nih.gov/sra/?term=SRP011365).

Author contributions

PV, GF, and VM conceived and designed the study and analysed the data. AK performed the DNA extractions. GF performed the bioinformatic analyses. PV, GF, EG, and VM wrote the main manuscript text. All authors reviewed the manuscript.

Funding

This project had received funding from the European Union's Horizon 2020 Research and Innovation Programme under the Marie Skłodowska-Curie actions grant agreement no. 704956. Sampling expeditions and sample analysis were provided by the Icelandic Centre for Research (Contract No. 080222023). Partial support for fieldwork was provided by the National Aeronautics and Space Administration through the NASA Astrobiology Institute under Cooperative Agreement No. NNA04CC08A issued through the Office of Space Science.

Acknowledgments

We would like to thank the Meteorological Office of Iceland (Veðurstofa Íslands) for realising the original and later collections of samples. The Illumina sequencings were made possible by the Deep Carbon Observatory's Census of Deep Life supported by the Alfred P. Sloan Foundation. Sequencing was performed at the Marine Biological Laboratory (Woods Hole, MA, United States) and we are grateful for the assistance of Mitch Sogin, Susan Huse, Joseph Vineis, Andrew Voorhis, Sharon Grim, and Hilary Morrison at MBL.

Conflict of interest

The authors declare that the research was conducted in the absence of any commercial or financial relationships that could be construed as a potential conflict of interest.

Publisher's note

All claims expressed in this article are solely those of the authors and do not necessarily represent those of their affiliated organizations, or those of the publisher, the editors and the reviewers. Any product that may be evaluated in this article, or claim that may be made by its manufacturer, is not guaranteed or endorsed by the publisher.

Supplementary material

The Supplementary Material for this article can be found online at: https://www.frontiersin.org/articles/10.3389/fmicb.2023.1122184/full#supplementary-material

References

Achberger, A. M., Christner, B. C., Michaud, A. B., Priscu, J. C., Skidmore, M. L., Vick-Majors, T. J., et al. (2016). Microbial community structure of subglacial lake whillans. West Antarctica. *Front. Microbiol.* 7:1457. doi: 10.3389/fmicb.2016.01457

Agustsdottir, A. M., and Brantley, S. L. (1994). Volatile fluxes integrated over 4 decades at Grímsvötn volcano, Iceland. *J. Geophys. Research-Solid Earth* 99, 9505–9522. doi: 10.1029/93JB03597

Alneberg, J., Bjarnason, B. S., De Bruijn, I., Schirmer, M., Quick, J., Ijaz, U. Z., et al. (2014). Binning metagenomic contigs by coverage and composition. *Nat. Methods* 11, 1144–1146. doi: 10.1038/nmeth.3103

Balch, W. E., Fox, G. E., Magrum, L. J., Woese, C. R., and Wolfe, R. S. (1979). Methanogens: re-evaluation of a unique biological group. *Microbiol. Rev.* 43, 260–296. doi: 10.1128/mr.43.2.260-296.1979

Bankevich, A., Nurk, S., Antipov, D., Gurevich, A. A., Dvorkin, M., Kulikov, A. S., et al. (2012). SPAdes: a new genome assembly algorithm and its applications to single-cell sequencing. *J. Comp. Biol.* 19, 455–477. doi: 10.1089/cmb.2012.0021

Bjornsson, H. (2003). Subglacial lakes and jokulhlaups in Iceland. *Global Plan. Change* 35, 255–271. doi: 10.1016/S0921-8181(02)00130-3

Brown, C. T., Hug, L. A., Thomas, B. C., Sharon, I., Castelle, C. J., Singh, A., et al. (2015). Unusual biology across a group comprising more than 15% of domain Bacteria. *Nature* 523:208. doi: 10.1038/nature14486

Brumfield, K. D., Huq, A., Colwell, R. R., Olds, J. L., and Leddy, M. B. (2020). Microbial resolution of whole genome shotgun and 16S amplicon metagenomic sequencing using publicly available NEON data. *PLoS One* 15:e0228899. doi: 10.1371/journal.pone.0228899

Buchfink, B., Xie, C., and Huson, D. H. (2015). Fast and sensitive protein alignment using DIAMOND. *Nat. Methods* 12:59. doi: 10.1038/nmeth.3176

Bulat, S. A. (2016). Microbiology of the subglacial Lake Vostok: first results of borehole-frozen lake water analysis and prospects for searching for lake inhabitants. *Philos. Trans. R. Soc. Mathematical Phys. Eng. Sci.* 374:20140292. doi: 10.1098/rsta.2014.0292

Camacho, C., Coulouris, G., Avagyan, V., Ma, N., Papadopoulos, J., Bealer, K., et al. (2009). BLAST+: architecture and applications. *BMC Bioinformatics* 10:421. doi: 10.1186/1471-2105-10-421

Chinn, T. (1993). Physical hydrology of the dry valley lakes. *Phys. Biogeochem. Proc. Antarctic Lakes* 59, 1–51. doi: 10.1029/AR059p0001

Christner, B. C., Mosley-Thompson, E., Thompson, L. G., and Reeve, J. N. (2001). Isolation of bacteria and 16S rDNAs from Lake Vostok accretion ice. *Environ. Microbiol.* 3, 570–577. doi: 10.1046/j.1462-2920.2001.00226.x

Christner, B. C., Priscu, J. C., Achberger, A. M., Barbante, C., Carter, S. P., Christianson, K., et al. (2014). A microbial ecosystem beneath the West Antarctic ice sheet. *Nature* 512, 310–313. doi: 10.1038/nature13667

Dartnell, L. R., Hunter, S. J., Lovell, K. V., Coates, A. J., and Ward, J. M. (2010). Low-temperature ionizing radiation resistance of *Deinococcus radiodurans* and Antarctic Dry Valley bacteria. *Astrobiology* 10, 717–732. doi: 10.1089/ast.2009.0439

Davies, B. J., Hambrey, M. J., Glasser, N. F., Holt, T., Rodés, A., Smellie, J. L., et al. (2017). Ice-dammed lateral lake and epishelf lake insights into Holocene dynamics of marguerite trough ice stream and george VI Ice Shelf, Alexander Island, Antarctic Peninsula. *Quaternary Sci. Rev.* 177, 189–219. doi: 10.1016/j.quascirev.2017.10.016

Degryse, E., Glansdorff, N., and Pierard, A. (1978). Comparative analysis of extreme thermophilic bacteria belonging to genus Thermus. *Arch. Microbiol.* 117, 189–196. doi: 10.1007/BF00402307

Eisenmann, E., Beuerle, J., Sulger, K., Kroneck, P. M., and Schumacher, W. (1995). Lithotrophic growth of *Sulfurospirillum deleyianum* with sulfide as electron donor coupled to respiratory reduction of nitrate to ammonia. *Arch. Microbiol.* 164, 180–185. doi: 10.1007/BF02529969

Ferrari, B., Winsley, T., Ji, M., and Neilan, B. (2014). Insights into the distribution and abundance of the ubiquitous candidatus Saccharibacteria phylum following tag pyrosequencing. *Sci. Rep.* 4:3957. doi: 10.1038/srep03957

Gaidos, E., Lanoil, B., Thorsteinsson, T., Graham, A., Skidmore, M., Han, S. K., et al. (2004). A viable microbial community in a subglacial volcanic crater lake. Iceland. *Astrobiology* 4, 327–344. doi: 10.1089/ast.2004.4.327

Gaidos, E., Marteinsson, V., Thorsteinsson, T., Johannesson, T., Runarsson, A. R., Stefansson, A., et al. (2009). An oligarchic microbial assemblage in the anoxic bottom waters of a volcanic subglacial lake. *ISME J.* 3, 486–497. doi: 10.1038/ismej.2008.124

González-Toril, E., Amils, R., Delmas, R. J., Petit, J.-R., Komárek, J., and Elster, J. (2009). Bacterial diversity of autotrophic enriched cultures from remote, glacial Antarctic, Alpine and Andean aerosol, snow and soil samples. *Biogeosciences* 6, 33–44. doi: 10.5194/bg-6-33-2009

Gudmundsson, M. T., Larsen, G., Höskuldsson, Á, and Gylfason, ÁG. (2008). Volcanic hazards in Iceland. *Jokull* 58, 251–268. doi: 10.33799/jokull2008.58.251

Gura, C., and Rogers, S. O. (2020). Metatranscriptomic and metagenomic analysis of biological diversity in subglacial lake vostok (Antarctica). *Biology* 9:55. doi: 10.3390/biology9030055

Han, C., Kotsyurbenko, O., Chertkov, O., Held, B., Lapidus, A., Nolan, M., et al. (2012). Complete genome sequence of the sulfur compounds oxidizing chemolithoautotroph *Sulfuricurvum kujiense* type strain (YK-1 T). *Standards Genomic Sci.* 6:94. doi: 10.4056/sigs.2456004

Howard-Williams, C., Schwarz, A.-M., Hawes, I., and Priscu, J. (1998). Optical properties of the McMurdo Dry Valley lakes. *Antarctic Res. Ser.* 72, 189–203. doi: 10.1029/AR072p0189

Huang, Y., Gilna, P., and Li, W. (2009). Identification of ribosomal RNA genes in metagenomic fragments. *Bioinformatics* 25, 1338–1340. doi: 10.1093/bioinformatics/btp161

Johannesson, T., Thorsteinsson, T., Stefansson, A., Gaidos, E. J., and Einarsson, B. (2007). Circulation and thermodynamics in a subglacial geothermal lake under the Western Skafta cauldron of the Vatnajokull ice cap, Iceland. *Geophys. Res. Lett.* 34, 502–508. doi: 10.1029/2007GL030686

Kanehisa, M., and Goto, S. (2000). KEGG: kyoto encyclopedia of genes and genomes. *Nucleic Acids Res.* 28, 27–30. doi: 10.1093/nar/28.1.27

Kanehisa, M., Sato, Y., Kawashima, M., Furumichi, M., and Tanabe, M. (2015). KEGG as a reference resource for gene and protein annotation. *Nucleic Acids Res.* 44, D457–D462. doi: 10.1093/nar/gkv1070

Karl, D., Bird, D., Björkman, K., Houlihan, T., Shackelford, R., and Tupas, L. (1999). Microorganisms in the accreted ice of Lake Vostok, Antarctica. *Science* 286, 2144–2147. doi: 10.1126/science.286.5447.2144

Kirschvink, J. L., Gaidos, E. J., Bertani, L. E., Beukes, N. J., Gutzmer, J., Maepa, L. N., et al. (2000). Paleoproterozoic snowball Earth: extreme climatic and geochemical global change and its biological consequences. *Proc. Natl. Acad. Sci. U S A.* 97, 1400–1405. doi: 10.1073/pnas.97.4.1400

Kivelson, M. G., Khurana, K. K., Russell, C. T., Volwerk, M., Walker, R. J., and Zimmer, C. (2000). Galileo magnetometer measurements: a stronger case for a subsurface ocean at Europa. *Science* 289, 1340–1343. doi: 10.1126/science.289.5483.1340

Kivelson, M. G., Khurana, K. K., and Volwerk, M. (2002). The permanent and inductive magnetic moments of ganymede. *Icarus* 157, 507–522. doi: 10.1006/icar.2002.6834

Kodama, Y., and Watanabe, K. (2004). *Sulfuricurvum kujiense* gen. nov., sp nov., a facultatively anaerobic, chemolithoautotrophic, sulfur-oxidizing bacterium isolated from an underground crude-oil storage cavity. *Int. J. Systematic Evol. Microbiol.* 54, 2297–2300. doi: 10.1099/ijs.0.63243-0

Kristjansson, J. K., Schönheit, P., and Thauer, R. K. (1982). Different K s values for hydrogen of methanogenic bacteria and sulfate reducing bacteria: an explanation for the apparent inhibition of methanogenesis by sulfate. *Arch. Microbiol.* 131, 278–282. doi: 10.1007/BF00405893

Laanbroek, H. J., Abee, T., and Voogd, I. L. (1982). Alcohol conversion by *Desulfobulbus propionicus* Lindhorst in the presence and absence of sulfate and hydrogen. *Arch. Microbiol.* 133, 178–184. doi: 10.1007/BF00414998

Lauro, S. E., Pettinelli, E., Caprarelli, G., Guallini, L., Rossi, A. P., Mattei, E., et al. (2020). Multiple subglacial water bodies below the south pole of Mars unveiled by new MARSIS data. *Nat. Astronomy* 5, 63–70. doi: 10.1038/s41550-020-1200-6

Livingstone, S. J., Li, Y., Rutishauser, A., Sanderson, R. J., Winter, K., Mikucki, J. A., et al. (2022). Subglacial lakes and their changing role in a warming climate. *Nat. Rev. Earth Environ.* 3, 106–124. doi: 10.1038/s43017-021-00246-9

Lloyd, K. G., Steen, A. D., Ladau, J., Yin, J., and Crosby, L. (2018). Phylogenetically novel uncultured microbial cells dominate earth microbiomes. *mSystems* 3:e00055-18. doi: 10.1128/mSystems.00055-18

Logares, R., Sunagawa, S., Salazar, G., Cornejo-Castillo, F. M., Ferrera, I., Sarmento, H., et al. (2014). Metagenomic 16S rDNA I llumina tags are a powerful alternative to amplicon sequencing to explore diversity and structure of microbial communities. *Environ. Microbiol.* 16, 2659–2671. doi: 10.1111/1462-2920.12250

Magoč, T., and Salzberg, S. L. (2011). FLASH: fast length adjustment of short reads to improve genome assemblies. *Bioinformatics* 27, 2957–2963. doi: 10.1093/bioinformatics/btr507

Marteinsson, V. T., Birrien, J. L., and Prieur, D. (1997). In situ enrichment and isolation of thermophilic microorganisms from deep-sea vent environments. *Canadian J. Microbiol.* 43, 694–697. doi: 10.1139/m97-100

Marteinsson, V. T., Kristjansson, J. K., Kristmannsdottir, H., Dahlkvist, M., Saemundsson, K., Hannington, M., et al. (2001). Discovery and description of giant submarine smectite cones on the seafloor in Eyjafjordur, northern Iceland, and a novel thermal microbial habitat. *Appl. Environ. Microbiol.* 67, 827–833. doi: 10.1128/AEM.67.2.827-833.2001

Marteinsson, V. T., Runarsson, A., Stefansson, A., Thorsteinsson, T., Johannesson, T., Magnusson, S. H., et al. (2013). Microbial communities in the subglacial waters of the Vatnajokull ice cap. Iceland. *ISME J.* 7, 427–437. doi: 10.1038/ismej.2012.97

Mori, K., Yamaguchi, K., Sakiyama, Y., Urabe, T., and Suzuki, K.-I. (2009). Caldisericum exile gen. nov., sp. nov., an anaerobic, thermophilic, filamentous bacterium of a novel bacterial phylum, *Caldiserica phyl*. nov., originally called the candidate phylum OP5, and description of *Caldisericaceae fam*. nov., *Caldisericales ord*. nov. and *Caldisericia classis* nov. *Int. J. Systematic Evol. Microbiol.* 59, 2894–2898. doi: 10.1099/ijs.0.010033-0

Muyzer, G., and Stams, A. J. M. (2008). The ecology and biotechnology of sulphate-reducing bacteria. *Nat. Rev. Microbiol.* 6, 441–454. doi: 10.1038/nrmicro1892

Nozhevnikova, A. N., Kotsyurbenko, O. R., and Simankova, M. V. (1994). "Acetogenesis at low temperature," in *Acetogenesis. Chapman & Hall Microbiology Series*, ed. H. L. Drake (Boston, MA: Springer), 416–431. doi: 10.1007/978-1-4615-1777-1_15

Palmer, S. J., Dowdeswell, J. A., Christoffersen, P., Young, D. A., Blankenship, D. D., Greenbaum, J. S., et al. (2013). Greenland subglacial lakes detected by radar. *Geophys. Res. Lett.* 40, 6154–6159. doi: 10.1002/2013GL058383

Parada, A. E., Needham, D. M., and Fuhrman, J. A. (2016). Every base matters: assessing small subunit rRNA primers for marine microbiomes with mock communities, time series and global field samples. *Environ. Microbiol.* 18, 1403–1414. doi: 10.1111/1462-2920.13023

Peng, Y., Leung, H. C., Yiu, S.-M., and Chin, F. Y. (2012). IDBA-UD: a de novo assembler for single-cell and metagenomic sequencing data with highly uneven depth. *Bioinformatics* 28, 1420–1428. doi: 10.1093/bioinformatics/bts174

Peter, H., and Sommaruga, R. (2016). Shifts in diversity and function of lake bacterial communities upon glacier retreat. *ISME J.* 10:1545. doi: 10.1038/ismej.2015.245

Poehlein, A., Schmidt, S., Kaster, A.-K., Goenrich, M., Vollmers, J., Thürmer, A., et al. (2012). An ancient pathway combining carbon dioxide fixation with the generation and utilization of a sodium ion gradient for ATP synthesis. *PLoS One* 7:e33439. doi: 10.1371/journal.pone.0033439

Priscu, J. C., Adams, E. E., Lyons, W. B., Voytek, M. A., Mogk, D. W., Brown, R. L., et al. (1999). Geomicrobiology of subglacial ice above Lake Vostok. Antarctica. *Science* 286, 2141–2144. doi: 10.1126/science.286.5447.2141

Priscu, J. C., Kalin, J., Winans, J., Campbell, T., Siegfried, M. R., Skidmore, M., et al. (2021). Scientific access into Mercer Subglacial Lake: scientific objectives, drilling operations and initial observations. *Ann. Glaciol.* 62, 340–352. doi: 10.1017/aog.2021.10

Quast, C., Pruesse, E., Yilmaz, P., Gerken, J., Schweer, T., Yarza, P., et al. (2012). The SILVA ribosomal RNA gene database project: improved data processing and web-based tools. *Nucleic Acids Res.* 41, D590–D596. doi: 10.1093/nar/gks1219

Ragsdale, S. W., and Pierce, E. (2008). Acetogenesis and the Wood–Ljungdahl pathway of CO2 fixation. *Biochim. Biophys. Acta (BBA)-Proteins Proteom.* 1784, 1873–1898. doi: 10.1016/j.bbapap.2008.08.012

Reasoner, D. J., and Geldreich, E. E. (1985). A new medium for the enumeration and subculture of bacteria from potable water. *Appl. Environ. Microbiol.* 49, 1–7. doi: 10.1128/aem.49.1.1-7.1985

Rogers, S., Shtarkman, Y., Koçer, Z., Edgar, R., Veerapaneni, R., and Elia, T. (2013). Ecology of subglacial lake vostok (Antarctica), based on metagenomic/metatranscriptomic analyses of accretion ice. *Biology* 2, 629. doi: 10.3390/biology2020629

Rutishauser, A., Blankenship, D. D., Sharp, M., Skidmore, M. L., Greenbaum, J. S., Grima, C., et al. (2018). Discovery of a hypersaline subglacial lake complex beneath Devon Ice Cap, Canadian Arctic. *Sci. Adv.* 4:eaar4353. doi: 10.1126/sciadv.aar4353

Schönheit, P., Kristjansson, J. K., and Thauer, R. K. (1982). Kinetic mechanism for the ability of sulfate reducers to out-compete methanogens for acetate. *Arch. Microbiol.* 132, 285–288. doi: 10.1007/BF00407967

Simon, J., and Klotz, M. G. (2013). Diversity and evolution of bioenergetic systems involved in microbial nitrogen compound transformations. *Biochim. Biophys. Acta (BBA)-Bioenergetics* 1827, 114–135. doi: 10.1016/j.bbabio.2012.07.005

Stams, A. J., and Plugge, C. M. (2009). Electron transfer in syntrophic communities of anaerobic bacteria and archaea. *Nat. Rev. Microbiol.* 7, 568–577. doi: 10.1038/nrmicro2166

Stoddard, S. F., Smith, B. J., Hein, R., Roller, B. R., and Schmidt, T. M. (2014). rrnDB: improved tools for interpreting rRNA gene abundance in bacteria and archaea and a new foundation for future development. *Nucleic Acids Res.* 43, D593–D598. doi: 10.1093/nar/gku1201

Stolz, J. F., Ellis, D. J., Blum, J. S., Ahmann, D., Lovley, D. R., and Oremland, R. S. (1999). *Sulfurospirillum barnesii* sp nov and *Sulfurospirillum arsenophilum* sp nov., new members of the *Sulfurospirillum clade* of the epsilon Proteobacteria. *Int. J. Systematic Bacteriol.* 49, 1177–1180. doi: 10.1099/00207713-49-3-1177

Thauer, R. K., Kaster, A.-K., Seedorf, H., Buckel, W., and Hedderich, R. (2008). Methanogenic archaea: ecologically relevant differences in energy conservation. *Nat. Rev. Microbiol.* 6, 579–591. doi: 10.1038/nrmicro1931

Thomas, P. C., Tajeddine, R., Tiscareno, M. S., Burns, J. A., Joseph, J., Loredo, T. J., et al. (2016). Enceladus's measured physical libration requires a global subsurface ocean. *Icarus* 264, 37–47. doi: 10.1016/j.icarus.2015.08.037

Thorsteinsson, T., Elefsen, S. O., Gaidos, E., Lanoil, B., Johannesson, T., Kjartansson, V., et al. (2008). A hot water drill with built-in sterilization: design, testing and performance. *Jokull* 51, 71–82. doi: 10.33799/jokull2007.57.071o

Trivedi, C. B., Lau, G. E., Grasby, S. E., Templeton, A. S., and Spear, J. R. (2018). Low-temperature sulfidic-ice microbial communities, borup fiord pass, Canadian high Arctic. *Front. Microbiol.* 9:1622. doi: 10.3389/fmicb.2018.01622

Tulaczyk, S., Mikucki, J. A., Siegfried, M. R., Priscu, J. C., Barcheck, C. G., Beem, L. H., et al. (2014). WISSARD at Subglacial Lake Whillans, West Antarctica: scientific operations and initial observations. *Ann. Glaciol.* 55, 51–58. doi: 10.3189/2014AoG65A009

Vick-Majors, T. J., Mitchell, A. C., Achberger, A. M., Christner, B. C., Dore, J. E., Michaud, A. B., et al. (2016). Physiological ecology of microorganisms in subglacial lake whillans. *Front. Microbiol.* 7:1705. doi: 10.3389/fmicb.2016.01705

Wang, Q., Garrity, G. M., Tiedje, J. M., and Cole, J. R. (2007). Naive Bayesian classifier for rapid assignment of rRNA sequences into the new bacterial taxonomy. *Appl. Environ. Microbiol.* 73, 5261–5267. doi: 10.1128/AEM.00062-07

Webster, G., Newberry, C. J., Fry, J. C., and Weightman, A. J. (2003). Assessment of bacterial community structure in the deep sub-seafloor biosphere by 16S rDNA-based techniques: a cautionary tale. *J. Microbiol. Methods* 55, 155–164. doi: 10.1016/S0167-7012(03)00140-4

Yilmaz, P., Parfrey, L. W., Yarza, P., Gerken, J., Pruesse, E., Quast, C. et al. (2013). The SILVA and "All-species Living Tree Project (LTP)" taxonomic frameworks. *Nucleic Acids Res.* 42, D643–D648. doi: 10.1093/nar/gkt1209

Zhou, Z., Jiang, F., Wang, S., Peng, F., Dai, J., Li, W., et al. (2012). *Pedobacter arcticus* sp. nov., a facultative psychrophile isolated from Arctic soil, and emended descriptions of the genus *Pedobacter*, *Pedobacter heparinus*, *Pedobacter daechungensis*, *Pedobacter terricola*, *Pedobacter glucosidilyticus* and *Pedobacter lentus*. *Int. J. Systematic Evol. Microbiol.* 62, 1963–1969. doi: 10.1099/ijs.0.031104-0

Zhu, W., Lomsadze, A., and Borodovsky, M. (2010). Ab initio gene identification in metagenomic sequences. *Nucleic Acids Res.* 38:e132. doi: 10.1093/nar/gkq275

frontiers | Frontiers in Microbiology

TYPE Review
PUBLISHED 26 April 2023
DOI 10.3389/fmicb.2023.1152847

OPEN ACCESS

EDITED BY
Prashant Kumar Singh,
Mizoram University, India

REVIEWED BY
Zothanpuia,
Pachhunga University College, India
Rajan Kumar Gupta,
Banaras Hindu University, India

*CORRESPONDENCE
Sitong Zhang
✉ 18943132269@163.com

RECEIVED 28 January 2023
ACCEPTED 06 April 2023
PUBLISHED 26 April 2023

CITATION
Liu Y, Zhang N, Ma J, Zhou Y, Wei Q, Tian C, Fang Y, Zhong R, Chen G and Zhang S (2023) Advances in cold-adapted enzymes derived from microorganisms.
Front. Microbiol. 14:1152847.
doi: 10.3389/fmicb.2023.1152847

Advances in cold-adapted enzymes derived from microorganisms

Yehui Liu[1,2], Na Zhang[1,2], Jie Ma[1,2], Yuqi Zhou[1,2], Qiang Wei[1,2], Chunjie Tian[3], Yi Fang[3], Rongzhen Zhong[3], Guang Chen[1,2] and Sitong Zhang[1,2,3]*

[1]College of Life Science, Jilin Agricultural University, Changchun, China, [2]Key Laboratory of Straw Comprehensive Utilization and Black Soil Conservation, Ministry of Education, Changchun, China, [3]Key Laboratory of Mollisols Agroecology, Northeast Institute of Geography and Agroecology, Chinese Academy of Sciences, Changchun, China

Cold-adapted enzymes, produced in cold-adapted organisms, are a class of enzyme with catalytic activity at low temperatures, high temperature sensitivity, and the ability to adapt to cold stimulation. These enzymes are largely derived from animals, plants, and microorganisms in polar areas, mountains, and the deep sea. With the rapid development of modern biotechnology, cold-adapted enzymes have been implemented in human and other animal food production, the protection and restoration of environments, and fundamental biological research, among other areas. Cold-adapted enzymes derived from microorganisms have attracted much attention because of their short production cycles, high yield, and simple separation and purification, compared with cold-adapted enzymes derived from plants and animals. In this review we discuss various types of cold-adapted enzyme from cold-adapted microorganisms, along with associated applications, catalytic mechanisms, and molecular modification methods, to establish foundation for the theoretical research and application of cold-adapted enzymes.

KEYWORDS

cold-adapted enzymes, psychrophile, cold-adapted catalytic mechanism, molecular modification, application of cold-adapted enzymes

1. Introduction

Cold-adapted enzymes, also called psychrophilic enzymes, are enzymes that can effectively catalyze low temperature reactions and are very temperature sensitive (Kulakova et al., 1999). As defined by Margesin and Schinner (1992) enzymes that optimally catalyze at about 30°C and still have some catalytic efficiency at 0°C are usually called cold-adapted enzymes. Unlike mesophilic and thermophilic enzymes, cold-adapted enzymes have the following characteristics: (1) The optimal reaction temperature is low, with an optimal catalytic temperature generally between 20°C to 45°C. (2) The enzymatic reaction activation energy is low and can be reduced by increasing substrate turnover or affinity. (3) Thermal stability is low, with rapid, easily lost activity at high temperatures (more than half of activity is lost after 10 min at 50°C to 60°C or several hours at 37°C) (Feller et al., 1997; Berchet et al., 2000; D'Amico et al., 2003; Santiago et al., 2016).

Baldwin and Hochachka (1970) discovered the existence of a cold-adapted enzyme in trout brains and began theoretical and applied research on it. The first paper to biochemically

characterize cold-adapted enzymes was published in 1984, in which the optimal temperature and substrate preferences of a thermosensitive alkaline phosphatase from an Antarctic bacterium were analyzed in detail (Kobori et al., 1984). Through continued biotechnological development, cold-adapted enzymes have been applied in food processing, detergent production, basic molecular biology research, and other areas.

Cold-adapted enzymes, because their loose structure and high flexibility, reduce the activation energy required for enzymatic reactions at lower temperatures. But this also results in the disadvantage of increased sensitivities to metallic ions and organic solvents, and a low variability of thermal stability. Furthermore, a lack of enzymatic sources and difficulty in separating and purifying these enzymes seriously limit the industrial application of cold-adapted enzymes. Regardless, compared with cold-adapted enzymes from animals and plants, cold-adapted enzymes from microorganisms have the positive characteristics of abundant source, short production cycle, high yield, and simple separation and purification, and thus have attracted much attention (Georlette et al., 2000; Kim et al., 2018; Ge et al., 2020).

Cold-adapted enzymes have been observed in *Pseudomonas*, *Penicillium*, and the yeast *Rhodotorula*, among many microorganisms. Investigations into cold-adapted catalytic mechanisms and the molecular modifications of cold-adapted enzymes have frequently been reported (Kumar et al., 2021). However, research and reports on applications of cold-adapted enzymes from microorganisms are dispersed and unsystematic to date. This review systematically discusses the types, applications, catalytic mechanisms, and molecular modifications of cold-adapted enzymes from microorganisms, providing a theoretical basis for the research and comprehensive application of cold-adapted enzymes.

2. Principal types of cold-adapted enzymes from microorganisms

Approximately 100 types of cold-adapted enzymes have been reported over the last few years (Santiago et al., 2016; Pereira et al., 2017; DangThu et al., 2020). According to International Commission of Enzymes nomenclature, these enzymes can be classified into six primary categories: hydrolase, oxidoreductases, ransferases, lyases, isomerases, and synthetases. Because there are six types of cold-adapted enzymes involved, we selected typical cold-adapted enzymes for introduction.

2.1. α-Amylases from cold-adapted hydrolases

Hydrolases are the most common commercially used cold-adapted enzyme of the six primary categories. These include cold-adapted proteases, lipases, and amylases. Among them, α-amylases was the first cold-adapted hydrolase to be crystallized and analyzed. *Bacillus*, *Cryptococcus*, *Penicillium*, *Pseudomonas*, and the yeast *Rhodotorula* are principal representative genera used for the production of cold-adapted α-amylases. Commercial cold-adapted microbial α-amylases and associated characteristics are overviewed in Table 1.

Aghajari et al. (1998) analyzed the structure of an *Alteromonas haloplanctis* cold-adapted α-amylase (AHA) and explained its cold catalytic mechanism at a molecular level by comparison with the structure of human pancreatic α-amylase (HPA) (Figure 1). AHA is a typical monomeric enzyme, with three domains A, B, and C. Unlike HPA, AHA has a large number of amino acid residues that are eliminated. The number of hydrogen bonds, glutamate residues, aspartate residues, and proline residues in domains A consisting of a $(\beta/\alpha)_8$-barrel structures, and in domain C consisting of eight β-strands, and in its N-terminal domain, are significantly lower than so in HPA. The number of disulfide bonds in the B domain is also significantly lower. This makes AHA's structure looser than HPA's, increasing AHA's affinity for substrates (Aghajari et al., 1998). Unlike mesophilic and thermophilic α-amylases, most cold-adapted α-amylases are highly active at 25–37°C and pH 4.0–8.0, are inactivated at 50°C for 10–15 min, and are sensitive to metal and salt ions, and organic solvents (Lu et al., 2010; Kim et al., 2017). However, cold-adapted enzyme resource development has found some cold-adapted α-amylases that possess a degree of tolerance to metal and salt ions. For instance, Wang Y. et al. (2018) and Wang X. et al. (2018) analyzed and characterized a cold-adapted α-amylase from an Antarctic bacterium and found the enzyme to be extremely salt-tolerant. It also possesses a degree of tolerance to other metal ions, such as potassium, calcium, and manganese, and to solvents, including sodium dodecyl sulfate (SDS), and dimethyl sulfoxide (DMSO). Therefore, this cold-adapted α-amylase is more suitable for use in detergents than most other α-amylases (Wang Y. et al., 2018; Wang X. et al., 2018).

2.2. Superoxide dismutase from cold-adapted oxidoreductase

To date, cold-adapted oxidoreductases derived from microorganisms mainly consist of sorbitol dehydrogenase, glutathione reductase, hydrogen peroxide reductase, and superoxide dismutase. Of these, cold-adapted superoxide dismutase is commonly used in clinical debridement and for other therapeutic purposes (DangThu et al., 2020; Wang Z. P. et al., 2020; Wang Q. et al., 2020; Krumova et al., 2021). Presently, *Pseudoalteromonas*, *Salmonella*, and the fungi *Aspergillus* are the primary sources of cold-adapted superoxide dismutases. Most show high activity at 25°C–35°C and pH 7.0–8.0 (Abrashev et al., 2016; Wang Z. P. et al., 2020; Wang Q. et al., 2020). Major features of microbial cold-adapted superoxide dismutases are summarized in Table 2.

Pedersen et al. (2009) reported the structure of cold-adapted iron superoxide dismutase from *Aliivibrio salmonicida* analyzing its active site and pocket area (Figure 2), and found that the number of disulfide and hydrogen bonds in the region were significantly lower than that of homologous mesophilic iron superoxide dismutases. They attribute this decrease in the number of disulfide and hydrogen bonds to be the main factor in maintaining the flexibility of its structure (Pedersen et al., 2009). Interestingly, in contrast to other types of cold-adapted enzymes, the cold-adapted superoxide dismutase from *Halomonas* sp. ANT108 (rHsSOD) is itself a metalloenzyme, so that it is tolerant to Cu^{2+} and other metal ions. Therefore, Cu^{2+} and Zn^{2+} ions can promote rHsSOD activity in this bacterium, thus avoiding breaks in DNA

TABLE 1 Cold-adapted α-amylases from various microorganisms and associated characteristics.

Enzyme	Microorganism	Optimal temperature	Optimal pH	Deactivation conditions	Activator	Inhibitors	Reference
α-Amylase	*Arthrobacter agilis* PAMC 27388	30°C	3.0	50°C, 10 min	Co^{2+}, Fe^{3+}, Na^{+}, K^{+}, β-ME	Mg^{2+}, Zn^{2+}, urea, SDS, EDTA	Kim et al. (2017)
Amy175	*Pseudoalteromonas* sp. M175	25°C	8.0	55°C, 10 min	Ca^{2+}, Mg^{2+}, Zn^{2+}, K^{+}, EDTA, SDS, Triton X-100	Co^{2+}, β-ME	Wang Y. et al. (2018); Wang X. et al. (2018)
Amy SH3	*Exiguobacterium.*	37°C	7.0	50°C, 20 min	Co^{2+}	Ca^{2+}, Mg^{2+}, Urea, Zn^{2+}, Fe^{3+}, SDS, β-ME, EDTA	Mojallali et al. (2014)
Amylase	*Nocardiopsis* sp. 7,326	35°C	8.0	60°C, 10 min	Co^{2+}, Ca^{2+}, K^{+}, Mg^{2+}, Zn^{2+}	EDTA	Zhang and Zeng (2008)
Amylase GS230	*Pseudoalteromonas arctica* GS230	30°C	7.5	50°C, 10 min	Co^{2+}, Urea, Ca^{2+}, Mg^{2+}, Na^{+}, K^{+}	Fe^{3+}, Zn^{2+}, EDTA, SDS	Lu et al. (2010)

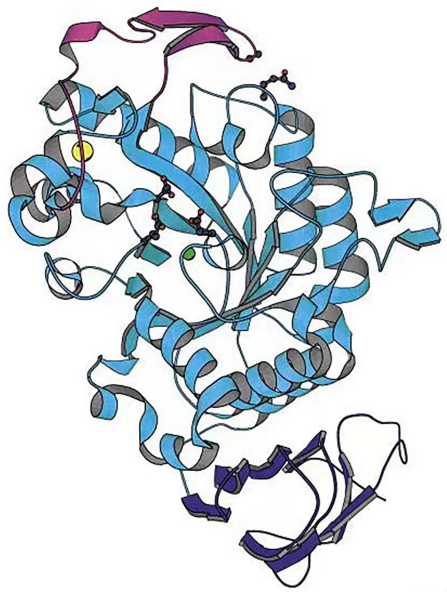

FIGURE 1
Cold-adapted α-amylase from *Alteromonas haloplantis* structure (Aghajari et al., 1998).

strands caused by metal-catalyzed oxidation (Wang Z. P. et al., 2020; Wang Q. et al., 2020).

2.3. Alginate lyase from cold-adapted lyase

Cold-adapted lyases from microbes predominantly include glycosaminoglycan lyase, alginate lyase, and DNA photolyase. Among these, cold-adapted alginate lyases can cleave alginate to produce trehalase, which is an enzyme of high value with broad applications in industrial production processes (Munshi et al., 2017; Gao et al., 2018; Zhang et al., 2022). Researchers have studied cold-adapted alginate lyases from *Vibrio*, *Flavobacterium*, *Pseudoalteromonas* spp., and *Alteromonas portus*, finding that optimal catalytic conditions are generally between 25°C and 35°C and pH 7.0–8.0 (Chen et al., 2016; Wang Z. P. et al., 2020; Wang Q. et al., 2020; Zhou et al., 2020; Huang et al., 2021). Table 3 summarizes connercial cold-adapted alginate lyases of microbial origin and associated characteristics.

Yang et al. (2021) reported the AlgSH17 structure, a cold-adapted alginate lyase with both endolytic and exolytic cleavage activities from *Microbulbifer* sp. SH-1 (Figure 3). The enzyme is composed of two domains. Asparagine, histidine, tyrosine, and arginine jointly constitute the binding pocket, and a Zn^{2+} binding site is near this binding pocket. Consequently, Zn^{2+} competitively binds to the enzyme inhibiting its activity, but Mn^{2+} and Fe^{2+} have activation effects. This research shows that AlgSH17 has good tolerance to some metal ions, suggesting that it has great potential in industrial applications (Yang et al., 2021). Most cold-adapted alginate lyases are neutral enzymes. Enzymatic activity is reduced or even inactivated under hypoacidic or hyperacidic conditions. However, the cold-adapted alginate lyase TAPL7B from *Thalassotalea algicola* has an optimum pH of 11.0, and retains 75% activity at pH 4.0, probably because of the presence of both acidic and basic catalytic domains in its conserved structural fold (Chen et al., 2023).

2.4. γ-Glutamylcysteine ligase from cold-adapted synthetase

DNA ligase, glutathione synthase, and γ-glutamylcysteine ligase are the primary cold-adapted synthetases, with γ-glutamylcysteine ligase being the most often employed (Albino et al., 2012; Munshi et al., 2017). Glutathione synthesized by γ-glutamylcysteine ligase functions in repairing cell damage caused by reactive oxygen species *in vivo*. It is widely used in clinical medicine and has good potential for biopharmaceutical industrial applications (Pallardo et al., 2009; Narayanankutty et al., 2019). Albino et al. (2014) studied the structure and associated phenotype of γ-glutamylcysteine ligase from the psychrophilic bacterium *Pseudoalteromonas haloplanktis*

TABLE 2 Cold-adapted superoxide dismutases from various microorganisms and associated characteristics.

Enzyme	Microorganism	Optimal temperature	Optimal pH	Deactivation conditions	Activator	Inhibitors	Reference
rHsSOD	*Halomonas* sp. ANT108	35°C	7.5	60°C, 20 min	Cu^{2+}, Zn^{2+}	Ca^{2+}, Fe^{3+}, Cd^{2+}, Co^{2+}, Cr^{3+}, Ni^{2+}, Mg^{2+}, DTT, TritonX-100	Wang Z. P. et al. (2020); Wang Q et al. (2020)
PsSOD	*Pseudoalteromonas* sp. ANT506	30°C	8.0	70°C, 20 min	Ca^{2+}, Mg^{2+}, Cu^{2+}, Zn^{2+}, Tween-80	Ni^{2+}, Fe^{3+}, SDS, Urea	Wang et al. (2016)
PhSOD	*Pseudoalteromonas haloplanktis*	25°C	6.9	54°C, 10 min	Na^{+}, EDTA	K^{+}	Castellano et al. (2006)

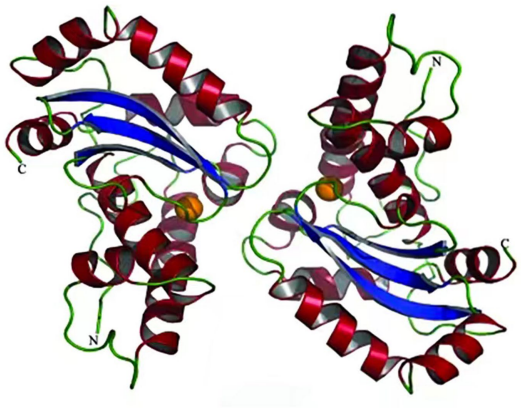

FIGURE 2
Superoxide dismutase from *Aliivibrio salmonicida* structure (Pedersen et al., 2009).

(Figure 4). The enzyme has maximum activity at 15°C and pH 8.0 and is heavily dependent on Mg^{2+}. Further analysis of its amino acid sequence and structure found that amino acids without five-membered ring side chain such as cysteine and glutamic acid, and a reduction in the number of disulfide bonds, in its catalytic domain are more conducive to maintaining the enzyme's structural flexibility (Albino et al., 2014).

2.5. Peptidylprolyl isomerase from cold-adapted isomerase

Currently, cold-adapted isomerases mainly include cold-adapted phosphotriester isomerase and peptidylprolyl isomerase from *Vibrio* and *Swaniella* sp. SIB1, respectively (Budiman et al., 2011; Aqvist, 2017). *Shewanella* peptidylprolyl isomerase is a folding enzyme that helps intracellular molecular assembly and improves overall low temperature catalytic abilities in this organism. This enzyme, FK506-binding protein 22 (FKBP22) is a typical cold-adapted enzyme, consisting of an N-terminal domain and C-terminal domain, forming a 'V' dimer structure, with the N-terminal domain mainly involved in its catalytic reactions (Figure 5). The enzyme's optimum catalytic temperature is 20°C; therefore, its study helps in the understanding of cold-adapted microorganism catalytic mechanisms overall, and provides a theoretical basis for the improvement of industrial microorganisms microorganism utilization (Budiman et al., 2011).

2.6. ATP phosphoribosyl transferase from cold-adapted transferase

ATP phosphoribosyl transferase is representative and the most commonly reported cold-adapted transferase. Two ATP phosphoribosyl transferase subfamilies from *Thermotoga maritima* and *Lactococcus lactis* are descriptive. One is $HisG_L$ which contains a catalytic domain, and the other is $HisG_S$, which does not and needs to bind HisZ to function (Champagne et al., 2005; Vega et al., 2005). Subsequently, Stroek et al. (2017) analyzed the crystal structure of an $HisG_S$ and HisZ complex from the psychrophilic polar bacterium *Psychrobacter arcticus* (Figure 6), and found that the existence of HisZ made $HisG_S$ more sensitive to temperature rise, and that the flexibility of its structure increased after the combination of HisZ and $HisG_S$. Unlike the cold-adapted enzymes mentioned above, this enzyme may increase the contact surface of the enzyme with the solvent *via* HisZ and $HisG_S$ binding, thereby increasing enzyme flexibility, which in turn increases substrate affinity and enzymatic reaction rates of at low temperatures (Isaksen et al., 2016).

3. Microorganism cold-adapted enzyme applications

Cold-adapted enzymes have numerous industrial benefits. These include easily managed reaction conditions, easy monitoring and control of the production processes, and a wide variety of commercial applications. Therefore, these enzymes are widely studied and have been applied in various areas, including food processing, detergent production, bioremediation, environmental protection, straw resourcing, and in basic molecular biology research (Cavicchioli et al., 2011; Yadav et al., 2022).

3.1. Applications in food processing

Cold-adapted enzymes are often used in the food processing industry to help maintain the nutritional value and flavor of particular

TABLE 3 Cold-adapted alginate lyases from various microorganisms and associated characteristics.

Enzyme	Microorganism	Optimal temperature	Optimal pH	Deactivation conditions	Activator	Inhibitors	Reference
ALG2951	*Alteromonas portus*	25°C	8.0	60°C, 20 min	Na^+, K^+, Na^+	Mn^{2+}, Fe^{2+}, Ba^{2+}, SDS	Huang et al. (2021)
AlyS02	*Flavobacterium* sp.	30°C	7.6	50°C, 20 min	Na^+, K^+, Ca^{2+}, Mg^{2+}	Fe^{3+},Al^{3+},Mn^{2+}, Cu^{2+}, SDS, EDTA	Zhou et al. (2020)
AlgSH17	*Microbulbifer* sp. SH- 1	30°C	7.0	60°C, 20 min	Mg^{2+}, Mn^{2+}, Fe^{3+}, Co^{2+}, Ni^{2+}	Ba^{2+}, Cu^{2+}, Al^{3+}	Yang et al. (2021)
Alys1	*Tamlana* sp. s12	35°C	7.0	60°C,20 min	Mg^{2+}, glycerol	Ca^{2+}, Mn^{2+}, Fe^{2+}, Fe^{3+}, SDS, EDTA	Yin et al. (2021)

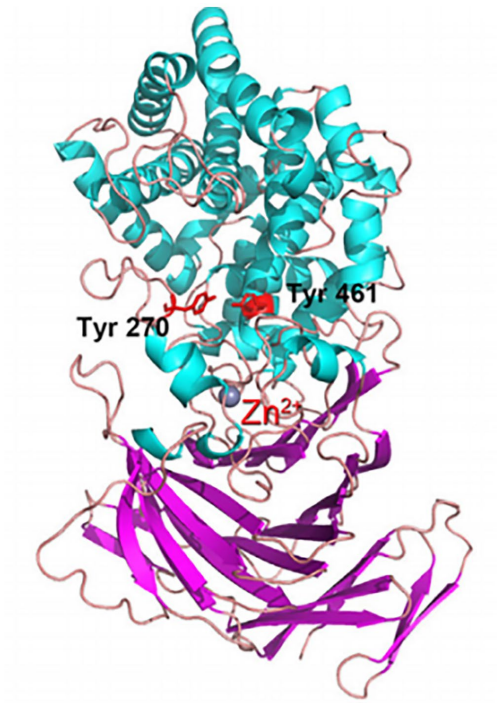

FIGURE 3
Alginate lyase from yeast *Yarrowia lipolytica* structure (Yang et al., 2021).

ingredients during processing and treatment, and to replace mesophilic or thermophilic enzymes in the processing and treatment of food materials. Representative examples include cold-adapted β-galactosidases, esterases, xylanases, and proteases (Kumar et al., 2021).

β-galactosidase can hydrolyze the lactose in dairy products, which effectively resolves the issue of human lactose sensitivity in dairy products (Ugidos-Rodriguez et al., 2018). However, dairy product treatment with β-galactosidase combined with pasteurization or ultra-high temperature sterilization is not conducive to preserving the taste and nutrition of dairy products (Krishna et al., 2021). In contrast, the cold-adapted β-galactosidase BsGal1332, can hydrolyze lactose at 0°C and loses its activity at 50°C (Liu et al., 2021). These special properties may effectively solve the nutrient loss problem caused by conventional lactose treatment in dairy products.

Esterase can maintain the characteristic flavor of cheese during cheese ripening, but mesophilic and higher temperature-adapted esterases can decompose certain amino acids causing a loss of flavor during the usual higher temperatures required for dry cheese fermentation. Whereas a cold-adapted esterase from *Lactobacillus plantarum* can catalyze at 5°C is inactivate after 30 min at 55°C, and has some acid and salt resistance, and therefore, can be used as an exogenous esterase to maintain cheese flavor in fully ripened cheeses (Esteban-Torres et al., 2014).

The addition of xylanase can improve the water holding capacity and improve the quality of wheat bread, but thermophilic xylanase can cause the excessive release of water and gelatinization during baking (Jiang et al., 2005). Li et al. (2022) found that a recombinant cold-adapted xylanase originally from *Sorangium cellulosum* (XYNSC8) at a low dose (0.05–0.2 mg/kg flour) can effectively improve the quality of bread, and its effect was obviously better than that of mesophilic xylanases available on the market.

Proteases can improve the tenderness of meat while processing meat products (Mangiagalli et al., 2020). Currently, commercial meat tenderizer proteases such as papain are mesophilic or thermophilic. Zhao et al. (2012) studied a cold-adapted collagenolytic enzyme from *Pseudoalteromonas* (MCP-01) and found that it can selectively degrade muscle fiber protein at 4°C, improving beef tenderness, while keeping meat quality and color.

3.2. Applications in the detergent industry

In traditional laundry applications, chemical detergents are often stirred at high temperatures with fabrics to remove stains. But long-term stirring at high temperatures reduces the lifespan of clothing, and also increases energy consumption. However, adding an enzyme preparation to the detergent can produce ideal washing effects in more gentle conditions (Kuddus and Ahmad, 2012; Sarmiento et al., 2015). Proteases can decompose adsorbed protein residues into small molecular peptides, consequently dissolving the residue into detergent laden water, thus removing protein stains. Unfortunately, mesophilic and thermophilic proteases have low activity at low temperatures, so it is difficult to obtain the ideal benefits of cold water washing (Kuddus and Ramteke, 2009).

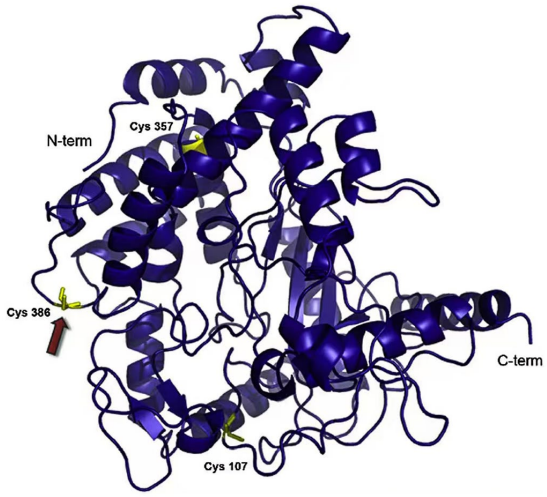

FIGURE 4
γ-Glutamylcysteine ligase from *Pseudoalteromonas alobanktis* structure (Albino et al., 2014).

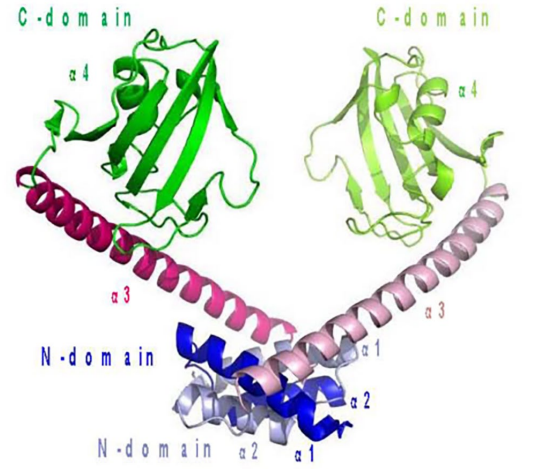

FIGURE 5
Peptidylprolyl isomerase from *Shewanella* sp. SIB1 structure (Budiman et al., 2011).

The cold-adapted alkaline protease of *Stenotrophomonas maltophilia* has good activity at 20°C, high stability, good compatibility with commercial detergents, and good stain removal at low temperatures. Therefore, it can be added to commercial detergents to remove protein-containing stains such as milk and blood (Mohammed and Pramod, 2011).

Adding lipases to detergents can effectively remove grease, but the maximal activity temperature of commonly used lipases is generally between 30°C and 50°C. Adding mesophilic or thermophilic lipases to detergents not only increases energy consumption, but also increases garment damage due to high temperature washing. The cold-adapted lipase "Lipoclean" produced by Novozymes can remove lipid substances at low temperatures. When mixed with detergent this enzyme can even achieve good cleaning effects on porous building materials (Mhetras et al., 2021).

Cold-adapted amylases can effectively remove starch-containing stains such as chocolate and tomato sauce. Adding *Pseudoalteromonas* Amy175 can greatly improve the ability of commercial detergents to remove stains (Wang Y. et al., 2018; Wang X. et al., 2018). The DuPont Bioscience Company developed "PREFERENZ" cold-adapted amylase to add todetergent. It has a high activity at 16°C and effectively removes starch stains (Edser, 2004).

3.3. Applications in bioremediation and environmental protection

Soil and water pollution are currently major problems worldwide. Antibiotic and dye pollution in soils and water resources seriously affects ecology and accumulates in heterotrophic bodies through the food chain, including hemans, resulting in irreversible harm. Cold-adapted laccase can degrade aromatic compounds, including most antibiotics under mild conditions. Unlike mesophilic and thermophilic laccase, cold-adapted laccase can be inactivated immediately at a lower temperature (40°C) after a reaction, without affecting subsequent reactions. The degradation rate of crystal violet using a coupling system of cold-adapted laccase from *Kabatiella bupleuri* G3 IBMiP and 2,2′-azino-bis (3-ethylbenzothiazoline-6-sulfonic acid) diammonium salt (ABTS) can reach 48% (Wiśniewska et al., 2021). Tetracycline and oxytetracycline can be degraded effectively at 0°C with a cold-adapted laccase-ABTS coupling system from the white-rot fungus *Pycnoporus* sp. SYBC-L10 (Tian et al., 2020).

As demand for fossil fuels grows, oil spills are an increasingly greater threat to the environment. The cold-adapted lipase produced by *Bacillus cereus* HSS can effectively remove oil from wastewater; using sponge immobilized cells, it can achieve an oil removal elimination efficiency of 94.7% (Hassan et al., 2018). Another good choice for the treatment of waste oil is to produce biodiesel. Novozymes produces a cold-adapted lipase named "Novozyme 435" that can be used convert waste oil into biodiesel (Mhetras et al., 2021). Unfortunately, "Novozyme 435" is not stable in high methanol concentration environments. However, the cold-adapted lipase M37 from *Photobacterium lipolyticum* retains high activity in a methanol concentration of 10% and can be used to produce biodiesel (Yang et al., 2009). M37 showed significantly higher stability and conversion rates than "Novozyme 435" in both one and two methanol feed reactions demonstrating good application prospects in waste oil biodiesel production.

3.4. Applications in molecular biology

Gentle thermal treatment of cold-adapted enzymes causes irreversible enzymatic inactivation without interfering with subsequent reactions during *in vitro* molecular biology. Moran et al. (2001) isolated a strain of psychrophilic bacteria from seawater that secreted a cold-adapted protease (A9) that could digest restriction endonuclease PvuII to prevent it from cleaving DNA without interfering with DNA quality. However, the enzyme can also interfere with Taq polymerase activity, so A9 protease can be added to a reaction, then the enzyme can be inactivated to terminate its reaction

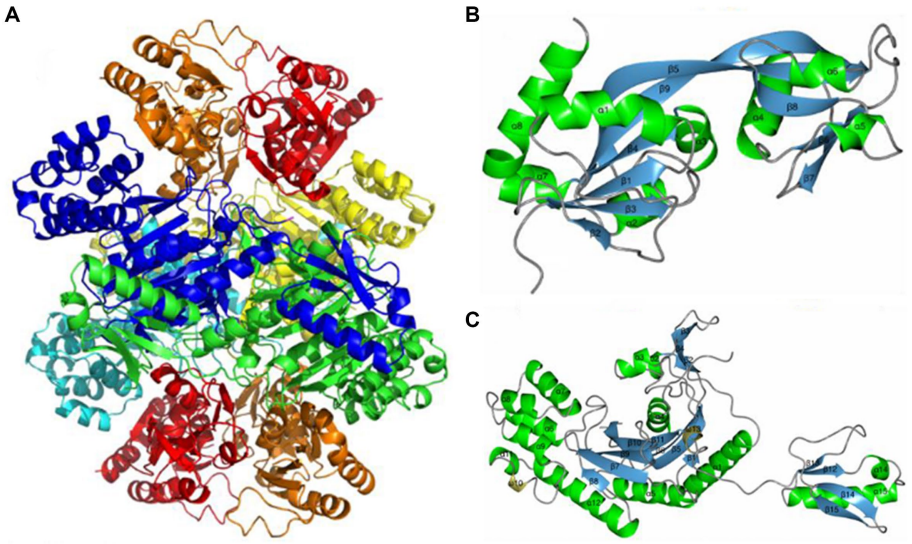

FIGURE 6
ATP phosphoribosyl transferase from Psychrobacter arcticus structure. **(A)** HisGS and HisZ heterooctamer structure; **(B)** HisGS monomer structure; **(C)** HisZ monomer structure (Stroek et al., 2017).

under mild thermal conditions and ensure the subsequent reactions are not interfered with (Moran et al., 2001).

Alkaline phosphatase dephosphorylates DNA and is often used to clean up PCR products and prevent multiple cycles before cloning, but persistence of alkaline phosphatase activity can interfere with subsequent reactions. Most commercially available alkaline phosphatases are mesophilic enzymes, which generally require medium-high inactivation temperatures. This can lead to DNA degradation and affect nucleic acid quality. However, alkaline phosphatase from the Antarctic psychrophilic bacterium TAB5 can be inactivated after incubation at 50°C for 20 min. Inactivating the phosphatase at this temperature does not affect the quality of the sample (Rina et al., 2000).

DNA ligase catalyzes the ligature of DNA fragments by phosphodiester bonds. When used *in vitro* in molecular biology it is usually derived from a bacteriophage and has optimal activity at a fairly low temperature. The cold-adapted T4 DNA Ligase of Takara Bioscience Company is widely used in research (Kumar et al., 2021). Berg et al. (2019) isolated three cold-adapted ATP-dependent DNA ligases from psychrophilic bacteria. Among them, Vib-Lig from *Aliivibrio salmonicida* retained 60% of its activity at 20°C and 80% of its substrate bonding efficiency at 10°C, demonstrating good application prospects for basic research.

3.5. Applications for straw resourcing

Making full use of biomass such as agricultural waste to produce ethanol helps solve environmental pollution problems caused by agricultural waste and help ease energy shortage problems. A primary agriculture waste is straw. However, the conversion efficiency of lignocellulose to fermentable sugars is low and the cost is high because of straw's structure, which limits the large-scale industrialization of cellulosic ethanol. Currently, optimal activity temperature of the enzymes, xylanase, and cellulase, associated with straw degradation is about 55°C. Normal environmental temperatures do not meet the requirements of straw degradation enzymes (Wang et al., 2021). Thus, the development of cold-adapted enzymes to degrade straw is central to the overall utilization of straw resources. Sun et al. (2018) expressed and purified a β-glucosidase from a marine bacterium with maximal activity at 25°C and pH 6–8 that is rapidly inactivated after incubation at 40°C. The enzyme is not affected by NaCl nor organic solvents, and the activity of the enzyme can be increased in the presence of reducing agents. These cold-adapted characteristics provide great potential for the large-scale production of cellulosic ethanol at room temperature. Cold-adapted laccases, xylanases, and β-xylosidases also have great potential in the industrial application of straw degradation to produce cellulose ethanol (Kim et al., 2021). Owing to the particular composition of straw, the effect of a single enzyme is not evident in its breakdown. The synergistic synergistic effect of the *Cladosporium cladosporioides* cold-adapted catalytic enzyme system for lignocellulose degradation with commercial xylanase is impressive. Having maximal activity at 28°C, and a sugar yield of 10.1 mg/ml, this method can greatly reduce the cost of straw conversion to ethanol (Ji et al., 2014).

With the development of modern biotechnology, cold-adapted enzymes are playing a major role in an increasing number of fields. Representative cold-adapted enzymes of all types different microorganisms with associated application potentials are summarized in Table 4.

4. Mechanisms for cold-adapted catalysis in cold-adapted enzymes

Cold-adapted enzymes usually enhance the affinity of the enzyme substrate by reducing the amount of activation energy needed for the enzyme-substrate complex. This is accomplished by increasing the flexibility of all or part of the enzyme's structure, which increases the rate of the enzymatic reaction at low temperatures, consequently

TABLE 4 Cold-adapted enzymes from various microorganisms and associated applications.

Enzyme	Microorganism	Source	Field of application	References
DNA Ligase	*Pseudoalteromonas haloplanktis*	Deep sea	basic Biology Research	Georlette et al. (2000)
Glucose Oxidase	*Cladosporium neopsychrotolerans* SL16	Alpine soil	feed production, pharmaceutical technology, food industry	Ge et al. (2020)
Protease	*Janthinobacterium lividum*	Polar soil	detergent production, food industry, pharmaceutical process, environmental bioremediation	Kim et al. (2018)
Alginate Lyase	*Vibrio* sp. W2	Deep sea	food industry, clinical medicine, basic biological research	Wang Z. P. et al. (2020); Wang Q. et al. (2020)
Chitosanase CsnS	*Serratia* sp. QD07	Deep sea	clinical medicine, industrial production	Zheng et al. (2021)
β-1,4-glucanase	*citrisub* sp.	Mountain plant pathogens	food industry	de Melo et al. (2021)
Glucoamylase	*Tetracladium* sp.	Polar soil	Biofuels, food industry	Carrasco et al. (2017)
Pullulanase	*Bacillus methanolicus* PB1	Polar soil	food industry	Zhang et al. (2020)
α-Amylase	*Arthrobacter agilis*	Polar soil	Food industry, basic biology research	Kim et al. (2017)
Dextranase	*Catenovulum* sp. DP03	Deep sea	food industry	Deng et al. (2020)
Lipase	*Pseudomonas* sp. KE38	Deep sea	Food Industry, detergent production, environmental bioremediation	Salwoom et al. (2019)
Superoxide Dismutase	*Paelopatides* sp.	Deep sea	Cosmetic production, clinical medicine research	Li et al. (2019)
FK506-Binding Protein	*Shewanella* sp.	Deep sea	Basic biological research	Budiman et al. (2011)

reducing energy consumption. Presently, the catalytic mechanism of cold-adapted enzymes is generally explained in two respects: (1) The structure is different from that of a mesophilic or thermophilic enzyme possessing greater structural flexibility. (2) The enzyme has a lower activation energy level, such that enzyme molecule energy consumption is low in low temperature conditions (Cavicchioli et al., 2011; Siddiqui, 2015).

4.1. Cold-adapted enzymes structural flexibility

Structurally, compared with the mesophilic and thermophilic enzymes, cold-adapted enzymes have obvious differences in the number of glycine, arginine, and proline residues, as well as in the number of salt bridges, hydrogen bonds, disulfide bonds, and overall hydrophobicity and hydrophobic surfaces. The number of proline residues, salt bridges, hydrogen bonds, and disulfide bonds are decreased, and an increase in the number of glycine residues and in overall hydrophobicity and hydrophobic surfaces are common features of most cold-adapted enzymes (Siddiqui and Cavicchioli, 2006).

4.1.1. Primary structure

Cold-adapted enzyme amino acid sequence analysis shows that the number of proline residues in cold-adapted enzymes is much lower than that in mesophilic and thermophilic enzymes (Wang Y. et al., 2018; Wang X. et al., 2018; Hou et al., 2019). Proline's α-carbon atom is connected to its five-membered ring structure side chain group, which makes it difficult for the main chain carbon atom to rotate This limits the rotation of the carbon main chain during the formation of a peptide chain (Figure 7B), increases the rigidity of the peptide chain, and reduces local flexibility of the protein, but to a certain extent, it improves the stability of a protein, namely the 'proline law' (Watanabe et al., 1996). Studies on the homologs of mesophilic and thermophilic oligosaccharidases show that proline content of high temperature oligosaccharidases is significantly higher than that of mesophilic homologs (Land et al., 2019). The absence of proline increases the flexibility of a cold enzyme structure, thus facilitating attachment to its substrate. Additionally, the presence of cysteine can increase the stability of proteins by generating disulfide bonds during the formation of higher structure (Aghajari et al., 1998). The effect of disulfide bonds on protein stability will be discussed further below.

Glycine, serine, and histidine are often found in the central domain of cold-adapted enzymes (Mahdavi et al., 2011; Raymond-Bouchard et al., 2018). This may be because no amino acid has a five-membered ring side chain structure other than proline. Therefore, substitution by these amino acids reduces restriction on the rotation of the main chain (Figure 7A), thus increasing molecular conformation flexibility (Raymond-Bouchard et al., 2018). The proportion of amino acids with simple side chains in the primary structure of cold-adapted enzymes determines the flexibility of the

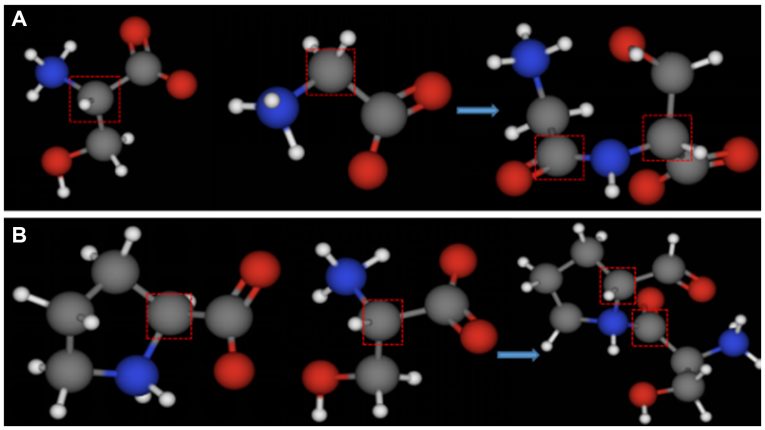

FIGURE 7
Ball-and-stick models of the dipeptide formed by the condensation of different amino acids. **(A)** Ball-and-stick model of serine and glycine dipeptide; **(B)** ball-and-stick model of proline and serine dipeptide (the gray part in the red box represents the main chain carbon atom of each amino acid).

structure. However, increased structural flexibility inevitably leads to reduced thermal stability. Therefore, in the modification of cold-adapted enzymes, proline is often used as an alternative to other amino acids to improve the stability of cold-adapted biomodified enzymes (Xu et al., 2020).

Arginine's structure allows it to form five hydrogen bonds and two salt bridges in tertiary structure with other amino acid residues. The existence of hydrogen bonds and salt bridges rendera protein structure more stable. Nonetheless, in most cold-adapted enzymes, the level of arginine residues on the surface of the protein is often higher than that of mesophilic or thermophilic homologs (Zheng et al., 2016). The presence of arginine on the structural surface of cold-adapted enzymes may facilitate interaction with solvents instead of forming hydrogen bonds and salt bridges with other residues on that protein surface, actually contributing more flexibility to the molecular structure of cold-adapted enzymes (Siddiqui and Cavicchioli, 2006).

4.1.2. Advanced structure and surface properties

Hydrogen bonding plays an important role in protein folding, and a main driving force of protein folding is the formation of hydrophobic cores (Lee et al., 2017). A reduction in the number of hydrogen bonds leads to a sharp decrease in the hydrophobicity of an enzyme, but at the same time, increases its flexibility parameters to some extent (Bentahir et al., 2000). Furthermore, the existence of amino acid residues such as arginine and glutamic acid in enzyme structure may lead to the formation of salt bridges when an enzyme molecule interacts with substrate molecules. Although these salt bridges are non-covalent interactions with weak binding force, the existence of a large number of these amino acids will produce more salt bridges, which will increase the stability yet reduce the flexibility of an enzyme molecule. This is why the salt bridge content in the structure of cold-adapted enzymes is lower than that of homologous mesophilic enzymes (Wang et al., 2016).

The disulfide bond is a stable covalent bond that can make protein structures more complex and enhance protein stability under certain conditions (Siddiqui et al., 2005). The Cys70-Cys115 disulfide bond is unique to mammalian α-amylase. The number of disulfide bonds decreases gradually in thermophilic, mesophilic, and psychrophilic α-amylase, and the Cys70-Cys115 disulfide bond is always absent in the cold-adapted α-amylase produced by low temperature microorganisms (Janecek, 1997; Aghajari et al., 1998). Disulfide bonds often form between peptide chains over much of the molecule, so the absence of disulfide bonds leads to a decrease in the thermal stability of an enzyme while increasing the flexibility of the molecule (Siddiqui et al., 2005). Protein folding also affects the cold catalytic activity of cold-adapted enzymes. Some enzymes have similar amino acid sequences yet possess different thermodynamic effects. The weakening of interactions between N-terminal, C-terminal, and various internal domains all affects the flexibility and stability of an enzyme (Feller et al., 1999).

Hydrophobicity and hydrophobic surface area also receive particular attention in the study of cold-adapted enzyme structure and mechanism. Hydrophobic pockets in an enzyme molecule can reduce the interference of water in an enzymatic reaction, facilitate enzymatic reaction transition states, and reduce the activation energy of an enzymatic reaction, thereby reducing the energy consumption of an enzymatic reaction at low temperature. An analysis of many cold-adapted enzyme structures found that the overall hydrophobicity and number of hydrophobic surfaces of cold-adapted enzymes is significantly higher than that of homologous mesophilic or thermophilic enzymes (Zheng et al., 2016; Rutkiewicz et al., 2019). This confirms that the existence of hydrophobic pockets enables cold-adapted enzymes to catalyze reactions at lower temperature more easily.

4.2. Activation energy and cold catalysis of cold-adapted enzymes

In severely low temperature conditions, the main problem faced by cold-adapted enzymes is maintaining normal catalytic function. The catalytic efficiency of a cold-adapted enzyme is higher and the activation energy lower than that of mesophilic and thermophilic enzymes.

According to the Arrhenius equation:

$$k_{\text{cat}} = Ake^{-E_a/RT} \quad (1)$$

where "A" represents an exponential factor; "k" is the dynamic transfer coefficient (generally 1); "E_a" is the activation energy; "R" is the gas constant; and "T" is the absolute temperature. Reaction rates decrease sharply as temperature decreases. Furthermore, the viscosity of culture medium increases and the molecular diffusion rate decreases at low temperature, which also leads to a decrease in the reaction rate, that is, low temperatures influence the smooth progress of an enzymatic reaction (Siddiqui and Cavicchioli, 2006). In this case, the value of dynamic transfer coefficient "k" is not set to 1. Based on mean viscosity and transition state theory, the following results are obtained:

$$k_{\text{cat}} = \sqrt{1+(\eta'/\eta_1)} - (\eta'/\eta_1) \quad (2)$$

wherein, "η" is relative viscosity, and "η_1" is an unknown parameter that is determined according to experimental fitting. When "η_1" is greater than or equal to 10, the value "k" is close to 1 and can be obtained from Equation 1 and transitional state theory:

$$k_{\text{cat}} = (K_B T/h)e^{-\Delta G/RT} \quad (3)$$

Here "k_{cat}" is the enzymatic reaction rate; "K_B" is the Boltzmann constant ($\sim 1.38\times10^{-23}$ J·K^{-1}); "h" is Planck constant ($\sim 6.63\times10^{-34}$ J·Hz^{-1}), and "ΔG" is the activation energy.

The rate of an enzymatic reaction can be increased by lowering ΔG. This can be achieved by stabilizing an activated substrate in a transitional state or by destabilizing an enzyme–substrate complex (increasing the Michaelis constant k_m). Cold-adapted enzymes reduce activation energy at low temperatures by increasing the turnover number (k_{cat}) or by increasing enzyme–substrate complex affinity. This maintains reaction equilibrium and overcomes chemical reaction rate decreases caused by low temperatures (Zanphorlin et al., 2016).

The k_{cat}/k_m value can be used to measure the catalytic efficiency of an enzyme and the affinity of an enzyme to its substrate. Sometimes an increase in catalytic rate indicates that the activation energy of an enzyme is lower than that of other enzymes. Iyo and Forsberg (1999) compared the k_{cat}/k_m of two endoglucanases from *Fibrobacter succinogenes* S85 at different temperatures CelG was designated the cold-adapted version. The k_{cat}/k_m of CelG was 75 times and 10 times higher than that of the other endoglucanase at 4°C and 25°C, respectively, and the catalytic efficiency of CelG was also higher at these lower temperatures (Iyo and Forsberg, 1999; Table 5). Under similar low temperature conditions, the higher the k_{cat}/k_m value, the lower the activation energy. The activation energy of cold-adapted enzymes is lower than that of mesophilic or thermophilic enzymes, and this lower activation energy reduces the energy consumption of cold-adapted enzyme catalytic reactions.

TABLE 5 Kinetic parameters of Fibrobacter succinogenes S85 CelG and EGD (Iyo and Forsberg, 1999).

Enzyme	Temperature	Kinetic parameter		
		K_{cat} (s^{-1})	K_m (mg/mL)	K_{cat}/K_m
CelG	4	20.1	6.8	3.0
	25	93	55	1.7
EGD	4	0.6	16.1	0.04
	25	4.0	23.8	0.17

Enzyme molecules can assume a variety of different conformations, in which natural conformations dominate while alternate conformations can be transformed from one to another. An increase in the flexibility of an enzyme molecule can increase its number of conformational isomers, which relates to the catalytic function of the enzyme. This is because increased flexibility reduces energy consumption required for the induction of the enzyme to bind to the substrate and makes control of the isomer easier to achieve (Zecchinon et al., 2001).

Zavodsky et al. used infrared spectroscopy to detect the exchange of hydrogen and heavy hydrogen in two 3-isopropyl malate dehydrogenases, one mesophilic, one thermophilic. By comparing the relative flexibility of the two 3-isopropyl malate dehydrogenases, they found that under the most appropriate catalytic conditions, the two 3-isopropyl malate dehydrogenase structures have similar flexibility. However at room temperature, the mesophilic enzymes has a looser molecular structure compared with the thermophilic counterpart (Zavodszky et al., 1998). That is, thermophilic enzymes are less efficient at room temperature, perhaps because a more closed conformation at room temperature hinders the interactions in between enzyme-substrate complexes. In contrast, mesophilic or cold-adapted enzymes have higher conformational flexibility at room or low temperatures. These enzymes bind to substrates easier consuming less energy in the process which subsequently reduces the activation energy required for catalytic reaction and improves over efficiency.

To investigate relationships between cold-adapted enzyme structure and enzymatic reaction at cryogenic temperatures, several researchers have compared the crystal structure of a variety of cold-adapted enzymes with that of homologous mesophilic or thermophilic enzymes. Trypsin, citric acid synthase, α-amylase, and malate dehydrogenase are representative of those studied. The active sites of the cold-adapted enzymes all possess a larger cavity than homologous mesophilic and thermophilic counterparts. Therefore substrates are more easily brought closer together, thus reducing the activation energy required for enzyme-substrate complex formation. However, large active cavities may cause a reduction in enzyme-substrate affinity. This means that cold-adapted enzymes can increase the probability of complex enzyme-substrate formation by possessing a larger active site cavity, thereby increasing the rate of enzymatic reaction (Smalas et al., 1994; Russell et al., 1998; Kim et al., 1999; Aghajari et al., 2002; Voigt et al., 2002).

In summary, at low temperatures, cold-adapted enzymes ensure the smooth progress of catalytic reactions through the following three strategies: (1) Flexibility of the structural domain in the molecule is increased which increases the affinity of the enzyme-substrate complex, thereby reducing the activation energy required by the chemical reaction and ensuring the smooth progress of the catalytic reaction at low temperature. (2) Hydrophobic surface area within the hydrophobic pocket is increased, which reduces the interference of water on the enzymatic reaction thus the enzymatic reaction more easily to forms a transition state, t the activation energy required by

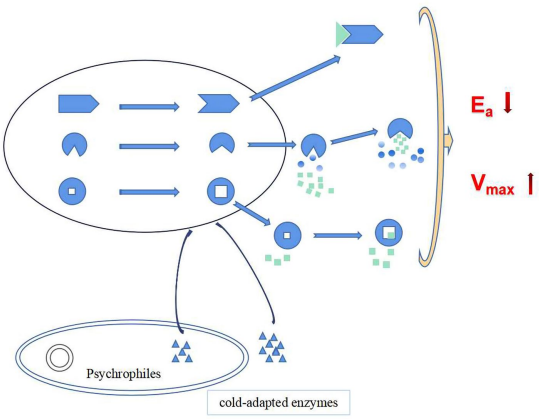

FIGURE 8
Cold catalytic mechanism of cold-adapted enzymes (green square and triangle as substrate molecules, gradient color round as water molecules).

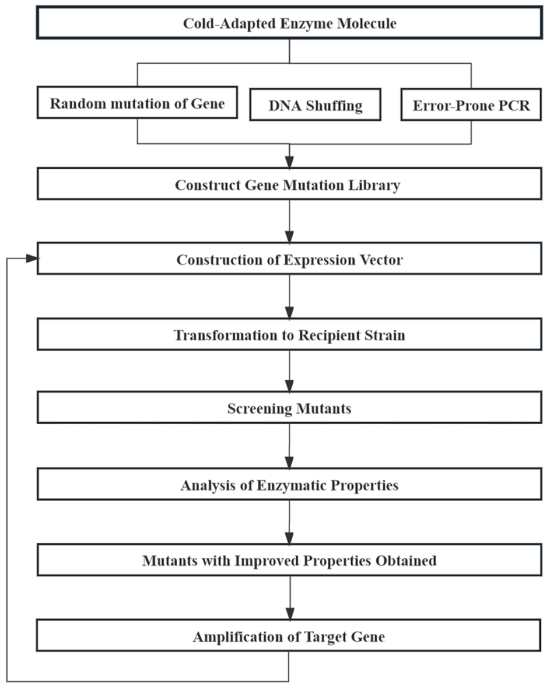

FIGURE 9
Basic process of enzyme molecules irrational design.

the enzymatic reaction is reduced, and energy consumption of the enzymatic reaction at low temperature is reduced. (3) Formation of a larger cavity in the active site increases the probability for the formation of an enzyme-substrate complex, thereby increasing the enzymatic reaction rate (Figure 8; Mangiagalli and Lotti, 2021).

5. Cold-adapted enzyme molecular modification

Cold-adapted enzymes can catalyze biological reactions at low temperatures. These enzymes have the advantage of requiring low temperatures to achieve activation, and so are widely used in industry. However, owing to inherent structural characteristics, naturally low-temperature enzymes have greater sensitivity to pH, metal ions, and organic solvents, which confer the characteristics of low thermodynamic stability, and easy inactivation. Furthermore the reaction condition requirements of cold-adapted enzymes are often difficult to meet in industrial production processes resulting in enzymatic inactivation. Therefore, the molecular modification of cold-adapted enzymes has become a hot topic (Shemsi et al., 2019). Molecular modification of naturally cold-adapted enzymes can be achieved using rational or irrational design.

5.1. Irrational design

Irrational design of enzyme molecules is also known as directed evolution. Using known structural information and the catalytic mechanism of enzyme molecules, by simulating random mutation, and by using recombination and other natural evolutionary mechanisms, directional pressure can be exerted in later screening process to obtain desired mutants with excellent performance (Jackel et al., 2008). Irrational design needs to construct an efficient mutant library and screening system using error-prone PCR, DNA shuffling, or other technologies to obtain target enzyme molecules (Figure 9; Yang et al., 2014). LipC, a cold-catalyzed lipase derived from a psychrophilic strain of *Pseudomonas aeruginosa*, is a cold-acting lipase that tolerates elevated concentrations of ions and heavy metals. The enzyme has strong substrate specificity at elevated temperatures but loses stability at those temperatures. Cesarini et al. (2012) constructed eight LipC mutant libraries with two point mutations using error-prone PCR technology and then screened for a mutant with both cold catalytic properties and thermal stability from more than 3,000 mutant clones.

DNA shuffling technology can obtain a large number of mutations through *in vitro* recombination. Wintrode et al. (2001) performed eight cycles of mutation recombination on subtilisin S41 using DNA shuffling technology, and inactivation temperatures of an obtained mutant increased by 25°C. Furthermore, constructing mutant libraries using multi-technology is common in the irrational modification of cold-adapted enzymes. Arrizubieta and Polaina (2000) combined error-prone PCR and DNA shuffling technology to increase the half-life of *Paenibacillus polymyxa* β-galactosidase by 20 times at 55°C. The irrational design of enzymatic molecules does not target a specific targeted modification, rather it is random. Therefore, owing to its large workload and low probability of obtaining positive mutants, it is seldom applied to the modification of cold-adapted enzymes.

5.2. Rational design

Rational design attempts to derive and design a specific amino acid sequence that corresponds to a specific function based on the secondary and tertiary structure of representative enzymatic molecules. Site-directed mutagenesis is used to achieve the amino acid substitutions necessary for the desired structure (Figure 10; Oskarsson and Kristjansson, 2019; Oskarsson et al., 2020). Several strategies, including homologous sequence alignment, disulfide bond-based design, and SCHEMA simulation, have been used to improve the thermostability of cold-adapted enzymes (Voigt et al., 2002; Veno et al., 2019).

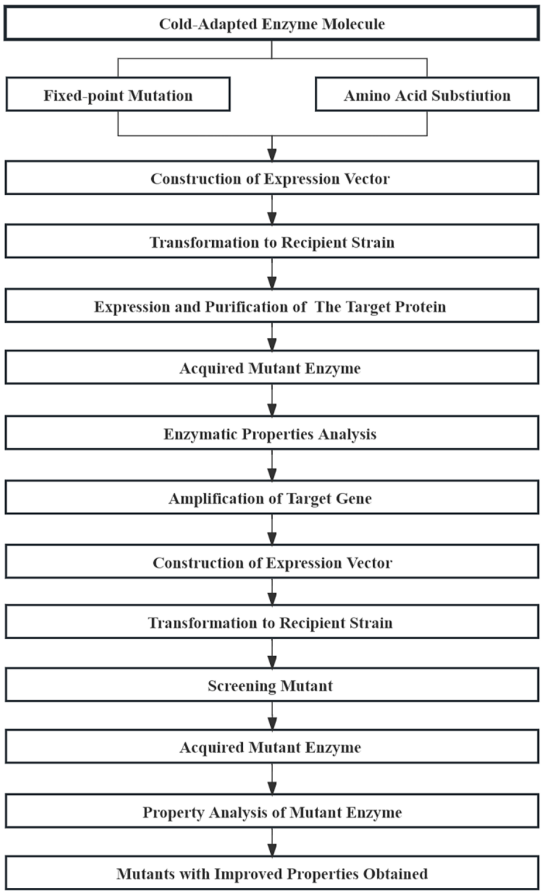

FIGURE 10
Basic process of enzyme molecule rational design.

Chang et al. (2016) analyzed the pullulanase sequence of *Bacillus naganoensis* using homologous sequence alignment. Six site-directed mutants were obtained and three screened positive for higher thermostability after mutagenesis. Thermal stability is an ideal characteristic for the preservation and application of various cold-adapted lipases. The thermal stability of a cold-adapted lipase can be improved by introducing a cysteine residue into the "cap region" of a cold-adapted lipase (Veno et al., 2019). According to the proline law, Yang et al. (2017) introduced proline residues into the A and B domains of the surface loop of α-amylase from the Antarctic ciliated protozoon *Euplotes focardii* (EfAmy), which greatly improved the thermostability and catalytic efficiency of the enzyme. Presently, most enzyme molecule modifications rely on the crystal structure of that enzyme or homologous molecules and ignore the influence of enzymatic molecular dynamics. Li et al. (2020) combined molecular dynamics simulations and energy optimization methods to design unconserved residue mutants of cold-adapted α-amylase (PHA) from *Pseudoalteromonas haloplanktis* and was able to obtain double mutants with higher thermal stability than the native enzyme.

6. Discussion

In nature, more than 80% of ambient temperatures are below 5°C, while in the north and south poles, the average sea temperature is −1.8°C, and even in summer, the average soil temperature does not exceed 10°C. A large variety of microorganisms exist at such low temperatures, of which bacteria are the most diverse. Cold-adapted, also know as psychrophilic, bacteria have adapted to these cold environments. These bacteria have unique metabolic mechanisms, controlled by unique enzymes. Cold-adapted bacteria have gained the ability to produce cold-adapted enzymes during long-term evolutionary processes. Cold-adapted enzymes have high molecular structural flexibilities and low activation energies and, therefore, can catalyze enzymatic reactions at high rates at low temperatures. Consequently these enzymes have a wide range of applications in various fields.

More than 100 cold-adapted enzymes have been successfully expressed so far, and these cold-adapted enzymes have very good application prospects in food processing, the detergents industry, medical field, environmental protection, and basic molecular biology research. But most cold-adapted enzymes have been found from cultured microorganisms or from the metagenomes of uncultured microorganisms and are primarily derived from deep-sea oceans, high-elevation plains and mountain soils, or polar region habitats. Owing to these extreme environments, many of these psychrophilic microorganisms are difficult to culture, which makes the isolation, purification, and catalytic mechanism research of cold-adapted enzymes from these microorganisms particularly difficult. In addition, presently the unsolved problem remains that most cold-adapted enzymes are quite unstable in structure making it difficult to fully realize industrial production and application. The amino acid sequence, secondary structure, and the higher structure of cold-adapted enzymes are different from those of mesophilic and thermophilic enzymes. It is these structural characteristics that lead to a looser structure, less stability, and higher modification requirements of cold-adapted enzymes.

Enzyme immobilization and chemical and physical modification methods to address these issues affect the catalytic efficacy of the enzymes to a certain extent. Most modifications of cold-adapted enzymes are based on molecular biology and use rational or irrational design protocols. Modification methods for mesophilic and thermophilic enzymes have often been reported using these methods. However, cold-adapted enzyme modification by saturation mutagenesis and fixed-point mutation based on computer prediction and irrational design are less reported. This severely limits the development of cold-adapted enzyme modification and application. Therefore, we discuss cold catalysis mechanisms and strategies for improving the stability of cold enzymes in this review, hoping to lay a theoretical foundation for the research and application of cold-adapted enzymes in the future.

Author contributions

YL, NZ, QZ, and SZ: conceptualization. YL, NZ, JM, QW, QZ, and SZ: visualization. YL: writing-original draft. YL, SZ, CT, YF, GC, and RZ: writing-review and editing. All authors contributed to the article and approved the submitted version.

Funding

This work was supported by the Natural Science Foundation of Science and Technology Department of Jilin Province (grant number: 20220101334JC), the Chinese Academy of Sciences Strategic Pilot Science and Technology Project XDA28020400, the Key Projects of

the Jilin Province Science and Technology Development Plan (grant number: 20210203117SF).

Conflict of interest

The authors declare that the research was conducted in the absence of any commercial or financial relationships that could be construed as a potential conflict of interest.

Publisher's note

References

Abrashev, R., Feller, G., Kostadinova, N., Krumova, E., Alexieva, Z., Gerginova, M., et al. (2016). Production, purification, and characterization of a novel cold-active superoxide dismutase from the Antarctic strain *Aspergillus glaucus* 363. *Fungal Biol.* 120, 679–689. doi: 10.1016/j.funbio.2016.03.002

Aghajari, N., Feller, G., Gerday, C., and Haser, R. (1998). Structures of the psychrophilic *Alteromonas haloplanctis* alpha-amylase give insights into cold adaptation at a molecular level. *Structure* 6, 1503–1516. doi: 10.1016/s0969-2126(98)00149-x

Aghajari, N., Roth, M., and Haser, R. (2002). Crystallographic evidence of a transglycosylation reaction: ternary complexes of a psychrophilic alpha-amylase. *Biochemistry* 41, 4273–4280. doi: 10.1021/bi0160516

Albino, A., de Angelis, A., Marco, S., Severino, V., Chambery, A., di Maro, A., et al. (2014). The cold-adapted gamma-glutamyl-cysteine ligase from the psychrophile *Pseudoalteromonas haloplanktis*. *Biochimie* 104, 50–60. doi: 10.1016/j.biochi.2014.05.003

Albino, A., Marco, S., Di Maro, A., Chambery, A., Masullo, M., and De Vendittis, E. (2012). Characterization of a cold-adapted glutathione synthetase from the psychrophile *Pseudoalteromonas haloplanktis*. *Mol. BioSyst.* 8, 2405–2414. doi: 10.1039/c2mb25116g

Aqvist, J. (2017). Cold adaptation of triosephosphate isomerase. *Biochemistry* 56, 4169–4176. doi: 10.1021/acs.biochem.7b00523

Arrizubieta, M. J., and Polaina, J. (2000). Increased thermal resistance and modification of the catalytic properties of a β-glucosidase by random mutagenesis andin vitro recombination. *J. Biol. Chem.* 275, 28843–28848. doi: 10.1074/jbc.M003036200

Baldwin, J., and Hochachka, P. W. (1970). Functional significance of isoenzymes in thermal acclimatization. Acetylcholinesterase from trout brain. *Biochem. J.* 116, 883–887. doi: 10.1042/bj1160883

Bentahir, M., Feller, G., Aittaleb, M., Lamotte-Brasseur, J., Himri, T., Chessa, J. P., et al. (2000). Structural, kinetic, and calorimetric characterization of the cold-active phosphoglycerate kinase from the Antarctic *Pseudomonas* sp. Tacii18. *J. Biol. Chem.* 275, 11147–11153. doi: 10.1074/jbc.275.15.11147

Berchet, V., Boulanger, D., and Gounot, A. M. (2000). Use of gel electrophoresis for the study of enzymatic activities of cold-adapted bacteria. *J. Microbiol. Methods* 40, 105–110. doi: 10.1016/S0167-7012(99)00141-4

Berg, K., Leiros, I., and Williamson, A. (2019). Temperature adaptation of DNA ligases from psychrophilic organisms. *Extremophiles* 23, 305–317. doi: 10.1007/s00792-019-01082-y

Budiman, C., Koga, Y., Takano, K., and Kanaya, S. (2011). Fk506-binding protein 22 from a psychrophilic bacterium, a cold shock-inducible peptidyl prolyl isomerase with the ability to assist in protein folding. *Int. J. Mol. Sci.* 12, 5261–5284. doi: 10.3390/ijms12085261

Carrasco, M., Alcaino, J., Cifuentes, V., and Baeza, M. (2017). Purification and characterization of a novel cold adapted fungal glucoamylase. *Microb. Cell Factories* 16:75. doi: 10.1186/s12934-017-0693-x

Castellano, I., Di Maro, A., Ruocco, M. R., Chambery, A., Parente, A., Di Martino, M. T., et al. (2006). Psychrophilic superoxide dismutase from *Pseudoalteromonas haloplanktis*: biochemical characterization and identification of a highly reactive cysteine residue. *Biochimie* 88, 1377–1389. doi: 10.1016/j.biochi.2006.04.005

Cavicchioli, R., Charlton, T., Ertan, H., Mohd, O. S., Siddiqui, K. S., and Williams, T. J. (2011). Biotechnological uses of enzymes from psychrophiles. *Microb. Biotechnol.* 4, 449–460. doi: 10.1111/j.1751-7915.2011.00258.x

Cesarini, S., Bofill, C., Pastor, F. I. J., Reetz, M. T., and Diaz, P. (2012). A thermostable variant of *P. aeruginosa* cold-adapted LipC obtained by rational design and saturation mutagenesis. *Process Biochem.* 47, 2064–2071. doi: 10.1016/j.procbio.2012.07.023

Champagne, K. S., Sissler, M., Larrabee, Y., Doublie, S., and Francklyn, C. S. (2005). Activation of the hetero-octameric ATP phosphoribosyl transferase through subunit interface rearrangement by a tRNA synthetase paralog. *J. Biol. Chem.* 280, 34096–34104. doi: 10.1074/jbc.M505041200

Chang, M., Chu, X., Lv, J., Li, Q., Tian, J., and Wu, N. (2016). Improving the thermostability of acidic pullulanase from *Bacillus naganoensis* by rational design. *PLoS One* 11:11. doi: 10.1371/journal.pone.0165006

Chen, C., Cao, S., Zhu, B., Jiang, L., and Yao, Z. (2023). Biochemical characterization and elucidation the degradation pattern of a new cold-adapted and ca(2+) activated alginate lyase for efficient preparation of alginate oligosaccharides. *Enzym. Microb. Technol.* 162:110146. doi: 10.1016/j.enzmictec.2022.110146

Chen, X. L., Dong, S., Xu, F., Dong, F., Li, P. Y., Zhang, X. Y., et al. (2016). Characterization of a new cold-adapted and salt-activated polysaccharide lyase family 7 alginate lyase from *Pseudoalteromonas* sp. Sm0524. *Front Microbiol.* 7:1120. doi: 10.3389/fmicb.2016.01120

D'Amico, S., Marx, J. C., Gerday, C., and Feller, G. (2003). Activity-stability relationships in extremophilic enzymes. *J. Biol. Chem.* 278, 7891–7896. doi: 10.1074/jbc.M212508200

DangThu, Q., Jang, S. H., and Lee, C. (2020). Biochemical comparison of two glucose 6-phosphate dehydrogenase isozymes from a cold-adapted *Pseudomonas mandelii*. *Extremophiles* 24, 501–509. doi: 10.1007/s00792-020-01171-3

de Melo, R. R., de Lima, E. A., Persinoti, G. F., Vieira, P. S., de Sousa, A. S., Zanphorlin, L. M., et al. (2021). Identification of a cold-adapted and metal-stimulated beta-1,4-glucanase with potential use in the extraction of bioactive compounds from plants. *Int. J. Biol. Macromol.* 166, 190–199. doi: 10.1016/j.ijbiomac.2020.10.137

Deng, T., Feng, Y., Xu, L., Tian, X., Lai, X., Lyu, M., et al. (2020). Expression, purification and characterization of a cold-adapted dextranase from marine bacteria and its ability to remove dental plaque. *Protein Expr. Purif.* 174:105678. doi: 10.1016/j.pep.2020.105678

Edser, C. (2004). Dupont preferenz preferred stain removal technoiogy for laundry. Focus on Surfactants.

Esteban-Torres, M., Santamaría, L., de Las Rivas, B., and Muñoz, R. (2014). Characterisation of a cold-active and salt-tolerant esterase from *Lactobacillus plantarum* with potential application during cheese ripening. *Int. Dairy J.* 39, 312–315. doi: 10.1016/j.idairyj.2014.08.004

Feller, G., Arpigny, J. L., Narinx, E., and Gerday, C. (1997). Molecular adaptations of enzymes from psychrophilic organisms. *Comp. Biochem. Physiol. A Physiol.* 118, 495–499. doi: 10.1016/S0300-9629(97)00011-X

Feller, G., D'Amico, D., and Gerday, C. (1999). Thermodynamic stability of a cold-active alpha-amylase from the Antarctic bacterium *Alteromonas haloplanctis*. *Biochemistry* 38, 4613–4619. doi: 10.1021/bi982650+

Gao, S., Zhang, Z., Li, S., Su, H., Tang, L., Tan, Y., et al. (2018). Characterization of a new endo-type polysaccharide lyase (pl) family 6 alginate lyase with cold-adapted and metal ions-resisted property. *Int J Biol Macromol. Pt A* 120, 729–735. doi: 10.1016/j.ijbiomac.2018.08.164

Ge, J., Jiang, X., Liu, W., Wang, Y., Huang, H., Bai, Y., et al. (2020). Characterization, stability improvement, and bread baking applications of a novel cold-adapted glucose oxidase from *Cladosporium neopsychrotolerans* sl16. *Food Chem.* 310:125970. doi: 10.1016/j.foodchem.2019.125970

Georlette, D., Jónsson, Z. O., van Petegem, F., Chessa, J., van Beeumen, J., Hübscher, U., et al. (2000). A dna ligase from the psychrophile *Pseudoalteromonas haloplanktis* gives insights into the adaptation of proteins to low temperatures. *Eur. J. Biochem.* 267, 3502–3512. doi: 10.1046/j.1432-1327.2000.01377.x

Hassan, S., Abd, E. L. H., and Ali, S. M. (2018). Production of cold-active lipase by free and immobilized marine *Bacillus cereus* HSS: application in wastewater treatment. *Front. Microbiol.* 9:2377. doi: 10.3389/fmicb.2018.02377

Hou, Y., Qiao, C., Wang, Y., Wang, Y., Ren, X., Wei, Q., et al. (2019). Cold-adapted glutathione s-transferases from Antarctic psychrophilic bacterium *Halomonas* sp. Ant108: heterologous expression, characterization, and oxidative resistance. *Mar. Drugs* 17:17. doi: 10.3390/md17030147

Huang, H., Li, S., Bao, S., Mo, K., Sun, D., and Hu, Y. (2021). Expression and characterization of a cold-adapted alginate lyase with exo/endo-type activity from a novel marine bacterium *Alteromonas portus* hb161718(t). *Mar. Drugs* 19:19. doi: 10.3390/md19030155

Isaksen, G. V., Aqvist, J., and Brandsdal, B. O. (2016). Enzyme surface rigidity tunes the temperature dependence of catalytic rates. *Proc. Natl. Acad. Sci. U. S. A.* 113, 7822–7827. doi: 10.1073/pnas.1605237113

Iyo, A. H., and Forsberg, C. W. (1999). A cold-active glucanase from the ruminal bacterium *Fibrobacter succinogenes* s85. *Appl. Environ. Microbiol.* 65, 995–998. doi: 10.1128/AEM.65.3.995-998.1999

Jackel, C., Kast, P., and Hilvert, D. (2008). Protein design by directed evolution. *Annu. Rev. Biophys.* 37, 153–173. doi: 10.1146/annurev.biophys.37.032807.125832

Janecek, S. (1997). Alpha-amylase family: molecular biology and evolution. *Prog. Biophys. Mol. Biol.* 67, 67–97. doi: 10.1016/s0079-6107(97)00015-1

Ji, L., Yang, J., Fan, H., Yang, Y., Li, B., Yu, X., et al. (2014). Synergy of crude enzyme cocktail from cold-adapted *Cladosporium cladosporioides* ch2-2 with commercial xylanase achieving high sugars yield at low cost. *Biotechnol. Biofuels* 7:130. doi: 10.1186/s13068-014-0130-x

Jiang, Z. Q., Yang, S. Q., Tan, S. S., Li, L. T., and Li, X. T. (2005). Characterization of a xylanase from the newly isolated thermophilic *Thermomyces lanuginosus* cau44 and its application in bread making. *Lett. Appl. Microbiol.* 41, 69–76. doi: 10.1111/j.1472-765X.2005.01725.x

Kim, S. Y., Hwang, K. Y., Kim, S. H., Sung, H. C., Han, Y. S., and Cho, Y. (1999). Structural basis for cold adaptation. Sequence, biochemical properties, and crystal structure of malate dehydrogenase from a psychrophile *Aquaspirillium arcticum*. *J. Biol. Chem.* 274, 11761–11767. doi: 10.1074/jbc.274.17.11761

Kim, H. D., Kim, S. M., and Choi, J. I. (2018). Purification, characterization, and cloning of a cold-adapted protease from antarctic *Janthinobacterium lividum*. *J. Microbiol. Biotechnol.* 28, 448–453. doi: 10.4014/jmb.1711.11006

Kim, D. Y., Kim, J., Lee, Y. M., Lee, J. S., Shin, D. H., Ku, B. H., et al. (2021). Identification and characterization of a novel, cold-adapted d-xylobiose- and d-xylose-releasing endo-beta-1,4-xylanase from an Antarctic soil bacterium, *Duganella* sp. PAMC 27433. *Biomolecules* 11:11. doi: 10.3390/biom11050680

Kim, S. M., Park, H., and Choi, J. I. (2017). Cloning and characterization of cold-adapted alpha-amylase from Antarctic *Arthrobacter agilis*. *Appl. Biochem. Biotechnol.* 181, 1048–1059. doi: 10.1007/s12010-016-2267-5

Kobori, H., Sullivan, C. W., and Shizuya, H. (1984). Heat-labile alkaline phosphatase from Antarctic bacteria: rapid 5′ end-labeling of nucleic acids. *Proc. Natl. Acad. Sci. U. S. A.* 81, 6691–6695. doi: 10.1073/pnas.81.21.6691

Krishna, T. C., Najda, A., Bains, A., Tosif, M. M., Papliński, R., Kapłan, M., et al. (2021). Influence of ultra-heat treatment on properties of milk proteins. *Polymers (Basel)* 13:13. doi: 10.3390/polym13183164

Krumova, E., Abrashev, R., Dishliyska, V., Stoyancheva, G., Kostadinova, N., Miteva-Staleva, J., et al. (2021). Cold-active catalase from the psychrotolerant fungus *Penicillium griseofulvum*. *J. Basic Microbiol.* 61, 782–794. doi: 10.1002/jobm.202100209

Kuddus, M.,Roohi,Saima,Ahmad, I. Z. (2012). Cold-active extracellular α-amylase production from novel bacteria microbacterium foliorum ga2 and *Bacillus cereus* ga6 isolated from *Gangotri glacier*, Western Himalaya. *J. Genet. Eng. Biotechnol.* 10:151–159. doi: 10.1016/j.jgeb.2012.03.002

Kuddus, M., and Ramteke, P. W. (2009). Cold-active extracellular alkaline protease from an alkaliphilic *Stenotrophomonas maltophilia*: production of enzyme and its industrial applications. *Can. J. Microbiol.* 55, 1294–1301. doi: 10.1139/w09-089

Kulakova, L., Galkin, A., Kurihara, T., Yoshimura, T., and Esaki, N. (1999). Cold-active serine alkaline protease from the psychrotrophic bacterium *Shewanella* strain ac10: gene cloning and enzyme purification and characterization. *Appl. Environ. Microbiol.* 65, 611–617. doi: 10.1128/AEM.65.2.611-617.1999

Kumar, A., Mukhia, S., and Kumar, R. (2021). Industrial applications of cold-adapted enzymes: challenges, innovations and future perspective, Industrial applications of cold-adapted enzymes: challenges, innovations and future perspective 11, 426. doi: 10.1007/s13205-021-02929-y

Land, H., Campillo-Brocal, J. C., Svedendahl, H. M., and Berglund, P. (2019). B-factor guided proline substitutions in chromobacterium violaceum amine transaminase: evaluation of the proline rule as a method for enzyme stabilization. *Chembiochem* 20, 1297–1304. doi: 10.1002/cbic.201800749

Lee, S., Wang, C., Liu, H., Xiong, J., Jiji, R., Hong, X., et al. (2017). Hydrogen bonds are a primary driving force for de novo protein folding. *Acta. Crystallogr. D Struct. Biol. Pt* 73, 955–969. doi: 10.1107/S2059798317015303

Li, Y., Kong, X., and Zhang, H. (2019). Characteristics of a novel manganese superoxide dismutase of a hadal sea cucumber (*Paelopatides* sp.) from the mariana trench. *Mar. Drugs* 17:17. doi: 10.3390/md17020084

Li, Q., Yan, Y., Liu, X., Zhang, Z., Tian, J., and Wu, N. (2020). Enhancing thermostability of a psychrophilic alpha-amylase by the structural energy optimization in the trajectories of molecular dynamics simulations. *Int. J. Biol. Macromol.* 142, 624–633. doi: 10.1016/j.ijbiomac.2019.10.004

Li, X., Zhang, L., Jiang, Z., Liu, L., Wang, J., Zhong, L., et al. (2022). A novel cold-active gh8 xylanase from cellulolytic myxobacterium and its application in food industry. *Food Chem.* 393:133463. doi: 10.1016/j.foodchem.2022.133463

Liu, Y., Wu, Z., Zeng, X., Weng, P., Zhang, X., and Wang, C. (2021). A novel cold-adapted phospho-beta-galactosidase from *Bacillus velezensis* and its potential application for lactose hydrolysis in milk. *Int. J. Biol. Macromol.* 166, 760–770. doi: 10.1016/j.ijbiomac.2020.10.233

Lu, M., Wang, S., Fang, Y., Li, H., Liu, S., and Liu, H. (2010). Cloning, expression, purification, and characterization of cold-adapted alpha-amylase from *Pseudoalteromonas arctica* gs230. *Protein J.* 29, 591–597. doi: 10.1007/s10930-010-9290-0

Mahdavi, A., Sajedi, R. H., Asghari, S. M., Taghdir, M., and Rassa, M. (2011). An analysis of temperature adaptation in cold active, mesophilic and thermophilic bacillus alpha-amylases. *Int. J. Biol. Macromol.* 49, 1038–1045. doi: 10.1016/j.ijbiomac.2011.08.030

Mangiagalli, M., Brocca, S., Orlando, M., and Lotti, M. (2020). The "cold revolution". Present and future applications of cold-active enzymes and ice-binding proteins. *New Biotechnol.* 55, 5–11. doi: 10.1016/j.nbt.2019.09.003

Mangiagalli, M., and Lotti, M. (2021). Cold-active beta-galactosidases: insight into cold adaption mechanisms and biotechnological exploitation. *Mar. Drugs* 19:19. doi: 10.3390/md19010043

Margesin, R., and Schinner, F. (1992). Extracellular protease production by psychrotrophic bacteria from glaciers. *Int. Biodeterior. Biodegradation* 29, 177–189. doi: 10.1016/0964-8305(92)90015-G

Mhetras, N., Mapare, V., and Gokhale, D. (2021). Cold active lipases: biocatalytic tools for greener technology. *Appl. Biochem. Biotechnol.* 193, 2245–2266. doi: 10.1007/s12010-021-03516-w

Mohammed, K., and Pramod, W. R. (2011). Production optimization of an extracellular cold-active alkaline protease from *Stenotrophomonas maltophilia* mtcc 7528 and its application in detergent industry. *Afr. J. Microbiol. Res.* 5, 809–816. doi: 10.5897/AJMR10.806

Mojallali, L., Shahbani, Z. H., Rajaei, S., Akbari, N. K., and Haghbeen, K. (2014). A novel approximately 34-kda alpha-amylase from psychrotroph *Exiguobacterium* sp. Sh3: production, purification, and characterization. *Biotechnol. Appl. Biochem.* 61, 118–125. doi: 10.1002/bab.1140

Moran, A. J., Hills, M., Gunton, J., and Nano, F. E. (2001). Heat-labile proteases in molecular biology applications. *FEMS Microbiol. Lett.* 197, 59–63. doi: 10.1111/j.1574-6968.2001.tb10583.x

Munshi, S., Rajamoorthi, A., and Stanley, R. J. (2017). Characterization of a cold-adapted DNA photolyase from c. psychrerythraea 34h. *Extremophiles* 21, 919–932. doi: 10.1007/s00792-017-0953-z

Narayanankutty, A., Job, J. T., and Narayanankutty, V. (2019). Glutathione, an antioxidant tripeptide: dual roles in carcinogenesis and chemoprevention. *Curr. Protein Pept. Sci.* 20, 907–917. doi: 10.2174/1389203720666190206130003

Oskarsson, K. R., and Kristjansson, M. M. (2019). Improved expression, purification and characterization of vpr, a cold active subtilisin-like serine proteinase and the effects of calcium on expression and stability. *Biochim. Biophys. Acta Proteins Proteom.* 1867, 152–162. doi: 10.1016/j.bbapap.2018.11.010

Oskarsson, K. R., Saevarsson, A. F., and Kristjansson, M. M. (2020). Thermostabilization of VPR, a kinetically stable cold adapted subtilase, via multiple proline substitutions into surface loops. *Sci. Rep.* 10:10. doi: 10.1038/s41598-020-57873-3

Pallardo, F. V., Markovic, J., Garcia, J. L., and Vina, J. (2009). Role of nuclear glutathione as a key regulator of cell proliferation. *Mol. Asp. Med.* 30, 77–85. doi: 10.1016/j.mam.2009.01.001

Pedersen, H. L., Willassen, N. P., and Leiros, I. (2009). The first structure of a cold-adapted superoxide dismutase (SOD): biochemical and structural characterization of iron SOD from *Aliivibrio salmonicida*. *Acta Crystallogr sect F Struct biol Cryst Commun* 65, 84–92. doi: 10.1107/S1744309109001110

Pereira, J. Q., Ambrosini, A., Passaglia, L., and Brandelli, A. (2017). A new cold-adapted serine peptidase from Antarctic *Lysobacter* sp. A03: insights about enzyme activity at low temperatures. *Int. J. Biol. Macromol.* 103, 854–862. doi: 10.1016/j.ijbiomac.2017.05.142

Raymond-Bouchard, I., Goordial, J., Zolotarov, Y., Ronholm, J., Stromvik, M., Bakermans, C., et al. (2018). Conserved genomic and amino acid traits of cold adaptation in subzero-growing arctic permafrost bacteria. *FEMS Microbiol. Ecol.* 94. doi: 10.1093/femsec/fiy023

Rina, M., Pozidis, C., Mavromatis, K., Tzanodaskalaki, M., Kokkinidis, M., and Bouriotis, V. (2000). Alkaline phosphatase from the antarctic strain tab5. Properties and psychrophilic adaptations. *Eur. J. Biochem.* 267, 1230–1238. doi: 10.1046/j.1432-1327.2000.01127.x

Russell, R. J., Gerike, U., Danson, M. J., Hough, D. W., and Taylor, G. L. (1998). Structural adaptations of the cold-active citrate synthase from an antarctic bacterium. *Structure* 6, 351–361. doi: 10.1016/s0969-2126(98)00037-9

Rutkiewicz, M., Bujacz, A., and Bujacz, G. (2019). Structural features of cold-adapted dimeric gh2 beta-d-galactosidase from *Arthrobacter* sp. 32cb. *Biochim. Biophys. Acta Proteins Proteom.* 1867, 776–786. doi: 10.1016/j.bbapap.2019.06.001

Salwoom, L., Raja, A. R. R., Salleh, A. B., Mohd, S. F., Convey, P., and Mohamad, A. M. (2019). New recombinant cold-adapted and organic solvent tolerant lipase from psychrophilic *Pseudomonas* sp. Lsk25, isolated from signy island Antarctica. *Int. J. Mol. Sci.* 20:20. doi: 10.3390/ijms20061264

Santiago, M., Ramirez-Sarmiento, C. A., Zamora, R. A., and Parra, L. P. (2016). Discovery, molecular mechanisms, and industrial applications of cold-active enzymes. *Front. Microbiol.* 7:1408. doi: 10.3389/fmicb.2016.01408

Sarmiento, F., Peralta, R., and Blamey, J. M. (2015). Cold and hot extremozymes: industrial relevance and current trends. *Front. Bioeng. Biotechnol.* 3:148. doi: 10.3389/fbioe.2015.00148

Shemsi, A. M., Khanday, F. A., Qurashi, A., Khalil, A., Guerriero, G., and Siddiqui, K. S. (2019). Site-directed chemically-modified magnetic enzymes: fabrication, improvements, biotechnological applications and future prospects. *Biotechnol. Adv.* 37, 357–381. doi: 10.1016/j.biotechadv.2019.02.002

Siddiqui, K. S. (2015). Some like it hot, some like it cold: temperature dependent biotechnological applications and improvements in extremophilic enzymes. *Biotechnol. Adv.* 33, 1912–1922. doi: 10.1016/j.biotechadv.2015.11.001

Siddiqui, K. S., and Cavicchioli, R. (2006). Cold-adapted enzymes. *Annu. Rev. Biochem.* 75, 403–433. doi: 10.1146/annurev.biochem.75.103004.142723

Siddiqui, K. S., Poljak, A., Guilhaus, M., Feller, G., D'Amico, S., Gerday, C., et al. (2005). Role of disulfide bridges in the activity and stability of a cold-active alpha-amylase. *J. Bacteriol.* 187, 6206–6212. doi: 10.1128/JB.187.17.6206-6212.2005

Smalas, A. O., Heimstad, E. S., Hordvik, A., Willassen, N. P., and Male, R. (1994). Cold adaption of enzymes: structural comparison between salmon and bovine trypsins. *Proteins* 20, 149–166. doi: 10.1002/prot.340200205

Stroek, R., Ge, Y., Talbot, P. D., Glok, M. K., Bernas, K. E., Thomson, C. M., et al. (2017). Kinetics and structure of a cold-adapted hetero-octameric ATP phosphoribosyltransferase. *Biochemistry* 56, 793–803. doi: 10.1021/acs.biochem.6b01138

Sun, J., Wang, W., Yao, C., Dai, F., Zhu, X., Liu, J., et al. (2018). Overexpression and characterization of a novel cold-adapted and salt-tolerant gh1 beta-glucosidase from the marine bacterium *Alteromonas* sp. L82. *J. Microbiol.* 56, 656–664. doi: 10.1007/s12275-018-8018-2

Tian, Q., Dou, X., Huang, L., Wang, L., Meng, D., Zhai, L., et al. (2020). Characterization of a robust cold-adapted and thermostable laccase from *Pycnoporus* sp. Sybc-l10 with a strong ability for the degradation of tetracycline and oxytetracycline by laccase-mediated oxidation. *J. Hazard. Mater.* 382:121084. doi: 10.1016/j.jhazmat.2019.121084

Ugidos-Rodriguez, S., Matallana-Gonzalez, M. C., and Sanchez-Mata, M. C. (2018). Lactose malabsorption and intolerance: a review. *Food Funct.* 9, 4056–4068. doi: 10.1039/c8fo00555a

Vega, M. C., Zou, P., Fernandez, F. J., Murphy, G. E., Sterner, R., Popov, A., et al. (2005). Regulation of the hetero-octameric atp phosphoribosyl transferase complex from thermotoga maritima by a trna synthetase-like subunit. *Mol. Microbiol.* 55, 675–686. doi: 10.1111/j.1365-2958.2004.04422.x

Veno, J., Rahman, R., Masomian, M., Ali, M., and Kamarudin, N. (2019). Insight into improved thermostability of cold-adapted staphylococcal lipase by glycine to cysteine mutation. *Molecules* 24:24. doi: 10.3390/molecules24173169

Voigt, C. A., Martinez, C., Wang, Z. G., Mayo, S. L., and Arnold, F. H. (2002). Protein building blocks preserved by recombination. *Nat. Struct. Biol.* 9, 553–558. doi: 10.1038/nsb805

Wang, Z. P., Cao, M., Li, B., Ji, X. F., Zhang, X. Y., Zhang, Y. Q., et al. (2020). Cloning, secretory expression and characterization of a unique pH-stable and cold-adapted alginate lyase. *Mar. Drugs* 18:18. doi: 10.3390/md18040189

Wang, Y., Hou, Y., Wang, Y., Zheng, L., Xu, X., Pan, K., et al. (2018). A novel cold-adapted leucine dehydrogenase from Antarctic sea-ice bacterium *Pseudoalteromonas* sp. Ant178. *Mar. Drugs* 16:16. doi: 10.3390/md16100359

Wang, X., Kan, G., Ren, X., Yu, G., Shi, C., Xie, Q., et al. (2018). Molecular cloning and characterization of a novel alpha-amylase from Antarctic sea ice bacterium *Pseudoalteromonas* sp. M175 and its primary application in detergent. *Biomed Res Int.* 2018:3258383. doi: 10.1155/2018/3258383

Wang, Q., Nie, P., Hou, Y., and Wang, Y. (2020). Purification, biochemical characterization and dna protection against oxidative damage of a novel recombinant superoxide dismutase from psychrophilic bacterium *Halomonas* sp. Ant108. *Protein Expr. Purif.* 173:105661. doi: 10.1016/j.pep.2020.105661

Wang, Q. F., Wang, Y. F., Hou, Y. H., Shi, Y. L., Han, H., Miao, M., et al. (2016). Cloning, expression and biochemical characterization of recombinant superoxide dismutase from Antarctic psychrophilic bacterium *Pseudoalteromonas* sp. Ant506. *J. Basic Microbiol.* 56, 753–761. doi: 10.1002/jobm.201500444

Wang, Z., Wu, S., Fan, C., Zheng, X., Zhang, W., Wu, D., et al. (2021). Optimisation of enzymatic saccharification of wheat straw pre-treated with sodium hydroxide. *Sci. Rep.* 11:23234. doi: 10.1038/s41598-021-02693-2

Watanabe, K., Kitamura, K., and Suzuki, Y. (1996). Analysis of the critical sites for protein thermostabilization by proline substitution in oligo-1,6-glucosidase from *Bacillus coagulans* atcc 7050 and the evolutionary consideration of proline residues. *Appl. Environ. Microbiol.* 62, 2066–2073. doi: 10.1128/aem.62.6.2066-2073.1996

Wintrode, P. L., Miyazaki, K., and Arnold, F. H. (2001). Patterns of adaptation in a laboratory evolved thermophilic enzyme. *Biochim. Biophys. Acta.* 1:1549. doi: 10.1016/s0167-4838(01)00226-6

Wiśniewska, K. M., Twarda-Clapa, A., and Białkowska, A. M. (2021). Screening of novel laccase producers—isolation and characterization of cold-adapted laccase from *Kabatiella bupleuri* g3 capable of synthetic dye decolorization. *Biomol. Ther.* 11:11. doi: 10.3390/biom11060828

Xu, Z., Cen, Y. K., Zou, S. P., Xue, Y. P., and Zheng, Y. G. (2020). Recent advances in the improvement of enzyme thermostability by structure modification. *Crit. Rev. Biotechnol.* 40, 83–98. doi: 10.1080/07388551.2019.1682963

Yadav, P., Singh, R. P., Rana, S., Joshi, D., Kumar, D., Bhardwaj, N., et al. (2022). Mechanisms of stress tolerance in cyanobacteria under extreme conditions. *Stress* 4:2. doi: 10.3390/STRESSES2040036

Yang, J., Cui, D., Ma, S., Chen, W., Chen, D., and Shen, H. (2021). Characterization of a novel pl 17 family alginate lyase with exolytic and endolytic cleavage activity from marine bacterium *Microbulbifer* sp. Sh-1. *Int. J. Biol. Macromol.* 169, 551–563. doi: 10.1016/j.ijbiomac.2020.12.196

Yang, H., Li, J., Shin, H. D., Du, G., Liu, L., and Chen, J. (2014). Molecular engineering of industrial enzymes: recent advances and future prospects. *Appl. Microbiol. Biotechnol.* 98, 23–29. doi: 10.1007/s00253-013-5370-3

Yang, K. S., Sohn, J. H., and Kim, H. K. (2009). Catalytic properties of a lipase from photobacterium lipolyticum for biodiesel production containing a high methanol concentration. *J. Biosci. Bioeng.* 107, 599–604. doi: 10.1016/j.jbiosc.2009.01.009

Yang, G., Yao, H., Mozzicafreddo, M., Ballarini, P., Pucciarelli, S., and Miceli, C. (2017). Rational engineering of a cold-adapted alpha-amylase from the Antarctic ciliate Euplotes focardii for simultaneous improvement of thermostability and catalytic activity. *Appl. Environ. Microbiol.* 83:e00449-17. doi: 10.1128/AEM.00449-17

Yin, R., Yi, Y. J., Chen, Z., Wang, B. X., Li, X. H., and Zhou, Y. X. (2021). Characterization of a new biofunctional, exolytic alginate lyase from *Tamlana* sp. S12 with high catalytic activity and cold-adapted features. *Mar. Drugs* 19:19. doi: 10.3390/md19040191

Zanphorlin, L. M., de Giuseppe, P. O., Honorato, R. V., Tonoli, C. C., Fattori, J., Crespim, E., et al. (2016). Oligomerization as a strategy for cold adaptation: structure and dynamics of the gh1 beta-glucosidase from *Exigzuobacterium antarcticum* b7. *Sci. Rep.* 6:23776. doi: 10.1038/srep23776

Zavodszky, P., Kardos, J., and Svingor Petsko, G. A. (1998). Adjustment of conformational flexibility is a key event in the thermal adaptation of proteins. *Proc. Natl. Acad. Sci. U. S. A.* 95, 7406–7411. doi: 10.1073/pnas.95.13.7406

Zecchinon, L., Claverie, P., Collins, T., D'Amico, S., Delille, D., Feller, G., et al. (2001). Did psychrophilic enzymes really win the challenge? *Extremophiles* 5, 313–321. doi: 10.1007/s007920100207

Zhang, S. Y., Guo, Z. W., Wu, X. L., Ou, X. Y., Zong, M. H., and Lou, W. Y. (2020). Recombinant expression and characterization of a novel cold-adapted type I pullulanase for efficient amylopectin hydrolysis. *J. Biotechnol.* 313, 39–47. doi: 10.1016/j.jbiotec.2020.03.007

Zhang, S., Li, Y., Han, F., and Yu, W. (2022). Yshyl8a, an alkalophilic cold-adapted glycosaminoglycan lyase cloned from pathogenic *Yersinia* sp. 298. *Molecules* 27:27. doi: 10.3390/molecules27092897

Zhang, J. W., and Zeng, R. Y. (2008). Purification and characterization of a cold-adapted alpha-amylase produced by *Nocardiopsis* sp. 7326 isolated from Prydz Bay, Antarctic. *Mar. Biotechnol. (N.Y.)* 1:10. doi: 10.1007/s10126-007-9035-z

Zhao, G. Y., Zhou, M. Y., Zhao, H. L., Chen, X. L., Xie, B. B., Zhang, X. Y., et al. (2012). Tenderization effect of cold-adapted collagenolytic protease mcp-01 on beef meat at low temperature and its mechanism. *Food Chem.* 134, 1738–1744. doi: 10.1016/j.foodchem.2012.03.118

Zheng, Y., Li, Y., Liu, W., Chen, C. C., Ko, T. P., He, M., et al. (2016). Structural insight into potential cold adaptation mechanism through a psychrophilic glycoside hydrolase family 10 endo-beta-1,4-xylanase. *J. Struct. Biol.* 193, 206–211. doi: 10.1016/j.jsb.2015.12.010

Zheng, Q., Meng, X., Cheng, M., Li, Y., Liu, Y., and Chen, X. (2021). Cloning and characterization of a new chitosanase from a deep-sea *Bacterium serratia* sp. QD07. *Front Microbiol.* 12:619731. doi: 10.3389/fmicb.2021.619731

Zhou, H. X., Xu, S. S., Yin, X. J., Wang, F. L., and Li, Y. (2020). Characterization of a new bifunctional and cold-adapted polysaccharide lyase (pl) family 7 alginate lyase from *Flavobacterium* sp. *Mar. Drugs* 18:18. doi: 10.3390/md18080388

frontiers | Frontiers in Microbiology

TYPE Original Research
PUBLISHED 12 May 2023
DOI 10.3389/fmicb.2023.1156033

OPEN ACCESS

EDITED BY
Trista J. Vick-Majors,
Michigan Technological University,
United States

REVIEWED BY
Wei Li,
Lawrence Livermore National Laboratory (DOE), United States
Pablo Almela,
University of Minnesota Twin Cities,
United States

*CORRESPONDENCE
Jill A. Mikucki
jmikucki@utk.edu

RECEIVED 01 February 2023
ACCEPTED 20 April 2023
PUBLISHED 12 May 2023

CITATION
Shaffer JMC, Giddings L-A, Samples RM and Mikucki JA (2023) Genomic and phenotypic characterization of a red-pigmented strain of *Massilia frigida* isolated from an Antarctic microbial mat.
Front. Microbiol. 14:1156033.
doi: 10.3389/fmicb.2023.1156033

Genomic and phenotypic characterization of a red-pigmented strain of *Massilia frigida* isolated from an Antarctic microbial mat

Jacob M. C. Shaffer[1], Lesley-Ann Giddings[2], Robert M. Samples[2] and Jill A. Mikucki[1]*

[1]Department of Microbiology, University of Tennessee, Knoxville, TN, United States, [2]Department of Chemistry, Smith College, Northampton, MA, United States

The McMurdo Dry Valleys of Antarctica experience a range of selective pressures, including extreme seasonal variation in temperature, water and nutrient availability, and UV radiation. Microbial mats in this ecosystem harbor dense concentrations of biomass in an otherwise desolate environment. Microbial inhabitants must mitigate these selective pressures *via* specialized enzymes, changes to the cellular envelope, and the production of secondary metabolites, such as pigments and osmoprotectants. Here, we describe the isolation and characterization of a Gram-negative, rod-shaped, motile, red-pigmented bacterium, strain DJPM01, from a microbial mat within the Don Juan Pond Basin of Wright Valley. Analysis of strain DJMP01's genome indicates it can be classified as a member of the *Massilia frigida* species. The genome contains several genes associated with cold and salt tolerance, including multiple RNA helicases, protein chaperones, and cation/proton antiporters. In addition, we identified 17 putative secondary metabolite gene clusters, including a number of nonribosomal peptides and ribosomally synthesized and post-translationally modified peptides (RiPPs), among others, and the biosynthesis pathway for the antimicrobial pigment prodigiosin. When cultivated on complex agar, multiple prodiginines, including the antibiotic prodigiosin, 2-methyl-3-propyl-prodiginine, 2-methyl-3-butyl-prodiginine, 2-methyl-3-heptyl-prodiginine, and cycloprodigiosin, were detected by LC–MS. Genome analyses of sequenced members of the *Massilia* genus indicates prodigiosin production is unique to Antarctic strains. UV-A radiation, an ecological stressor in the Antarctic, was found to significantly decrease the abundance of prodiginines produced by strain DJPM01. Genomic and phenotypic evidence indicates strain DJPM01 can respond to the ecological conditions of the DJP microbial mat, with prodiginines produced under a range of conditions, including extreme UV radiation.

KEYWORDS

prodigiosin biosynthesis, Antarctic *Massilia*, psychrophilic bacteria, whole-genome sequencing, Don Juan Pond Basin

1. Introduction

Upwards of 80% of Earth's environments are permanently cold (<5°C), including polar, alpine, maritime, and atmospheric regions (De Maayer et al., 2014). Understanding how life survives at low temperatures is crucial to our understanding of life itself, as well as how life might exist on other planets. On the Antarctic continent, the McMurdo Dry Valleys (MDV) constitute

the largest ice-free region (Levy, 2013). The MDV region is the coldest, driest desert on our planet, and experiences average annual air and absolute surficial soil temperatures ranging from −26.8 to −16.5°C and −59.8 to +31.1°C, respectively (Obryk et al., 2020), and receive a maximum of ~50 mm of precipitation in the form of snowfall annually (Fountain et al., 2009). Additionally, the MDV experiences long periods of sustained light and dark, due to its extreme southern latitude, and high levels of UV-A and UV-B radiation from thinning in the ozone layer (Frederick and Snell, 1988).

Antarctic microbial mats provide a unique system for studying the effects of UV radiation and other adaptations due to their high biomass compared to other microbial niches within the MDV (Davey and Clarke, 1992). The formation of these communities is reliant on photosynthetic cyanobacteria, including either *Nostoc* species or *Phormidium* and *Oscillatoria* species, depending on the geomorphology and hydrology of the niche (Alger et al., 1997). Other photosynthetic organisms, such as green algae and diatoms, can be found in Antarctic mats, as well as heterotrophic bacteria and microscopic invertebrates (Andriuzzi et al., 2018). Microbial mats that occupy perennial stream channels and shallow ponds are particularly exposed to extremes of seasonal variation and experience fluctuations in meltwater flow from glaciers due to changes in temperature and solar angle, which in turn can lead to changes in nutrient availability and community structure (Zoumplis et al., 2023). In the winter, communities are exposed to months of darkness, desiccation, and subzero temperatures. MDV mats in stream channels and surface ponds lie dormant for ~10 months of the year due to the lack of water and sunlight, followed by rapid reactivation in response to rehydration by glacial meltwater (McKnight et al., 2007). In addition to freezing and dehydration, MDV mats are exposed to intense ultraviolet (UV) radiation. This UV exposure causes DNA damage and the production of reactive oxygen species (ROS; Castenholz and Garcia-Pichel, 2012). UV radiation has been proposed as a major limiting factor on growth for communities within the MDV (Tosi et al., 2005).

Microbial mats are scattered throughout the MDV, largely concentrated in meltwater streams and lake margins (Power et al., 2020) that wax and wane in volume in response to climate (Mikucki et al., 2010). Within the South Fork of the Wright Valley is a near-saturated $CaCl_2$ brine pond, known as Don Juan Pond (DJP). DJP is bounded to the west by a rock glacier, which provides a source of meltwater to the basin (Figure 1). While there are conflicting reports regarding the habitability of the brine (Toner et al., 2017), the DJP basin hosts a dense microbial mat that borders the rock glacier (Figure 1B). This mat was first described as approximately 500–600 m^2 and 2–5 mm thick (Siegel et al., 1979). Microscopic investigation of the mat revealed an abundance of cyanobacteria phenotypically similar to *Oscillatoria*, in addition to the green algae *Chlorella* and *Dunaliella*, diatoms, invertebrates, and bacteria (Siegel et al., 1983). The extent to which the saturated brine of DJP might influence the mat is currently unknown, though it is possible that dried salts are deposited in the mat by aeolian processes (Diaz et al., 2018).

The genus *Massilia* was first described in 1998 in a report on the isolation of *Massilia timonae* from the blood sample of an immunocompromised patient (La Scola et al., 1998). The genus belongs to the Oxalobacteraceae family and to date includes 61 validly published species (January 2023).[1] *Massilia* species have been isolated from disparate environments across the globe and have been implicated in human disease (La Scola et al., 1998; Van Craenenbroeck et al., 2011; Kämpfer et al., 2012; Chiquet et al., 2015) and as a common member of rhizosphere communities of *Arabidopsis* (Tkacz et al., 2015) and wheat (Schlatter et al., 2020). Rhizosphere *Massilia* are of interest due to their possible role in plant development through the production of phytohormones and solubilization of phosphates, among other activities (Ofek et al., 2012; Schlatter et al., 2020). Several *Massilia* have also been isolated from the cryosphere, including from Arctic (Son et al., 2021; Dahal et al., 2021a), Antarctic (Holochová et al., 2020; Sedláček et al., 2022), and alpine regions (Shen et al., 2013, 2015; Guo et al., 2016; Gu et al., 2017; Wang et al., 2018).

While their ecological role in polar environments is not as well understood, *Massilia* species have been detected in diverse Antarctic niches. For example, *Massilia* ranged from 54 to 79% of culturable community members in both closed and open cryoconite holes in the Larsemann Hills, Dronning Maud Land, and Amery Ice Shelf regions (Sanyal et al., 2018). Sommers et al. (2019) identified *Massilia* as one of the ten most abundant sequences in cryoconite water collected from Taylor Glacier, a glacier within the MDV. These authors suggested that *Massilia* may play a role in cryoconite colonization. *Massilia* have also been isolated from microbial mats in both peninsular and continental Antarctica, including other ice-free regions such as the Schirmacher and Syowa Oasis (Peeters et al., 2012).

Here we characterize a red-pigmented *Massilia* species, strain DJPM01, isolated from the DJP microbial mat. We identified genomic evidence for environmental adaptations in strain DJPM01 and compared these findings with other Antarctic *Massilia* species as well as the taxonomic distribution of secondary metabolite biosynthetic gene clusters (BGCs) within the *Massilia* genus. We then analyzed cultures of strain DJPM01 for the presence and relative abundance of pigments when grown under ecologically relevant UV-A radiation exposure to further our understanding of microbial responses in extreme environments.

2. Materials and methods

2.1. Site description and sample collection

Samples of a microbial mat were collected in the South Fork of the Wright Valley at the terminus of a rock glacier in the Don Juan Pond (DJP) basin, Victoria Land, Antarctica (77.56293 S, 161.1751 E; Figure 1). Mat material was collected on 5 December 2018 using individually wrapped sterile scoops (SP Bel-Art; Wayne, NJ) and transferred into sterile Whirl-Pak bags (Whirl-Pak; Madison, WI). *In situ* temperature, pH, and salinity were measured at the time of collection using a vented Aqua TROLL 500 Multiparameter Sonde (*in-situ*), configured with pH/ORP, conductivity, rugged dissolved oxygen (RDO), and turbidity modules. Samples were stored and shipped cool (4°C) until later processing at the University of Tennessee (Knoxville, TN, United States).

1 https://lpsn.dsmz.de/genus/massilia

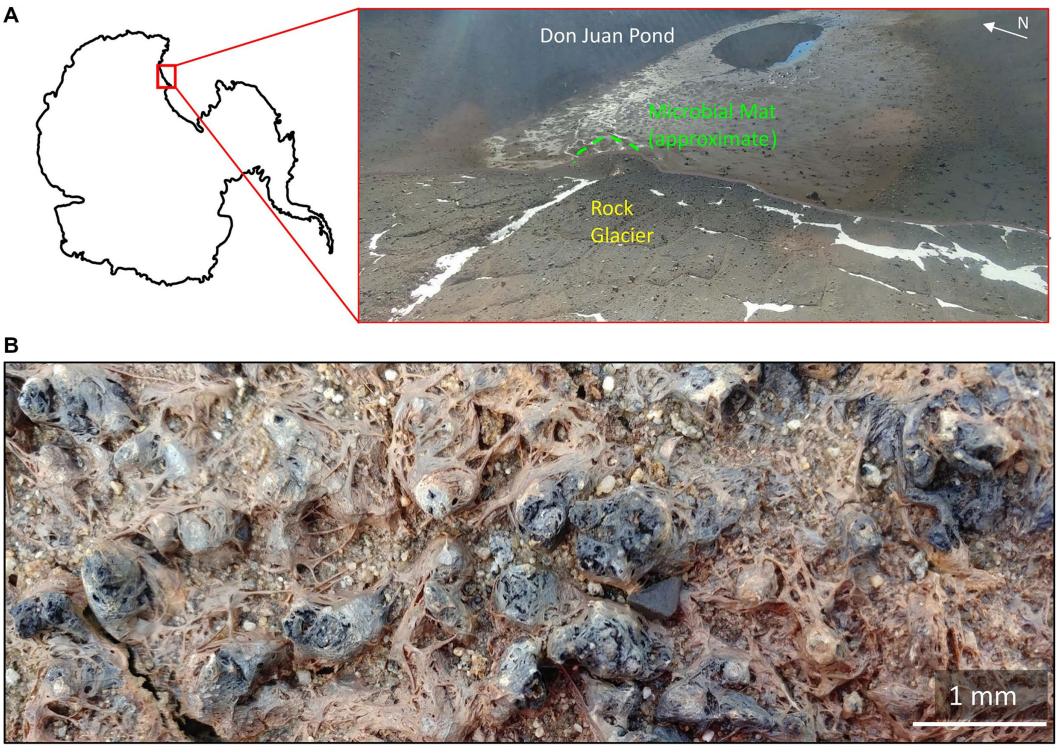

FIGURE 1
The Don Juan Pond (DJP) microbial mat **(A)** Location of the microbial mat within DJP basin. Approximate location of the basin in Antarctica is inset. **(B)** Close up of the DJP basin microbial mat collected for enrichment cultures that yielded strain DJPM01.

2.2. Isolation and incubation conditions

Mat material was incubated in R2A broth (Difco; Becton, Dickinson and Company; Franklin, NJ) at ~10°C for 10 days, after which the broth was used to inoculate R2A agar plates (BD Difco; Franklin, NJ). Bright red-pigmented colonies appeared on the plate after 4 days of incubation at 10°C and were selected for further isolation through multiple restreaks on R2A agar. Gram staining and microscopy was performed on strain DJPM01 using the American Society of Microbiology Gram stain protocol (Smith and Hussey, 2005) and observed with an Axio Imager M2 microscope (Zeiss; Oberkochen, Germany). Motility assays were conducted by spot inoculation of strain DJPM01 onto 0.5% agar R2A plates. To assess resistance to UV-C light, R2A agar plates of strain DJPM01 were prepared and exposed UV light (254 nm) as described by Hirsch et al. (2004). Plates were exposed for 10, 20, 30, 60, 120, and 300 s and left to incubate in the dark at 10°C for 10 days. Strain DJPM01 was incubated in R2A broth under a nitrogen headspace to test for anaerobic growth. To test the effects of temperature on the growth rate of strain DJPM01, incubations were performed in 96-well plates. Briefly, 180 µL R2A broth was aliquoted into each well. Strain DJPM01 was grown to late log phase and inoculated into 48 wells of a 96-plate (10% inoculum). Plates were incubated at 4, 10, 15, 20, and 25°C, and full spectra were collected for each plate once per day for 14 days. Outer wells were removed from analysis to control for unequal levels of evaporation.

2.3. Phylogenetic analysis and whole genome comparison

For taxonomic identification, DNA was extracted from bacterial colonies using a DNeasy PowerSoil PowerLyzer Kit (Qiagen; Hilden, Germany) following the manufacturer's protocol with the addition of a modified bead beating step as follows: 45 m sec^{-1} for 25 sec followed by 5 min rest at 10°C (FastPrep-24 Bead Lysis System; MP Biomedical; Santa Anna, CA). The 16S ribosomal RNA (rRNA) gene was amplified from extracted DNA using the following combination of primers: bacterial 27F (5'-AGAGTTTGATCCTGGCTCAG-3′; Weisburg et al., 1991) and 806R primers (5'-GGACTACNVGGGTWTCTAAT-3′; Apprill et al., 2015) and 515F (5'-GTGCCAGCMGCCGCGGTA-3′; Caporaso et al., 2011) and 1492R primers (5'-GGTTACCTTGTTACGACTT-3′; Weisburg et al., 1991). The resulting PCR products were purified using a Wizard SV Gel and PCR Clean-Up System Kit (Promega; Madison, WI) before Sanger sequencing, performed by Eurofins Genomics (Louisville, KY). Returned sequences were aligned using Geneious v6.1.8 (for a sequence length of 1,388 bp; Kearse et al., 2012) and compared to the NCBI nucleotide collection type material database (Federhen, 2012). Publicly available sequences for *Massilia* 16S rRNA genes were obtained from the RefSeq database (O'Leary et al., 2016), aligned, trimmed to the length of the shortest sequence (1,335 bp), and used to construct a maximum likelihood tree in MEGA v11.0.13 (Tamura et al., 2021). Additionally, strain DJPM01 was compared to all NCBI reference genomes within the Oxalobacteraceae family using

whole genome average nucleotide identity (ANI) through the enveomics collection (Rodriguez-R and Konstantinidis, 2016). Digital DNA–DNA hybridization (DDH) for all reference genomes available in the Oxalobacteraceae family was calculated using the Genome-to-Genome Distance Calculator (GGDC) v3.0 (Meier-Kolthoff et al., 2022). A final phylogenetic tree of RefSeq reference genomes was generated using OrthoFinder v2.5.4 (Emms and Kelly, 2019) with default settings. Estimation of abundance was performed using a 16S community amplicon sequence variant (ASV) library generated from the DJP mat (Schuler, 2022) using the Basic Local Alignment Search Toolkit (BLAST; Altschul et al., 1990). The final 16S rRNA gene sequence for strain DJPM01 was uploaded to GenBank under accession number OQ346149.

2.4. Genome sequencing, assembly, and annotation

Total genomic DNA was extracted from microbial biomass using a cetrimonium bromide (CTAB) buffer/organic phase extraction protocol (as described by Campen, 2015) for whole genome sequencing. Quality and quantity of extracted DNA was determined by a Qubit 4 fluorometer (Invitrogen Carlsbad, CA) and NanoDrop 2000 spectrophotometer (Thermo Scientific; Waltham, MA, United States). High molecular weight genomic DNA (25 ng/μL) was sequenced by MR DNA (Shallowater, TX). Library preparation was performed using the Nextera DNA Flex Library Preparation Kit (Illumina Inc.; San Diego, CA) and quality was confirmed using the Agilent 2,100 Bioanalyzer (Agilent Technologies; Santa Clara, CA). The library was diluted to 0.6 nM before sequencing on the NovoSeq platform (Illumina; San Diego, CA; paired end, 500 cycles). Sequencing adapters and low-quality reads were trimmed from using Trimmomatic v0.36 (Bolger et al., 2014) on default parameters. Trimmed reads were assembled using Unicycler v0.4.8 (Wick et al., 2017) with a maximum contig size of 500 bp and assembly quality was assessed using QUAST v5.0.2 (Gurevich et al., 2013) and checkM v1.1.3 (Parks et al., 2015). The genome draft was annotated by Prokka v1.13.7 (Seemann, 2014) and the resulting annotation was analyzed using GhostKOALA v2.2 (Kanehisa et al., 2016). Putative CRISPR-Cas sequences were identified using CRISPRCasFinder v4.2.20 (Couvin et al., 2018) and putative prophage sequences were identified by VirSorter2 v2.2.3 (Guo et al., 2021), both using the Proksee interface.[2] Putative secondary metabolite BGCs were identified *via* antiSMASH v6.0.0 (Blin et al., 2021) using default parameters. RefSeq *Massilia* genomes were annotated using Prokka v1.13.7, GhostKOALA v2.2, and antiSMASH v6.0.0 and all *Massilia* genomes in both NCBI and JGI databases were aligned against the *pig* operon of *Serratia* sp. strain ATCC 39006 to search for prodigiosin-specific biosynthetic genes (Harris et al., 2004). Putative prodigiosin operons were compared by pairwise alignment using SimpleSynteny v1.5 (Veltri et al., 2016). Statistical analyses of gene abundance were performed using R v4.1.2 (R Core Team, 2018). The final draft genome assembly was uploaded to GenBank under accession number JAQOZV000000000.

2 https://proksee.ca/

2.5. Biomass irradiation and extraction of pigments produced under UV light

A lawn of strain DJPM01 was grown on R2A agar plates in quadruplicate and incubated under a UV-A light (320–400 nm, peak absorbance 395 nm; Supplementary Figure S1; SANSI Lighting; Shanghai, China). Nalgene petri dishes (Thermo Scientific; Waltham, MA) made of polymethylpentene were utilized to increase UV penetration compared to standard polystyrene petri dishes (Peng et al., 2011). Control plates were inoculated, wrapped in foil, and placed inside two black bags prior to incubation. Uninoculated media controls were also incubated under both light and dark treatments. All plates were incubated at 10°C for 11 days. Following incubation, agar was sterilely sliced into strips for storage at −80°C. Agar strips from each plate were extracted four times with 10 mL of high performance liquid chromatography (HPLC)-grade ethyl acetate (Fisher Scientific; Hampton, NH) and sonicated for 10 min. Organic phases were pooled and diluted to 50 mL with ethyl acetate. Authentic prodigiosin (1) standard (P0103; Sigma-Aldrich, St. Louis, MO) was diluted 100 μg mL^{-1} in liquid chromatography/mass spectrometry (LC/MS)-grade methanol (Fisher Scientific; Hampton, NH) and exposed to UV-A radiation overnight to investigate potential breakdown products. UV-A exposed and unexposed prodigiosin (1) standard solutions were diluted to 10 μg mL^{-1} prior to LC/MS analysis.

2.6. LC/MS analyses

Extracts were analyzed on a Thermo Scientific (Waltham, MA) Q-exactive HF-X Hybrid Quadrupole-Orbitrap mass spectrometer interfaced with a Vanquish Horizon Ultra high performance liquid chromatography (UHPLC) system and VH-D10-A UV detector using a Waters (Milford, MA) HSS T3 C18 column (1.8 μm, 2.1 × 100 mm) with a VanGuard FIT precolumn. Using a flow rate of 0.5 mL min^{-1}, samples (2 μL) were injected onto the column prewarmed to 40°C. UHPLC separation was achieved using the following parameters: 2% acetonitrile: 98% water with 0.1% formic acid for 1 min, 2–40% over 4 min, 40–98% over 3 min, 98–2% over 0.2 min, and 2% for 2 min. The UV–Vis data were collected at 534 nm. The following electrospray ionization (ESI) settings were used in probe position D: 40 sheath gas flow, 8 auxiliary gas flow, 1 sweep gas flow, 3.5 kV spray voltage, 380°C capillary temperature, 50 radiofrequency (RF) funnel level, and 350°C auxiliary gas temperature. Data were evaluated using MS-DIAL (Tsugawa et al., 2015) and MPACT (Samples et al., 2022). See supplementary information for data processing methods.

A Waters Synapt G2-Si Q-ToF mass spectrometer coupled to an Acquity H-Class ultra performance liquid chromatography (UPLC) system was employed for LC/MS analysis of select samples and prodigiosin (1) standard using the previously described column and gradient. Positive mode MS^E acquisition was used, using 0.1 s MS1 survey scans from *m/z* 150–2000 in resolution mode, followed by 0.1 s high energy MS2 scan from *m/z* 50–2000. Data were acquired using the following parameters: 2 kV capillary voltage, 100°C source temperature, 20 V sampling cone, 800 L h^{-1} desolvation gas flow, 80 V source offset, and 30 V MS2 collision energy. Real-time mass correction used a lockspray of 400 pg μL^{-1} leucine enkephalin solution (1:1 methanol to water solution with 0.1% formic acid). A 10 μL injection volume was used in the closed loop configuration.

3. Results

3.1. Sample collection and isolation

At time of collection, the water within the mat was 7.7°C; collection site pH was 7.2 and salinity was 0.4 parts per thousand (ppt). Following isolation, the purity of the resulting axenic culture was confirmed by 16S rRNA gene analyses and microscopy, which revealed a single rod-shaped morphology. The resulting red-pigmented isolate was designated strain DJPM01.

3.2. Characterization and growth

Growth of strain DJPM01 on R2A yielded tall, convex, scarlet colonies with entire margins that spread outwards over time (Figure 2). Colonies were resistant to removal from the surface of the agar and remained aggregated when transferred to broth culture, unless thoroughly agitated through vortexing. Strain DJPM01 was determined to be Gram-negative using the standard Gram stain protocol (Smith and Hussey, 2005). Cells were rod-shaped and 4.65 µm in length on average (Figure 2A). Cultures exhibited growth from 4 to 25°C, but not at 30°C (Supplemental Figure S2). The fastest growth occurred at 10°C with a rate (µ) of $0.25 \pm 0.04\ day^{-1}$. Colonies were pigmented under all culture conditions, with some variation in color intensity and hue at warmer temperatures (Supplemental Figure S2). Growth was not detected under anaerobic conditions. Strain DJPM01 grew on R2A agar adjusted to pH 10.5. Abundance of colony forming units decreased following 30 s of exposure to UV-C radiation, however colonies were present on plates irradiated for up to 120 s. Evidence for motility was observed when grown on low density R2A agar. When grown in R2A broth, strain DJPM01 formed a robust pellicle at the surface and produced extracellular polymeric substances (Figure 2D).

3.3. Phylogenetic analysis

Analysis of the trimmed 16S rRNA gene sequence (1,335 bp) placed strain DJPM01 within the *Massilia* genus (Supplementary Figure S3). Strain DJPM01 shared highest sequence identity with *M. violaceinigra* strain B2 (CP024608, 99.87%) originally isolated from glacial permafrost in the Xinjiang region of China (Wang et al., 2018). Strain DJPM01 also shared high sequence identity with several other cryosphere associated *Massilia* species, including *M. aquatica* strain CCM 8693 (MN612031, 99.87%), *M. rubra* strain CCM 8692 (MN611986, 99.80%), *M. frigida* strain CCM 8695 (MN612047, 99.80%), *M. mucilaginosa* strain 8,733 (MN612043, 99.67%), and *M. atriviolacea* strain SOD (NR_171529, 99.40%). Of these six isolates, four were isolated from James Ross Island on the Antarctic Peninsula (*M. frigida, M. aquatica, M. rubra,* and *M. mucilaginosa*; Holochová et al., 2020). *M. atriviolacea,* was first isolated from agricultural soils from Hefei, China (Yang et al., 2019). Comparison of the 16S rRNA sequence to the available DJP basin mat 16S ASV library suggests that strain DJPM01 is present in low abundance with 2,110 reads or ~0.03% relative abundance (Schuler, 2022).

Whole genome comparison placed strain DJPM01 within a distinct clade (≥87% ANI between clade members) including all currently identified *Massillia* with either a red or purple pigmented phenotype (Figure 3; Supplementary Table S1). This clade includes the six *Massilia* strains with highest 16S rRNA gene similarity to strain DJPM01, as well as *M. antarctica* strain P9640 (OM243919; Sedláček et al., 2022), which was also isolated from James Ross Island. All members of this clade have been shown to grow at or below 4°C, regardless of isolation locale. Strain DJPM01 shared highest ANI with *M. frigida* strain CCM8695 (97.36% identity). High sequence identity of strain DJPM01 to *M. antarctica* strain P9640 (91.92%) and *M. violaceinigra* strain B2 (91.38%) were also noted. Additionally, *M. mucilaginosa* strain CCM8733, *M. atriviolacea* strain SOD, *M. rubra* CCM 8692 (GCF 011682065), and *M. aquatica* CCM 8693 had relatively high sequence identity (87.94–88.41% similarity to strain DJPM01). Digital DNA–DNA hybridization (DDH) showed 75.6% similarity between strain DJPM01 and *M. frigida* strain CCM8695 (Supplementary Table S1).

3.4. Genomic analyses

Whole-genome sequencing resulted in 8,995,221 paired reads of which 8,693,443 (96.6%) pairs survived trimming with 0 N's. Assembly yielded a genome 7.7 Gb in size across 236 contigs with 99.80% completeness (573 of 574 marker genes present) and 1.64% contamination (10 marker genes with two copies each; Figure 4). Following annotation, 6,626 predicted protein coding genes were identified, 3,037 of which had a non-hypothetical function (45.8% functional annotation). Of these genes, the largest functional categories within the KEGG database were protein families: signaling and cellular processes (361 genes), environmental information processing (339 genes), genetic information processing (339 genes), and carbohydrate metabolism (248 genes). The genome contains complete pathways for glycolysis and the TCA cycle, oxidative phosphorylation, flagellar motility, and denitrification. Additionally, we detected 9 putative CRISPR arrays and 4 Cas clusters (Figure 4). Both putative single- and double-stranded DNA phage sequences were found throughout the genome.

Strain DJPM01 has genomic evidence for adaptation to cold environments (Figure 4; Supplementary Table S2). The genome contains genes homologous to those encoding protein chaperones, including two copies of ClpB (Mogk et al., 2003) and DnaJ (Qiu et al., 2006), three copies of DnaK (Thompson et al., 2012), and one copy each of GroEL (Lenz and Ron, 2014), GroES (Takei et al., 2012), and GrpE (Wu et al., 1996). There was also evidence for genes encoding cold shock proteins involved in repairing misfolded mRNA, such as ATP-dependent RNA helicases DpbA (Tsu et al., 2001), DeaD (Prud'homme-Généreux et al., 2004), and three copies of RhlE (Bizebard et al., 2004). Strain DJPM01 contained two copies of genes putatively encoding the cold shock protein CspA (La Teana et al., 1991). Three genes were also associated with the formation of unsaturated fatty acids, including a Δ9-desaturase (Li et al., 2009) and two acyl-CoA thioesterases, TesA (Cho and Cronan, 1993) and YciA (Postle and Good, 1985).

Several genes putatively involved in osmotic and oxidative stress were present as well (Figure 4; Supplementary Table S2). Strain DJPM01 has genomic evidence of several cation/proton antiporters in the NhaA (Vimont and Berche, 2000) and CPA1 families (Utsugi et al., 1998). Both the biosynthetic pathway and transporters for the compatible solute glutamate are present (Saum et al., 2006). Strain DJPM01 also contained genes for superoxide dismutase (Fee, 1991)

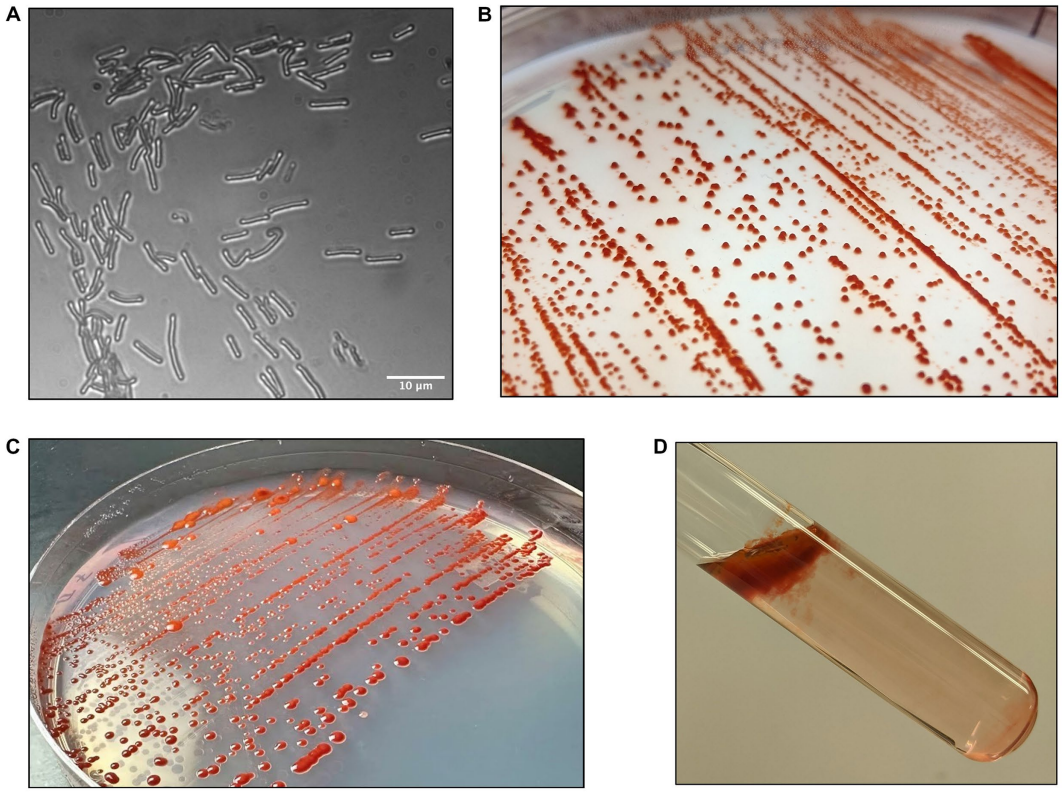

FIGURE 2
Morphology of strain DJPM01. **(A)** Light microscopy image of strain DJPM01 using phase shift. Cells were rods and 4.65µm in length on average. **(B,C)** Strain DJPM01 grown on R2A agar at 10 **(B)** and 15 **(C)** °C. Colonies were robust and resisted removal from the agar. Bright red pigmentation was present at all temperatures. **(D)** Pellicle formation by strain DJPM01 in R2A broth, held at an angle.

and peroxiredoxin (Weber et al., 2006), which are enzymes known to combat oxidative stress, in addition to six copies of the catalase gene (von Ossowski et al., 1991). Several genes were associated with DNA repair (Figure 4; Supplementary Table S2). Strain DJPM01 encodes for several copies of genes for nucleotide excision, mismatch repair, and homologous and non-homologous recombination. The genome also encodes for two proteins associated with light-dependent DNA repair, deoxyribodipyrimidine photolyase (Sancar et al., 1984) and DNA photolyase (Zhang et al., 2013).

Annotation by antiSMASH (Blin et al., 2021) revealed a total of 17 putative biosynthetic gene clusters (BGCs), including high similarity matches to characterized gene clusters for aryl polyene APE_{Ec} (36%), violacein (100%), cephamycin C (36%), myxochelin (41%), iso-migrastatin (45%), and prodigiosin (42%; Supplementary Table S3). Of these genes, aryl polyenes have been proposed to mediate oxidative stress (Cimermancic et al., 2014), myxochelins are iron-chelating siderophores (Li et al., 2008), cephamycin C is a β-lactam antimicrobial (Alexander and Jensen, 1998), and iso-migrastatin is a glutaride-containing cytotoxic agent (Ju et al., 2005). The pigments violacein (blue-violet) and prodigiosin (1; red) have both been described to have antibiotic properties and UV-protective effects (Danevčič et al., 2016; Cauz et al., 2019). Closer analysis of the iso-migrastatin BGC using PRISM v4.4.5 (Skinnider et al., 2020) revealed this cluster encodes genes which are 58–72% identical (based on amino acid sequence) to those involved in the biosynthesis of the antifungal gladiofungin, however the cluster was on the end of a contig, missing roughly 15% of the third polyketide synthase gene (Supplemental Figure S4; Niehs et al., 2020).

To understand how the diversity of BGCs in DJPM01 compares to other *Massilia* genomes, putative secondary metabolite BGCs were identified in representative *Massilia* genomes from RefSeq using antiSMASH (Figure 5; O'Leary et al., 2016; Blin et al., 2021). Antarctic *Massilia* genomes contained an average of 14.5 secondary metabolite BGCs per genome, significantly higher than both mesophilic *Massilia* (9.2 BGCs per genome; Tukey, $t = -4.95$, $p < 0.001$) and Arctic and alpine *Massilia* (7.8 BGCs per genome; Tukey, $t = -4.31$, $p < 0.001$). This trend was still significant when normalized to genome size (ANOVA, $F = 4.27$, $p = 0.023$) and number of coding sequences per genome (ANOVA, $F = 4.38$, $p = 0.021$; Supplementary Table S4). Strain DJPM01 was the only *Massilia* to contain the putative gladiofungin polyketide gene cluster. The BGC for prodigiosin was only identified in Antarctic *Massilia* species (*M. aquatica* CCM 8693, *M. frigida* CCM 8695, *M. mucilaginosa* CCM 8733, and *M. rubra* CCM 8692).

Genes for *Serratia* sp. strain ATCC 39006 prodigiosin BGC were aligned to all *Massilia* genomes available on NCBI (Harris et al., 2004). Only five genomes were identified to contain BGCs with high sequence identity to the prodigiosin BGC, with the highest bit scores for *pigC*, *pigD*, and *pigE* (Supplementary Figure S5A). Of these five organisms, four were *Massilia* species originally isolated from James Ross Island. The fifth genome was reported as *M. violaceinigra* strain sipir (GCF 022811105.1) in NCBI; the metadata associated with this entry indicated it was isolated from freshwater. Our analyses indicated

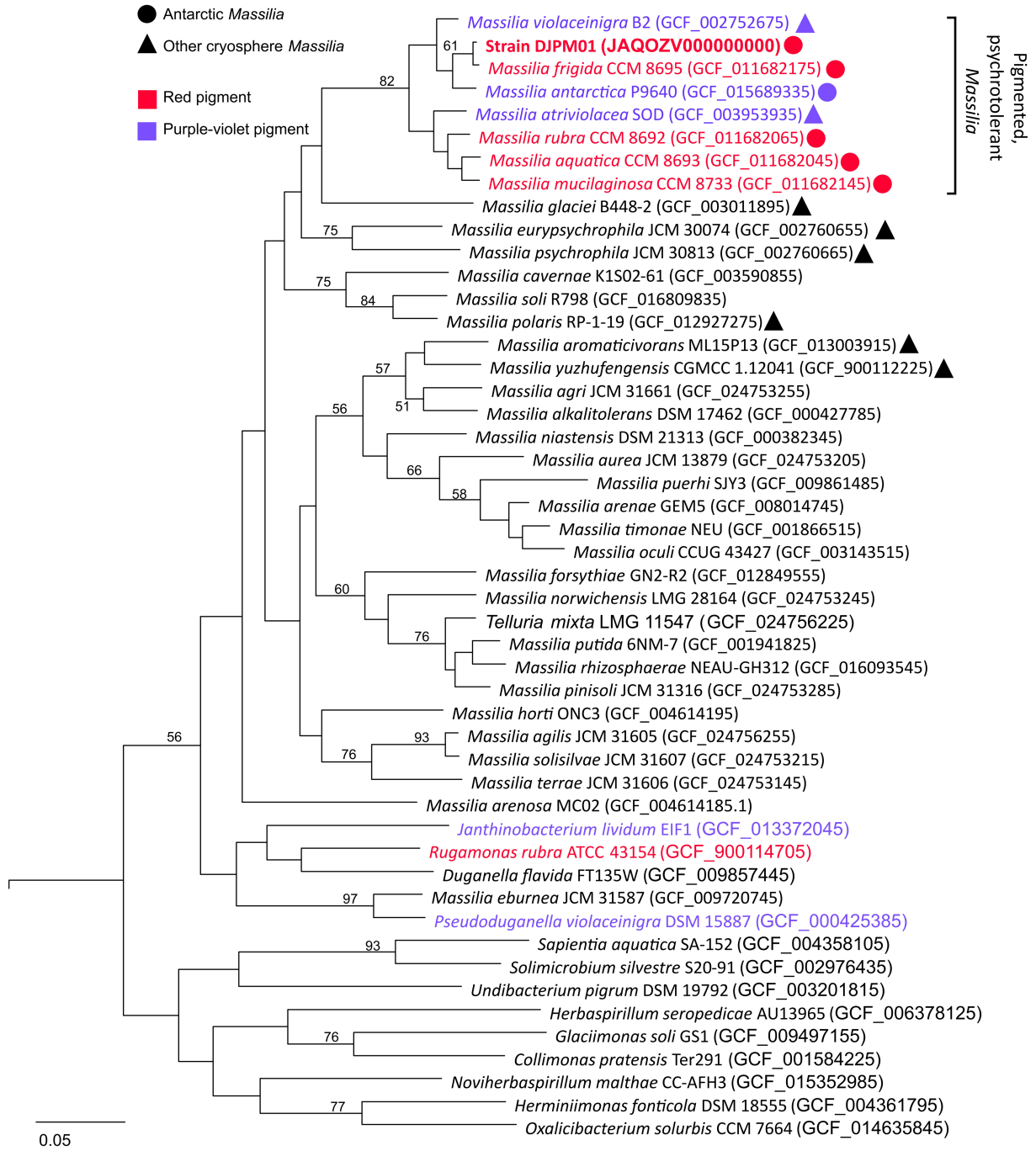

FIGURE 3
Multiple-gene tree of Oxalobacteraceae family members. Tree constructed using OrthoFinder v2.5.4 (Emms and Kelly, 2019). All *Massilia* with phenotypic and genotypic evidence for red (prodigiosin) or purple-violet (violacein) pigment production form a clade with >87% ANI between any given pair. All members of this clade were isolated cryosphere environments, including all five Antarctic *Massilia*. All *Massilia* genomes cluster into a single clade, with the exception of *M. eburnea*, originally identified as a species of *Pseudoduganella* (Lu et al., 2020). Node values represent bipartition support values >50. An Antarctic *Shewanella* species (strain BF02_Schw) was used as an outgroup (DQ677870.1).

this genome had >97% ANI to the Antarctic *M. aquatica* CCM 8693, which also has genotypic and phenotypic evidence for prodigiosin production. Given the uncertainty about the phylogeny of this strain we excluded it from further analyses. The four Antarctic *Massilia* prodigiosin BGCs had high sequence identity (93.59–100.00% identity) at the hypothetical gene level to strain DJPM01 (Supplementary Figure S5B).

Gene annotations were compared between strain DJPM01 and *M. frigida* stain CCM 8695. Both strains shared 1990 genes with non-hypothetical functions (97.9%), with 41 genes unique to strain DJPM01 and 51 genes unique to *M. frigida*. Genes unique to strain DJPM01 included two genes associated with lipopolysaccharide biosynthesis (*hddA* and *hddC*), one copy of fatty acid elongation gene *fabI*, and three genes associated with toxin-antitoxin systems (*fitA*,

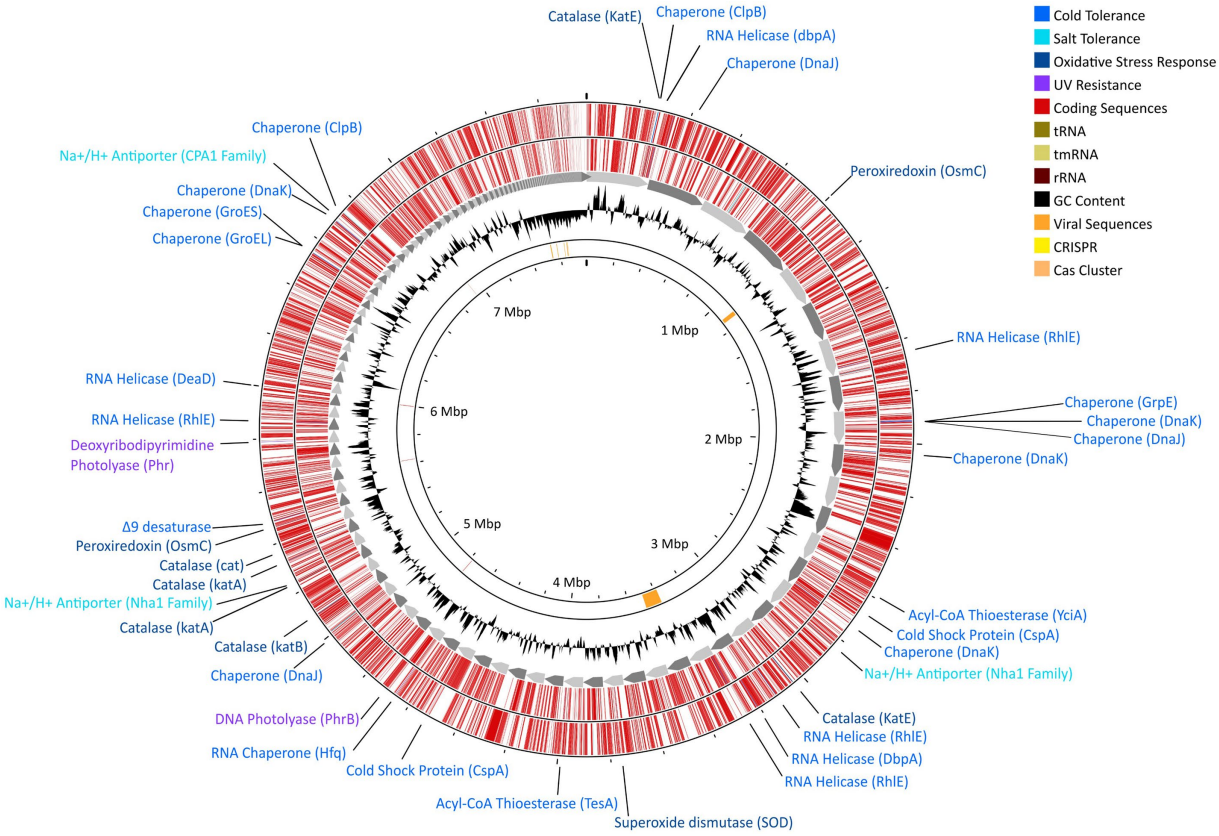

FIGURE 4
Gene map for strain DJPM01 highlighting proposed environmentally-relevant genes. Contigs are sorted by length and represented by grey arrows. Outer tracks depict coding sequences as annotated by Prokka v1.13.7 (Seemann, 2014), separated by strand. Genes related to environmentally-relevant stress adaptation and response are highlighted and labeled. Results of VirSorter2 v2.2.3 (Guo et al., 2021) and CRISPRCasFinder v4.2.20 (Couvin et al., 2018) are present on the inner ring.

fitB, and *yefM*). Both genomes contain genes associated with type IV pilin production, multifunctional fibers produced on cell surfaces, though *M. frigida* does not have a copy of *mshC* (Toma et al., 2002). An additional 91 genes had a higher copy number in strain DJPM01 and 102 genes had lower copy number in strain DJPM01. Strain DJPM01 had 2 additional copies of genes for catalase, and four fewer copies of the fatty acid biosynthesis gene *fabB*. When compared to non-Antarctic species, Antarctic *Massilia* tended to, on average, have slightly more genes associated with fatty acid biosynthesis (especially *fab* genes; 4 more genes), protein chaperones (1.4 more genes), and catalase (1.4 more genes).

3.5. Confirmation of prodigiosin in strain DJPM01

LC/MS and UV–Vis spectroscopic analyses of extracted DJPM01 agar plates resulted in the detection of prodigiosin (1), which was confirmed with an authentic standard (Figures 6A,B). Prodigiosin (1, *m/z* 324.2072; calculated for $C_{20}H_{26}N_3O$ $[M+H]^+$, 324.2076) was detected with a characteristic UV–Vis spectrum (λ_{max} = 540 nm; Figures 6A,B; Supplementary Figure S6; Andreyeva and Ogorodnikova, 2015). MS/MS spectra of the peak identified as prodigiosin (1) were congruent with the fragmentation pattern of the authentic standard. Furthermore, a number of distinct peaks with similar UV–Vis absorbances were detected in chromatograms with masses consistent with prodiginines based on mass defect values and even $[M+H]^+$ masses. Metabolomic analyses indicated the presence of numerous features consistent with those of 2-methyl-3-propyl prodiginine (2), 2-methyl-3-butyl prodiginine (3), 2-methyl-3-heptylprodiginine (4), cycloprodigiosin (5), and other uncharacterized prodiginines (Figure 6D; Supplementary Table S5).

3.6. Effects of UV light on the production of prodigiosin and other secondary metabolites

Incubation under UV light yielded a less-saturated, darker-hued pigmentation compared to control plates grown in the dark, with no UV exposure (Figure 6C). LC/MS analyses of UV-treated strain DJPM01 indicated statistically significant differences between UV-treated, control, and media blank samples (Supplementary Figure S7). A statistically significant decrease was observed in prodigiosin (1; $q < 0.001$) and other metabolites (Figures 6C, 7). Mass spectral analyses suggested that these uncharacterized prodiginines may be cyclized, reduced, oxygenated, and otherwise modified variations of prodigiosin. LC/MS analysis of

10.3389/fmicb.2023.1156033

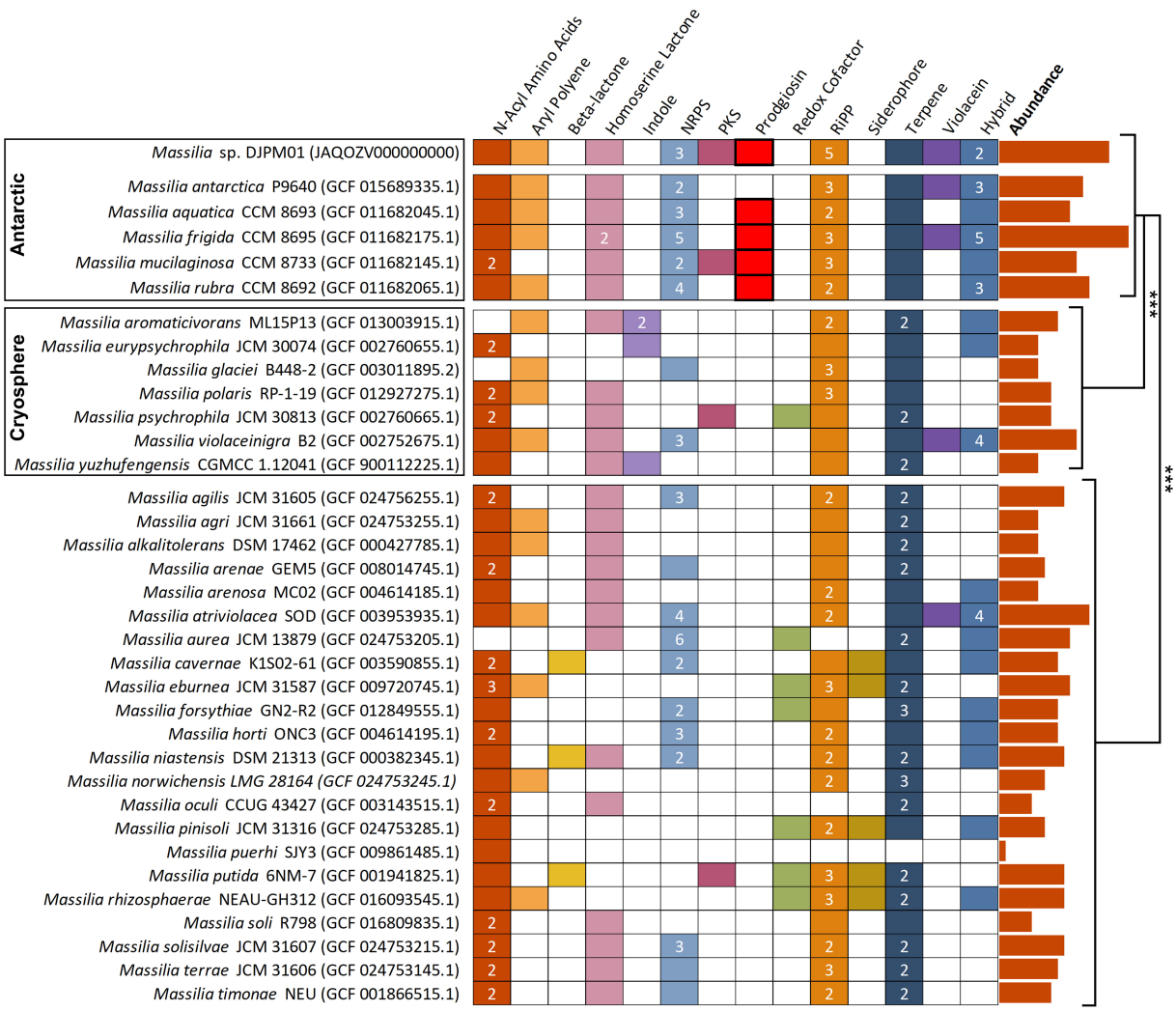

FIGURE 5
Annotated secondary metabolite BGS in *Massilia* reference genomes, sorted by isolation environment. Clusters have been sorted into broad categories, with hybrid clusters containing motifs of multiple categories (i.e., PKS-NRPS). Numbers represent the total abundance of clusters when multiple are present within the genome. Prodigiosin and violacein BGCs were confirmed *via* BLAST. Absolute abundance of clusters are plotted to the right of the figure and are significantly different between isolation environments (Tukey). NRPS, nonribosomal peptide synthetase; PKS, polyketide synthase; RiPP, ribosomally synthesized and post-translationally modified peptide.

a UV-treated prodigiosin (1) standard indicated a conversion of the compound to a non-pigmented degradation product with an *m/z* of 354.2169 $[M+H]^+$ and probable molecular formula of $C_{21}H_{28}N_3O_2$ (Supplementary Figure S8). Additionally, several other features with mass shifts consistent with addition of CH_2O to major prodiginines were observed. The only compound unique to the UV-treated strain DJPM01 was glycerophosphoserine (*m/z* 522.2831; calculated $[M+H]^+$ for $C_{24}H_{45}NO_9P$, 522.2832;). Masses congruent to those of arylpolyenes and migrastatin (*m/z* 512.2617; calculated $[M+H]^+$ for $C_{24}H_{45}NO_9P$, 522.2832) were also detected. No LC/MS or UV–Vis spectroscopic evidence of other pigments was found.

4. Discussion

Massilia species have been identified in diverse ecological niches across Antarctica, though little is known about their function within cold systems. We isolated strain DJPM01 from a microbial mat which sits adjacent to one of the saltiest aquatic features on Earth, the hypersaline Don Juan Pond in the McMurdo Dry Valleys (Toner et al., 2017). We identified this aerobic, Gram negative bacterium as a member of the *M. frigida* species. This strain was isolated on R2A agar, which is commonly utilized to cultivate bacteria from Antarctic environments, though growth on this medium is not an indicator of abundance or importance to a given system (Pulschen et al., 2017). Strain DJPM01 is estimated to be present at low abundance (~0.03%) in the established microbial mat community; however, abundance and ecological importance are not mutually exclusive, as highlighted with the rare biosphere concept (Lynch and Neufeld, 2015). Members of the *Massilia* genus have been of interest for their agricultural and pharmaceutical applications (Lewin et al., 2021; Dahal et al., 2021b). Thus, we examined both potential adaptations to ecologically relevant conditions and production of microbial secondary metabolites, including the pigment prodigiosin, in strain DJPM01.

10.3389/fmicb.2023.1156033

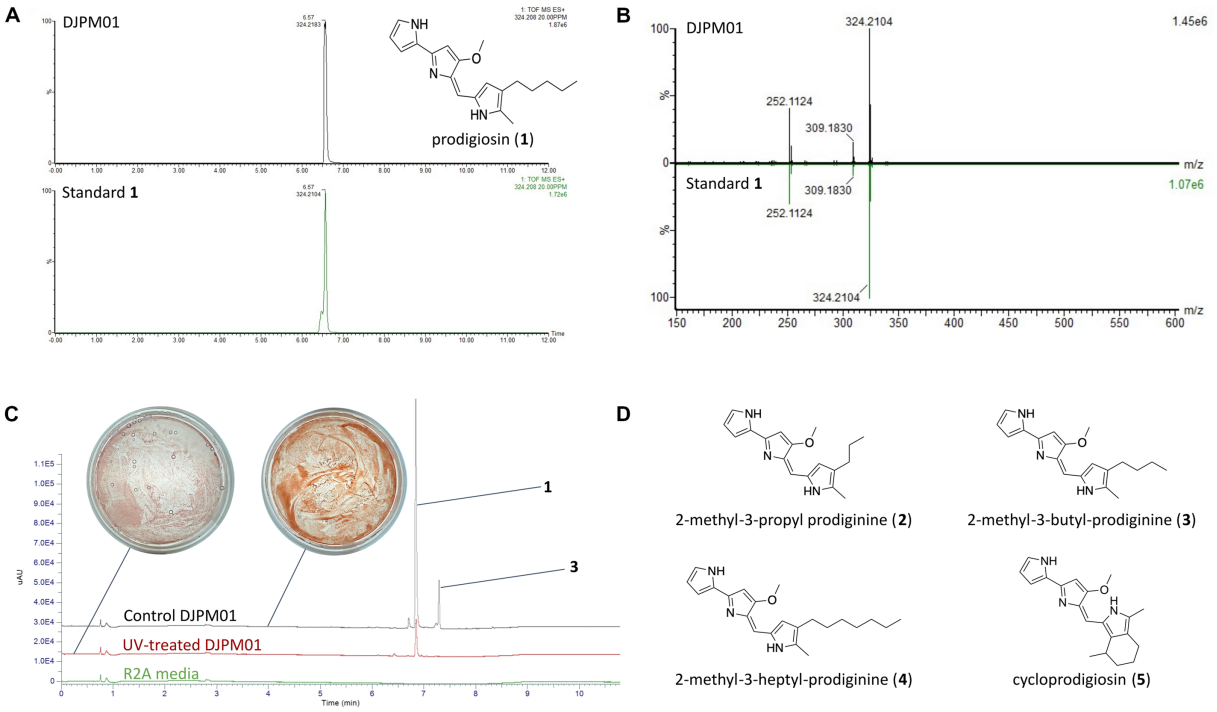

FIGURE 6
Detection of prodigiosin and derivatives in strain DJPM01 extracts. **(A)** Extracted ion chromatograms (m/z 324.208) of prodigiosin (1) in DJPM01 R2A agar extracts (black) compared to a prodigiosin standard (green). **(B)** Mirrored MS/MS mass spectra of prodigiosin (1) in DJPM01 agar extracts and prodigiosin standard. UV–Vis spectra of prodigiosin (1) in DJPM01 agar extracts (black) and prodigiosin standard (green) showing identical spectra. **(C)** Stacked UV trace diagram for plate extracts from control and UV-treated cultures. Dominant peaks corresponding to prodigiosin (1) and 2-methyl-3-butyl-prodiginine (3). Images of UV-exposed (left) and control (right) plates following 11days of incubation. **(D)** Molecular structures of detected prodigiosin derivatives.

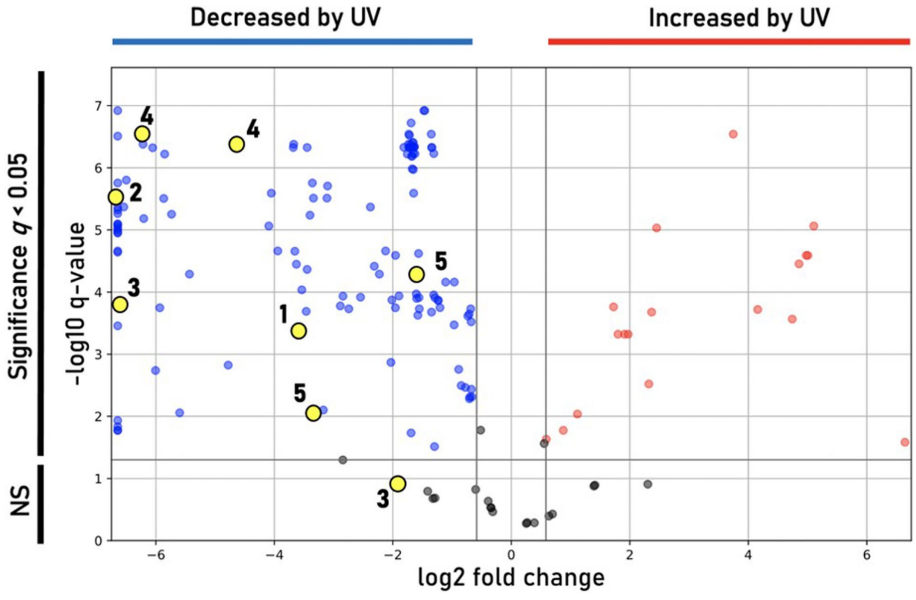

FIGURE 7
Differential features observed under UV treatment. Volcano plot showing statistically significant (q <0.05) features in DJPM01 grown on R2A agar that are either increased (red) or decreased (blue) relative to control samples that were not irradiated with UV-A light. Numbered and unnumbered yellow dots correspond to known features and unknown, prodiginine-related features, respectively.

4.1. Phylogeny and ecophysiology of an Antarctic *Massilia* strain

Modern prokaryotic species concepts strive to incorporate both the advanced sequencing tools available to interrogate microbial genomes as well as phenotypic assays (Rosselló-Móra and Amann, 2015). While specifics may be debated, it is generally agreed that species exhibit a large degree of genomic and phenotypic coherence (Rosselló-Móra and Amann, 2015). Conservative estimates indicate that a DDH of >70% (Tindall et al., 2010), ANI threshold of 95–96% (e.g., Konstantinidis and Tiedje, 2005; Konstantinidis et al., 2006), and 16S rRNA gene sequence identity of >98% (Kim et al., 2014) is appropriate for delineating prokaryotic species for taxonomic purposes. While strain DJPM01 has >99% sequence identity with several *Massilia* type strains, highest ANI (97.36%) and DDH (75.6%) were found with *M. frigida* strain CCM8695. Thus, we conclude that strain DJPM01 is a strain of this species group.

Strain DJPM01 shares phenotypic similarities with *M. frigida* strain CCM 8695 and other psychrotolerant strains, including colony morphology, motility, inability to grow at temperatures at or above 30°C, and sensitivity to UV-C irradiation (Holochová et al., 2020). Strain DJPM01 was more tolerant of alkaline growth conditions compared to reported observations of both psychrotolerant and mesophilic *Massilia*, though several *Massilia* species are also able to grow on media above pH 10, including *M. alkalitolerans*, which can survive on media adjusted to pH 12 (Xu et al., 2005). Based on 16S rRNA gene and whole-genome comparisons, strain DJPM01 forms a clade with seven named psychrotolerant *Massilia*, including the five described Antarctic species (Wang et al., 2018; Yang et al., 2019; Holochová et al., 2020; Sedláček et al., 2022). Of the Antarctic *Massilia* with published genome sequences, four have been described as producing a pink-red pigment when grown on R2A agar (Holochová et al., 2020) and contain the complete pathway for prodigiosin biosynthesis. The fifth, *M. antarctica* strain P9640, produces a blue-purple pigment, likely violacein (Sedláček et al., 2022). However, *Massilia* isolates beyond this clade (<82% ANI) have only been described as either unpigmented or as producing a yellow pigment, which could be carotenoids based on the putative BGCs present in their genomes (Gallego et al., 2006; Zhang et al., 2006).

4.2. Genomic adaptations to life in an Antarctic microbial mat

The genome of strain DJPM01 contains several adaptations to life in an Antarctic microbial mat. Low temperatures can negatively impact transcription and translation, both through decreases in reaction rate and through changes in the secondary structure of DNA, RNA, and proteins (De Maayer et al., 2014). Strain DJPM01 encodes multiple sets of genes associated with either preventing the formation of transcription-inhibiting RNA secondary structures (cold shock proteins) or unraveling the structures that do form (RNA helicases; Siddiqui et al., 2013). Similarly, strain DJPM01 has genes encoding for several protein chaperones to ensure correct folding of polypeptide chains. Other genes, such as *fab* genes and a putative Δ9-desaturase, are involved in the biosynthesis of unsaturated fatty acids to increase membrane fluidity at low temperature (De Maayer et al., 2014). Cold-adapted organisms synthesize compatible solutes to prevent the formation of ice crystals within the cell and combat changes in salinity associated with freezing temperatures (Chin et al., 2010). Genes involved in the biosynthesis and transport of the compatible solute glutamate are present within the genome, as well as several cation/proton antiporters, all of which are utilized to counteract changes in osmotic pressure (Kuroda et al., 2005; Saum and Müller, 2008).

UV irradiation can lead to both DNA damage and the generation of ROS (Castenholz and Garcia-Pichel, 2012). Strain DJPM01 contained several genes for reducing ROS (e.g., catalase and peroxiredoxin) and for DNA repair, including two photolyases, which may enable photo-repair of DNA during long Antarctic days in the austral summer. UV stress can also be mediated through the production of radiation-absorbing pigments. Strain DJPM01 contains BGCs for prodigiosin and violacein, pigments associated with UV survival in other organisms, such as *Serratia, Streptomyces*, and *Vibrio* species (Borić et al., 2011; Stankovic et al., 2012; Cediel Becerra et al., 2022), and increases the UV-screening ability of commercial sunscreen (Suryawanshi et al., 2015). Violacein has been described in a number of *Massilia* species, including *M. antarctica* from James Ross Island and *M. violaceinigra* from Tianshan glacier, China (Agematu et al., 2011; Myeong et al., 2016; Wang et al., 2018; Yang et al., 2019; Sedláček et al., 2022). To date, prodigiosin has only been described in Antarctic *Massilia* species (Holochová et al., 2020). The prevalence of pigment biosynthesis genes in Antarctic *Massilia* suggests that both violacein and prodigiosin could play a role in adaptation to the environment. However, it remains unclear why only the Antarctic *Massilia* appear to possess genes for prodigiosin. Regardless, climatic change in the MDV likely involves dynamic changes in solar radiation (Obryk et al., 2018), thus the production of UV-screening pigments may not provide a universal advantage to the organisms in question.

In addition to pigments, several other putative secondary metabolite BGCs were identified in the genome, including a homoserine lactone BGC potentially involved in quorum sensing, and a putative siderophore with similarity to myxochelin, shown to play a role in iron acquisition (Kunze et al., 1989; Montgomery et al., 2013). Several RiPP clusters are also present, which produce diverse molecules with a wide variety of functions, including antibacterial or enzyme inhibiting activities (Arnison et al., 2013). Notably, strain DJPM01 contained a putative BGC involved in the biosynthesis of the antifungal polyketide gladiofungin (Niehs et al., 2020). Further analysis of PKS modules in this gene cluster supported its identification as encoding for gladiofungin biosynthetic machinery (Supplementary Figure S4). This is the first report of a *Massilia* with the genetic potential to produce this antifungal. Gladiofungin has been shown to inhibit the fungus *Purpureocillium lilacinum* (Niehs et al., 2020), which has been isolated from the Antarctic peninsula (Gonçalves et al., 2015). The gladiofungin BGC in strain DJPM01 may play a role in inhibition of fungal competitors.

Strain DJPM01 has a similar abundance of genes associated with cold adaptation when compared to other psychrotolerant *Massilia* species, including genes for protein chaperones, RNA helicases, and fatty acid biosynthesis. Minor differences exist between strain DJPM01 and the closely related *M. frigida*, including the presence of specific toxin-antitoxin genes, which are believed to play a role in stress response (Fucich and Chen, 2020). Compared to non-Antarctic *Massilia*, the six *Massilia* isolated from Antarctic regions contained a significantly greater abundance of secondary metabolite BGCs (Supplementary Table S4). The genetic potential to synthesize a wide

arsenal of molecules in response to specific stressors under poly-extreme conditions would impart an ecological advantage (Giddings and Newman, 2015b; Sayed et al., 2020). Of the putatively identified BGCs, the myxochelin cluster is present across all six genomes, suggesting a strong selection pressure for iron acquisition (Kunze et al., 1989). Other gene clusters that are only present in one or two genomes, such as cephamycin and the gladiofungin we identified here, may play more specialized roles in competitive inhibition of other community members *in situ*. Secondary metabolism of Antarctic microbes remains poorly characterized and the abundance of putative BGCs that encode for yet uncharacterized molecules may be of interest in the search for novel bioactive compounds (Correa and Abreu, 2020). Extreme environments likely offer an untapped wealth of secondary metabolites that may prove useful in a number of industrial or biomedical applications (Giddings and Newman, 2015a; Sayed et al., 2020).

4.3. Prodigiosin, a molecule involved in environmental adaptation

Our work provides the first molecular characterization of prodiginines produced by a member of the *Massilia* genus. Holochová et al. (2020) noted the pigmentation and BGC for prodigiosin in four Antarctic *Massilia* species, and Woodhams et al. (2018) examined a mesophilic *Massilia* (now *Pseudoduganella*; Lu et al., 2022) for the production of prodigiosins, however none were detected. In our study, mass defect analysis (Figure 8) identified several metabolites congruent with prodiginines detected within similar retention times (5–8 min), including analogs formed from either the addition of oxygen, reduction, or cyclization. Some of these metabolites are known compounds; however, most are unknown and warrant further investigation (He et al., 2022). Due to the high sequence similarity between putative prodigiosin BGCs in *M. frigida*, *M. rubra*, *M. mucilaginosa*, and *M. aquatica*, it is likely that all five red-pigmented Antarctic *Massilia* are genetically capable of producing related pigments.

The biosynthesis of prodigiosin may provide numerous advantages to the cold-adapted *Massilia*, which may serve as pioneer species during microbial mat establishment (Sommers et al., 2019). Given prodigiosin's role as a UV-protectant in other microbial species (Borić et al., 2011; Stankovic et al., 2012; Cediel Becerra et al., 2022), we sought to determine the effect of intense UV-A radiation on pigment production by strain DJPM01. Following irradiation, we saw a decrease in the abundance of most metabolites, including prodigiosin (1), with the exception of an increase in an oxygenated prodiginine (*m/z* 340.2020), which may represent a UV photolysis product of 2-methyl-3-butyl-prodiginine (3). We did not detect the pigment violacein under any growth condition tested, despite strong genomic evidence for a violacein BGC. Thus, it is likely that this molecule may be produced under yet-unknown conditions, such as in response to predation by metazoans (Choi et al., 2015). The color change (Figure 6C) of UV-treated strain DJPM01 was likely related to prodiginine degradation, as the irradiated prodigiosin standard was observed to lose color intensity following 24-h of UV-A exposure (Supplementary Figure S8). As pigment degradation is likely the result of UV-A exposure, and the rate of photolysis is independent from molecular synthesis, transcriptional or translational response in prodigiosin biosynthesis upon UV exposure should be further investigated. Alternatively, *Massilia* within the natural mat environment may also benefit from other photoprotective mechanisms. Photoprotective compounds can provide a shielding effect to the entire community within microbial mats, so that not only the producers benefit from the UV protection (Gareia-Pichel and Castenholz, 1994).

In addition to UV-protection, prodigiosin has been linked to numerous bioactivities. For example, prodigiosin has been shown to function as an antimicrobial agent against both Gram positive and Gram negative bacteria (Danevčič et al., 2016), and thus may serve as a mediator of interspecies competition within the microbial mat environment. Prodigiosin has also been reported as a nematicidal agent (Habash et al., 2020). Nematodes in the MDV function as grazers within microbial mats, and have been identified as present within the DJP mat (Siegel et al., 1979; Andriuzzi et al., 2018), thus prodigiosin may serve as a defense against overgrazing. Additionally, psychrophilic organisms increase intracellular ATP concentrations to support metabolic activity at low temperatures (Amato and Christner, 2009). In high-density cultures of *S. marcescens*, accumulation of intracellular ATP occurred at a higher rate in prodigiosin pigmented cells, compared to non-pigmented cells (Haddix and Shanks, 2018). Thus, prodigiosin may also play an undescribed role in energetics and adaptation to low temperatures. More directed experiments are necessary to elucidate the ecological function of prodiginines in strain DJPM01 *in situ*.

In the coming decades, changes in solar radiation will impact MDV communities through both direct and indirect processes. The low albedo of MDV soils leads to increased levels of energy absorption compared to the surrounding ice (Dana et al., 1998) resulting in higher summer *in situ* temperatures (Fountain et al., 2014), which could lead to possible hydrological and geochemical changes, such as enhanced permafrost melting and salt mobilization (Ball and Virginia, 2012). Additionally, both anthropogenic and natural (i.e., volcanoes and wildfire) emissions drive variations in solar flux in the MDV, potentially resulting in a decrease UV radiation (Obryk et al., 2018). Thus, microbial community response to UV irradiation will likely vary with local climatic trends. Investigating the responses of individual community members to simulated stressors (i.e., UV radiation) can inform how natural microbial communities may respond to environmental variation associated with anthropogenic climate change.

5. Conclusion

Our characterization of *Massilia frigida* strain DJPM01 provides insight into the complex microbial interactions occurring in an Antarctic microbial mat and suggests multiple avenues for future research. In Antarctic *Massilia*, both pigment production and the high number of BGCs suggests *Massilia* may play a role in mediating microbial interactions in Antarctic ecosystems and highlights the importance of investigating Antarctic microbial isolates for their production of bioactive compounds. Prodigiosin has been implicated in bactericidal, nematocidal, and UV-screening activities, though the role it plays *in situ* in complex, multi-species Antarctic microbial mats warrants further investigation. Our data demonstrate that UV radiation impacts the accumulation of this pigment in *Massilia*, thus the abundance of this molecule may be influenced by increased variation in solar radiation. The changing climate in the MDV system is complex with effects on microbial communities uncertain; understanding the role of secondary metabolites in the MDV

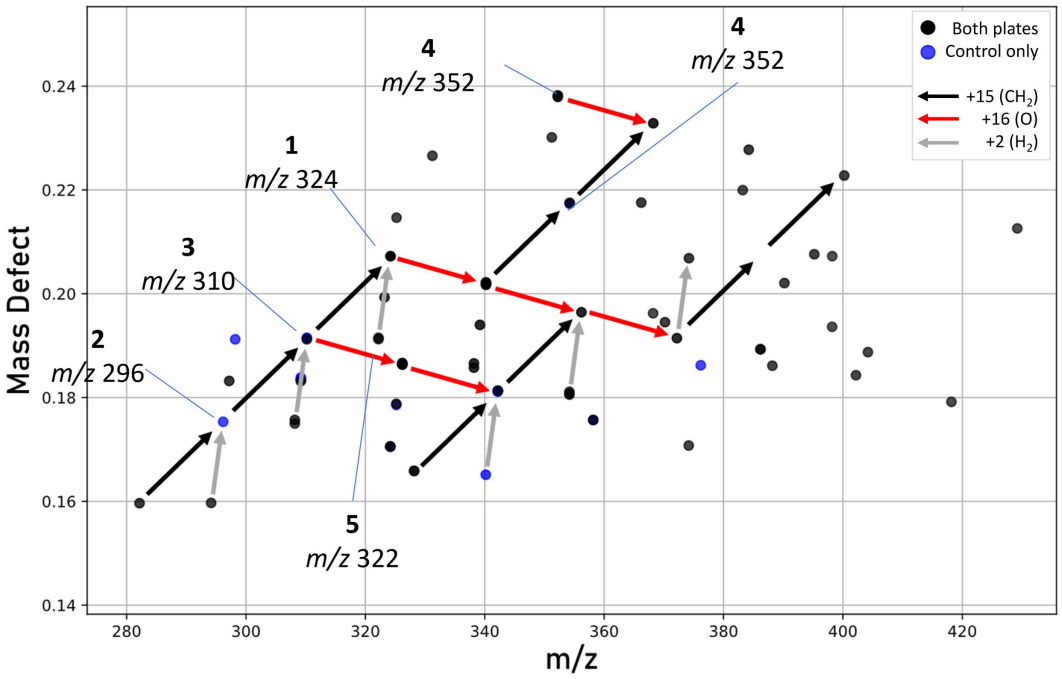

FIGURE 8
Mass defect plot showing features hypothesized to be prodiginines. Features seen in either both extracts (black dots) or control plate extracts only (blue dots). No unique prodiginine features were seen in UV-treated plates. Arrows represent mass defect vectors, with red denoting the addition of oxygen (+16), black the addition of a methyl group (+15), and gray a loss of hydrogen possibly indicating cyclization.

communities, especially under ecologically relevant conditions can inform how these communities will respond to environmental change.

Data availability statement

The datasets presented in this study can be found in online repositories. The names of the repository/repositories and accession number(s) can be found at: https://www.ncbi.nlm.nih.gov/genbank/, JAQOZV000000000. https://www.ncbi.nlm.nih.gov/genbank/, OQ346149.

Author contributions

JAM and L-AG conceived of the project and acquired funding and resources. JAM collected and processed the samples. JS, L-AG, RS, and JAM contributed to the design of the experiments. JS performed the culture work, DNA extraction, genomic analyses, and wrote the first draft of the manuscript. JS and L-AG extracted samples for metabolomics. RS analyzed the metabolite samples. L-AG and RS interpreted the metabolomics data. All authors contributed to the article and approved the submitted version.

Funding

This work was funded by the National Science Foundation OPP #2148730 and OPP #1643687 (to JAM) and OPP #2148731 (to L-AG) with additional support from the University of Tennessee Office of Research, Innovation and Economic Development (to JAM).

Acknowledgments

We are grateful to the Antarctic Support Contractor and ANTAEM Team members for logistical support during sample collection. In addition, we thank Teresa Mccarrell for initiating enrichments and Thomas Hyde for his assistance with culture work.

Conflict of interest

The authors declare that the research was conducted in the absence of any commercial or financial relationships that could be construed as a potential conflict of interest.

Publisher's note

All claims expressed in this article are solely those of the authors and do not necessarily represent those of their affiliated organizations, or those of the publisher, the editors and the reviewers. Any product that may be evaluated in this article, or claim that may be made by its manufacturer, is not guaranteed or endorsed by the publisher.

Supplementary material

The Supplementary material for this article can be found online at: https://www.frontiersin.org/articles/10.3389/fmicb.2023.1156033/full#supplementary-material

References

Agematu, H., Suzuki, K., and Tsuya, H. (2011). *Massilia* sp. BS-1, a novel violacein-producing bacterium isolated from soil. *Biosci. Biotechnol. Biochem.* 75, 2008–2010. doi: 10.1271/bbb.100729

Alexander, D. C., and Jensen, S. E. (1998). Investigation of the *Streptomyces clavuligerus* cephamycin C gene cluster and its regulation by the CcaR proteinbize. *J. Bacteriol.* 180, 4068–4079. doi: 10.1128/JB.180.16.4068-4079.1998

Alger, A. S., McKnight, D. M., Spaulding, S. A., Tate, C. M., Shupe, G. H., Welch, K. A., et al. (1997). *Ecological Processes in a Cold Desert Ecosystem: The Abundance and Species Distribution of Algal Mats in Glacial Meltwater Streams in Taylor Valley*. Boulder, CO: University of Colorado: Institute of Arctic and Alpine Research, Occasional Paper 51.

Altschul, S. F., Gish, W., Miller, W., Myers, E. W., and Lipman, D. J. (1990). Basic local alignment search tool. *J. Mol. Biol.* 215, 403–410. doi: 10.1016/S0022-2836(05)80360-2

Amato, P., and Christner, B. C. (2009). Energy metabolism response to low-temperature and frozen conditions in *Psychrobacter cryohalolentis*. *Appl. Environ. Microbiol.* 75, 711–718. doi: 10.1128/AEM.02193-08

Andreyeva, I. N., and Ogorodnikova, T. I. (2015). Pigmentation of Serratia marcescens and spectral properties of prodigiosin. *Microbiology* 84, 28–33. doi: 10.1134/S0026261715010026

Andriuzzi, W. S., Adams, B. J., Barrett, J. E., Virginia, R. A., and Wall, D. H. (2018). Observed trends of soil fauna in the Antarctic dry valleys: early signs of shifts predicted under climate change. *Ecology* 99, 312–321. doi: 10.1002/ecy.2090

Apprill, A., McNally, S., Parsons, R., and Weber, L. (2015). Minor revision to V4 region SSU rRNA 806R gene primer greatly increases detection of SAR11 bacterioplankton. *Aquat. Microb. Ecol.* 75, 129–137. doi: 10.3354/ame01753

Arnison, P. G., Bibb, M. J., Bierbaum, G., Bowers, A. A., Bugni, T. S., Bulaj, G., et al. (2013). Ribosomally synthesized and post-translationally modified peptide natural products: overview and recommendations for a universal nomenclature. *Nat. Prod. Rep.* 30, 108–160. doi: 10.1039/c2np20085f

Ball, B. A., and Virginia, R. A. (2012). Meltwater seep patches increase heterogeneity of soil geochemistry and therefore habitat suitability. *Geoderma* 189–190, 652–660. doi: 10.1016/j.geoderma.2012.06.028

Bizebard, T., Ferlenghi, I., Iost, I., and Dreyfus, M. (2004). Studies on three *E. coli* DEAD-box helicases point to an unwinding mechanism different from that of model DNA helicases. *Biochemistry* 43, 7857–7866. doi: 10.1021/bi049852s

Blin, K., Shaw, S., Kloosterman, A. M., Charlop-Powers, Z., van Wezel, G. P., Medema, M. H., et al. (2021). antiSMASH 6.0: improving cluster detection and comparison capabilities. *Nucleic Acids Res.* 49, W29–W35. doi: 10.1093/nar/gkab335

Bolger, A. M., Lohse, M., and Usadel, B. (2014). Trimmomatic: a flexible trimmer for Illumina sequence data. *Bioinformatics* 30, 2114–2120. doi: 10.1093/bioinformatics/btu170

Borić, M., Danevčič, T., and Stopar, D. (2011). Prodigiosin from *Vibrio* sp. DSM 14379; a new UV-protective pigment. *Microb. Ecol.* 62, 528–536. doi: 10.1007/s00248-011-9857-0

Campen, R. L. (2015). Investigating the Mode of Action of Tuberculosis Drugs Using Hypersensitive Mutants of *Mycobacterium smegmatis*. *Dissertation*. Wellington, NZ: Victoria University of Wellington.

Caporaso, J. G., Lauber, C. L., Walters, W. A., Berg-Lyons, D., Lozupone, C. A., Turnbaugh, P. J., et al. (2011). Global patterns of 16S rRNA diversity at a depth of millions of sequences per sample. *Proc. Natl. Acad. Sci.* 108, 4516–4522. doi: 10.1073/pnas.1000080107

Castenholz, R. W., and Garcia-Pichel, F. (2012). "Cyanobacterial responses to UV radiation" in *Ecology of Cyanobacteria II*. ed. B. A. Whitton (Dordrecht: Springer Netherlands), 481–499.

Cauz, A. C. G., Carretero, G. P. B., Saraiva, G. K. V., Park, P., Mortara, L., Cuccovia, I. M., et al. (2019). Violacein targets the cytoplasmic membrane of Bacteria. *ACS Infect. Dis.* 5, 539–549. doi: 10.1021/acsinfecdis.8b00245

Cediel Becerra, J. D. D., Suescún Sepúlveda, J. A., and Fuentes, J. L. (2022). Prodigiosin production and Photoprotective/Antigenotoxic properties in *Serratia marcescens* indigenous strains from eastern cordillera of Colombia. *Photochem. Photobiol.* 98, 254–261. doi: 10.1111/php.13507

Chin, J. P., Megaw, J., Magill, C. L., Nowotarski, K., Williams, J. P., Bhaganna, P., et al. (2010). Solutes determine the temperature windows for microbial survival and growth. *Proc. Natl. Acad. Sci. U. S. A.* 107, 7835–7840. doi: 10.1073/pnas.1000557107

Chiquet, C., Boisset, S., Pechinot, A., Creuzot-Garcher, C., Aptel, F., and Bron, A. M. (2015). *Massilia timonae* as cause of chronic endophthalmitis following cataract surgery. *J Cataract Refract Surg* 41, 1778–1780. doi: 10.1016/j.jcrs.2015.07.016

Cho, H., and Cronan, J. E. (1993). *Escherichia coli* thioesterase I, molecular cloning and sequencing of the structural gene and identification as a periplasmic enzyme. *J. Biol. Chem.* 268, 9238–9245. doi: 10.1016/S0021-9258(18)98341-9

Choi, S. Y., Yoon, K., Lee, J. I., and Mitchell, R. J. (2015). Violacein: properties and production of a versatile bacterial pigment. *Biomed. Res. Int.* 2015, 1–8. doi: 10.1155/2015/465056

Cimermancic, P., Medema, M. H., Claesen, J., Kurita, K., Wieland Brown, L. C., Mavrommatis, K., et al. (2014). Insights into secondary metabolism from a global analysis of prokaryotic biosynthetic gene clusters. *Cells* 158, 412–421. doi: 10.1016/j.cell.2014.06.034

Correa, T., and Abreu, F. (2020). "Antarctic microorganisms as sources of Q21 biotechnological products" in *Physiological and Biotechnological Aspects of Extremophiles*. eds. R. Salwan and V. Sharma (Cambridge, MA: Academic Press), 269–284.

Couvin, D., Bernheim, A., Toffano-Nioche, C., Touchon, M., Michalik, J., Néron, B., et al. (2018). CRISPRCasFinder, an update of CRISRFinder, includes a portable version, enhanced performance and integrates search for Cas proteins. *Nucleic Acids Res.* 46, W246–W251. doi: 10.1093/nar/gky425

Dahal, R. H., Chaudhary, D. K., and Kim, J. (2021b). Genome insight and description of antibiotic producing *Massilia antibiotica* sp. nov., isolated from oil-contaminated soil. *Sci. Rep.* 11:6695. doi: 10.1038/s41598-021-86232-z

Dahal, R. H., Chaudhary, D. K., Kim, D.-U., and Kim, J. (2021a). Cold-shock gene cspC in the genome of *Massilia polaris* sp. nov. revealed cold-adaptation. *Antonie Van Leeuwenhoek* 114, 1275–1284. doi: 10.1007/s10482-021-01600-z

Dana, G. L., Wharton, R. A. Jr., and Dubayah, R. A. (1998). "Solar radiation in the Mcmurdo dry valleys, Antarctica" in *Ecosystem Dynamics in a Polar Desert: The Mcmurdo Dry Valleys* (Washington DC: American Geophysical Union), 39–64.

Danevčič, T., Vezjak, M. B., Zorec, M., and Stopar, D. (2016). Prodigiosin – a multifaceted *Escherichia coli* antimicrobial agent. *PLoS One* 11:e0162412. doi: 10.1371/journal.pone.0162412

Davey, M. C., and Clarke, K. J. (1992). Fine structure of a terrestrial cyanobacterial mat from Antarctica1. *J. Phycol.* 28, 199–202. doi: 10.1111/j.0022-3646.1992.00199.x

De Maayer, P., Anderson, D., Cary, C., and Cowan, D. A. (2014). Some like it cold: understanding the survival strategies of psychrophiles. *EMBO Rep.* 15, 508–517. doi: 10.1002/embr.201338170

Diaz, M. A., Adams, B. J., Welch, K. A., Welch, S. A., Opiyo, S. O., Khan, A. L., et al. (2018). Aeolian material transport and its role in landscape connectivity in the McMurdo dry valleys, Antarctica. *J. Geophys. Res. Earth* 123, 3323–3337. doi: 10.1029/2017JF004589

Emms, D. M., and Kelly, S. (2019). OrthoFinder: phylogenetic orthology inference for comparative genomics. *Genome Biol.* 20:238. doi: 10.1186/s13059-019-1832-y

Federhen, S. (2012). The NCBI taxonomy database. *Nucleic Acids Res.* 40, D136–D143. doi: 10.1093/nar/gkr1178

Fee, J. A. (1991). Regulation of sod genes in *Escherichia coli*: relevance to superoxide dismutase function. *Mol. Microbiol.* 5, 2599–2610. doi: 10.1111/j.1365-2958.1991.tb01968.x

Fountain, A. G., Levy, J. S., Gooseff, M. N., and Van Horn, D. (2014). The McMurdo Dry Valleys: A landscape on the threshold of change. *Geomorphology* 225, 25–35. doi: 10.1016/j.geomorph.2014.03.044

Fountain, A. G., Nylen, T. H., Monaghan, A., Basagic, H. J., and Bromwich, D. (2009). Snow in the McMurdo dry valleys, Antarctica. *Int. J. Climatol.* doi: 10.1002/joc.1933

Frederick, J. E., and Snell, H. E. (1988). Ultraviolet radiation levels during the Antarctic spring. *Science* 241, 438–440. doi: 10.1126/science.241.4864.438

Fucich, D., and Chen, F. (2020). Presence of toxin-antitoxin systems in picocyanobacteria and their ecological implications. *ISME J.* 14, 2843–2850. doi: 10.1038/s41396-020-00746-4

Gallego, V., Sánchez-Porro, C., García, M. T., and Ventosa, A. (2006). *Massilia aurea* sp. nov., isolated from drinking water. *Int. J. Syst. Evol. Microbiol.* 56, 2449–2453. doi: 10.1099/ijs.0.64389-0

Gareia-Pichel, F., and Castenholz, R. W. (1994). "On the significance of solar ultraviolet radiation for the ecology of microbial mats" in *Microbial Mats NATO ASI Series*. eds. L. J. Stal and P. Caumette (Berlin, Heidelberg: Springer), 77–84.

Giddings, L.-A., and Newman, D. J. (2015a). "Bioactive compounds from extremophiles" in *SpringerBriefs in Microbiology: Extremophilic Bacteria*. eds. S. M. Tiquia-Arashiro and M. Mormile (Cham, Germany: Springer).

Giddings, L.-A., and Newman, D. J. (2015b). "Bioactive compounds from terrestrial extremophiles" in *Springer Briefs in Microbiology: Extremophilic Bacteria*. eds. S. M. Tiquia-Arashiro and M. Mormile (Cham, Germany: Springer).

Gonçalves, V. N., Carvalho, C. R., Johann, S., Mendes, G., Alves, T. M. A., Zani, C. L., et al. (2015). Antibacterial, antifungal and antiprotozoal activities of fungal communities present in different substrates from Antarctica. *Polar Biol.* 38, 1143–1152. doi: 10.1007/s00300-015-1672-5

Gu, Z., Liu, Y., Xu, B., Wang, N., Jiao, N., Shen, L., et al. (2017). *Massilia glaciei* sp. nov., isolated from the Muztagh glacier. *Int. J. Syst. Evol. Microbiol.* 67, 4075–4079. doi: 10.1099/ijsem.0.002252

Guo, J., Bolduc, B., Zayed, A. A., Varsani, A., Dominguez-Huerta, G., Delmont, T. O., et al. (2021). VirSorter2: a multi-classifier, expert-guided approach to detect diverse DNA and RNA viruses. *Microbiome* 9:37. doi: 10.1186/s40168-020-00990-y

Guo, B., Liu, Y., Gu, Z., Shen, L., Liu, K., Wang, N., et al. (2016). *Massilia psychrophila* sp. nov., isolated from an ice core. *Int. J. Syst. Evol. Microbiol.* 66, 4088–4093. doi: 10.1099/ijsem.0.001315

Gurevich, A., Saveliev, V., Vyahhi, N., and Tesler, G. (2013). QUAST: quality assessment tool for genome assemblies. *Bioinformatics* 29, 1072–1075. doi: 10.1093/bioinformatics/btt086

Habash, S. S., Brass, H. U. C., Klein, A. S., Klebl, D. P., Weber, T. M., Classen, T., et al. (2020). Novel Prodiginine derivatives demonstrate bioactivities on plants, nematodes, and Fungi. *Front. Plant Sci.* 11:579807. doi: 10.3389/fpls.2020.579807

Haddix, P. L., and Shanks, R. M. Q. (2018). Prodigiosin pigment of *Serratia marcescens* is associated with increased biomass production. *Arch. Microbiol.* 200, 989–999. doi: 10.1007/s00203-018-1508-0

Harris, A. K. P., Williamson, N. R., Slater, H., Cox, A., Abbasi, S., Foulds, I., et al. (2004). The Serratia gene cluster encoding biosynthesis of the red antibiotic, prodigiosin, shows species- and strain-dependent genome context variation. *Microbiology* 150, 3547–3560. doi: 10.1099/mic.0.27222-0

He, S., Li, P., Wang, J., Zhang, Y., Lu, H., Shi, L., et al. (2022). Discovery of new secondary metabolites from marine bacteria *Hahella* based on an omics strategy. *Mar. Drugs* 20:269. doi: 10.3390/md20040269

Hirsch, P., Gallikowski, C. A., Siebert, J., Peissl, K., Kroppenstedt, R., Schumann, P., et al. (2004). *Deinococcus frigens* sp. nov., *Deinococcus saxicola* sp. nov., and *Deinococcus marmoris* sp. nov., low temperature and draught-tolerating, UV-resistant bacteria from continental Antarctica. *Syst. Appl. Microbiol.* 27, 636–645. doi: 10.1078/0723202042370008

Holochová, P., Mašlaňová, I., Sedláček, I., Švec, P., Králová, S., Kovařovic, V., et al. (2020). Description of *Massilia rubra* sp. nov., *Massilia aquatica* sp. nov., *Massilia mucilaginosa* sp. nov., *Massilia frigida* sp. nov., and one *Massilia* genomospecies isolated from Antarctic streams, lakes and regoliths. *Syst. Appl. Microbiol.* 43:126112. doi: 10.1016/j.syapm.2020.126112

Ju, J., Lim, S.-K., Jiang, H., and Shen, B. (2005). Migrastatin and Dorrigocins are shunt metabolites of iso-Migrastatin. *J. Am. Chem. Soc.* 127, 1622–1623. doi: 10.1021/ja043808i

Kämpfer, P., Lodders, N., Martin, K., and Falsen, E. (2012). *Massilia oculi* sp. nov., isolated from a human clinical specimen. *Int. J. Syst. Evol. Microbiol.* 62, 364–369. doi: 10.1099/ijs.0.032441-0

Kanehisa, M., Sato, Y., and Morishima, K. (2016). BlastKOALA and GhostKOALA: KEGG tools for functional characterization of genome and metagenome sequences. *J. Mol. Biol.* 428, 726–731. doi: 10.1016/j.jmb.2015.11.006

Kearse, M., Moir, R., Wilson, A., Stones-Havas, S., Cheung, M., Sturrock, S., et al. (2012). Geneious basic: an integrated and extendable desktop software platform for the organization and analysis of sequence data. *Bioinformatics* 28, 1647–1649. doi: 10.1093/bioinformatics/bts199

Kim, M., Oh, H.-S., Park, S.-C., and Chun, J. (2014). Towards a taxonomic coherence between average nucleotide identity and 16S rRNA gene sequence similarity for species demarcation of prokaryotes. *Int. J. Syst. Evol. Microbiol.* 64, 346–351. doi: 10.1099/ijs.0.059774-0

Konstantinidis, K. T., Ramette, A., and Tiedje, J. M. (2006). The bacterial species definition in the genomic era. *Philos Trans R Soc B Biol Sci* 361, 1929–1940. doi: 10.1098/rstb.2006.1920

Konstantinidis, K. T., and Tiedje, J. M. (2005). Genomic insights that advance the species definition for prokaryotes. *Proc. Natl. Acad. Sci.* 102, 2567–2572. doi: 10.1073/pnas.0409727102

Kunze, B., Bedorf, N., Kohl, W., Höfle, G., and Reichenbach, H. (1989). Myxochelin a, a new iron-chelating compound from *Angiococcus disciformis* (myxobacterales). Production, isolation, physico-chemical and biological properties. *J. Antibiot.* 42, 14–17. doi: 10.7164/antibiotics.42.14

Kuroda, T., Mizushima, T., and Tsuchiya, T. (2005). Physiological roles of three Na+/H+ Antiporters in the Halophilic bacterium *Vibrio parahaemolyticus*. *Microbiol. Immunol.* 49, 711–719. doi: 10.1111/j.1348-0421.2005.tb03662.x

la Scola, B., Birtles, R. J., Mallet, M.-N., and Raoult, D. (1998). *Massilia timonae* gen. Nov., sp. nov., isolated from blood of an immunocompromised patient with cerebellar lesions. *J. Clin. Microbiol.* 36, 2847–2852. doi: 10.1128/JCM.36.10.2847-2852.1998

La Teana, A., Brandi, A., Falconi, M., Spurio, R., Pon, C. L., and Gualerzi, C. O. (1991). Identification of a cold shock transcriptional enhancer of the *Escherichia coli* gene encoding nucleoid protein H-NS. *Proc. Natl. Acad. Sci.* 88, 10907–10911. doi: 10.1073/pnas.88.23.10907

Lenz, G., and Ron, E. Z. (2014). Novel interaction between the major bacterial heat shock chaperone (GroESL) and an RNA chaperone (CspC). *J. Mol. Biol.* 426, 460–466. doi: 10.1016/j.jmb.2013.10.018

Levy, J. (2013). How big are the McMurdo dry valleys? Estimating ice-free area using Landsat image data. *Antarct. Sci.* 25, 119–120. doi: 10.1017/S0954102012000727

Lewin, S., Francioli, D., Ulrich, A., and Kolb, S. (2021). Crop host signatures reflected by co-association patterns of keystone Bacteria in the rhizosphere microbiota. *Environ Microbiome* 16:18. doi: 10.1186/s40793-021-00387-w

Li, Y., Weissman, K. J., and Müller, R. (2008). Myxochelin biosynthesis: direct evidence for two- and four-Electron reduction of a carrier protein-bound Thioester. *J. Am. Chem. Soc.* 130, 7554–7555. doi: 10.1021/ja8025278

Li, Y., Xu, X., Dietrich, M., Urlacher, V. B., Schmid, R. D., Ouyang, P., et al. (2009). Identification and functional expression of a Δ9 fatty acid desaturase from the marine bacterium *Pseudoalteromonas* sp. MLY15. *J. Mol. Catal. B Enzym.* 56, 96–101. doi: 10.1016/j.molcatb.2008.07.012

Lu, H.-B., Cai, Z.-P., Yang, Y.-G., and Xu, M.-Y. (2020). *Duganella rivus* sp. nov., *Duganella fentianensis* sp. nov., *Duganella qianjiadongensis* sp. nov. and *Massilia guangdongensis* sp. nov., isolated from subtropical streams in China and reclassification of all species within genus *Pseudoduganella*. *Antonie Van Leeuwenhoek* 113, 1155–1165. doi: 10.1007/s10482-020-01422-5

Lu, H., Song, D., Deng, T., Mei, C., and Xu, M. (2022). *Duganella vulcania* sp. nov., *Rugamonas fusca* sp. nov., *Rugamonas brunnea* sp. nov. and *Rugamonas apoptosis* sp. nov., isolated from subtropical streams, and phylogenomic analyses of the genera *Janthinobacterium, Duganella, Rugamonas, Pseudoduganella* and *Massilia*. *Int. J. Syst. Evol. Microbiol.* 72:005407. doi: 10.1099/ijsem.0.005407

Lynch, M. D. J., and Neufeld, J. D. (2015). Ecology and exploration of the rare biosphere. *Nat. Rev. Microbiol.* 13, 217–229. doi: 10.1038/nrmicro3400

McKnight, D. M., Tate, C. M., Andrews, E. D., Niyogi, D. K., Cozzetto, K., Welch, K., et al. (2007). Reactivation of a cryptobiotic stream ecosystem in the McMurdo dry valleys, Antarctica: a long-term geomorphological experiment. *Geomorphology* 89, 186–204. doi: 10.1016/j.geomorph.2006.07.025

Meier-Kolthoff, J. P., Carbasse, J. S., Peinado-Olarte, R. L., and Göker, M. (2022). TYGS and LPSN: a database tandem for fast and reliable genome-based classification and nomenclature of prokaryotes. *Nucleic Acids Res.* 50, D801–D807. doi: 10.1093/nar/gkab902

Mikucki, J., Lyons, W. B., Hawes, I., Lanoil, B. D., and Doran, P. T. (2010). "Saline lakes and ponds in the McMurdo dry valleys: ecological analogs to martian paleolake environments" in *Life in Antarctic Deserts and Other Cold Dry Environments: Astrobiological Analogs*. eds. P. T. Doran, W. B. Lyons and D. M. McKnight (Cambridge, Massachusetts: Cambridge University Press), 160–194.

Mogk, A., Schlieker, C., Strub, C., Rist, W., Weibezahn, J., and Bukau, B. (2003). Roles of individual domains and conserved motifs of the AAA+ chaperone ClpB in Oligomerization, ATP hydrolysis, and chaperone activity*. *J. Biol. Chem.* 278, 17615–17624. doi: 10.1074/jbc.M209686200

Montgomery, K., Charlesworth, J. C., LeBard, R., Visscher, P. T., and Burns, B. P. (2013). Quorum sensing in extreme environments. *Life* 3, 131–148. doi: 10.3390/life3010131

Myeong, N. R., Seong, H. J., Kim, H.-J., and Sul, W. J. (2016). Complete genome sequence of antibiotic and anticancer agent violacein producing *Massilia* sp. strain NR 4-1. *J. Biotechnol.* 223, 36–37. doi: 10.1016/j.jbiotec.2016.02.027

Niehs, S. P., Kumpfmüller, J., Dose, B., Little, R. F., Ishida, K., Flórez, L. V., et al. (2020). Insect-associated Bacteria assemble the antifungal Butenolide Gladiofungin by non-canonical polyketide chain termination. *Angew. Chem. Int. Ed.* 59, 23122–23126. doi: 10.1002/anie.202005711

Obryk, M. K., Doran, P. T., Fountain, A. G., Myers, M., and McKay, C. P. (2020). Climate from the McMurdo dry valleys, Antarctica, 1986–2017: surface air temperature trends and redefined summer season. *J. Geophys. Res. Atmos.* 125:e2019JD032180. doi: 10.1029/2019JD032180

Obryk, M. K., Fountain, A. G., Doran, P. T., Lyons, W. B., and Eastman, R. (2018). Drivers of solar radiation variability in the McMurdo dry valleys, Antarctica. *Sci Rep* 8:5002. doi: 10.1038/s41598-018-23390-7

Ofek, M., Hadar, Y., and Minz, D. (2012). Ecology of root colonizing *Massilia* (Oxalobacteraceae). *PLoS One* 7:e40117. doi: 10.1371/journal.pone.0040117

O'Leary, N. A., Wright, M. W., Brister, J. R., Ciufo, S., Haddad, D., McVeigh, R., et al. (2016). Reference sequence (RefSeq) database at NCBI: current status, taxonomic expansion, and functional annotation. *Nucleic Acids Res.* 44, D733–D745. doi: 10.1093/nar/gkv1189

Parks, D. H., Imelfort, M., Skennerton, C. T., Hugenholtz, P., and Tyson, G. W. (2015). CheckM: assessing the quality of microbial genomes recovered from isolates, single cells, and metagenomes. *Genome Res.* 25, 1043–1055. doi: 10.1101/gr.186072.114

Peeters, K., Verleyen, E., Hodgson, D. A., Convey, P., Ertz, D., Vyverman, W., et al. (2012). Heterotrophic bacterial diversity in aquatic microbial mat communities from Antarctica. *Polar Biol.* 35, 543–554. doi: 10.1007/s00300-011-1100-4

Peng, J., Chou, K., Li, C., and Lee, S. (2011). Generation kinetics of color centers in irradiated poly(4-methyl-1-pentene). *J. Appl. Phys.* 110:063529. doi: 10.1063/1.3642957

Postle, K., and Good, R. F. (1985). A bidirectional rho-independent transcription terminator between the *E. coli* tonB gene and an opposing gene. *Cells* 41, 577–585. doi: 10.1016/s0092-8674(85)80030-1

Power, S. N., Salvatore, M. R., Sokol, E. R., Stanish, L. F., and Barrett, J. E. (2020). Estimating microbial mat biomass in the McMurdo dry valleys, Antarctica using satellite imagery and ground surveys. *Polar Biol.* 43, 1753–1767. doi: 10.1007/s00300-020-02742-y

Prud'homme-Généreux, A., Beran, R. K., Iost, I., Ramey, C. S., Mackie, G. A., and Simons, R. W. (2004). Physical and functional interactions among RNase E, polynucleotide phosphorylase and the cold-shock protein, CsdA: evidence for a 'cold shock degradosome'. *Mol. Microbiol.* 54, 1409–1421. doi: 10.1111/j.1365-2958.2004.04360.x

Pulschen, A. A., Bendia, A. G., Fricker, A. D., Pellizari, V. H., Galante, D., and Rodrigues, F. (2017). Isolation of uncultured Bacteria from Antarctica using long

incubation periods and low nutritional media. *Front. Microbiol.* 8:1346. doi: 10.3389/fmicb.2017.01346

Qiu, X.-B., Shao, Y.-M., Miao, S., and Wang, L. (2006). The diversity of the DnaJ/Hsp40 family, the crucial partners for Hsp70 chaperones. *Cell. Mol. Life Sci.* 63, 2560–2570. doi: 10.1007/s00018-006-6192-6

R Core Team (2018). R: A Language and Environment for Statistical Computing. R Foundation for Statistical Computing, Vienna, Austria. Available at: https://www.R-project.org/ (Accessed January 28, 2023).

Rodriguez-R, L. M., and Konstantinidis, K. T. (2016). The enveomics collection: a toolbox for specialized analyses of microbial genomes and metagenomes. *PeerJ* 4:e1900v1. doi: 10.7287/peerj.preprints.1900v1

Rosselló-Móra, R., and Amann, R. (2015). Past and future species definitions for bacteria and archaea. *Syst. Appl. Microbiol.* 38, 209–216. doi: 10.1016/j.syapm.2015.02.001

Samples, R., Puckett, S., and Balunas, M. (2022). MPACT: An advanced informatics tool for metabolomics and data visualization of specialized metabolites from complex microbial samples. *ChemRxiv*. [Preprint]. doi: 10.26434/chemrxiv-2022-r0xbx

Sancar, G. B., Smith, F. W., Lorence, M. C., Rupert, C. S., and Sancar, A. (1984). Sequences of the *Escherichia coli* photolyase gene and protein. *J. Biol. Chem.* 259, 6033–6038. doi: 10.1016/S0021-9258(18)91118-X

Sanyal, A., Antony, R., Samui, G., and Thamban, M. (2018). Microbial communities and their potential for degradation of dissolved organic carbon in cryoconite hole environments of Himalaya and Antarctica. *Microbiol. Res.* 208, 32–42. doi: 10.1016/j.micres.2018.01.004

Saum, S. H., and Müller, V. (2008). Regulation of osmoadaptation in the moderate halophile *Halobacillus halophilus*: chloride, glutamate and switching osmolyte strategies. *Saline Systems* 4:4. doi: 10.1186/1746-1448-4-4

Saum, S. H., Sydow, J. F., Palm, P., Pfeiffer, F., Oesterhelt, D., and Müller, V. (2006). Biochemical and molecular characterization of the biosynthesis of glutamine and glutamate, two major compatible solutes in the moderately Halophilic bacterium *Halobacillus halophilus*. *J. Bacteriol.* 188, 6808–6815. doi: 10.1128/JB.00781-06

Sayed, A. M., Hassan, M. H. A., Alhadrami, H. A., Hassan, H. M., Goodfellow, M., and Rateb, M. E. (2020). Extreme environments: microbiology leading to specialized metabolites. *J. Appl. Microbiol.* 128, 630–657. doi: 10.1111/jam.14386

Schlatter, D. C., Yin, C., Hulbert, S., and Paulitz, T. C. (2020). Core Rhizosphere microbiomes of Dryland wheat are influenced by location and land use history. *Appl. Environ. Microbiol.* 86:e02135-19. doi: 10.1128/AEM.02135-19

Schuler, C. (2022). Astrobiological Analogs: Exploring the Microbial Ecology of Cryptic Cryosphere Habitats. *Dissertation*. Knoxville, TN: University of Tennessee.

Sedláček, I., Holochová, P., Busse, H.-J., Koublová, V., Králová, S., Švec, P., et al. (2022). Characterisation of waterborne psychrophilic *Massilia* isolates with Violacein production and description of *Massilia antarctica* sp. nov. *Microorganisms* 10:704. doi: 10.3390/microorganisms10040704

Seemann, T. (2014). Prokka: rapid prokaryotic genome annotation. *Bioinformatics* 30, 2068–2069. doi: 10.1093/bioinformatics/btu153

Shen, L., Liu, Y., Gu, Z., Xu, B., Wang, N., Jiao, N., et al. (2015). *Massilia eurypsychrophila* sp. nov. a facultatively psychrophilic bacteria isolated from ice core. *Int. J. Syst. Evol. Microbiol.* 65, 2124–2129. doi: 10.1099/ijs.0.000229

Shen, L., Liu, Y., Wang, N., Yao, T., Jiao, N., Liu, H., et al. (2013). *Massilia yuzhufengensis* sp. nov., isolated from an ice core. *Int. J. Syst. Evol. Microbiol.* 63, 1285–1290. doi: 10.1099/ijs.0.042101-0

Siddiqui, K. S., Williams, T. J., Wilkins, D., Yau, S., Allen, M. A., Brown, M. V., et al. (2013). Psychrophiles. *Annu. Rev. Earth Planet. Sci.* 41, 87–115. doi: 10.1146/annurev-earth-040610-133514

Siegel, B. Z., Mcmurty, G., Siegel, S. M., Chen, J., and Larock, P. (1979). Life in the calcium chloride environment of Don Juan pond, Antarctica. *Nature* 280, 828–829. doi: 10.1038/280828a0

Siegel, B. Z., Siegel, S. M., Chen, J., and LaRock, P. (1983). An extraterrestrial habitat on earth: the algal mat of Don Jaun pond. *Adv. Space Res.* 3, 39–42. doi: 10.1016/0273-1177(83)90171-0

Skinnider, M. A., Johnston, C. W., Gunabalasingam, M., Merwin, N. J., Kieliszek, A. M., MacLellan, R. J., et al. (2020). Comprehensive prediction of secondary metabolite structure and biological activity from microbial genome sequences. *Nat. Commun.* 11:6058. doi: 10.1038/s41467-020-19986-1

Smith, A. C., and Hussey, M. A. (2005). *Gram Stain Protocols*. American Society for Microbiology, 1:14.

Sommers, P., Darcy, J. L., Porazinska, D. L., Gendron, E. M. S., Fountain, A. G., Zamora, F., et al. (2019). Comparison of microbial communities in the sediments and water columns of frozen Cryoconite holes in the McMurdo dry valleys, Antarctica. *Front Microbiol* 10:65. doi: 10.3389/fmicb.2019.00065

Son, J., Lee, H., Kim, M., Kim, D.-U., and Ka, J.-O. (2021). *Massilia aromaticivorans* sp. nov., a BTEX degrading bacterium isolated from Arctic soil. *Curr. Microbiol.* 78, 2143–2150. doi: 10.1007/s00284-021-02379-y

Stankovic, N., Radulovic, V., Petkovic, M., Vuckovic, I., Jadranin, M., Vasiljevic, B., et al. (2012). Streptomyces sp. JS520 produces exceptionally high quantities of undecylprodigiosin with antibacterial, antioxidative, and UV-protective properties. *Appl. Microbiol. Biotechnol.* 96, 1217–1231. doi: 10.1007/s00253-012-4237-3

Suryawanshi, R. K., Patil, C. D., Borase, H. P., Narkhede, C. P., Stevenson, A., Hallsworth, J. E., et al. (2015). Towards an understanding of bacterial metabolites prodigiosin and violacein and their potential for use in commercial sunscreens. *Int. J. Cosmet. Sci.* 37, 98–107. doi: 10.1111/ics.12175

Takei, Y., Iizuka, R., Ueno, T., and Funatsu, T. (2012). Single-molecule observation of protein folding in symmetric GroEL-(GroES)2 complexes*. *J. Biol. Chem.* 287, 41118–41125. doi: 10.1074/jbc.M112.398628

Tamura, K., Stecher, G., and Kumar, S. (2021). MEGA11: molecular evolutionary genetics analysis version 11. *Mol. Biol. Evol.* 38, 3022–3027. doi: 10.1093/molbev/msab120

Thompson, A. D., Bernard, S. M., Skiniotis, G., and Gestwicki, J. E. (2012). Visualization and functional analysis of the oligomeric states of *Escherichia coli* heat shock protein 70 (Hsp70/DnaK). *Cell Stress Chaperones* 17, 313–327. doi: 10.1007/s12192-011-0307-1

Tindall, B. J., Rosselló-Móra, R., Busse, H.-J., Ludwig, W., and Kämpfer, P. (2010). Notes on the characterization of prokaryote strains for taxonomic purposes. *Int. J. Syst. Evol. Microbiol.* 60, 249–266. doi: 10.1099/ijs.0.016949-0

Tkacz, A., Cheema, J., Chandra, G., Grant, A., and Poole, P. S. (2015). Stability and succession of the rhizosphere microbiota depends upon plant type and soil composition. *ISME J.* 9, 2349–2359. doi: 10.1038/ismej.2015.41

Toma, C., Kuroki, H., Nakasone, N., Ehara, M., and Iwanaga, M. (2002). Minor pilin subunits are conserved in *Vibrio cholerae* type IV pili. *FEMS Immunol Med Microbiol* 33, 35–40. doi: 10.1111/j.1574-695X.2002.tb00569.x

Toner, J. D., Catling, D. C., and Sletten, R. S. (2017). The geochemistry of Don Juan pond: evidence for a deep groundwater flow system in Wright Valley, Antarctica. *Earth Planet. Sci. Lett.* 474, 190–197. doi: 10.1016/j.epsl.2017.06.039

Tosi, S., Onofri, S., Brusoni, M., Zucconi, L., and Vishniac, H. (2005). Response of Antarctic soil fungal assemblages to experimental warming and reduction of UV radiation. *Polar Biol.* 28, 470–482. doi: 10.1007/s00300-004-0698-x

Tsu, C. A., Kossen, K., and Uhlenbeck, O. C. (2001). The *Escherichia coli* DEAD protein DbpA recognizes a small RNA hairpin in 23S rRNA. *RNA* 7, 702–709. doi: 10.1017/S1355838201010135

Tsugawa, H., Cajka, T., Kind, T., Ma, Y., Higgins, B., Ikeda, K., et al. (2015). MS-DIAL: data-independent MS/MS deconvolution for comprehensive metabolome analysis. *Nat. Methods* 12, 523–526. doi: 10.1038/nmeth.3393

Utsugi, J., Inaba, K., Kuroda, T., Tsuda, M., and Tsuchiya, T. (1998). Cloning and sequencing of a novel Na+/H+ antiporter gene from *Pseudomonas aeruginosa*. *Biochim. Biophys. Acta* 1398, 330–334. doi: 10.1016/s0167-4781(98)00058-x

Van Craenenbroeck, A. H., Camps, K., Zachée, P., and Wu, K. L. (2011). *Massilia timonae* infection presenting as generalized lymphadenopathy in a man returning to Belgium from Nigeria▽. *J. Clin. Microbiol.* 49, 2763–2765. doi: 10.1128/JCM.00160-11

Veltri, D., Wight, M. M., and Crouch, J. A. (2016). SimpleSynteny: a web-based tool for visualization of microsynteny across multiple species. *Nucleic Acids Res.* 44, W41–W45. doi: 10.1093/nar/gkw330

Vimont, S., and Berche, P. (2000). NhaA, an Na(+)/H(+) antiporter involved in environmental survival of *Vibrio cholerae*. *J. Bacteriol.* 182, 2937–2944. doi: 10.1128/JB.182.10.2937-2944.2000

von Ossowski, I., Mulvey, M. R., Leco, P. A., Borys, A., and Loewen, P. C. (1991). Nucleotide sequence of *Escherichia coli* katE, which encodes catalase HPII. *J. Bacteriol.* 173, 514–520. doi: 10.1128/jb.173.2.514-520.1991

Wang, H., Zhang, X., Wang, S., Zhao, B., Lou, K., and Xing, X.-H. (2018). *Massilia violaceinigra* sp. nov., a novel purple-pigmented bacterium isolated from glacier permafrost. *Int. J. Syst. Evol. Microbiol.* 68, 2271–2278. doi: 10.1099/ijsem.0.002826

Weber, A., Kögl, S. A., and Jung, K. (2006). Time-dependent proteome alterations under osmotic stress during aerobic and anaerobic growth in *Escherichia coli*. *J. Bacteriol.* 188, 7165–7175. doi: 10.1128/JB.00508-06

Weisburg, W. G., Barns, S. M., Pelletier, D. A., and Lane, D. J. (1991). 16S ribosomal DNA amplification for phylogenetic study. *J. Bacteriol.* 173, 697–703. doi: 10.1128/jb.173.2.697-703.1991

Wick, R. R., Judd, L. M., Gorrie, C. L., and Holt, K. E. (2017). Unicycler: resolving bacterial genome assemblies from short and long sequencing reads. *PLoS Comput. Biol.* 13:e1005595. doi: 10.1371/journal.pcbi.1005595

Woodhams, D. C., LaBumbard, B. C., Barnhart, K. L., Becker, M. H., Bletz, M. C., Escobar, L. A., et al. (2018). Prodigiosin, Violacein, and volatile organic compounds produced by widespread cutaneous Bacteria of amphibians can inhibit two *Batrachochytrium* fungal pathogens. *Microb. Ecol.* 75, 1049–1062. doi: 10.1007/s00248-017-1095-7

Wu, B., Wawrzynow, A., Zylicz, M., and Georgopoulos, C. (1996). Structure-function analysis of the *Escherichia coli* GrpE heat shock protein. *EMBO J.* 15, 4806–4816. doi: 10.1002/j.1460-2075.1996.tb00861.x

Xu, P., Li, W.-J., Tang, S.-K., Zhang, Y.-Q., Chen, G.-Z., Chen, H.-H., et al. (2005). *Naxibacter alkalitolerans* gen. Nov., sp. nov., a novel member of the family 'Oxalobacteraceae' isolated from China. *Int. J. Syst. Evol. Microbiol.* 55, 1149–1153. doi: 10.1099/ijs.0.63407-0

Yang, E., Zhao, M., Li, S., Wang, Y., Sun, L., Liu, J., et al. (2019). *Massilia atriviolacea* sp. nov., a dark purple-pigmented bacterium isolated from soil. *Int. J. Syst. Evol. Microbiol.* 69, 2135–2141. doi: 10.1099/ijsem.0.003449

Zhang, Y.-Q., Li, W.-J., Zhang, K.-Y., Tian, X.-P., Jiang, Y., Xu, L.-H., et al. (2006). *Massilia dura* sp. nov., *Massilia albidiflava* sp. nov., *Massilia plicata* sp. nov. and *Massilia lutea* sp. nov., isolated from soils in China. *Int. J. Syst. Evol. Microbiol.* 56, 459–463. doi: 10.1099/ijs.0.64083-0

Zhang, F., Scheerer, P., Oberpichler, I., Lamparter, T., and Krauß, N. (2013). Crystal structure of a prokaryotic (6-4) photolyase with an Fe-S cluster and a 6,7-dimethyl-8-ribityllumazine antenna chromophore. *Proc. Natl. Acad. Sci. U. S. A.* 110, 7217–7222. doi: 10.1073/pnas.1302377110

Zoumplis, A., Kolody, B., Kaul, D., Zheng, H., Venepally, P., McKnight, D. M., et al. (2023). Impact of meltwater flow intensity on the spatiotemporal heterogeneity of microbial mats in the McMurdo dry valleys, Antarctica. *ISME Commun* 3, 3–11. doi: 10.1038/s43705-022-00202-8

frontiers | Frontiers in Microbiology

TYPE Original Research
PUBLISHED 18 May 2023
DOI 10.3389/fmicb.2023.1168507

OPEN ACCESS

EDITED BY
Trista J. Vick-Majors,
Michigan Technological University,
United States

REVIEWED BY
Connie Lovejoy,
Laval University, Canada
Alexis Marshall,
University of Waikato, New Zealand
Maria Rovisco Monteiro,
University of Waikato, New Zealand
Pauline Vannier,
Matis Ltd., Iceland

*CORRESPONDENCE
Avishek Dutta
✉ avishek.dutta@uga.edu;
✉ avishekdutta14@gmail.com

RECEIVED 17 February 2023
ACCEPTED 25 April 2023
PUBLISHED 18 May 2023

CITATION
Dutta A, Connors E, Trinh R, Erazo N, Dasarathy S, Ducklow HW, Steinberg DK, Schofield OM and Bowman JS (2023) Depth drives the distribution of microbial ecological functions in the coastal western Antarctic Peninsula.
Front. Microbiol. 14:1168507.
doi: 10.3389/fmicb.2023.1168507

Depth drives the distribution of microbial ecological functions in the coastal western Antarctic Peninsula

Avishek Dutta[1,2,3]*, Elizabeth Connors[1], Rebecca Trinh[4], Natalia Erazo[1], Srishti Dasarathy[1], Hugh W. Ducklow[4], Deborah K. Steinberg[5], Oscar M. Schofield[6] and Jeff S. Bowman[1,7]

[1]Integrative Oceanography Division, Scripps Institution of Oceanography, University of California, San Diego, La Jolla, CA, United States, [2]Department of Geology, University of Georgia, Athens, GA, United States, [3]Savannah River Ecology Laboratory, University of Georgia, Aiken, SC, United States, [4]Department of Earth and Environmental Sciences, Lamont-Doherty Earth Observatory, Columbia University, Palisades, NY, United States, [5]Department of Biological Science, College of William & Mary, Virginia Institute of Marine Science, Gloucester Point, VA, United States, [6]Department of Marine and Coastal Sciences, Rutgers University, New Brunswick, NJ, United States, [7]Center for Microbiome Innovation, University of California, San Diego, La Jolla, CA, United States

The Antarctic marine environment is a dynamic ecosystem where microorganisms play an important role in key biogeochemical cycles. Despite the role that microbes play in this ecosystem, little is known about the genetic and metabolic diversity of Antarctic marine microbes. In this study we leveraged DNA samples collected by the Palmer Long Term Ecological Research (LTER) project to sequence shotgun metagenomes of 48 key samples collected across the marine ecosystem of the western Antarctic Peninsula (wAP). We developed an *in silico* metagenomics pipeline (iMAGine) for processing metagenomic data and constructing metagenome-assembled genomes (MAGs), identifying a diverse genomic repertoire related to the carbon, sulfur, and nitrogen cycles. A novel analytical approach based on gene coverage was used to understand the differences in microbial community functions across depth and region. Our results showed that microbial community functions were partitioned based on depth. Bacterial members harbored diverse genes for carbohydrate transformation, indicating the availability of processes to convert complex carbons into simpler bioavailable forms. We generated 137 dereplicated MAGs giving us a new perspective on the role of prokaryotes in the coastal wAP. In particular, the presence of mixotrophic prokaryotes capable of autotrophic and heterotrophic lifestyles indicated a metabolically flexible community, which we hypothesize enables survival under rapidly changing conditions. Overall, the study identified key microbial community functions and created a valuable sequence library collection for future Antarctic genomics research.

KEYWORDS

metagenomics, Antarctic microbiome, Palmer LTER, metagenome-assembled genomes (MAGs), microbial community function

1. Introduction

Marine microorganisms play an important role in regulating biogeochemical cycles (Green et al., 2008). They are key drivers of the transformation of carbon-, nitrogen-, and sulfur-containing compounds in the environment. Changes in environmental conditions impact microbial communities, which in turn exert control over many environmental parameters (Thompson et al., 2017; Dutta et al., 2022). The ecological outcomes of the rapid environmental change are well documented for the western Antarctic Peninsula (wAP) (Meredith and King, 2005; Clarke et al., 2007; Bowman et al., 2016, 2017), home to multiple long-term observing programs. Large shifts in bacterial production relative to primary production signal radically different outcomes for primary production from one year to another (Bowman et al., 2016). The metabolic potential of the heterotrophic bacterial community is presumed to play a strong role in determining what primary production gets recycled by the microbial food web. However, we know little about the genomic makeup of the bacteria and archaea responsible for bacterial production and other marine microbial processes along the wAP (Bowman et al., 2018).

Heterotrophic bacterial populations are intimately linked to phytoplankton blooms and play an essential role in the transformation of phytoplankton-derived organic matter (Buchan et al., 2014). Phytoplankton are a direct source of dissolved organic carbon (DOC) for heterotrophic bacteria in the photic zone. Below the photic zone, heterotrophs reprocess DOC and degrade sinking particles to generate new DOC. The timing of the seasonal phytoplankton bloom, its composition, and its intensity are strongly influenced by physical processes along the wAP. For example, conditions that favor large diatoms are thought to transfer carbon more efficiently to krill and upper trophic-level consumers (Saba et al., 2014). Alternatively, strong winds and reduced sea ice cover can lead to lower levels of primary production and smaller phytoplankton cells, in turn leading to high rates of bacterial production compared to primary production (Bowman et al., 2016). Recent trends and future climate scenarios suggest an increase in wind and a reduction in sea ice for the Antarctic Peninsula (Siegert et al., 2019) and, presumably, a strengthened microbial food web. To better understand the metabolic capabilities of wAP marine bacterial communities, we applied metagenomics to a historic sample library of microbial DNA collected by the Palmer Long Term Ecological Research (LTER) project to better understand how bacterial communities will respond to future environmental change along the wAP.

Most primary production along the wAP is attributed to eukaryotic phytoplankton (Schofield et al., 2018; Lin et al., 2021). However, dark carbon fixation is likely to be a significant process below the photic zone and during the polar night. Though well appreciated for the global ocean (Baltar and Herndl, 2019), surprisingly little is known about the distribution of prokaryotic carbon fixation mechanisms in the Antarctic marine environment. Previous analysis of fosmid libraries from contrasting summer and winter communities along the wAP identified gammaproteobacterial sulfur-oxidizing (GSO) chemolithotrophs (Grzymski et al., 2012). Other works using 16S rRNA gene surveys have shown these taxa to be widely distributed in the coastal Antarctic (Bowman et al., 2017; Bowman and Deming, 2017). Alternate prokaryotic carbon fixation strategies for the wAP may rely on energy obtained from nitrification (Bowman et al., 2016). This study aimed to understand the microbial community functions in the marine ecosystem of coastal wAP. We applied a novel analytical approach based on gene coverage to investigate the distribution of genes and reconstructed metagenome-assembled genomes (MAGs) to understand the pathways associated with prokaryotic carbon fixation and utilization. We combined observations of genes diagnostic of carbon fixation with genes for catabolic processes to identify autotrophic, mixotrophic, and heterotrophic guilds among wAP marine prokaryotes.

2. Methods

2.1. Sample collection

Forty-eight samples were selected covering different depth horizons (0–275 m) on the Palmer LTER sampling grid (lines 100–600, covering latitudes 67.566533°S to 63.96565°S) (Waters and Smith, 1992) and locations of special significance such as Palmer Canyon, Armstrong Reef, and the coastal LTER time-series near Palmer Station (Figure 1). The selection of samples was made based on three different parameters: (i) higher abundances of unclassified taxa based on 16S rRNA amplicon sequence data (16S rRNA gene sequence data submitted under NCBI BioProject ID PRJNA901488), (ii) depth profile, and (iii) variations in latitude. A detailed description of the samples used in this study is given in Supplementary Table S1. Forty-two samples were collected during the austral summer of 2019–2020, and four samples were collected during the austral summer of 2018–2019. The remaining two samples were collected in January 2017 and November 2018. We grouped the samples into three depth horizons: shallow (0–40 m), medium (50–75 m), and deep (100–275 m). The depth categorization was done based on mixed layer depth, temperature, and salinity, as reported previously in Schofield et al. (2018) and Seyitmuhammedov et al. (2022). There were 23 samples collected from the shallower depth, whereas 11 and 14 samples were collected from the medium-depth and deeper horizons, respectively. The samples were also categorized into three regions based on Palmer LTER lines: Northern (Line 400 and north of Line 400), Southern (south of Line 400), and Palmer Canyon (near Palmer Station on Anvers Island) (Supplementary Table S1). There were 14 samples collected from the Northern region, whereas 16 and 18 samples were collected from Palmer Canyon and the Southern region, respectively. For each sample, approximately 1 L of seawater was filtered through a sterile 0.2 µm Supor membrane disc filter (Pall Corporation, Port Washington, NY, United States) and stored at −80°C until extraction.

2.2. DNA extraction, sequencing, and metagenome analysis

DNA was extracted from the filters using the MagMAX Microbiome Ultra nucleic acid extraction kit and KingFisher Flex extraction system following the manufacturer's protocols. The extracted DNA was sequenced at the UC San Diego Microbiome Core for shotgun metagenome sequencing on the Illumina NovaSeq platform. Sequencing was done across multiple lanes in two runs (24 samples for each run). The average depth of sequencing for the second run (an average of ~427 million paired-end reads per sample) was higher compared to the first run (an average of ~55 million paired-end reads per sample) to facilitate a separate analysis that will be reported

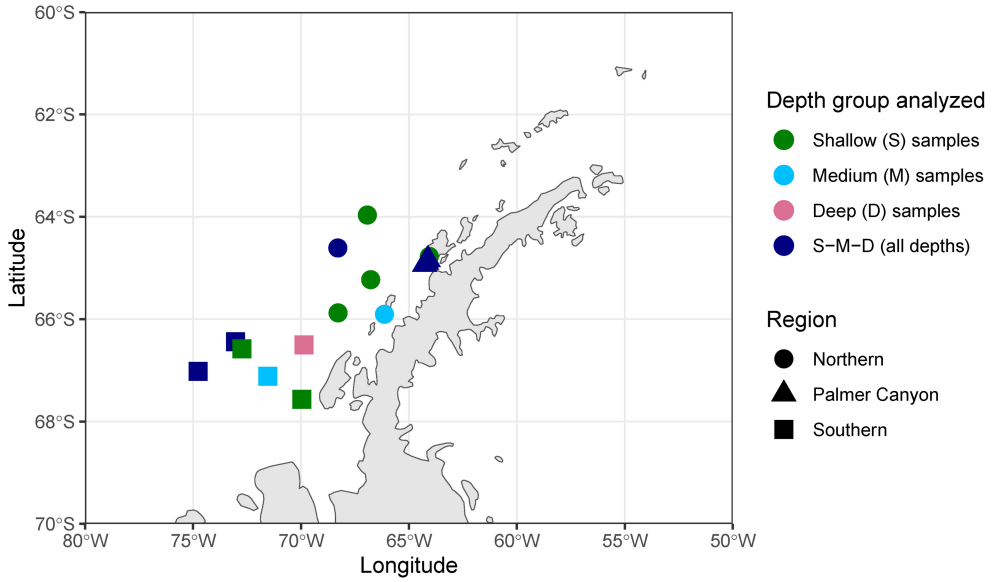

FIGURE 1
Sample locations in the western Antarctic Peninsula. S, only shallower samples analyzed; M, only medium-depth samples analyzed; D, only deeper samples analyzed; S-M-D, samples collected from deep, medium, and shallow environments analyzed.

elsewhere. To avoid memory limitation, samples from the second run were down-sampled using reformat.sh, a script from the BBMap package (Bushnell, 2014), to ~55 million paired-end reads per sample. The raw metagenomic data for 48 samples were processed and analyzed using the *in silico* Metagenomics Pipeline (iMAGine) using default parameters.[1] iMAGine uses fastp (Chen et al., 2018) for filtering, metaSPAdes (Nurk et al., 2017) for assembling the reads, QUAST (Gurevich et al., 2013) for analyzing the assembly quality, bwa-mem (v0.7.17) for aligning the raw reads to the assembly (Li, 2013), samtools for modifying alignment files (Li et al., 2009), metabat2 (Kang et al., 2019) for binning contigs, and checkM (Parks et al., 2015) for quality assessment of the bins. The assembled contigs from iMAGine were used for further analyses.

Genes were predicted from contigs with Prodigal v2.6.3 (Hyatt et al., 2010) using the "meta" flag. The predicted genes were annotated using emapper v2.1.5 (Cantalapiedra et al., 2021) based on a Diamond search (Buchfink et al., 2014). The following arguments were used for search filtering in emapper: --evalue 0.001 (e-value threshold), --score 60 (minimum hit bit score), --pident 40 (minimum percentage identity), --query_cover 20 (minimum percentage query coverage), and --subject_cover 20 (minimum percentage subject coverage). The database used for annotation was eggNOG DB v5.0.2 (Huerta-Cepas et al., 2019). For this study, taxfin.sh (a part of iMAGine) was used for filtering out genes not affiliated to domain bacteria and archaea. Coverage of each gene (average gene fold) was determined using gene_fold_counter.sh (a part of iMAGine), which takes in the alignment map file (sam output from iMAGine), removes unmapped reads and reads mapped to multiple locations using samtools (with parameters -F 0×904), uses pileup.sh script from the BBMap package to calculate the average coverage of the contigs and maps back average contig coverage to the genes on those contigs. To enable comparison across metagenomes, all the genes were scaled based on Equation (1):

$$\frac{\textit{Normalized gene coverage of a sample}}{\textit{Total average gene coverage}} = \frac{\textit{Total average gene coverage}}{\textit{Total rpoB}\,(K03043)\,\textit{coverage}} \quad (1)$$

For gene-specific analysis, KEGG orthologs from the emapper outputs were considered. Genes mapping to more than one ortholog were not considered for the analysis. Key genes involved in different processes of carbon, nitrogen, and sulfur cycles were selected based on KEGG pathways, whereas genes involved in carbohydrate transformation were selected based on previously published literature (Bergauer et al., 2018). Detailed gene inventories, along with the associated pathways considered in this study, are mentioned in Supplementary Table S2 and Supplementary Figures S1–S4. The KEGG ortholog for *rpoB*, i.e., K03043 was used as a reference for normalization in this study. The genes involved in methane oxidation considered in this study (*pmoA-amoA*, *pmoB-amoB*, and *pmoC-amoC*) also play an important role in ammonia oxidation (a key step in nitrification). Similarly, it has been seen before that the variations of the same gene responsible for dissimilatory sulfate reduction (considered in this study) are also involved in sulfur oxidation (Loy et al., 2009).

Bins with completeness higher than 70% and contamination lower than 5% were considered MAGs. Similar cutoffs were used in a previous study (Parks et al., 2017). For further analysis, MAGs were dereplicated with dRep v3.2.2 (Olm et al., 2017) using a secondary ANI threshold of 0.96 and goANI as the algorithm for secondary clustering. The minimum genome completeness was set to 70%, and the maximum genome contamination was set to 5% for dereplication. All the other dereplication parameters were kept default. The taxonomy of the dereplicated MAGs was assessed using the GTDB-Tk v1.5.0 based on reference database version release 202 (Chaumeil

1 https://github.com/avishekdutta14/iMAGine

et al., 2020). The multiple sequence alignment output of domain-specific marker genes from GTDB-Tk was used for constructing a phylogenomic tree with RAxML-ng (Kozlov et al., 2019). Tree construction used the WAG amino-acid substitution model and MAGs belonging to Chloroflexota and Thermoproteota as outgroups for bacteria- and archaea-specific phylogenomic trees, respectively. The default number of starting trees was used (10 random and 10 parsimony-based) and 1,000 bootstrap replicates were used for confidence scoring of the final tree.

The number of reads mapped to each MAG was calculated using the mag_abund.py script present in the iMAGine repository,[2] and the average reads per secondary cluster (as obtained from dRep analyses) was obtained to understand average reads mapped per dereplicated MAGs.

Sequence data for metagenomics reads from 48 samples, along with 137 dereplicated MAGs, can be found under NCBI BioProject ID PRJNA894514. The MAGs have been deposited at GenBank under the accession JAPKAB000000000- JAPKFH000000000.

2.3. Determination of putative metabolic lifestyle in MAGs

Functional annotation of MAGs was conducted using two different methods. To identify functional guilds, genes were predicted using Prodigal v2.6.3 and annotated using Ghost Koala (Kanehisa et al., 2016), whereas DRAM 1.4.0 was used to assess pathway completeness and categorize different microbial metabolisms (Shaffer et al., 2020). Though it is hard to ascertain the exact metabolic lifestyle of the MAGs given the limitation imposed by genome completeness, we described the putative metabolisms based on combinations of diagnostic metabolic pathways. All the annotations for metabolic lifestyle assessment were based on DRAM analysis. Glucose utilization (GU) and carbon fixation (CF) pathways having greater than 70% completeness in a MAG were considered in this study. GU, indicative of the use of exogenous fixed carbon, was assessed by the presence of the Embden-Meyerhof pathway and/or the Entner-Doudoroff pathway. CF was assessed based on the presence of either of the three carbon fixing pathways (3-Hydroxypropionate bicycle, Arnon–Buchanan cycle, and Calvin cycle) found in the MAGs. Sulfur oxidation (SO) capability was determined based on the presence of the SOX system and/or the presence of the *dsr* gene. Nitrification (NI) capability was determined based on the presence of either ammonia oxidation genomic repertoire and/or gene involved in the conversion of nitrite to nitrate. Denitrification (DNR) capability was determined based on the presence of either one of the genes involved in the following processes: (i) genes involved in the conversion of nitrate to nitrite, (ii) genes involved in the conversion of nitrite to nitric oxide, and/or (iii) genes involved in the conversion of nitric oxide to nitrous oxide. We described each MAG as a putative autotroph, mixotroph, or heterotroph based on the presence of diagnostic metabolic pathways. Autotrophs were determined by the presence of CF and absence of GU, heterotrophs by the presence of GU and absence of CF, and mixotrophs by the presence of both GU and CF.

2.4. Statistical analyses

All the statistical analyses were carried out in R and R Studio (RStudio Team, 2015). Principal Coordinates Analysis (PCoA) of Bray-Curtis dissimilatory based on the normalized gene coverage across different samples was performed using the phyloseq package (McMurdie and Holmes, 2013). For this PCoA, we considered key genes responsible for carbon, nitrogen, sulfur, and carbohydrate transformations (Supplementary Figures S1–S4). A PERMANOVA test was conducted using the "adonis2" function of the Vegan package (Oksanen et al., 2007) to test whether different sample groups had different centroids. The average distance from the median was calculated based on a dispersion test using the "betadisper" function of the Vegan package, which was followed by a permutation test of multivariate homogeneity of group dispersions using the "permutest" function of the Vegan package. Boxplots were made to analyze the differences in process abundances across different depth profiles. The Kruskal-Wallis test for significance was used to determine whether the overall changes were significant, whereas the Wilcoxon test was used to find the pairwise significance. Heatmap and cluster analyses were carried out with the pheatmap package (Kolde, 2019) and based on normalized gene coverage. Column clustering, which displayed the clustering of different samples, was based on Bray–Curtis dissimilatory. Each row, depicting normalized gene coverage, was scaled using min-max scaling and clustered based on correlation. To understand the clustering of MAGs based on genomic repertoire, genes obtained from Ghost Koala analysis were mapped to each dereplicated MAGs using custom R scripts, and Non-Metric Multidimensional Scaling (NMDS) of a binary matrix based on the presence or absence of all genes constraining different metabolic categories were performed using Vegan. All the statistical analyses for the MAGs were conducted based on dereplicated MAGs, except for the mapped read coverage analysis. For mapped read coverage, all the MAGs were considered. A web-based tool[3] was used to generate Venn diagrams to find the overlap across different metabolic categories to determine the metabolic lifestyle of the MAGs.

3. Results

3.1. Microbial community function

Microbial community functions varied across depths (Figure 2). Three distinct clusters were observed for deep, medium-deep, and shallow samples with minor overlaps based on normalized gene coverage (PERMANOVA, $p = 0.001$). One of the medium-deep samples (Armstrong Reef) clustered with the shallower-depth samples. Dispersion among sample groups differed according to depth ($p = 0.001$). The average distance from the median was highest for shallower depth samples, followed by medium-deep and deeper samples. The samples were also significantly different (PERMANOVA, $p = 0.011$) based on region (Southern, Northern, and Palmer Canyon). However, the separation of samples was more pronounced for depth than region according to the PERMANOVA F-ratio ($F_{depth} = 10.224$;

2 https://github.com/avishekdutta14/iMAGine/blob/main/Utilities/mag_abund.py

3 https://bioinformatics.psb.ugent.be/webtools/Venn/

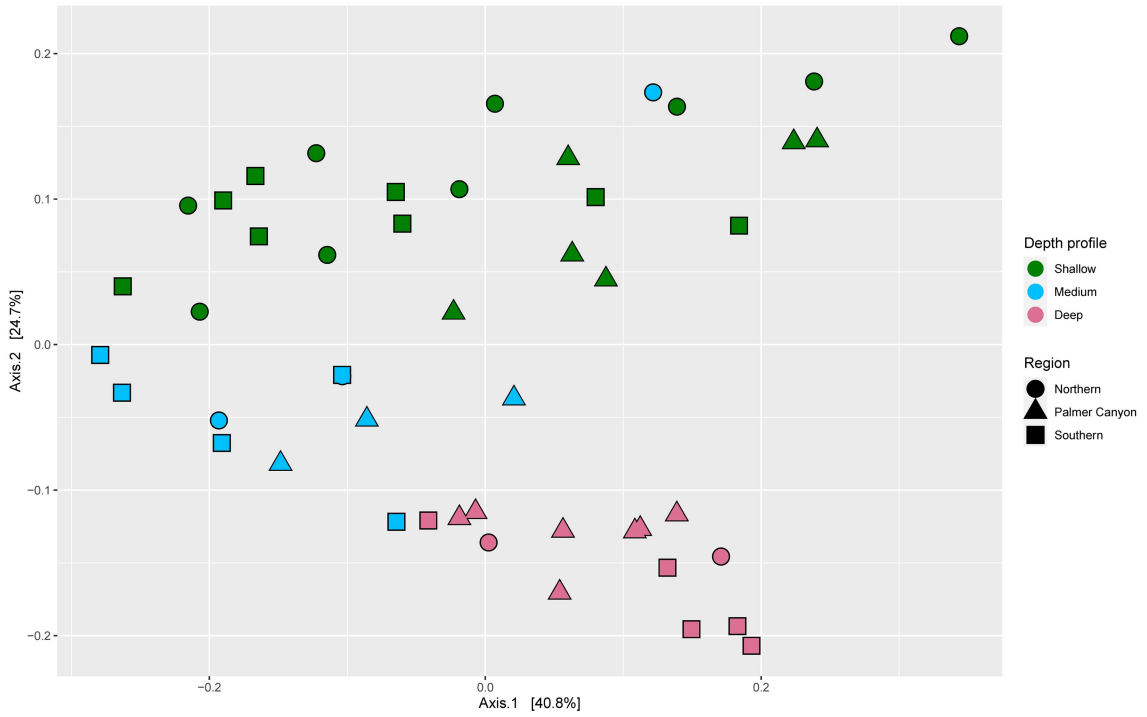

FIGURE 2
Principal coordinates analysis (PCoA) of Bray-Curtis dissimilatory based on normalized gene coverage across 48 samples. Symbol shape and color indicates sample region and depth, respectively.

$p = 0.001$ and $F_{region} = 2.6985$; $p = 0.011$). We conducted a detailed study of carbon, nitrogen, sulfur, and carbohydrate metabolism-specific genes based on normalized gene coverage to understand the differential abundances of functional genes across different depth horizons and regions.

3.1.1. Carbon cycle

Key genes involved in prokaryotic dark carbon fixation, carbon monoxide oxidation, fermentation, methane oxidation, and photoheterotrophy were explored to understand carbon transformation and their distribution in the wAP. Varied abundances of groups of genes involved in different carbon transformation processes were observed across different depths (Supplementary Figure S1). Genes associated with dark carbon fixation were found to be significantly higher in the deeper samples compared to medium-depth ($p = 9 \times 10^{-7}$) and shallower samples ($p = 0.00085$) (Figure 3A). The abundance of the genes involved in CO oxidation varied across depths. The deeper samples harbored significantly greater CO oxidation gene coverages compared to shallower ($p = 0.00096$) and medium-deep samples ($p = 4.4 \times 10^{-5}$) (Figure 3B). A similar trend was observed for genes involved in fermentation and methane metabolism (Figures 3C,D).

3.1.2. Sulfur cycle

The abundance of genes involved in the oxidation and reduction of sulfur species varied across depths (Supplementary Figure S2). Normalized coverages of genes involved in sulfur oxidation were found to be significantly higher in the shallower samples compared to medium-depth ($p = 0.0051$) and deeper samples ($p = 3.9 \times 10^{-5}$) (Figure 4A). On the contrary, normalized coverage of genes involved in dissimilatory sulfate reduction was found to be significantly higher in the deeper samples compared to medium-depth ($p = 9 \times 10^{-7}$) and shallower samples ($p = 6.9 \times 10^{-6}$) (Figure 4B). Normalized coverage of genes involved in thiosulfate to sulfide reduction was found to be the highest in the deeper samples, followed by medium-depth and shallower samples (Figure 4C).

3.1.3. Nitrogen cycle

The abundances of the genes involved in oxidation and reduction of nitrogen species also varied with depth (Supplementary Figure S3). The average coverages of the genes involved in nitrification were significantly higher in the deeper horizons of the water column compared to medium-depth ($p = 0.0051$) and shallower horizons ($p = 4.1 \times 10^{-7}$) (Figure 5A). Similarly, the abundance of genes involved in denitrification and dissimilatory nitrate reduction to ammonia (DNRA) was found to be significantly higher in deeper samples compared to medium-deep (Denitrification: $p = 5.4 \times 10^{-6}$; DNRA: $p = 0.00012$) and shallower depth (Denitrification: $p = 3.9 \times 10^{-9}$; DNRA: $p = 0.026$) samples (Figures 5B,C). Genes involved in urea utilization were also observed in all the wAP samples. Urea-utilizing gene coverages were found to be significantly higher in the deeper horizon samples compared to samples from the medium depth ($p = 4.5 \times 10^{-7}$) and shallower depth ($p = 0.00013$) horizons (Figure 5D).

3.1.4. Carbohydrate transformations

We further analyzed genes involved in the transformation of glycoprotein, cellulose, chitin, pectin, starch, xylans, and xyloglucans to understand the carbohydrate pool and

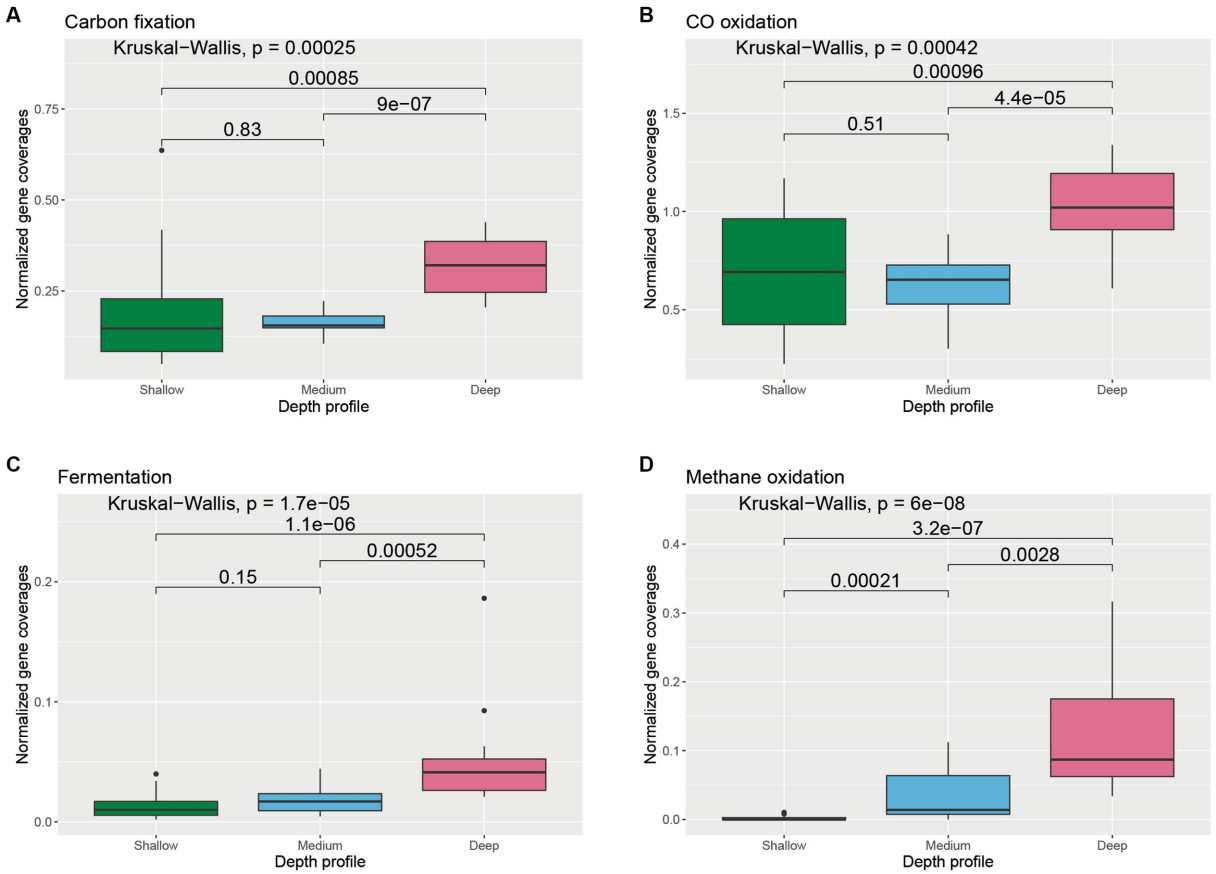

FIGURE 3
Boxplot showing the distribution of different carbon cycle genes related to **(A)** carbon fixation, **(B)** CO oxidation, **(C)** fermentation, and **(D)** methane oxidation across different depth horizons of the wAP. Normalized coverages of genes grouped in each of these categories are listed in Supplementary Figure S1. A pairwise comparison for significance was conducted using the Wilcoxon test.

transformation capabilities of microorganisms across different depth horizons of the wAP (Supplementary Figure S4). Cellulose, pectin (RGI), starch, and xyloglucans metabolizing gene coverages were found to be significantly higher in the shallower depth samples compared to medium-deep [Cellulose: $p = 0.00033$; pectin (RGI): $p = 8.6 \times 10^{-5}$; starch: $p = 0.0095$; and xyloglucans: $p = 0.0051$] and deeper samples [cellulose: $p = 2.7 \times 10^{-5}$; pectin (RGI): $p = 1.8 \times 10^{-6}$; starch: $p = 0.00074$; and xyloglucans: $p = 2.3 \times 10^{-5}$] (Figures 6A–D). Abundances of chitin metabolizing genes were significantly higher in deeper samples compared to the samples from medium depth ($p = 8.7 \times 10^{-5}$) and shallow samples ($p = 0.0029$) (Figure 6E).

3.2. Distribution, taxonomy, and metabolic profiles of MAGs

A total of 2,940 bins were obtained from 48 samples. Of these, 612 bins with genome completeness of more than 70% and contamination of less than 5% were considered MAGs and used for further analysis. These 612 MAGs were filtered down to 609 MAGs by dRep based on genome quality and were dereplicated to a final set of 137 MAGs. 137 MAGs (representing 609 MAGs) covered 13.11, 5.96, and 2.12% of the total filtered reads from deep, medium-deep, and shallow samples, respectively (Figure 7). Among these 137 MAGs, 64 MAGs were unique to deep samples, whereas 19 and 15 MAGs were unique to the medium and shallow horizons, respectively. 11 MAGs were found in all three depth horizons, and the remaining 28 MAGs were found in two of the three horizons (medium and deep: 18, shallow and medium: 9, and shallow and deep: 1). When sorted by region, 33 MAGs represented MAGs unique to the Southern region, whereas 32 and 4 MAGs represented MAGs unique to the Palmer Canyon and Northern region, respectively. 21 MAGs were found in all three regions, and the remaining 47 MAGs were found in two of the three regions (Southern—Palmer Canyon: 30, Southern—Northern: 14, and Northern—Palmer Canyon: 3). The most abundant MAG found in the shallower waters was affiliated with Bacteroidota (represented by ANT-68) (Figure 7A). This MAG was exclusively observed in the shallow environments of the coastal wAP. The most abundant MAG found in the medium-depth waters was affiliated with family SAR324 (represented by ANT-96) (Figure 7B). This MAG was observed in the medium-depth and deeper samples. ANT-96 was also found to be the most abundant MAG in deeper waters (Figure 7C). Considering the proportion of reads that mapped to each MAG, the overall highest average mapped read percentage was also found in ANT-96 ($2.11\% \pm 1.22\%$; representing 7 MAGs from different samples). Detailed genome statistics of the 137 MAGs are present in Supplementary Table S3.

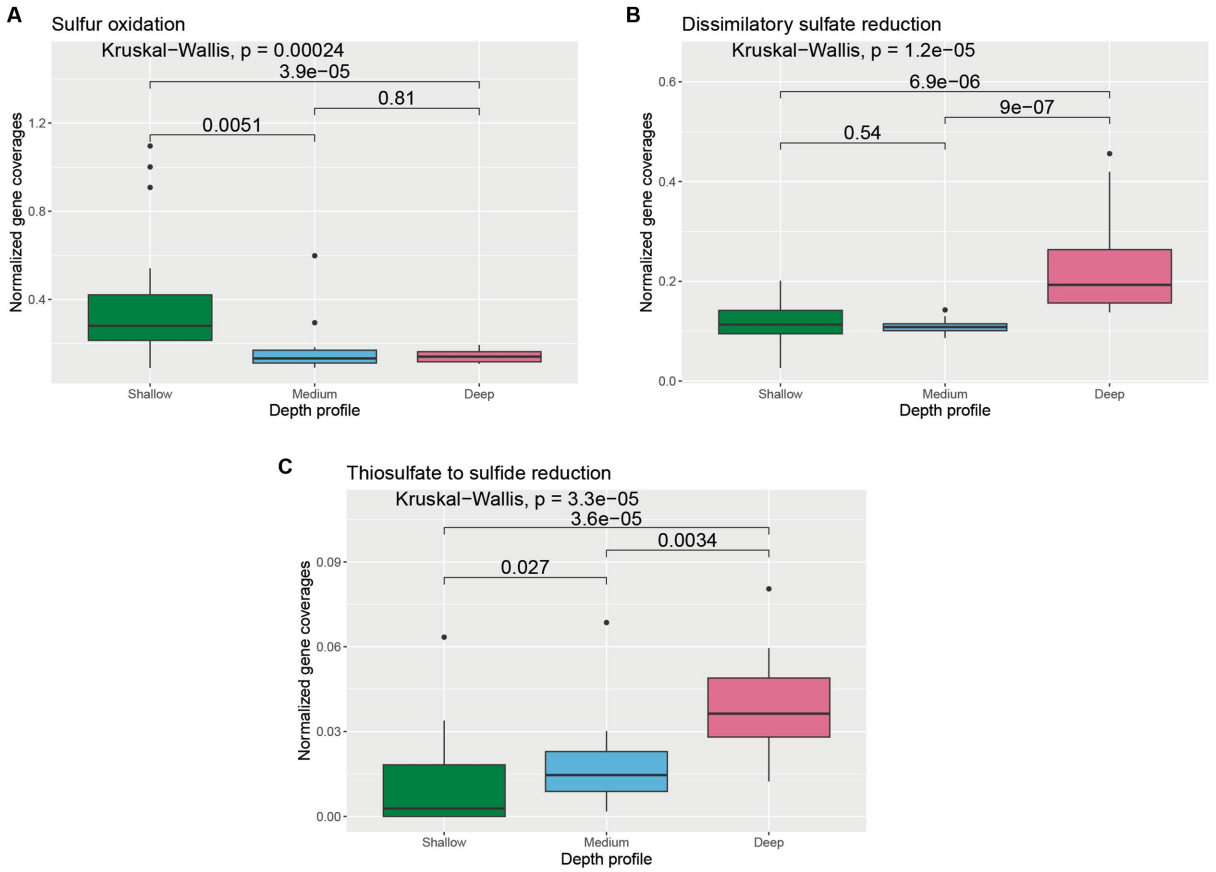

FIGURE 4
Boxplot showing the distribution of different sulfur cycle genes related to **(A)** sulfur oxidation, **(B)** dissimilatory sulfate reduction, and **(C)** thiosulfate to sulfide reduction across different depth horizons of the wAP. Normalized coverages of genes grouped in each of these categories are listed in Supplementary Figure S2. A pairwise comparison for significance was conducted using the Wilcoxon test.

The MAGs were taxonomically diverse. Of 137 MAGs, 10 MAGs were affiliated with the domain Archaea, and 127 MAGs were affiliated with Bacteria. Average nucleotide identity (ANI) or relative evolutionary divergence (RED) values were analyzed for each MAG based on reference genomes from GTDB using GTDB-Tk. RED values were calculated when the MAGs were unable to be classified based on ANI. ANI values greater than 0.95 were obtained for 40 MAGs (2 archaeal MAGs and 38 bacterial MAGs), whereas RED values (ranging between 0.660 to 0.998) were obtained for the rest of the MAGs (Supplementary Table S4). Nine of the archaeal MAGs were affiliated with the phylum Thermoplasmatota whereas one was affiliated with Thermoproteota (Figure 8A). Among the ten archaeal MAGs, two MAGs had formal taxonomic nomenclature (as indicated in the International Code of Nomenclature of Prokaryotes) at the genus level (*Nitrosopumilus* and *Thalassarchaeum*), and one of the Thermoplasmatota MAGs had a separate branch from the root of the phylogenomic tree. Bacterial MAGs were assigned to 13 different phyla (Figure 8B). The highest number of MAGs were affiliated with Proteobacteria (53 MAGs), followed by 17 and 14 MAGs affiliated with Planctomycetota and Verrucomicrobiota, respectively. Out of 127 bacterial MAGs, 61, 28, and 5 MAGs had a formal taxonomic nomenclature at the family, genus, and species levels, respectively. Two bacterial MAGs affiliated with class Alphaproteobacteria (ANT-120) and phylum Planctomycetota (ANT-49) had RED values lower than 0.70. Detailed taxonomy classifications of all 137 MAGs are present in Supplementary Table S4. It was interesting to note that one of the MAGs classified as Myxococcota by GTDB-Tk clustered with Proteobacterial MAGs on the phylogenomic tree (Figure 8B).

Distinct groups of MAGs were observed when clustered according to their metabolic profiles. The NMDS plot indicated that the metabolic profiles of bacterial populations were phylum-specific, with minor overlaps among phyla (Figure 9). Distinct clusters for archaeal and bacterial MAGs were observed on the PCoA plot based on genomic repertoire (PERMANOVA, $p = 0.001$) (Supplementary Figure S5). Specific gene sets, and pathways were studied to determine the metabolic capabilities of the MAGs (Supplementary Table S5 and Supplementary Figure S6).

3.2.1. Role of MAGs in carbon transformation

Capabilities of glucose utilization and carbon fixation were analyzed based on different pathways. Since these pathways have multiple enzymes involved in them, pathways having ≥70% completeness in a MAG were considered as the presence of the pathway in the MAG. The details of the pathways and the completeness profiles are described in Supplementary Table S5. The capability to use externally fixed carbon was studied based on the presence of the Embden-Meyerhof and Entner–Doudoroff pathways. These two pathways help in the conversion of glucose into pyruvate. 75 MAGs

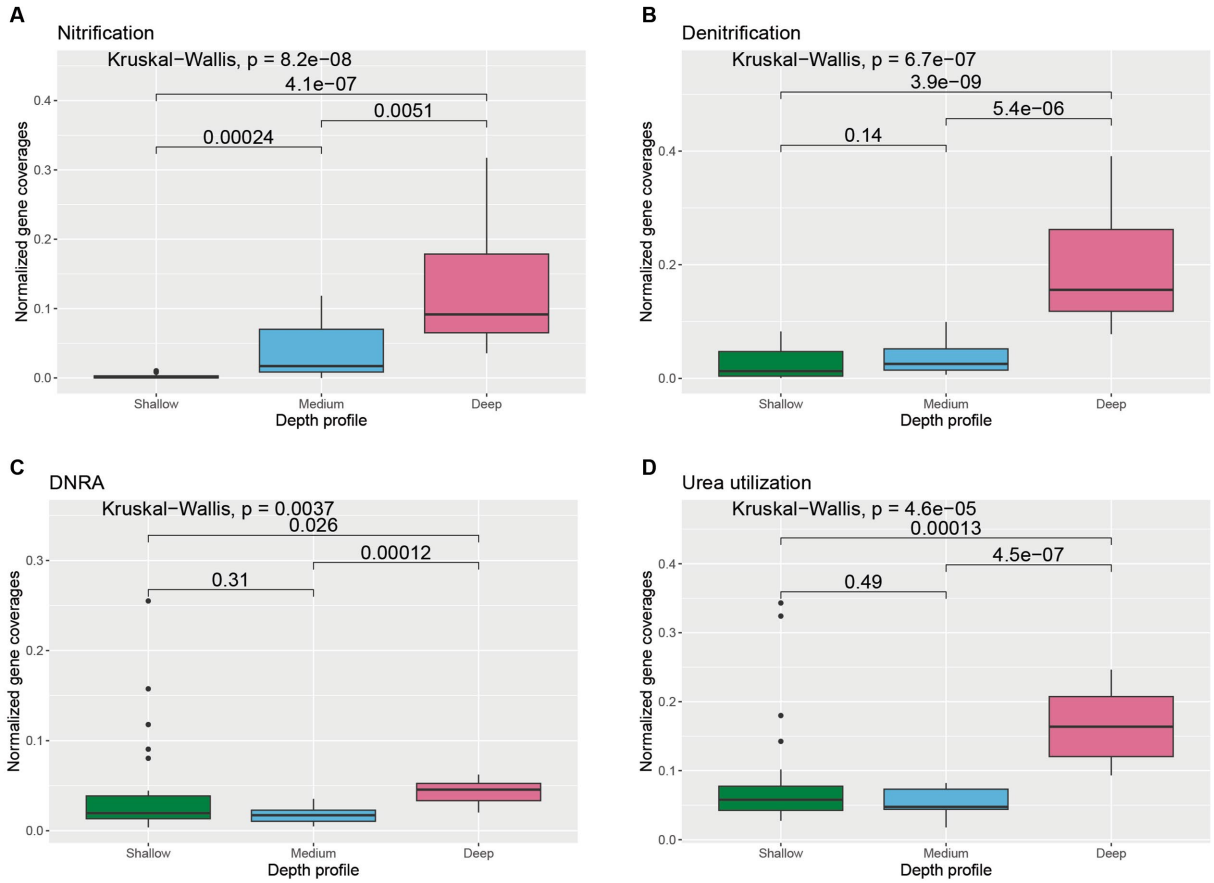

FIGURE 5
Boxplot showing the distribution of different nitrogen cycle genes related to **(A)** nitrification, **(B)** denitrification, **(C)** dissimilatory nitrate reduction to ammonia (DNRA), and **(D)** urea utilization across different depth horizons of the wAP. Normalized coverages of genes grouped in each of these categories are listed in Supplementary Figure S3. A pairwise comparison for significance was conducted using the Wilcoxon test.

covering 10 phyla had the capability of performing the Embden Meyerhof pathway, whereas 42 MAGs covering seven phyla had genomic repertoires for the Entner–Doudoroff pathway. The pentose phosphate pathway was observed in 88 MAGs covering 11 phyla. The citric acid cycle (Krebs cycle) was observed in 112 MAGs, whereas the glyoxylate cycle was observed in 40 MAGs. Three carbon fixation pathways *viz.* 3-Hydroxypropionate bicycle, Arnon–Buchanan cycle (reductive citrate cycle), and Calvin cycle (reductive pentose phosphate cycle) were observed among the MAGs. Capabilities of the Arnon–Buchanan cycle were present in a higher number of MAGs (56 MAGs) compared to the Calvin cycle (present in 26 MAGs) and 3-Hydroxypropionate bicycle (present in 8 MAGs). 3-Hydroxypropionate bicycle was only present in Proteobacterial MAGs, whereas Arnon–Buchanan cycle was distributed over MAGs affiliated to Proteobacteria, Verrucomicrobiota, Actinobacteriota, Planctomycetota, Chloroflexota, Thermoplasmatota, SAR324, and Latescibacterota. Calvin cycle was present in MAGs affiliated to Proteobacteria, Actinobacteriota, Chloroflexota, Bacteroidota, Planctomycetota, Gemmatimonadota, and SAR324.

The ability to produce or catabolize small-chain fatty acids and alcohols was studied based on the presence of certain genes in the genomic inventories of the MAGs. Capabilities of alcohol production (EC 1.1.1.1) were found in 53 MAGs, with the majority of the MAGs affiliated with Proteobacteria. The presence of genes encoding for phosphate acetyltransferase (EC 2.3.1.8) and/or acetate kinase (EC 2.7.2.1) was studied to understand acetate metabolism in the MAGs. Genes encoding for acetate metabolizing enzymes were found in 21 MAGs which were affiliated with six different phyla (Proteobacteria, Verrucomicrobiota, Planctomycetota, Actinobacteriota, Latescibacterota, and Bacteroidota). Genes encoding for L-lactate metabolizing enzyme (L-lactate dehydrogenase) were found in 19 MAGs, which were affiliated with the Proteobacteria, Actinobacteriota, Verrucomicrobiota, and Planctomycetota, whereas genes encoding for D-lactate metabolizing enzyme (D-lactate dehydrogenase) were found in five MAGs affiliated with Proteobacteria, Verrucomicrobiota, and Bacteroidota. The gene encoding for propionate metabolism (propionate CoA transferase) was found in three MAGs affiliated with two different phyla (Proteobacteria and Verrucomicrobiota).

Genes encoding for carbohydrate-active enzymes were studied to understand the polysaccharide-degrading capabilities of the MAGs. Genes encoding for enzymes involved in breaking down amorphous cellulose were found in 30 MAGs affiliated with seven different phyla (Proteobacteria, Planctomycetota, Bacteroidota, Myxococcota, Verrucomicrobiota, Actinobacteriota, and Latescibacterota), whereas genes encoding for the enzyme involved in breaking down crystalline cellulose was found in 11 MAGs covering five phyla (Planctomycetota,

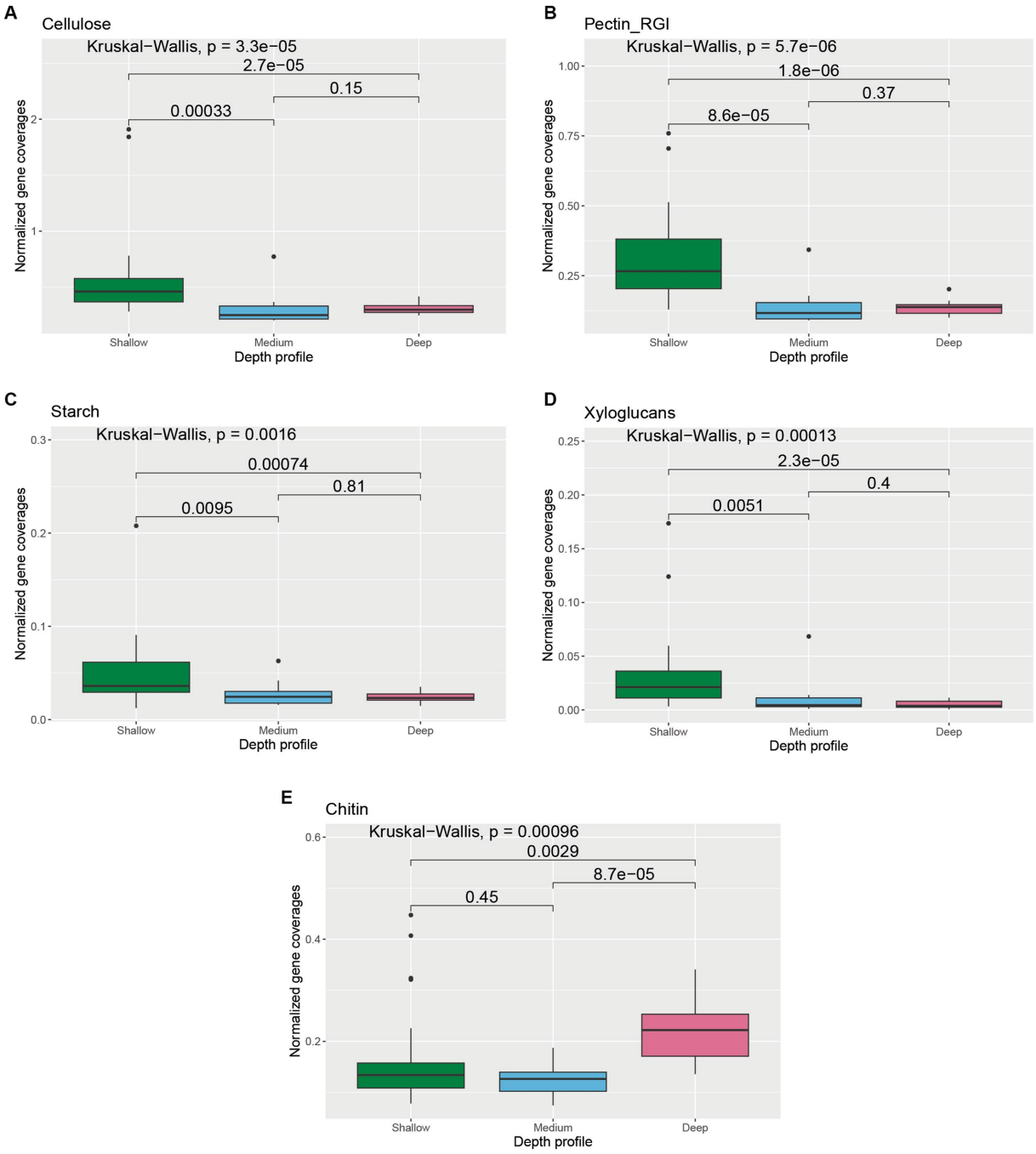

FIGURE 6
Boxplot showing the distribution of different carbohydrate transformation genes related to **(A)** cellulose, **(B)** pectin RGI, **(C)** starch, **(D)** xyloglucan, and **(E)** chitin degradation across different depth horizons of the wAP. Normalized coverages of genes grouped in each of these categories are listed in Supplementary Figure S4. A pairwise comparison for significance was conducted using the Wilcoxon test.

Proteobacteria, Verrucomicrobiota, Actinobacteriota, and Myxococcota). Genes coding for chitin-degrading enzymes were found in 85 MAGs (found in all phyla detected in this study except for MAGs affiliated with Thermoproteota, Chloroflexota, and Thermoplasmatota), whereas genes for starch-degrading enzymes were found in 15 MAGs having affiliation with five phyla (Proteobacteria, Verrucomicrobiota, Planctomycetota, Actinobacteriota, and Latescibacterota). Genes encoding enzymes that can perform xylan and xyloglucan (major components of hemicellulose) degradation were found in 23 and 40 MAGs, respectively. MAGs with the ability to degrade xylan were affiliated with Proteobacteria, Bacteroidota, Myxococcota, Planctomycetota, Actinobacteriota, and Latescibacterota, whereas MAGs with the ability to degrade xyloglucan were affiliated to Proteobacteria, Bacteroidota, Verrucomicrobiota, Planctomycetota, Myxococcota, Latescibacterota, and Marinisomatota. Genes encoding pectin degradation enzymes were found in 31 MAGs (having affiliation with Proteobacteria, Verrucomicrobiota, Planctomycetota, Bacteroidota, Latescibacterota, Marinisomatota, Gemmatimonadota, Acidobacteriota, and Chloroflexota).

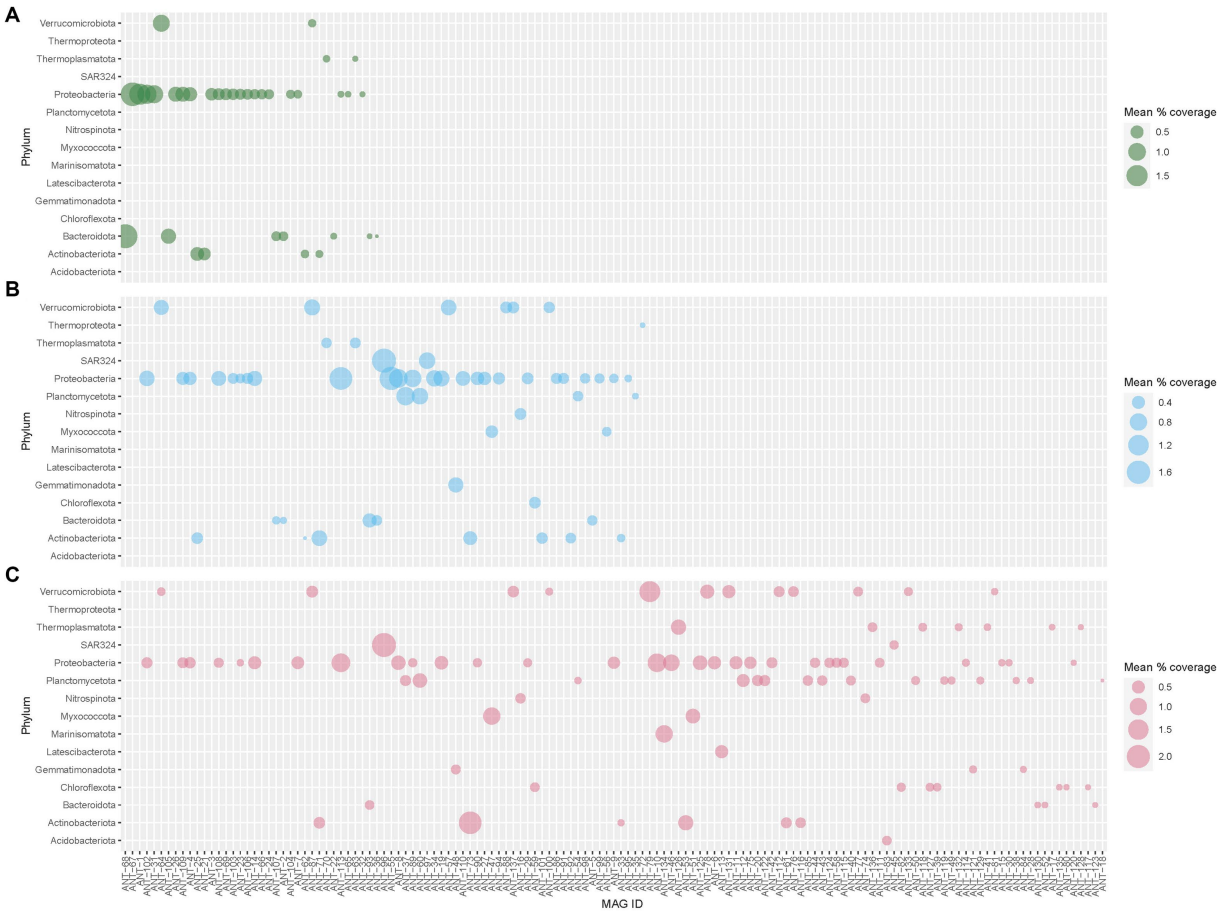

FIGURE 7
Average abundance of 137 dereplicated MAGs across **(A)** shallow, **(B)** medium, and **(C)** deep waters of the coastal wAP. Each dereplicated MAG represents multiple MAGs from different samples. The average abundance of each dereplicated MAG represents the average abundance of all the MAGs it represents from a particular depth horizon.

3.2.2. Role of MAGs in sulfur and nitrogen transformation

Genes involved in thiosulfate oxidation were found in 26 MAGs having affiliations with four phyla (Proteobacteria, Gemmatimonadota, Acidobacteriota, and SAR324) (Supplementary Figure S6). Three proteobacterial MAGs were found to harbor genes for dissimilatory sulfate reduction.

Genes involved in ammonia oxidation were found in two proteobacterial MAGs and in one archaeal MAG (affiliated to Thermoproteota). Genes involved in the conversion of nitrite to nitrate (one of the steps in nitrification) were found in two proteobacterial MAGs. Genes involved in the conversion of nitrate to nitrite (one of the steps in denitrification or dissimilatory nitrate reduction to ammonia) were found in two proteobacterial MAGs. Enzymes involved in the conversion of nitrite to nitric oxide (a key step in denitrification) were found in 14 different MAGs covering eight phyla (Proteobacteria, Actinobacteriota, Thermoproteota, Gemmatimonadota, Verrucomicrobiota, Acidobacteriota, Bacteroidota, and Nitrospinota), whereas enzymes involved in the conversion of nitric oxide to nitrous oxide (an additional step in denitrification) were found in two proteobacterial MAGs.

3.3. Putative metabolic lifestyles of MAGs

Overlaps across different metabolic categories are reported in Figures 8, 10A. It was found that the average genome sizes of the mixotrophs were significantly higher compared to heterotrophs ($p = 0.0001$) and autotrophs ($p = 0.02$) (Figure 10B). In the shallower depth samples, a significantly high mapped read percentage was observed in the mixotrophic MAGs ($n = 37$ MAGs), while compared to the autotrophic ($n = 2$ MAGs) and heterotrophic MAGs ($n = 52$ MAGs) (mixotroph vs. autotrophs, $p = 0.054$; mixotroph vs. heterotroph, $p = 1.5 \times 10^{-5}$) (Figure 10C). In the medium and deeper samples, the mapped read percentages for mixotrophic, autotrophic, and heterotrophic MAGs were not significantly different.

3.3.1. Putative mixotrophs

Four categories of mixotrophs covering 52 dereplicated MAGs were obtained (Supplementary Figure S6 and Supplementary Table S5). Only one MAG (ANT-6) recovered from a deeper horizon sample and classified as *Paraburkholderia* was found to harbor genes from all four categories of metabolism (GU, CF, SO, and NI). There were 12 MAGs that

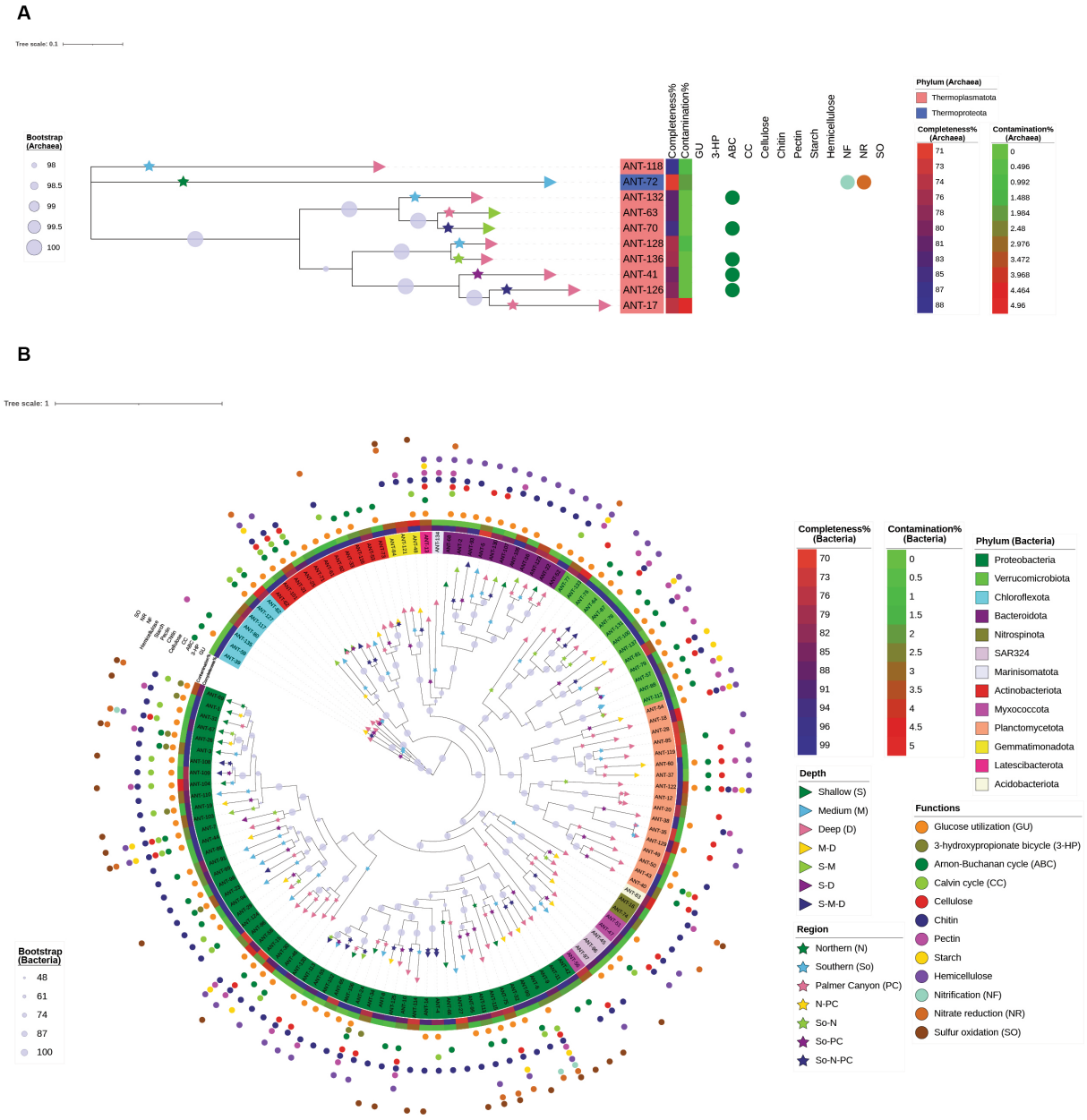

FIGURE 8
Maximum-likelihood phylogenomic analysis of 137 dereplicated MAGs based on **(A)** archaeal and **(B)** bacterial marker genes from GTDB-Tk analysis. Detailed genome statistics and taxonomy are provided in Supplementary Tables S3, S4, and the detailed pathways and functions are provided in Supplementary Table S5. Phylum, completeness %, contamination %, and bootstrap legends are domain-specific, whereas depth, region, and function are common for bacteria and archaea. Depth (represented by a right triangle) and region (represented by a star) symbols are present on the terminal node and terminal branch, respectively. The circle symbols in the outermost layer depict the functional capabilities of each MAG. All the carbohydrates mentioned represent the presence of enzymes capable of degrading them. Xylan and/or xyloglucan degrading enzymes are represented by hemicellulose in this figure. The hyphenated legends for depth represent MAGs found in multiple depth horizons, whereas hyphenated legends for regions represent MAGs found in multiple regions.

harbored genes from GU, CF, and SO (11 affiliated to Proteobacteria and one affiliated to Gemmatimonadota), whereas there was only one MAG that harbored genes from GU, CF, and NI (affiliated to Proteobacteria). There were 38 MAGs that harbored the genes from GU and CF metabolism categories only (affiliated to Proteobacteria, Actinobacteriota, Verrucomicrobiota, Planctomycetota, Chloroflexota, Bacteroidota, Latescibacterota, and SAR324).

3.3.2. Putative autotrophs

Three categories of autotrophs covering 20 dereplicated MAGs were obtained (Supplementary Table S5). There were three MAGs harboring genes for CF and SO (affiliated with Gammaproteobacteria), whereas there was only one MAG harboring gene for CF and NI (affiliated with Gammaproteobacteria). There were 16 MAGs that had genomic repertoire for CF but lacked genes for SO and NI (affiliated

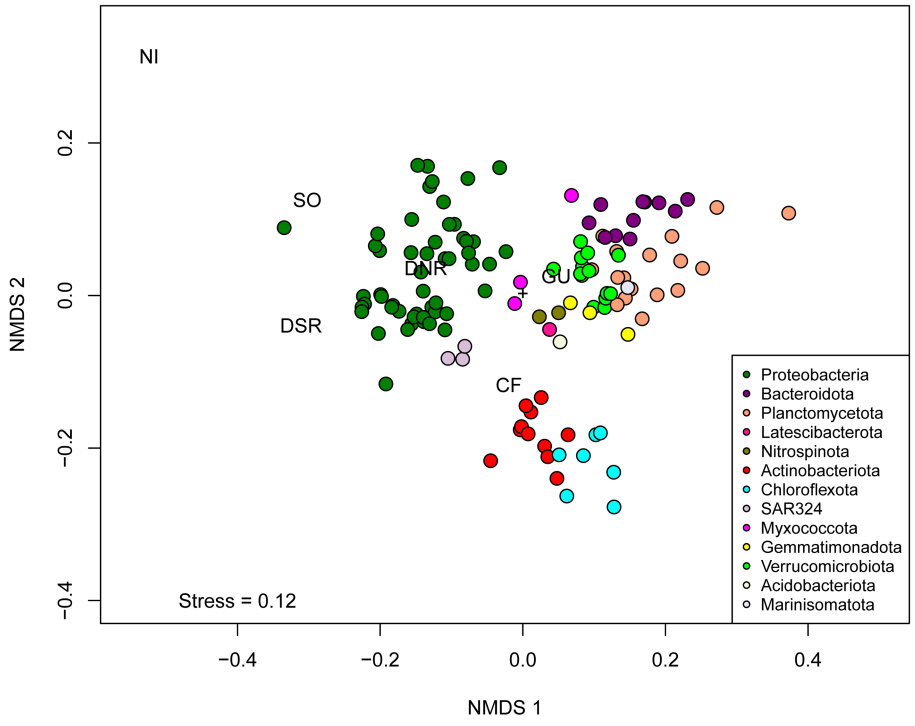

FIGURE 9
Non-Metric Multidimensional Scaling (NMDS) of binary matrix based on the presence or absence of genes predicted by Ghost Koala across 127 dereplicated bacterial MAGs. Abbreviations of metabolic categories as used in the NMDS analysis are as follows: GU, Glucose utilization; CF, carbon fixing pathways; NI, nitrification; SO, sulfur oxidation; DNR, Denitrification; DSR, Dissimilatory sulfate reduction.

with Proteobacteria, Thermoplasmatota, Planctomycetota, Chloroflexota, Actinobacteriota, and Verrucomicrobiota).

3.3.3. Putative heterotrophs

Two categories of heterotrophs covering 35 dereplicated MAGs were observed in this study (Supplementary Figure S6 and Supplementary Table S5). One of the categories harbored genes for GU and SO, which was found in five different MAGs (affiliated to Proteobacteria and SAR324). The other category solely harbored genes for GU and was found in 30 MAGs (affiliated to Proteobacteria, Bacteroidota, Verrucomicrobiota, Planctomycetota, Actinobacteriota, SAR324, and Myxococcota).

4. Discussion

Our analysis reveals the diverse genomic repertoire contained among marine bacteria and archaea along the coastal wAP. PCoA based on normalized gene coverage across 48 samples suggested that microbial community functions were strongly partitioned by depth, with the highest variation in microbial community function observed in the shallower samples (0–40 m). A possible explanation is that this higher variance results from a more dynamic environment in the shallower waters than in the deeper environments (Carranza et al., 2018).

Primary production in the coastal Antarctic is attributed primarily to phytoplankton (Arrigo et al., 2008). However, prokaryotic dark carbon fixation can be significant in deep and polar oceans (Alonso-Sáez et al., 2010; Williams et al., 2012; Connelly et al., 2014), and previous work has identified the genomic signatures of dark carbon fixation along the wAP (Grzymski et al., 2012). We observed genes indicative of dark carbon fixation in numerous MAGs representing multiple phyla. This suggests that in addition to eukaryotic carbon fixation, prokaryotic dark carbon fixation can also be a source of fixed carbon in the Antarctic marine ecosystem, expanding the conventional viewpoint of marine primary production (Buchan et al., 2014). We are not aware of any studies that attempt to quantify dark carbon fixation inputs to coastal Antarctic ecosystems. However, previous work suggests oceanic primary production estimates would increase by 5–22% when total dark DOC fixation is included (Baltar and Herndl, 2019). Moreover, the normalized coverage of genes related to dark carbon fixation was found to be higher in deeper waters compared to the waters from medium-deep and shallower horizons in the coastal wAP suggesting that the dearth of phytoplankton-fixed carbon in the deeper waters selects for microorganisms capable of fixing carbon in the dark. This lack of photosynthate as an electron donor in deeper water is further supported by the presence of higher normalized gene coverage of CO oxidation genes. Lappan et al. (2023) previously reported an enrichment of CO hydrogenase (an enzyme involved in CO oxidation) in temperate mesopelagic waters and suggested that CO oxidation is favored in energy-limited waters at depths where primary production is low.

The normalized gene coverages for processes preferred in hypoxic/anoxic environments, such as fermentation, dissimilatory sulfate reduction, thiosulfate to sulfide reduction, denitrification,

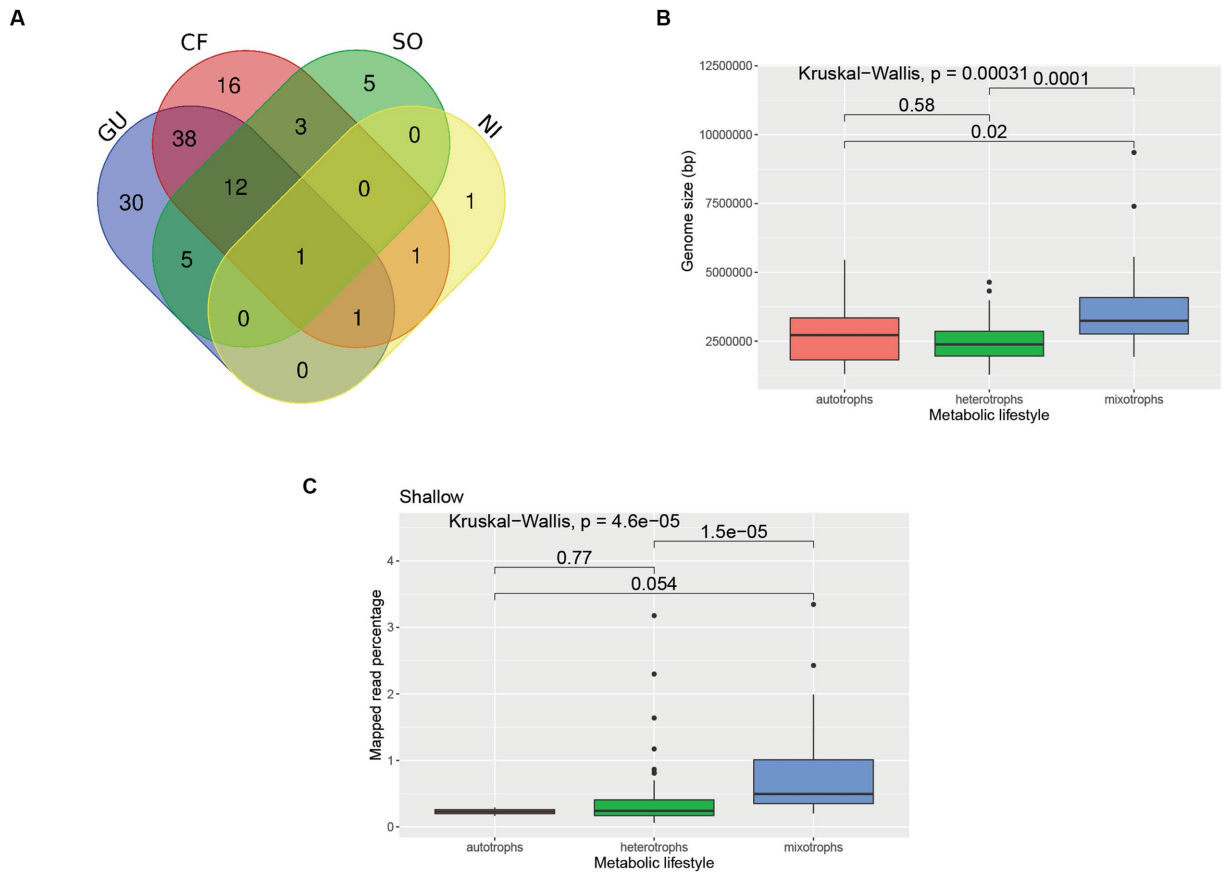

FIGURE 10
Comparison of MAGs having different metabolic lifestyles. **(A)** Venn Diagram showing overlaps among different metabolic categories of the MAGs. The numbers depicted in the Venn diagram represent the number of MAGs affiliated to each category. GU, Glucose utilization; CF, carbon fixing pathways; NI, nitrification; SO, sulfur oxidation. **(B)** Boxplot showing genome sizes of MAGs related to different metabolic lifestyles. The details of the genome sizes and metabolic lifestyle of each MAG are reported in Supplementary Table S3. **(C)** Boxplot showing mapped read percentage of MAGs having different metabolic lifestyles in shallower depth samples. For the boxplots, a pairwise comparison for significance was conducted using the Wilcoxon test.

and DNRA, were found to be higher in the water samples from the deeper horizons (>100 m). Although oxygen drawdown is observed below the photic zone in the wAP (Cape et al., 2019), the water column typically remains sufficiently oxic to support aerobic processes, including nitrification and methane oxidation in deeper waters. We suggest two explanations for the presence of anaerobic pathways here. First, the organisms harboring these pathways may be facultative anaerobes that can dwell in multiple environments of the wAP. This is supported by the presence of certain MAGs capable of using oxygen (presence of cytochrome c oxidase and F-Type ATPases genes) and nitrate (presence of genes involved in denitrification) as terminal electron acceptors. Second, these microbial populations may come from fecal pellets and sinking detritus that harbor microenvironments that support the growth of anaerobic microbial populations.

Due to high levels of primary production, the coastal wAP harbors a diverse and abundant carbohydrate pool. The source of these carbohydrates includes phytoplankton or zooplankton such as krill (van Oijen et al., 2003; Yu et al., 2020). We observed a diverse genomic repertoire for degrading carbohydrates derived from phytoplankton and zooplankton. This suggests a link between the microeukaryotic and prokaryotic populations in the Antarctic. Moreover, higher abundances of microorganisms capable of degrading cellulose, xyloglucans, pectin, and starch were observed in the upper water column, consistent with the greater phytoplankton biomass expected there. This distribution suggests that carbohydrates are readily turned over in the upper water column, possibly reducing vertical export. This is further supported by the presence of prokaryotic dark carbon fixing pathways in the deeper environment of coastal wAP. Several MAGs having the capability to degrade polysaccharide was also observed in the medium-deep and deeper horizon of the wAP. This suggests that these microbial populations may be associated with the sinking detritus material, which helps in the conversion of complex carbohydrates to simpler carbon compounds that can be used by other heterotrophs.

Varied metabolic flexibility was observed in several MAGs. ANT-6, affiliated to *Paraburkholderia fungorum* was found to have the most diverse genomic repertoire based on the presence of heterotrophic and autotrophic pathways. The genomic repertoire suggests that they can perform carbon fixation and also utilize glucose. The mixotrophic behavior of *Paraburkholderia* has been

reported previously (Herpell et al., 2020). Interestingly, ANT-6 also harbored genes involved in thiosulfate oxidation, nitrification, and denitrification. Sulfite oxidation was previously observed in *Paraburkholderia caledonica* PHRS4 (BioCyc ID: PWY-5276). Even though varied metabolic traits of the genus *Paraburkholderia* are well known, the presence of genomic machinery related to autotrophic and heterotrophic lifestyle, along with the presence of thiosulfate oxidation, nitrification, and denitrification capability in a single strain, is not reported elsewhere to the best of our knowledge. The genome size of ANT-6 was found to be the highest (9.3 Mbp) among all the other MAGs constructed. The genome size of ANT-6 is in the range of genome sizes of other *Paraburkholderia* strains (Wang et al., 2021), which is bigger than "typical" bacterial genomes (Land et al., 2015). The metabolic flexibility of *Paraburkholderia* is consistent with its bigger genomes size. Previous reports of the presence of *Paraburkholderia* in the Antarctic environment (Malard et al., 2022) also support the presence of ANT-6 in the Antarctic.

A high number of mixotrophic MAGs (52 MAGs) were observed compared to exclusively heterotrophic (35) and autotrophic (20) MAGs. The prevalence of mixotrophy was also previously reported in Arctic prokaryotic genomes (Royo-Llonch et al., 2021). In the shallow samples of the coastal wAP, the abundances of mixotrophic MAGs were found to be significantly higher compared to heterotrophic and autotrophic MAGs, whereas, in the deeper samples, the abundances of the mixotrophic MAGs were not significantly different compared to autotrophic and heterotrophic MAGs. This suggests a strong pressure for metabolic flexibility, potentially a response to the seasonal boom-bust cycle of photosynthetic primary production. This is in line with the higher variations of genomic repertoire in the shallower samples compared to medium-depth and deeper samples. We hypothesize that dynamic environments select microbial populations with a diverse genomic repertoire, including the capacity to switch between heterotrophic and autotrophic lifestyles. Moreover, the genome size of the mixotrophs was found to be significantly larger compared to the autotrophs and heterotrophs. This is in accordance with a previous study where they reported larger genome sizes of the generalist compared to the specialist (Sriswasdi et al., 2017). However, it should be taken into account that higher completeness of MAGs is required to ascertain a particular function or metabolic lifestyle with greater confidence.

Several of our MAGs were only distantly related to the genomes of type strains. A MAG classified as Myxococcota (ANT-56) by GTDB-Tk clustered with Proteobacterial MAGs on the phylogenomic tree (Figure 8B), which might be due to its novel taxonomy. There might also be two other reasons for this: (i) lower completeness of the Myxococcota genome (75.54% completeness) and/or (ii) close relatedness of Myxococcota genome with Proteobacterial genomes, which can be supported by the recent classification of Myxococcota as a new separate phylum, which was earlier assigned to class Deltaproteobacteria (Murphy et al., 2021). Only 40 MAGs had ANI values higher than 0.95 when compared to the genomes from the GTDB reference database. Based on our current analyses, we found that only 70, 30, and 5 MAGs had a formal taxonomic nomenclature at the family, genus, and species levels, respectively. We were unable to determine the metabolic lifestyle of the MAG (ANT-120, affiliated to Alphaproteobactria) having the lowest RED value (0.66). Similarly, there were 29 other MAGs for which we were unable to determine the metabolic lifestyle based on the criteria we used in this study.

This study used high-throughput metagenomics to understand the microbial role in the marine ecosystem of the wAP. A streamlined metagenomic sequence analysis pipeline (iMAGine) was developed to process data and reconstruct MAGs. Our pipeline enabled a coverage-based approach to understand how genes were partitioned by depth and region. With this approach, we identified diverse groups of microorganisms contributing to the carbon, sulfur, and nitrogen cycle along the coastal wAP. Distinct microbial metabolisms were observed across different depth horizons. In particular, higher abundances of mixotrophic MAGs compared to heterotrophic and autotrophic MAGs were found in the shallower waters, suggesting that the dynamic pelagic environment of the coastal wAP has selected microbial populations which can adapt to rapidly changing nutrient availability. Metabolic profiles of the MAGs were phylum specific, indicating a strong link between functional guilds and taxonomy. Our results highlight the novel genetic and metabolic diversity present within Antarctic marine ecosystems and the need for future studies based on cultivable microbes to better understand the distribution of phenotypic and genotypic traits.

Data availability statement

The datasets presented in this study can be found in online repositories. The names of the repository/repositories and accession number(s) can be found in the article/Supplementary material.

Author contributions

AD and JB designed the study and developed the first draft of the manuscript. AD developed the iMAGine pipeline and conducted the analysis with assistance from JB. EC, RT, NE, and SD collected the samples and edited the manuscript. EC conducted DNA extractions and processed samples for sequencing. HD, DS, and OS contributed to the study design and writing. All authors contributed to the article and approved the submitted version.

Funding

This work was funded by NSF-OPP 1846837 to JB, NSF-OPP 1440435 to HD, and NSF-OPP 2023425 to OS. JB was partly supported by the Simons Foundation Early Career Marine Microbial Ecology and Evolution fellowship. NE was funded through a SENESCYT graduate fellowship. This publication includes data generated at the UC San Diego IGM Genomics Center utilizing an Illumina NovaSeq 6000 that was purchased with funding from a National Institutes of Health SIG grant (#S10 OD026929).

Acknowledgments

We would like to thank the staff of Palmer Station and the crew of *ARSV Laurence Gould* for their assistance.

Conflict of interest

The authors declare that the research was conducted in the absence of any commercial or financial relationships that could be construed as a potential conflict of interest.

Publisher's note

All claims expressed in this article are solely those of the authors and do not necessarily represent those of their affiliated organizations, or those of the publisher, the editors and the reviewers. Any product that may be evaluated in this article, or claim that may be made by its manufacturer, is not guaranteed or endorsed by the publisher.

Supplementary material

The Supplementary material for this article can be found online at: https://www.frontiersin.org/articles/10.3389/fmicb.2023.1168507/full#supplementary-material

SUPPLEMENTARY TABLE S1
Sample metadata for 48 samples.

SUPPLEMENTARY TABLE S2
Genes considered for whole metagenome analysis.

SUPPLEMENTARY TABLE S3
Detailed genome statistics of 137 MAGs.

SUPPLEMENTARY TABLE S4
Detailed taxonomic classification-based genome summary.

SUPPLEMENTARY TABLE S5
Metabolic profiles of 137 MAGs.

References

Alonso-Sáez, L., Galand, P. E., Casamayor, E. O., Pedrós-Alió, C., and Bertilsson, S. (2010). High bicarbonate assimilation in the dark by Arctic bacteria. *ISME J.* 4, 1581–1590. doi: 10.1038/ismej.2010.69

Arrigo, K. R., van Dijken, G. L., and Bushinsky, S. (2008). Primary production in the Southern Ocean, 1997-2006. *J. Geophys. Res. Oceans* 113:C08004. doi: 10.1029/2007JC004551

Baltar, F., and Herndl, G. J. (2019). Ideas and perspectives: is dark carbon fixation relevant for oceanic primary production estimates? *Biogeosciences* 16, 3793–3799. doi: 10.5194/bg-16-3793-2019

Bergauer, K., Fernandez-Guerra, A., Garcia, J. A. L., Sprenger, R. R., Stepanauskas, R., Pachiadaki, M. G., et al. (2018). Organic matter processing by microbial communities throughout the Atlantic water column as revealed by metaproteomics. *Proc. Natl. Acad. Sci. U. S. A.* 115, E400–E408. doi: 10.1073/pnas.1708779115

Bowman, J. S., Amaral-Zettler, L. A., Rich, J. J., Luria, C. M., and Ducklow, H. W. (2017). Bacterial community segmentation facilitates the prediction of ecosystem function along the coast of the western Antarctic Peninsula. *ISME J.* 11, 1460–1471. doi: 10.1038/ismej.2016.204

Bowman, J. S., and Deming, J. W. (2017). Wind-driven distribution of bacteria in coastal Antarctica: evidence from the Ross Sea region. *Polar Biol.* 40, 25–35. doi: 10.1007/s00300-016-1921-2

Bowman, J. S., Kavanaugh, M. T., Doney, S. C., and Ducklow, H. W. (2018). Recurrent seascape units identify key ecological processes along the western Antarctic Peninsula. *Glob. Chang. Biol.* 24, 3065–3078. doi: 10.1111/gcb.14161

Bowman, J. S., van Mooy, B. A. S., Lowenstein, D. P., Fredricks, H. F., Hansel, C. M., Gast, R., et al. (2021). Whole community metatranscriptomes and lipidomes reveal diverse responses among Antarctic phytoplankton to changing ice conditions. *Front. Mar. Sci.* 8:593566. doi: 10.3389/fmars.2021.593566

Bowman, J. S., Vick-Majors, T. J., Morgan-Kiss, R., Takacs-Vesbach, C., Ducklow, H. W., and Priscu, J. C. (2016). Microbial community dynamics in two polar extremes: the lakes of the McMurdo dry valleys and the West Antarctic Peninsula marine ecosystem. *Bioscience* 66, 829–847. doi: 10.1093/biosci/biw103

Buchan, A., LeCleir, G. R., Gulvik, C. A., and González, J. M. (2014). Master recyclers: features and functions of bacteria associated with phytoplankton blooms. *Nat. Rev. Microbiol.* 12, 686–698. doi: 10.1038/nrmicro3326

Buchfink, B., Xie, C., and Huson, D. H. (2014). Fast and sensitive protein alignment using DIAMOND. *Nat. Methods* 12, 59–60. doi: 10.1038/nmeth.3176

Bushnell, B. (2014). *BBMap: a fast, accurate, splice-aware aligner*. Lawrence Berkeley National Laboratory, Berkeley, CA.

Cantalapiedra, C. P., Hernández-Plaza, A., Letunic, I., Bork, P., and Huerta-Cepas, J. (2021). eggNOG-mapper v2: functional annotation, orthology assignments, and domain prediction at the metagenomic scale. *Mol. Biol. Evol.* 38, 5825–5829. doi: 10.1093/molbev/msab293

Cape, M. R., Vernet, M., Pettit, E. C., Wellner, J., Truffer, M., Akie, G., et al. (2019). Circumpolar deep water impacts glacial meltwater export and coastal biogeochemical cycling along the West Antarctic Peninsula. *Front. Mar. Sci.* 6:144. doi: 10.3389/fmars.2019.00144

Carranza, M. M., Gille, S. T., Franks, P. J. S., Johnson, K. S., Pinkel, R., and Girton, J. B. (2018). When mixed layers are Not mixed. Storm-driven mixing and bio-optical vertical gradients in mixed layers of the Southern Ocean. *J. Geophys. Res. Oceans* 123, 7264–7289. doi: 10.1029/2018JC014416

Chaumeil, P. A., Mussig, A. J., Hugenholtz, P., and Parks, D. H. (2020). GTDB-Tk: a toolkit to classify genomes with the genome taxonomy database. *Bioinformatics* 36, 1925–1927. doi: 10.1093/bioinformatics/btz848

Chen, S., Zhou, Y., Chen, Y., and Gu, J. (2018). fastp: an ultra-fast all-in-one FASTQ preprocessor. *Bioinformatics* 34, i884–i890. doi: 10.1093/bioinformatics/bty560

Clarke, A., Murphy, E. J., Meredith, M. P., King, J. C., Peck, L. S., Barnes, D. K. A., et al. (2007). Climate change and the marine ecosystem of the western Antarctic Peninsula. *Philos. Trans. R. Soc. B Biol. Sci.* 362, 149–166. doi: 10.1098/rstb.2006.1958

Connelly, T. L., Baer, S. E., Cooper, J. T., Bronk, D. A., and Wawrik, B. (2014). Urea uptake and carbon fixation by marine pelagic bacteria and archaea during the Arctic summer and winter seasons. *Appl. Environ. Microbiol.* 80, 6013–6022. doi: 10.1128/AEM.01431-14

Dutta, A., Goldman, T., Keating, J., Burke, E., Williamson, N., Dirmeier, R., et al. (2022). Machine learning predicts biogeochemistry from microbial community structure in a complex model system. Available at: https://journals.asm.org/journal/spectrum.

Green, J. L., Bohannan, B. J. M., and Whitaker, R. J. (2008). Microbial biogeography: from taxonomy to traits. *Science* 320, 1039–1043. doi: 10.1126/science.1153475

Grzymski, J. J., Riesenfeld, C. S., Williams, T. J., Dussaq, A. M., Ducklow, H., Erickson, M., et al. (2012). A metagenomic assessment of winter and summer bacterioplankton from Antarctica Peninsula coastal surface waters. *ISME J.* 6, 1901–1915. doi: 10.1038/ismej.2012.31

Gurevich, A., Saveliev, V., Vyahhi, N., and Tesler, G. (2013). QUAST: quality assessment tool for genome assemblies. *Bioinformatics* 29, 1072–1075. doi: 10.1093/bioinformatics/btt086

Herpell, J. B., Schindler, F., Bejtović, M., Fragner, L., Diallo, B., Bellaire, A., et al. (2020). The potato yam phyllosphere ectosymbiont *Paraburkholderia* sp. Msb3 is a potent growth promotor in tomato. *Front. Microbiol.* 11:581. doi: 10.3389/fmicb.2020.00581

Huerta-Cepas, J., Szklarczyk, D., Heller, D., Hernández-Plaza, A., Forslund, S. K., Cook, H., et al. (2019). EggNOG 5.0: a hierarchical, functionally and phylogenetically annotated orthology resource based on 5090 organisms and 2502 viruses. *Nucleic Acids Res.* 47, D309–D314. doi: 10.1093/nar/gky1085

Hyatt, D., Chen, G.-L., Locascio, P. F., Land, M. L., Larimer, F. W., and Hauser, L. J. (2010). Prodigal: prokaryotic gene recognition and translation initiation site identification. Available at: http://www.biomedcentral.com/1471-2105/11/119.

Kanehisa, M., Sato, Y., and Morishima, K. (2016). BlastKOALA and GhostKOALA: KEGG tools for functional characterization of genome and metagenome sequences. *J. Mol. Biol.* 428, 726–731. doi: 10.1016/j.jmb.2015.11.006

Kang, D. D., Li, F., Kirton, E., Thomas, A., Egan, R., An, H., et al. (2019). MetaBAT 2: an adaptive binning algorithm for robust and efficient genome reconstruction from metagenome assemblies. *PeerJ* 7, –e7359. doi: 10.7717/peerj.7359

Kolde, R.. (2019). Package 'pheatmap.' Available at: https://cran.r-project.org/web/packages/pheatmap/pheatmap.pdf.

Kozlov, A. M., Darriba, D., Flouri, T., Morel, B., and Stamatakis, A. (2019). RAxML-NG: a fast, scalable and user-friendly tool for maximum likelihood phylogenetic inference. *Bioinformatics* 35, 4453–4455. doi: 10.1093/bioinformatics/btz305

Land, M., Hauser, L., Jun, S. R., Nookaew, I., Leuze, M. R., Ahn, T. H., et al. (2015). Insights from 20 years of bacterial genome sequencing. *Funct. Integr. Genomics* 15, 141–161. doi: 10.1007/s10142-015-0433-4

Lappan, R., Shelley, G., Islam, Z. F., Leung, P. M., Lockwood, S., Nauer, P. A., et al. (2023). Molecular hydrogen in seawater supports growth of diverse marine bacteria. *Nat. Microbiol.* 8, 581–595. doi: 10.1038/s41564-023-01322-0

Li, H.. (2013). Aligning sequence reads, clone sequences and assembly contigs with BWA-MEM. Available at: http://arxiv.org/abs/1303.3997.

Li, H., Handsaker, B., Wysoker, A., Fennell, T., Ruan, J., Homer, N., et al. (2009). The sequence alignment/map format and SAMtools. *Bioinformatics* 25, 2078–2079. doi: 10.1093/bioinformatics/btp352

Lin, Y., Moreno, C., Marchetti, A., Ducklow, H., Schofield, O., Delage, E., et al. (2021). Decline in plankton diversity and carbon flux with reduced sea ice extent along the Western Antarctic Peninsula. *Nat. Commun.* 12:4948. doi: 10.1038/s41467-021-25235-w

Loy, A., Duller, S., Baranyi, C., Mußmann, M., Ott, J., Sharon, I., et al. (2009). Reverse dissimilatory sulfite reductase as phylogenetic marker for a subgroup of sulfur-oxidizing prokaryotes. *Environ. Microbiol.* 11, 289–299. doi: 10.1111/j.1462-2920.2008.01760.x

Malard, L. A., Avila-Jimenez, M. L., Schmale, J., Cuthbertson, L., Cockerton, L., and Pearce, D. A. (2022). Aerobiology over the Southern Ocean – implications for bacterial colonization of Antarctica. *Environ. Int.* 169:107492. doi: 10.1016/j.envint.2022.107492

McLeod, D. J., Hallegraeff, G. M., Hosie, G. W., and Richardson, A. J. (2012). Climate-driven range expansion of the red-tide dinoflagellate *Noctiluca scintillans* into the Southern Ocean. *J. Plankton Res.* 34, 332–337. doi: 10.1093/plankt/fbr112

McMurdie, P. J., and Holmes, S. (2013). Phyloseq: an R package for reproducible interactive analysis and graphics of microbiome census data. *PLoS One* 8:e61217. doi: 10.1371/journal.pone.0061217

Meredith, M. P., and King, J. C. (2005). Rapid climate change in the ocean west of the Antarctic Peninsula during the second half of the 20th century. *Geophys. Res. Lett.* 32, 1–5. doi: 10.1029/2005GL024042

Murphy, C. L., Yang, R., Decker, T., Cavalliere, C., Andreev, V., Bircher, N., et al. (2021). Genomes of novel myxococcota reveal severely curtailed machineries for predation and cellular differentiation. *Appl. Environ. Microbiol.* 87:e0170621. doi: 10.1128/AEM.01706-21

Nurk, S., Meleshko, D., Korobeynikov, A., and Pevzner, P. A. (2017). metaSPAdes: a new versatile metagenomic assembler. *Genome Res.* 27, 824–834. doi: 10.1101/gr.213959.116

Oksanen, J., Kindt, R., Legendre, P., O'Hara, B., Stevens, M. H. H., Oksanen, M. J., et al. (2007). The vegan package. *Community Ecol. Package* 10, 631–637.

Olm, M. R., Brown, C. T., Brooks, B., and Banfield, J. F. (2017). DRep: a tool for fast and accurate genomic comparisons that enables improved genome recovery from metagenomes through de-replication. *ISME J.* 11, 2864–2868. doi: 10.1038/ismej.2017.126

Parks, D. H., Imelfort, M., Skennerton, C. T., Hugenholtz, P., and Tyson, G. W. (2015). CheckM: assessing the quality of microbial genomes recovered from isolates, single cells, and metagenomes. *Genome Res.* 25, 1043–1055. doi: 10.1101/gr.186072.114

Parks, D. H., Rinke, C., Chuvochina, M., Chaumeil, P. A., Woodcroft, B. J., Evans, P. N., et al. (2017). Recovery of nearly 8,000 metagenome-assembled genomes substantially expands the tree of life. *Nat. Microbiol.* 2, 1533–1542. doi: 10.1038/s41564-017-0012-7

Plum, C., Hillebrand, H., and Moorthi, S. (2020). Krill vs salps: dominance shift from krill to salps is associated with higher dissolved N:P ratios. *Sci. Rep.* 10:5911. doi: 10.1038/s41598-020-62829-8

Royo-Llonch, M., Sánchez, P., Ruiz-González, C., Salazar, G., Pedrós-Alió, C., Sebastián, M., et al. (2021). Compendium of 530 metagenome-assembled bacterial and archaeal genomes from the polar Arctic Ocean. *Nat. Microbiol.* 6, 1561–1574. doi: 10.1038/s41564-021-00979-9

RStudio Team (2015). *RStudio: integrated development for R*. RStudio, Inc., Boston, MA. Available at: http://www.rstudio.com

Saba, G. K., Fraser, W. R., Saba, V. S., Iannuzzi, R. A., Coleman, K. E., Doney, S. C., et al. (2014). Winter and spring controls on the summer food web of the coastal West Antarctic Peninsula. *Nat. Commun.* 5:4318. doi: 10.1038/ncomms5318

Schofield, O., Brown, M., Kohut, J., Nardelli, S., Saba, G., Waite, N., et al. (2018). Changes in the upper ocean mixed layer and phytoplankton productivity along the West Antarctic Peninsula. *Philos. Trans. R. Soc. A Math. Phys. Eng. Sci.* 376:20170173. doi: 10.1098/rsta.2017.0173

Seyitmuhammedov, K., Stirling, C. H., Reid, M. R., van Hale, R., Laan, P., Arrigo, K. R., et al. (2022). The distribution of Fe across the shelf of the Western Antarctic Peninsula at the start of the phytoplankton growing season. *Mar. Chem.* 238:104066. doi: 10.1016/j.marchem.2021.104066

Shaffer, M., Borton, M. A., McGivern, B. B., Zayed, A. A., la Rosa, S. L., Solden, L. M., et al. (2020). DRAM for distilling microbial metabolism to automate the curation of microbiome function. *Nucleic Acids Res.* 48, 8883–8900. doi: 10.1093/nar/gkaa621

Siegert, M., Atkinson, A., Banwell, A., Brandon, M., Convey, P., Davies, B., et al. (2019). The Antarctic Peninsula under a 1.5°C global warming scenario. *Front Environ. Sci.* 7:102. doi: 10.3389/fenvs.2019.00102

Sriswasdi, S., Yang, C. C., and Iwasaki, W. (2017). Generalist species drive microbial dispersion and evolution. *Nat. Commun.* 8:1162. doi: 10.1038/s41467-017-01265-1

Thompson, L. R., Sanders, J. G., McDonald, D., Amir, A., Ladau, J., Locey, K. J., et al. (2017). A communal catalogue reveals Earth's multiscale microbial diversity. *Nature* 551, 457–463. doi: 10.1038/nature24621

van Oijen, T., van Leeuwe, M. A., and Gieskes, W. W. C. (2003). Variation of particulate carbohydrate pools over time and depth in a diatom-dominated plankton community at the Antarctic polar front. *Polar Biol.* 26, 195–201. doi: 10.1007/s00300-002-0456-x

Wang, K., Wu, Y., Ye, M., Yang, Y., Asiegbu, F. O., Overmyer, K., et al. (2021). Comparative genomics reveals potential mechanisms of plant beneficial effects of a novel bamboo-endophytic bacterial isolate Paraburkholderia sacchari Suichang626. *Front. Microbiol.* 12:686998. doi: 10.3389/fmicb.2021.686998

Waters, K. J., and Smith, R. C. (1992). Palmer LTER: a sampling grid for the palmer LTER program. *Antarct. J. US* 27, 236–239.

Williams, T. J., Long, E., Evans, F., Demaere, M. Z., Lauro, F. M., Raftery, M. J., et al. (2012). A metaproteomic assessment of winter and summer bacterioplankton from Antarctic Peninsula coastal surface waters. *ISME J.* 6, 1883–1900. doi: 10.1038/ismej.2012.28

Yu, Y., Liu, X., Miao, J., and Leng, K. (2020). Chitin from Antarctic krill shell: eco-preparation, detection, and characterization. *Int. J. Biol. Macromol.* 164, 4125–4137. doi: 10.1016/j.ijbiomac.2020.08.244

frontiers | Frontiers in Microbiology

TYPE Review
PUBLISHED 16 June 2023
DOI 10.3389/fmicb.2023.1197797

OPEN ACCESS

EDITED BY
Prashant Kumar Singh,
Mizoram University, India

REVIEWED BY
Alysson Wagner Fernandes Duarte,
Federal University of Alagoas, Brazil
Garvita Singh,
University of Delhi, India

*CORRESPONDENCE
Kesava Priyan Ramasamy
✉ kesava.ramasamy@umu.se

RECEIVED 31 March 2023
ACCEPTED 31 May 2023
PUBLISHED 16 June 2023

CITATION
Ramasamy KP, Mahawar L, Rajasabapathy R, Rajeshwari K, Miceli C and Pucciarelli S (2023) Comprehensive insights on environmental adaptation strategies in Antarctic bacteria and biotechnological applications of cold adapted molecules.
Front. Microbiol. 14:1197797.
doi: 10.3389/fmicb.2023.1197797

Comprehensive insights on environmental adaptation strategies in Antarctic bacteria and biotechnological applications of cold adapted molecules

Kesava Priyan Ramasamy[1]*, Lovely Mahawar[2], Raju Rajasabapathy[3], Kottilil Rajeshwari[4], Cristina Miceli[5] and Sandra Pucciarelli[5]

[1]Department of Ecology and Environmental Science, Umeå University, Umeå, Sweden, [2]Department of Plant Physiology, Faculty of Agrobiology and Food Resources, Slovak University of Agriculture, Nitra, Slovakia, [3]Department of Marine Science, Bharathidasan University, Tiruchirappalli, Tamilnadu, India, [4]Department of Zoology, Goa University, Taleigão, Goa, India, [5]School of Biosciences and Veterinary Medicine, University of Camerino, Camerino, Italy

Climate change and the induced environmental disturbances is one of the major threats that have a strong impact on bacterial communities in the Antarctic environment. To cope with the persistent extreme environment and inhospitable conditions, psychrophilic bacteria are thriving and displaying striking adaptive characteristics towards severe external factors including freezing temperature, sea ice, high radiation and salinity which indicates their potential in regulating climate change's environmental impacts. The review illustrates the different adaptation strategies of Antarctic microbes to changing climate factors at the structural, physiological and molecular level. Moreover, we discuss the recent developments in "omics" approaches to reveal polar "blackbox" of psychrophiles in order to gain a comprehensive picture of bacterial communities. The psychrophilic bacteria synthesize distinctive cold-adapted enzymes and molecules that have many more industrial applications than mesophilic ones in biotechnological industries. Hence, the review also emphasizes on the biotechnological potential of psychrophilic enzymes in different sectors and suggests the machine learning approach to study cold–adapted bacteria and engineering the industrially important enzymes for sustainable bioeconomy.

KEYWORDS

Antarctic bacteria, climate change, psychrophiles, omics, machine learning, biotechnological applications

Introduction

Approximately 70% of the Earth's surface is covered by ice which includes ice caps, ice sheets, glaciers, sea ice and high mountain ranges (Yusof et al., 2021). Antarctica, the least populated continent placed at the southernmost of the Earth, contains about 90% of the world's ice and is continually blanketed in ice sheets. Around 15% part of the continent is covered by sea ice. However, the ongoing climate change and stratospheric ozone consistently impact the continent and the residing organisms by rapidly altering environmental factors including

temperature, precipitation, UV radiation etc. (Yusof et al., 2021). Climate change is influenced by anthropogenic emissions of greenhouse gasses (GHGs), which result in an increase in global temperature of up to 1.5°C or even 2°C (IPCC, 2021). The increase in average temperature leads to the amplification of permafrost thawing, melting of the Antarctic ice sheet (Dietz and Koninx, 2022), and changes in ice mass (Stokes et al., 2022). An increase in Antarctic ice sheet loss enhances the penetration of light and energy levels into water that changes plankton productivity and composition, including microbes (Barnes et al., 2021). Hence, climate-induced disturbances are major threats to the Antarctic ecosystem, especially to microbial composition and functions (Gutt et al., 2021).

Microbes are important components that generate the base of polar food webs in both terrestrial and freshwater Antarctic ecosystems, hence affecting all trophic levels. They play a crucial role in the biogeochemical cycle (especially in carbon and nitrogen cycling) and functioning of an extreme Antarctic environment (Anesio et al., 2009). Microbes thriving in polar cryosphere, which comprises 14% of the Earth's surface for more than 33 million kilometers (Malard and Pearce, 2018) are called psychrophilic *sensu stricto* and psychrotolerant organisms, based on the optimum growth temperature. The minimum, optimum and maximum growth temperatures for psychrophiles are <0, <15 and < 20°C, and for psychrotrophs >0, >20 and > 30°C, respectively (Moyer and Morita, 2007). To persist in extreme environment and inhospitable conditions, these microbes are thriving and displaying striking adaptive characteristics towards severe external factors including low humidity, precipitation, freezing temperature, sea ice, high radiation and salinity, nutrients limitation and strong winds (Feller and Gerday, 2003). This indicates the potential of polar microbes in regulating climate change's environmental impacts and represents their distinctive adaptability of primitive life-forms. Therefore, it is crucial to find how Antarctic microorganisms adapt to different climate-induced environmental stresses.

Several previous studies reported that distinctive adaptive characteristics of psychrophiles are due to the specific protein adaptations and enzymes they secrete (Kohli et al., 2020). The different types of bonding (covalent and H-bond), amino acid composition, G + C content and folding pattern of proteins are responsible for the improved stability and adaptation of psychrophiles (Dutta and Chaudhuri, 2010). However, due to the difficulty in direct cultivation of psychrophiles from extreme Antarctic environment, the research on their adaptation is still on the elementary phase and most of the adaptation strategies and their underlying mechanisms (freezing tolerance/avoidance, regulation of protein synthesis and membrane fluidity) have not been fully understood.

In this review, we focus on the different adaptation strategies of Antarctic marine bacteria to environmental changes at morphological, physiological, and molecular level. Moreover, the review highlights the biotechnological applications of Antarctic bacteria and their enzymes and sourced proteins in different industries. To unlock "blackbox" of Antarctic bacteria and engineer cold adapted molecules including psychrozymes, in the last section of the review, we discussed the possible use of recent technologies such as omics and machine learning as an effective, fast and less labor- intensive approach. Additionally, we emphasize the existing research gaps and illustrate our view on future research directions on Antarctic microbes, an unexplored ecosystem.

Adaptation strategies of Antarctic bacteria

The adaptation of psychrophilic bacteria to the multitude of environmental stressors including low temperature is achieved via complex range of structural and physiological changes (Table 1) during long term evolution (Collins and Margesin, 2019). Several new emerging omics techniques including genomics, transcriptomics, metagenomics, metabolomics, etc. have increased our understanding of bacterial cold adaptation. These technologies demonstrated that psychrophilic bacteria employ various survival strategies to cope with the challenges confronted in their habitat. The following section includes the strategic tools adapted by bacteria at morphological, physiological and molecular level to enable life in the harsh Antarctic environment.

Structural adaptation

The cell envelope is a complex multi-layered (outer, peptidoglycan and inner membrane) structure of bacteria that provides protection from the unpredictable and hostile environment. Several studies reported the thickening of outer cell surfaces in particular, peptidoglycan layer (Figure 1) (gram positive) and lipopolysaccharide (gram negative bacteria) in cold adapted bacteria (Di Lorenzo et al., 2020). The thick cell surface strengthens the psychrophiles against cell disruption by ice formation, increased osmotic pressure and freezing/thawing at low/subzero temperature (Figure 1). Recent study on the structural elucidation of the highly heterogenous lipid A (LPS' glycolipid moiety) in the three Antarctic bacteria strains *Pseudoalteromonas tetraodonis* SY174, *Psychromonas arctica* SY204b, and *Psychrobacter cryohalolentis* SY185 showed that structural alterations in the LPS' glycolipid moiety increase the membrane flexibility and stability of these psychrophiles in Antarctica (Di Lorenzo et al., 2020). To tolerate the negative effect of temperature stress, bacteria alter the composition of cell membrane fatty acids (Hassan et al., 2020). Cold-adapted bacteria usually increases the polyunsaturated to saturated fatty acid ratio in membrane phospholipids to maintain optimal fluidity and membrane permeability (homeoviscous adaptation) (De Maayer et al., 2014). In this regard Králová (2017) studied the role of membrane fatty acids in adaptation of *Flavobacterium* sp. towards harsh Antarctic environment (Table 1). The study suggested that Antarctic *Flavobacterium* sp. mostly utilizes two mechanisms of homeoviscous adaptation in cold-adaptive response- unsaturation of fatty acids and synthesis of branched fatty acids (Králová, 2017). Similarly, Bajerski et al. (2017) investigated the biomembrane polar fatty acid adaptation of *Chryseobacterium frigidisoli* PB4T isolated from an Antarctic glacier in response to varying temperature (0°C to 20°C) and pH (5.5 to 8.5). Another strategy adopted by the Antarctic bacteria is the production of extracellular polymeric substances (EPSs) that protects the cell from sub-freezing temperature by forming a protective covering around the bacterial cell that act as a barrier to solutes diffusion and ice formation (Collins and Margesin, 2019) (Figure 1). In this context, Caruso et al. (2018) studied the EPS synthesis in four Antarctic sponge-associated bacteria (*Shewanella* sp. strain CAL606, *Colwellia* sp. strain GW185, and *Winogradskyella* sp. strains CAL384 and CAL396). EPS production by psychrophilic bacteria has an ecological role in cell

TABLE 1 Adaptation strategies in Antarctic bacteria in response to different stress environment.

Environmental conditions	Bacterial adaptation	Taxa	Reference
Temperature	Membrane fatty acids	*Flavobacterium* spp.	Královά (2017)
	EPS production	*Pedobacter polysaccharеus* sp.	Wang et al. (2023)
	Transcriptional changes	*Pseudoalteromonas haloplanktis* TAC125	Riccardi et al. (2023)
	Expression of diguanylate cyclase (DGC) gene, biofilm formation	*Rhodococcus* sp. NJ-530	Wang et al. (2022)
	Chemical modifications of the lipopolysaccharide (LPS)	*Pseudoalteromonas tetraodonis* strain SY174, *Psychromonas arctica* strain SY204b, *Psychrobacter cryohalolentis* strain SY185	Di Lorenzo et al. (2020)
	Increase of saturated fatty acid	*Rhodococcus* sp. JG-3	García-Descalzo et al. (2023)
	Hydrolases, a clp protease, and novel YraN family endonuclease upregulation	*Cryobacterium* sp. SO1	Teoh et al. (2021)
	GH42 β-galactosidase	*Marinomonas* ef1	Mangiagalli et al. (2021)
	Ice-binding proteins (IBPs)	*Flavobacterium frigoris* PS1, *Nostoc* sp. HG1	Kim et al. (2019), Raymond et al. (2007)
	Extracellular polymeric substrates	*Nostoc* sp. strain SO-36	Effendi et al. (2022)
	Endolysins	*Pseudomonas* ef1	Orlando et al. (2020)
	Changes in the gene expression profile	*Shewanella baltica*	Kloska et al. (2020)
	Polyhydroxyalkanoates synthesis	*Pseudomonas* sp. MPC6	Orellana-Saez et al. (2019)
Salinity	Variation in fatty acids types composition	*Rhodococcus* sp. JG-3	García-Descalzo et al. (2023)
	Intracellular laccase-like protein	*Halomonas* sp. strain M68	Bisaccia et al. (2023)
	Biofilm formation, expression of diguanylate cyclase (DGC) gene	*Rhodococcus* sp. NJ-530	Wang et al. (2022)
UV	Pyomelanin production	*Pseudomonas* sp. ANT_H4	Styczynski et al. (2022)
	Role of DEAD-box RNA helicase	*Pseudomonas syringae* Lz4W	Hussain and Ray (2022)
	Production of polyhydroxyalkanoates	*Pseudomonas extremaustralis*	Tribelli et al. (2020)
	DNA photolyase	*Rhodococcus* sp. NJ-530	He et al. (2021)
	Production of carotenoids	*Planococcus* sp. ANT_H30, *Rhodococcus sp.* ANT_H53B	Styczynski et al. (2020)
	Expression of light reactive proteins	*Hymenobacter nivis* P3T	Terashima et al. (2019)
	Pigment production	*Hymenobacter* sp. *strain* UV11	Marizcurrena et al. (2019)
Hydrocarbon	Bio emulsifier production	*Paenibacillus antarcticus* IPAC21	de Lemos et al. (2023)
	Trinitrotoluene metabolic genes, xenobiotic reductases	*Pseudomonas* sp. TNT3, TNT11, and TNT19	Cabrera et al. (2020), Cabrera et al. (2022)
	Biosurfactant	*Bacillus* sp. ANT_WA51	Krucoń et al. (2023)
	Contains genes for aromatic compounds degradation	*Pseudomonas* sp. MPC6	Orellana-Saez et al. (2019)
Phenol	Phenol degradation	*Rhodococcus* sp. strain AQ5-14	Tengku-Mazuki et al. (2020)
Polyethylene	Laccase catalytic structure	*Psychrobacter* sp. NJ228	Zhang et al. (2022)
Heavy metal pollution	Increasing antioxidant enzymes (Super oxide dismutase, glutathione reductase) and antioxidant substances (glutathione, carotenoid)	*Planococcus* sp. O5	Cheng et al. (2022)
	Molybdenum reduction	*Arthrobacter* sp. *Strain* AQ5-05	Darham et al. (2021)
	Heavy metal tolerance genes	*Dietzia psychralcaliphila* JI1D	Ausuri et al. (2022)
Nutrients	Carbon metabolism	*Arthrobacter*	Gushgari-Doyle et al. (2022)
	Biofilm formation	*Pseudoalteromonas haloplanktis* TAC125	Ricciardelli et al. (2019)
	Production of extracellular hydrolytic enzymes	*Hymenobacter* sp. *strain* UV11	Marizcurrena et al. (2019)
High hydrostatic pressure	Antioxidant defenses and energy regulation	*Halomonas titanicae* ANRCS81	Li et al. (2023)
	Metabolic adaptation	*Microbacterium sediminis*	Xiao et al. (2023)

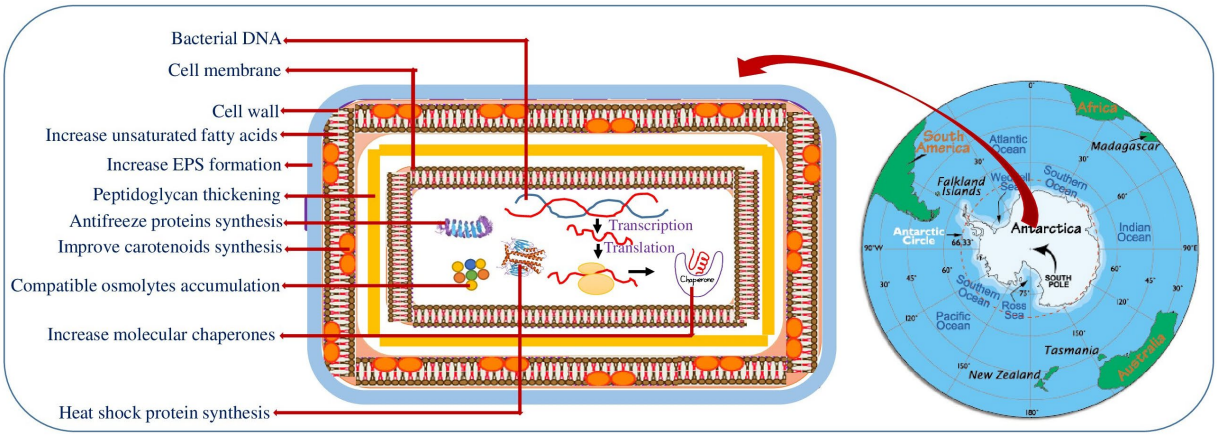

FIGURE 1
Schematic representation of the various cold adaptation strategies of Antarctic bacteria. Map of Antarctica retrieved from worldatlas.com.

adhesion to surfaces and cell protection due to their chemical composition (Lo Giudice et al., 2020). In addition, EPS also plays a vital role in biofilm formation that enhances access to nutrients and cell survivability. The adaptation of haloarchaea *Halorubrum lacusprofundi* in Deep Lake (Antarctica) is a good example of cold adaptation by biofilm (Liao et al., 2016). Moreover, EPS secreted from cold adapted microbes shows ice binding functions and ice recrystallization inhibitors (IRI) activity (Casillo et al., 2017). Additionally, cold adapted microbes produce a substantial amount of biosurfactants that play a potential role in their survival.

Physiological adaptation

Psychrophilic bacteria developed several physiological adaptations such as metabolic alterations, synthesis of pigments, compatible osmolytes and ice binding proteins to optimize their metabolism in harsh Antarctic environment (Figure 1) (Collins and Margesin, 2019). Pigment formation is a common feature in cold-adapted microbes thriving in diverse habitat including glaciers, high altitude, marine water and ice cores (Pandey et al., 2018). Pigments, in particular polar carotenoids, have been suggested to serve in maintaining the membrane fluidity and rigidity. Moreover, these pigments act as a photoprotector, antioxidants, cryoprotectants, antimicrobials and light harvesters in psychrophilic microbes to counteract the low temperature and other environmental stresses (Pandey et al., 2018). The pigment production by cold adapted bacteria including Antarctic environment have been extensively reviewed by Sajjad et al. (2020). Accumulation of compatible osmolytes (glycine betaine, trehalose, glycerol, sucrose, mannitol etc.) is the other way of Antarctic bacteria to prevent cell shrinkage and water loss during sub-zero temperature (Goordial et al., 2016). Improved concentration of compatible osmolytes restore osmotic balance by reducing the freezing point of the cell cytoplasm (Fonseca et al., 2016). The osmolytes were also found to be involved in scavenging free radicals, counteracting protein aggregation, improving protein folding and stabilizing membranes and proteins at chilling temperatures (Collins and Margesin, 2019).

Additionally, psychrophiles synthesize several proteins namely ice binding, cold shock and heat shock proteins to sustain their physiological state in changing environment (Figure 1) (Kim et al., 2018). Ice binding proteins are antifreeze proteins (AFPs) that on binding to ice inhibits the growth of ice crystals and lower freezing temperature. The proteins were initially reported in Antarctic fish and in various cold organisms including bacteria. Bar Dolev et al. (2016) identified the multidomain ice adhesion AFP in the Antarctic bacterium *Marinomonas primoryensis*. AFPs causes thermal hysteresis (TH) in which the freezing temperature of water drops below the melting temperature. This ceases ice growth by creating a thermal hysteresis gap (Mangiagalli et al., 2017). Antifreeze proteins are also found to display ice recrystallisation inhibitors (IRI) activity. A study by Raymond et al. (2007) suggested the role of AFPs isolated from Antarctic Gram-negative bacteria *Colwellia*, strain SLW05 in ice recrystallization inhibition and ice-binding. The cold shock proteins are a family of widely distributed low molecular weight highly conserved proteins, synthesized under normal environment but strongly induced when exposed to cold conditions. The cold shock gene homologous to *cspA* of *E. coli* has been isolated in two isolates of Antarctic psychrotrophs- Gram-positive bacterium *Arthrobacter protophormiae* and Gram-negative *Pseudomonas fluorescens* which expressed constitutively at two different temperatures (4°C and 22°C) (Ray et al., 1994). Kim et al. (2007) characterized cold shock protein A of the Antarctic bacterium *Streptomyces* sp. AA8321 and depicted its role in inhibiting DNA replication during cold adaptation. Similarly, characterization and expression of three cold shock protein (CSP) genes under different stress conditions is studied in the Antarctic bacteria *Psychrobacter* sp. G (Song et al., 2012). A comparative proteomic study of cold-repressed proteins in the *Pseudoalteromonas haloplanktis* TAC125 located in Antarctic environment at 4°C and 18°C demonstrated that majority of these proteins expressed at 4°C were heat shock proteins associated to folding (Piette et al., 2011). Furthermore, the increase accretion of heat shock proteins has been observed in Antarctic psychrophiles during ocean warming and acidification. Recently, Yusof et al. (2021) characterized two Hsp70 genes in the Antarctic yeast, *Glaciozyma antarctica* PI12 that protect the functional activity of the yeast under different temperature stress (4°,15°, 25 ° and 37°C). The Antarctic ciliated protozoon *E. focardii* maintains a constitutive synthesis of some Hsp70 genes to preserve protein functions in the cold and

induces high expression of other Hsp70 genes in response to the oxidative stress increased by the Antarctic ozone hole (Mozzicafreddo et al., 2021).

Immunoblot analysis indicated the accumulation of DnaK protein (homolog of eukaryotic Hsp 70 that plays vital role in several abiotic stresses, including thermal stress) in the Antarctic psychrotroph *Shewanella* sp. Ac10 at 24°C (Yoshimune et al., 2005). The study also suggested that recombinant SheDnaK gene facilitates the growth of mutant *E. coli* at 15°C. Similarly, García-Descalzo et al. (2014) studied the thermal adaptation in Antarctic bacteria *Shewanella frigidimarina* towards different temperature ranges, from 0°C to 30°C. The significant accumulation in heat shock and other stress proteins is observed in bacterial cells cultured at 28°C (García-Descalzo et al., 2014).

Moreover, studies have indicated that psychrophiles at chilling temperature alter their metabolic pathways to conserve energy and thrive in cold environment. For long term survival, psychrophiles either down regulate their primary metabolic pathways (glycolysis, tricarboxylic acid (TCA) cycle, electron transport chain, pentose phosphate pathway etc.) or substitute them with abridged alternative pathways (glyoxylate, methylglyoxal, acetate metabolism, ethanol oxidation pathway etc.) (Collins and Margesin, 2019).

Molecular adaptation

Molecular chaperones (RNA/DNA/protein) play an important role in stabilization of RNA/DNA and protein molecules at freezing temperature and in reducing protein aggregation and misfolding. These molecules are constitutively produced and expressed in psychrophiles as cold -adapted proteins. Several molecular chaperone proteins are identified from the Antarctic green alga *Chlamydomonas* sp. ICE-L shows high similarity with the genes of the psychrophilic bacterium *Psychroflexus torquis* and appears to be involved in tolerance to freezing, changing light and saline conditions in bacteria (Liu et al., 2016). Recently, Ijaq et al. (2022) investigated the functional role of hypothetical proteins from *Pseudomonas* sp. Lz4W, a Gram-negative psychrophilic bacterium adapted to survive in Antarctica. The study categorized two hypothetical proteins, HP AUB76544.1 and HP AUB76897, as chaperones that are important for correct folding and insertion of outer membrane proteins (HP AUB76544.1) as well as in sustaining the structural integrity and protein functions (HP AUB76897) (Ijaq et al., 2022). Furthermore, Solar Venero et al. (2022) studied the role of small non-coding RNAs (sRNAs) as genetic regulators in the adaptation of the Antarctic bacterium *Pseudomonas extremaustralis* towards changing climatic conditions and stress environment. The study showed the expression of novel sRNA, sRNA40 (identified by RNA-seq experiments) in response to different oxygen availability and oxidative stress and demonstrated that sRNA40 gene expression (associated to upregulation of selected secretory proteins) is triggered under aerobiosis/microaerobiosis conditions (Solar Venero et al., 2022).

Cold adapted enzymes are more flexible as compared to mesophilic enzymes due to the presence of relative low arginine content. Recently, one peroxidase named DyP (dye-decolorizing peroxidase) from an Antarctic bacteria *Pseudomonas* sp. AU10 was found to contain low arginine content (Cagide et al., 2023). Another study by Tang et al. (2019) characterized a cold-active alkaline pectate lyase from Antarctic bacterium *Massilia eurypsychrophila* with a low arginine content, suggesting that this is a distinctive property of cold adaptation. Petratos et al. (2020) studied the molecular dynamics of alcohol dehydrogenase (MoADH) from the cold-adapted bacterium *Moraxella* sp. TAE123 compared with the *Escherichia coli* (EcADH), *Geobacillus stearothermophilus* (GsADH), *Thermus* sp. ATN1 (ThADH). The cold adapted GH42 has also been identified in some microbes such as *Halobacterium lacusprofundi*, *Arthrobacter* sp. and *Marinomonas* sp. BSi20414 (Sheridan and Brenchley, 2000; Karan et al., 2013; Ding et al., 2017). Experimental study by Mangiagalli et al. (2021) on the cold adaptation of β-galactosidase from the psychrophilic *Marinomonas* ef1 shows the cold activity of this enzyme at 5°C and maintains stability up to 50°C, which suggests the origin of GH42 from the different evolutionary pathway. The biochemical and molecular features of GH42 and its biotechnological applications have been described in the recent review by Mangiagalli and Lotti (2021). Another study by Fan et al. (2016) reveals the structure of cold-active β-galactosidase from psychrotrophic *Rahnella* sp. R3. However, the glycoside hydrolase family (GH42) of other psychrophilic microbes is still poorly known. Thus, very little knowledge is available on the role of these enzymes in psychrophilic bacteria and adaptation to climate change in the Antarctic environment.

Another adaptation strategy by psychrophile bacteria is through horizontal gene transfer (HGT), which is considered as one of the important forces that regulates bacterial evolution (Martínez-Rosales et al., 2012). The occurrence of HGT was found in various Antarctic bacteria such as *Marinomonas* sp. ef1, *Pseudomonas* spp., *Collimonas* sp. (Martínez-Rosales et al., 2012; John et al., 2020; Hwang et al., 2021). Recently, Abe et al. (2020) used neural network called Batch Learning Self-Organizing Maps BLSOM method to detect HGTs in the genomes of two Antarctic bacteria (*Sphingomonas* sp. HMP6 and HMP9) compared with other continents.

Though, the various adaptation strategies have been studied in Antarctic psychrophiles in response to changing climate as evident from the previous studies stated above. However, the research is still on the elementary phase and there are many unexplored areas including the underlying mechanism of adaptation, molecular pathways and key components involved which will give better understanding of Antarctic psychrophiles adaptation towards ongoing changing environment. Upcoming research on cold -adapted bacteria needs to be emphasized on these aspects by using novel techniques such as metagenomics and machine learning. These methods could serve as a dynamic tool to decipher adaptation mechanisms in the Antarctic psychrophiles, as they are difficult to culture in laboratory conditions.

Industrial applications of Antarctic bacteria

Cold active enzymes

The last few decades witnessed extensive research on microbial diversity inhabiting harsh extreme environmental conditions. Bacteria inhabiting extreme environments, like in Antarctica regions, are undergoing several stress factors and to withstand such conditions they have developed numerous physiological and molecular strategies (Hamid et al., 2022). These psychrophilic bacteria can survive and

grow at a temperature range from −2 to 20°C, and express cold-adapted enzymes with distinctive properties that allow higher catalytic efficiency, improved flexibility, and lower thermal stability (Bruno et al., 2019). The advantages of cold-adapted enzymes over mesophilic enzymes are illustrated in various research articles (Kuddus, 2015; Javed and Qazi, 2016). Cold-active enzymes isolated from microorganisms are classified into three groups.

Group 1: Heat-sensitive with other enzymatic characteristics similar to mesophilic enzymes.

Group 2: Heat-sensitive and relatively more active than mesophilic enzymes at a low temperature.

Group 3: Same thermostability as mesophilic enzymes but more active than mesophilic enzymes at a low temperature.

Since low temperatures are required for some industrial processes, there is a huge demand for cold-adapted enzymes in different biotechnological and industrial area, such as bioremediation, detergents, food and beverage processing, molecular biology and in textile industries (Figure 2) (Kuddus, 2018). Cold-active enzymes such as amylases, cellulases, lipases, pectinases, proteases, etc. from Antarctic bacteria establish an evident resource for several biotechnological applications. Many of the above enzymes are enormously used at commercial level, with special reference to hydrolases sourced from psychrophilic microorganisms (Hamid et al., 2022).

Food industry

Most of the Antarctic microbial enzymes have high catalytic competence at low and moderate temperatures when compared to mesophilic enzymes. This makes the cold-active enzymes unique in the food industry for their less biochemical requirements, reduction in process times, save energy costs and easy inactivation by gentle heat (Kuddus, 2018).

In dairy industries, the use of cold-active β-galactosidases is effectively operational in milk at lower temperatures that lead to lactose breakdown. Antarctic marine bacteria especially *Pseudoalteromonas haloplanktis*, has been proven to produce cold-active β-galactosidase with high efficacy in the hydrolysis of lactose under cold conditions (Cieśliński et al., 2005). Similarly, cold-active

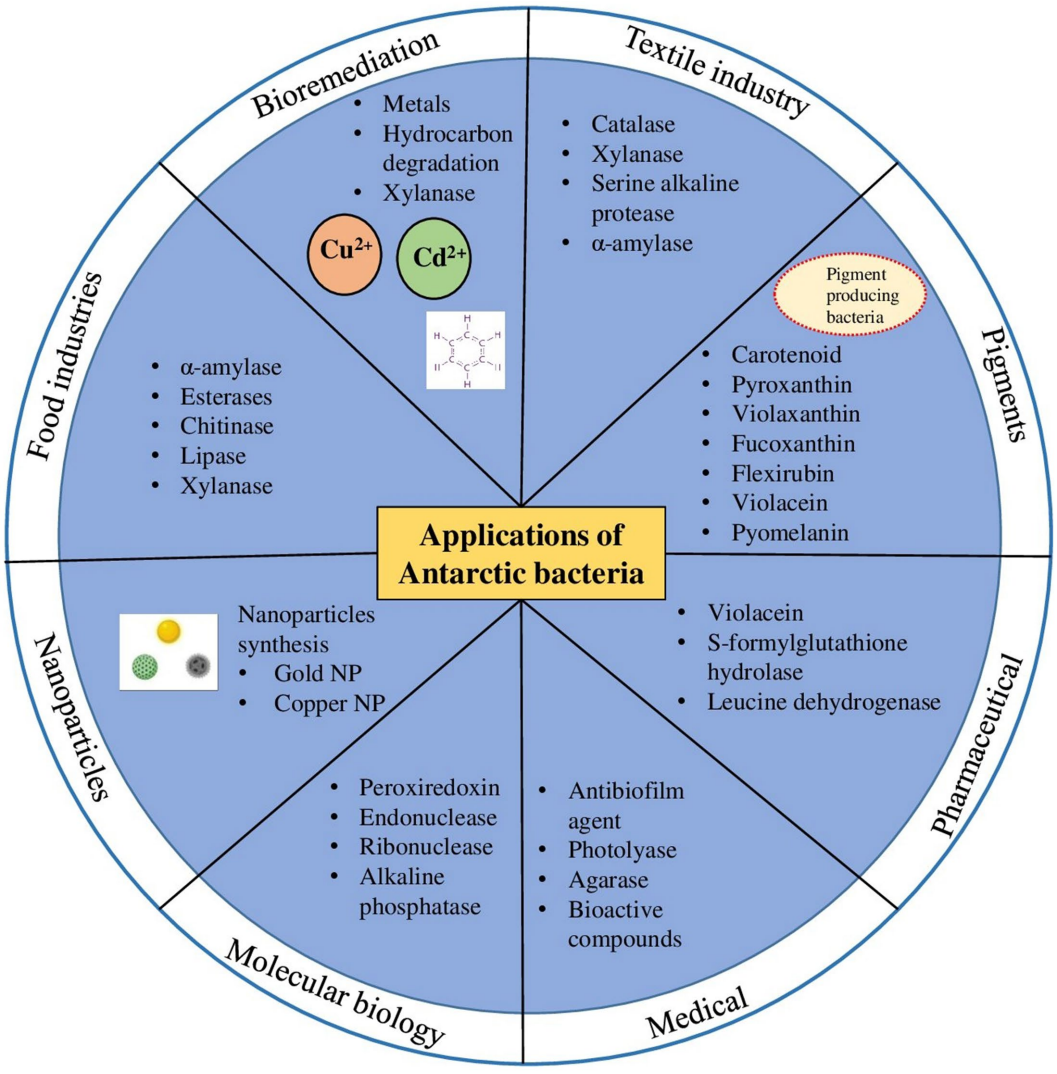

FIGURE 2
Biotechnological applications of cold-adapted molecules from Antarctic bacteria in different industrial sectors.

polygalacturonase isolated from *P. haloplanktis* can be used in juice manufacturing industries for degradation of pectin. Many other cold-active enzymes such as α-amylase, esterases, chitinases, and lipase have important applications in the food (Figure 2) and brewing industries, for cheese ripening, cheese flavoring, meat tenderizing, production of fatty acids and interesterification of fats, wheat bread making, improvement in food texture, etc. The gene encoding the cold active enzymes can be cloned into a suitable host to produce recombinant enzymes which are already proved to show high catalytic activity and stability at low temperatures (Table 2 and references therein). In case of food and brewage industries, low-temperature processing is highly favorable since it provides many advantages, for instances, prevention of bacterial contamination and occurrence of unwanted chemical responses, higher food quality, and persistence of flavor (Al-Maqtari et al., 2019).

Detergent industry

The removal of stains (lipids, polysaccharides, and proteins) by manual heating and beating of the clothes reduces the life of the fabrics and also decolorization (Kumar et al., 2021). On the other hand, harmful chemicals are most widely used in the chemical industries for removal of dirt which ultimately contaminates the environment. To overcome these issues, cold-active enzymes are the best alternative to the chemicals and moreover they increase the life of the fabrics, as manual heating is no longer required. The use of cold active enzymes such as lipases, amylases and proteases active at alkaline pH, with thermostability has solved the problems arising in the detergent industries. Switching mesophilic to cold-adaptive enzymes in the cleaning process ensures lowers wash temperatures and greater energy protection. A 10°C reduction in wash temperature created a 30% reduction in the consumption of electricity (Nielsen, 2005).

Proteases are found to be the most widely used enzymes in detergents and most of the cold-active proteases have shown remarkable stability and activity in a wide-ranging alkaline condition (Hamid et al., 2022). Cold-active proteases from *Bacillus* TA41, *Colwellia* sp. NJ341, *Pseudoalteromonas* sp. NJ276, *P. haloplanktis* etc. can be used as detergent additives for cold washing (Table 2 and references therein). The detergent manufacturers are seeking novel cold-active enzymes that may improve efficiency of detergents and retain the quality of fabrics (Al-Ghanayem and Joseph, 2020). Hence more studies on this aspect may lead to the discovery of many novel cold-active enzymes.

Molecular biology

Alkaline phosphatases which catalyze the hydrolysis of phosphate monoesters have a significant role in molecular cloning for dephosphorylation of DNA at the 5′ end to avoid its re-circularization. Based on this importance, New England Biolabs developed a recombinant alkaline phosphatase isolated from the Antarctic bacterial strain TAB5.[1] In addition, cold active alkaline phosphatase from an Antarctic *Vibrio* sp., was reported to have a higher turnover number (k_{cat}) and higher apparent Michaelis–Menten factor (K_m) as compared with enzyme from *E. coli* (Hauksson et al., 2000). Similarly, to cold adapted alkaline phosphatases, uracil DNA N-glycosylases have been recently commercialized as a molecular biological tool by various companies (New England Biolabs Inc., Takara-Clontech, Affymetrix, Inc.) (Awazu et al., 2011; Muller-Greven et al., 2013).

DNA ligases are enzymes involved in DNA replication, DNA recombination and DNA repair. These enzymes are commonly used in molecular biology to catalyze the formation of a phosphodiester bond between adjacent 5′-phosphoryl and 3′-hydroxyl groups in double stranded DNA (Bruno et al., 2019). The well-established psychrophile *P. haloplanktis* TAE72, was also reported to produce DNA ligase and exhibit activity at temperatures as low as 4°C (Georlette et al., 2000).

Bioremediation

Bioremediation by mesophilic and thermophilic enzymes is ineffective in cold environmental conditions hence cold active enzymes are valuable tools for removal or biodegradation of pollutants. The use of cold-active enzymes could be more feasible and result oriented than the use of whole bacterial cells, since the whole cells requires multiple parameters of optimal growth (Kumar and Bharadvaja, 2019). Many cold adapted microorganisms, such as *Pseudomonas* sp., *Rhodococcus* sp., *Oleispira antarctica* and *Sphingomonas* spp. are proficient in degradation of petroleum hydrocarbons (Aislabie et al., 2006; Miri et al., 2019). Many cold active enzymes such as lipases, proteases, xylanase (Figure 2) etc. are regularly explored for various applications in bioremediation (Miri et al., 2019).

Bacterial pigments

Pigments of natural origin play an important role in the physiology and molecular processes of microorganisms because they act as a strategy of adaptation to various extreme environments, have a protective function against solar radiation, and are also involved in functional processes like photosynthesis (Sutthiwong et al., 2014). Bacteria also produce a wide range of pigments such as carotenoids, melanin, violacein, prodigiosin, pyocyanin, actinorhodin, and zeaxanthin (Venil et al., 2013). Antarctica environment is also well known for richness of bacterial species producing various pigments such as carotenoids, flexirubin, violaceins, tetrapyrroles, quinones, biochromes, etc. (Figure 2).

Antarctic bacteria are able to produce not only different kinds of carotenoids but other pigments as well. This is supposedly due to the harsh conditions to which they are exposed. Therefore, these microorganisms may be regarded as promising potential targets for further research on the growing market of biotechnological pigments for industrial applications, not only focusing on long established compounds, but also on unconventional pigments. *Arthrobacter*, *Citricoccus*, and *Microbacterium* from the phylum Actinobacteria, *Chryseobacterium* and *Flavobacterium* from the phylum Bacteroidetes, and *Janthinobacterium*, *Pseudomonas*, *Lysobacter*, and *Serratia* from the phylum Proteobacteria are among the main pigment-producing bacteria reported in Antarctic environments (Silva et al., 2021 and references therein).

The carotenoid content, pyroxanthin, violaxanthin, fucoxanthin, and nostoxanthine 3-sulfate from the Antarctic bacterium *Pedobacter*

1 https://www.neb.com/products/m0289-antarctic-phosphatase#Product%20Information

TABLE 2 Polar-active enzymes isolated from Antarctic bacteria and their potential industrial applications (Reproduced from Bruno et al. (2019) and updated until recent literature).

Marine polar active enzymes	Organism source	Source of isolation	Potential industrial applications	References
EC3: Hydrolases				
β-galactosidase	*Pseudoalteromonas* sp. 22b	*Alimentary tract of Antarctic krill* Thyssanoessa macrura	Candidates for lactose removal from dairy products at low temperatures	Turkiewicz et al. (2003), Cieśliński et al. (2005)
	Pseudoalteromonas haloplanktis TAE 79	Antarctic seawater		Hoyoux et al. (2001)
	Pseudoalteromonas haloplanktis LMG P-1	Antarctic seawater		Gerday et al. (2000)
α-Amylase	*Pseudoalteromonas* sp. M175	Antarctic sea-ice	Detergent additive for stain removal in efficient way	Wang et al. (2018a)
	Alteromonas sp. TAC 240B	Antarctic seawater	Additives in processed food, in detergents for cold washing, in waste-water treatment, in bioremediation in cold climates and in molecular biology applications	Chessa et al. (1999)
	Pseudoalteromonas haloplanktis	Antarctic seawater		Feller et al. (1999), Kuddus et al. (2011)
Xylanase	*Flavobacterium frigidarium* sp.	Antarctic shallow-water marine sediment	Additives in textile and food industries, and bioremediation	Humphry et al. (2001)
Serine protease (Subtilisin)	*Bacillus* TA39	Antarctic seawater	Additives in low-temperature food processing, food and textile industries, leather processing, detergent industry	Narinx et al. (1992), Miyazaki et al. (2000)
	Bacillus TA41	Antarctic seawater		Davail et al. (1994), Miyazaki et al. (2000)
Serine protease	*Colwellia* sp. NJ341	Antarctic sea-ice		Wang et al. (2005)
Serine alkaline protease	*Shewanella* sp. Ac10u	Antarctic seawater		Kulakova et al. (1999)
Subtilisin-like serine protease	*Pseudoalteromonas* sp., *Marinobacter* sp., *Psychrobacter* sp., *Polaribacter* sp.	Antarctic seawater and thorax, abdomen and head of krill (*Euphausia superba* Dana)		Acevedo et al. (2013)
Protease	*Pseudoalteromonas* sp. NJ276	Antarctic sea-ice		Wang Q. et al. (2008)
	Lysobacter sp. A03	*Elephant Island, Antarctic*		Millan et al. (2022)
Aminopeptidase	*Pseudoalteromonas haloplanktis* TAC125	Antarctic seawater		De Pascale et al. (2010)
Serine peptidase	*Lysobacter* sp. A03	Penguin feathers in Antarctica		Pereira et al. (2017)
Metalloprotease	*Sphingomonas paucimobilis*	Stomach of Antarctic krill, *Euphausia superba* Dana		Turkiewicz et al. (1999)
	Psychrobacter proteolyticus sp. strain 116	Stomach of Antarctic krill, *Euphausia superba* Dana		Denner et al. (2001)

(Continued)

10.3389/fmicb.2023.1197797

TABLE 2 (Continued)

Marine polar active enzymes	Organism source	Source of isolation	Potential industrial applications	References
Lipase	*Pseudoalteromonas haloplanktis* TAC125	Antarctic seawater	Detergent additives used at low temperatures and biocatalysts for the biotransformation of heat-labile compounds	De Pascale et al. (2008)
	Polaromonas vacuolata	Antarctic seawater		Irgens et al. (1996)
	Psychrobacter sp.	Antarctic seawater		Parra et al. (2008), Xuezheng et al. (2010)
	Shewanella frigidimarina	Antarctic seawater		Parra et al. (2015)
	Psychrobacter sp. TA144	Antarctic seawater		Feller et al. (1991)
	Psychrobacter sp. 7,195	Antarctic deep-sea sediment (Prydz Bay)		Zhang et al. (2007)
	Moritella sp. 2–5–10-1	Antarctic deep-sea water		Yang et al. (2008)
	Pseudoalteromonas sp., *Psychrobacter* sp., *Vibrio* sp.	Antarctic seawater samples (Ross Sea)		Lo Giudice et al. (2006)
	Moraxella sp.	King George Island		Morozova et al. (2022)
	Bacillus altitudinis Ant19 strain	Antarctic soil	Detergent additives and useful for oil stain removal	Nimkande et al. (2023)
Esterase	*Oleispira antarctica*	Antarctic coastal water	Additives in laundry detergents and biocatalysts for the biotransformation of labile compounds at low temperatures	Lemak et al. (2012), Kube et al. (2013)
	Pseudoalteromas haloplanktis TAC125	Antarctic seawater		Aurilia et al. (2007), D'Auria et al. (2009)
	Pseudoalteromas sp. 643A	Alimentary tract of Antarctic krill *Euphasia superba*		Cieśliński et al. (2007)
Polyesterase	Moraxella sp.	Antarctic seawater	Bioremediation	Nikolaivits et al. (2022)
S-formylglutathione hydrolase	*Pseudoalteromonas haloplanktis* TAC125	Antarctic seawater	Candidates for chemical synthesis and industrial pharmaceutics	Alterio et al. (2010)
	Shewanella frigidimarina	Antarctic marine environment		Lee J. et al. (2019)
Polygalacturonas (pectin depolymerase)	*Pseudoalteromonas haloplanktis*	Antarctic seawater	Additive in food industries, such as clarification of juice, in the process of vinification, yield and color enhancement and in the mashing of fruits	Ramya and Pulicherla (2015)
RNA polymerase	*Pseudomonas syringae Lz4W*	Antarctic soil sample	Candidate for molecular biology application	Uma et al. (1999)
Cellulase	*Pseudoalteromonas haloplanktis*	Antarctic seawater	Additive in detergent industry	Violot et al. (2005)
	Flavobacterium sp. AUG42	Antarctic oligochaete	Food processing, textile processing and detergent industries	Herrera et al. (2019)
	Nocardiopsis sp.	Antarctic seawater	Cellulose hydrolysis efficiency	Sivasankar et al. (2022)
Alkaline phosphatase	TAB5 strain	Antarctica	Candidate for molecular biology application such as DNA dephosphorylation	Rina et al. (2000), Koutsioulis et al. (2008)
	Shewanella sp.	Intestine of Antarctic shellfish	Candidate for molecular biology application	Tsuruta et al. (2010)
	Vibrio sp.	North-Atlantic coastal waters	Candidate for molecular biology application	Hauksson et al. (2000)
	Shewanella frigidimarina W32-2	Antarctic sediments	Candidate for molecular biology application	Chen et al. (2021)
Acid phosphatase	*Shewanella frigidimarina W32-2*	Antarctic sediments	Candidate for molecular biology application	Chen et al. (2021)

(Continued)

10.3389/fmicb.2023.1197797

TABLE 2 (Continued)

Marine polar active enzymes	Organism source	Source of isolation	Potential industrial applications	References
Gelatin hydrolase	*Shewanella frigidimarina W32-2*	Antarctic sediments	Candidate for food and pharmaceutical industries	Chen et al. (2021)
Endonuclease (Cryonase)	*Shewanella sp. Ac10*	Antarctic seawater	Candidate for molecular biology application such as digestion of all types of DNA and RNA at cold temperatures (Takara-Clontech)	Takara-Clontech (n.d.)
Ribonuclease	*Psychrobacter* sp. ANT206	Antarctic sea-ice	Candidate for molecular biology applications	Wang et al. (2019)
Chitinase	*Arthrobacter psychrochitiniphilus, Arthrobacter cryoconite and Curtobacterium luteum*	Maritime Antarctica	Candidate for food industry, cosmetics and medicine	Vasquez et al. (2021)
EC1: Oxidoreductases				
Alcohol dehydrogenase	*Moraxella* sp. TAE123	Antarctic seawater	Candidate for asymmetric synthesis	Tsigos et al. (1998)
Aldehyde dehydrogenase	*Flavobacterium PL002*	Antarctic seawater	Potent catalyst for acetaldehyde determination in wine	Paun et al. (2022)
Alanine dehydrogenase	*Shewanella* sp. Ac10u, *Carnobacterium* sp. St2	Antarctic seawater	Candidate for enantioselective production of optically active amino acids	Galkin et al. (1999)
Leucine dehydrogenase	*Pseudoalteromonas* sp. ANT178	Antarctic sea-ice	Candidate for medical and pharmaceutical industry applications	Wang et al. (2018b)
Malate dehydrogenase	*Flavobacterium frigidimaris* KUC-1	Antarctic seawater	Candidate for detection and production of malate under cold conditions	Oikawa et al. (2005)
Superoxide dismutase	*Pseudoalteromonas haloplanktis*	Antarctic seawater	Candidates for applications in agriculture, cosmetics, food, healthcare products and medicines	Merlino et al. (2010)
	Marinomonas sp. NJ522	Antarctic sea-ice		Zheng et al. (2006)
	Pseudoalteromonas sp. ANT506	Antarctic sea-ice		Wang et al. (2017)
	Halomonas sp. ANT108	Antarctic sea-ice		Wang et al. (2020)
Catalase	*Bacillus* sp. N2a	Antarctic seawater	*Candidate for textile and cosmetic industry*	Wang W. et al. (2008), Sarmiento et al. (2015)
Glutathione reductase	*Colwellia psychrerythraea*	Antarctic seawater	Candidate as an antioxidant enzyme in heterologous systems	Ji et al. (2015)
Peroxiredoxin	*Psychrobacter* sp. ANT206	Antarctic sea-ice	Candidate for food and pharmaceutical industries	Wang et al. (2019)
Lignin peroxidase	Geobacter spp.	Antarctic soils	Bioenergy and bioremediation	Merino et al. (2021)
Manganese peroxidase	Geobacter spp.	Antarctic soils	Bioenergy and bioremediation	Merino et al. (2021)
Laccase	*Psychrobacter sp. NJ228*	Antarctic sea-ice	Candidate for Bioremediation	Zhang et al. (2022)
	Halomonas sp. M68	Antarctic seawater		Bisaccia et al. (2023)

(Continued)

10.3389/fmicb.2023.1197797

TABLE 2 (Continued)

Marine polar active enzymes	Organism source	Source of isolation	Potential industrial applications	References
Nitrate reductase	*Shewanella frigidimarina W32-2*	Antarctic sediments	Candidate for applications in agriculture and bioremediation	Chen et al. (2021)
Nitroreductase	*Psychrobacter sp. ANT206*	Antarctic sea-ice	Candidate for bioremediation	Wang J. et al. (2019)
EC6: Ligases				
DNA ligase	*Pseudoalteromonas haloplanktis* TAE 72	Antarctic seawater	Candidate for applications in molecular biology	Georlette et al. (2000)
EC4: Lyases				
γ-carbonic anhydrase	*Colwellia psychrerythraea*	Antarctic cold ice sediments	Candidates for biomedical applications	De Luca et al. (2016)
	Pseudoalteromonas haloplanktis	Antarctic seawater		De Luca et al. (2015), Angeli et al. (2019)
Pectate lyase	*Pseudoalteromonas haloplanktis* ANT/505	Antarctic sea-ice	Candidate for detergent industry	Sarmiento et al. (2015), Van Truong et al. (2001)
EC5: Isomerases				
Triose phosphate isomerase	*Pseudomonas* sp. π9	Antarctic sea-ice	Candidate for biocatalysis under low water conditions	See Too and Few (2010)
	Moraxella sp. TA137	Intestine of Antarctic fish		Rentier-Delrue et al. (1993)
CPD-photolyases	*Hymenobacter sp. UV11*	King George Island, Antarctica	Candidates for biomedical applications	Acosta et al. (2022)

showed strong antioxidant capacity and protects the bacterium against oxidative damage caused by high levels of UV-B radiation (Correa-Llanten et al., 2012).

Microbial pigments are of great interest in cosmetic, dairy, food, pharmaceutical and textile industries (Figure 2), mainly due to its new chemical structures and most importantly they are natural. A recent report from the global food colorants market showed that natural products represent one third of the total colorants approximately, and three fourths of these natural colorants are used in food in beverages.

Other applications

Antarctic bacteria are a source of a wide range of applications in the medical sector due to their capacity of producing numerous compounds/metabolites (presence of diverse metabolic pathways resulting from evolutionary adaptation to subzero and nutrient deficient conditions) (Figure 2). Recently, a new anti-biofilm agent called "CATASAN" has been found in Antarctic bacteria *Psychrobacter* sp. TAE2020 which can be used against the human pathogen *Staphylococcus epidermidis* (D'Angelo et al., 2022). Similarly, another Antarctic bacteria *Pseudomonas* sp. TAE6080 is capable of inhibiting biofilm formation by the opportunistic pathogen *Staphylococcus epidermidis* (Riccardi et al., 2022). Several studies have shown that Antarctic microbes produce bioactive compounds to treat various diseases (Murray et al., 2021; Xiao et al., 2023). Quinones from orange-yellow pigmented *Sphingomonas aerolata* (Busse et al., 2003), isolated from the ice of Taylor dome and hydrocarbon-contaminated soils around Scott Base is used to treat Alzheimer's, Huntington's, Parkinson's, and cardiovascular diseases (Nair and Abraham, 2020). Previous analysis showcased that the Antarctic pigments also have various biological activities such as antioxidant, antibacterial, antimalarial, antifungal, anticancer and many others (Silva et al., 2021). Experimental studies by Maeda et al. (2009) on fucoxanthin (characteristic carotenoid of brown algae) have revealed various applications of the compound in producing anti lymphangiogenic, antitumoral, neuroprotective, antidiabetic, anti-obesity, and anti-inflammatory effects. In addition, fucoxanthin prevents carcinogenesis and depressive behavior, such as the attenuation of bleomycin-induced lung fibrosis and ulcerative colitis (Wang Y. et al., 2019). Another pigment violaxanthin has proved to have antiproliferative and anti-inflammatory effects (Pasquet et al., 2011; Soontornchaiboon et al., 2012). Decaprenoxanthin from *Arthrobacter psychrochitiniphilus* strain 366 isolated from a biofilm formed on the surface of defrost water in Whalers Bay, Deception Island, Silva et al. (2019) has strong antioxidant properties. Apart from pigments, a variety of antimicrobial lipid-based substances have been isolated from Antarctic microorganisms with potential to be used in treatments of bacterial infections. Rhamnolipids, a special class of bacterial lipids purified form Antarctic marine sediment bacteria, *Pseudomonas* sp. BTN1 displayed antibacterial activity against *Burkholderia cenocepacia* (isolated from cystic fibrosis patient) and *Staphylococcus aureus* (Tedesco et al., 2016). Aminolipids, another category of microbial lipids purified from shallow-sea-sediment bacterium *Aequorivita* sp. is effective against methycilin-resistant *Staphylococcus aureus* (Chianese et al., 2018).

Besides bioactive compounds, Antarctic bacteria synthesizes metal nanoparticles (Figure 2) through biomineralization process.

The biosynthesis of metal nanoparticles using Antarctic bacteria is a cost-effective, environmentally friendly process, without using toxic chemicals in the synthesis and purification steps. In recent years, synthesis of metal nanoparticles using cold adapted bacterial strains have gained attention due to the high stability (even at psychrophilic conditions) and diverse biomedical applications (Das et al., 2020; John et al., 2021, 2022). Das et al. (2020) biosynthesize gold nanoparticle (GNP) at different temperatures (4°, 10°, 25°, 30° and 37° C) using psychrotolerant Antarctic bacteria *Bacillus* sp. GL1.3. The synthesized gold nanoparticles exhibit antibacterial activity against sulfate-reducing bacteria (*Desulfovibrio* sp.) (Das et al., 2020). A similar study by Javani et al. (2015) identified four psychrophilic Antarctic bacteria namely *Aeromonas salmonicida*, *Pseudomonas veronii*, *Psychrobacter* sp. and *Yersinia kristensenii* that extracellularly biosynthesize nanosilver at 4°C and 30°C. The study demonstrated that the most active and stable nanoparticles with highest antibacterial activity were those prepared at 4°C. These nanoparticles possess high stability even after 10 months of incubation under light (Javani et al., 2015). An efficient novel approach is used by Plaza et al. (2016) to synthesize quantum dots (CdS and CdTe quantum dots) at room temperature by using heavy metal (cadmium and tellurite) resistant Antarctic bacteria, *Pseudomonas*, *Psychrobacter* and *Shewanella*. Recently, John et al. (2022) synthesizes silver nanoparticles (AgNPs) using three bacterial strains *Rhodococcus*, *Brevundimonas* and *Bacillus* isolated from an Antarctic consortium. Biosynthetic AgNPs show promising effects against common nosocomial pathogens and can be replaced with conventional antibiotics (John et al., 2022). Thus, despite being underexplored, Antarctic bacteria constitute a promising platform for biosynthesis of nanomaterials.

Advanced strategies to study Antarctic bacterial adaptation

Omics

To gain a comprehensive picture of bacterial communities, several "omics" approaches should be applied to reveal polar "blackbox" microbes (Figure 3). The development of genomic technologies in recent years has gained knowledge on microbial communities and their adaptation in the Antarctic ecosystem. The most common technique to reveal the taxonomical composition of cold adapted bacteria is 16S rRNA gene sequencing (Bowman and Ducklow, 2015), but the functional role of many other genes remains unknown. However, new technologies are being developed in high -throughput sequencing, which provides high quality data with short or long read sequences. To date, several genomes from psychrophilic bacteria and archaea have been sequenced (Pucciarelli et al., 2015; Ramasamy et al., 2019; John et al., 2020; Wang et al., 2021; Lee et al., 2022; Riccardi et al., 2022; Otur et al., 2023). The advantage of whole genome sequencing of Antarctic bacteria is to analyze and characterize the genes in the entire genome, especially genes coding industrially relevant enzymes using DNA sequencing methods and bioinformatics tools (assemble and analyze the structure and functions of specific gene). However, the whole genome is limited to cultivable bacteria which can grow as pure cultures in the laboratory conditions (Figure 3). Due to lack of cultivation methods in laboratory conditions, the majority of bacteria on our planet are uncultured and hence unidentified (Hug et al., 2016).

Up till now the whole genome sequence of Antarctic bacteria is available for a few taxa. The advancement in sequencing methods and bioinformatic approach could provide the understanding of their physiological and metabolic roles. The portable sequencers of Oxford Nanopore Technologies MinION could be used as an *in situ* sequencing tool for community composition and functional profiling of microbes thrive in Antarctic environment. Although, the high error rate of Nanopore sequencing compared to the amplicon sequencing technology by the Illumina platform is gradually decreasing, the hybrid assembly strategy (i.e., Illumina short reads assembled together with Nanopore long reads) is considered the best to cover the novel taxa and their functions in various Antarctic microbial communities.

The use of long-read metagenomic sequencing by Waschulin et al. (2022) revealed the biosynthetic potential of uncultured bacterial phyla such as *Acidobacteriota*, *Verrucomicrobiota* and *Gemmatimonadota*. Additionally, the uncultivable bacteria and their genetic functions can be explored through the metagenomic approach (genetic material of mixed community directly recovered from natural environment without obtaining the pure culture) which can either be sequence based, including high-throughput sequencing and bioinformatic analysis (high quality metagenome-assembled genomes, obtained through combination of binning approaches), or function based by involving functional expression of metagenomic libraries to identify target genes/gene clusters (Figure 3) (Alneberg et al., 2018).

Uncultivated microbial clades (candidate phyla) belonging to Genome Taxonomy Database (GTDB) in the Antarctic Ace Lake may play an important role in nutrient cycling (Williams et al., 2022). Similar studies have been reported by Williams et al. (2021) on microbial "dark matter" i.e. *Candidatus* bacterial phyla of metagenome-assembled genomes (MAGs) obtained from an Antarctic Lake. Recently, Fonseca et al. (2022) identified the bacterial family *Woeseiaceae* for the first time in Antarctic sediments, but the cellular and molecular adaptation of this family to the cold environment is unknown. Although the metagenomic approach reveals the taxonomic composition, to deeply understand the expression of genes in the microbes to environmental changes, the metatranscriptome provides the information about microbial functions associated with the environment (Sutherland et al., 2022). The functional diversity of the microbial communities has been recently investigated under the Antarctic ice shelf using multiomics approach such as metagenomics, metatranscriptomics, single-cell genomics by Martínez-Pérez et al. (2022).

A study by Médigue et al. (2005) sequenced the genome of the Antarctic bacterium *Pseudoalteromonas haloplanktis* TAC125 and using *in silico* analysis revealed the composition of the proteome for cold adaptation. Similarly, Fondi et al. (2015) investigated several metabolic features of *Pseudoalteromonas haloplanktis* TAC125 and variations in cellular metabolic fluxes through *in silico* modeling.

Recent developments in the omics era will open a remarkable milestone in structural and functional metagenomics (Prayogo et al., 2020). In fact, metagenome mining is applied to bacterial communities to screen novel classes of cold adapted enzymes for biotechnological applications (Kumar et al., 2021). A recent study by Blázquez-Sánchez et al. (2022) found Antarctic bacteria *Moraxella* sp. strain TA144 (Mors1) and *Oleispira antarctica* RB-8 (OaCut) hydrolyze aliphatic and aromatic polyesters at moderate temperatures. In addition,

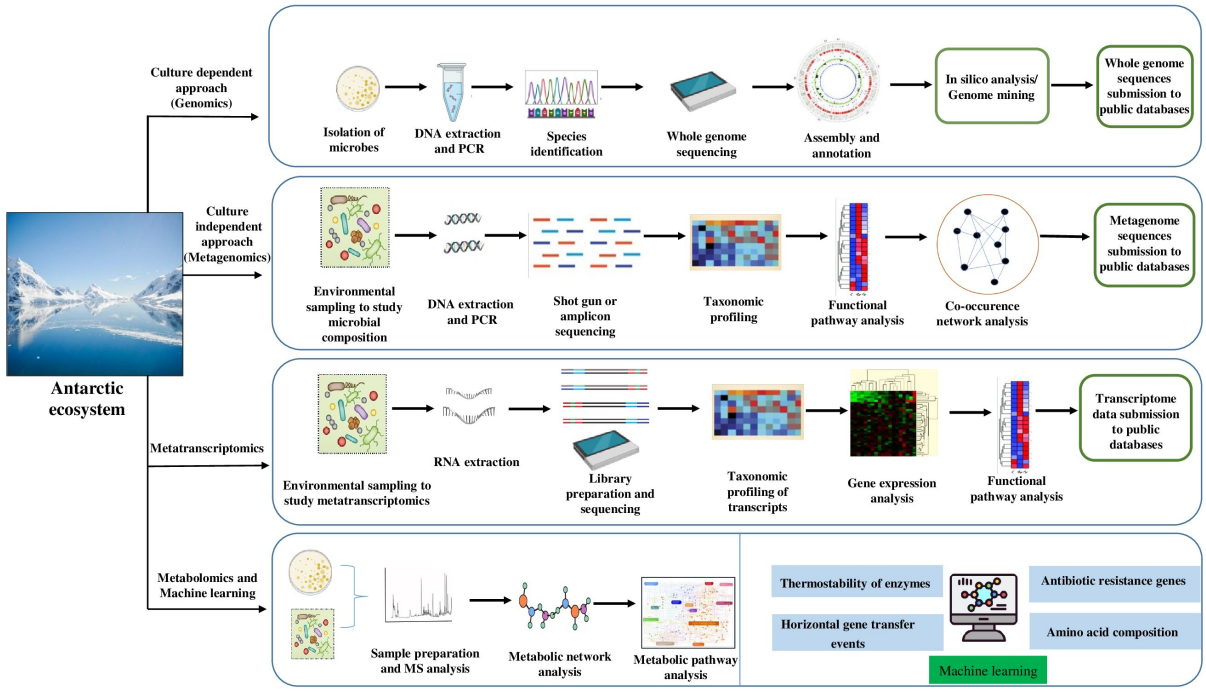

FIGURE 3
Advanced technologies – omics tools and machine learning approach to study the adaptation mechanism and potential of cold-adaptive molecules of Antarctic bacteria.

metagenome analysis revealed the members of the *Moraxellaceae* family harbors candidate genes for polyethylene terephthalate (PET) hydrolases (Blázquez-Sánchez et al., 2022). The majority of bacteria living in the cold expresses certain genes as adaptation strategies. Dall Agnol et al. (2014), using transcriptomes (Figure 3) and proteomes, unveiled global gene expression in response to thermal adaptation of *E. antarcticum* B7 at different temperatures (0°C and 37°C). In a recent study by Ijaq et al. (2022), *Pseudomonas* sp. Lz4W genome analysis revealed 743 CDS annotated as hypothetical proteins, including 61 hypothetical proteins at translational level. However, with the current global climate crisis, there is the urgent need to understand all the adaptation mechanisms to the changing environmental conditions, particularly in the polar region. Recent developments in proteomics along with gene expression profiling have been coupled for the discovery of various biomolecules in psychrophilic bacteria. Garcia-Lopez et al. (2021) presented a review of the current knowledge on psychrophiles for their biomolecules and metabolic pathways. Understanding the adaptation strategies of Antarctic bacteria using the omics approach will help to reveal their metabolic changes (Figure 3) to future climate change scenario.

Machine learning approach

Machine learning (ML) is a branch of artificial intelligence (AI) that designs mathematical models to execute certain tasks from assembled information in less time and cost. Generally, two ML models – supervised (also known as predictive) and unsupervised (descriptive)- have been extensively used in most research areas in the field of microbiology (Goodswen et al., 2021; Greener et al., 2022). The supervised model requires to be trained using the training data set which includes text, images, and alphanumeric data. The most used supervised model algorithms are classification and regression. While the unsupervised algorithm uses unlabeled data which involves clustering and association rule mining (Goodswen et al., 2021). The ML approach has evolved rapidly in recent years to understand microbial and molecular processes using high-throughput data. Considering the various applications of this approach in biology, very scarce studies are available for psychrophilic microbes, especially bacteria. Previously, Lee C. et al. (2019) used ML method (classification and regression tree machine learning algorithms called CART) to study the bacterial communities and geochemical variables. The study provides a clue to unravel the bacterial communities link to changing environmental conditions using ML approach in other habitats of the Antarctic environment. Later, the mobilized colistin resistance (*mcr*) gene, that is a type of antibiotic resistance gene (ARG), has been identified using machine learning tools (Figure 3) in polar *Psychrobacter* (Cuadrat et al., 2020). Similarly, Arango-Argoty et al. (2018) developed a tool called DeepARG using a deep learning approach for the prediction of antibiotic resistance genes from metagenomic data. Recent study by Marcoleta et al. (2022) employ DeepARG tool to detect ARG from North Antarctic soils microbial communities (*Pseudomonas*, *Streptomyces*, *Gemmatimonas*, *Paenibacillus*, and *Polaromonas*). Yet, sparse information is available for antibiotic resistance genes (ARG) of resistome profile of Antarctic bacteria. Moreover, genomic, and metabolic pathways of novel taxa of bacteria are poorly known. The ML is a promising approach and can be widely used in omics data to explore the presence of ARGs in Antarctic habitats.

Furthermore, studies based on machine learning have been reported on thermophilic and mesophilic bacterial proteins, however little is known about the application of ML approach in psychrophilic enzymes. Recent study on psychrophilic amino acid composition (AAC) using machine learning (ML) algorithm showed that psychrophiles proteins contains high frequency of Ala, Gly, Ser, and Thr, compared to Glu, Lys, Arg, Ile, Val, and Leu amino acids (Huang et al., 2023a). The support vector machine learning model (SVM) in combination with molecular dynamics (MD) is employed to study the thermostability of psychrophilic alpha-amylase (Figure 3) (exhibited high activity at low temperature) isolated from *Pseudoalteromonas haloplanktis* (Li et al., 2020). The study revealed the presence of two single point mutations (S255K and S340P) and one double mutation (S255K/S340P) at non-conserved residues that enhanced thermostability of enzyme without altering its catalytic activity (Li et al., 2020). Similarly, to understand the antifreeze peptides and proteins interactions to ice crystals, several computational predictors have been used (Jiang et al., 2022). Recently, ML-guided robotic strain isolation platform for the isolation of diverse microbes from human feces have been used by Huang et al. (2023b). These ML approaches can be applicable to bridge the knowledge gap on genes functions in bacterial genome in response to climate change adaptation (Figure 3). Hence, we think this algorithm can be extendable to the Antarctic ecosystem in the upcoming studies to develop the understanding on bacterial dark matter and their adaptation.

ML has the potential to accelerate HIV drug discovery by narrowing down the number of antiviral compounds selected for *in vitro* and *in vivo* testing.

Conclusion and future perspectives

The cold-adapted Antarctic psychrophilic bacteria represent excellent model organisms to study climate change induced stress adaptation. These bacteria are thriving in harsh and inhospitable Antarctic environment and displaying immense potential of regulating climate change factors. Therefore, the comprehensive review on Antarctic bacteria highlighted the adaptation strategies of psychrophiles at various levels (structural, physiological and molecular) in response to the changing environment. Many of these adaptation tools including biosurfactants, EPS, PUFA, membrane pigments, molecular chaperones and the underlying mechanisms are superficially studied due to the difficulty in some bacterial cultivation. The aid of ML and omics approach, particularly metagenomics, could provide insight into how psychrophilic bacteria adapt to cope with cellular and molecular mechanisms as survival strategies. Extensive research using these approaches needs to be done to better understand the bacterial adaptation in Antarctic environment and implementing this knowledge for improving the tolerance ability of other bacteria, for an environmentally sustainable future. The multi-omics tools coupled with ML algorithms might explore the industrial potential of biomolecules from Antarctic bacteria effectively in less time and labor. This is another aspect of upcoming research that needs to be emphasized. In recent years, the exploitation of psychrophilic enzymes (amylase, lipase, protease, hydrolase, pectinase, cellulase etc.) has been increased in different biotechnological industries due to their improved catalytic efficiency, flexibility, and low thermal stability. The cold-active enzymes are the best eco-friendly alternative to synthetic chemicals and moreover it increases the shelf life of the products (fabrics, foods etc.). Therefore, the manufacturers are seeking novel cold-active enzymes that further improve the efficiency and quality of products (particularly in the detergents industry). Hence, this is an additional aspect of research that needs to be explored. Overall, the review discusses the most recent studies on Antarctic bacterial adaptation as future climate model and suggested novel approaches for upcoming research in this direction.

Author contributions

KPR and LM conceptualized the idea and constructed figures. RR and KPR constructed tables. KPR, LM, RR, and KR wrote the original draft. CM and SP revised the manuscript. KPR wrote the final draft with all other authors. All authors contributed to the article and approved the submitted version.

Funding

The authors are thankful to Umeå University for the funding provided for Open access fee.

Conflict of interest

The authors declare that the research was conducted in the absence of any commercial or financial relationships that could be construed as a potential conflict of interest.

Publisher's note

References

Abe, T., Akazawa, Y., Toyoda, A., Niki, H., and Baba, T. (2020). Batch-learning self-organizing map identifies horizontal gene transfer candidates and their origins in entire genomes. *Front. Microbiol.* 11:1486. doi: 10.3389/fmicb.2020.01486

Acevedo, J. P., Rodriguez, V., Saavedra, M., Munoz, M., Salazar, O., Asenjo, J. A., et al. (2013). Cloning, expression and decoding of the cold adaptation of a new widely represented thermolabile subtilisin-like protease. *J. Appl. Microbiol.* 114, 352–363. doi: 10.1111/jam.12033

Acosta, S., Canclini, L., Marizcurrena, J. J., Castro-Sowinski, S., and Hernández, P. (2022). Photo-repair effect of a bacterial Antarctic CPD-photolyase on UVC-induced DNA lesions in human keratinocytes. *Environ. Toxicol. Pharmacol.* 96:104001. doi: 10.1016/j.etap.2022.104001

Aislabie, J., Saul, D. J., and Foght, J. M. (2006). Bioremediation of hydrocarbon-contaminated polar soils. *Extremophiles* 10, 171–179. doi: 10.1007/s00792-005-0498-4

Al-Ghanayem, A. A., and Joseph, B. (2020). Current prospective in using cold-active enzymes as eco-friendly detergent additive. *Appl. Microbiol. Biotechnol.* 104, 2871–2882. doi: 10.1007/s00253-020-10429-x

Al-Maqtari, Q. A., Waleed, A. A., and Mahdi, A. A. (2019). Cold-active enzymes and their applications in industrial fields-a review. *Int. J. Res. Agric. Sci.* 6, 2348–3997.

Alneberg, J., Karlsson, C. M., Divne, A. M., Bergin, C., Homa, F., Lindh, M. V., et al. (2018). Genomes from uncultivated prokaryotes: a comparison of metagenome-assembled and single-amplified genomes. *Microbiome* 6, 1–14. doi: 10.1186/s40168-018-0550-0

Alterio, V., Aurilia, V., Romanelli, A., Parracino, A., Saviano, M., D'Auria, S., et al. (2010). Crystal structure of an S-formylglutathione hydrolase from *Pseudoalteromonas haloplanktis* TAC125. *Biopolymers* 93, 669–677. doi: 10.1002/bip.21420

Anesio, A. M., Hodson, A. J., Fritz, A., Psenner, R., and Sattler, B. (2009). High microbial activity on glaciers: importance to the global carbon cycle. *Glob. Chang. Biol.* 15, 955–960. doi: 10.1111/j.1365-2486.2008.01758.x

Angeli, A., Del Prete, S., Osman, S. M., AlOthman, Z., Donald, W. A., Capasso, C., et al. (2019). Activation studies of the γ-carbonic anhydrases from the Antarctic marine bacteria Pseudoalteromonas haloplanktis and *Colwellia psychrerythraea* with amino acids and amines. *Mar. Drugs* 17:238. doi: 10.3390/md17040238

Arango-Argoty, G., Garner, E., Pruden, A., Heath, L. S., Vikesland, P., and Zhang, L. (2018). Deep ARG: a deep learning approach for predicting antibiotic resistance genes from metagenomic data. *Microbiome* 6, 1–15. doi: 10.1186/s40168-018-0401-z

Aurilia, V., Parracino, A., Saviano, M., and D'Auria, S. (2007). The psychrophilic bacterium Pseudoalteromonas halosplanktis TAC125 possesses a gene coding for a cold-adapted feruloyl esterase activity that shares homology with esterase enzymes from γ-proteobacteria and yeast. *Gene* 397, 51–57. doi: 10.1016/j.gene.2007.04.004

Ausuri, J., Dell'Anno, F., Vitale, G. A., Palma Esposito, F., Funari, V., Franci, G., et al. (2022). Bioremediation of Multiple Heavy Metals Mediated by Antarctic Marine Isolated Dietzia psychralcaliphila JI1D. *JMSE* 10:1669. doi: 10.3390/jmse10111669

Awazu, N., Shodai, T., Takakura, H., Kitagawa, M., Mukai, H., and Kato, I. (2011). U.S. patent no. 8, 034, 597. Washington, DC: U.S. patent and trademark office.

Bajerski, F., Wagner, D., and Mangelsdorf, K. (2017). Cell membrane fatty acid composition of Chryseobacterium frigidisoli PB4T, isolated from Antarctic glacier forefield soils, in response to changing temperature and pH conditions. *Front. Microbiol.* 8:677. doi: 10.3389/fmicb.2017.00677

Bar Dolev, M., Bernheim, R., Guo, S., Davies, P. L., and Braslavsky, I. (2016). Putting life on ice: bacteria that bind to frozen water. *J. R. Soc. Interface* 13:20160210. doi: 10.1098/rsif.2016.0210

Barnes, D. K., Sands, C. J., Paulsen, M. L., Moreno, B., Moreau, C., Held, C., et al. (2021). Societal importance of Antarctic negative feedbacks on climate change: blue carbon gains from sea ice, ice shelf and glacier losses. *Sci. Nat.* 108, 1–14. doi: 10.1007/s00114-021-01748-8

Bisaccia, M., Binda, E., Rosini, E., Caruso, G., Dell'Acqua, O., Azzaro, M., et al. (2023). A novel promising laccase from the psychrotolerant and halotolerant Antarctic marine Halomonas sp. M68 strain. *Front. Microbiol.* 14:1078382. doi: 10.3389/fmicb.2023.1078382

Blázquez-Sánchez, P., Engelberger, F., Cifuentes-Anticevic, J., Sonnendecker, C., Griñén, A., Reyes, J., et al. (2022). Antarctic polyester hydrolases degrade aliphatic and aromatic polyesters at moderate temperatures. *Appl. Environ. Microbiol.* 88, e01842–e01821. doi: 10.1128/aem.01842-21

Bowman, J. S., and Ducklow, H. W. (2015). Microbial communities can be described by metabolic structure: a general framework and application to a seasonally variable, depth-stratified microbial community from the coastal West Antarctic peninsula. *PLoS One* 10:e0135868. doi: 10.1371/journal.pone.0135868

Bruno, S., Coppola, D., di Prisco, G., Giordano, D., and Verde, C. (2019). Enzymes from marine polar regions and their biotechnological applications. *Mar. Drugs* 17:544. doi: 10.3390/md17100544

Busse, H. J., Denner, E. B., Buczolits, S., Salkinoja-Salonen, M., Bennasar, A., and Kampfer, P. (2003). *Sphingomonas aurantiaca* sp. nov., *Sphingomonas aerolata* sp. nov. and *Sphingomonas faeni* sp. nov., air-and dustborne and Antarctic, orange-pigmented, psychrotolerant bacteria, and emended description of the genus Sphingomonas. *Int. J. Syst. Evol. Microbiol.* 53, 1253–1260. doi: 10.1099/ijs.0.02461-0

Cabrera, M. Á., Márquez, S. L., and Pérez-Donoso, J. M. (2022). Comparative genomic analysis of Antarctic Pseudomonas isolates with 2, 4, 6-trinitrotoluene transformation capabilities reveals their unique features for xenobiotics degradation. *Genes* 13:1354. doi: 10.3390/genes13081354

Cabrera, M. Á., Márquez, S. L., Quezada, C. P., Osorio, M. I., Castro-Nallar, E., González-Nilo, F. D., et al. (2020). Biotransformation of 2, 4, 6-trinitrotoluene by Pseudomonas sp. TNT3 isolated from deception island, Antarctica. *Environ. Pollut.* 262:113922. doi: 10.1016/j.envpol.2020.113922

Cagide, C., Marizcurrena, J. J., Vallés, D., Alvarez, B., and Castro-Sowinski, S. (2023). A bacterial cold-active dye-decolorizing peroxidase from an Antarctic Pseudomonas strain. *Appl. Microbiol. Biotechnol.* 107, 1707–1724. doi: 10.1007/s00253-023-12405-7

Caruso, C., Rizzo, C., Mangano, S., Poli, A., Di Donato, P., Finore, I., et al. (2018). Production and biotechnological potential of extracellular polymeric substances from sponge-associated Antarctic bacteria. *Appl. Environ. Microbiol.* 84, e01624–e01617. doi: 10.1128/aem.01624-17

Casillo, A., Parrilli, E., Sannino, F., Mitchell, D. E., Gibson, M. I., Marino, G., et al. (2017). Structure-activity relationship of the exopolysaccharide from a psychrophilic bacterium: a strategy for cryoprotection. *Carbohydr. Polym.* 156, 364–371. doi: 10.1016/j.carbpol.2016.09.037

Cheng, Z., Shi, C., Gao, X., Wang, X., and Kan, G. (2022). Biochemical and Metabolomic responses of Antarctic bacterium Planococcus sp. O5 induced by copper ion. *Toxics* 10:302. doi: 10.3390/toxics10060302

Chen, Y., Gao, P., Tang, X., and Xu, C. (2021). Characterisation and bioactivities of an exopolysaccharide from an Antarctic bacterium *Shewanella frigidimarina* W32–2. *Aquaculture* 530:735760. doi: 10.1016/j.aquaculture.2020.735760

Chessa, J. P., Feller, G., and Gerday, C. (1999). Purification and characterization of the heat-labile α-amylase secreted by the psychrophilic bacterium TAC 240B. *Can. J. Microbiol.* 45, 452–457. doi: 10.1139/w99-021

Chianese, G., Esposito, F. P., Parrot, D., Ingham, C., De Pascale, D., and Tasdemir, D. (2018). Linear aminolipids with moderate antimicrobial activity from the Antarctic gram-negative bacterium Aequorivita sp. *Mar. Drugs* 16:187. doi: 10.3390/md16060187

Cieśliński, H., Białkowska, A. M., Długołęcka, A., Daroch, M., Tkaczuk, K. L., Kalinowska, H., et al. (2007). A cold-adapted esterase from psychrotrophic Pseudoalteromas sp. strain 643A. *Arch. Microbiol.* 188, 27–36. doi: 10.1007/s00203-007-0220-2

Cieśliński, H., Kur, J., Białkowska, A., Baran, I., Makowski, K., and Turkiewicz, M. (2005). Cloning, expression, and purification of a recombinant cold-adapted β-galactosidase from Antarctic bacterium Pseudoalteromonas sp. 22b. *Protein Expr. Purif.* 39, 27–34. doi: 10.1016/j.pep.2004.09.002

Collins, T., and Margesin, R. (2019). Psychrophilic lifestyles: mechanisms of adaptation and biotechnological tools. *Appl. Microbiol. Biotechnol.* 103, 2857–2871. doi: 10.1007/s00253-019-09659-5

Correa-Llanten, D. N., Amenabar, M. J., and Blamey, J. M. (2012). Resistance to hypoosmotic shock of liposomes containing novel pigments from an Antarctic bacterium. *Microbiol. Biotechnol. Lett.* 40, 215–219. doi: 10.4014/kjmb.1205.05018

Cuadrat, R. R., Sorokina, M., Andrade, B. G., Goris, T., and Davila, A. M. (2020). Global Ocean resistome revealed: exploring antibiotic resistance gene abundance and distribution in TARA oceans samples. *Gigascience* 9:giaa046. doi: 10.1093/gigascience/giaa046

D'Angelo, C., Casillo, A., Melchiorre, C., Lauro, C., Corsaro, M. M., Carpentieri, A., et al. (2022). CATASAN is a new anti-biofilm agent produced by the marine Antarctic bacterium Psychrobacter sp. TAE2020. *Mar. Drugs* 20:747. doi: 10.3390/md20120747

D'Auria, S., Aurilia, V., Marabotti, A., Gonnelli, M., and Strambini, G. (2009). Structure and dynamics of cold-adapted enzymes as investigated by phosphorescence spectroscopy and molecular dynamics studies. 2. The case of an esterase from *Pseudoalteromonas haloplanktis*. *J. Phys. Chem. B* 113, 13171–13178. doi: 10.1021/jp9043286

Dall Agnol, H. P., Baraúna, R. A., de Sá, P. H., Ramos, R. T., Nóbrega, F., Nunes, C. I., et al. (2014). Omics profiles used to evaluate the gene expression of *Exiguobacterium antarcticum* B7 during cold adaptation. *BMC Genomics* 15, 1–12. doi: 10.1186/1471-2164-15-986

Darham, S., Syed-Muhaimin, S. N., Subramaniam, K., Zulkharnain, A., Shaharuddin, N. A., Khalil, K. A., et al. (2021). Optimisation of Various Physicochemical Variables Affecting Molybdenum Bioremediation Using Antarctic Bacterium, Arthrobacter sp. Strain AQ5-05. *Water* 13:2367. doi: 10.3390/w13172367

Das, K. R., Tiwari, A. K., and Kerkar, S. (2020). Psychrotolerant Antarctic bacteria biosynthesize gold nanoparticles active against sulphate reducing bacteria. *Prep. Biochem. Biotechnol.* 50, 438–444. doi: 10.1080/10826068.2019.1706559

Davail, S., Feller, G., Narinx, E., and Gerday, C. (1994). Cold adaptation of proteins. Purification, characterization, and sequence of the heat-labile subtilisin from the Antarctic psychrophile Bacillus TA41. *J. Biol. Chem.* 269, 17448–17453.

De Lemos, E. A., Procópio, L., Da Mota, F. F., Jurelevicius, D., Rosado, A. S., and Seldin, L. (2023). Molecular characterization of *Paenibacillus antarcticus* IPAC21, a bioemulsifier producer isolated from Antarctic soil. *Front. Microbiol.* 14:1142582. doi: 10.3389/fmicb.2023.1142582

De Luca, V., Vullo, D., Del Prete, S., Carginale, V., Osman, S. M., AlOthman, Z., et al. (2016). Cloning, characterization and anion inhibition studies of a γ-carbonic anhydrase from the Antarctic bacterium *Colwellia psychrerythraea*. *Bioorg. Med. Chem.* 24, 835–840. doi: 10.1016/j.bmc.2016.01.005

De Luca, V., Vullo, D., Del Prete, S., Carginale, V., Scozzafava, A., Osman, S. M., et al. (2015). Cloning, characterization and anion inhibition studies of a new γ-carbonic anhydrase from the Antarctic bacterium *Pseudoalteromonas haloplanktis*. *Bioorg. Med. Chem.* 23, 4405–4409. doi: 10.1016/j.bmc.2015.06.021

De Maayer, P., Anderson, D., Cary, C., and Cowan, D. A. (2014). Some like it cold: understanding the survival strategies of psychrophiles. *EMBO Rep.* 15, 508–517. doi: 10.1002/embr.201338170

Denner, E. B., Mark, B., Busse, H. J., Turkiewicz, M., and Lubitz, W. (2001). *Psychrobacter proteolyticus* sp. nov., a psychrotrophic, halotolerant bacterium isolated

from the Antarctic krill *Euphausia superba* Dana, excreting a cold-adapted metalloprotease. *Syst. Appl. Microbiol.* 24, 44–53. doi: 10.1078/0723-2020-00006

De Pascale, D., Cusano, A. M., Autore, F., Parrilli, E., Di Prisco, G., Marino, G., et al. (2008). The cold-active Lip1 lipase from the Antarctic bacterium *Pseudoalteromonas haloplanktis* TAC125 is a member of a new bacterial lipolytic enzyme family. *Extremophiles* 12, 311–323. doi: 10.1007/s00792-008-0163-9

De Pascale, D., Giuliani, M., De Santi, C., Bergamasco, N., Amoresano, A., Carpentieri, A., et al. (2010). PhAP protease from *Pseudoalteromonas haloplanktis* TAC125: gene cloning, recombinant production in E. coli and enzyme characterization. *Pol. Sci.* 4, 285–294. doi: 10.1016/j.polar.2010.03.009

Dietz, S., and Koninx, F. (2022). Economic impacts of melting of the Antarctic ice sheet. *Nat. Commun.* 13:5819. doi: 10.1038/s41467-022-33406-6

Di Lorenzo, F., Crisafi, F., La Cono, V., Yakimov, M. M., Molinaro, A., and Silipo, A. (2020). The structure of the lipid a of gram-negative cold-adapted Bacteria isolated from Antarctic environments. *Mar. Drugs* 18:592. doi: 10.3390/md18120592

Ding, H., Zeng, Q., Zhou, L., Yu, Y., and Chen, B. (2017). Biochemical and structural insights into a novel thermostable β-1, 3-galactosidase from Marinomonas sp. BSi20414. *Mar. Drugs* 15:13. doi: 10.3390/md15010013

Dutta, A., and Chaudhuri, K. (2010). Analysis of tRNA composition and folding in psychrophilic, mesophilic and thermophilic genomes: indications for thermal adaptation. *FEMS Microbiol. Lett.* 305, 100–108. doi: 10.1111/j.1574-6968.2010.01922.x

Effendi, D. B., Sakamoto, T., Ohtani, S., Awai, K., and Kanesaki, Y. (2022). Possible involvement of extracellular polymeric substrates of Antarctic cyanobacterium Nostoc sp. strain SO-36 in adaptation to harsh environments. *J. Plant Res.* 135, 771–784. doi: 10.1007/s10265-022-01411-x

Fan, Y., Yi, J., Hua, X., Feng, Y., Yang, R., and Zhang, Y. (2016). Structure analysis of a glycosides hydrolase family 42 cold-adapted β-galactosidase from Rahnella sp R3. *RSC Adv.* 6, 37362–37369. doi: 10.1039/c6ra04529d

Feller, G., d'Amic, D., and Gerday, C. (1999). Thermodynamic stability of a cold-active α-amylase from the Antarctic bacterium Alteromonas haloplanctis. *Biochemistry* 38, 4613–4619. doi: 10.1021/bi982650+

Feller, G., and Gerday, C. (2003). Psychrophilic enzymes: hot topics in cold adaptation. *Nat. Rev. Microbiol.* 1, 200–208. doi: 10.1038/nrmicro773

Feller, G., Thiry, M., Arpigny, J. L., and Gerday, C. (1991). Cloning and expression in *Escherichia coli* of three lipase-encoding genes from the psychrotrophic Antarctic strain Moraxella TA144. *Gene* 102, 111–115. doi: 10.1016/0378-1119(91)90548-p

Fondi, M., Maida, I., Perrin, E., Mellera, A., Mocali, S., Parrilli, E., et al. (2015). Genome-scale metabolic reconstruction and constraint-based modelling of the Antarctic bacterium *Pseudoalteromonas haloplanktis* TAC 125. *Environ. Microbiol.* 17, 751–766. doi: 10.1111/1462-2920.12513

Fonseca, F., Meneghel, J., Cenard, S., Passot, S., and Morris, G. J. (2016). Determination of intracellular vitrification temperatures for unicellular microorganisms under conditions relevant for cryopreservation. *PLoS One* 11:e0152939. doi: 10.1371/journal.pone.0152939

Fonseca, V. G., Kirse, A., Giebner, H., Vause, B. J., Drago, T., Power, D. M., et al. (2022). Metabarcoding the Antarctic peninsula biodiversity using a multi-gene approach. *ISME Commun.* 2:37. doi: 10.1038/s43705-022-00118-3

Galkin, A., Kulakova, L., Ashida, H., Sawa, Y., and Esaki, N. (1999). Cold-adapted alanine dehydrogenases from two Antarctic bacterial strains: gene cloning, protein characterization, and comparison with mesophilic and thermophilic counterparts. *Appl. Environ. Microbiol.* 65, 4014–4020. doi: 10.1128/aem.65.9.4014-4020.1999

García-Descalzo, L., García-López, E., Alcázar, A., Baquero, F., and Cid, C. (2014). Proteomic analysis of the adaptation to warming in the Antarctic bacteria *Shewanella frigidimarina*. *Biochim Biophys Acta* 1844, 2229–2240. doi: 10.1016/j.bbapap.2014.08.006

García-Descalzo, L., Lezcano, M. Á., Carrizo, D., and Fairén, A. G. (2023). Changes in membrane fatty acids of a halo-psychrophile exposed to magnesium perchlorate and low temperatures: implications for Mars habitability. *Front. Astron. Space Sci.* 10:65. doi: 10.3389/fspas.2023.1034651

Garcia-Lopez, E., Alcazar, P., and Cid, C. (2021). Identification of biomolecules involved in the adaptation to the environment of cold-loving microorganisms and metabolic pathways for their production. *Biomol. Ther.* 11:1155. doi: 10.3390/biom11081155

Georlette, D., Jonsson, Z. O., Van Petegem, F., Chessa, J. P., Van Beeumen, J., Hübscher, U., et al. (2000). A DNA ligase from the psychrophile *Pseudoalteromonas haloplanktis* gives insights into the adaptation of proteins to low temperatures. *Eur. J. Biochem.* 267, 3502–3512. doi: 10.1046/j.1432-1327.2000.01377.x

Gerday, C., Aittaleb, M., Bentahir, M., Chessa, J. P., Claverie, P., Collins, T., et al. (2000). Cold-adapted enzymes: from fundamentals to biotechnology. *Trends Biotechnol.* 18, 103–107. doi: 10.1016/s0167-7799(99)01413-4

Goodswen, S. J., Barratt, J. L., Kennedy, P. J., Kaufer, A., Calarco, L., and Ellis, J. T. (2021). Machine learning and applications in microbiology. *FEMS Microbiol. Rev.* 45:fuab015. doi: 10.1093/femsre/fuab015

Goordial, J., Raymond-Bouchard, I., Zolotarov, Y., de Bethencourt, L., Ronholm, J., Shapiro, N., et al. (2016). Cold adaptive traits revealed by comparative genomic analysis of the eurypsychrophile Rhodococcus sp. JG3 isolated from high elevation McMurdo Dry Valley permafrost, Antarctica. *FEMS Microbiol. Ecol.* 92:fiv154. doi: 10.1093/femsec/fiv154

Greener, J. G., Kandathil, S. M., Moffat, L., and Jones, D. T. (2022). A guide to machine learning for biologists. *Nat. Rev. Mol. Cell Biol.* 23, 40–55. doi: 10.1038/s41580-021-00407-0

Gushgari-Doyle, S., Lui, L. M., Nielsen, T. N., Wu, X., Malana, R. G., Hendrickson, A. J., et al. (2022). Genotype to ecotype in niche environments: adaptation of Arthrobacter to carbon availability and environmental conditions. *ISME Commun.* 2:32. doi: 10.1038/s43705-022-00113-8

Gutt, J., Isla, E., Xavier, J. C., Adams, B. J., Ahn, I. Y., Cheng, C. H. C., et al. (2021). Antarctic ecosystems in transition–life between stresses and opportunities. *Biol. Rev.* 96, 798–821. doi: 10.1111/brv.12679

Hamid, B., Bashir, Z., Yatoo, A. M., Mohiddin, F., Majeed, N., Bansal, M., et al. (2022). Cold-active enzymes and their potential industrial applications—a review. *Molecules* 27:5885. doi: 10.3390/molecules27185885

Hassan, N., Anesio, A. M., Rafiq, M., Holtvoeth, J., Bull, I., Haleem, A., et al. (2020). Temperature driven membrane lipid adaptation in glacial psychrophilic bacteria. *Front. Microbiol.* 11:824. doi: 10.3389/fmicb.2020.00824

Hauksson, J. B., Andrésson, Ó. S., and Ásgeirsson, B. (2000). Heat-labile bacterial alkaline phosphatase from a marine Vibrio sp. *Enzym. Microb. Technol.* 27, 66–73. doi: 10.1016/s0141-0229(00)00152-6

Herrera, L. M., Braña, V., Fraguas, L. F., and Castro-Sowinski, S. (2019). Characterization of the cellulase-secretome produced by the Antarctic bacterium Flavobacterium sp. AUG42. *Microbiol. Res.* 223, 13–21. doi: 10.1016/j.micres.2019.03.009

He, Y., Qu, C., Zhang, L., and Miao, J. (2021). DNA photolyase from Antarctic marine bacterium Rhodococcus sp. NJ-530 can repair DNA damage caused by ultraviolet. 3. *Biotech* 11, 1–9. doi: 10.1007/s13205-021-02660-8

Hoyoux, A., Jennes, I., Dubois, P., Genicot, S., Dubail, F., François, J. M., et al. (2001). Cold-adapted β-galactosidase from the Antarctic psychrophile *Pseudoalteromonas haloplanktis*. *Appl. Environ. Microbiol.* 67, 1529–1535. doi: 10.1128/aem.67.4.1529-1535.2001

Huang, A., Lu, F., and Liu, F. (2023a). Discrimination of psychrophilic enzymes using machine learning algorithms with amino acid composition descriptor. *Front. Microbiol.* 14:1130594. doi: 10.3389/fmicb.2023.1130594

Huang, Y., Sheth, R. U., Zhao, S., Cohen, L. A., Dabaghi, K., Moody, T., et al. (2023b). High-throughput microbial culturomics using automation and machine learning. *Nat. Biotechnol.*, 1–10. doi: 10.1038/s41587-023-01674-2

Hug, L. A., Baker, B. J., Anantharaman, K., Brown, C. T., Probst, A. J., Castelle, C. J., et al. (2016). A new view of the tree of life. *Nat. Microbiol.* 1, 1–6. doi: 10.1038/nmicrobiol.2016.48

Humphry, D. R., George, A., Black, G. W., and Cummings, S. P. (2001). *Flavobacterium frigidarium* sp. nov., an aerobic, psychrophilic, xylanolytic and laminarinolytic bacterium from Antarctica. *Int. J. Syst. Evol. Microbiol.* 51, 1235–1243. doi: 10.1099/00207713-51-4-1235

Hussain, A., and Ray, M. K. (2022). DEAD box RNA helicases protect Antarctic *Pseudomonas syringae* Lz4W against oxidative stress. *Infect. Genet. Evol.* 106:105382. doi: 10.1016/j.meegid.2022.105382

Hwang, K., Choe, H., Nasir, A., and Kim, K. M. (2021). Complete genome of *Polaromonas vacuolata* KCTC 22033T isolated from beneath Antarctic Sea ice. *Mar. Genomics* 55:100790. doi: 10.1016/j.margen.2020.100790

Ijaq, J., Chandra, D., Ray, M. K., and Jagannadham, M. V. (2022). Investigating the functional role of hypothetical proteins from an Antarctic bacterium Pseudomonas sp. Lz4W: emphasis on identifying proteins involved in cold adaptation. *Front. Genet.* 13:825269. doi: 10.3389/fgene.2022.825269

IPCC (2021). *Climate Change 2021: The Physical Science Basis. Contribution of Working Group I to the Sixth Assessment Report of the Intergovernmental Panel on Climate Change* (Cambridge: Cambridge University Press).

Irgens, R. L., Gosink, J. J., and Staley, J. T. (1996). *Polaromonas vacuolata* gen. Nov., sp. nov., a psychrophilic, marine, gas vacuolate bacterium from Antarctica. *Int. J. Syst. Bacteriol.* 46, 822–826. doi: 10.1099/00207713-46-3-822

Javani, S., Marín, I., Amils, R., and Abad, J. P. (2015). Four psychrophilic bacteria from Antarctica extracellularly biosynthesize at low temperature highly stable silver nanoparticles with outstanding antimicrobial activity. *Colloids Surf. A Physicochem. Eng. Asp.* 483, 60–69. doi: 10.1016/j.colsurfa.2015.07.028

Javed, A., and Qazi, J. I. (2016). Psychrophilic microbial enzymes implications in coming biotechnological processes. *Am. Sci. Res. J. Eng. Technol. Sci.* 23, 103–120.

Jiang, W., Yang, F., Chen, X., Cai, X., Wu, J., Du, M., et al. (2022). Molecular simulation-based research on antifreeze peptides: advances and perspectives. *J. Future Food* 2, 203–212. doi: 10.1016/j.jfutfo.2022.06.002

Ji, M., Barnwell, C. V., and Grunden, A. M. (2015). Characterization of recombinant glutathione reductase from the psychrophilic Antarctic bacterium *Colwellia psychrerythraea*. *Extremophiles* 19, 863–874. doi: 10.1007/s00792-015-0762-1

John, M. S., Nagoth, J. A., Ramasamy, K. P., Ballarini, P., Mozzicafreddo, M., Mancini, A., et al. (2020). Horizontal gene transfer and silver nanoparticles production in a new Marinomonas strain isolated from the Antarctic psychrophilic ciliate Euplotes focardii. *Sci. Rep.* 10, 1–14. doi: 10.1038/s41598-020-66878-x

John, M. S., Nagoth, J. A., Ramasamy, K. P., Mancini, A., Giuli, G., Miceli, C., et al. (2022). Synthesis of bioactive silver nanoparticles using new bacterial strains from an Antarctic consortium. *Mar. Drugs* 20:558. doi: 10.3390/md20090558

John, M. S., Nagoth, J. A., Zannotti, M., Giovannetti, R., Mancini, A., Ramasamy, K. P., et al. (2021). Biogenic synthesis of copper nanoparticles using bacterial strains isolated from an Antarctic consortium associated to a psychrophilic marine ciliate: characterization and potential application as antimicrobial agents. *Mar. Drugs* 19:263. doi: 10.3390/md19050263

Karan, R., Capes, M. D., DasSarma, P., and DasSarma, S. (2013). Cloning, overexpression, purification, and characterization of a polyextremophilic β-galactosidase from the Antarctic haloarchaeon *Halorubrum lacusprofundi*. *BMC Biotechnol.* 13, 1–11. doi: 10.1186/1472-6750-13-3

Kim, E. J., Kim, J. E., Hwang, J. S., Kim, I. C., Lee, S. G., Kim, S., et al. (2019). Increased productivity and antifreeze activity of ice-binding protein from *Flavobacterium frigoris* PS1 produced using *Escherichia coli* as bioreactor. *Appl. Biochem. Microbiol.* 55, 489–494. doi: 10.1134/S0003683819050077

Kim, J., Ha, S., and Park, W. (2018). Expression and deletion analyses of cspE encoding cold-shock protein E in Acinetobacter oleivorans DR1. *Res. Microbiol.* 169, 244–253. doi: 10.1016/j.resmic.2018.04.011

Kim, M. J., Lee, Y. K., Lee, H. K., and Im, H. (2007). Characterization of cold-shock protein a of Antarctic Streptomyces sp. AA8321. *Protein J.* 26, 51–59. doi: 10.1007/s10930-006-9044-1

Kloska, A., Cech, G. M., Sadowska, M., Krause, K., Szalewska-Pałasz, A., and Olszewski, P. (2020). Adaptation of the marine bacterium *Shewanella baltica* to low temperature stress. *Int. J. Mol. Sci.* 21:4338. doi: 10.3390/ijms21124338

Kohli, I., Joshi, N. C., Mohapatra, S., and Varma, A. (2020). Extremophile–an adaptive strategy for extreme conditions and applications. *Curr. Genomics* 21, 96–110. doi: 10.2174/1389202921666200401105908

Koutsioulis, D., Wang, E., Tzanodaskalaki, M., Nikiforaki, D., Deli, A., Feller, G., et al. (2008). Directed evolution on the cold adapted properties of TAB5 alkaline phosphatase. *Protein Eng. Des. Sel.* 21, 319–327. doi: 10.1093/protein/gzn009

Králová, S. (2017). Role of fatty acids in cold adaptation of Antarctic psychrophilic Flavobacterium spp. *Syst. Appl. Microbiol.* 40, 329–333. doi: 10.1016/j.syapm.2017.06.001

Krucoń, T., Ruszkowska, Z., Pilecka, W., Szych, A., and Drewniak, Ł. (2023). Bioprospecting of the Antarctic *Bacillus subtilis* strain for potential application in leaching hydrocarbons and trace elements from contaminated environments based on functional and genomic analysis. *Environ. Res.* 227:115785. doi: 10.1016/j.envres.2023.115785

Kube, M., Chernikova, T. N., Al-Ramahi, Y., Beloqui, A., Lopez-Cortez, N., Guazzaroni, M. E., et al. (2013). Genome sequence and functional genomic analysis of the oil-degrading bacterium *Oleispira antarctica*. *Nat. Commun.* 4:2156. doi: 10.1038/ncomms3156

Kuddus, M. (2015). Cold-active microbial enzymes. *Biochem. Physiol.* 4:e132. doi: 10.4172/2168-9652.1000e132

Kuddus, M. (2018). Cold-active enzymes in food biotechnology: an updated mini review. *J. Appl. Biol.* 6, 58–63. doi: 10.7324/jabb.2018.60310

Kuddus, M., Arif, J. M., and Ramteke, P. W. (2011). An overview of cold-active microbial a-amylase: adaptation strategies and biotechnological potentials. *Biotechnology* 10, 246–258. doi: 10.3923/biotech.2011.246.258

Kulakova, L., Galkin, A., Kurihara, T., Yoshimura, T., and Esaki, N. (1999). Cold-active serine alkaline protease from the psychrotrophic bacterium Shewanella strain Ac10: gene cloning and enzyme purification and characterization. *Appl. Environ. Microbiol.* 65, 611–617. doi: 10.1128/aem.65.2.611-617.1999.5

Kumar, A., Mukhia, S., and Kumar, R. (2021). Industrial applications of cold-adapted enzymes: challenges, innovations and future perspective. *Biotech* 11, 1–18. doi: 10.1007/s13205-021-02929-y

Kumar, L., and Bharadvaja, N. (2019). "Enzymatic bioremediation: a smart tool to fight environmental pollutants" in *Smart Bioremediation Technologies* (Cambridge: Academic Press), 99–118.

Lee, C. W., Yoo, W., Park, S. H., Le, L. T. H. L., Jeong, C. S., Ryu, B. H., et al. (2019). Structural and functional characterization of a novel cold-active S-formylglutathione hydrolase (SfSFGH) homolog from *Shewanella frigidimarina*, a psychrophilic bacterium. *Microb. Cell Factories* 18, 1–13. doi: 10.1186/s12934-019-1190-1

Lee, G. L. Y., Zakaria, N. N., Futamata, H., Suzuki, K., Zulkharnain, A., Shaharuddin, N. A., et al. (2022). Metabolic pathway of phenol degradation of a cold-adapted Antarctic Bacteria, Arthrobacter sp. *Catalysts* 12:1422. doi: 10.3390/catal12111422

Lee, J., Cho, J., Cho, Y. J., Cho, A., Woo, J., Lee, J., et al. (2019). The latitudinal gradient in rock-inhabiting bacterial community compositions in Victoria land, Antarctica. *Sci. Total Environ.* 657, 731–738. doi: 10.1016/j.scitotenv.2018.12.073

Lemak, S., Tchigvintsev, A., Petit, P., Flick, R., Singer, A. U., Brown, G., et al. (2012). Structure and activity of the cold-active and anion-activated carboxyl esterase OLEI01171 from the oil-degrading marine bacterium *Oleispira antarctica*. *Biochem. J.* 445, 193–203. doi: 10.1042/bj20112113

Liao, Y., Williams, T. J., Ye, J., Charlesworth, J., Burns, B. P., Poljak, A., et al. (2016). Morphological and proteomic analysis of biofilms from the Antarctic archaeon, *Halorubrum lacusprofundi*. *Sci. Rep.* 6, 1–17. doi: 10.1038/srep37454

Li, J., Xiao, X., Zhou, M., and Zhang, Y. (2023). Strategy for the adaptation to stressful conditions of the novel isolated conditional Piezophilic strain *Halomonas titanicae* ANRCS81. *Appl. Environ. Microbiol.* 89, e01304–e01322. doi: 10.1128/aem.01304-22

Li, Q., Yan, Y., Liu, X., Zhang, Z., Tian, J., and Wu, N. (2020). Enhancing thermostability of a psychrophilic alpha-amylase by the structural energy optimization in the trajectories of molecular dynamics simulations. *Int. J. Biol. Macromol.* 142, 624–633. doi: 10.1016/j.ijbiomac.2019.10.004

Liu, C., Wang, X., Wang, X., and Sun, C. (2016). Acclimation of Antarctic Chlamydomonas to the sea-ice environment: a transcriptomic analysis. *Extremophiles* 20, 437–450. doi: 10.1007/s00792-016-0834-x

Lo Giudice, A., Michaud, L., De Pascale, D., De Domenico, M., Di Prisco, G., Fani, R., et al. (2006). Lipolytic activity of Antarctic cold-adapted marine bacteria (Terra Nova Bay, Ross Sea). *J. Appl. Microbiol.* 101, 1039–1048. doi: 10.1111/j.1365-2672.2006.03006.x

Lo Giudice, A., Poli, A., Finore, I., and Rizzo, C. (2020). Peculiarities of extracellular polymeric substances produced by Antarctic bacteria and their possible applications. *Appl. Microbiol. Biotechnol.* 104, 2923–2934. doi: 10.1007/s00253-020-10448-8

Maeda, H., Hosokawa, M., Sashima, T., Murakami-Funayama, K., and Miyashita, K. (2009). Anti-obesity and anti-diabetic effects of fucoxanthin on diet-induced obesity conditions in a murine model. *Mol. Med. Rep.* 2, 897–902. doi: 10.3892/mmr_00000189

Malard, L. A., and Pearce, D. A. (2018). Microbial diversity and biogeography in Arctic soils. *Environ. Microbiol. Rep.* 10, 611–625. doi: 10.1111/1758-2229.12680

Mangiagalli, M., Bar-Dolev, M., Tedesco, P., Natalello, A., Kaleda, A., Brocca, S., et al. (2017). Cryo-protective effect of an ice-binding protein derived from Antarctic bacteria. *FEBS J.* 284, 163–177. doi: 10.1111/febs.13965

Mangiagalli, M., Lapi, M., Maione, S., Orlando, M., Brocca, S., Pesce, A., et al. (2021). The co-existence of cold activity and thermal stability in an Antarctic GH42 β-galactosidase relies on its hexameric quaternary arrangement. *FEBS J.* 288, 546–565. doi: 10.1111/febs.15354

Mangiagalli, M., and Lotti, M. (2021). Cold-active β-galactosidases: insight into cold adaptation mechanisms and biotechnological exploitation. *Mar. Drugs* 19:43. doi: 10.3390/md19010043

Marcoleta, A. E., Arros, P., Varas, M. A., Costa, J., Rojas-Salgado, J., Berríos-Pastén, C., et al. (2022). The highly diverse Antarctic peninsula soil microbiota as a source of novel resistance genes. *Sci. Total Environ.* 810:152003. doi: 10.1016/j.scitotenv.2021.152003

Marizcurrena, J. J., Herrera, L. M., Costábile, A., Morales, D., Villadóniga, C., Eizmendi, A., et al. (2019). Validating biochemical features at the genome level in the Antarctic bacterium Hymenobacter sp. strain UV11. *FEMS Microbiology Letters* 366. doi: 10.1093/femsle/fnz177

Martínez-Pérez, C., Greening, C., Bay, S. K., Lappan, R. J., Zhao, Z., De Corte, D., et al. (2022). Phylogenetically and functionally diverse microorganisms reside under the Ross ice shelf. *Nat. Commun.* 13:117. doi: 10.1038/s41467-021-27769-5

Martínez-Rosales, C., Fullana, N., Musto, H., and Castro-Sowinski, S. (2012). Antarctic DNA moving forward: genomic plasticity and biotechnological potential. *FEMS Microbiol. Lett.* 331, 1–9. doi: 10.1111/j.1574-6968.2012.02531.x

Médigue, C., Krin, E., Pascal, G., Barbe, V., Bernsel, A., Bertin, P. N., et al. (2005). Coping with cold: the genome of the versatile marine Antarctica bacterium *Pseudoalteromonas haloplanktis* TAC125. *Genome Res.* 15, 1325–1335. doi: 10.1101/gr.4126905

Merino, C., Kuzyakov, Y., Godoy, K., Jofré, I., Nájera, F., and Matus, F. (2021). Iron-reducing bacteria decompose lignin by electron transfer from soil organic matter. *Sci. Total Environ.* 761:143194. doi: 10.1016/j.scitotenv.2020.143194

Merlino, A., Krauss, I. R., Castellano, I., De Vendittis, E., Rossi, B., Conte, M., et al. (2010). Structure and flexibility in cold-adapted iron superoxide dismutases: the case of the enzyme isolated from *Pseudoalteromonas haloplanktis*. *J. Struct. Biol.* 172, 343–352. doi: 10.1016/j.jsb.2010.08.008

Millan, G. C. L., Veras, F. F., Stincone, P., Pailliè-Jiménez, M. E., and Brandelli, A. (2022). Biological activities of whey protein hydrolysate produced by protease from the Antarctic bacterium Lysobacter sp. A03. Biocatalysis and agricultural. *Biotechnology* 43:102415. doi: 10.1016/j.bcab.2022.102415

Miri, S., Naghdi, M., Rouissi, T., Kaur Brar, S., and Martel, R. (2019). Recent biotechnological advances in petroleum hydrocarbons degradation under cold climate conditions: a review. *Crit. Rev. Environ. Sci. Technol.* 49, 553–586. doi: 10.1080/10643389.2018.1552070

Miyazaki, K., Wintrode, P. L., Grayling, R. A., Rubingh, D. N., and Arnold, F. H. (2000). Directed evolution study of temperature adaptation in a psychrophilic enzyme. *J. Mol. Biol.* 297, 1015–1026. doi: 10.1006/jmbi.2000.3612

Morozova, O. V., Andreeva, I. S., Zhirakovskiy, V. Y., Pechurkina, N. I., Puchkova, L. I., Saranina, I. V., et al. (2022). Antibiotic resistance and cold-adaptive enzymes of Antarctic culturable bacteria from King George Island. *Pol. Sci.* 31:100756. doi: 10.1016/j.polar.2021.100756

Moyer, C. L., and Morita, R. Y. (2007). *Psychrophiles and psychrotrophs. Encyclopedia of Life Science, 1*. John Wiley & Sons, Ltd. Hoboken, NJ

Mozzicafreddo, M., Pucciarelli, S., Swart, E. C., Piersanti, A., Emmerich, C., Migliorelli, G., et al. (2021). The macronuclear genome of the Antarctic psychrophilic marine ciliate Euplotes focardii reveals new insights on molecular cold adaptation. *Sci. Rep.* 11:18782. doi: 10.1038/s41598-021-98168-5

Muller-Greven, J. C., Post, M. A., and Kubu, C. J. (2013). U.S. patent no. 8,486,665. Washington, DC: U.S. patent and trademark office

Murray, A. E., Lo, C. C., Daligault, H. E., Avalon, N. E., Read, R. W., Davenport, K. W., et al. (2021). Discovery of an Antarctic ascidian-associated uncultivated Verrucomicrobia with antimelanoma palmerolide biosynthetic potential. *Msphere* 6, e00759–e00721. doi: 10.1128/mSphere.00759-21

Nair, S., and Abraham, J. (2020). "Natural products from actinobacteria for drug discovery" in *Advances in Pharmaceutical Biotechnology: Recent Progress and Future Applications*. eds. J. K. Patra, A. C. Shukla and G. Das (Singapore: Springer), 333–363.

Narinx, E., Davail, S., Feller, G., and Gerday, C. (1992). Nucleotide and derived amino acid sequence of the subtilisin from the Antarctic psychrotroph Bacillus TA39. *Biochim. Biophys. Acta* 1131, 111–113. doi: 10.1016/0167-4781(92)90108-c

Nielsen, P. H. (2005). Life cycle assessment supports cold-wash enzymes. *SÖFW-J.* 131, 24–26.

Nikolaivits, E., Taxeidis, G., Gkountela, C., Vouyiouka, S., Maslak, V., Nikodinovic-Runic, J., et al. (2022). A polyesterase from the Antarctic bacterium Moraxella sp. degrades highly crystalline synthetic polymers. *J. Hazard. Mater.* 434:128900. doi: 10.1016/j.jhazmat.2022.128900

Nimkande, V. D., Sivanesan, S., and Bafana, A. (2023). Screening, identification, and characterization of lipase-producing halotolerant *Bacillus altitudinis* Ant19 from Antarctic soil. *Arch. Microbiol.* 205:113. doi: 10.1007/s00203-023-03453-8

Oikawa, T., Yamamoto, N., Shimoke, K., Uesato, S., Ikeuchi, T., and Fujioka, T. (2005). Purification, characterization, and overexpression of psychrophilic and thermolabile malate dehydrogenase of a novel Antarctic psychrotolerant, *Flavobacterium frigidimaris* KUC-1. *Biosci. Biotechnol. Biochem.* 69, 2146–2154. doi: 10.1271/bbb.69.2146

Orellana-Saez, M., Pacheco, N., Costa, J. I., Mendez, K. N., Miossec, M. J., Meneses, C., et al. (2019). In-Depth Genomic and Phenotypic Characterization of the Antarctic Psychrotolerant Strain Pseudomonas sp. MPC6 Reveals Unique Metabolic Features, Plasticity, and Biotechnological Potential. *Front. Microbiol.* 10. doi: 10.3389/fmicb.2019.01154

Orlando, M., Pucciarelli, S., and Lotti, M. (2020). Endolysins from Antarctic Pseudomonas display lysozyme activity at low temperature. *Mar. Drugs* 18:579. doi: 10.3390/md18110579

Otur, Ç., Okay, S., and Kurt-Kızıldoğan, A. (2023). Whole genome analysis of Flavobacterium aziz-sancarii sp. nov., isolated from Ardley Island (Antarctica), revealed a rich resistome and bioremediation potential. *Chemosphere* 313:137511. doi: 10.1016/j.chemosphere.2022.137511

Pandey, N., Jain, R., Pandey, A., and Tamta, S. (2018). Optimisation and characterisation of the orange pigment produced by a cold adapted strain of Penicillium sp. (GBPI_P155) isolated from mountain ecosystem. *Mycology* 9, 81–92. doi: 10.1080/21501203.2017.1423127

Parra, L. P., Espina, G., Devia, J., Salazar, O., Andrews, B., and Asenjo, J. A. (2015). Identification of lipase encoding genes from Antarctic seawater bacteria using degenerate primers: expression of a cold-active lipase with high specific activity. *Enzym. Microb. Technol.* 68, 56–61. doi: 10.1016/j.enzmictec.2014.10.004

Parra, L. P., Reyes, F., Acevedo, J. P., Salazar, O., Andrews, B. A., and Asenjo, J. A. (2008). Cloning and fusion expression of a cold-active lipase from marine Antarctic origin. *Enzym. Microb. Technol.* 42, 371–377. doi: 10.1016/j.enzmictec.2007.11.003

Pasquet, V., Morisset, P., Ihammouine, S., Chepied, A., Aumailley, L., Berard, J. B., et al. (2011). Antiproliferative activity of violaxanthin isolated from bioguided fractionation of *Dunaliella tertiolecta* extracts. *Mar. Drugs* 9, 819–831. doi: 10.3390/md9050819

Paun, V. I., Banciu, R. M., Lavin, P., Vasilescu, A., Fanjul-Bolado, P., and Purcarea, C. (2022). Antarctic aldehyde dehydrogenase from Flavobacterium PL002 as a potent catalyst for acetaldehyde determination in wine. *Sci. Rep.* 12:17301. doi: 10.1038/s41598-022-22289-8

Pereira, J. Q., Ambrosini, A., Passaglia, L. M. P., and Brandelli, A. (2017). A new cold-adapted serine peptidase from Antarctic Lysobacter sp. A03: insights about enzyme activity at low temperatures. *Int. J. Biol. Macromol.* 103, 854–862. doi: 10.1016/j.ijbiomac.2017.05.142

Petratos, K., Gessmann, R., Daskalakis, V., Papadovasilaki, M., Papanikolau, Y., Tsigos, I., et al. (2020). Structure and dynamics of a thermostable alcohol dehydrogenase from the Antarctic Psychrophile Moraxella sp. TAE123. ACS. *Omega* 5, 14523–14534. doi: 10.1021/acsomega.0c01210

Piette, F., D'Amico, S., Mazzucchelli, G., Danchin, A., Leprince, P., and Feller, G. (2011). Life in the cold: a proteomic study of cold-repressed proteins in the Antarctic bacterium *Pseudoalteromonas haloplanktis* TAC125. *Appl. Environ. Microbiol.* 77, 3881–3883. doi: 10.1128/aem.02757-10

Plaza, D. O., Gallardo, C., Straub, Y. D., Bravo, D., and Pérez-Donoso, J. M. (2016). Biological synthesis of fluorescent nanoparticles by cadmium and tellurite resistant Antarctic bacteria: exploring novel natural nanofactories. *Microb. Cell Factories* 15, 1–11. doi: 10.1186/s12934-016-0477-8

Prayogo, F. A., Budiharjo, A., Kusumaningrum, H. P., Wijanarka, W., Suprihadi, A., and Nurhayati, N. (2020). Metagenomic applications in exploration and development of novel enzymes from nature: a review. *J. Genet. Eng. Biotechnol.* 18, 1–10. doi: 10.1186/s43141-020-00043-9

Pucciarelli, S., Devaraj, R. R., Mancini, A., Ballarini, P., Castelli, M., Schrallhammer, M., et al. (2015). Microbial consortium associated with the Antarctic marine ciliate Euplotes focardii: an investigation from genomic sequences. *Microb. Ecol.* 70, 484–497. doi: 10.1007/s00248-015-0568-9

Ramasamy, K. P., Telatin, A., Mozzicafreddo, M., Miceli, C., and Pucciarelli, S. (2019). Draft genome sequence of a new Pseudomonas sp. strain, ef1, associated with the psychrophilic Antarctic ciliate Euplotes focardii. *Microbiol. Resour. Announc.* 8, e00867–e00819. doi: 10.1128/mra.00867-19

Ramya, L. N., and Pulicherla, K. K. (2015). Molecular insights into cold active polygalacturonase enzyme for its potential application in food processing. *J. Food Sci. Technol.* 52, 5484–5496. doi: 10.1007/s13197-014-1654-6

Ray, M. K., Sitaramamma, T., Ghandhi, S., and Shivaji, S. (1994). Occurrence and expression of cspA, a cold shock gene, in Antarctic psychrotropic bacteria. *FEMS Microbiol. Lett.* 116, 55–60. doi: 10.1111/j.1574-6968.1994.tb06675.x

Raymond, J. A., Fritsen, C., and Shen, K. (2007). An ice-binding protein from an Antarctic Sea ice bacterium. *FEMS Microbiol. Ecol.* 61, 214–221. doi: 10.1111/j.1574-6941.2007.00345.x

Rentier-Delrue, F., Mande, S. C., Moyens, S., Terpstra, P., Mainfroid, V., Goraj, K., et al. (1993). Cloning and overexpression of the triosephosphate isomerase genes from psychrophilic and thermophilic bacteria: structural comparison of the predicted protein sequences. *J. Mol. Biol.* 229, 85–93. doi: 10.1006/jmbi.1993.1010

Riccardi, C., Calvanese, M., Ghini, V., Alonso-Vásquez, T., Perrin, E., Turano, P., et al. (2023). Metabolic robustness to growth temperature of a cold-adapted marine bacterium. *Msystems* 8, e01124–e01122. doi: 10.1128/msystems.01124-22

Riccardi, C., D'Angelo, C., Calvanese, M., Ricciardelli, A., Tutino, M. L., Parrilli, E., et al. (2022). Genome analysis of a new biosurfactants source: the Antarctic bacterium Psychrobacter sp. TAE2020. *Mar. Genomics* 61:100922. doi: 10.1016/j.margen.2021.100922

Ricciardelli, A., Casillo, A., Vergara, A., Balasco, N., Corsaro, M. M., Tutino, M. L., et al. (2019). Environmental conditions shape the biofilm of the Antarctic bacterium *Pseudoalteromonas haloplanktis* TAC125. *Microbiol. Res.* 218, 66–75. doi: 10.1016/j.micres.2018.09.010

Rina, M., Pozidis, C., Mavromatis, K., Tzanodaskalaki, M., Kokkinidis, M., and Bouriotis, V. (2000). Alkaline phosphatase from the Antarctic strain TAB5: properties and psychrophilic adaptations. *Eur. J. Biochem.* 267, 1230–1238. doi: 10.1046/j.1432-1327.2000.01127.x

Sajjad, W., Din, G., Rafiq, M., Iqbal, A., Khan, S., Zada, S., et al. (2020). Pigment production by cold-adapted bacteria and fungi: colorful tale of cryosphere with wide range applications. *Extremophiles* 24, 447–473. doi: 10.1007/s00792-020-01180-2

Sarmiento, F., Peralta, R., and Blamey, J. M. (2015). Cold and hot extremozymes: industrial relevance and current trends. *Front. Bioeng. Biotechnol.* 3:148. doi: 10.3389/fbioe.2015.00148

See Too, W. C., and Few, L. L. (2010). Cloning of triose phosphate isomerase gene from an Antarctic psychrophilic Pseudomonas sp. by degenerate and splinkerette PCR. *World J. Microbiol. Biotechnol.* 26, 1251–1259. doi: 10.1007/s11274-009-0295-9

Sheridan, P. P., and Brenchley, J. E. (2000). Characterization of a salt-tolerant family 42 β-galactosidase from a psychrophilic Antarctic Planococcus isolate. *Appl. Environ. Microbiol.* 66, 2438–2444. doi: 10.1128/AEM.66.6.2438-2444.2000

Silva, T. R. E., Silva, L. C. F., de Queiroz, A. C., Alexandre Moreira, M. S., de Carvalho Fraga, C. A., de Menezes, G. C. A., et al. (2021). Pigments from Antarctic bacteria and their biotechnological applications. *Crit. Rev. Biotechnol.* 41, 809–826. doi: 10.1080/07388551.2021.1888068

Silva, T. R., Tavares, R. S., Canela-Garayoa, R., Eras, J., Rodrigues, M. V., Neri-Numa, I. A., et al. (2019). Chemical characterization and biotechnological applicability of pigments isolated from Antarctic bacteria. *Mar. Biotechnol.* 21, 416–429. doi: 10.1007/s10126-019-09892-z

Sivasankar, P., Poongodi, S., Sivakumar, K., Al-Qahtani, W. H., Arokiyaraj, S., and Jothiramalingam, R. (2022). Exogenous production of cold-active cellulase from polar Nocardiopsis sp. with increased cellulose hydrolysis efficiency. *Arch. Microbiol.* 204:218. doi: 10.1007/s00203-022-02830-z

Solar Venero, E. C., Matera, G., Vogel, J., López, N. I., and Tribelli, P. M. (2022). Small RNAs in the Antarctic bacterium *Pseudomonas extremaustralis* responsive to oxygen availability and oxidative stress. *Environ. Microbiol. Rep.* 14, 604–615. doi: 10.1111/1758-2229.13084

Song, W., Lin, X., and Huang, X. (2012). Characterization and expression analysis of three cold shock protein (CSP) genes under different stress conditions in the Antarctic bacterium Psychrobacter sp. *G. Polar Biology* 35, 1515–1524. doi: 10.1007/s00300-012-1191-6

Soontornchaiboon, W., Joo, S. S., and Kim, S. M. (2012). Anti-inflammatory effects of violaxanthin isolated from microalga *Chlorella ellipsoidea* in RAW 264.7 macrophages. *Biol. Pharm. Bull.* 35, 1137–1144. doi: 10.1248/bpb.b12-00187

Stokes, C. R., Abram, N. J., Bentley, M. J., Edwards, T. L., England, M. H., Foppert, A., et al. (2022). Response of the East Antarctic ice sheet to past and future climate change. *Nature* 608, 275–286. doi: 10.1038/s41586-022-04946-0

Styczynski, M., Rogowska, A., Gieczewska, K., Garstka, M., Szakiel, A., and Dziewit, L. (2020). Genome-based insights into the production of carotenoids by Antarctic bacteria,

Planococcus sp. ANT_H30 and Rhodococcus sp. ANT_H53B. *Molecules* 25:4357. doi: 10.3390/molecules25194357

Styczynski, M., Rogowska, A., Nyabayo, C., Decewicz, P., Romaniuk, F., Pączkowski, C., et al. (2022). Heterologous production and characterization of a pyomelanin of Antarctic Pseudomonas sp. ANT_H4: a metabolite protecting against UV and free radicals, interacting with iron from minerals and exhibiting priming properties toward plant hairy roots. *Microb. Cell Factories* 21, 1–17. doi: 10.1186/s12934-022-01990-3

Sutherland, B. J., Finke, J. F., Saunders, R., Warne, S., Schulze, A. D., Strohm, J. H., et al. (2022). Metatranscriptomics reveals a shift in microbial community composition and function during summer months in a coastal marine environment. *Environ. DNA*. doi: 10.1002/edn3.353

Sutthiwong, N., Fouillaud, M., Valla, A., Caro, Y., and Dufossé, L. (2014). Bacteria belonging to the extremely versatile genus Arthrobacter as novel source of natural pigments with extended hue range. *Food Res. Int.* 65, 156–162. doi: 10.1016/j.foodres.2014.06.024

Takara-Clontech. Available at: https://www.takarabio.com/products/cloning/modifying-enzymes/nucleases/cryonasecold-active-nuclease

Tang, Y., Wu, P., Jiang, S., Selvaraj, J. N., Yang, S., and Zhang, G. (2019). A new cold-active and alkaline pectate lyase from Antarctic bacterium with high catalytic efficiency. *Appl. Microbiol. Biotechnol.* 103, 5231–5241. doi: 10.1007/s00253-019-09803-1

Tedesco, P., Maida, I., Palma Esposito, F., Tortorella, E., Subko, K., Ezeofor, C. C., et al. (2016). Antimicrobial activity of monoramnholipids produced by bacterial strains isolated from the Ross Sea (Antarctica). *Mar. Drugs* 14:83. doi: 10.3390/md14050083

Tengku-Mazuki, T. A., Subramaniam, K., Zakaria, N. N., Convey, P., Abdul Khalil, K., Lee, G. L. Y., et al. (2020). Optimization of phenol degradation by Antarctic bacterium Rhodococcus sp. *Antarctic Science* 32, 486–495. doi: 10.1017/s0954102020000358

Teoh, C. P., Lavin, P., Lee, D. J. H., González-Aravena, M., Najimudin, N., Lee, P. C., et al. (2021). Genomics and transcriptomics analyses provide insights into the cold adaptation strategies of an Antarctic bacterium, Cryobacterium sp. SO1. *Polar. Biol.* 44, 1305–1319. doi: 10.1007/s00300-021-02883-8

Terashima, M., Ohashi, K., Takasuka, T. E., Kojima, H., and Fukui, M. (2019). Antarctic heterotrophic bacterium Hymenobacter nivis P3T displays light-enhanced growth and expresses putative photoactive proteins. *Environ. Microbiol. Rep.* 11, 227–235. doi: 10.1111/1758-2229.12702

Tribelli, P. M., Pezzoni, M., Brito, M. G., Montesinos, N. V., Costa, C. S., and López, N. I. (2020). Response to lethal UVA radiation in the Antarctic bacterium *Pseudomonas extremaustralis*: polyhydroxybutyrate and cold adaptation as protective factors. *Extremophiles* 24, 265–275. doi: 10.1007/s00792-019-01152-1

Tsigos, I., Velonia, K., Smonou, I., and Bouriotis, V. (1998). Purification and characterization of an alcohol dehydrogenase from the Antarctic psychrophile Moraxella sp. TAE123. *Eur. J. Biochem.* 254, 356–362. doi: 10.1046/j.1432-1327.1998.2540356.x

Tsuruta, H., Mikami, B., Higashi, T., and Aizono, Y. (2010). Crystal structure of cold-active alkaline phosphatase from the psychrophile Shewanella sp. *Biosci. Biotechnol. Biochem.* 74, 69–74. doi: 10.1271/bbb.90563

Turkiewicz, M., Gromek, E., Kalinowska, H., and Zielińska, M. (1999). Biosynthesis and properties of an extracellular metalloprotease from the Antarctic marine bacterium *Sphingomonas paucimobilis*. *J. Biotechnol.* 70, 53–60. doi: 10.1016/s0168-1656(99)00057-7

Turkiewicz, M., Kur, J., Białkowska, A., Cieśliński, H., Kalinowska, H., and Bielecki, S. (2003). Antarctic marine bacterium Pseudoalteromonas sp. 22b as a source of cold-adapted β-galactosidase. *Biomol. Eng.* 20, 317–324. doi: 10.1016/s1389-0344(03)00039-x

Uma, S., Jadhav, R. S., Seshu Kumar, G., Shivaji, S., and Ray, M. K. (1999). A RNA polymerase with transcriptional activity at 0 °C from the Antarctic bacterium *Pseudomonas syringae*. *FEBS Lett.* 453, 313–317. doi: 10.1016/s0014-5793(99)00660-2

Van Truong, L., Tuyen, H., Helmke, E., Binh, L. T., and Schweder, T. (2001). Cloning of two pectate lyase genes from the marine Antarctic bacterium *Pseudoalteromonas haloplanktis* strain ANT/505 and characterization of the enzymes. *Extremophiles* 5, 35–44. doi: 10.1007/s007920000170

Vasquez, Y. M. S. C., Gomes, M. B., E Silva, T. RDuarte, A. W. F., Rosa, L. H., and de Oliveira, V. M. (2021). Cold-adapted chitinases from Antarctic bacteria: taxonomic assessment and enzyme production optimization. *Biocatal. Agric. Biotechnol.* 34:102029. doi: 10.1016/j.bcab.2021.102029

Venil, C. K., Zakaria, Z. A., and Ahmad, W. A. (2013). Bacterial pigments and their applications. *Process Biochem.* 48, 1065–1079. doi: 10.1016/j.procbio.2013.06.006

Violot, S., Aghajari, N., Czjzek, M., Feller, G., Sonan, G. K., Gouet, P., et al. (2005). Structure of a full length psychrophilic cellulase from *Pseudoalteromonas haloplanktis* revealed by X-ray diffraction and small angle X-ray scattering. *J. Mol. Biol.* 348, 1211–1224. doi: 10.1016/j.jmb.2005.03.026

Wang, J., Ma, Y., Yang, J., Jin, L., Gao, Z., Xue, L., et al. (2019). Fucoxanthin inhibits tumour-related lymphangiogenesis and growth of breast cancer. *J. Cell. Mol. Med.* 23, 2219–2229. doi: 10.1111/jcmm.14151

Wang, Q. F., Hou, Y. H., Xu, Z., Miao, J. L., and Li, G. Y. (2008). Purification and properties of an extracellular cold-active protease from the psychrophilic bacterium Pseudoalteromonas sp. NJ276. *Biochem. Eng. J.* 38, 362–368. doi: 10.1016/j.bej.2007.07.025

Wang, Q. F., Miao, J. L., Hou, Y. H., Ding, Y., Wang, G. D., and Li, G. Y. (2005). Purification and characterization of an extracellular cold-active serine protease from the psychrophilic bacterium Colwellia sp. NJ341. *Biotechnol. Lett.* 27, 1195–1198. doi: 10.1007/s10529-005-0016-x

Wang, Q., Nie, P., Hou, Y., and Wang, Y. (2020). Purification, biochemical characterization and DNA protection against oxidative damage of a novel recombinant superoxide dismutase from psychrophilic bacterium Halomonas sp. ANT108. *Protein Expr. Purif.* 173:105661. doi: 10.1016/j.pep.2020.105661

Wang, W., Mu, H., Ren, X., Ouyang, Q., and Li, J. (2023). Genome-based classification of Pedobacter polysaccharideus sp. nov., isolated from Antarctic soil producing exopolysaccharide. *FEMS Microbiol. Lett.* 370, fnad031. doi: 10.1093/femsle/fnad031

Wang, W., Sun, M., Liu, W., and Zhang, B. (2008). Purification and characterization of a psychrophilic catalase from Antarctic Bacillus. *Can. J. Microbiol.* 54, 823–828. doi: 10.1139/w08-066

Wang, X., He, Y., Deng, Y., Zuo, Z., Li, D., Chen, F., et al. (2022). A diguanylate cyclase regulates biofilm formation in Rhodococcus sp. NJ-530 from Antarctica. *Biotech* 12, 1–10. doi: 10.1007/s13205-021-03093-z

Wang, X., Kan, G., Ren, X., Yu, G., Shi, C., Xie, Q., et al. (2018a). Molecular cloning and characterization of a novel α-amylase from Antarctic Sea ice bacterium Pseudoalteromonas sp. M175 and its primary application in detergent. *Biomed. Res. Int.* 2018:3258383. doi: 10.1155/2018/3258383

Wang, Y., Han, H., Cui, B., Hou, Y., Wang, Y., and Wang, Q. (2017). A glutathione peroxidase from Antarctic psychrotrophic bacterium Pseudoalteromonas sp. ANT506: cloning and heterologous expression of the gene and characterization of recombinant enzyme. *Bioengineered* 8, 742–749. doi: 10.1080/21655979.2017.1373534

Wang, Y., Hou, Y., Nie, P., Wang, Y., Ren, X., Wei, Q., et al. (2019). A novel cold-adapted and salt-tolerant RNase R from Antarctic Sea-ice bacterium Psychrobacter sp. Ant206. *Molecules* 24:2229. doi: 10.3390/molecules24122229

Wang, Y., Hou, Y., Wang, Y., Zheng, L., Xu, X., Pan, K., et al. (2018b). A novel cold-adapted leucine dehydrogenase from Antarctic Sea-ice bacterium Pseudoalteromonas sp. ANT178. *Mar. Drugs* 16:359. doi: 10.3390/md16100359

Wang, Y., Ma, L., He, J., Liu, Z., Weng, S., Wang, L., et al. (2021). Whole genome sequencing and comparative genomic analyses of Planococcus alpniumensis MSAK28401T, a new species isolated from Antarctic krill. *BMC Microbiol.* 21, 1–15. doi: 10.1186/s12866-021-02347-3

Waschulin, V., Borsetto, C., James, R., Newsham, K. K., Donadio, S., Corre, C., et al. (2022). Biosynthetic potential of uncultured Antarctic soil bacteria revealed through long read metagenomic sequencing. *ISME J.* 16, 101–111. doi: 10.1038/s41396-021-01052-3

Williams, T. J., Allen, M. A., Ivanova, N., Huntemann, M., Haque, S., Hancock, A. M., et al. (2021). Genome analysis of a verrucomicrobial endosymbiont with a tiny genome discovered in an Antarctic Lake. *Front. Microbiol.* 12:674758. doi: 10.3389/fmicb.2021.674758

Williams, T. J., Allen, M. A., Panwar, P., and Cavicchioli, R. (2022). Into the darkness: the ecologies of novel 'microbial dark matter'phyla in an Antarctic Lake. *Environ. Microbiol.* 24, 2576–2603. doi: 10.1111/1462-2920.16026

Xiao, Y., Yan, F., Cui, Y., Du, J., Hu, G., Zhai, W., et al. (2023). A symbiotic bacterium of Antarctic fish reveals environmental adaptability mechanisms and biosynthetic potential towards antibacterial and cytotoxic activities. *Front. Microbiol.* 13:1085063. doi: 10.3389/fmicb.2022.1085063

Xuezheng, L., Shuoshuo, C., Guoying, X., Shuai, W., Ning, D., and Jihong, S. (2010). Cloning and heterologous expression of two cold-active lipases from the Antarctic bacterium Psychrobacter sp. *G. Polar Res.* 29, 421–429. doi: 10.1111/j.1751-8369.2010.00189.x

Yang, X., Lin, X., Fan, T., Bian, J., and Huang, X. (2008). Cloning and expression of lipP, a gene encoding a cold-adapted lipase from Moritella sp. 2-5-10-1. *Curr. Microbiol.* 56, 194–198. doi: 10.1007/s00284-007-9051-2

Yoshimune, K., Galkin, A., Kulakova, L., Yoshimura, T., and Esaki, N. (2005). Cold-active DnaK of an Antarctic psychrotroph Shewanella sp. Ac10 supporting the growth of dnaK-null mutant of *Escherichia coli* at cold temperatures. *Extremophiles* 9, 145–150. doi: 10.1007/s00792-004-0429-9

Yusof, N. A., Hashim, N. H. F., and Bharudin, I. (2021). Cold adaptation strategies and the potential of psychrophilic enzymes from the Antarctic yeast, Glaciozyma antarctica PI12. *J. Fungi* 7:528. doi: 10.3390/jof7070528

Zhang, A., Hou, Y., Wang, Q., and Wang, Y. (2022). Characteristics and polyethylene biodegradation function of a novel cold-adapted bacterial laccase from Antarctic Sea ice psychrophile Psychrobacter sp. NJ228. *J. Hazard. Mater.* 439:129656. doi: 10.1016/j.jhazmat.2022.129656

Zhang, J., Lin, S., and Zeng, R. (2007). Cloning, expression, and characterization of a cold-adapted lipase gene from an Antarctic deep-sea psychrotrophic bacterium, Psychrobacter sp. 7195. *J. Microbiol. Biotechnol.* 17, 604–610.

Zheng, Z., Jiang, Y. H., Miao, J. L., Wang, Q. F., Zhang, B. T., and Li, G. Y. (2006). Purification and characterization of a cold-active iron superoxide dismutase from a psychrophilic bacterium, Marinomonas sp. NJ522. *Biotechnol. Lett.* 28, 85–88. doi: 10.1007/s10529-005-4951-3

frontiers | Frontiers in Microbiology

TYPE Original Research
PUBLISHED 31 August 2023
DOI 10.3389/fmicb.2023.1241826

OPEN ACCESS

EDITED BY
Trista J. Vick-Majors,
Michigan Technological University,
United States

REVIEWED BY
Alessandra Norici,
Marche Polytechnic University, Italy
Charles Bachy,
GEOMAR Helmholtz Center for Ocean Research Kiel, Helmholtz Association of German Research Centres (HZ), Germany
Josef Elster,
University of South Bohemia in České Budějovice, Czechia

*CORRESPONDENCE
Ulf Karsten
✉ ulf.karsten@uni-rostock.de

†These authors have contributed equally to this work and share first authorship

RECEIVED 17 June 2023
ACCEPTED 08 August 2023
PUBLISHED 31 August 2023

CITATION
Juchem DP, Schimani K, Holzinger A, Permann C, Abarca N, Skibbe O, Zimmermann J, Graeve M and Karsten U (2023) Lipid degradation and photosynthetic traits after prolonged darkness in four Antarctic benthic diatoms, including the newly described species *Planothidium wetzelii* sp. nov. *Front. Microbiol.* 14:1241826. doi: 10.3389/fmicb.2023.1241826

Lipid degradation and photosynthetic traits after prolonged darkness in four Antarctic benthic diatoms, including the newly described species *Planothidium wetzelii* sp. nov.

Desirée P. Juchem[1†], Katherina Schimani[2†], Andreas Holzinger[3], Charlotte Permann[3], Nélida Abarca[2], Oliver Skibbe[2], Jonas Zimmermann[2], Martin Graeve[4] and Ulf Karsten[1*]

[1]Applied Ecology and Phycology, Institute of Biological Sciences, University of Rostock, Rostock, Germany, [2]Botanischer Garten und Botanisches Museum Berlin, Freie Universität Berlin, Berlin, Germany, [3]Department of Botany, Functional Plant Biology, University of Innsbruck, Innsbruck, Austria, [4]Alfred-Wegener-Institute Helmholtz-Center for Polar and Marine Research, Ecological Chemistry, Bremerhaven, Germany

In polar regions, the microphytobenthos has important ecological functions in shallow-water habitats, such as on top of coastal sediments. This community is dominated by benthic diatoms, which contribute significantly to primary production and biogeochemical cycling while also being an important component of polar food webs. Polar diatoms are able to cope with markedly changing light conditions and prolonged periods of darkness during the polar night in Antarctica. However, the underlying mechanisms are poorly understood. In this study, five strains of Antarctic benthic diatoms were isolated in the field, and the resulting unialgal cultures were identified as four distinct species, of which one is described as a new species, *Planothidium wetzelii* sp. nov. All four species were thoroughly examined using physiological, cell biological, and biochemical methods over a fully controlled dark period of 3 months. The results showed that the utilization of storage lipids is one of the key mechanisms in Antarctic benthic diatoms to survive the polar night, although different fatty acids were involved in the investigated taxa. In all tested species, the storage lipid content declined significantly, along with an ultrastructurally observable degradation of the chloroplasts. Surprisingly, photosynthetic performance did not change significantly despite chloroplasts decreasing in thylakoid membranes and an increased number of plastoglobules. Thus, a combination of biochemical and cell biological mechanisms allows Antarctic benthic diatoms to survive the polar night.

KEYWORDS

Antarctica, benthic diatoms, photosynthesis, polar night, lipid consumption, plastid degradation

1. Introduction

The polar regions represent unique ecosystems characterized by low temperatures, ice and snow cover, and pronounced seasonal fluctuations in light availability with long periods of complete darkness during the polar night. The abiotic factor of light is especially challenging for autotrophic primary producers living in polar regions. Regional ice and snow cover can further extend the dark period for organisms (Cottier and Potter, 2020). If sea ice is covered with snow, photon fluence rates can be reduced to 2% of the solar surface radiation, leaving the organisms underneath exposed to extremely low light conditions or even darkness for up to 10 months in certain regions (Karsten et al., 2019a). Polar algae must, therefore, tolerate both very high light conditions after ice break-up and extremely low irradiances (Gómez et al., 2009; Zacher et al., 2009) and must have high adaptability to such fluctuating conditions in combination with always enhanced photosynthetic efficiency and plasticity (Longhi et al., 2003).

Diatoms are the most species-rich group of microalgae and dominate well-mixed water columns across all oceans as well as benthic algal communities of shallow-water soft bottoms, and rocky substrates (Lacour et al., 2019). They are responsible for ~20–25% of the global and 40–45% of the marine primary production (Nelson et al., 1995; Field et al., 1998), which reflects their important role in marine food webs and in the global carbon cycle as well as other biochemical cycles (Field et al., 1998; Armbrust, 2009). In depths down to 30 m, the primary production of microphytobenthic communities forms the main food source for benthic suspension or deposit feeders and thus plays a major role in the ecology of polar coastal habitats (Glud et al., 2009). Carbon budget measurements in Young Sound, Greenland, showed almost 50% of primary production originating from microphytobenthos (Glud et al., 2002), which could also be confirmed for the Arctic Kongsfjorden (Svalbard, Norway; Woelfel et al., 2010). In Antarctica, McMinn et al. (2012) described that in <5 m of water depth, benthic primary production exceeds that of phytoplankton or sea ice algae. Consequently, benthic diatoms play a crucial role in polar ecosystems and coastal food chains (Glud et al., 2009) but are still less studied compared to their planktonic or ice-associated counterparts. Marine Antarctic benthic diatoms are still poorly studied in terms of biodiversity, biogeography, and ecology, while for freshwater habitats, comprehensive datasets exist (Verleyen et al., 2021; Al-Handal et al., 2022).

Diatom taxa from different Arctic and Antarctic habitats, such as sea ice, water column, and soft bottom, are reported to survive long periods of complete darkness (Schaub et al., 2017, and literature therein). The species-specific maximum survival periods are highly variable, ranging from 3 months to 1 year, and benthic diatoms have been reported with the longest survival times (Antia, 1976). Experiments on the dark survival potential of different Arctic benthic diatom species indicated a high tolerance, i.e., survival for up to 5 months without light. Although chloroplast volume was strongly reduced with increasing dark treatment, *Cylindrotheca closterium* (Ehrenberg) Reimann and J. C. Lewin and *Surirella* cf. *minuta* showed high growth rates after a few days of lag phase after re-irradiation (Karsten et al., 2012; Schlie and Karsten, 2017). During the polar night, the reallocation of energy toward maintenance metabolism through the decomposition of organelle components or lipid droplets seems to be a key process for survival in benthic polar diatoms. The lag phase after transfer to light can be interpreted as a recovery period, in which diatom cells rebuild cellular structures and metabolic activity (Karsten et al., 2012). In order to maintain viability, not only organelles but also membranes and DNA must remain intact (McMinn and Martin, 2013). Benthic diatoms with intact plasmalemma can be distinguished from those with permeabilized membranes using the nucleic acid stain SYTOX Green, which only passes through compromised or damaged membranes, and stains the nucleus, leading to enhanced fluorescence under blue light excitation (Karsten et al., 2019a,b, and references therein). Application of the SYTOX Green stain to dark-incubated Arctic *Navicula directa* (W. Smith) Brébisson indicated that >95% of all cells exhibited intact membranes, even after 5 months of darkness, and hence, the high degree of membrane integrity contributed to long-term dark tolerance (Karsten et al., 2019a,b). Lower temperatures generally reduce the metabolic activity of all organisms, thereby enhancing the dark survival potential of polar benthic diatoms. Reeves et al. (2011) reported for Antarctic sea ice diatoms a reduced dark survival time at 10°C compared to −2°C but no negative effect at 4°C. *Fragilariopsis cylindrus* (Grunow ex Cleve) Helmcke and Krieger survived 60 days of darkness at both −2 and 4°C but only 7 days at 10°C (Reeves et al., 2011).

The physiological state in which polar diatoms survive the darkness and the underlying metabolic processes is still almost unstudied. In the few diatoms studied, different mechanisms have been described for coping with the polar night (McMinn and Martin, 2013). Those include the reduction of metabolic activity (Palmisano and Sullivan, 1982), the utilization of stored energy products (Palmisano and Sullivan, 1982; Schaub et al., 2017), formation of resting stages (Durbin, 1978; McQuoid and Hobson, 1996), and a mixotrophic lifestyle (Hellebust and Lewin, 1977; Tuchman et al., 2006). These adaptive mechanisms are not considered to be mutually exclusive, as they probably vary in relative importance among polar algae (Palmisano and Sullivan, 1983). The utilization of energy storage products, such as the typical reserve carbohydrate chrysolaminarin or lipids (triacylglycerol), the latter being stored in cell vacuoles and/or in cytoplasmic lipid droplets, could sustain the cellular maintenance metabolism during long periods of darkness. Schaub et al. (2017) confirmed in the Arctic benthic diatom *Navicula* cf. *perminuta* the preferential utilization of the stored lipid compound triacylglycerol during prolonged dark periods, but also the pool of free fatty acids.

Diatoms are well-known for their metabolic strategy to store energy as lipids, often as neutral triacylglycerol, which consist of a glycerin backbone esterified with three fatty acids and which are deposited in densely packed lipid droplets intracellularly located in the cytoplasm (Hu et al., 2008; Leyland et al., 2020). Lipids can store more energy per molecule compared to carbohydrates or proteins (Morales et al., 2021), and hence, high proportions of such lipid bodies have been described in polar diatoms from the water column and sea ice, particularly in late autumn prior to the onset of the polar night (Fryxell, 1989; Fahl and Kattner, 1993; Zhang et al., 1998), while Antarctic benthic diatoms are almost unstudied.

For the present study, five benthic diatom strains from King George Island, Antarctic Peninsula, were morphologically and molecularly identified and examined using physiological, cell biological, and biochemical methods to better understand the underlying mechanisms for coping with the polar night. Over a period of 3 months of experimental dark treatment, we evaluated photosynthesis, respiration, and chlorophyll *a* content, as well as ultrastructure, lipid body size, and volume in combination with fatty acid concentrations prior to and after the dark treatment. Based on previous studies in Arctic benthic diatoms (Schaub et al., 2017, and references therein), we expected a strong involvement of storage lipids in the survival of the polar night in Antarctic benthic diatoms. In addition, our study provides transmission electron microscopic images of these ecologically important primary producers to our knowledge for the first time.

2. Materials and methods

2.1. Description of the study site with ecological characterization

Sediment surface samples were taken from 28 January to 15 February 2020 from four study sites near the Argentinian research station Carlini Base (S 62°14′17.45", W 58°40′2.19") at Potter Cove on King George Island, Antarctic Peninsula, and used for benthic diatom isolation (Figure 1, Table 1). The marine culture D288_003 originated from sample location D288 (62° 14′ 30.55" S, 58° 40′ 54.96" W) and was isolated from a biofilm of an intertidal rock pool. D296_001 was isolated from a marine sample at the inner part of Potter Cove (62° 13′ 43.61" S, 58° 39′ 49.36" W), at 15 m depth, from an epipsammic community. The marine culture D323_018 originated from a sample location closer to the glacier front in the inner part of the bay at 10 m water depth from an epipsammic community (62°13′25.68" S, 58°38′33.50" W). Both limnic isolates (D300_015 and D300_025) were established from biofilms on top of stones in a freshwater drinking reservoir (62° 14′ 16.30" S, 58° 39′ 44.10" W).

At Carlini Base, various abiotic parameters were recorded. The minimum water temperature was −1.69°C in the inner part of Potter Cove and −1.4°C in the outer part, while the maximum temperature at both sites was 2.89 and 1.98°C, respectively. Furthermore, the salinity of the outer cove was stable at ∼33.5 S_A, while the salinity in the inner cove can decline to 29.6 S_A because of meltwater run-off (Hernández et al., 2019). Light conditions are diurnally and seasonally highly variable, and more recent data were published by Hoffmann et al. (2019).

2.2. Culture establishment

The diatom cells were isolated from aliquots of environmental samples to establish clonal cultures. Under an inverse light microscope (Olympus, Hamburg, Germany), single cells were transferred using microcapillary glass pipettes onto microwell plates containing culture medium [Guillard's f/2 medium (Guillard and Ryther, 1962) or Walne's medium (Walne, 1970), 34 S_A for marine samples and 1 S_A for freshwater samples]. All samples and isolated diatom cells from Antarctica were maintained at 5–7°C at the Botanische Museum Berlin. Irradiation was accomplished by white LEDs with 5,000 K under a 16/8 day/night cycle with several dark phases during the day to prevent photo-oxidative stress. After the successful establishment of clonal cultures, they were separated into subsamples for DNA extraction, morphological analysis, and ecophysiological, biochemical, and cell biological experiments. For all experimental approaches, diatom cultures were transferred to the University of Rostock and cultured in sterile-filtered Baltic Sea water, enriched with Guillard's f/2 medium (Guillard and Ryther, 1962) and metasilicate ($Na_2SiO_3 \bullet 5\ H_2O$; 10 g 100 mL^{-1}) to a final concentration of 0.6 mM (further referred to as culture media). The salinity of 33 S_A for the marine cultures was adjusted by adding artificial sea salt (hw-Marinemix® professional, Wiegandt GmbH, Germany), while 1 S_A for the limnic cultures was achieved by dilution with deionized water. The media were regularly changed to replenish nutrients.

All stock cultures at the University of Rostock were kept at 8–9°C and 15–20 μmol photons m^{-2} s^{-1} under a 16/8-h light/dark cycle [Osram Daylight Lumilux Cool White lamps L36W/840 (Osram, Munich, Germany)].

2.3. Taxonomic identification

In order to obtain clean diatom frustules for species identification, material harvested from the clonal cultures was treated with 35% (v/v) hydrogen peroxide at room temperature to oxidize the organic material, followed by several washing steps with distilled water. To prepare permanent slides for light microscopy (LM) analyses, the cleaned material (frustules and valves) was dispersed on cover glasses, dried at room temperature, and embedded with the high refraction index mounting medium Naphrax®.

For each culture, 15–20 cells were measured for morphometry. Observations were conducted with a Zeiss Axioplan Microscope equipped with differential interference contrast (DIC) using a Zeiss 100x/1.30 Plan Apochromat objective, while microphotographs were taken with an AXIOAM MRc camera. Aliquots of cleaned sample material for scanning electron microscopy (SEM) observations were mounted on stubs and observed under a Hitachi FE 8010 scanning electron microscope operated at 1.0 kV.

2.3.1. DNA extraction, amplification, sequencing, and processing

Clonal diatom material from log phase cultures was transferred to 1.5 mL tubes. DNA was isolated using the NucleoSpin® Plant II Mini Kit (Macherey and Nagel, Düren, Germany), following the manufacturer's instructions. DNA fragment size and concentrations were evaluated via gel electrophoresis (1.5% agarose gel) and NanoDrop® (Peqlab Biotechnology LLC; Erlangen, Germany), respectively. DNA samples were stored at −20°C until further use and finally deposited in the Berlin collection of the DNA Bank Network (Gemeinholzer et al., 2011).

DNA amplification was conducted by polymerase chain reaction (PCR) after Zimmermann et al. (2011) for the V4 region

10.3389/fmicb.2023.1241826

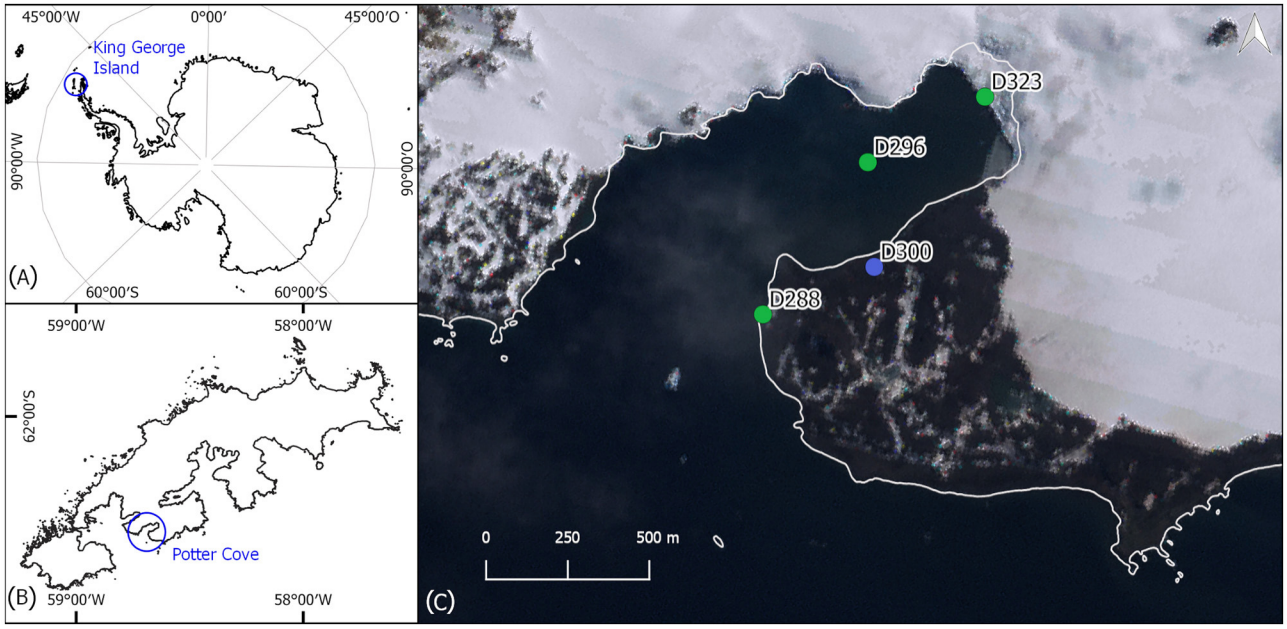

FIGURE 1
(A) Map of Antarctica; **(B)** map of King George Island; **(C)** map of Potter Cove, with the four sampling locations. The blue point represents the freshwater sampling site and green points represent marine sampling locations. Base map: Landsat Image Mosaic of Antarctica (LIMA).

TABLE 1 List of benthic diatom strains established from Antarctic marine and freshwater samples with scientific names, information on dimensions of the valves, striae density, sequenced marker genes, and accession numbers, RV, raphe valve; SV, sternum valve.

Strain	Scientific name	Water type	Length/ diameter (μm)	Width/ pervalvar axis (μm)	Striae in 10 μm	Marker genes	Accession number *rbc*L	Accession number 18SV4/18S
D288_003	*Navicula criophiliforma*	Marine	24.2–52.4	5.8–8.5	11–12	18S V4, *rbc*L	OX258986	OX259166
D296_001	*Chamaepinnularia gerlachei*	Marine	17.1–20.6	4.1–5.4	18–20	18S, *rbc*L	OX258987	OX258985
D323_018	*Melosira* sp.	Marine	18.6–20.9	19.4–22.0	-	18S V4, *rbc*L	OR036645	OR042180
D300_015	*Planothidium wetzelii* sp. nov.	Freshwater	10.9–11.3	5.6–6.1	16–18 (RV)	18S V4, *rbc*L	OX258989	OX259168
					17–18 (SV)			
D300_025	*Planothidium wetzelii* sp. nov.	Freshwater	17.8–18.8	6.0–6.3	14–15 (RV)	18S V4, *rbc*L	OR036646	OR042181
					15–16 (SV)			
D300_019*	*Planothidium wetzelii* sp. nov.	Freshwater	11.1–11.8	5.8–6.7	16–18 (RV)	18S V4, *rbc*L	OR036648	OR042183
					16–17 (SV)			
D300_020*	*Planothidium wetzelii* sp. nov.	Freshwater	17.5–18.5	5.8–6.5	14–15 (RV)	18S V4, *rbc*L	OR036647	OR042182
					14–15 (SV)			

*Strains were only used for the description of the new species.

of 18S. For strain D296_001, the whole 18S gene was amplified after Jahn et al. (2017). The protein-coding plastid gene *rbc*L was amplified by Abarca et al. (2014). PCR products were visualized on a 1.5% agarose gel and cleaned with MSB Spin PCRapace® (Invitek Molecular GmbH; Berlin, Germany) following the manufacturer's instructions. DNA content was measured using NanoDrop® (Peqlab Biotechnology). The samples were normalized to a total DNA content >100 ng μL^{-1} for sequencing. Sanger sequencing of the PCR products was conducted bidirectionally by StarSEQ® (GENterprise LLC; Mainz, Germany).

Electropherograms obtained by Sanger sequencing were checked manually. The resulting reads from both sequencing

directions overlapped, and the fragments were assembled in PhyDE® (Müller et al., 2010) to obtain the final sequences of the amplified markers.

The genetic differences of the newly described *Planothidium* to other species of this genus were investigated based on the 18S V4 and *rbc*L sequence matrices using MEGA 11 (Tamura et al., 2021) and the implemented p-distance option. Therefore, our dataset was complemented with 21 sequences of *Planothidium* from NCBI (Supplementary Tables 1, 2) and that of *P. tujii* C. E. Wetzel and Ector (molecular data supplied by A. Tuji). The alignments were trimmed to 437 bp for 18S V4 and 988 bp for *rbc*L.

2.3.2. Data curation

Vouchers and DNA of all strains were deposited in the collections at Botanischer Garten und Botanisches Museum Berlin, Freie Universität Berlin (B). DNA samples were stored in the Berlin DNA bank and were available via the Genome Biodiversity Network (GGBN; Droege et al., 2016). All sequences were submitted to GenBank. All cultures were available from the authors at the culture collection of the Department of Applied Ecology and Phycology, University of Rostock.

2.4. Experimental part

After cultivation for 4–6 weeks to achieve sufficient biomass for the experiments, each strain was divided into different Erlenmeyer flasks. From the control condition (T0, control), three replicate samples were harvested for evaluation, and an additional three replicates were transferred to 3 months of darkness (T3) at 5°C. Cells from both T0 and T3 treatments were investigated concerning physiological, biochemical, and cell biological traits.

2.4.1. Photosynthetic efficiency

The efficiency of energy transfer in the diatom chloroplasts from the antenna to photosystem II (PS II) allows conclusions about the cell viability and the physiological state of the cells. It was measured using a pulse amplitude modulation (PAM) fluorimeter (PAM-2500, Heinz Walz GmbH, Effeltrich, Germany). The maximum quantum yield [$Y(II)_{max}$] of PS II was calculated by detecting the ground fluorescence (F_0) of the dark-adapted samples and the maximal fluorescence (F_m) after an oversaturating light pulse:

$$Y\,(II)_{\max} = \frac{F_v}{F_m} = \frac{(F_m - F_0)}{F_m}$$

For measurements, a cooling block was used and set to the dark incubation temperature of 5°C to avoid temperature stress in the Antarctic benthic diatom samples. On the cooling block, 25-mm glass fiber filters (GF/6, Whatman, Little Chalfont, UK) were wetted with the respective culture medium. In a dark working space, a uniformly dense diatom cell layer was dripped on the filter and immediately measured. For detecting F_0 of the dark-adapted samples, a weak measuring light (<0.5 µmol photons m^{-2} s^{-1}) was applied, while for F_m, an oversaturating light pulse (>10 000 µmol photons m^{-2} s^{-1}) was used (Malapascua et al., 2014).

2.4.2. Photometric chlorophyll *a* measurement

Five milliliters of algal biomass at T0 and T3 were filtered onto a Whatman GF/6 glass fiber filter (Ø 25 mm; $n = 3$), and chlorophyll *a* was extracted using 96% ethanol (v/v) and measured spectrophotometrically using the equation given by HELCOM (2019).

To obtain a reference value for the chlorophyll *a* concentration, 5 mL of algal suspension from each culture ($n = 3$) was fixed with Lugol solution at T0 and T3, and the cell number was determined in 1 mL, using a sedimentation chamber at 100x or 200x magnification and an inverted microscope (Olympus IX70, Hamburg, Germany). Always 400 morphologically intact cells were counted, and empty or half-empty valves were ignored. The final amount of cells per mL suspension was calculated as follows:

$$\frac{cells}{mL} = \frac{counted\ cells \times D \times A \times 1mL}{a \times Sq}$$

[D = dilution factor; **A** = total area of the chamber (mm^2); Sq = amount of counted squares; **a** = area of one square (according to used magnification) (mm^2)].

Chlorophyll *a* measurements were then correlated with the cell counts ($n = 3$ replicates).

2.4.3. Photosynthesis–irradiance curves (P–I curve)

The photosynthetic oxygen production and respiratory oxygen consumption of each strain were determined at 10 different light levels (0–~1,500 µmol photons m^{-2} s^{-1}) generated by LEDs (LUXEON Rebel1 LXML-PWN1-0100, neutral-white, Phillips, Amsterdam, Netherlands) implemented into a self-constructed P–I box as described by Prelle et al. (2019). Always, 3 mL of algal suspension was measured in airtight chambers [DW1 oxygen electrode chambers each placed on a magnetic stirrer (Hansatech Instruments, King's Lynn, United Kingdom)] using oxygen dipping probe DP sensors (PreSens Precision Sensing GmbH, Regensburg, Germany) connected to an Oxy 4-mini meter (PreSens Precision Sensing GmbH, Regensburg, Germany) in combination with the PreSens software OXY4v2_30 for measuring and calibration (two-point calibration, 0 and 100% oxygen saturation). The chambers were tempered at 5°C, and 30 µL of sodium bicarbonate ($NaHCO_3$, final concentration 2 mM) was added to each sample to avoid carbon deficiency (for details, see Prelle et al., 2019). After each P–I curve, diatom suspension from each cuvette was filtered onto an individual Whatman GF/6 glass fiber filter (Ø 25 mm) for chlorophyll *a* determination as reference parameter (Method see above). The photosynthetic model of Walsby (1997) was used for fitting and calculating different P–I curve parameters.

Since all clonal cultures were not axenic, we estimated the potential influence of bacterial respiration on the diatom net photosynthesis determination. The bacterial volume and the respective diatom volume of T0 samples were determined using DAPI (4′6-diamidine-2-phenylindole) staining. A measure

of 500 μL of each glutaraldehyde-fixed T0 sample was filtered on a blackened Polycarbonate Track-Etched Filter (Ø 25 mm, pore size 0.2 μm, Sartorius Lab Instruments GmbH & Co. KG, Goettingen) and stained for 5 min with DAPI (Kapuscinski, 1995). Micrographs of different locations of the filter were taken using an epifluorescence microscope BX-51 (Olympus, Hamburg, Germany) with a 40x lens and CellSens Standard imaging software (Olympus, Hamburg, Germany). For each culture, five micrographs were analyzed using Fiji–ImageJ (version 2.3.0; open source), detecting the area of the blue signal after deleting the shapes of diatoms and determining the area of diatoms in each picture. Additionally, the average diameter of the bacterial cells and the diatoms was measured and used to calculate the volume of both groups. The resulting volume data should, therefore, be regarded as a rough approximation to evaluate the bacterial influence on the oxygen values.

2.4.4. Cell biology

To investigate changes in cell integrity after 3 months of dark incubation, 1 mL of algae suspension was taken ($n = 3$) from T0 and T3 without further fixation and was directly stained with 1 μL of SYTOX Green (Catalog no. S7020, Thermo Fisher Scientific, Waltham, Massachusetts, USA; diluted in culture medium from a 5 mM solution in DMSO). After 5 min of dark incubation, stained and unstained cells were quantified with an epifluorescence microscope (BX-51, Olympus, Hamburg, Germany) under blue excitation (U-MWB, Olympus, Hamburg, Germany). At least 400 unstained cells and the corresponding number of compromised cells were counted in each replicate.

The effects of dark incubation on the volume of lipid droplets were determined using Nile red lipid staining according to Greenspan et al. (1985). Twenty-five cells of each culture at T0 and T3, preferably in the same orientation, were imaged using epifluorescence microscopy (BX-51) under blue excitation (U-MWB) along with a digital camera UC30 and CellSens standard imaging software (all from Olympus, Hamburg, Germany). The width and length of each cell and the respective sizes of lipid droplets were measured with Fiji–ImageJ (version 2.3.0; open source). The cell volume and the volume of a lipid droplet were modulated by an ellipsoid shape. Height and width were assumed to be identical, except for the centric species *Melosira* sp. D323_018, which exhibited numerous lipid droplets. In this study, the number of lipid droplets was counted, and the average diameter of the spherical lipid droplets was determined to calculate the total lipid volume. The cell volume of this culture was idealized and calculated using two hemispheres and a cylinder.

To obtain a more detailed picture of the cell biological changes in darkness, T0 and T3 samples were prepared and fixed by standard chemical fixation for transmission electron microscopy (TEM) according to Holzinger et al. (2009), using 2.5% glutaraldehyde (25% glutaraldehyde diluted with 50 mM cacodylic acid buffer, pH 6.8) and osmium tetroxide (OsO_4 diluted in cacodylic acid buffer) fixatives. These samples were dehydrated by increasing the alcohol series, embedded in modified Spurr resin according to Holzinger et al. (2009) before being sectioned using an ultra-microtome. Ultrathin sections were stained with uranyl acetate and lead citrate and were investigated with a Zeiss LIBRA 120 transmission electron microscope at 80 kV. Images were captured with a TRS 2k SSCCD camera and further processed using Adobe Photoshop software (Adobe Systems Inc., San José, CA, USA).

2.4.5. GC-MS analysis

For fatty acid analysis of diatom samples at T0 and T3, a gas chromatograph connected to a mass spectrometer (GC-MS) was used according to Schaub et al. (2017). Since this analytical approach is time-consuming, we used only one replicate with three individual injections to identify at least the most conspicuous changes in the main fatty acids. Diatom samples were filtered onto Whatman GF/6 glass fiber filter (Ø 25 mm), freeze-dried and extracted with dichloromethane:methanol (2:1, v/v), and evaporated under nitrogen in a heat block (30°C), and the residue was re-dissolved in dichloromethane:methanol (2:1, v/v) and stored at −20°C until further analysis (Schaub et al., 2017).

For transesterification, 1 mL of lipid extract was evaporated under nitrogen to dryness, dissolved in 250 μL of hexane and heated for 4 h at 80°C with 1 mL of a 3% concentrated sulfuric acid in methanol. Subsequently, fatty acid methyl esters (FAMEs) were extracted three times with hexane, transferred to GC vials, and concentrated under nitrogen down to ∼80 μL. GC analysis was carried on a fused silica capillary column (WCOT; 60 m × 0.25 mm I.D.; film thickness 0.25 μm; liquid phase: DB-FFAP; J&W, Germany) with a HP 6890 gas-liquid chromatograph coupled with a 5,970 Series mass selective detector (MSD; Hewlett–Packard GmbH, Germany) and a temperature program according to Kattner and Fricke (1986). The samples were injected at 60°C in splitless mode, with helium as carrier gas. Identification and quantification of fatty acids were according the protocol in Schaub et al. (2017).

2.4.6. Statistics and calculations

All calculations were performed using Microsoft Office Excel (2016). To calculate the P–I curves according to the Walsby model, the solver function was used to minimize the normalized deviation squares. The statistical analysis was performed using SPSS Statistics (version 27). To calculate significance levels among all means, one-way ANOVA was used followed by a *post-hoc* Tukey test. If the data did not fulfill the assumptions of variance homogeneity or normal distribution for one-way ANOVA, the Mann–Whitney test was used in case of two independent groups—in case of three or more independent groups, the Kruskal–Wallis one-factor ANOVA was applied. The significance level was set to $\alpha < 0.05$ for all analyses.

3. Results

3.1. Species identification and the description of a new benthic diatom taxon

Five strains from the four sample locations were investigated in this study. The morphological and molecular analyses confirmed the assignment to four distinct species. The taxonomic identity of

some strains was already published before (D288_003, D296_001, D300_015; Prelle et al., 2022; Schimani et al., 2023).

D288_003 was identified as *Navicula criophiliforma* Witkowski, Riaux-Gob. and Daniszewska-Kowalczyk. This taxon was first published by Witkowski et al. (2010) from the Kerguelen Islands coastal area, Southern Ocean, and more recently also reported from Livingston Island, north of the Antarctic Peninsula (Zidarova et al., 2022). LM and SEM pictures of this strain can be found in Prelle et al. (2022).

D296_001 was identified as *Chamaepinnularia gerlachei* Van de Vijver and Sterken. This species was first published by Van de Vijver et al. (2010) from dry soil samples from James Ross Island, near the northeastern extremity of the Antarctic Peninsula, and has been observed until now just from maritime Antarctica (Kopalová et al., 2012; Sterken et al., 2015; Zidarova et al., 2016). A thorough examination of this strain can be found in Schimani et al. (2023).

D323_018 (Figure 2) could only be identified at the genus level as *Melosira* sp. Cells are subcylindrical with a diameter ranging between 18.6 and 20.9 µm and a pervalvar axis ranging between 19.4 and 22.0 µm (Figures 2A–E). The hypovalve is more rounded than the epivalve (Figure 2H), which exhibits at the mantel a more cylindrical shape. Our strain resembles *Melosira moniliformis* C. Agardh in Crawford (1977), who examined the type and new material. However, in *M. moniliformis*, ridges on the outer mantle surface fuse to form bigger spines, which are not visible in our strain. Therefore, unambiguous taxonomic assignment of this strain to a particular *Melosira* species is not possible at this stage.

D300_015 was only identified at the genus level as *Planothidium* sp. in Prelle et al. (2022). Morphological and molecular investigations showed that strain D300_025 is the same species. With the new data generated from those strains and two other strains obtained from the same location (D300_019, D300_020), this species is described as new.

***Planothidium wetzelii* Schimani, N. Abarca et R. Jahn sp. nov.**

Description:

Living material (Figures 3Q–AB, AP–BA): One plate of the C-shaped plastid lies appressed to the valve face. The concavity of the plastid is visible on the valve side lacking the cavum. Pyrenoids are not clearly visible, but Figures 3AR, AT suggest that there is one pyrenoid located in the vicinity of the cavum. In the girdle view, especially in the larger cells before cell division (Figure 3BA), two lobes of the chloroplast are visible appressed to the valves, and connected in the center of the cell.

LM (Figures 3A–P, AC–AO, BB–BN): The outline ranged from elliptic with slightly protracted rostrate apices in smaller valves to elliptic or lanceolate with protracted, rostrate to capitate apices in larger valves. One valve side—especially strain D300_020—appeared more convex than the other. The length of the valves varied between 10.9 and 18.8 µm and the width between 5.6 and 6.7 µm ($n = 43$). Sternum valve (SV): Axial area narrow, becoming wider toward the center of the valve. Central area asymmetrical with an oblong cavum with parallel sides, extending slightly over the axial area on one side and with shortened striae on the other side. The parallel margins of the cavum widen just shortly before the mantle, and its aperture is seen as a roundish line close to the mantle. Striae parallel or weakly radiating in the center, becoming more radiate near the apices (16–18 in 10 µm in smaller valves and 14–16 in 10 µm in larger valves). Raphe valve (RV): Axial area narrow. The central area widened due to three to four shortened striae on both sides. Raphe straight with enlarged proximal endings. Distal endings are not visible in light microscopy. Striae are parallel or weakly radiating in the center, becoming more radiating near the apices (16–18 in 10 µm in smaller valves and 14–15 in 10 µm in larger valves).

SEM (Figures 4A–W) SV: The striae are composed of three to four rows of small rounded areolae exceeding the width of the virgae. Striae near the center of the valve become pointed with one or two areolae near the axial area. Externally, striae reach over the mantle with up to four rows of areolae. Irregularly rounded depressions are externally present along the axial area and concentrated in the central area. Internally, areolae are covered by hymenate occlusions. The broad cavum had a tight hood opening close to the mantle. Cingulum is composed of unperforated girdle bands. RV: The striae are composed of usually three to four rows of rounded areolae exceeding the width of the virgae. Similar to the central striae on the SV, the shortened central striae on the RV gradually narrow toward the axial area. At each stria, one to three areolae reach over the edge of the valve face. Internally, areolae are covered with the same hymenate occlusions as in SV. Externally, the raphe straight with drop-like expanded proximal ends and distal raphe fissures unilaterally deflected, not or just shortly continuing onto the valve mantle. Internally, proximal raphe endings are slightly bent to opposite sides, and raphe endings terminate on a small helictoglossae not continuing on the valve mantle.

Holotype: Slide B 40 0045341a, Botanic Garden and Botanical Museum, Berlin, Figure 3BJ for SV and Figure 3BK for RV from the strain D300_025 illustrate the holotype. SEM-stub deposited as B 40 0045341b. For molecular material and data, see Methods.

Type locality: Drinking water reservoir of Carlini Station, Potter Cove, King George Island, South Shetland Islands, collected by J. Zimmermann on 01 February 2020, coordinates: S 62.237861, W 58.662250.

Registration: http://phycobank.org/103793.

For INSDC Accession numbers see Table 1.

Habitat: Freshwater biofilm on stones.

Etymology: With this name, we would like to acknowledge the morphological and taxonomic work on the genus *Planothidium* done by Carlos Wetzel (Luxembourg Institute of Science and Technology, Luxembourg) in recent years, as well as his help in finding the identity of this species.

Differential diagnosis: *Planothidium wetzelii* shares similarities with several cavum-bearing species and species with external shallow rounded depressions on the rapheless valve (as defined by Wetzel et al., 2019): The smaller valves of *P. wetzelii* share similarities in shape with the small valves of *P. frequentissimum* (Lange-Bertalot), Lange-Bertalot as illustrated from type material in Wetzel et al. (2019). However, they can be distinguished by the form of the cavum, which is oblong with parallel sides and extending slightly over the axial area, vs. a round cavum in *P. frequentissimum*. The shape of the central area on the RV is much smaller in *P. wetzelii* compared to the type of *P. frequentissimum*. In SEM, the virgae in the SL and to some extent on the RV are wider in *P. wetzelii* compared to images of the type of *P. frequentissimum*. Additionally, the striae on the RV do not

10.3389/fmicb.2023.1241826

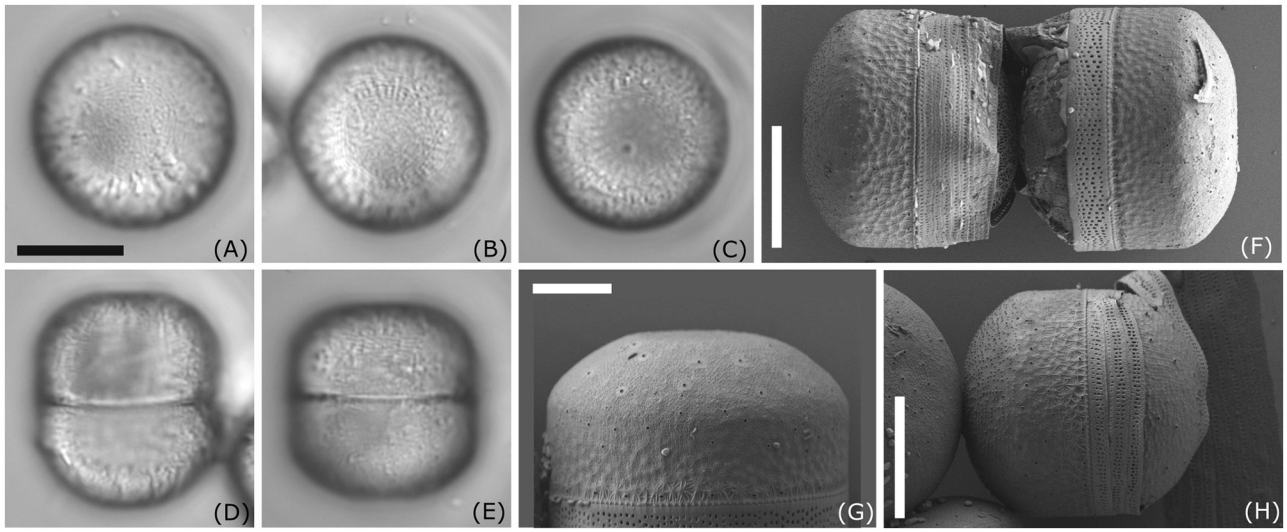

FIGURE 2
Morphology of *Melosira* sp. D332_018. **(A–E)** Light microscopy images; **(F–H)** scanning electron microscopy images external view; Scale bar: **(A–E, H)** 10 μm; **(G)** 5 μm.

continue over the mantle in *P. frequentissimum* as they do in *P. wetzelii*. Larger valves of *P. frequentissimum* are lanceolate with less developed rostrate apices than those of *P. wetzelii*. Valves of *P. victorii* Novis, Braidwood et Kilroy (syn. *P. caputium*) are in contrast to *P. wetzelii* lanceolate to weakly elliptic-lanceolate with protracted but never capitate apices (Jahn et al., 2017; Wetzel et al., 2019). The species can be differentiated by the form of the cavum too as it is rounder or has a V-shape in *P. victorii*. In addition, the tight hood opening in *P. wetzelii* (SEM), seen as a roundish line close to the mantle (LM), differs from the wider hood opening (SEM) in *P. victorii*, which is present as an almost straight line distant from the mantle (LM). The axial area is narrower in this species and the cavum has a wider aperture toward the mantle than *P. wetzelii*. Some of the medium sized valves could be confused with *P. naradoense* R.Jahn et J.Zimmermann but differ from *P. wetzelii* by the outline, as *P. naradoense* is lanceolate to elliptic-lanceolate and somewhat asymmetric with slightly rostrate and rounded apices. The axial area is narrow on both valves (Jahn et al., 2017). Larger valves of *P. wetzelii* share similarities with *P. tujii* and *P. gallicum* C. E. Wetzel et Ector (Wetzel et al., 2019). However, the valves of *P. tujii* are shorter, while the width is almost in the same range. The central area in the RV of *P. tujii* is bowtie-shaped instead of the smaller rounded central area in *P. wetzelii*. The virgae are wider in *P. tujii* and have almost the same width as the striae; the helictoglossa is continuing onto the valve mantle. *P. gallicum* has clear broadly elliptic-lanceolate shaped valves with markedly rostrate apices. Furthermore, *P. gallicum* has a more prominent aperture of the cavum toward the mantle, and the striae located in the central area are not becoming narrower toward the axial areal as in *P. wetzelii*. *P. straubianum* C. E. Wetzel, Van de Vijver et Ector has elliptic-lanceolate valves with slightly parallel margins and round, obtuse ends with smaller dimensions than *P. wetzelii* (length 6.0–14.0 μm vs. 10.9–18.8 μm and width 4.0–5.5 μm vs. 5.6–6.7 μm; Wetzel et al., 2019). Striae are composed of four to five rows of areolae, in contrast to three to four in *P. wetzelii*. *P. biporomum* (M. H. Hohn et Hellerman) Lange-Bertalot can be differentiated from *P. wetzelii* in SEM by the striae on the rapheless valve (Wetzel et al., 2013). The striae start externally with one, rarely two, areolae at the axial area and end in two or three rows toward the valve face/mantle junction. Additionally, they are interrupted at the junction with the valve mantle. Furthermore, the cavum aperture is wide with its borders linked to the neighboring striae. *P. alekseevae* Gogorev et E. K. Lange has smaller dimensions (length 9.5–13.5 μm, width 4.5–5.0 μm) and wider apices in relation to the valve width. This feature is more apparent in smaller valves (Wetzel et al., 2019).

Molecular results: The four strains of *P. wetzelii* showed no intraspecific variability in the 18S V4 and the *rbc*L sequences (Supplementary Tables 1, 2). Compared to the available sequences of other *Planothidium* species, genetic distances are apparent in both marker genes. It is placed within the F2 subclade (Jahn et al., 2017, p. 84, Figure 1): strains of *P. victorii* (e.g., type strain from New Zealand), *P. straubianum* (strain B86_3 from Lake Baikal, renamed by Wetzel et al., 2019), and *P. tujii* show the smallest genetic divergence: in 18S V4 0.5–1.1, 0.7–0.9, and 0.9–1.1%, respectively, which corresponds to 3–5 bp differences, and in *rbc*L 0.5–0.8, 0.5, and 0.5% (3–7 bp). Higher genetic differences are evident for *P. naradoense* and *P. frequentissimum*: in 18S V4 2.5% and 2.5–3.2% (11 bp) and in *rbc*L 2.2 and 1.8–2.3%, respectively (8–22 bp). Species with a sinus instead of a cavum [*P. lanceolatum* (Brébisson ex Kützing) Lange-Bertalot, *P.* cf. *subantarcticum*, *P. taeansa* R. Jahn and N. Abarca, *P. cryptolanceolatum* R. Jahn and N. Abarca, and *P. suncheonmanense* R. Jahn and J. Zimmermann] exhibit the highest divergence with a p-distance of 4.3–7.8% (19–38 bp) in 18S V4 and 3.0–6.2% (30–61 bp) in *rbc*L.

10.3389/fmicb.2023.1241826

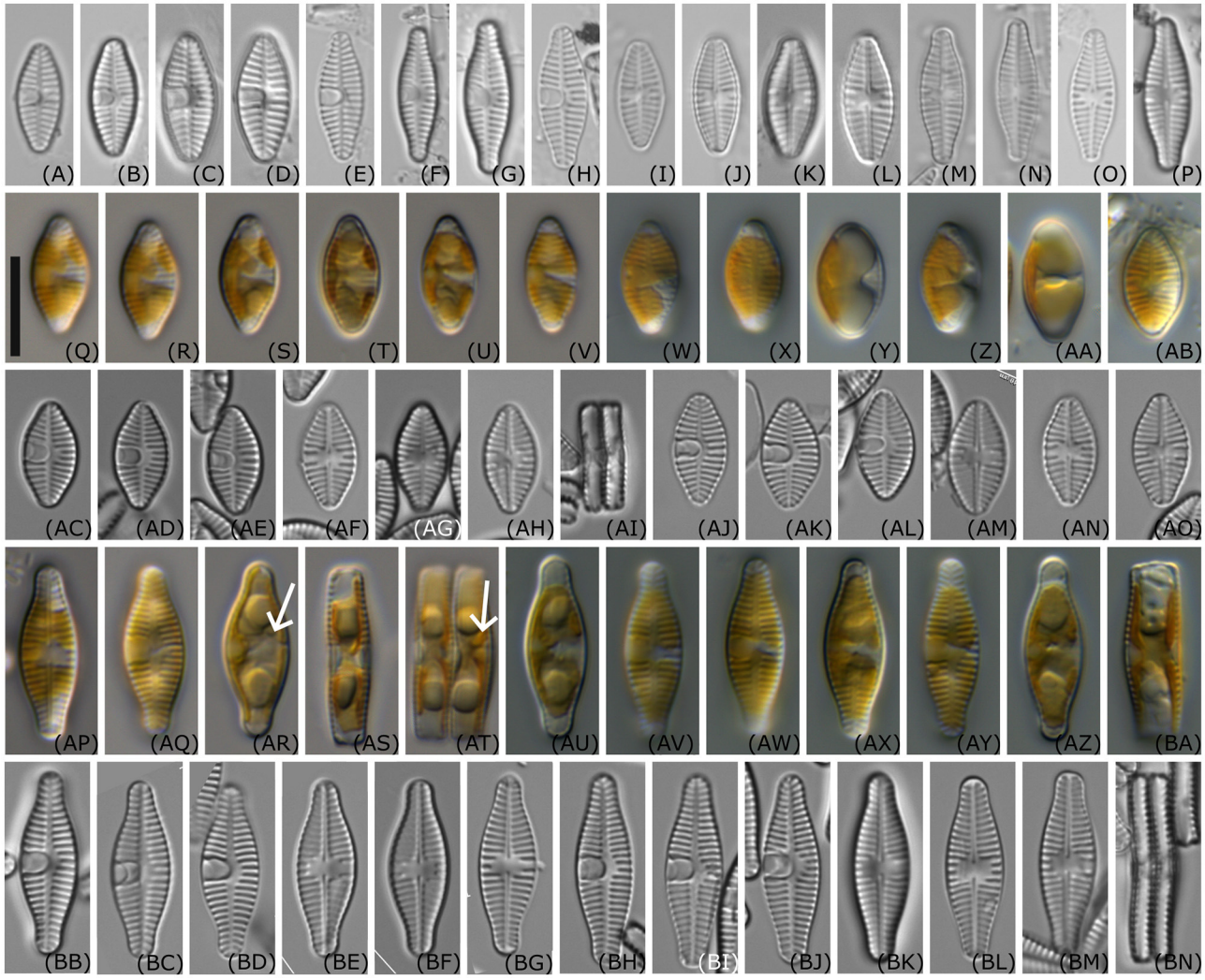

FIGURE 3
Light microscopy images of *Planothidium wetzelii* sp. nov. **(A–P)** valves of environmental samples; **(Q–V)** live material of strain D300_015; **(W–AB)** live material of strain D300_019; **(AC–AI)** oxidized material of strain D300_015; **(AJ–AO)** oxidized material of strain D300_019; **(AP–AT)** live material of strain D300_020, **(AR, AT)** arrows indicate possible location of one pyrenoid in vicinity of the cavum; **(AU–BA)** live material of strain D300_025; **(BB–BG)** oxidized material of D300_020; **(BH–BN)** oxidized material of strain D300_025; Scale bar: 10 μm.

3.2. Photosynthesis and respiration

The values for $Y(II)_{max}$ at T0 and T3 are shown in Table 2 (mean values ± SD, $n = 3$). All results were between 0.53 (*P. wetzelii* (D300_025) at T3) and 0.63 (*N. criophiliforma* and *C. gerlachei* at T0) and therefore within a range reflecting "good" physiological activity of all diatom cells during the dark incubation. Small, but significant differences in $Y(II)_{max}$ between T0 and T3 were found only in both cultures of the limnic species *P. wetzelii* (Table 2).

The results of the chlorophyll *a* measurements, which were referenced to cell counts, showed species-specific responses (Table 2). In both strains of *P. wetzelii*, the chlorophyll *a* content per cell did not significantly change during 3 months of dark treatment. In contrast, *N. criophiliforma* and *C. gerlachei* exhibited a pronounced chlorophyll *a* decline up to 74% after dark incubation compared to the control, while the *Melosira sp.* decreased chlorophyll *a* by ~46% (Table 2).

All measured P–I curves exhibited a typical shape without photoinhibition, as already reported for some of the species in detail in Prelle et al. (2022). The key parameters NPP_{max} and respiration were selected for all species before and after dark incubation (Table 2), and species-specific responses could be outlined. At T0, the highest value for NPP_{max} was determined in the marine species *N. criophiliforma* (80.0 ± 20.2 μmol O_2 mg^{-1} Chl *a* h^{-1}), while *P. wetzelii* (D200_015) showed the lowest NPP_{max} (16.7 ± 4.0 μmol O_2 mg^{-1} Chl *a* h^{-1}). While some species (*N. criophiliforma*, both *P. wetzelii* isolates) did not exhibit any significant NPP_{max} decline ($p < 0.05$) during dark treatment at T3, *C. gerlachei* and *Melosira* sp. showed a strong and significant decrease ($p < 0.05$) in NPP_{max} by 39.9 and 44.6%, respectively (Table 2).

Although respiration rates were also species-specifically different and variable, we could not detect any significant difference in respiration between T0 and T3 among all benthic diatom

10.3389/fmicb.2023.1241826

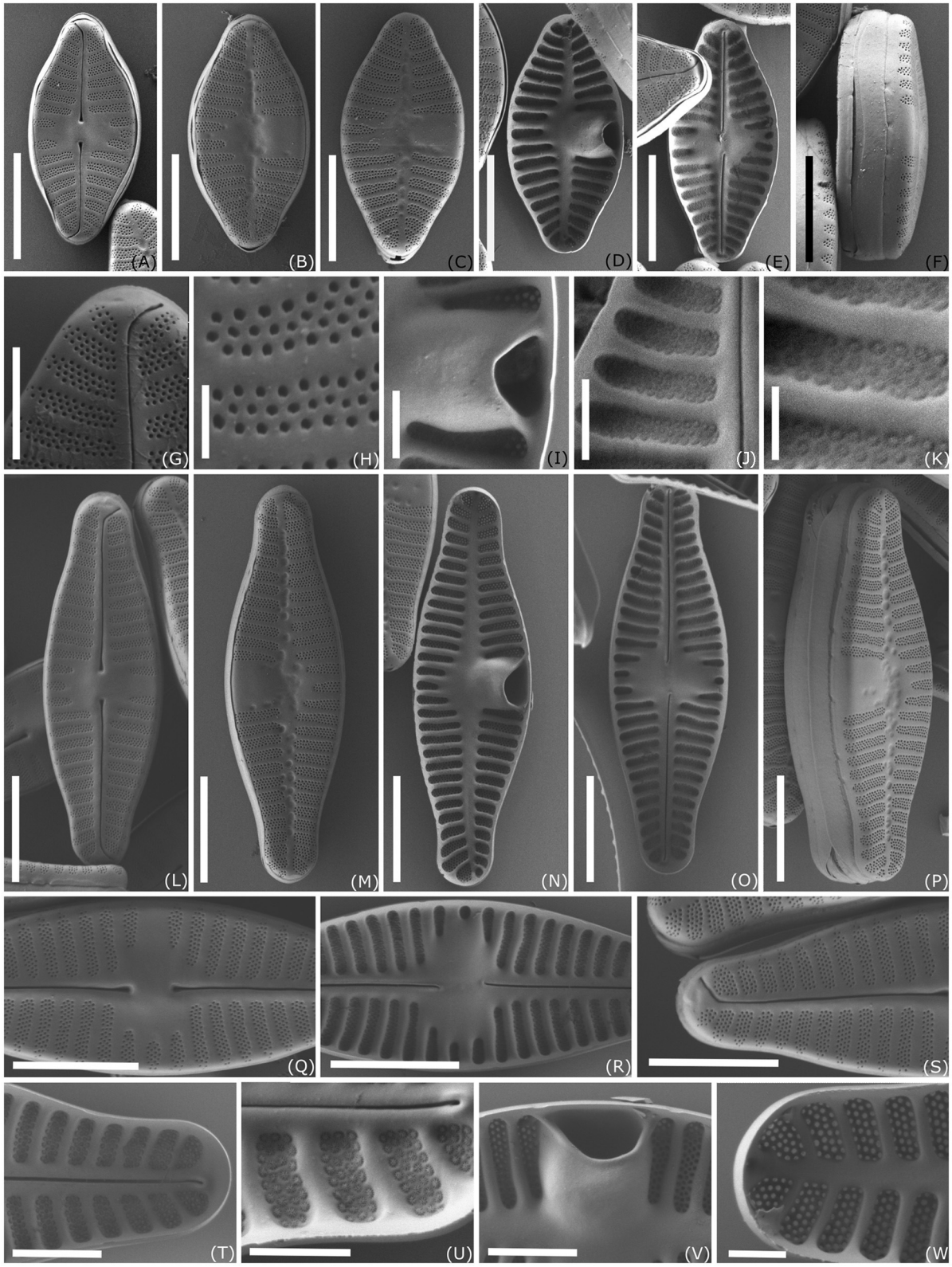

FIGURE 4
Scanning electron microscopy images of *Planothidium wetzelii* sp. nov. **(A–K)** strain D300_015; **(L–W)** strain D300_025; **(A, E, G, H, J–L, O–T)** raphe valve (RV); **(B–D, F, I, M, N, P, V, W)** sternum valve (SV); **(A–C, F–H, L, M, P, Q, S)** external view; **(J, K, U)** internal view of RV, showing three to four rows of same sized hymenate areolae in one stria; **(I, V)** internal view of central area in RLV showing cavum; Scale bar: **(A–F, L–P)** 5 μm; **(Q–S)** 4 μm; **(G, T, V)** 2 μm; **(I, J, U, W)** 1 μm; **(H, K)** 0.5 μm.

10.3389/fmicb.2023.1241826

TABLE 2 Results of different photosynthesis-related measurements before dark incubation (T0) and after 3 months of dark incubation (T3) of five Antarctic benthic diatom species.

Culture	Treatment	F_v/F_m	Chl a per cell (ng Chl per cell)	NPPmax (μmol O_2 mg^{-1} Chl *a* h^{-1})	Respiration (μmol O_2 mg^{-1} Chl *a* h^{-1})	NPP_{max}: respiration
Navicula criophiliforma	T0	0.63 ± 0.01	8.18 ± 8.86	80.0 ± 20.2	−72.2 ± 70.3	2.1 ± 1.5
		a	*a*	*a*	*a*	*a*
	T3	0.6 ± 0.02	2.21 ± 1.67	76.9 ± 8.4	−35.8 ± 14.5	2.3 ± 0.6
		a	*a*	*a*	*a*	*a*
Chamaepinnularia gerlachei	T0	0.63 ± 0.01	0.43 ± 0.51	33.9 ± 2.2	−30.9 ± 10.0	1.2 ± 0.4
		a	*a*	*a*	*a*	*a*
	T3	0.57 ± 0.02	0.13 ± 0.02	20.4 ± 2.9	−26.3 ± 1.8	0.8 ± 0.1
		a	*b*	*b*	*a*	*a*
Melosira sp.	T0	0.57 ± 0.01	4.16 ± 2.69	76.1 ± 9.4	−16 ± 8.4	6.6 ± 5.0
		a	*a*	*a*	*a*	*a*
	T3	0.55 ± 0	2.22 ± 1.57	42.2 ± 7.2	−9.4 ± 2.9	5.0 ± 2.2
		a	*b*	*b*	*a*	*a*
Planothidium wetzelii (D300_015)	T0	0.61 ± 0	0.93 ± 0.08	16.7 ± 4.0	−7.8 ± 6.2	9.0 ± 14.0
		a	*a*	*a*	*a*	*a*
	T3	0.57 ± 0.01	0.95 ± 0.4	13.4 ± 4.7	−15.4 ± 2.4	0.9 ± 0.4
		b	*a*	*a*	*a*	*a*
Planothidium wetzelii (D300_025)	T0	0.57 ± 0.03	1.53 ± 1.37	39.6 ± 9.8	−31.0 ± 4.3	1.3 ± 0.5
		a	*a*	*a*	*a*	*a*
	T3	0.53 ± 0	1.345 ± 0.56	25.3 ± 11.2	−30.5 ± 19	1.2 ± 0.8
		b	*b*	*a*	*a*	*a*

Maximum quantum yield (F_v/ F_m) of PS II measured by pulse amplitude modulation (PAM) fluorimetry. Data are shown as mean ± standard deviation (n = 3). Chlorophyll a content is given as ng Chl a per cell (n = 3). NPP_{max} represents the maximum net primary production rate derived from P–I curves in the PI box at 5°C (n = 4, D300_025 n = 3). Different lowercase letters (a, b) represent significance levels among all means as calculated by one-way ANOVA (Tukey's test, $p < 0.05$). Significance concerning NPP_{max}, respiration, and NPP_{max}: Respiration was analyzed by Kruskal–Wallis analysis ($p < 0.05$) due to non-normally distributed data points.

species (Table 2). While the highest respiration values occurred in the marine species *N. criophiliforma* (−72.2 ± 70.3 O_2 mg^{-1} Chl *a* h^{-1}), the lowest respiration rates were measured in the limnic culture *P. wetzelii* (D300_015, −7.8 ± 6.2 O_2 mg^{-1} Chl *a* h^{-1}). The NPP_{max}: Respiration ratios were relatively low for all isolates between 0.8 ± 0.1 and 2.9 ± 4.0 at T0 and T3, except for *Melosira* sp. which exhibited higher ratios of 6.6 ± 5.0 and 5.0 ± 2.2, respectively, due to proportionally lower respiration rates (Table 2). All diatom cultures were not axenic, and the bacterial abundance ranged from a very low 1.7% bacteria volume when compared with the diatom volume in *Melosira* sp. to 23.7% in *P. wetzelii* (D300_25; Table 2). All other species showed bacterial contamination between these extreme percentages.

3.3. Membrane integrity and ultrastructure

SYTOX Green staining was applied as a cell biological approach to evaluate membrane integrity during dark incubation. The percentage of damaged cells increased significantly in four out of the five tested benthic diatom species (Figure 5). In *N. criophiliforma*, *C. gerlachei*, and *Melosira* sp. at T0 only <5% of the cells were damaged pointing to highly viable cell populations. After 3 months, dark incubation membrane integrity decreased in all three species, i.e., cells with compromised membranes accounted for between 16.4 and 39.0% (Figure 5). Both *P. wetzelii* strains were already at T0 and less viable as reflected in approximately one-third of the damaged cells. While isolate D300_025 exhibited 71.5% compromised membranes, *P. wetzelii* (D300_015) maintained membrane integrity over 3 months of dark incubation (Figure 5).

Figures 6, 7 show the first transmission electron micrographs (TEMs) of benthic diatom species from Antarctica under control (T0, Figure 6) conditions and after 3 months of dark incubation (T3, Figure 7). The three pennate (*N. criophiliforma*, *C. gerlachei*, and *P. wetzelii*) and one-centric diatom species (*Melosira* sp.) exhibited the typical cellular ultrastructure of a diatom cell. All cells contained a central nucleus, several chloroplasts, and, most conspicuously, one or more large lipid droplets that occupied large parts of the cell volume (Figure 6). After the dark

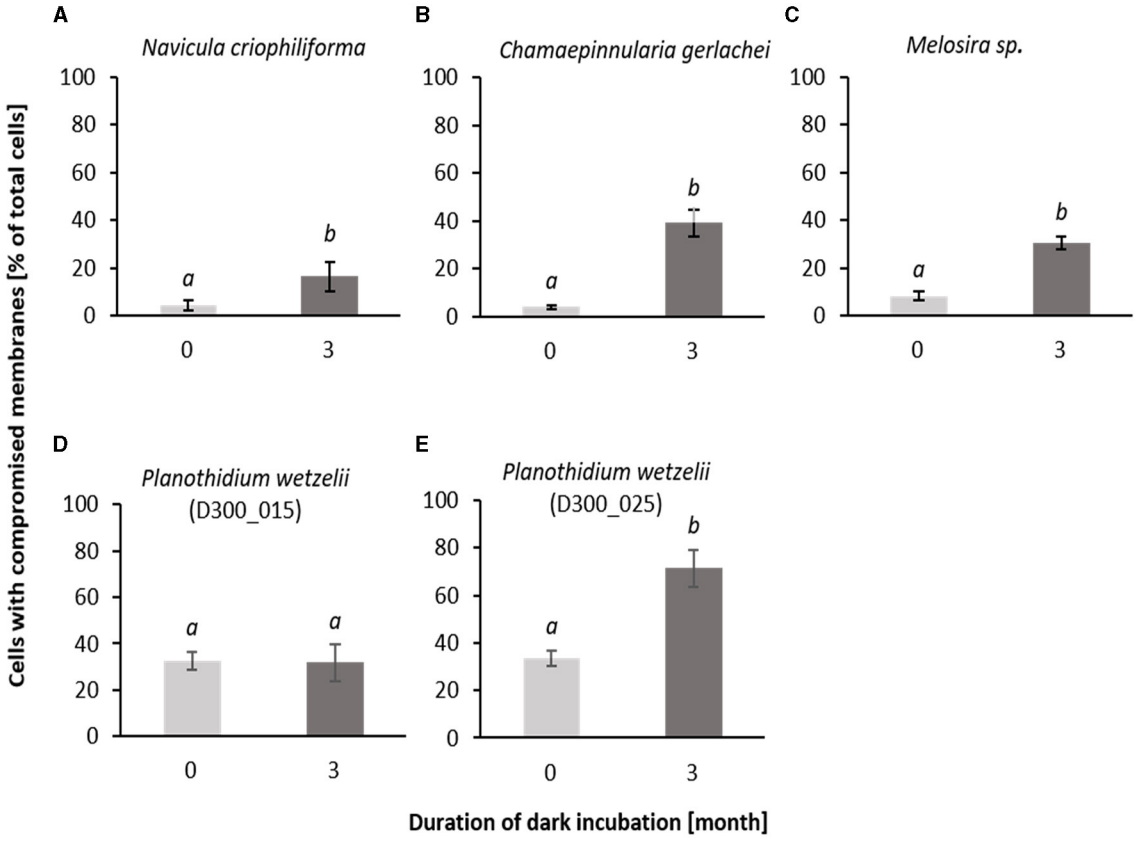

FIGURE 5
Stained cells of all investigated Antarctic benthic diatoms **(A–E)** with SYTOX Green as the percentage of total counted cells (stained and not stained) before and after 3 months of dark incubation. 400–700 cells were counted for each treatment and taxon. Data are shown as mean ± standard deviation ($n = 3$). Different lower case letters (*a* and *b*) represent significance differences calculated by one-way ANOVA (Tukey's test, $p < 0.05$).

treatment, ultrastructural changes could be detected (Figure 7). The most conspicuous observations were degraded chloroplasts with plastoglobules (PGs) in all species and partially more endoplasmic reticulum (ER). In addition, the volume or number of lipid droplets drastically decreased (Figure 7). In *N. criophiliforma*, lipid droplets were virtually absent (Figures 7A, B) and only observed in a few cases. Similarly, in *Melosira* sp., no or only very small lipid droplets occurred at T3. In contrast, in *C. gerlachei* and *P. wetzelii* (D300_015), well-developed lipid droplets could be identified. However, in Figure 7C of *C. gerlachei* beginning, the degradation of a lipid droplet was observed (marked by an arrow). In addition, *N. criophiliforma* and *P. wetzelii* (D300_015) exhibited multivesicular bodies (MVBs) after 3 months of darkness (Figures 7A, H), a typical sign of apoptosis. Additionally, in *P. wetzelii*, several larger electron-dense bodies were observed (Figures 7G, H). While the origin of these bodies remains unknown, they might resemble the degradation products of the chloroplasts.

3.4. Lipid volume and composition

The visual differences of the species-specific lipid content after Nile red staining of the diatom cells before and after 3 months of dark incubation are summarized in Figure 8. In this study, a clear decrease in the size of the stained lipid droplets can be seen. The corresponding calculated lipid volume changes in the examined diatom cells are shown in Figure 9 as boxplots of 25 measured cells each. A significant decrease in the lipid content over 3 months of dark incubation could be documented for all species. The marine isolates *N. criophiliforma*, *C. gerlachei*, and *Melosira* sp. exhibited >95% the strongest decrease in the total lipid content per cell within 3 months of darkness, and in the first and third species only traces of lipids remained detectable (Figure 9). In contrast, in both *P. wetzelii* strains, the lipid content changed much less, with a decrease to only 58.7–60.7% of the control, i.e., these cells contained at T3 still detectable amounts of lipids.

The chemical GC-MS analysis of the total lipid content supports the results shown in Figures 8, 9, i.e., the marine isolates *N. criophiliforma*, *C. gerlachei*, and *Melosira* sp. exhibited concentration declines between 90.0 and 94.5% (Table 3). In both limnic *P. wetzelii* strains, the lipid content decreased by 20.6 and 35.2% after 3 months of darkness (Table 3). Saturated fatty acids (SFAs), monounsaturated fatty acids (MUFAs), and polyunsaturated fatty acids (PUFAs) before and after 3 months of dark incubation were also evaluated, but a clear trend is not

10.3389/fmicb.2023.1241826

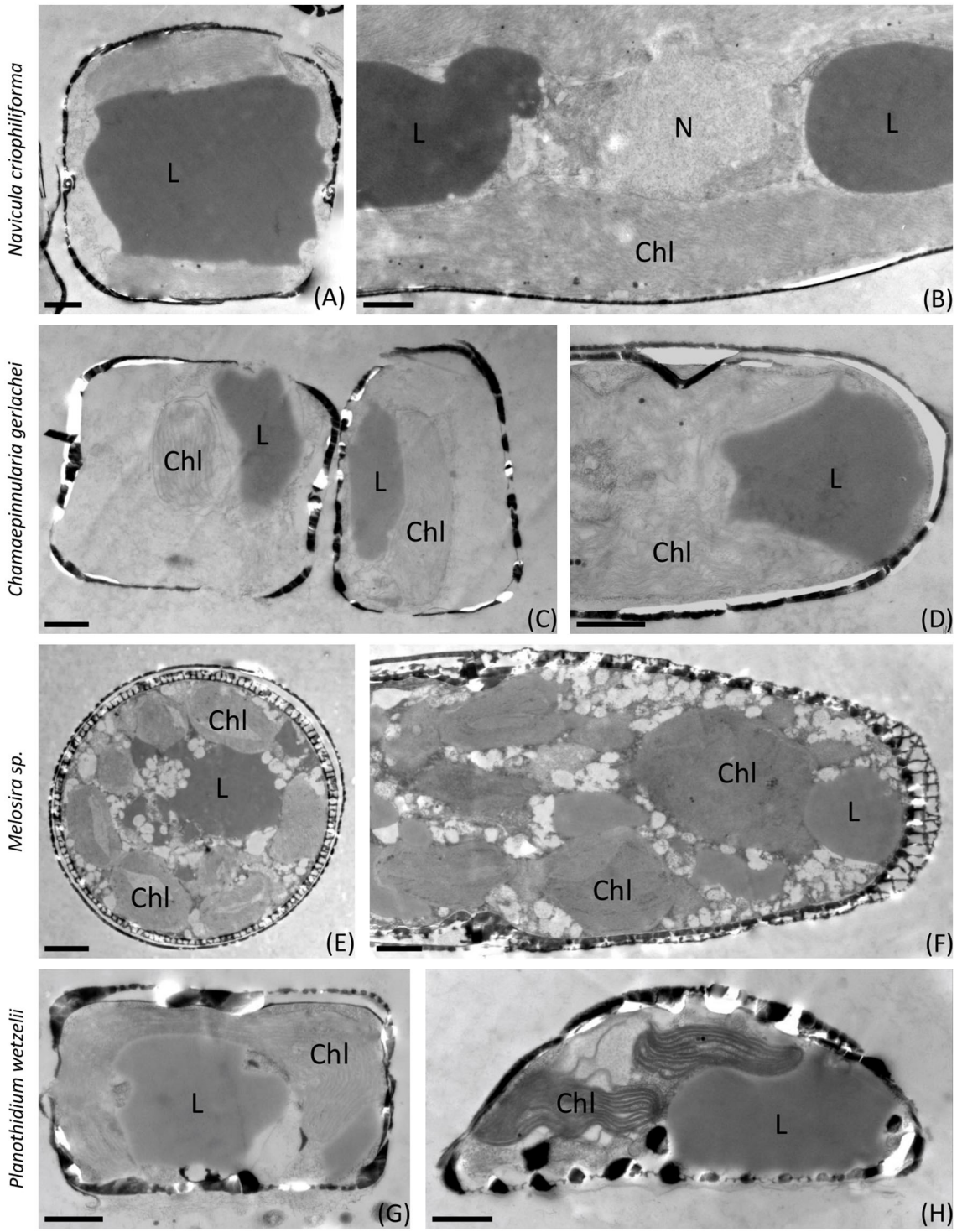

FIGURE 6
Transmission electron micrographs of control samples (T0). **(A, B)** *Navicula criophiliforma*, massive lipid droplets on both sides of the nucleus, intact chloroplast with thylakoid membranes; **(C, D)** *Chamaepinnularia gerlachei*, lipid droplets and intact chloroplasts; **(E, F)** *Melosira* sp., several small chloroplasts visible, lipid droplets and small electron translucent particles in the cell lumen, characteristic cell wall pattern; **(G, H)** *Planothidium wetzelii* (D300_015). Chl, chloroplast; L, lipid droplet; N, nucleus. Scale bars: 1 μm.

visible, since all species showed different response patterns. The quantitatively most abundant fatty acids in all benthic diatoms were the saturated 16:0 and the monosaturated 16:1n7 (Table 3). While the percentage proportion of 16:0 in relation to all measured fatty acids increased in *N. criophiliforma* (from 43.6 to 58.4%) and *C. gerlachei* (from 38.3 to 48.1%) after 3 months of darkness, it

10.3389/fmicb.2023.1241826

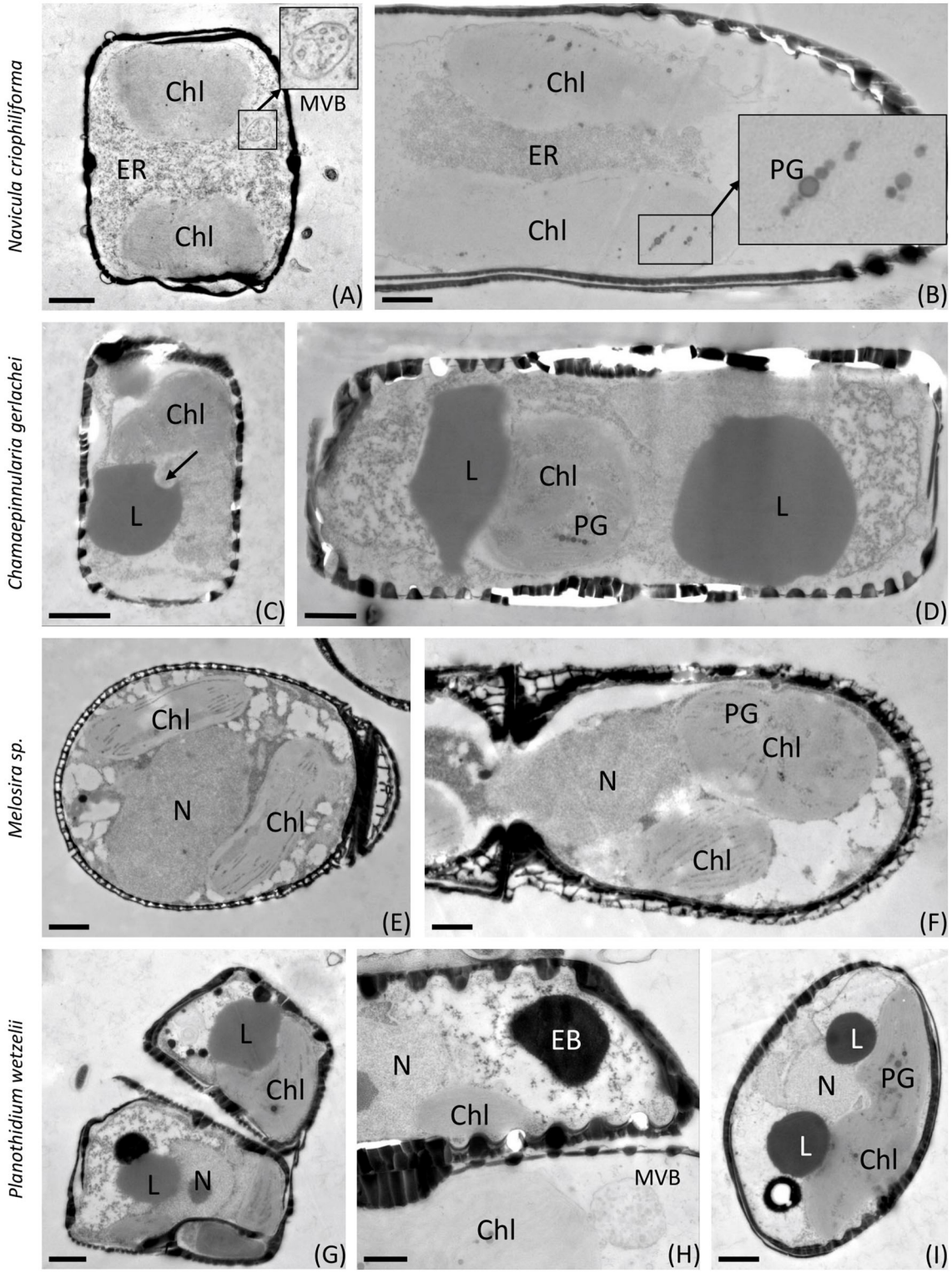

FIGURE 7
Transmission electron micrographs of 3 months of dark-treated samples (T3). **(A, B)** *Navicula criophiliforma*, chloroplasts are virtually lacking thylakoids, rows of plastoglobules are visible, massive accumulations of ER in the cell center, no lipid droplets are visible; **(C, D)** *Chamaepinnularia gerlachei*, lipid droplets are visible, and signs of lipid degradation are marked with an arrow; **(E, F)** *Melosira* sp., chloroplasts with reduced thylakoid membranes, containing plastoglobules; **(G–I)** *Planothidium wetzelii* (D300_015), chloroplasts reduced, lipid droplets visible, sometimes in close contact with electron-dense bodies. Chl, chloroplast; EB, electron-dense body; ER, endoplasmic reticulum; L, lipid droplet; MVB, multivesicular body; N, nucleus; PG, plastoglobules. Scale bars: 1 μm; (insets) 250 nm.

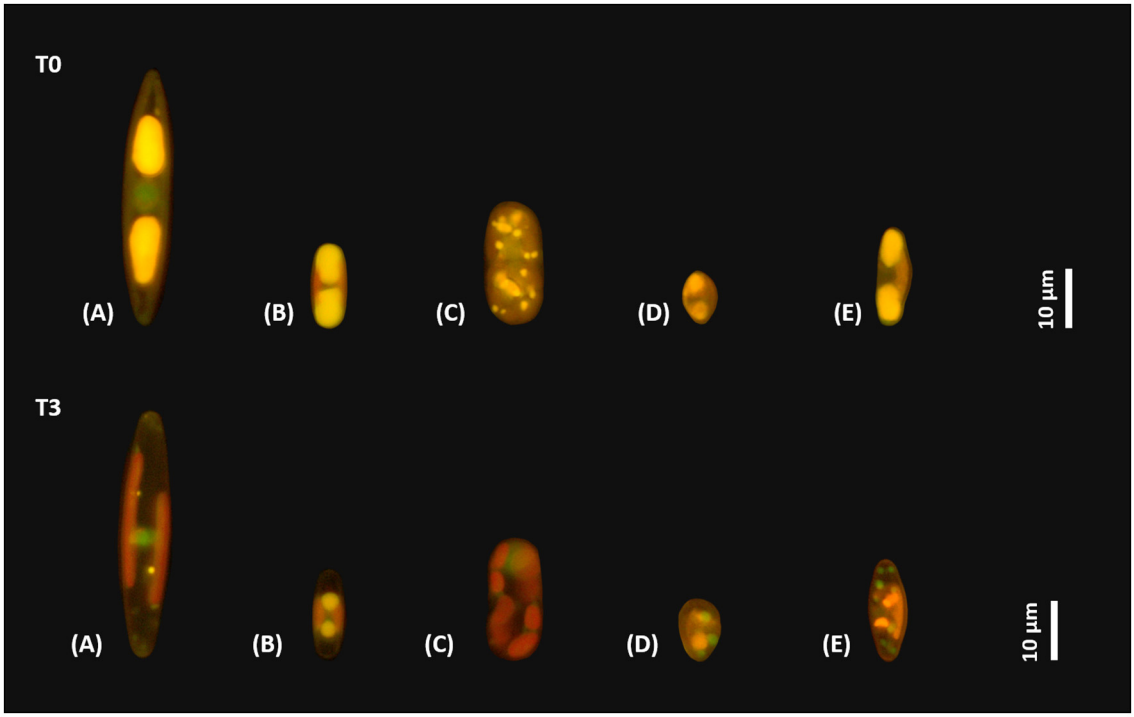

FIGURE 8
Micrographs of five Antarctic benthic diatom strains stained with Nile red. Upper row shows lipid droplets of the control, and lower row shows lipid droplets after 3 months of dark incubation. **(A)** *Navicula criophiliforma*; **(B)** *Chamaepinnularia gerlachei*; **(C)** *Melosira* sp.; **(D)** *Planothidium wetzelii* (D300_015); **(E)** *Planothidium wetzelii* (D300_025).

strongly decreased in the remaining species (e.g., in *Melosira* sp. from 36.2 to 16.9%). Reversely, the percentage proportion of 16:1n7 in relation to all fatty acids strongly declined in *N. criophiliforma*, *C. gerlachei*, and *Melosira* sp., while both *P. wetzelii* strains exhibited a slight increase (Table 3).

4. Discussion

Since Antarctic benthic diatoms are regularly confronted with the polar night, we isolated five strains at Potter Cove, established clonal cultures, and investigated their physiological, biochemical, and cell biological traits after 3 months of darkness to better understand the underlying tolerance mechanisms.

4.1. Importance of taxonomy as baseline for ecophysiological investigations

However, the first step, prior to ecophysiological experiments, is always to carefully address the taxonomic position of freshly collected field material. Two of the investigated diatom species were morphologically and molecular-genetically identified as species only known from maritime Antarctica (*Chamaepinnularia gerlachei*) or the Southern Indian Ocean (*Navicula criophiliforma*). Two additional cultures belong to the newly described freshwater species *Planothidium wetzelii*, which is so far unknown in any other region of the world. Finally, one centric species was investigated in this study, which does not fit morphologically and genetically to any described *Melosira* species, and most probably represents a new taxon, which was not further investigated in the present study.

Due to a thorough identification of the investigated cultures, a restricted geographical distribution in the southern hemisphere could be verified for all of them, and some might even be endemic to the Antarctic region. Morphological variability of the newly described species *Planothidium wetzelii* shows that valves from environmental samples need to be complemented with molecular and morphological information gained by cultures. This case highlights once again the importance of integrative taxonomy for the investigation of diatom biodiversity. In addition to an integrated taxonomy, the establishment of clonal cultures is the prerequisite for a combined taxonomical and physiological investigation of benthic diatoms. The two *P. wetzelii* strains D300_015 and D300_025 exhibit some variability in valve morphology. They might be considered two separate species when just examined by light microscopy, based on their differences in shape and size. However, diatoms can exhibit phenotypic plasticity due to environmental changes (Andrejić et al., 2018) or when observed over long time in culture (Mohamad et al., 2022). Both strains represent the same species based on molecular markers and micromorphology, and the results from this study show very similar response patterns during dark incubation.

10.3389/fmicb.2023.1241826

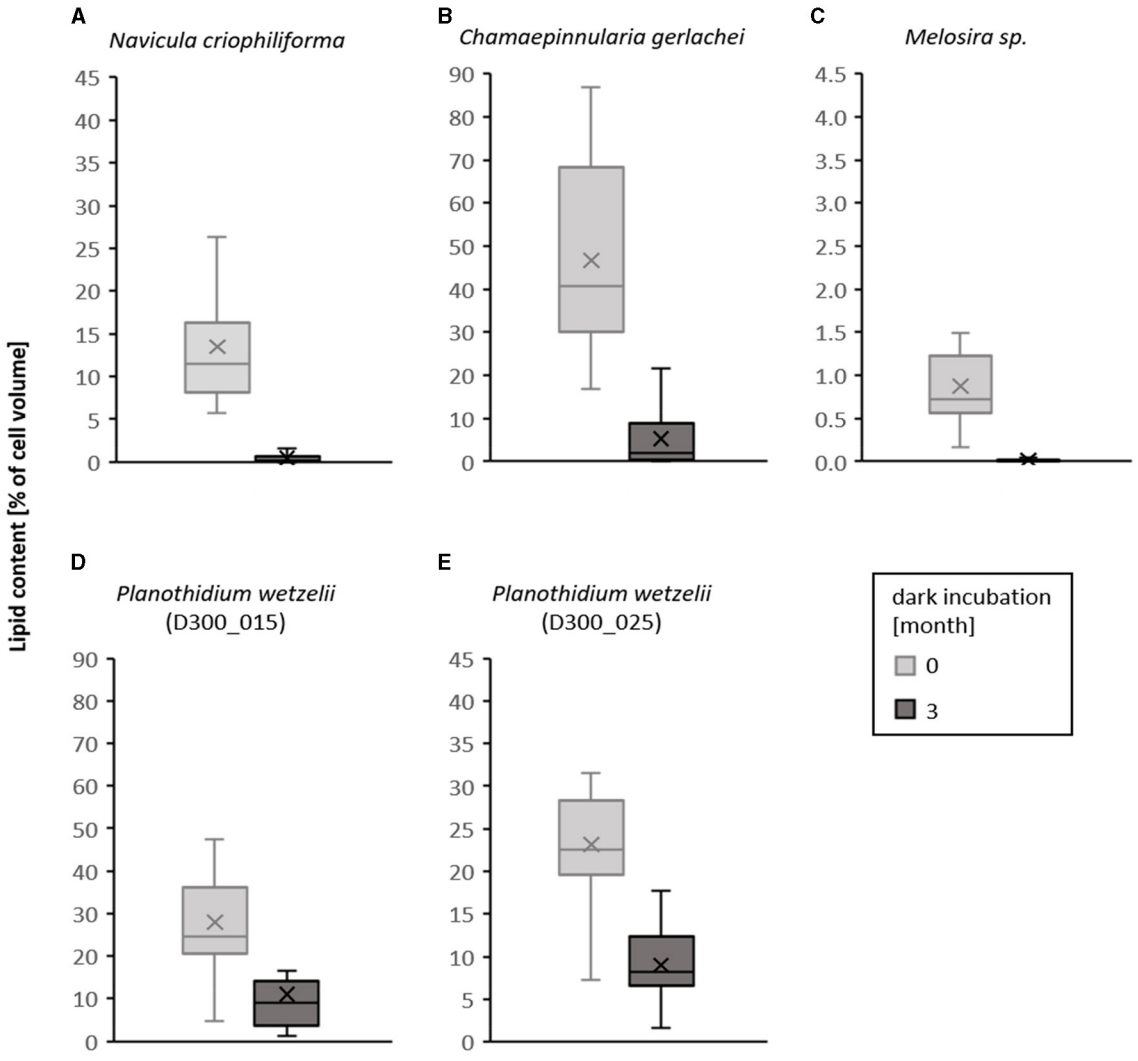

FIGURE 9
Boxplots of lipid content per cell calculated as percentage cell volume before dark incubation (light gray) and after 3 months of dark incubation (dark gray) in five Antarctic benthic diatom strains **(A–E)**. For each culture and time, 25 cells were measured. Scaling of the Y-axis is proportional but different as the lipid content differs. Different lower case letters represent significance differences calculated by Mann–Whitney *U*-test ($p < 0.05$).

As a result of the inaccessibility of Antarctica, the diversity of benthic diatoms is still poorly known. Considerable taxonomic work needs to be done in polar regions, which can then be used as a baseline for physiological, biochemical, and cell biological studies, allowing important conclusions, such as, for example, if geographic boundaries and environmental conditions led to many endemic taxa.

4.2. Variable light conditions and photosynthesis

Phototrophic organisms in the polar regions such as benthic diatoms cope with strong diurnally and seasonally fluctuating light conditions. The review of Pavlov et al. (2019) comprehensively summarized the underwater light climate and all main controlling factors in the Arctic Kongsfjorden, one of the best studied polar field sites, which is discussed here as a representative high latitude coastal habitat since adequate data for Antarctica are missing. In addition to the seasonal changes from midnight sun to polar night, clouds, sea ice conditions, and the optical seawater properties further strongly influence dose and spectral composition of solar radiation penetrating into the water column, thus defining the underwater light conditions. In addition, input of local run-off and glacial meltwater introducing inorganic and organic matter into the system, and phytoplankton blooms at diverse times and locations. Together, these factors result in a complex underwater light climate with high variability in time and space (Pavlov et al., 2019). Although not comprehensively investigated, similar processes and physico-chemical properties can be assumed for

10.3389/fmicb.2023.1241826

TABLE 3 Lipid analysis using gas chromatography connected to a mass spectrometer (GC-MS).

Dark incubation [months]	*Navicula criophiliforma*		*Chamaepinnularia gerlachei*		*Melosira* sp.		*Planothidium wetzelii* (D300_015)		*Planothidium wetzelii* (D300_025)	
	T0	T3	T0	T3	T0	T3	T0	T3	T0	T3
Total lipid content [pg/cell]	43.6 ± 59.5	2.4 ± 1.2	9.6 ± 6.1	1.2 ± 0.3	27.8 ± 17.3	2.8 ± 2.2	6.5 ± 2.5	4.2 ± 1.7	21.9 ± 6.6	17.4 ± 4.8
Decrease in total lipid content [%]	−94.5		−87.6		−90		−35.2		−20.6	
Saturated fatty acids (SFAs) [%]	52.8	73.8	43.9	58.3	55.6	34.7	47.9	36.4	79.0	43.8
Monounsaturated fatty acids (MUFAs) [%]	29.0	11.7	46.4	24.8	32.9	31.7	37.1	43.6	10.7	18.8
Polyunsaturated fatty acids (PUFAs) [%]	18.2	14.5	9.7	16.9	11.5	33.7	15.0	20.0	10.3	37.4
(SFA+MUFA) $(PUFA)^{-1}$	4.5	5.9	9.3	4.9	7.7	2.0	5.7	4.0	8.7	1.7
16:0 [%]	43.6	58.4	38.3	48.1	36.2	16.9	41.0	31.9	53.3	25.0
16:1n7	23.5	1.3	40.3	13.0	24.0	8.7	33.3	36.5	8.8	11.5

Total fatty acid content was normalized to cell number and is shown before dark incubation (T0) and after 3 months of dark incubation (T3) in five Antarctic benthic diatom species. Standard deviation was calculated according to Gaussian error propagation (n = 3). The percentage decrease in the total fatty acid content during this time was calculated. Saturated fatty acids (SFAs), monounsaturated (MUFA), and polyunsaturated (PUFA) fatty acids at T0 and T3 are given as the percentage of the total lipid content, as well as the ratio (SFA+MUFA)/(PUFA). In addition, the most abundant fatty acids detected in all strains, 16:0 and 16:1n7 are shown in the percentage proportion of all measured fatty acids.

Potter Cove (Hoffmann et al., 2019) and other bays around the Antarctic Peninsula. Polar benthic diatoms are additionally affected by huge amounts of particles released into the water column due to coastal glacier retreat and melt under global change conditions, resulting in increased turbidity and hence less available light (Hoffmann et al., 2019).

Photosynthesis is the essential mechanism for the energy metabolism and, thus, not only responsible for viability and survival of benthic diatoms, but also primarily dependent on light availability. All benthic diatom species examined in this study showed $Y(II)_{max}$ of 0.57–0.63 before dark incubation as physiological marker for photosynthetic activity. Other studies on Antarctic benthic diatoms reported similar maximum $Y(II)_{max}$ values between 0.6 and 0.7, indicating that the strains were in good physiological conditions prior to dark incubation (Longhi et al., 2003; Wulff et al., 2008a).

Prelle et al. (2022) used for their P–I curves various Antarctic benthic diatoms, including the species also investigated in the present study: *Navicula criophiliforma*, *Chamaepinnularia gerlachei*, and *P. wetzelii* strain D300_015, and demonstrated generally low light requirements, as light-saturated photosynthesis was reached at <70 μmol photons m^{-2} s^{-1}. A similarly low light demand was observed for *Melosira* sp. and *P. wetzelii* strain D300_025 (data not shown). Other polar benthic diatoms are also known for their shade acclimation with low light compensation (I_c) and light saturation points (I_k) as well as steep initial slopes (α value) in their P–I curves (Wulff et al., 2008a). At the same time, they are also described as phototrophic microorganisms with a pronounced photophysiological plasticity, allowing them to cope with high solar radiation (Prelle et al., 2022).

Remarkable are the relatively high respiration rates, which were about as high as the net photosynthetic rates in some of the studied benthic diatom species, resulting in low ratios of NPP_{max}: respiration, and which can be explained by co-occurring bacteria in the cultures. Overall, we cannot rule out that diatom-associated bacteria could affect the results of the P–I curves through their respiration, particularly when present in high cell numbers. However, bacteria and diatoms are known to have complex biotic interactions that affect each other's viability, and diatoms can even control their own phycosphere (microbiome; Amin et al., 2012). Therefore, the often-applied antibiotic treatment prior to experiments could potentially not only reduce essential bacteria but also affect diatom viability with unforeseen consequences for dark survival.

4.3. Physiological traits during darkness

Three months of darkness did not negatively affect $Y(II)_{max}$ values in the studied benthic diatom species, which provides at least a crude measure for still-existing photosynthetic viability, which is confirmed by the oxygen data. Previous studies on the dark survival of polar diatoms showed a decrease in various photosynthetic parameters during dark incubation (Wulff et al., 2008a; Reeves et al., 2011; Karsten et al., 2012; Lacour et al., 2019). The only study on Antarctic benthic diatoms was performed by Wulff et al. (2008b) on semi-natural cultures with a dark period of 64 days. Their results revealed significant decreases in the parameters F_v/F_m, rETR (relative electron transport rate), and α (light-using efficiency).

All species revealed oxygen production after the dark period but to different degrees. While *C. gerlachei* and *Melosira* sp. showed a moderate decline in NPP_{max} (39.9 and 44.6%, respectively), the remaining species (*N. criophiliforma*, both *P. wetzelii* isolates) exhibited unaffected NPP_{max} values. Furthermore, the chlorophyll *a* data pointed to species-specific responses. While chlorophyll *a* decreased in *N. criophiliforma, C. gerlachei*, and *Melosira sp.* after 3 months of dark incubation, it remained more or less stable in both *P. wetzelii* strains. This observation is further supported by the TEM observations, which showed that some of the thylakoid membranes remained intact in this species. In contrast, in *N. criophiliforma*, much more degradation of the thylakoid system was observed with an increased number of plastoglobules. The lower NPP_{max} values can be related to the decline in chlorophyll *a* content as discussed by Wulff et al. (2008a) and Reeves et al. (2011), who explained the decrease in photosynthetic potential in Antarctic diatoms with a progressive degradation of the antenna complex and the reaction center. The decline in chlorophyll *a* concentration in some of the benthic diatom species can also be explained by chloroplast degradation after 3 months of darkness, but remarkably, this did not seem to have an effect neither on the physiological performance nor on the viability. Apparently, parts of the thylakoid membranes are degraded in darkness, but a functional part seems to remain intact and thus contributes to a basal level of photosynthetic activity. Kennedy et al. (2019) found similar results in Antarctic sea ice diatoms during 4 months of dark incubation and reported a rapid reduction of light-harvesting complexes and photosystems while maintaining photosynthetic capacity.

Applying SYTOX Green to the Arctic benthic diatoms *Surirella* cf. *minuta* and *Navicula directa* during 5 months of darkness indicated that an increasing number of cells exhibited damaged membranes over time in the first species (Karsten et al., 2019a), while the latter one was almost unaffected (Karsten et al., 2019b). In the present study, SYTOX Green staining was applied for the first time to Antarctic benthic diatoms, and the results are comparable to those on both Arctic species. While the percentage of damaged cells increased significantly in *N. criophiliforma*, *C. gerlachei, Melosira* sp., and *P. wetzelii* (D300_025) after 3 months of dark incubation, *P. wetzelii* (D300_015) maintained membrane integrity over this period of darkness. Although some diatom cells could not cope with longer darkness, others maintained viability and hence guaranteed the survival of the population after re-irradiation.

4.4. Cell biological traits during darkness

These are the first transmission electron micrographs of Antarctic benthic diatoms after dark treatment. They showed degraded chloroplasts in all benthic diatom species after 3 months of dark incubation with a markedly increased amount of plastoglobules (PGs) in the stroma of the plastids. PG appearance is a common response of plant cells to high light stress (Meier and Lichtenthaler, 1981) or any other stress, leading to a reduction of thylakoid membranes, as PGs contain the building blocks for thylakoids, including the enzymatic setting. The increase in PG in the Antarctic benthic diatoms can thus also be interpreted as a stress response; in this case, however, it is a response to long-term darkness. Schwarz et al. (2017) reported in the green microalga *Micrasterias* sp. how lipid droplets are released from the chloroplast into the cytoplasm during starvation, where they are degraded by autophagy. In addition, multivesicular bodies (MVBs) were also found in the cytoplasm after 7 weeks of starvation in darkness in *Micrasterias* sp., confirming autophagy (Schwarz et al., 2017). In the literature, it has been discussed that apoptosis and autophagy are both distinct processes but strongly interlinked (Mariño et al., 2014). In our study, the observable TEM structures are MVBs, which were present in *N. criophiliforma* and *P. wetzelii* (D300_015). Along with the numerous PGs and the degradation of the chloroplasts, this could indicate a mobilization of energy reserves by the autophagy of chloroplast components to survive the polar night. Furthermore, the chlorophyll *a* content per cell after 3 months of darkness strongly decreased in *N. criophiliforma, C. gerlachei*, and *Melosira sp.*, supporting the ultrastructural results.

The cell biological data on Antarctic benthic diatoms confirm the few results on their Arctic pendants, which also reported, for example, a 30–50% decrease in chloroplast length (Karsten et al., 2012, 2019b). In addition, Wulff et al. (2008a) demonstrated condensed chloroplasts after dark treatment, which recovered within hours after re-exposure to light. Thus, no long-term damage appears to have been caused by the partial decomposition of chloroplasts during the prolonged darkness. According to Karsten et al. (2019b), the degradation of chloroplast compounds seems to be a key mechanism in Arctic benthic diatoms to survive the polar night and generate energy for their maintenance metabolism. The results of this study confirm that this is also a survival strategy for the examined Antarctic benthic diatoms.

4.5. Lipid content after 3 months of dark incubation

Both the light microscopic and the TEM images indicated significant differences in the lipid content of all species between control and after 3 months of dark incubation, which was additionally supported by the GC-MS analysis. *N. criophiliforma* and *Melosira* sp. consumed most of their lipid reserves in darkness, *C. gerlachei* depleted ~85% of their lipids, and both *P. wetzelii* strains still exhibited lipid droplets even after 3 months of darkness, which could suggest that this species might survive additional months in darkness. Enhanced lipid content, as well as the consumption of storage substances during darkness to maintain the cellular metabolism, have been described before for Arctic diatoms (Zhang et al., 1998; McMinn and Martin, 2013; Karsten et al., 2019b). Only a few studies on Arctic benthic diatoms quantified the decrease of lipid storage compounds during darkness (Schaub et al., 2017; Karsten et al., 2019a). Investigations on Antarctic benthic diatoms in this regard are entirely lacking so far.

Diatoms carry two pathways of β-oxidation for the breakdown of lipid compounds, the plant-like and the animal-like metabolic capabilities (Armbrust et al., 2004; Schaub et al., 2017). In the darkness, the mechanism of animal-like β-oxidation, located in the mitochondria, is upregulated and thus can provide energy from lipid storages during the polar night (Chauton et al., 2013), which probably allows diatoms to survive long periods

of darkness, thereby maintaining their metabolism and the fundamental functions of their organelles (Armbrust et al., 2004). Thus, the results of the present study confirm the described metabolic pathway in Armbrust et al. (2004) and Chauton et al. (2013). In addition, in the more recent review of Leyland et al. (2020), the authors describe the storage of lipids in droplets and characterize these structures as organelles composed of a core of neutral lipids, mostly triacylglycerol (TAG), surrounded by a polar lipid monolayer. Most interestingly, lipid droplets can store not only reserves of energy but also membrane components, carbon skeletons, carotenoids, and even proteins (Leyland et al., 2020, and references therein).

While the membrane lipids of polar diatoms are mainly composed of polyunsaturated fatty acids in order to maintain membrane fluidity at low temperatures (Murata and Los, 1997), the storage lipids are mainly formed by triacylglycerol (TAG), which has three fatty acids that are mainly saturated or monounsaturated (Schaub et al., 2017). The latter authors carefully investigated qualitatively and quantitatively the lipid classes of the Arctic benthic diatom *Navicula perminuta* during 2 months of dark incubation. Schaub et al. (2017) demonstrated by the ratio of SFA and MUFA to PUFA that, indeed, lipid reserves were depleted, while membrane lipids remained unchanged, including thylakoid membranes. In the Antarctic *C. gerlachei*, *Melosira* sp., and both *P. wetzelii* strains, a decline in the ratio of fatty acids groups was observed, indicating enhanced degradation of storage lipids. In contrast, *N. criophiliforma* showed a slight increase in the ratio of fatty acids after 12 weeks, which points to a stronger increase in membrane degradation compared to lipid consumption. Apparently, both the consumption of storage lipids and the partial degradation of chloroplasts took place in the investigated Antarctic benthic diatoms during prolonged darkness in order to obtain energy for the maintenance metabolism.

5. Conclusion

In conclusion, all Antarctic benthic diatom species exhibited similar response patterns after 3 months of darkness. The combination of ecophysiological, biochemical, and cell biological data led to a better understanding of the underlying mechanisms. All benthic diatoms degrade parts of their chloroplasts and utilize their lipid energy reserves but at the same time maintained a functional photosynthetic apparatus that guarantees rapid recovery after re-irradiation. The combination of both mechanisms, presumably using storage lipids and degrading chloroplasts, is a key strategy for dark survival and hence for coping with the polar night.

Data availability statement

The datasets presented in this study can be found in online repositories. The names of the repository/repositories and accession number(s) can be found in the article/Supplementary material.

Author contributions

UK and JZ developed the concept for this manuscript. JZ sampled and OS isolated, purified, and established clonal cultures. DJ conducted the ecophysiological and biochemical parts of the manuscript. KS provided the light microscopic and scanning electron microscopic analyses. CP and AH undertook the transmission electron microscopy, combined the transmission electron micrographs, and edited the manuscript. KS and NA performed the taxonomic treatment. MG provided the GC-MS data. DJ and KS wrote the first version of the manuscript and prepared most of the figures. UK edited the first draft. All authors interpreted the data and edited and approved the final version of this manuscript.

Funding

This study was funded within the framework of the SPP 1158 Antarktisforschung by the DFG under grant numbers ZI 1628/2-1 and KA899/38-1. This study was further supported by the Austrian Science Fund Grant P34181-B to AH.

Acknowledgments

The authors would like to thank the team of the Argentinian Antarctic Research Station: Carlini of the Instituto Antártico Argentino (IAA) for their support and logistics, especially Gabriela L. Campana and María Liliana Quartino. The authors acknowledge the contribution of Regine Jahn to the description of the new species and thank Wolf-Henning Kusber for his support of the nomenclature act. Furthermore, the authors would like to thank Akihiro Tuji from the National Museum of Nature and Science, Japan, for sharing the sequence data of *P. tujii*. The authors are grateful to Jana Bansemer for work in the molecular laboratory and to Juliane Bettig for support at the SEM at the BGBM Berlin. The authors thank Matthias Woll, AWI Bremerhaven, for undertaking the GC-MS analysis. Moreover, the authors thank Sabrina Obwegeser, University of Innsbruck, for expert technical assistance in transmission electron microscopy.

Conflict of interest

The authors declare that the research was conducted in the absence of any commercial or financial relationships that could be construed as a potential conflict of interest.

Publisher's note

All claims expressed in this article are solely those of the authors and do not necessarily represent those of

their affiliated organizations, or those of the publisher, the editors and the reviewers. Any product that may be evaluated in this article, or claim that may be made by its manufacturer, is not guaranteed or endorsed by the publisher.

Supplementary material

The Supplementary Material for this article can be found online at: https://www.frontiersin.org/articles/10.3389/fmicb.2023.1241826/full#supplementary-material

References

Abarca, N., Jahn, R., Zimmermann, J., and Enke, N. (2014). Does the cosmopolitan diatom *Gomphonema parvulum* (Kützing) Kützing have a biogeography? *PLoS ONE* 9, e86885. doi: 10.1371/journal.pone.0086885

Al-Handal, A. Y., Torstensson, A., and Wulff, A. (2022). Revisiting Potter Cove, King George Island, Antarctica, 12 years later: new observations of marine benthic diatoms. *Bot. Mar.* 65, 81–103. doi: 10.1515/bot-2021-0066

Amin, S. A., Parker, M. S., and Armbrust, E. V. (2012). Interactions between diatoms and bacteria. *Microbiol. Mol. Biol. Rev.* 76, 667–684. doi: 10.1128/MMBR.00007-12

Andrejić, J. Z., Spaulding, S. A., Manoylov, K. M., and Edlund, M. B. (2018). Phenotypic plasticity in diatoms: Janus cells in four *Gomphonema* taxa. *Diatom Res.* 33, 453–470. doi: 10.1080/0269249X.2019.1572652

Antia, N. J. (1976). Effects of temperature on the darkness survival of marine microplanktonic algae. *Microb. Ecol.* 3, 41–54. doi: 10.1007/BF02011452

Armbrust, E. V. (2009). The life of diatoms in the world's oceans. *Nature* 459, 185–192. doi: 10.1038/nature08057

Armbrust, E. V., Berges, J. A., Bowler, C., Green, B. R., Martinez, D., Putnam, N. H., et al. (2004). The genome of the diatom *Thalassiosira pseudonana*: ecology, evolution, and metabolism. *Science* 306, 79–86. doi: 10.1126/science.1101156

Chauton, M. S., Winge, P., Brembu, T., Vadstein, O., and Bones, A. M. (2013). Gene regulation of carbon fixation, storage, and utilization in the diatom *Phaeodactylum tricornutum* acclimated to light; dark cycles. *Plant Physiol.* 161, 1034–1048. doi: 10.1104/pp.112.206177

Cottier, F., and Potter, M. (2020). "The marine physical environment during the polar night," in *Polar Night Marine Ecology, Life and Light in the Dead of Night*, eds G. Johnsen, E. Leu, and R. Gradinger (Cham: Springer), 17–36. doi: 10.1007/978-3-030-33208-2_2

Crawford, R. M. (1977). The taxonomy and classification of the diatom genus *Melosira* C. Ag. II. *M. moniliformis* (Müll.) C. Ag. *Phycologia* 16, 277–285. doi: 10.2216/i0031-8884-16-3-277.1

Droege, G., Barker, K., Seberg, O., Coddington, J., Benson, E., Berendsohn, W. G., et al. (2016). The Global Genome Biodiversity Network (GGBN) data standard specification. *Database* 2016, baw125. doi: 10.1093/database/baw125

Durbin, E. G. (1978). Aspects of the biology of resting spores of *Thalassiosira nordenskioeldii* and *Detonula confervacea*. *Mar. Biol.* 45, 31–37. doi: 10.1007/BF00388975

Fahl, K., and Kattner, G. (1993). Lipid content and fatty acid composition of algal communities in sea-ice and water from the Weddell Sea (Antarctica). *Polar Biol.* 13, 405–409. doi: 10.1007/BF01681982

Field, C. B., Behrenfeld, M. J., Randerson, J. T., and Falkowski, P. (1998). Primary production of the biosphere: integrating terrestrial and oceanic components. *Science* 281, 237–240. doi: 10.1126/science.281.5374.237

Fryxell, G. A. (1989). Marine phytoplankton at the Weddell Sea ice edge: seasonal changes at the specific level. *Polar Biol.* 10, 1–18. doi: 10.1007/BF00238285

Gemeinholzer, B., Droege, G., Zetzsche, H., Haszprunar, G., Klenk, H. P., Güntsch, A., et al. (2011). The DNA Bank Network: the start from a German initiative. *Biopreserv. Biobank* 9, 51–55. doi: 10.1089/bio.2010.0029

Glud, R. N., Kühl, M., Wenzhöfer, F., and Rysgaard, S. (2002). Benthic diatoms of a high Arctic fjord (Young Sound, NE Greenland): importance for ecosystem primary production. *Mar. Ecol. Prog. Ser.* 238, 15–29. doi: 10.3354/meps238015

Glud, R. N., Woelfel, J., Karsten, U., Kühl, M., and Rysgaard, S. (2009). Benthic microalgal production in the Arctic: applied methods and status of the current database. *Bot. Mar.* 52, 559–571. doi: 10.1515/BOT.2009.074

Gómez, I., Wulff, A., Roleda, M. Y., Huovinen, P., Karsten, U., Quartino, M. L., et al. (2009). Light and temperature demands of marine benthic microalgae and seaweeds in polar regions. *Bot. Mar.* 52, 593–608. doi: 10.1515/BOT.2009.073

Greenspan, P., Mayer, E. P., and Fowler, S. D. (1985). Nile red: a selective fluorescent stain for intracellular lipid droplets. *J. Cell Biol.* 100, 965–973. doi: 10.1083/jcb.100.3.965

Guillard, R. R. L., and Ryther, J. H. (1962). Studies of marine planktonic diatoms: I. *Cyclotella nana* Hustedt, and *Detonula confervacea* (Cleve) Gran. *Can. J. Microbiol.* 8, 229–239. doi: 10.1139/m62-029

HELCOM (2019). *Guidelines-for-Measuring-Chlorophyll-a*. Baltic Marine Environment Protection Commission. Available online at: https://helcom.fi/post_type_publ/guidelines-for-measuring-chlorophyll-a/ (accessed October 15, 2022).

Hellebust, J. A., and Lewin, J. (1977). "Heterotrophic nutrition," in *The Biology of Diatoms*, ed D. Werner (Berkeley, CA: University of California Press), 169–197.

Hernández, E. A., Lopez, J. L., Piquet, A. M. T., Mac Cormack, W. P., and Buma, A. G. J. (2019). Changes in salinity and temperature drive marine bacterial communities' structure at Potter Cove, Antarctica. *Polar Biol.* 42, 2177–2191. doi: 10.1007/s00300-019-02590-5

Hoffmann, R., Al-Handal, A. Y., Wulff, A., Deregibus, D., Zacher, K., Quartino, M. L., et al. (2019). Implications of glacial melt-related processes on the potential primary production of a microphytobenthic community in Potter Cove (Antarctica). *Front. Mar. Sci.* 6, 655. doi: 10.3389/fmars.2019.00655

Holzinger, A., Roleda, M. Y., and Lütz, C. (2009). The vegetative arctic freshwater green alga *Zygnema* is insensitive to experimental UV exposure. *Micron* 40, 831–838. doi: 10.1016/j.micron.2009.06.008

Hu, Q., Sommerfeld, M., Jarvis, E., Ghirardi, M., Posewitz, M., Seibert, M., et al. (2008). Microalgal triacylglycerols as feedstocks for biofuel production: perspectives and advances. *Plant J.* 54, 621–639. doi: 10.1111/j.1365-313X.2008.03492.x

Jahn, R., Abarca, N., Gemeinholzer, B., Mora, D., Skibbe, O., Kulikovskiy, M., et al. (2017). *Planothidium lanceolatum* and *Planothidium frequentissimum* reinvestigated with molecular methods and morphology: four new species and the taxonomic importance of the sinus and cavum. *Diatom Res.* 32, 75–107. doi: 10.1080/0269249X.2017.1312548

Kapuscinski, J. (1995). DAPI: a DNA-specific fluorescent probe. *Biotech. Histochem.* 70, 220–233. doi: 10.3109/10520299509108199

Karsten, U., Schaub, I., Woelfel, J., Sevilgen, D. S., Schlie, C., Becker, B., et al. (2019a). "Living on cold substrata: new insights and approaches in the study of microphytobenthos ecophysiology and ecology in Kongsfjorden," in *The Ecosystem of Kongsfjorden, Svalbard*, eds H. Hop and C. Wiencke (Cham: Springer International Publishing), 303–330. doi: 10.1007/978-3-319-46425-1_8

Karsten, U., Schlie, C., Woelfel, J., and Becker, B. (2012). Benthic diatoms in arctic seas—Ecological functions and adaptations. *Polarforschung* 81, 77–84. doi: 10.2312/polarforschung.81.2.77

Karsten, U., Schumann, R., and Holzinger, A. (2019b). "Ecophysiology, cell biology and ultrastructure of a benthic diatom isolated in the arctic," in *Diatoms. Fundamentals and Applications*, eds J. Seckbach and R. Gordon (Hoboken, NJ; Salem, MA: Wiley, Scrivener), 273–287. doi: 10.1002/9781119370741.ch12

Kattner, G., and Fricke, H. S. G. (1986). Simple gas–liquid chromatographic method for the simultaneous determination of fatty acids and alcohols in wax esters of marine organisms. *J. Chromatogr.* 361, 263–268. doi: 10.1016/S0021-9673(01)86914-4

Kennedy, F., Martin, A., Bowman, J. P., Wilson, R., and McMinn, A. (2019). Dark metabolism: a molecular insight into how the Antarctic sea-ice diatom *Fragilariopsis cylindrus* survives long-term darkness. *New Phytol.* 223, 675–691. doi: 10.1111/nph.15843

Kopalová, K., Veselá, J., Elster, J., Nedbalová, L., Komárek, J., and Van de Vijver, B. (2012). Benthic diatoms (Bacillariophyta) from seepages and streams on James Ross Island (NW Weddell Sea, Antarctica). *Plant Ecol. Evol.* 145, 190–208. doi: 10.5091/plecevo.2012.639

Lacour, T., Morin, P., Sciandra, T., Donaher, N., Campbell, D. A., Ferland, J., et al. (2019). Decoupling light harvesting, electron transport and carbon fixation during prolonged darkness supports rapid recovery upon re-illumination in the Arctic diatom *Chaetoceros neogracilis*. *Polar Biol.* 42, 1787–1799. doi: 10.1007/s00300-019-02507-2

Leyland, B., Boussiba, S., and Khozin-Goldberg, I. (2020). A review of diatom lipid droplets. *Biology* 9, 38. doi: 10.3390/biology9020038

Longhi, M. L., Schloss, I. R., and Wiencke, C. (2003). Effect of irradiance and temperature on photosynthesis and growth of two antarctic benthic

diatoms, *Gyrosigma subsalinum* and *Odontella litigiosa*. *Bot. Mar.* 46, 276–284. doi: 10.1515/BOT.2003.025

Malapascua, J. R. F., Jerez, C. G., Sergejevová, M., Figueroa, F. L., and Masojídek, J. (2014). Photosynthesis monitoring to optimize growth of microalgal mass cultures: application of chlorophyll fluorescence techniques. *Aquat. Biol.* 22, 123–140. doi: 10.3354/ab00597

Mariño, G., Niso-Santano, M., Baehrecke, E., and Kroemer, G. (2014). Self-consumption: the interplay of autophagy and apoptosis. *Nat. Rev. Mol. Cell Biol.* 15, 81–94. doi: 10.1038/nrm3735

McMinn, A., Ashworth, C., Bhagooli, R., Martin, A., Salleh, S., Ralph, P., et al. (2012). Antarctic coastal microalgal primary production and photosynthesis. *Mar. Biol.* 159, 2827–2837. doi: 10.1007/s00227-012-2044-0

McMinn, A., and Martin, A. (2013). Dark survival in a warming world. *Proc. Biol. Sci.* 280, 20122909. doi: 10.1098/rspb.2012.2909

McQuoid, M. R., and Hobson, L. A. (1996). Diatom resting stages. *J. Phycol.* 32, 889–902. doi: 10.1111/j.0022-3646.1996.00889.x

Meier, D., and Lichtenthaler, H. K. (1981). Ultrastructural development of chloroplasts in radish seedlings grown at high- and low-light conditions and in the presence of the herbicide bentazon. *Protoplasma* 107, 195–207. doi: 10.1007/BF01275618

Mohamad, H., Mora, D., Skibbe, O., Abarca, N., Deutschmeyer, V., Enke, N., et al. (2022). Morphological variability and genetic marker stability of 16 monoclonal pennate diatom strains under medium-term culture. *Diatom Res.* 37, 307–328. doi: 10.1080/0269249X.2022.2141346

Morales, M., Aflalo, C., and Bernard, O. (2021). Microalgal lipids: a review of lipids potential and quantification for 95 phytoplankton species. *Biomass Bioenergy* 150, 106108. doi: 10.1016/j.biombioe.2021.106108

Müller, J., Müller, K., Neinhuis, C., and Quandt, D. (2010). *PhyDE® -Phylogenetic Data Editor*. Available online at: http://www.phyde.de/

Murata, N., and Los, D. A. (1997). Membrane fluidity and temperature perception. *Plant Physiol.* 115, 875–879. doi: 10.1104/pp.115.3.875

Nelson, D. M., Tréguer, P., Brzezinski, M. A., Leynaert, A., and Quéguiner, B. (1995). Production and dissolution of biogenic silica in the ocean: revised global estimates, comparison with regional data and relationship to biogenic sedimentation. *Glob. Biogeochem. Cycles* 9, 359–372. doi: 10.1029/95GB01070

Palmisano, A. C., and Sullivan, C. W. (1982). Physiology of sea ice diatoms. I. Response of three polar diatoms to a simulated summer-winter transition. *J. Phycol.* 18, 489–498. doi: 10.1111/j.1529-8817.1982.tb03215.x

Palmisano, A. C., and Sullivan, C. W. (1983). Physiology of sea ice diatoms. II. Dark survival of three polar diatoms. *Can. J. Microbiol.* 29, 157–160. doi: 10.1139/m83-026

Pavlov, A., Leu, E., Hanelt, D., Bartsch, I., Karsten, U., Hudson, S. R., et al. (2019). "Underwater light regime in Kongsfjorden and its ecological implications," in *The Ecosystem of Kongsfjorden, Svalbard, Advances in Polar Ecology 2*, eds H. Hop and C. Wiencke (Cham: Springer), 137–170.

Prelle, L. R., Graiff, A., Gründling-Pfaff, S., Sommer, V., Kuriyama, K., and Karsten, U. (2019). Photosynthesis and respiration of Baltic Sea benthic diatoms to changing environmental conditions and growth responses of selected species as affected by an adjacent peatland (Hütelmoor). *Front. Microbiol.* 10, 1500. doi: 10.3389/fmicb.2019.01500

Prelle, L. R., Schmidt, I., Schimani, K., Zimmermann, J., Abarca, N., Skibbe, O., et al. (2022). Photosynthetic, respirational, and growth responses of six benthic diatoms from the antarctic peninsula as functions of salinity and temperature variations. *Genes* 13, 71264. doi: 10.3390/genes13071264

Reeves, S., McMinn, A., and Martin, A. (2011). The effect of prolonged darkness on the growth, recovery and survival of Antarctic sea ice diatoms. *Polar Biol.* 34, 1019–1032. doi: 10.1007/s00300-011-0961-x

Schaub, I., Wagner, H., Graeve, M., and Karsten, U. (2017). Effects of prolonged darkness and temperature on the lipid metabolism in the benthic diatom *Navicula perminuta* from the Arctic Adventfjorden, Svalbard. *Polar Biol.* 40, 1425–1439. doi: 10.1007/s00300-016-2067-y

Schimani, K., Abarca, N., Zimmermann, J., Skibbe, O., Jahn, R., Kusber, W. H., et al. (2023). Molecular phylogenetics coupled with morphological analyses of Arctic and Antarctic strains place *Chamaepinnularia* (Bacillariophyta) within the Sellaphoraceae. *Fottea* 24, 1–22. doi: 10.5507/fot.2023.002

Schlie, C., and Karsten, U. (2017). Microphytobenthic diatoms isolated from sediments of the Adventfjorden (Svalbard): growth as function of temperature. *Polar Biol.* 40, 1043–1051. doi: 10.1007/s00300-016-2030-y

Schwarz, V., Andosch, A., Geretschläger, A., Affenzeller, M., and Lütz-Meindl, U. (2017). Carbon starvation induces lipid degradation via autophagy in the model alga *Micrasterias*. *J. Plant Physiol.* 208, 115–127. doi: 10.1016/j.jplph.2016.11.008

Sterken, M., Verleyen, E., Jones, V., Hodgson, D., Vyverman, W., Sabbe, K., et al. (2015). An illustrated and annotated checklist of freshwater diatoms (Bacillariophyta) from Livingston, Signy and Beak Island (Maritime Antarctic Region). *Plant Ecol. Evol.* 148, 431–455. doi: 10.5091/plecevo.2015.1103

Tamura, K., Stecher, G., and Kumar, S. (2021). MEGA11: molecular evolutionary genetics analysis version 11. *Mol. Biol. Evol.* 38, 3022–3027. doi: 10.1093/molbev/msab120

Tuchman, N. C., Schollett, M. A., Rier, S. T., and Geddes, P. (2006). Differential heterotrophic utilization of organic compounds by diatoms and bacteria under light and dark conditions. *Hydrobiologia* 561, 167–177. doi: 10.1007/s10750-005-1612-4

Van de Vijver, B., Sterken, M., Vyverman, W., Mataloni, G., Nedbalová, L., Kopalová, K., et al. (2010). Four new non-marine diatom taxa from the Subantarctic and Antarctic regions. *Diatom Res.* 25, 431–443. doi: 10.1080/0269249X.2010.9705861

Verleyen, E., Van de Vijver, B., Tytgat, B., Pinseel, E., Hodgson, D. A., Kopalová, K., et al. (2021). Diatoms define a novel freshwater biogeography of the Antarctic. *Ecography* 44, 548–560. doi: 10.1111/ecog.05374

Walne, P. R. (1970). Studies on the food value of nineteen genera of algae to juvenile bivalves of the genera *Ostrea*, *Crassostrea*, *Mercenaria* and *Mytilus*. *Fish. Invest. Ser.* 2, 1–62.

Walsby, A. E. (1997). Numerical integration of phytoplankton photosynthesis through time and depth in a water column. *New Phytol.* 136, 189–209. doi: 10.1046/j.1469-8137.1997.00736.x

Wetzel, C. E., Van de Vijver, B., Blanco, S., and Ector, L. (2019). On some common and new cavum-bearing *Planothidium* (Bacillariophyta) species from freshwater. *Fottea* 19, 50–89. doi: 10.5507/fot.2018.016

Wetzel, C. E., Van de Vijver, B., Hoffmann, L., and Ector, L. (2013). *Planothidium incuriatum* sp. nov. a widely distributed diatom species (Bacillariophyta) and type analysis of *Planothidium biporomum*. *Phytotaxa* 138, 43–57. doi: 10.11646/phytotaxa.138.1.6

Witkowski, A., Riaux-Gobin, C., and Daniszewska-Kowalczyk, G. (2010). New marine diatom (Bacillariophyta) species described from Kerguelen Islands coastal area and pertaining to *Navicula* S.S. with some remarks on morphological variation of the genus. *Vie et Milieu* 60, 265–281.

Woelfel, J., Schumann, R., Peine, F., Flohr, A., Kruss, A., Tegowski, J., et al. (2010). Microphytobenthos of Arctic Kongsfjorden (Svalbard, Norway): biomass and potential primary production along the shore line. *Polar Biol.* 33, 1239–1253. doi: 10.1007/s00300-010-0813-0

Wulff, A., Roleda, M. Y., Zacher, K., and Wiencke, C. (2008a). Exposure to sudden light burst after prolonged darkness - a case study on benthic diatoms in Antarctica. *Diatom Res.* 23, 519–532. doi: 10.1080/0269249X.2008.9705774

Wulff, A., Roleda, M. Y., Zacher, K., and Wiencke, C. (2008b). UV radiation effects on pigments, photosynthetic efficiency and DNA of an Antarctic marine benthic diatom community. *Aquat. Biol.* 3, 167–177. doi: 10.3354/ab00076

Zacher, K., Rautenberger, R., Hanelt, D., Wulff, A., and Wiencke, C. (2009). The abiotic environment of polar marine benthic algae. *Bot. Mar.* 52, 483–490. doi: 10.1515/BOT.2009.082

Zhang, Q., Gradinger, R., and Spindler, M. (1998). Dark survival of marine microalgae in the high arctic (greenland sea). *Polarforschung* 65, 111–116.

Zidarova, R., Ivanov, P., Hineva, E., and Dzhembekova, N. (2022). Diversity and habitat preferences of benthic diatoms from South Bay (Livingston Island, Antarctica). *Plant Ecol. Evol.* 155, 70–106. doi: 10.5091/plecevo.84534

Zidarova, R., Kopalová, K., and Van de Vijver, B. (2016). Ten new Bacillariophyta species from James Ross Island and the South Shetland Islands (Maritime Antarctic Region). *Phytotaxa* 272, 37. doi: 10.11646/phytotaxa.272.1.2

Zimmermann, J., Jahn, R., and Gemeinholzer, B. (2011). Barcoding diatoms: evaluation of the V4 subregion on the 18S rRNA gene, including new primers and protocols. *Org. Divers. Evol.* 11, 173. doi: 10.1007/s13127-011-0050-6

frontiers | Frontiers in Microbiology

TYPE Original Research
PUBLISHED 18 October 2023
DOI 10.3389/fmicb.2023.1280775

OPEN ACCESS

EDITED BY
Prashant Kumar Singh,
Mizoram University, India

REVIEWED BY
Rakshak Kumar,
Institute of Himalayan Bioresource Technology (CSIR), India
Galyna Kufryk,
Grand Canyon University, United States

*CORRESPONDENCE
Tae-Jin Oh
✉ tjoh3782@sunmoon.ac.kr

†These authors have contributed equally to this work

RECEIVED 21 August 2023
ACCEPTED 05 October 2023
PUBLISHED 18 October 2023

CITATION
Shrestha P, Karmacharya J, Han S-R, Lee JH and Oh T-J (2023) Elucidation of cold adaptation in *Glaciimonas* sp. PAMC28666 with special focus on trehalose biosynthesis. *Front. Microbiol.* 14:1280775. doi: 10.3389/fmicb.2023.1280775

Elucidation of cold adaptation in *Glaciimonas* sp. PAMC28666 with special focus on trehalose biosynthesis

Prasansah Shrestha[1†], Jayram Karmacharya[1†], So-Ra Han[1,2,3], Jun Hyuck Lee[4] and Tae-Jin Oh[1,2,3,5*]

[1]Department of Life Sciences and Biochemical Engineering, Graduate School, SunMoon University, Asan, Republic of Korea, [2]Genome-Based Bio-IT Convergence Institute, Asan, Republic of Korea, [3]Bio Big Data-Based Chungnam Smart Clean Research Leader Training Program, SunMoon University, Asan, Republic of Korea, [4]Research Unit of Cryogenic Novel Materials, Korea Polar Research Institute, Incheon, Republic of Korea, [5]Department of Pharmaceutical Engineering and Biotechnology, SunMoon University, Asan, Republic of Korea

Glaciimonas sp. PAMC28666, an extremophilic bacterium thriving in Antarctic soil and belonging to the *Oxalobacteraceae* family, represents the only complete genome of its genus available in the NCBI database. Its genome measures 5.2Mb and comprises 4,476 genes (4,350 protein-coding and 72 non-coding). Phylogenetic analysis shows the strain PAMC28666 in a unique branch within the genus *Glaciimonas*, closely related to *Glaciimonas* alpine Cr9-12, supported by robust bootstrap values. In addition, strain PAMC28666 showed 77.08 and 23.3% ANI and DDH, respectively, with *Glaciimonas* sp. PCH181.This study focuses on how polar strain PAMC28666 responds to freeze–thaw conditions, Experimental results revealed a notable survival rate of 47.28% when subjected to a temperature of 15°C for a period of 10 days. Notably, two genes known to be responsive to cold stress, Trehalose 6-phosphate synthase (*otsA*) and Trehalose 6-phosphate phosphatase (*otsB*), exhibited increased expression levels as the temperature shifted from 25°C to 15°C. The upregulation of *otsAB* and the consequent synthesis of trehalose play pivotal roles in enhancing the cold resistance of strain PAMC28666, offering valuable insights into the correlation between trehalose production and adaptation to cold stress. Furthermore, research into this neglected cold-adapted variation, like *Glaciimonas* sp. PAMC28666, has the potential to shed light on how trehalose is produced in cold-adapted environments Additionally, there is potential to extract trehalose compounds from this strain for diverse biotechnological applications, including food and cosmetics, with ongoing research exploring its unique properties.

KEYWORDS

Antarctica, cold shock proteins, extremophiles, *Glaciimonas* sp., trehalose biosynthesis

Introduction

Glaciimonas are Gram-negative, rod shaped, and non-motile bacteria belonging to the family *Oxalobacteraceae* (Zhang et al., 2011). These bacteria can thrive in aerobic and microaerophilic conditions but cannot survive in anaerobic environments. Many strains of *Glaciimonas* have been found in glaciers (Zhang et al., 2011; Frasson et al., 2015; Margesin et al., 2016), as well as in water samples from a uranium mine (Chung et al., 2013). However, our Antarctica isolate, *Glaciimonas* sp. PAMC28666 was obtained from soil, and it is a complete genome. Microbes present in extreme environments such as Antarctica provide excellent opportunities to elucidate eco-physiological and

biochemical adaptations of such life forms (Pearce, 2012). Habitats with permanently low temperatures have been successfully inhabited by a wide variety of organisms, known as psychrophiles or cold-adapted organisms (Collins and Margesin, 2019).

In extreme environments, such as those with varying temperatures, salt concentration, and limited nutrients and oxygen, the presence and diversity of different metabolic pathways become essential for colonization and survival. Bacteria exposed to low-temperature conditions undergo various physiological changes. One such alteration is the synthesis of proteins, which are believed to aid bacteria in withstanding freezing temperatures. These proteins, known as cold shock proteins (CSPs), are induced, or enhanced during cold shock. Many of the proteins induced by cold shock belong to the cold shock family and are categorized as either cold-induced proteins (CIPs) or cold acclimation proteins (CAPs) (Klein et al., 1999). During the early stages of the cold shock response, CIPs show a short induction that is followed promptly by a decrease before reaching a stable state whereas CAPs are continuously synthesized at high levels during prolonged growth at low temperatures. In cold-adapted bacteria, there are fewer certain proteins called CIPs compared to bacteria that thrive in moderate temperatures (mesophiles). Instead, they rely on other proteins known as CAPs to help them grow in cold conditions (Roberts and Inniss, 1992; Berger et al., 1996; Bylund et al., 1998). This aligns with the observation that, unlike mesophiles where CIPs are the main proteins produced when exposed to cold, psychrotropic bacteria can continue making proteins with less hindrance (Hébraud and Potier, 1999).

Trehalose, a well-researched compatible solute, is accumulated through increased cold acclimatization (Kandror et al., 2002). Genes involved in trehalose biosynthesis, such as *otsA* and *otsB*, encode trehalose-6-phosphate synthase and trehalose-6-phosphate phosphatase, respectively. These genes can be induced during cold shock and osmotic stress when entering the stationary phase, and they are important for converting glucose into trehalose (Giaever et al., 1988). Furthermore, when *otsAB* mRNA is subjected to lower temperature (16°C), it demonstrates notably prolonged stability in comparison to higher temperatures (37°C) (Kandror et al., 2002). Additionally, *otsA* mutant (*ΔotsA*) cells exhibit a substantial decrease in cell viability when exposed to 4°C, suggesting that trehalose serves as a protective mechanism to combat stress in low-temperature conditions.

In the present study, we examined the complete genome of *Glaciimonas* sp. PAMC28666, which is the only complete genome of *Glaciimonas* to be reported in the NCBI database so far. The primary focus was on identifying genes responsible for a range of metabolic functions that facilitate environmental adaptability. These functions encompass aerobic metabolism, growth at low temperatures, osmoregulation, synthesis of exopolysaccharides, and chemical breakdown. Furthermore, we conducted experiments to assess the functionality of specific cold-induced proteins in *Glaciimonas* sp. PAMC28666.

Materials and methods

Bacterial strain and growth conditions

Glaciimonas sp. PAMC28666 was obtained from the Antarctica soil sample and deposited by the Korean Polar Research Institute. Using various medial like Tryptone Soya Broth (TSB), Marine Broth (MB), and Reasoner's 2A Broth (R2A), it was found that R2A broth medium showed the most favorable for seed culture. To initiate bacterial culture, the frozen sample was revived with a 1%(v/v) inoculum and allowed to grow for 48 h. For the preparation of bacterial suspension culture, the isolate was cultured on R2A agar medium to obtain single colony. Subsequently, these colonies were transferred to R2A broth and incubated at 15°C, 200 rpm for 48 h. Finally, the culture was preserved as 20% glycerol stocks at −80°C for later use.

Phenotypic characterization

To establish optimal growth conditions, the bacterial isolate was inoculated in R2A broth at different temperatures (8, 15, 25, and 37) °C maintaining a constant pH of 7.0 ± 0.2. The growth progress was tracked by assessing the optical density of the broth culture at 600 nm using the spectrophotometer. Once the optimal temperature was identified, the growth performance was examined across varying pH levels (ranging from 4 to 10 with 1.0 pH unit intervals) in R2A broth. Furthermore, growth rate was monitored under different NaCl concentrations (ranging from 0.5 to 2.5 with 0.5-unit intervals) while keeping temperature and pH constant. The growth curve was generated using Microsoft Corporation's Excel software.

Genome sequencing, assembly, and annotation

Glaciimonas sp. PAMC28666 was cultured in R2A broth at 15°C. Genomic DNA was extracted using a QIAamp DNAMini Kit (Qiagen, Valenciam CA) and assessed for quantity and purity using the Aglient 2,100 Bioanalyzer (Agilent Technologies, Santa Clara, CA). The extracted DNA's quality was confirmed through agarose gel electrophoresis. Subsequently, the genome was sequenced using PacBio Sequel single-molecule real-time (SMRT) sequencing technology from Pacific Biosciences (Menlo Park, CA). Raw sequence data underwent *de novo* assembly using the hierarchical genome-assembly process (HGAP v.4) protocol and HGAP4 assembly with SMRT analysis software (ver.2.3)[1] from Pacific Biosciences (Chin et al., 2013). The fully assembled genome was submitted to the NCBI WGS database with accession number ASM1691735v1.

16S rRNA gene sequence analysis and identification of *Glaciimonas* sp. PAMC28666

The phylogenetic analysis of the 16S rRNA gene sequence of *Glaciimonas* sp. PAMC28666 and sequences from the most closely related genera were determined. This analysis was performed using the MEGAX software, as detailed in the work by Kumar et al. (2018). The alignment of sequences was carried out using ClustalW (Larkin et al., 2007). The phylogenetic tree was then constructed using

1 http://github.com/pacificbiosciences/SMRT-Analysis

maximum likelihood analysis (Rogers and Swofford, 1998). To construct the phylogenetic tree, the sequences of 16S rRNA of related type strains were retrieved from the EzBioCloud database[2] (Yoon et al., 2017). The average nucleotide identity (ANI) values and the digital DNA–DNA hybridization (DDH) between the genome sequence of strain PAMC28666 and type strains of the genus *Collimonas* were also conducted. For ANI calculations, the ANI calculator available on EzBioCloud was used, while the Genome-to-Genome Distance Calculator by Meier-Kolthoff et al. (2013) was employed.[3] Additionally, the G+C mol. % content of DNA was determined from the complete sequence.

Genomic insights of *Glaciimonas* sp. PAMC28666

Further analysis was conducted and thoroughly reviewed prominent genes using RAST (Rapid Annotation using Subsystem Technology) (Aziz et al., 2008) platform to discover genes involved in *Glaciimonas* sp. PAMC28666 stress adaptation. To aid visualization, a circular map using the CGView^{BETA} comparison tool (Grant and Stothard, 2008) was also constructed. Based on previously published studies, cold shock proteins that are expressed in cold temperatures were predicted. The KEGG (Kyoto Encyclopedia of Genes and Genomes) (Kanehisa and Goto, 2000) pathway database was used to learn about a specific metabolic route, specifically the synthesis of trehalose. This approach allowed us to elucidate the intricate process of trehalose biosynthesis within *Glaciimonas* sp. PAMC28666.

Physiological characterization and tolerance of freeze–thaw cycles

Seed culture was diluted 1:100 into 100 mL of R2A broth to examine the growth patterns of *Glaciimonas* sp. PAMC28666. Following this, the diluted culture was divided across 250 mL flasks and incubated in a shaking incubator at 15°C, 25°C, and 37°C at 200 rpm. The optical density at 600 nm (OD_{600}) was measured every 24 h to monitor culture progression. It was determined that the exponential growth phase occurs when the relationship between log OD_{600} and time is linear. The Excel software was used to conduct a linear regression analysis and derive the equation of the best-fitting line in the linear function to calculate the growth rate.

To evaluate cold tolerance of strain PAMC28666, it was cultured at two distinct temperatures (15°C and 25°C) until it entered the exponential growth phase. Subsequently, cells grown at each temperature were individually suspended in a solution comprising 0.9% NaCl and 0.002% MgSO4, following the methodology outlined by Mei et al. (2016). This suspension was used to perform a freeze–thaw stress test that involved 24 h of freezing at −20°C and then 1 h of thawing at 25°C. Gradient dilutions up to 10^{-6} were created after each cycle in sterilized 0.9% NaCl containing 0.02% $MgSO_4$. To count colony-forming units (CFU), serial dilutions were plated on R2A agar and incubated for 96 h at 25°C. CFUs post-stress were compared to the starting CFU value at time zero to calculate the survival rate. With the average survival rates obtained from three separate studies, this resulted in the proportion of cells that survived the stress.

Trehalose production and assay

A medium containing 0.5 g of casamino acid hydrolysate, 0.5 g of yeast extract, and 0.5 g of peptone per liter was developed to produce trehalose (Difco™ R2A agar, Fisher scientific). The carbon source to produce trehalose in this medium was added as 2% glucose. The culture cell pellets were boiled at 95°C for 20 min to remove the trehalose from the pellets. After centrifuging the resulting mixes, the supernatant was collected. By continuing to boil the supernatant at 95°C until it lost half of its volume, the supernatant containing the extracted trehalose was concentrated. Furthermore, the trehalose extract sample was mixed with 495 mL of 50 mM sodium citrate buffer (pH 6.0) to create a total volume of 1,000 mL for the trehalose assay. Purified trehalase (Megazyme), with an enzyme concentration of 0.0009 UmL^{-1}, was added in a volume of 5 µL to start the reaction. The 3,5-dinitro salicylic acid colorimetric method (DNS method) (Miller et al., 1960) was used to evaluate the degradation of trehalose to glucose molecules. In this procedure, 1,000 µL of the reacted sample and 300 µL of the DNS solution were mixed and boiled for 5 min. The mixture was allowed to cool at room temperature, and the absorbance was measured at 540 nm using a spectrophotometer. Subsequently, by measuring the absorbance of a standard solution that contained 20 nmol of glucose instead of trehalose, glucose production was ascertained. A control sample devoid of trehalose was used in the measurement to gauge the level of pre-existing glucose in the tested sample. Additionally, a blank sample without trehalose extract was included as a reference.

Results

Physiological characterization of *Glaciimonas* sp. PAMC28666

In this study, *Glaciimonas* sp. PAMC28666 was subjected to various physiological conditions, including changes in salt concentrations, pH levels, and temperatures (Supplementary Figure S1). At different temperatures (8, 15, 25, and 37) °C explored, the strain PAMC28666 did not show growth at 8°C and 37°C whereas it showed highest growth at 25°C as compared to 15°C. Notably, it exhibited a wide range of pH from acidic to alkaline conditions (pH 4 to 10), with the most favorable pH for optimal growth being pH 6.0. Additionally, the strain revealed its endurance in NaCl concentrations of up to 2.0% (Supplementary Figure S1). To investigate the growth characteristics and cold tolerance of *Glaciimonas* sp. PAMC28666, a growth curve analysis was conducted at different temperatures. The species did not exhibit growth at 37°C. However, at 25°C, it reached the stationary phase after 72 h of incubation, and at 15°C, it reached the stationary phase after 96 h (Figure 1). Interestingly, it was found that there were no significant differences in the final cell density at the stationary phase between the two temperatures (data not shown). These results suggest that strain PAMC28666 might be categorized as a psychrotolerant bacterium.

2 http://www.ezbiocloud.net/

3 http://ggdc.dsmz.de/

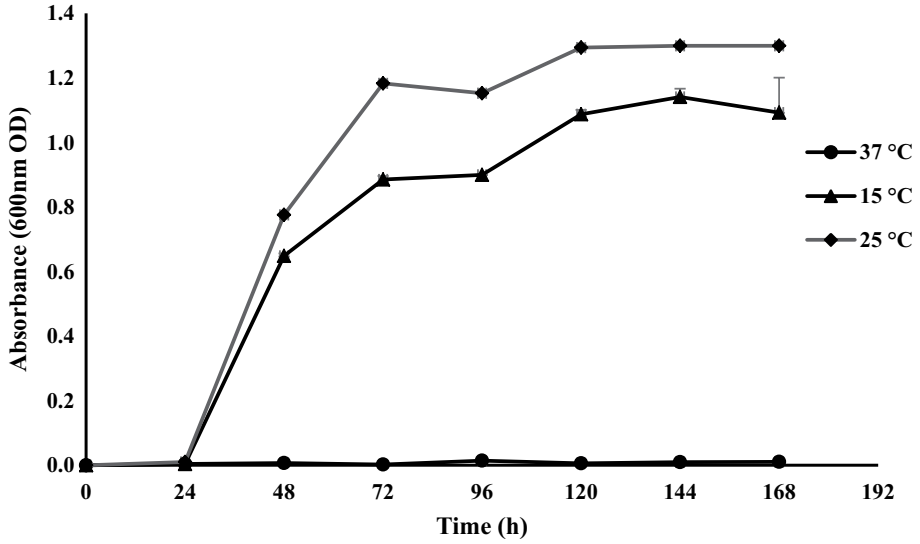

FIGURE 1
Growth curve of *Glaciimonas* sp. PAMC28666, grown at different temperatures for 168 h. Bacterial growth was evaluated by absorbance measurement at 600 nm using a spectrophotometer.

TABLE 1 Comparison of genomic features (ANI, DDH, G + C content, and 16 s rRNA) of *Glaciimonas* sp. PAMC28666 with the closest members.

Parameters	Microorganisms							
	G. sp. PAMC28666*	*G. imobilis*^{T}	*G. frigoris*^{T}	*G. alpina*^{T}	*G.* sp. PCH181	*C. fungivorans*Ter6^T	*C. pratensis* Ter91^T	*C. arenae* Ter10^T
Isolation source	Soil of Antarctica	Alpine glaciers	Permafrost sediment	Alpine glaciers	Glacier water of India	Dune grassland	Dune grassland	Dune grassland
RefSeq	GCF016917355.1	–	–	–	GCF003056055.1	GCF001584145.1	GCF001584185.1	GCF001584165.1
GS (Mb)	5.23	–	–	–	5.3	5.6	5.7	4.7
ANI (%)	100	–	–	–	77.08	74	73.91	73.91
DDH (%)	100	–	–	–	23.3	21.4	22	21.6
G + C (%)	51.5	51	53	49.2	51	59	58.7	56.38
16 s (%)	100	98.97	99.34	99.93	–	96.15	96.21	96.21

G., Glacimmonas; C., Collimonas; –, data not available; RefSeq, reference genome sequence; GS, genome size; and *, the studied strain.
Information: G + C content for G. frigoris, G. alpina and G, singularis were taken from the literature and for Glaciimonas sp. PCH181, and Collimonas G + C data were obtained from NCBI.

Genomic features of *Glaciimonas* sp. PAMC28666

The Antarctica isolate *Glaciimonas* sp. PAMC28666 is the only complete genome that has been deposited in the NCBI database until now. It comprises a single contig, with a total size of 5.2 Mb with 4,476 genes, a G + C content of 51.5% and genome coverage of 100.0X with reference sequences. Among these, 4,350 are protein-coding genes, while 12 are involved in ribosomal RNA (rRNA), along with 56 genes responsible for transfer RNA (tRNA), and 54 pseudogenes. It is noteworthy that the pseudogenes account for less than 2% of the entire gene set (See Supplementary Table S1). In the study conducted by Zhang et al. (2011) on *Glaciimonas immobilis*, a similar trait was noted within the genus *Glaciimonas* sp. PAMC28666. *Glaciimonas* sp. PAMC28666 showed a G + C content of 51.1% similar to *Glaciimonas immobilis* (Zhang et al., 2011) (Table 1). Additionally, as reported by Frasson et al. (2015) and Margesin et al. (2016), strain PAMC28666 shows an intermediate G + C content when compared to two *Glaciimonas* species, *Glaciimonas alpina* (49.2%) and *Glaciimonas frigoris* (53%). However, it is important to note that the G + C content within the genus *Collimonas* exhibits notable deviation, ranging from 56.06 to 59.6% (Song et al., 2015), significantly higher than that observed in the genus *Glaciimonas*.

Phylogenetic tree analysis of *Glaciimonas* sp. PAMC28666

When analyzing the 16S rRNA gene sequence of *Glaciimonas* sp. PAMC28666 isolate, its closest matches were *Glaciimonas aplina* and *Glaciimonas frigoris*, sharing a remarkably high similarity of 99%. The subsequent closest match was identified as *Glaciimonas immobilis*, showing a similarity of 98.97%. However, it is crucial to emphasize the 16S rRNA sequence-based similarity of *Glaciimonas* sp. PAMC28666

exceeds the defined threshold value of 98.65% which is recommended for species differentiation (Kim et al., 2014). Furthermore, during phylogenetic analysis, it became evident that strain PAMC28666 occupies a unique branch within the genus *Glaciimonas,* displaying a notable proximity to *Glaciimonas* alpine Cr9-12 in the same clade. The presence of robust bootstrap values strengthens the validity of this clustering and reinforces its close affiliation with the genus *Glaciimonas* (Figure 2). Due to the unavailable of complete genome for the genus *Glaciimonas* except our strain PAMC28666, additional computational analysis was carried out involving digital DNA–DNA hybridization (DDH) and average nucleotide identity (ANI), focusing on members of the genus *Collimonas*, specifically *Collimonas fungivorans* strain Ter6^{T}, *Collimonas pratensis* strain Ter91^{T}, and *Collimonas arenae* strain Ter10^{T}. The DDH values were found to vary between 21.4 and 22%, whereas the ANI values ranged from 73.91 to 74% (Table 1). In addition, strain PAMC28666 showed 77.08 and 23.3% ANI and DDH, respectively, with *Glaciimonas* sp. PCH181 (Kumar et al., 2020). These results suggest that strain PAMC28666 belongs to the genus to *Glaciimonas* rather than the genus *Collimonas.*

Genomic insights revealed stress adaptation strategies in *Glaciimonas* sp. PAMC28666

The stress adaptation mechanisms of *Glaciimonas* sp. PAMC28666 has been studied, revealing a range of proteins that could potentially be expressed in response to various stress conditions. These conditions include cold stress, which triggers the expression of proteins like cold-shock proteins (CSPs), as well as chaperonins (GroEL/GroES, HscA/HscB, and SurA), and cold-active chaperones. Additionally, for osmotic stress, proteins such as choline dehydrogenase, sarcosine oxidase, ABC transporters, and permease for glycine/betaine/choline were detected. Regarding oxidative stress, the strain possesses antioxidant genes like superoxide dismutase, catalase, alkyl hydro-peroxidase, glutathione-peroxidase, peroxiredoxin, and thioredoxin family proteins. Further details regarding stress-related proteins are outlined in Supplementary Table S2. A comprehensive examination of cold-shock proteins was conducted to better understand their role in the cold stress adaptation of strain PAMC28666. In comparison to the reference strain *Escherichia coli* K12, these proteins, which contribute to elevated protein synthesis at lower temperatures, displayed a similarity of more than 50% (Table 2). The key genes CSPs, such as *cspA*, *cspB*, *cspC*, *cspD*, and *cspE*, exhibited identities of 63.08, 64.25, 68.25, 68.75, and 70.49%, respectively, with strain PAMC28666. Besides the key genes of CSPs, trehalose biosynthetic genes like trehalose phosphate synthase (*otsA*) and trehalose phosphatase (*otsB*) were also identified. However, their similarities with the reference strain *Escherichia coli* K12 were comparatively lower, measuring 45.89 and 38.43%, respectively. The presence of these genes indicates the potential for trehalose production within strain PAMC28666.

In silico analysis of trehalose biosynthesis in the genome of *Glaciimonas* sp. PAMC28666

The Antarctica isolate *Glaciimonas* sp. PAMC28666 utilizes trehalose biosynthesis genes as a part of its response to cold stress through the analysis of the cold-shock protein was determined. To determine these genes involved in trehalose biosynthesis, several bioinformatics tools were employed. After conducting a RAST analysis, detected 325 subsystems. Among the prominent subsystems identified, the one with the most genes is the amino acid and derivatives system, totaling 333 genes. This is succeeded by carbohydrates with 252 genes, and respiration with 106 genes (Figure 3). Upon additional investigation, it was discovered that the studied strain possesses the di- and oligosaccharides metabolism under the carbohydrate subsystem, encompassing 3.6% of genes related to trehalose metabolism. Furthermore, the CGview web server is utilized to display the anticipated trehalose metabolism genes in the strain PAMC28666 (Figure 4). By using the KEGG annotation database, at first the pathways related to trehalose synthesis and their usefulness in this situation were evaluated. This study revealed that the trehalose biosynthetic pathways OtsA/B, TreYZ, and TS are present in the Antarctic isolate PAMC28666 (Supplementary Figure S2). It is significant that this mechanism also involves the OtsA/B pathway, which was previously identified as being essential to the cold shock protein's function. Additionally, the presence of *otsA* and *otsB* genes were identified within the RAST annotation using the seed viewer, spanning a length of 1,413 and 795 coding sequences (CDS) respectively (Figure 5). Therefore, this validated the existence of the OtsA/B pathway for trehalose synthesis in the Antarctic strain PAMC28666.

Freeze–thaw and cold shock effects on survival of *Glaciimonas* sp. PAMC28666

A freeze–thaw cycle was conducted on strain PAMC28666 to evaluate its viability when exposed to cold conditions. In exploring the survival mechanism in a cold environment, it was observed that strain PAMC28666 exhibited greater viability at 15°C when compared to 25°C following the execution of freeze–thaw cycles. Furthermore, upon conducting three freeze–thaw cycles, it revealed that survival rates of 75.65% at 15°C and 43.29% at 25°C (Figure 6). However, following five freeze–thaw cycles, the survival rate decreased to 47.28% at 15°C, whereas at 25°C, it dropped significantly to only 13.69%. significantly, a noticeable reduction in the survival rate was witnessed following freeze-thaw cycles at 25°C, suggesting an increased susceptibility to cold stress at this specific condition.

Determination the presence of trehalose

On further study, strain PAMC28666 showed the potential to synthesize trehalose at a lower temperature of 15°C. To confirm this finding, further conducted the thin layer chromatography (TLC) analysis which yielded a positive result with an Rf value correspondence with that of the standard trehalose (Figure 7). In addition, a commercial trehalase enzyme was utilized for verification. This observation indicated the possibility that strain PAMC28666 could be utilizing the OtsA/B pathway for trehalose production. Additionally, under the investigation of trehalose accumulation in strain PAMC28666 as a physiological response to a temperature decrease, it was noticed

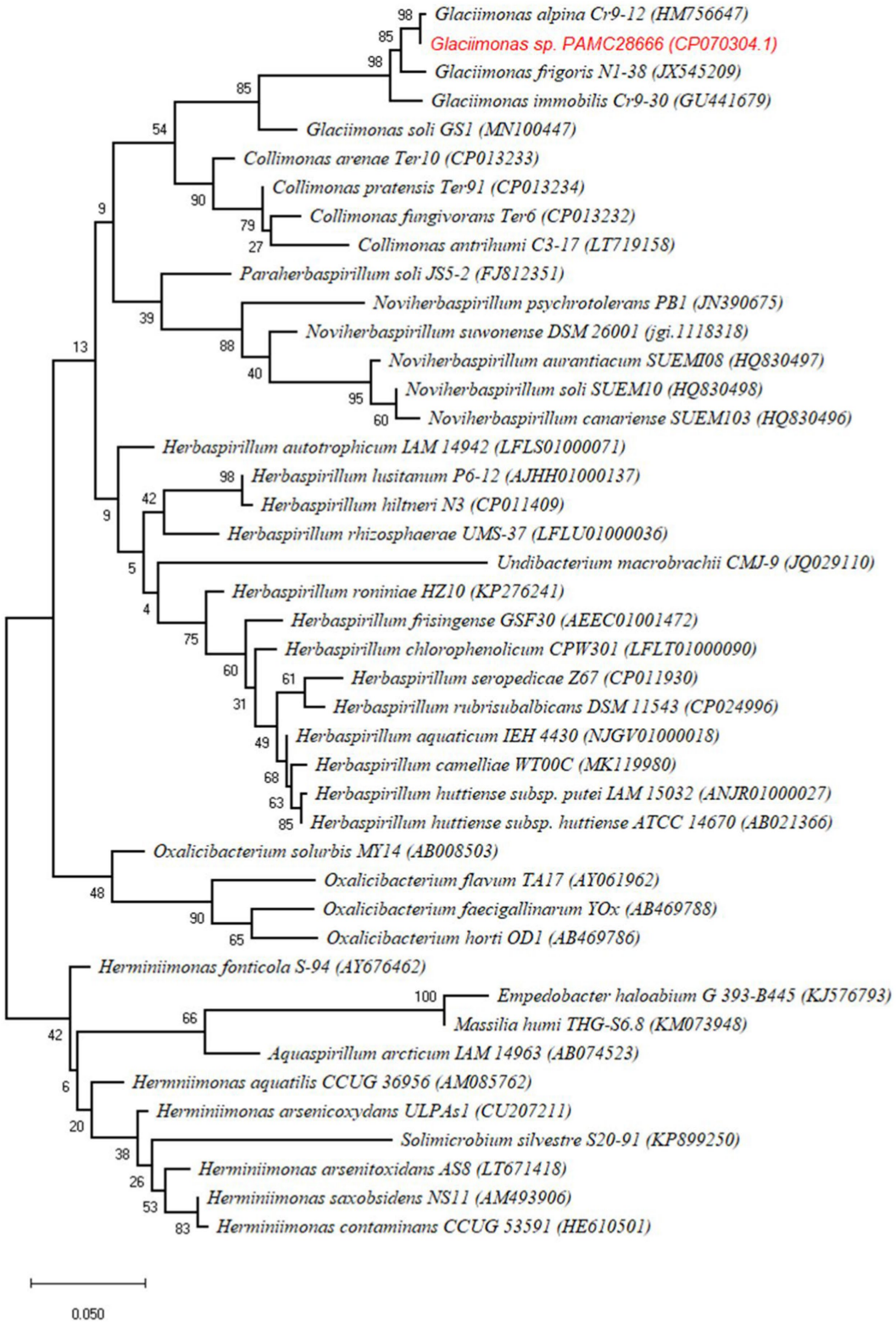

FIGURE 2
Phylogenetic tree of *Glaciimonas* sp. PAMC28666 with related strains based on 16 s rRNA sequences. The tree was constructed by maximum likelihood using MEGA X with 1,000 bootstrapping replications.

variations in the trehalose levels throughout the acclimation phase. Interestingly, as shifted the strain PAMC28666 cells from higher temperatures to lower ones, it showed two distinct outcomes. Initially, when transitioning from one psychrophilic condition (15°C) to another (8°C), strain PAMC28666 exhibited a negligible decrease in trehalose accumulation. Conversely, when transitioning from a

TABLE 2 List of genes encoding for proteins induced under cold stress conditions in the genome of *Glaciimonas* sp. PAMC28666.

NCBI reference sequence	Description	% identity with *E. coli* K12	References
WP_205319425.1	Pyruvate dehydrogenase, decarboxylase (AceE)	59.15	Jones and Inouye (1994)
WP_205319426.1	Pyruvate dehydrogenase, dihydrolipoamide acetyltransferase (AceF)	54.11	Jones and Inouye (1994)
WP_205321136.1	Cold-inducible RNA chaperone, transcriptional enhancer CspA	63.08	Goldstein et al. (1990) and Gualerzi et al. (2003)
WP_168052175.1	Function unknown (CspB)	64.52	Etchegaray et al. (1996)
WP_205319579.1	Regulation of expression of stress response proteins RpoS and UspA (CspcC)	68.25	Phadtare and Inouye (2001) and Shenhar et al. (2012)
WP_168057001.1	Biofilm development, inhibition of DNA replication (CspD)	68.75	Yamanaka and Inouye (2001a) and Kim et al. (2010)
WP_168052175.1	Regulation of expression of stress response proteins RpoS and UspA (CspE)	70.49	Phadtare and Inouye (2001), Shenhar et al. (2012), and Czapski and Trun (2014)
WP_205320165.1	Degradation of RNA (PNP)	64.97	Yamanaka and Inouye (2001b)
WP_205320931.1	Trehalose phosphate synthase (otsA)	45.89	Kandror et al. (2002)
WP_205320933.1	Trehalose phosphatase (OtsB)	38.43	Kandror et al. (2002)
WP_014004414.1	Protein chain initiation factor IF1 (InfA)	75.00	Gualerzi et al. (2003)
WP_205319525.1	Protein chain initiation factor IF2, binding of charged tRNA-fmet to 30S ribosomal subunit (InfB)	62.93	Gualerzi et al. (2003)
WP_108439777.1	Protein chain initiation factor IF3, mRNA translation stimulation (InfC)	64.53	Gualerzi et al. (2003)
WP_205321223.1	Protein-folding chaperone, ribosome binding (Tig)	40.71	Kandror et al. (2002)

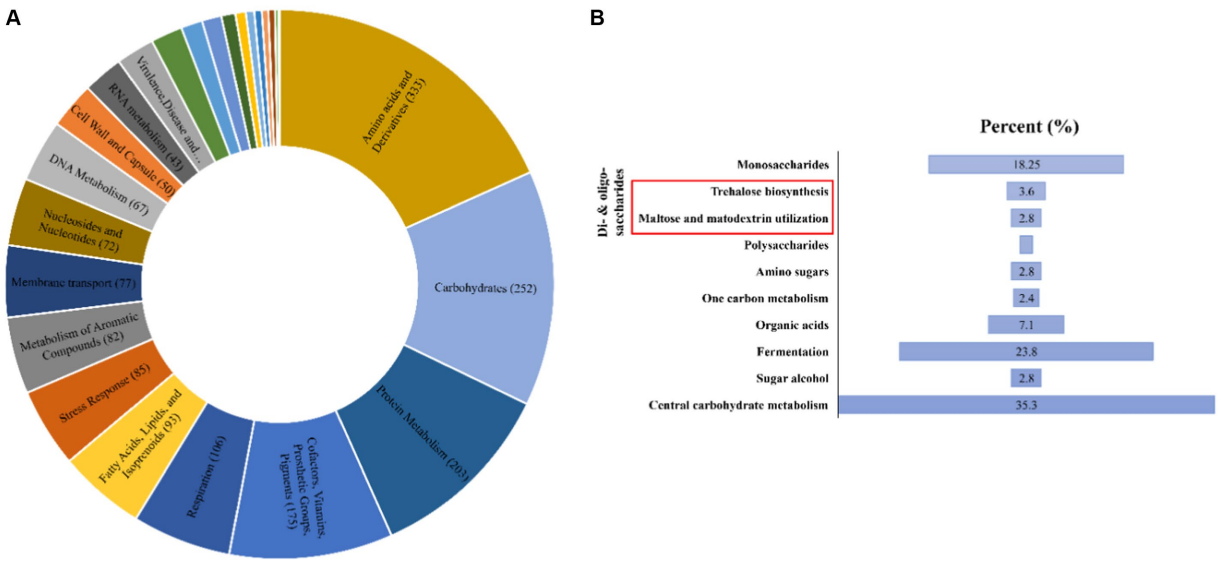

FIGURE 3
(A) A Pie chart illustrates the distribution of genes within different subsystem categories in the genome of *Glaciimonas* sp. PAMC28666; **(B)** A bar graph highlights the proportion of genes related to trehalose biosynthesis (indicated by a red box, constituting 3.6% of the total) within the Carbohydrate categories. The SEED viewer in the RAST server was used to gather data on the subsystem categories.

mesophilic state (25°C) to psychrophilic conditions (15°C), we witnessed a remarkable approximately 13-fold rise in trehalose accumulation (Figure 8). These results indicate that Antarctic isolate *Glaciimonas* sp. PAMC28666 could synthesize trehalose under temperature-induced stress conditions, thereby providing further confirmation of the involvement of the OtsA/B pathway.

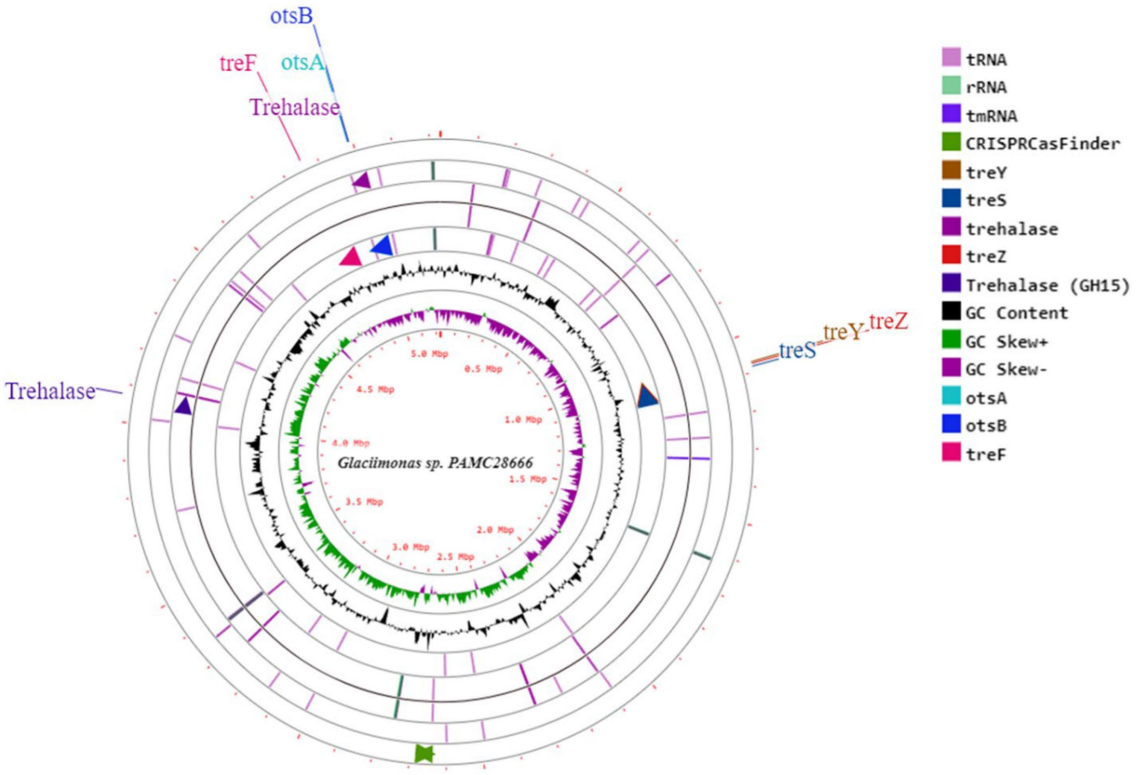

FIGURE 4
A circular depiction illustrates the genome and characteristics of *Glaciimonas* sp. PAMC28666. The components of the displayed rings (starting from the outermost to the center) are described as follows: Ring 1 contains CDS segments, encompassing tRNA and rRNA, along with Pokka annotation featuring genes linked to trehalose metabolism; Ring2 shows the combined ORFs in both forward and reverse strands; Ring 3 represents a plot indicating the GC content distribution; Ring 4 displays a GC skew plot, with values above average depicted in green and values below average depicted in purple; Ring 5 serves as a sequence ruler, offering a scale reference.

FIGURE 5
Genetic organizations of the *otsAB* gene clusters found in *Glaciimonas* sp. PAMC28666, i.e., *otsA* (encoding a trehalose-6-phosphate synthase) and *otsB* (encoding a trehalose-6-phosphate phosphatase). The arrows indicate the direction of gene transcription.

Discussion

The strain PAMC28666 from Antarctica was obtained from a soil sample from the Antarctica region. It comes from an environment with temperatures lower than 10°C. The identification of the strain PAMC28666 as a member of the genus *Glaciimonas* was based on comparing its 16S rRNA sequence with known sequences. The phylogenetic analysis further supported the relatedness of PAMC28666 to the genus *Glaciimonas*. According to the results of species classification using average nucleotide (ANI) and DNA–DNA hybridization (DDH) values, PAMC28666 did not meet the threshold for species classification (Richter and Rosselló-Móra, 2009). Moreover, the G+C content and 16S rRNA sequence similarity of PAMC28666 aligned with the phylogenetic groupings of strains *Glaciimonas*. The genus *Glaciimonas* is situated in the *Oxalobacteraceae* family within the Betaproteobacteria class. It encompasses four well-defined species: *Glaciimonas immobilis*, *Glaciimonas alpina*, *Glaciimonas frigoris*, and *Glaciimonas singularis*. These species have been isolated from diverse glacial environments globally (Zhang et al., 2011; Frasson et al., 2015; Margesin et al., 2016), and in the case of *Glaciimonas singularis*, from a water sample in a uranium mine (Chung et al., 2013). This information indicates that the *Glaciimonas* sp. PAMC28666 strain is a novel cold-adapted bacterium indigenous to the Antarctic region. Notably, it is the only complete genome of genus *Glaciimonas* deposited in the NCBI database until now. Although this strain was originally isolated from an extremely cold region, it has shown the ability to thrive in a culture medium at both 15°C and 25°C (Supplementary Figure S1).

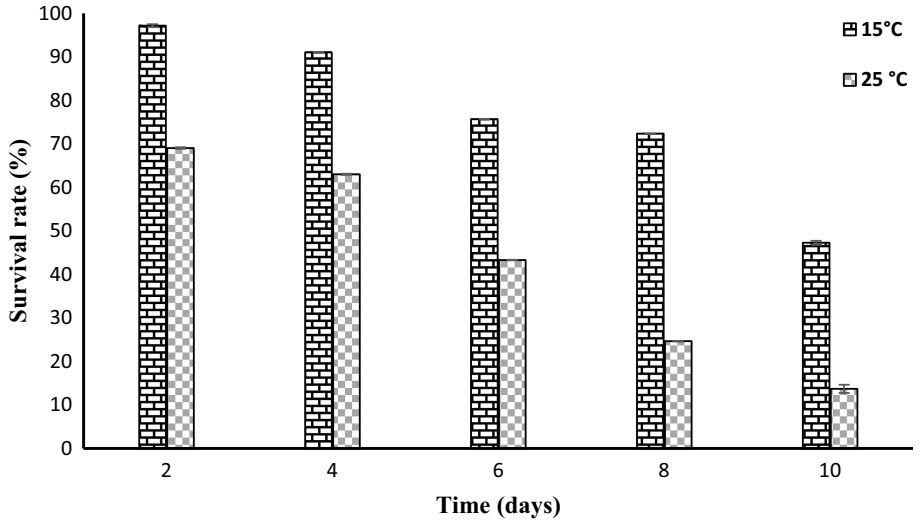

FIGURE 6
Effect of freeze–thaw times on the survival rates of *Glaciimonas* sp. PAMC28666.

This adaptability to grow under such diverse temperature conditions suggest its resilience to both cold and warm environments, classifying it as a psychrotroph. Moreover, strain PAMC28666 demonstrated resistance to salt which exhibited the potential to adapt to osmotic stress.

A noteworthy discovery related to the cold-resistant bacteria pertains to the existence of specific proteins that facilitate adaptation to cold conditions. Similar cold stress proteins have been identified within the Antarctic strain PAMC28666 (Table 2). In response to these challenges, bacteria induce the synthesis of diverse proteins, which encompass cold shock proteins, cold-active chaperones, and chaperonins. CSPs, characterized by their small size, engage with nucleic acids and are present across various microorganisms, including psychrophiles (organisms thriving in cold environments), mesophiles (organisms thriving in moderate temperatures), and thermophiles (organisms thriving in high temperatures) (Czapski and Trun, 2014; Jin et al., 2014). Different bacteria may exhibit varying types and levels of CSP expression in response to cold shock. Among the CSP genes, *cspA* is highly expressed and serves as an essential mRNA chaperone, regulating the transcription of other cold shock genes (Keto-Timonen et al., 2016) (Figure 6).

Moreover, there have been reports indicating that certain bacteria possess multiple paralogs (related genes) of CSPs within their genomes, and these paralogs can be regulated independently. Within this context, distinct paralogs might be induced by low temperatures, during the stationary growth phase, or could exhibit constitutive expression (Yamanaka et al., 1994; Yamanaka and Inouye, 1997; Graumann and Marahiel, 1998; Yamanaka et al., 1998; Graumann and Marahiel, 1999; Wang et al., 1999). In strain PAMC28666, significant genes associated with cold shock proteins, *including cspA, cspB, cspC, cspD,* and *cspE* were identified. Additionally, genes related to trehalose biosynthesis, such as trehalose phosphate synthase (*otsA*) and trehalose phosphatase (*otsB*) were also detected. This suggests that strain PAMC28666 possesses the capability to synthesize trehalose under conditions of cold stress. Additionally, cold acclimation proteins, often referred to as "CAPs," play a pivotal role in augmenting protein synthesis within bacteria under conditions of low temperatures (Margesin, 2007). These proteins are commonly present in bacteria inhabiting consistently cold environments and serve as markers for identifying psychrophiles (Mishra et al., 2010; Piette et al., 2011). As a result, it was hypothesized that strain PAMC28666 might have potentially to endure such extreme environments due to the presence of these CAPs. Furthermore, on further analysis into the mechanisms behind bacterial survival during cold stress, there have been prior investigations into the presence of compatible solutes within certain bacteria. Compatible solutes encompass a group of small molecules that can accumulate within cells without disrupting their essential biological functions. These solutes have been identified as cold-protective agents, including trehalose, glycine betaine, and carnitine. They are known to accumulate in response to cold shock, either through increased synthesis or uptake. In *Escherichia coli*, the genes *otsA* and *otsB* are responsible for the biosynthesis of trehalose from glucose, encoding trehalose 6-phosphate synthase and trehalose-6-phosphate phosphatase, respectively (Giaever et al., 1988). The OtsAB operon can be induced during cold shock, osmotic stress, and the stationary phase, and its expression is regulated by the Rpos protein (Giaever et al., 1988; Hengge-Aronis et al., 1991; White-Ziegler et al., 2008). In the case of *Glaciimonas* sp. PAMC28666, it was observed that trehalose also accumulates during cold shock, specifically at 15°C. While trehalose content did not impact growth at 25°C or 15°C, higher levels of trehalose enhanced viability under freezing and thawing conditions. Conversely, a lack of trehalose correlated with a reduced ability to survive under these conditions. Trehalose accumulation during the cold-shock response is thought to be part of the cell's adaptation to the temperature drop, and its accumulation follows a similar time course to known cold-shock proteins (Jones et al., 1987). Trehalose, a vital compound for organisms in stressful environments due to its distinct physiochemical properties, serves to safeguard cellular integrity against various environmental harms and nutritional limitations (Luyckx and Baudouin, 2011). In addition, it has been also reported

that trehalose biosynthetic pathways appear to be species-specific (Tournu et al., 2013).

It has been also reported that apart from transcriptional changes, the stability of mRNA molecules is an important factor in the induction of cold-shock mRNA expression at low temperatures (Fang et al., 1997). For example, the half-life of *otsAB* mRNA, responsible for trehalose synthesis, increases from less than 2 min at 37°C to approximately 20 min at 16°C (Kandror et al., 2002). This increase in *otsA/B* mRNA levels, occurring before trehalose accumulation, likely contributes to its buildup during cold shock and suggests enhanced transcription of the *otsA/B* genes. This might correlate to the findings as strain PAMC28666 was able to produce more trehalose when transferred from high temperature to low temperature.

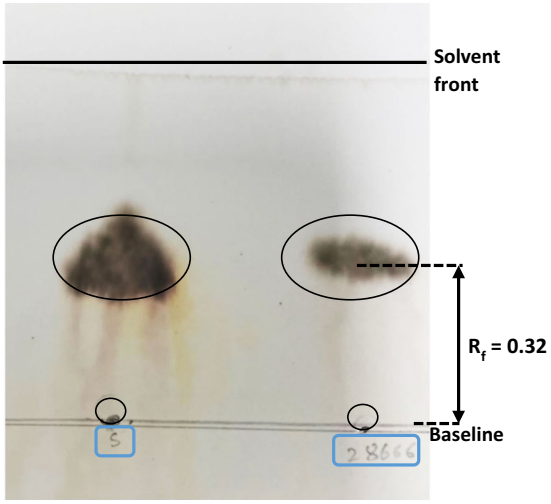

FIGURE 7
Analyses of the carbohydrates in the strain PAMC28666 cell extract. Note: To produce the cell extract, PAMC28666 cells cultured in R2A (100 mL, OD =2.0) were extracted with hot water. A TLC plate was spotted with ten microliters of the cell extract, which was then developed with n-butanol: ethanol: water = 5:3:2. Spraying 20% sulfuric acid in 5% ethanol was used to create the visualization. "Lane S" represents a standard sample of trehalose (Rf = 0.320), while "Lane 28666" corresponds to cell extracts from PAMC28666 (Rf = 0.32).

Trehalose has been extensively studied for its capacity to improve cell viability under diverse temperature conditions. At high temperatures, it acts as a "chemical chaperone," protecting cells by mitigating protein denaturation and aggregation induced by heat stress (De Virgilio et al., 1994; Welch and Brown, 1996; Singer and Lindquist, 1998). Moreover, trehalose may have a role in stabilizing cell membranes at 4°C, as lower temperatures lead to reduced fluidity (Figure 9). Interestingly, exogenous trehalose has been shown to safeguard various organisms from freezing (Lodato et al., 1999; Eroglu et al., 2000), and its maximum protective effect is observed when it is present on both sides of the cell membrane (Diniz-Mendes et al., 1999; Eroglu et al., 2000). The mechanisms underlying trehalose's ability to enhance cell viability at low temperatures likely involve multiple processes, potentially distinct from those proposed previously.

Conclusion

Glaciimonas sp. PAMC28666 is a unique aerobic bacterium that has been found in Antarctica and exhibits psychrotolerant characteristics. In this study, we present the complete genome of genus *Glaciimonas* that is deposited in the NCBI database as *Glaciimonas* sp. PAMC28666. The findings show that this bacterium could adapt to freezing temperatures while retaining its aerobic characteristics. Through complete genome analysis, a significant understanding of the complex physiological and metabolic

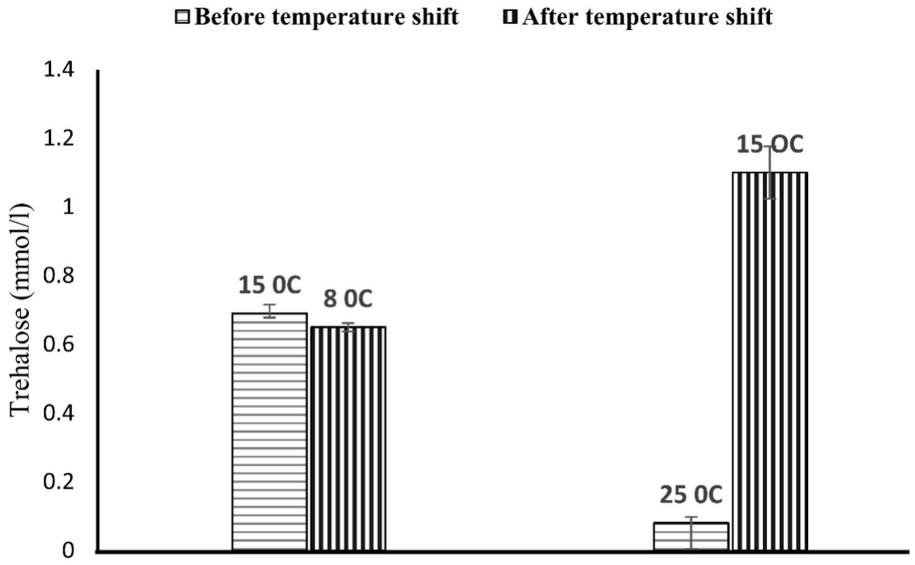

FIGURE 8
Accumulation of trehalose at 15 and 25°C correlates upon further temperature downshift to 8 and 15°C, respectively. The cells were grown to mid-logarithmic phase at each temperature 15 and 25°C, respectively, and then transferred to 8 and 15°C, respectively. At a steady growth phase at respective temperatures, aliquots were taken to measure intracellular trehalose content.

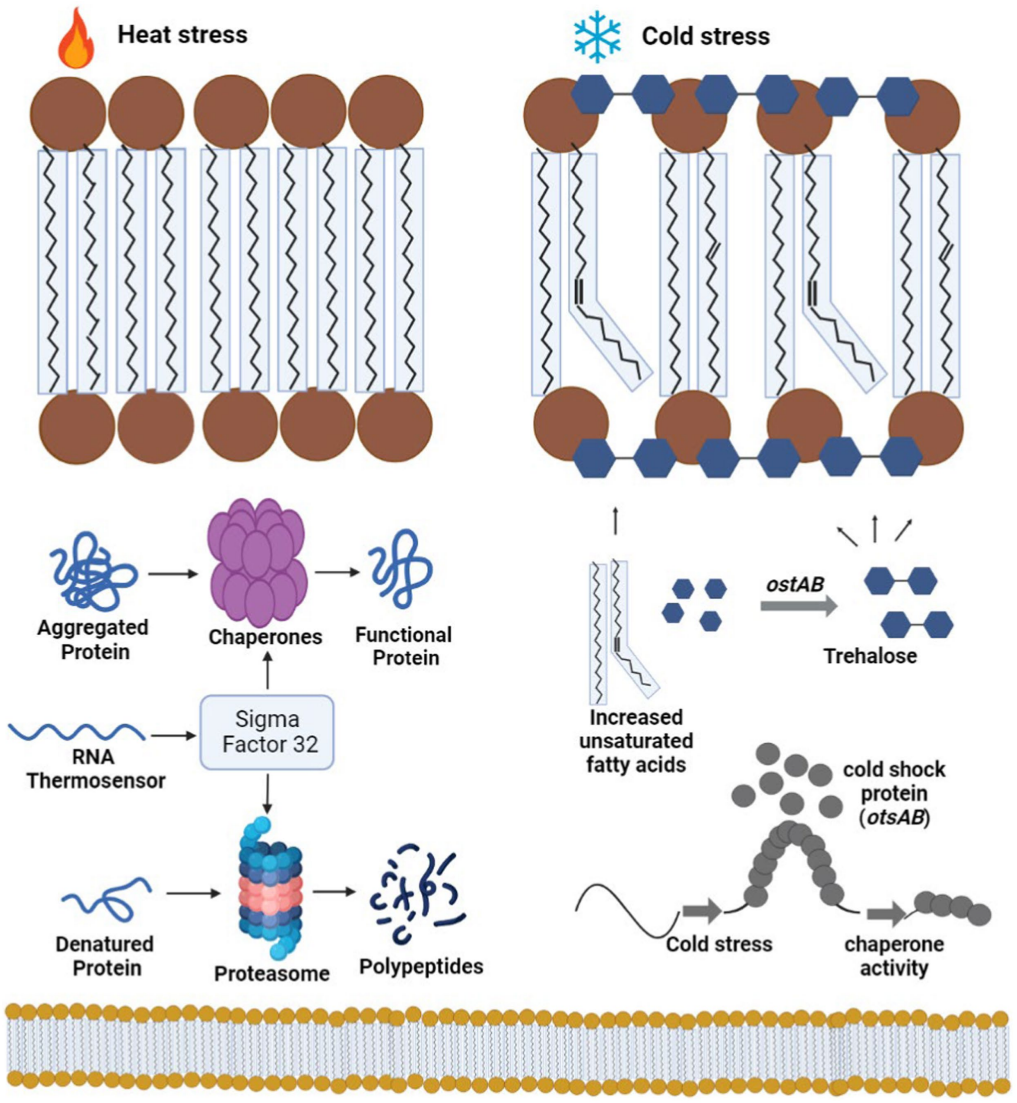

FIGURE 9
A schematic illustrates a simplified mode of action of cold shock proteins. When challenged with low-temperature stress, bacteria initiate a dramatic accumulation of cold shock proteins. Bacteria cold shock proteins function to effectively melt double-stranded regions of RNA transcripts. Cold shock genes, such *otsAB*, produce trehalose in the presence of glucose molecules, which acts as an intercalating agent between the membrane, protecting it from cold bursts. The figure was created with BioRender.com.

functions of *Glaciimonas* sp. PAMC28666 has been attained. The finding of genes linked to both oxidative and cold stress is particularly intriguing since it suggests that the bacterium can adapt to stressful environments. Furthermore, it was found that gene clusters are responsible for the biosynthesis of trehalose via the *otsAB* genes. Experimental validation has effectively confirmed the bacterium's capacity to adjust to cold conditions. Additionally, our investigation revealed the pivotal role of temperature as a determining factor that likely influences the regulation of key genes within bacterial systems. It is essential to highlight that this complete genome, the only one present in the NCBI repository, offers comprehensive insights into *Glaciimonas* genome. This information is pivotal for further deciphering the mechanisms behind its survival in extreme environments. Moreover, this knowledge could potentially pave the way for subsequent investigations into the importance of cold-adapted proteins in various biotechnological applications.

Data availability statement

The datasets presented in this study can be found in online repositories. The names of the repository/repositories and accession number(s) can be found in the article/Supplementary material.

Author contributions

PS: Conceptualization, Formal analysis, Investigation, Writing – original draft, Writing – review & editing. JK: Conceptualization, Formal analysis, Investigation, Writing – original draft, Writing – review & editing. S-RH: Investigation, Writing – original draft, Writing – review & editing. JL: Writing – original draft, Writing – review & editing. T-JO: Conceptualization, Funding acquisition, Project administration, Resources, Supervision, Writing – original draft, Writing – review & editing.

Funding

The author(s) declare financial support was received for the research, authorship, and/or publication of this article. This research was a part of the project titled "Development of potential antibiotic compounds using polar organism resources (20200610)," funded by the Ministry of Oceans and Fisheries, Korea.

Conflict of interest

The authors declare that the research was conducted in the absence of any commercial or financial relationships that could be construed as a potential conflict of interest.

Publisher's note

Supplementary material

The Supplementary material for this article can be found online at: https://www.frontiersin.org/articles/10.3389/fmicb.2023.1280775/full#supplementary-material

References

Aziz, R. K., Bartels, D., Best, A., DeJongh, M., Disz, T., Edwards, R. A., et al. (2008). The RAST server: rapid annotations using subsystems technology. *BMC Genomics* 9:75. doi: 10.1186/1471-2164-9-75

Berger, F., Morellet, N., Menu, F., and Potier, P. (1996). Cold shock and cold acclimation proteins in the psychrotrophic bacterium *Arthrobacter globiformis* SI55. *J. Bacteriol.* 178, 2999–3007. doi: 10.1128/jb.178.11.2999-3007.1996

Bylund, G. O., Wipemo, L. C., Lundberg, L. A. C., and Wikström, P. M. (1998). RimM and RbfA are essential for efficient processing of 16S rRNA in *Escherichia coli*. *J. Bacteriol.* 180, 73–82. doi: 10.1128/jb.180.1.73-82.1998

Chin, C. S., Alexander, D. H., Marks, P., Klammer, A. A., Drake, J., Heiner, C., et al. (2013). Nonhybrid, finished microbial genome assemblies from long-read SMRT sequencing data. *Nat. Methods* 10, 563–569. doi: 10.1038/nmeth.2474

Chung, A. P., Tiago, I., Nobre, M. F., Veríssimo, A., and Morais, P. V. (2013). *Glaciimonas singularis* sp. nov., isolated from a uranium mine wastewater treatment plant. *Int. J. Syst. Evol. Microbiol.* 63, 2344–2350. doi: 10.1099/ijs.0.046581-0

Collins, T., and Margesin, R. (2019). Psychrophilic lifestyles: mechanisms of adaptation and biotechnological tools. *Appl. Microbiol. Biotechnol.* 103, 2857–2871. doi: 10.1007/s00253-019-09659-5

Czapski, T. R., and Trun, N. (2014). Expression of *csp* genes in *E. coli* K-12 in defined rich and defined minimal media during normal growth, and after cold-shock. *Gene* 547, 91–97. doi: 10.1016/j.gene.2014.06.033

De Virgilio, C., Hottiger, T., Dominguez, J., Boller, T., and Wiemken, A. (1994). The role of trehalose synthesis for the acquisition of thermotolerance in yeast: I. Genetic evidence that trehalose is a thermoprotectant. *Eur. J. Biochem.* 219, 179–186. doi: 10.1111/j.1432-1033.1994.tb19928.x

Diniz-Mendes, L., Bernardes, E., De Araujo, P. S., Panek, A. D., and Paschoalin, V. M. F. (1999). Preservation of frozen yeast cells by trehalose. *Biotechnol. Bioeng.* 65, 572–578. doi: 10.1002/(SICI)1097-0290(19991205)65:5<572::AID-BIT10>3.0.CO;2-7

Eroglu, A., Russo, M. J., Bieganski, R., Fowler, A., Cheley, S., Bayley, H., et al. (2000). Intracellular trehalose improves the survival of cryopreserved mammalian cells. *Nat. Biotechnol.* 18, 163–167. doi: 10.1038/72608

Etchegaray, J. P., Jones, P. G., and Inouye, M. (1996). Differential thermoregulation of two highly homologous cold-shock genes, *cspA* and *cspB*, of *Escherichia coli*. *Genes Cells* 1, 171–178. doi: 10.1046/j.1365-2443.1996.d01-231.x

Fang, L., Jiang, W., Bae, W., and Inouye, M. (1997). Promoter-independent cold-shock induction of *cspA* and its derepression at 37°C by mRNA stabilization. *Mol. Microbiol.* 23, 355–364. doi: 10.1046/j.1365-2958.1997.2351592.x

Frasson, D., Udovičić, M., Frey, B., Lapanje, A., Zhang, D. C., Margesin, R., et al. (2015). *Glaciimonas alpina* sp. nov. isolated from alpine glaciers and reclassification of *Glaciimonas immobilis* Cr9-12 as the type strain of *Glaciimonas alpina* sp. nov. *Int. J. Syst. Evol. Microbiol.* 65, 1779–1785. doi: 10.1099/ijs.0.000174

Giaever, H. M., Styrvold, O. B., Kaasen, I., and Strøm, A. R. (1988). Biochemical and genetic characterization of osmoregulatory trehalose synthesis in *Escherichia coli*. *J. Bacteriol.* 170, 2841–2849. doi: 10.1128/jb.170.6.2841-2849.1988

Goldstein, J., Pollitt, N. S., and Inouye, M. (1990). Major cold shock protein of *Escherichia coli*. *Proc. Natl. Acad. Sci. U. S. A.* 87, 283–287. doi: 10.1073/pnas.87.1.283

Grant, J. R., and Stothard, P. (2008). The CGView server: a comparative genomics tool for circular genomes. *Nucleic Acids Res.* 36, W181–W184. doi: 10.1093/nar/gkn179

Graumann, P. L., and Marahiel, M. A. (1998). A superfamily of proteins that contain the cold-shock domain. *Trends Biochem. Sci.* 23, 286–290. doi: 10.1016/S0968-0004(98)01255-9

Graumann, P. L., and Marahiel, M. A. (1999). Cold shock proteins CspB and CspC are major stationary-phase-induced proteins in *Bacillus subtilis*. *Arch. Microbiol.* 171, 135–138. doi: 10.1007/s002030050690

Gualerzi, C. O., Giuliodori, A. M., and Pon, C. L. (2003). Transcriptional and post-transcriptional control of cold-shock genes. *J. Mol. Biol.* 331, 527–539. doi: 10.1016/S0022-2836(03)00732-0

Hébraud, M., and Potier, P. (1999). Cold shock response and low temperature adaptation in psychrotrophic bacteria. *J. Mol. Microbiol. Biotechnol.* 1, 211–219.

Hengge-Aronis, R., Klein, W., Lange, R., Rimmele, M., and Boos, W. (1991). Trehalose synthesis genes are controlled by the putative sigma factor encoded by *rpoS* and are involved in stationary-phase thermotolerance in *Escherichia coli*. *J. Bacteriol.* 173, 7918–7924. doi: 10.1128/jb.173.24.7918-7924.1991

Jin, B., Jeong, K. W., and Kim, Y. (2014). Structure and flexibility of the thermophilic cold-shock protein of *Thermus aquaticus*. *Biochem. Biophys. Res. Commun.* 451, 402–407. doi: 10.1016/j.bbrc.2014.07.127

Jones, P. G., and Inouye, M. (1994). The cold-shock response - a hot topic. *Mol. Microbiol.* 11, 811–818. doi: 10.1111/j.1365-2958.1994.tb00359.x

Jones, P. G., VanBogelen, R. A., and Neidhardt, F. C. (1987). Induction of proteins in response to low temperature in *Escherichia coli*. *J. Bacteriol.* 169, 2092–2095. doi: 10.1128/jb.169.5.2092-2095.1987

Kandror, O., DeLeon, A., and Goldberg, A. L. (2002). Trehalose synthesis is induced upon exposure of *Escherichia coli* to cold and is essential for viability at low temperatures. *Proc. Natl. Acad. Sci. U. S. A.* 99, 9727–9732. doi: 10.1073/pnas.142314099

Kanehisa, M., and Goto, S. (2000). KEGG: Kyoto encyclopedia of genes and genomes. *Nucleic Acids Res.* 28, 27–30. doi: 10.1093/nar/28.1.27

Keto-Timonen, R., Hietala, N., Palonen, E., Hakakorpi, A., Lindström, M., and Korkeala, H. (2016). Cold shock proteins: a minireview with special emphasis on Csp-family of enteropathogenic yersinia. *Front. Microbiol.* 7:1151. doi: 10.3389/fmicb.2016.01151

Kim, M., Oh, H. S., Park, S. C., and Chun, J. (2014). Towards a taxonomic coherence between average nucleotide identity and 16S rRNA gene sequence similarity for species demarcation of prokaryotes. *Int. J. Syst. Evol. Microbiol.* 64, 346–351. doi: 10.1099/ijs.0.059774-0

Kim, Y., Wang, X., Zhang, X. S., Grigoriu, S., Page, R., Peti, W., et al. (2010). *Escherichia coli* toxin/antitoxin pair MqsR/MqsA regulate toxin CspD. *Environ. Microbiol.* 12, 1105–1121. doi: 10.1111/j.1462-2920.2009.02147.x

Klein, W., Weber, M. H. W., and Marahiel, M. A. (1999). Cold shock response of *Bacillus subtilis*: isoleucine-dependent switch in the fatty acid branching pattern for membrane adaptation to low temperatures. *J. Bacteriol.* 181, 5341–5349. doi: 10.1128/jb.181.17.5341-5349.1999

Kumar, S., Stecher, G., Li, M., Knyaz, C., and Tamura, K. (2018). MEGA X: molecular evolutionary genetics analysis across computing platforms. *Mol. Biol. Evol.* 35, 1547–1549. doi: 10.1093/molbev/msy096

Kumar, V., Thakur, V., Ambika Kumar, V., Kumar, R., and Singh, D. (2020). Genomic insights revealed physiological diversity and industrial potential for *Glaciimonas* sp. PCH181 isolated from *Satrundi glacier* in Pangi-Chamba Himalaya. *Genomics* 112, 637–646. doi: 10.1016/j.ygeno.2019.04.016

Larkin, M. A., Blackshields, G., Brown, N. P., Chenna, R., Mcgettigan, P. A., McWilliam, H., et al. (2007). Clustal W and Clustal X version 2.0. *Bioinformatics* 23, 2947–2948. doi: 10.1093/bioinformatics/btm404

Lodato, P., Se Govia De Huergo, M., and Buera, M. P. (1999). Viability and thermal stability of a strain of *Saccharomyces cerevisiae* freeze-dried in different sugar and

polymer matrices. *Appl. Microbiol. Biotechnol.* 52, 215–220. doi: 10.1007/s002530051511

Luyckx, J., and Baudouin, C. (2011). Trehalose: an intriguing disaccharide with potential for medical application in ophthalmology. *Clin. Ophthalmol.* 5, 577–581. doi: 10.2147/OPTH.S18827

Margesin, R. (2007). Alpine microorganisms: useful tools for low-temperature bioremediation. *J. Microbiol.* 45, 281–285.

Margesin, R., Zhang, D. C., Frasson, D., and Brouchkov, A. (2016). *Glaciimonas frigoris* sp. nov., a psychrophilic bacterium isolated from ancient Siberian permafrost sediment, and emended description of the genus *Glaciimonas*. *Int. J. Syst. Evol. Microbiol.* 66, 744–748. doi: 10.1099/ijsem.0.000783

Mei, Y. Z., Huang, P. W., Liu, Y., He, W., and Fang, W. W. (2016). Cold stress promoting a psychrotolerant bacterium *Pseudomonas fragi* P121 producing trehaloase. *World J. Microbiol. Biotechnol.* 32:134. doi: 10.1007/s11274-016-2097-1

Meier-Kolthoff, J. P., Auch, A. F., Klenk, H. P., and Göker, M. (2013). Genome sequence-based species delimitation with confidence intervals and improved distance functions. *BMC Bioinformatics* 14:60. doi: 10.1186/1471-2105-14-60

Miller, G. L., Blum, R., Glennon, W. E., and Burton, A. L. (1960). Measurement of carboxymethylcellulase activity. *Anal. Biochem.* 1, 127–132. doi: 10.1016/0003-2697(60)90004-X

Mishra, P. K., Joshi, P., Bisht, S. C., Bisht, J. K., and Selvakumar, G. (2010). "Cold-Tolerant Agriculturally Important Microorganisms," in *Plant Growth and Health Promoting Bacteria. Microbiology Monographs*, Ed. D. Meheshwori (Berlin, Heidelberg: Springer), 18. doi: 10.1007/978-3-642-13612-2_12

Pearce, D. A. (2012). "Extremophiles in Antarctica: life at low temperatures" in *Adaption of microbial life to environmental extremes, novel research results and application*, 87–118.

Phadtare, S., and Inouye, M. (2001). Role of CspC and CspE in regulation of expression of RpoS and UspA, the stress response proteins in *Escherichia coli*. *J. Bacteriol.* 183, 1205–1214. doi: 10.1128/JB.183.4.1205-1214.2001

Piette, F., D'Amico, S., Mazzucchelli, G., Danchin, A., Leprince, P., and Feller, G. (2011). Life in the cold: a proteomic study of cold-repressed proteins in the antarctic bacterium *Pseudoalteromonas haloplanktis* TAC125. *Appl. Environ. Microbiol.* 77, 3881–3883. doi: 10.1128/AEM.02757-10

Richter, M., and Rosselló-Móra, R. (2009). Shifting the genomic gold standard for the prokaryotic species definition. *Proc. Natl. Acad. Sci. U. S. A.* 106, 19126–19131. doi: 10.1073/pnas.0906412106

Roberts, M. E., and Inniss, W. E. (1992). The synthesis of cold shock proteins and cold acclimation proteins in the psychrophilic bacterium *Aquaspirillum arcticum*. *Curr. Microbiol.* 25, 275–278. doi: 10.1007/BF01575861

Rogers, J. S., and Swofford, D. L. (1998). A fast method for approximating maximum likelihoods of phylogenetic trees from nucleotide sequences. *Syst. Biol.* 47, 77–89. doi: 10.1080/106351598261049

Shenhar, Y., Biran, D., and Ron, E. Z. (2012). Resistance to environmental stress requires the RNA chaperones CspC and CspE. *Environ. Microbiol. Rep.* 4, 532–539. doi: 10.1111/j.1758-2229.2012.00358.x

Singer, M. A., and Lindquist, S. (1998). Multiple effects of trehalose on protein folding in vitro and in vivo. *Mol. Cell* 1, 639–648. doi: 10.1016/S1097-2765(00)80064-7

Song, C., Schmidt, R., de Jager, V., Krzyzanowska, D., Jongedijk, E., Cankar, K., et al. (2015). Exploring the genomic traits of fungus-feeding bacterial genus Collimonas. *BMC Genomics* 16:1103. doi: 10.1186/s12864-015-2289-3

Tournu, H., Fiori, A., and Van Dijck, P. (2013). Relevance of trehalose in pathogenicity: some general rules, yet many exceptions. *PLoS Pathog.* 9:e1003447. doi: 10.1371/journal.ppat.1003447

Wang, N., Yamanaka, K., and Inouye, M. (1999). CspI, the ninth member of the CspA family of *Escherichia coli*, is induced upon cold shock. *J. Bacteriol.* 181, 1603–1609. doi: 10.1128/jb.181.5.1603-1609.1999

Welch, W. J., and Brown, C. R. (1996). Influence of molecular and chemical chaperones on protein folding. *Cell Stress Chaperones* 1, 109–115. doi: 10.1379/1466-1268(1996)001<0109:IOMACC>2.3.CO;2

White-Ziegler, C. A., Um, S., Pérez, N. M., Berns, A. L., Malhowski, A. J., and Young, S. (2008). Low temperature (23 °C) increases expression of biofilm-, cold-shock- and RpoS-dependent genes in *Escherichia coli* K-12. *Microbiology* 154, 148–166. doi: 10.1099/mic.0.2007/012021-0

Yamanaka, K., Fang, L., and Inouye, M. (1998). The CspA family in *Escherichia coli*: multiple gene duplication for stress adaptation. *Mol. Microbiol.* 27, 247–255. doi: 10.1046/j.1365-2958.1998.00683.x

Yamanaka, K., and Inouye, M. (1997). Growth-phase-dependent expression of *cspD*, encoding a member of the CspA family in *Escherichia coli*. *J. Bacteriol.* 179, 5126–5130. doi: 10.1128/jb.179.16.5126-5130.1997

Yamanaka, K., and Inouye, M. (2001a). Induction of CspA, an *E. coli* major cold-shock protein, upon nutritional upshift at 37°C. *Genes Cells* 6, 279–290. doi: 10.1046/j.1365-2443.2001.00424.x

Yamanaka, K., and Inouye, M. (2001b). Selective mRNA degradation by polynucleotide phosphorylase in cold shock adaptation in *Escherichia coli*. *J. Bacteriol.* 183, 2808–2816. doi: 10.1128/JB.183.9.2808-2816.2001

Yamanaka, K., Mitani, T., Ogura, T., Niki, H., and Hiraga, S. (1994). Cloning, sequencing, and characterization of multicopy suppressors of a *mukB* mutation in *Escherichia coli*. *Mol. Microbiol.* 13, 301–312. doi: 10.1111/j.1365-2958.1994.tb00424.x

Yoon, S. H., Ha, S. M., Kwon, S., Lim, J., Kim, Y., Seo, H., et al. (2017). Introducing EzBioCloud: a taxonomically united database of 16S rRNA gene sequences and whole-genome assemblies. *Int. J. Syst. Evol. Microbiol.* 67, 1613–1617. doi: 10.1099/ijsem.0.001755

Zhang, D. C., Redzic, M., Schinner, F., and Margesin, R. (2011). *Glaciimonas immobilis* gen. Nov., sp. nov., a member of the family Oxalobacteraceae isolated from alpine glacier cryoconite. *Int. J. Syst. Evol. Microbiol.* 61, 2186–2190. doi: 10.1099/ijs.0.028001-0

frontiers | Frontiers in Microbiology

TYPE Original Research
PUBLISHED 07 March 2024
DOI 10.3389/fmicb.2024.1362975

OPEN ACCESS

EDITED BY
Prashant Kumar Singh,
Mizoram University, India

REVIEWED BY
Céline Lavergne,
Universidad de Playa Ancha, Chile
W. Matthew Sattley,
Indiana Wesleyan University, United States

*CORRESPONDENCE
Prekrasna-Kviatkovska Yevheniia
✉ preckrasna@uac.gov.ua

RECEIVED 29 December 2023
ACCEPTED 21 February 2024
PUBLISHED 07 March 2024

CITATION
Prekrasna-Kviatkovska Y, Parnikoza I, Yerkhova A, Stelmakh O, Pavlovska M, Dzyndra M, Yarovyi O and Dykyi E (2024) From acidophilic to ornithogenic: microbial community dynamics in moss banks altered by gentoo penguins.
Front. Microbiol. 15:1362975.
doi: 10.3389/fmicb.2024.1362975

From acidophilic to ornithogenic: microbial community dynamics in moss banks altered by gentoo penguins

Yevheniia Prekrasna-Kviatkovska[1]*, Ivan Parnikoza[1,2,3], Anna Yerkhova[4], Olesia Stelmakh[5], Mariia Pavlovska[1,6], Marta Dzyndra[1], Oleksandr Yarovyi[1] and Evgen Dykyi[1]

[1]Biology and Ecology Department, State Institution National Antarctic Scientific Center, Kyiv, Ukraine, [2]Department of Cell Population Genetics, Institute of Molecular Biology and Genetics, Kyiv, Ukraine, [3]Faculty of Natural Science, National University of "Kyiv-Mohyla Academy", Kyiv, Ukraine, [4]Biomedical Institute, Open International University of Human Development Ukraine, Kyiv, Ukraine, [5]Faculty of Molecular Biology and Biotechnology, Kyiv Academic University, Kyiv, Ukraine, [6]Faculty of Plant Protection, Biotechnology and Ecology, National University of Life and Environmental Sciences of Ukraine, Kyiv, Ukraine

Introduction: The study explores the indirect impact of climate change driven by gentoo's penguin colonization pressure on the microbial communities of moss banks formed by Tall moss turf subformation in central maritime Antarctica.

Methods: Microbial communities and chemical composition of the differently affected moss banks (Unaffected, Impacted and Desolated) located on Galindez Island and Cape Tuxen on the mainland of Kyiv Peninsula were analyzed.

Results: The native microbiota of the moss banks' peat was analyzed for the first time, revealing a predominant presence of Acidobacteria (32.2 ± 14.4%), followed by Actinobacteria (15.1 ± 4.0%) and Alphaproteobacteria (9.7 ± 4.1%). Penguin colonization and subsequent desolation of moss banks resulted in an increase in peat pH (from 4.7 ± 0.05 to 7.2 ± 0.6) and elevated concentrations of soluble nitrogen (from 1.8 ± 0.4 to 46.9 ± 2.1 DIN, mg/kg) and soluble phosphorus compounds (from 3.6 ± 2.6 to 20.0 ± 1.8 DIP, mg/kg). The contrasting composition of peat and penguin feces led to the elimination of the initial peat microbiota, with an increase in Betaproteobacteria (from 1.3 ± 0.8% to 30.5 ± 23%) and Bacteroidota (from 5.5 ± 3.7% to 19.0 ± 3.7%) proportional to the intensity of penguins' impact, accompanied by a decrease in community diversity. Microbial taxa associated with birds' guts, such as *Gottschalkia* and *Tissierella*, emerged in Impacted and Desolated moss banks, along with bacteria likely benefiting from eutrophication. The changes in the functional capacity of the penguin-affected peat microbial communities were also detected. The nitrogen-cycling genes that regulate the conversion of urea into ammonia, nitrite oxide, and nitrate oxide (*ureC*, *amoA*, *nirS*, *nosZ*, *nxrB*) had elevated copy numbers in the affected peat. Desolated peat samples exhibit the highest nitrogen-cycle gene numbers, significantly differing from Unaffected peat ($p < 0.05$).

Discussion: The expansion of gentoo penguins induced by climate change led to the replacement of acidophilic microbiomes associated with moss banks, shaping a new microbial community influenced by penguin guano's chemical and microbial composition.

KEYWORDS

peat microbial communities, climate change, ornithogenic impact, Antarctica, moss banks

1 Introduction

The Western Antarctic Peninsula has experienced the fastest climate change than anywhere on Earth during the last 50 years. Such rapid changes inevitably affect the conditions for the functioning of Antarctica's terrestrial and marine biota (Smith et al., 1999; Vaughan et al., 2003; Bromwich et al., 2013). While climate changes threaten some species in the region, such as Adélie penguin or krill (Atkinson et al., 2004; Emmerson and Southwell, 2022), others benefit from these alterations. In the latter context, species adapted to the comparatively moderate subantarctic conditions can be mentioned. Examples include the growth of *Pygoscelis papua* or gentoo penguin population (Lynch et al., 2012; Korczak-Abshire et al., 2021), the salp expansion in the Southern Ocean (Atkinson et al., 2004), and the spread of crabs from Patagonia to the Southern Ocean (Hellberg et al., 2019).

For species such as gentoo penguins, salps, or krill, the impact of climate change—whether positive or negative—is directly linked to rising temperatures, ice retreat, or the expanding areas available for colonization. Nevertheless, climatic changes extend beyond direct impacts and have large-scale indirect consequences on Antarctic biota.

The indirect impact of climate change is reliably illustrated by the influence of the Southward expansion of the gentoo penguin (Lynch et al., 2012; LaRue et al., 2013; Younger et al., 2015). An example of such expansion is the first appearance of gentoo penguins on Galindez Island in central maritime Antarctica in 2006, followed by rapid colonization and population growth (Parnikoza et al., 2018). Though penguins can often occupy barren areas released after recent glacier retreat (LaRue et al., 2013; Younger et al., 2015), gentoo penguins also establish colonies on moss banks, which are the most developed forms of the Tall moss turf subformation, as it happened on Galindez Island. These cryptogamic communities are exclusive to the maritime Antarctic and are composed of one or two moss species capable of accumulating peat: *Polytrichum strictum* Brid. and *Chorisodontium aciphyllum* (Hook.f. & Wilson) Broth. (Wierzgoń et al., 2023). Eutrophication resulting from gentoo penguins' colonization leads to the desolation of moss banks and the flourishing of the nitrophilic *Prasiola crispa* (Lightfoot) Kützing (Parnikoza et al., 2018; Wierzgoń et al., 2023). It induces changes in the structure of plant communities, followed by a loss of diversity and the elimination of species poorly adapted to high eutrophication levels. This scenario was observed on Galindez Island, devoid of gentoo colonies until the 2007/08 season (Parnikoza et al., 2018). The authors have observed a similar process on Cape Tuxen since 2014. The ongoing loss of diversity on Galindez Island and other localities caused by ornithogenic eutrophication continues to unfold.

Besides the ornithogenic effect observable to the naked eye, penguin colonization is likely to affect the chemical and microbiological composition of the peat accumulated beneath the plant community. The peat in moss banks in Antarctica possesses distinctive characteristics, setting it apart from other substrates in the region, including acidity, aerobicity, slow decomposition, and the accumulation of partially decomposed plant organic matter (Fenton, 1980; Parnikoza et al., 2017). These unique properties likely support specific microbial communities. As illustrated earlier, penguin feces alter the composition of the soil microbial community (Wang et al., 2015; Santamans et al., 2017). The guano of penguins is highly enriched in nitrogen compounds, primarily represented by urea, proteins, and ammonium (Lindeboom, 1984; Zhu et al., 2009; Crittenden et al., 2015; Lorrain et al., 2017). Studies of the mineral and ornithogenic soils in Cape Hallet and Cape Bird in the Ross Sea region revealed the enrichment in organic carbon, nitrogen, phosphorus and microbial biomass (Aislabie et al., 2009). Similarly, there were enriched concentrations of total carbon, total organic carbon and total nitrogen content in ornithogenic soils formed by *P. papua* and *P. antarctica* compared to the mineral soils on the southern coast of the Barton Peninsula of King George Island (Kim et al., 2012), and water content, organic matter content, and phosphorus content were higher in bird-impacted soil from Fildes Peninsula, Ardley Peninsula, and Livingston Island (Ramírez-Fernández et al., 2021). Alongside nutrients, the microbiota from penguins' intestines is released into the Antarctic environment (Grzesiak et al., 2020). Bacterial community composition exhibited significant distinctions between soils influenced by penguins' activity and mineral soils on the southern coast of the Barton Peninsula (Kim et al., 2012). According to Aislabie et al. (2009) *Firmicutes* and *Psychrobacter* dominated the nest sites of the Adelie penguins, while *Xantomonadaceae*, *Rhodanobacter*, *Dokdonella*, and *Lysobacter* dominated the abandoned sites. Analysis of the bacterial metagenomically assembled genomes (MAGs) (Ramírez-Fernández et al., 2021) revealed that bird impact on Antarctic soil changes the functional activity of microbes. In particular, *nirK* and *nosZ* genes (encoding for nitrite reductase and nitrous oxide reductase) were more significantly abundant in bird-impacted soils than soils without animal influence. Ornithogenic eutrophication and the input of gut microbiota are likely to alter moss banks' peat and the specific microbial communities that inhabit this substrate.

In Antarctica, microbial communities typically constitute the dominant biomass component of terrestrial ecosystems. They play a pivotal role in controlling the biological flux of carbon, nutrients, and energy (Wynn-Williams, 1996), thereby influencing the functioning and development of terrestrial ecosystems (Yergeau and Kowalchuk, 2008; Teixeira et al., 2010; Yergeau et al., 2012). Given the crucial role of microorganisms in Antarctic terrestrial life, penguin-induced eutrophication can lead to the replacement of the peat microbiota, impairment or changes in its functional capabilities. The intense input of penguin guano rich in nitrogen compounds is likely to alter the functioning of nitrogen-cycling bacteria, initially leading to enrichment in nitrogen-cycling taxa.

Herewith, the study's objective was to investigate the gentoo penguin's increasing colonization influence on the microbial communities of peat moss banks in central maritime Antarctica. The particular tasks of the study were: (i) estimate changes in the chemical parameters of the peat; (ii) evaluate the changes in microbial composition as the result of the penguins' colonization; (iii) compare the abundance of the microbial nitrogen-cycling genes in the peat differentially affected by penguins.

2 Materials and methods

2.1 Study sites

Several moss banks influenced by penguin colonies expansion have been studied. These moss banks, namely moss banks 1 and 4 are located on Galindez Island, Argentine Islands (Figure 1, points 1 and 4 respectively). The other moss bank 5 is located on the Cape Tuxen on the mainland of Kyiv Peninsula (Figure 1, point 5). All studied

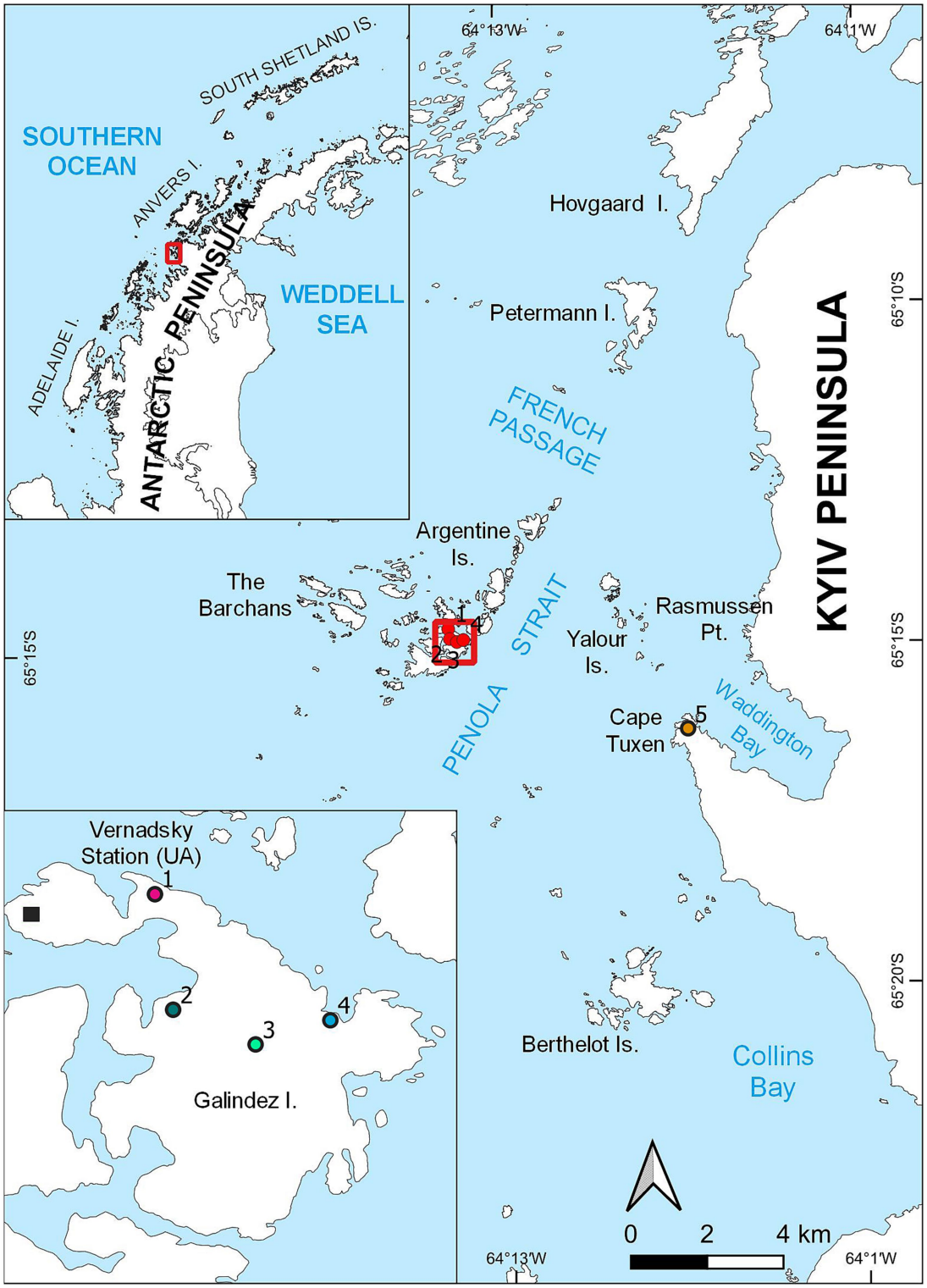

FIGURE 1
Locations of the moss banks located on Galindez Island and Cape Tuxen on the mainland of Kyiv Peninsula, where samples were collected.

moss banks were formed mainly by *Polytrichum strictum* (Schrader) but had significant diversity (Wierzgoń et al., 2023).

Penguin colonies appeared on the moss bank 1 in 2019, though birds abandoned this territory afterwards, leaving single nests. Both moss banks 4 and 5 were colonized by *P. papua* in 2020 and were considered newly penguin-disturbed territories at the moment of sampling. Moss banks 2 and 3 located on Galindez Island were not disturbed by penguins at the moment of sampling.

Moss banks were not evenly affected by penguins' direct impact, such as colonization, trampling, and excretion. The moss banks that

were not affected directly by the birds had no visual sign of the impact (Figure 2). We define 3 degrees of moss bank colonization by penguins (Figure 2).

(i) Unaffected: Intact moss banks that show no direct and visible penguin influence. Samples of unaffected peat were collected from moss banks 2 and 3 on Galindez Island [Figure 1, points 2 and 3, respectively (Wierzgoń et al., 2023)] in addition to moss banks 1, 4, and 5. These moss banks were not directly affected by *P. papua* in the study seasons.

(ii) Impacted: Moss banks with a moderate impact, consisting of live, beaten-up turfs neighboring the patches covered with feces and feathers. The dominant *P. strictum* moss was partially deceased in this condition. It was pink, probably due to the loss of chlorophyll. Samples were collected from moss banks 1, 4, 5.

(iii) Desolated: A moss bank with deceased *P. strictum* and other mosses entirely covered with guano. Subsequently, it can be colonized by nitrophilic algae such as *Prasiola crispa*. Samples were collected from moss banks 1, 4, 5.

We distinguished these degrees of the penguin impact as Unaffected, Impacted and Desolated moss cover (Figure 2) and used these definitions here and after in the manuscript.

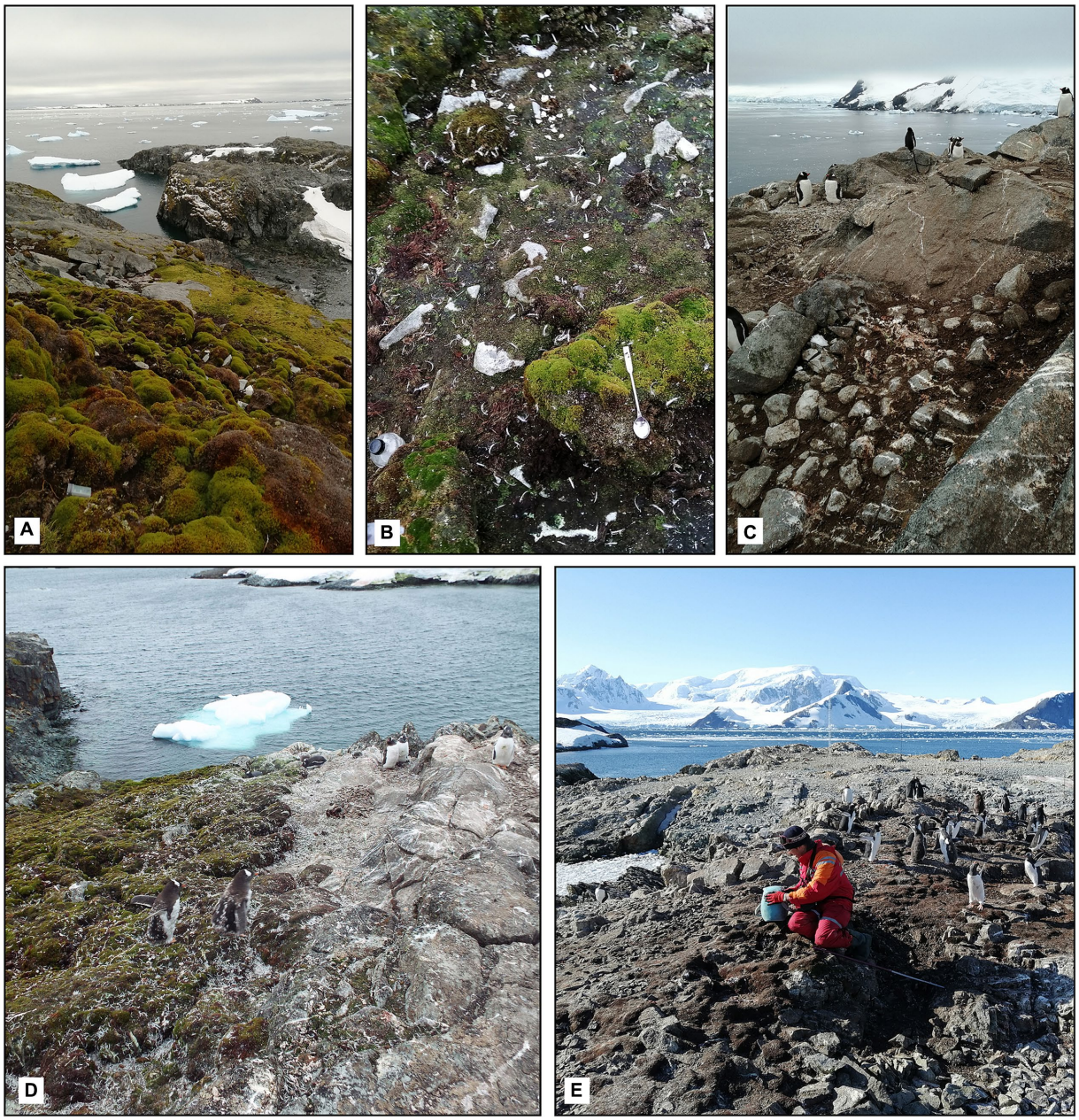

FIGURE 2
Levels of the ornithogenic impact on the moss banks: **(A)** Unaffected moss bank, moss bank 5; **(B)** impacted moss bank, moss bank 5; **(C)** desolated moss bank covered by guano, moss bank 5; **(D)** expansion of the penguin colony on the moss bank 4; **(E)** desolated part of moss bank 4 (2020).

In addition to these sample types, we collected peat samples that had perished for reasons other than penguin colonization (Control Dead) as control points the margin of moss bank 3. This moss had died before the first colonies of *P. papua* appeared on the island in 2007. The primary reason for this moss death was glaciation and prolonged snow coverage in the 20th century, as discussed by Yu et al. (2016). These samples were collected to compare microbiome composition with penguin-affected and Unaffected moss.

2.2 Samples collection

Samples of the peat were collected by sterile spatula in 15 mL polypropylene tubes and kept at the ambient temperature during the sampling campaign (several hours) until the laboratory at Vernadsky Station, where they were immediately frozen at −80°C for further microbiological analysis. Transportation of the samples from Antarctica was facilitated on the dry ice (−30°C).

About 50 g of peat samples were collected for the chemical analysis, which was performed immediately at the Vernadsky Station.

2.3 Measuring the biogenic elements' content and pH of the peat

Peat samples were homogenized and topped with distilled water in a 10:1 (H_2O: sample) v/w ratio. Samples were mixed with water and endured for 12 h. The suspension was filtered, and the filtrate was used for further chemical analysis. pH was measured by pH-meter HI 2550 (HANNA instruments, Italy). Concentrations of mineral nitrogen (NH_4^+, NO_2^+, NO_3^+) and soluble phosphates in the filtrate were measured by spectrophotometer Hach Lange DR3900 (Hach, USA) in 1 inch square glass cuvettes according to the standard manufacturers' instructions that correspond to the following methods of water analysis certified by EPA Environmental Protection Agency (USA) (Rice and Bridgewater, 2012). In brief, the concentration of NO_2^- was measured by the diazotization method (reagent set NitriVer 3, Hach), the concentration of NO_3− was measured by the cadmium reduction method (reagent set NitraVer 6, Hach), the salicylate method was used to measure NH_4^+ (Nitrogen-Ammonia Reagent Set, Hach), and ascorbic acid method was used to measure concentration of PO_4^{3-} (reagent set PhosVer 3). Nitrate Standard Solution (100 mg/L), Nitrite Standard Solution (250 mg/L NO_2^--N), Ammonium Standard Solution (50 mg/L), Phosphate Standard Solution (50 mg/L as PO_4^{3-}, NIST) provided by Hach (USA) were used to build the calibration curves. All measurements were performed in triplicates at 18°C.

2.4 DNA extraction

DNA was extracted from peat samples in duplicates by the DNeasy PowerSoil kit (Qiagen, Germany) according to the manufacturer's instructions. DNA concentration, 260/280 and 260/230 absorbance ratio were measured by spectrophotometer Denovix DS-11 FX (Denovix, USA). In the cases where the absorbance ratios indicated heavy impurity of the sample, DNA was precipitated in 96% ethanol (in the presence of 3 M sodium acetate) and dissolved in elution buffer from a DNeasy PowerSoil kit. As a result, the DNA concentration extracted from the peat samples varied from 5.8 to 112.7 ng/μl, and the 260/280 ratio was ~1.5–1.8.

2.5 16S rRNA amplicon sequencing

V3-V4 regions of 16S rRNA gene were amplified with universal primers 515F (GTGCCAGCMGCCGCGGTAA) and 806R (GGACTACHVGGGTWTCTAAT) with Phusion High-Fidelity PCR Master Mix (New England, Biolabs). PCR products were checked in 2% agarose gel. Samples with 400–450 bp amplicon lengths were used for further analysis. PCR products were purified by Qiagen Gel Extraction Kit (Qiagen, Germany) and used for sequencing. Libraries were prepared using NEB Next Ultra DNA Library Pre Kit for Illumina according to the manufacturer's instructions. Quality check of the libraries was performed by fluorimeter Qubit 2.0 (Thermo Scientific, USA) and 2,100 Bioanalyzer Instrument (Agilent Technologies, USA). A nucleotide sequence with a length of 250 bp was estimated on the NovaSeq 6000 platform.

Sequences were uploaded to the National Center for Biotechnology Information (NCBI) database under accession number PRJNA1057234.

2.6 qPCR analysis

Bacterial DNA extracted from peat was used to quantify the copy number of nitrogen cycle genes and 16S rRNA gene by quantitative real-time PCR. We quantified the following genes: *ureC*, *amoA*, *amoA* gene of comammox *Nitrospira* clade A, *amoA* gene of comammox *Nitrospira* clade B, *nxrB*, *nirS*, *nosZ*. The list of genes, their function and primers are presented in Supplementary Table S1.

PCR products were used as standards for each of the genes. PCR products were generated using the DNA isolated from the peat samples. The standards for each gene were agarose checked and purified with a Qiagen Gel Extraction Kit (Qiagen, Germany). The concentration of the DNA was measured by spectrophotometer Denovix DS-11 FX (Denovix, USA), and 10-fold serially diluted ranging from 1.0×10^{-3} to 1.0×10^{-7} ng/μl to be used for standard curve generation in quantitative PCR. The gene copy number per μl was calculated according to the formula:

$$\left(\frac{X\frac{g}{\mu l}DNA}{[product\ length\ in\ base\ pairs\times 660]}\right)\times 6.022\times10^{23} = Y\ molecules\ /\ \mu L$$

Each 25 μL PCR reaction contained the following components: 2x QuantiFast SYBR Green PCR Master Mix (Qiagen, Germany) – 12.5 μL, Primer Reverse – 2.5 μL, Primer Forward – 2.5 μL, template DNA – 1 μL, RNase-free water – 6.5 μL. The concentration of template DNA in each reaction was 20 ng/μL. The thermal conditions were different for all primers and can be found in Supplementary Table S2.

The negative control contained components for PCR reaction and RNase-free water without sample DNA. All reactions were run in triplicate on Rotor-Gene Q (Qiagen, Germany). Based on

10.3389/fmicb.2024.1362975

the standard curves, the threshold value (Ct) was used to determine the copy number of genes in the peat. Melting curve analysis was performed at the end of the amplification cycles to assess primer specificity and to ensure proper amplification of all target fragments.

The concentration of genes per mg of sample (wet weight) was calculated according to the formula

$$Y\ gene\ copy/mg = \frac{\begin{array}{l}(gene\ copies\ per\ reaction\ mix)\\ \times(volume\ of\ DNA,\mu L)\\ \times(dilution\ factor)\end{array}}{(sample\ weight,mg)}$$

2.7 Bioinformatic and statistical analysis

Sequences were grouped according to their barcodes, and barcodes and primers were trimmed. The paired ends of the sequences were joined by FLASH V1.2.7 (Magoč and Salzberg, 2011). Quality assessment and filtering were performed in QIIME V1.7.0 (Caporaso et al., 2010). Filtered data was compared to the Gold database by the UCHIME pipeline (Edgar et al., 2011). Filtered data were clustered into OTUs with a threshold of 97% in Uparse v7.0.1001 (Edgar, 2013). Each representative read was taxonomically annotated by comparison with Silva database v138.1 (Quast et al., 2013).

Data were analyzed in QIIME V1.7.0 and RStudio 4.0.4. Specifically, packages such as *vegan* (Oksanen et al., 2016), *ComplexHeatmap* (Gu et al., 2016), *ggplot2* (Wickham, 2016) and *edgeR* (Robinson et al., 2010) were used. Alpha diversity indices (OTU number, Shannon index, Faith PD index) were estimated by QIIME V1.7.0 functional and compared between groups by *t-test* ($p < 0.05$). Rarefaction analysis was performed in QIIME V1.7.0. The data on the bacterial taxa abundance and nitrogen gene number was tested for normality by the Shapiro–Wilk normality test, which revealed their non-normal distribution ($p < 0.05$). A general linear model with a negative binomial distribution ('EdgeR' package) was used to identify significant relationships between OTUs and intensity of the penguin impact. *p*-values were corrected to account for multiple comparisons using the false discovery rate (*q*-value) method (Benjamini and Hochberg, 1995). Results with $q < 0.05$ were considered to be significant.

A Mantel test, based on Spearman's rank correlation, was conducted to assess whether the variance in microbial composition is explained by the pH of the substrate, utilizing distance matrices calculated using the Bray–Curtis measure. ANOSIM tests, based on Bray–Curtis distance matrices, were applied to assess whether the variabilities between microbial communities are explained by the intensity of ornitogenic impact or the sampling place (moss bank). A Non-metric Multidimensional Scaling (NMDS) plot of the OTU abundance was built on the Bray-Curtis distance matrix. Welch *t-test* was applied to compare the chemical parameters of the different types of peat. Kruskal-Wallis and Dunn tests were used to compare the nitrogen-cycle gene numbers in different types of peat. Spearman's rank correlation coefficient was calculated to reveal a correlation between nitrogen-cycling genes and the relative abundance of bacterial taxa.

3 Results

3.1 Chemical parameters of the peat

All the samples were acidic except the Desolated peat. The Unaffected and Impacted peat had acidic pH (4.7 ± 0.05 and 5.4 ± 0.4), though Welch's two-sample *t-test* revealed a significant difference between these two groups of samples ($T = -4.45$, $p < 0.05$, $df = 15.0$). pH of the Desolated peat significantly differed from the Unaffected peat ($T = 5.8$, $p < 0.05$, $df = 14.4$) and comprised 7.2 ± 0.6. The moss bank affected by factors other than penguin colonization was similar to the Unaffected peat from this study (4.6 ± 0.03).

Concentrations of the NH_4^+, NO_2^-, NO_3^- and content of dissolved inorganic nitrogen (DIN) had the lowest concentrations in the Unaffected peat and Control Dead peat (Figure 3). The concentration of all these nutrients increased in the Impacted peat. On the contrary, the content of nitrogen compounds tended to decrease in the destroyed substrate. In particular, the concentration of NH_4^+ fell from 44.4 ± 10.6 mg/kg in Impacted peat to 35.5 ± 26.2 mg/kg in Desolated peat. Similarly, the concentration of NO_2^- and NO_3^- decreased from 2.9 ± 3.2 and 17.6 ± 16.1 mg/kg to 0.9 ± 0.9 and 10.4 ± 10.5 mg/kg, respectively.

The concentration of PO_4^{3-} and dissolved inorganic phosphorus (DIP) increased when ornithogenic impact grew with the highest estimates in the Desolated peat samples (Figure 3). The concentration of PO_4^{3-} increased from 49.3 ± 9.6 mg/kg in the Impacted peat to 61.4 ± 5.6 mg/kg in the Desolated peat. In contrast, it was 5.0 ± 2.9 mg/kg in the Control Dead samples. Similarly, the concentration of DIP increased from 16.1 ± 3.2 to 20.0 ± 1.8 mg/kg in the Impacted and Desolated peat. Control Dead peat samples contained lower DIP concentrations, numbering 1.6 ± 0.9 mg/kg.

The Unaffected peat sample group included an outlier taken from the moss bank 5, exhibiting elevated concentrations of all nitrogen compounds (Figure 3). NH_4^+ was 19 times higher than the average of the remaining Unaffected samples, NO_2^- was higher by 29 times, and NO_3^- was higher by 46 times. The total DIN exceeded the average values for the Unaffected samples by 29 times. An outlier within the Unaffected peat group also exhibited an elevated concentration of soluble phosphorus, represented by a sample collected from the moss bank 1 (Figure 3).

3.2 16S rRNA amplicon sequencing output

Illumina NovaSeq 6,000 identified between 6,032 to 126,755 reads of the partial 16S rRNA gene per sample, with an average length of 414 ± 5 bp. Based on rarefaction curves, significantly higher estimates would not be achievable by deeper sequencing (Supplementary Figure S1). After quality filtering and clustering (threshold 97%) of the sequencing data, we obtained from 813 to 1990 OTUs per sample. Averages of the OTU number and diversity indices are presented in Table 1.

The microbial communities in Unaffected and Control Dead samples exhibited comparable OTU numbers and diversity indices. In contrast, the Impacted peat microbiomes showed slightly elevated OTU, Shannon, and Faith values compared to the other microbial communities. Conversely, the Desolated peat microbial communities displayed lower diversity than those in the other three groups. Notably,

10.3389/fmicb.2024.1362975

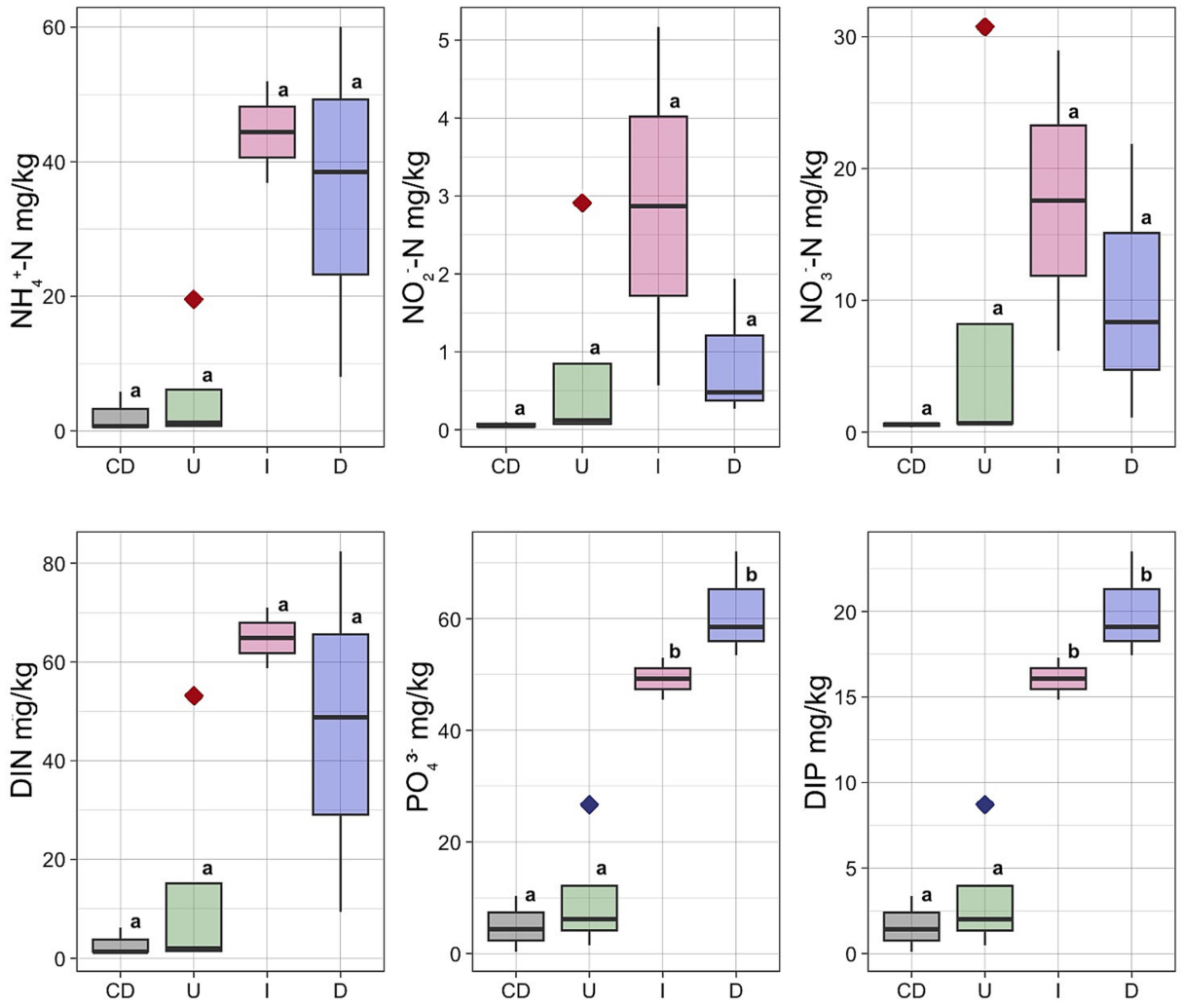

FIGURE 3
Concentrations of the NH_4^+, NO_2^-, NO_3^-, PO_4^{3-}, DIN and DIP in different types of the peat: U, Unaffected; I, Impacted; D, Desolated; CD, Control Dead; Outlier marked by red diamond – moss bank 5; Outlier marked by blue diamond – moss bank 1.

TABLE 1 Diversity indices of the microbial communities of the peat (average ± standard deviation).

	OTU number	Shannon, H	Faith, PD
Unaffected	1,276 ± 242	7.1 ± 0.9	129 ± 14
Impacted	1,564 ± 378	7.7 ± 0.6	143 ± 46
Desolated	1,185 ± 255	5.6 ± 1.5	117 ± 22
Control Dead	1,302 ± 187	7.5 ± 0.3	122 ± 18

a significant difference was only observed for the Shannon index between Impacted and Desolated peat ($t = -2.9$, $df = 5.4$, $p < 0.05$), indicating a distinct diversity pattern in these two peat types.

3.3 Taxonomic composition of moss banks' microbial communities

Proteobacteria, *Actinobacteria*, *Acidobacteria*, *Firmicutes*, *Chloroflexi*, *Cyanobacteria*, and *Bacterioidota* were identified as the most abundant phyla in the peat of moss banks affected by penguins' colonization (Figure 4). *Proteobacteria* dominated across all conditions, constituting 14.1 ± 3.9% in Unaffected, 23.9 ± 9.4% in Impacted, 38.6 ± 6.0% in Desolated, and 16.3 ± 3.8% in Control Dead peat. *Actinobacteria* exhibited variations with percentages of 15.1 ± 4.0%, 13.4 ± 4.4%, 14.7 ± 20.5%, and 10.3 ± 1.6% in the respective conditions. *Acidobacteria* represented 32.3 ± 14.4% in Unaffected, 20.4 ± 10.5% in Impacted, 3.1 ± 2.4% in Desolated, and 31.0 ± 11.6% in Control Dead peat. *Firmicutes* (9.7 ± 8.6%) and *Chloroflexi* (5.2 ± 7.8%) maintained consistent distributions across conditions. *Cyanobacteria* comprised 6.4 ± 8.5% in Unaffected, 1.5 ± 1.9% in Impacted, 6.8 ± 9.8% in Desolated, and 1.0 ± 0.9% in Control Dead peat, while *Bacterioidota*

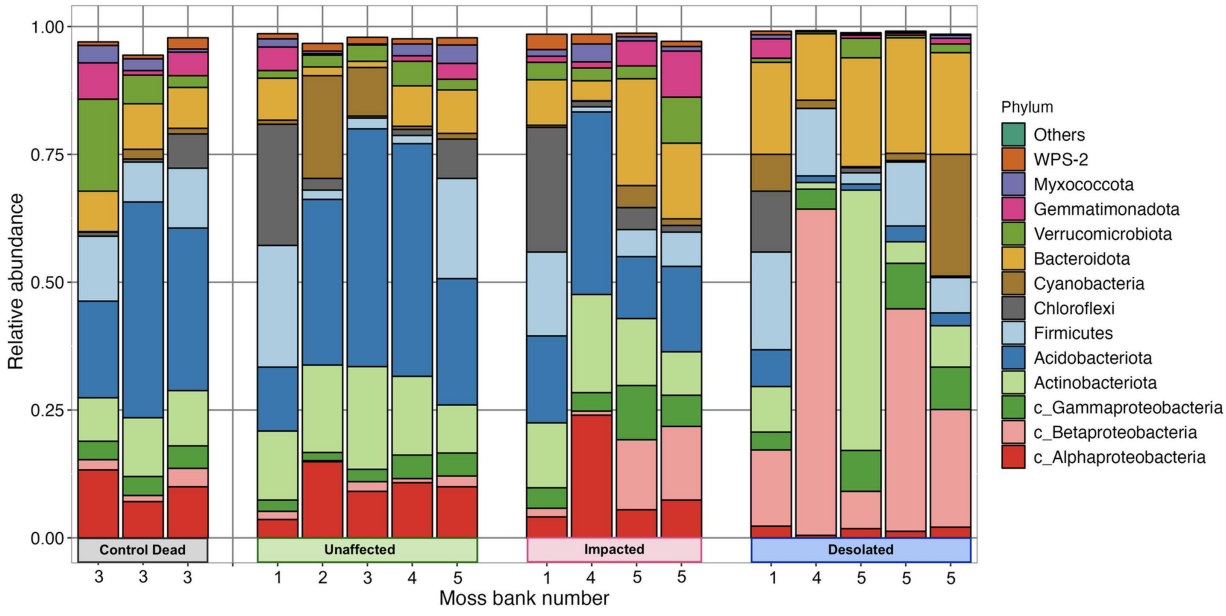

FIGURE 4
Abundance of bacterial phyla in different types of peat and different moss banks.

ratios were 5.5 ± 3.7% in Unaffected, 12.1 ± 7.4% in Impacted, 18.9 ± 3.7% in Desolated, and 8.3 ± 0.6% in Control Dead peat.

The ratio of some bacterial phyla, such as *Betaproteobacteria* and *Bacterioidota*, differed when the ornithogenic impact on the moss increased. The relative abundance of these phyla increased from 1.3 ± 0.8% and 5.5 ± 3.7% in the Unaffected peat to 30.5 ± 23.0% and 19.0 ± 3.7% in the Desolated peat. On the other hand, the relative abundance of *Acidobacteria* decreased from 32.2 ± 14.4% in Unaffected peat to 3.1 ± 2.4%.

A general linear model (GLM) with a negative binomial distribution identified OTUs with significantly differential abundance ($q < 0.05$) across Unaffected, Impacted, Desolated, and Control Dead peat samples (Supplementary Table S3). The heatmap in Figure 5 illustrates the relative abundance of taxa, the OTUs of which were identified as differentially abundant across various types of peat samples ($q < 0.05$).

Figure 5 showcases a distinctive microbial assemblage predominantly found in Unaffected moss:

(i) Acidobacteria: *Subgroup 1*, *Subgroup 2*, *Bryobacter*, *Granulicella*, *Occalatibacter*, *Candidatus Solibacter*, *Acidimicrobia*, *Acidobacteriaceae*, *Acidobacteriales*;
(ii) Actinobacteria: *Acidothermus*, *Conexibacter*, IMCC26256, *Solirubrobacteraceae*;
(iii) Alphaproteobacteria: *Pseudolabrys, Roseiarcus, Xanthobacteraceae, Caulobacteraceae, Acetobacteraceae, Micropepsaceae*, *Elsterales;*
(iv) Bacteroidota: *Puia*, *Mucilaginibacter*;
(v) Chloroflexi: AD3, JG30a-KF-32, *Ktedonobacteraceae*;
(vi) Gammaproteobacteria: WD260, *Acidibacter*;
(vii) Gemmatimonadota: *Gemmatimonadaceae*;
(viii) Myxococcota: *Pajaroellobacter*;
(ix) Verrucomicrobia: *Pedosphaeraceae*, *Methylacidiphilaceae*, *Opitutaceae*;
(x) WPS-2: WPS-2.

Genetic markers of these taxa were abundant in the Control Dead peat, suggesting that this microbial assemblage may represent an initial community for moss bank peat. These microbial taxa are present in Impacted moss, although they may be dormant or deceased in this case.

In contrast, the Impacted moss harbors a secondary microbial group alongside the initial assemblage. This secondary group comprises taxa such as:

(i) Actinobacteria: *Arthrobacter*;
(ii) Bacteroidota: *Tissierella*, *Pedobacter*;
(iii) Betaproteobacteria: *Simplicispira*, *Polaromonas*;
(iv) Cyanobacteria: *Tychonema*;
(v) Firmicutes: *Gottschalkia*, *Sporosarcina*;
(vi) Flavobacteria: *Chryseobacterium*, *Gelidibacter*, *Flavobacterium*, *Aequorivita*;
(vii) Gammaproteobacteria: *Psychrobacter*, *Luteoibacter*;
(viii) Verrucomicrobia: *Candidatus Udeobacter*.

This second microbial group becomes a core component in the Desolated mosses, where, unlike the Impacted mosses, the initial peat microbiota is nearly absent.

ANOSIM statistics revealed moderate correlation of the microbimes composition with the intensity of the penguins' impact ($R = 0.4$, $p < 0.05$) and moss bank ($R = 0.4$, $p < 0.05$). According to the Mantel test results based on Spearman correlation, there is strong correlation between the microbiome composition and pH of the substrate ($R = 0.65$, $p < 0.05$).

10.3389/fmicb.2024.1362975

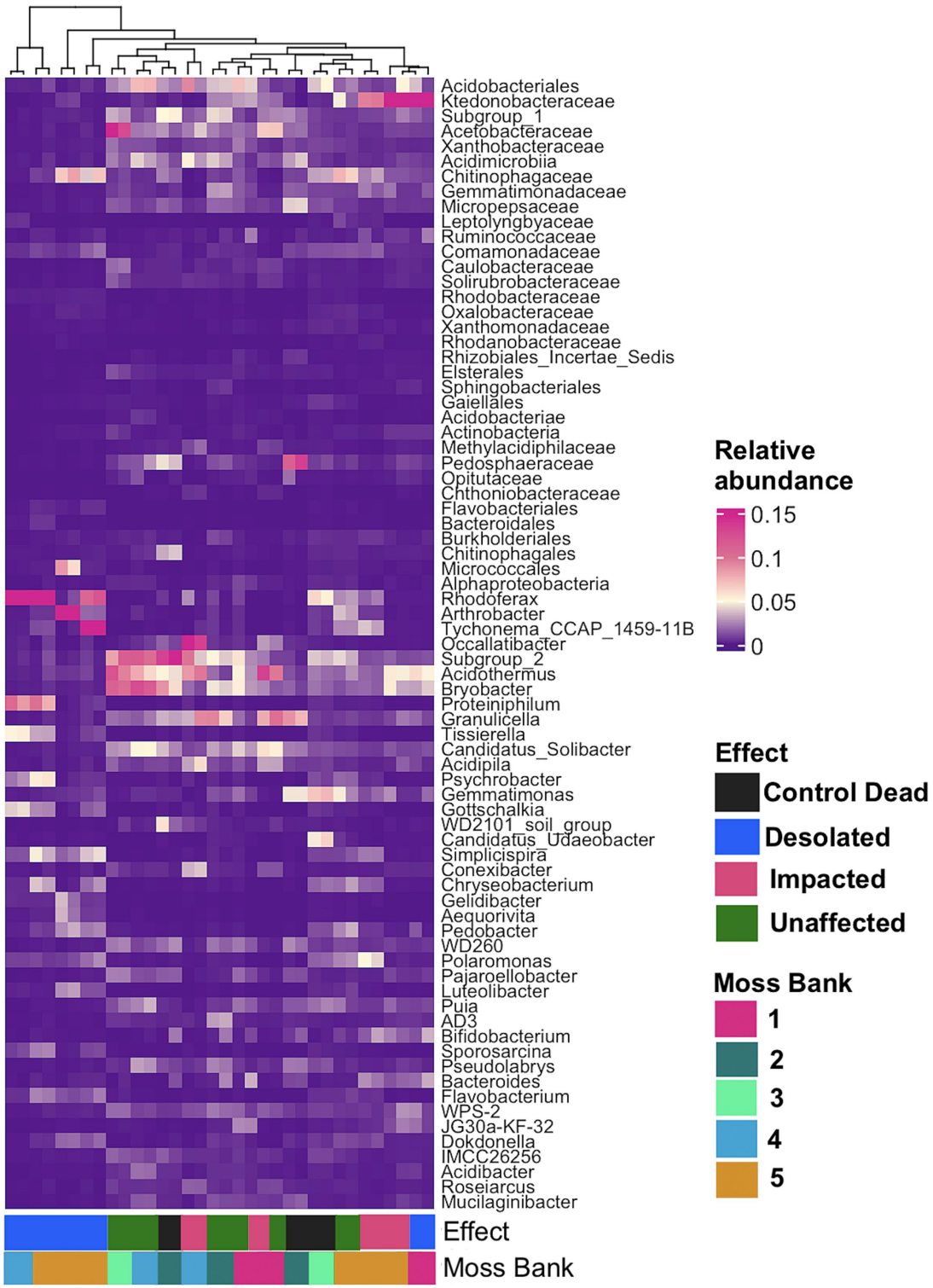

FIGURE 5
The relative abundance of bacterial taxa at the lowest taxonomic level, identified as differentially abundant OTUs ($q < 0.05$) across various types of peat samples using a general linear model (GLM) with a negative binomial distribution.

Non-metric multidimensional scaling (NMDS) ordination analysis was conducted using OTUs to visualize differences in microbiomes (Figure 6). The microbiomes of Desolated moss formed a distinct cluster, in contrast to the Unaffected moss. The microbial communities of Impacted moss represented a transitional state between the Unaffected and Desolated mosses' microbiomes. pH played a significant role ($p < 0.05$) in distinguishing microbial communities, as depicted in Figure 6A. Figure 6B illustrates the taxa ($p < 0.001$) that may contribute to the differences between microbiomes in different types of peat.

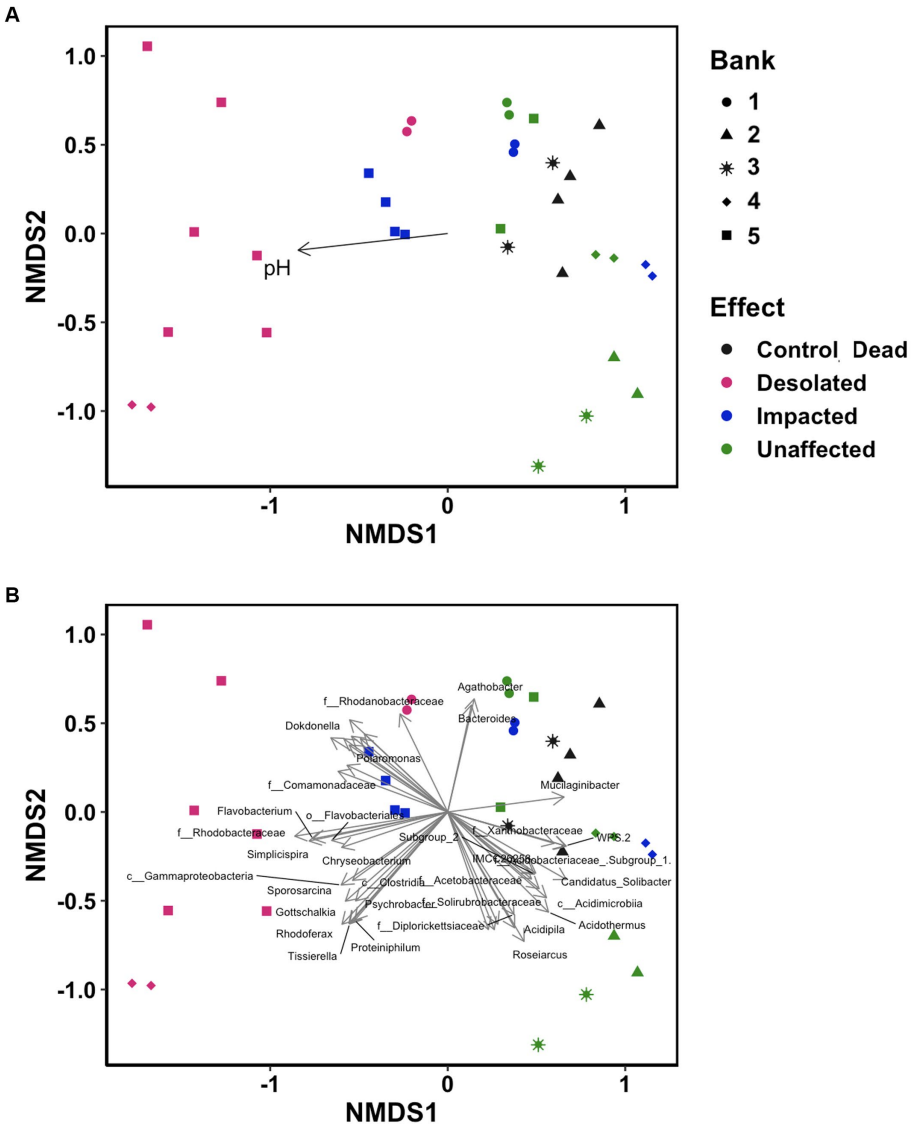

FIGURE 6
Non-metric multidimensional scaling (NMDS) ordination analysis on the distinctive distribution of OTU build on the Bray–Curtis dissimilarity matrix. Data points are color-coded by ornithogenic impact and symbolized by moss bank. **(A)** pH as intrinsic vector driving the distribution pattern ($p < 0.05$); **(B)** microbial taxa ($p < 0.001$) driving the distribution pattern.

3.4 Changes in the microbial communities functioning

The copy number of 16S rRNA gene and several genes related to the nitrogen cycle were quantified, such as *ureC*, bacterial *amoA*, *amoA* of the commamox *Nitrospira* clade A- and B, *nxrB*, *nirS* and *nosZ* (Figure 7; Supplementary Table S4).

The nitrogen cycle gene copy number increased in the Impacted and Desolated moss (Figure 7). The Kruskal-Wallis rank sum test supports the differential copy number of the *ureC*, *amoA*, commamox *amoA* of *Nitrospira* clades A and B, *nosZ* genes among the groups tested ($p < 0.05$). Dunn test revealed a significant difference ($p < 0.05$) in the abundance of all nitrogen cycle genes except for *nxrB* between the Unaffected and Desolated peat. The detailed *p-values* of the Dunn test are presented in the Supplementary Table S4. Differences in the abundance of the genes between the other groups of samples (as Unaffected and Impacted, Impacted and Desolated) were not significant according to the Dunn test.

The copy number of the 16S rRNA gene increased when the impact of the penguins on the moss banks intensified ($p < 0.05$). Unlike the Desolated moss banks, the copy number of nitrogen cycle genes and 16S rRNA genes in Control Dead samples remained comparable to the Unaffected samples.

The Spearman correlation was calculated to uncover what taxa are likely involved in the enrichment of the nitrogen-cycling genes. The group of taxa that had a negative correlation with the nitrogen cycling genes was native to Unaffected moss bank samples (Figure 8), which is likely the result of eliminating these bacteria.

A positive correlation between the abundance of taxa and the presence of nitrogen-cycling genes may suggest that enrichment with

10.3389/fmicb.2024.1362975

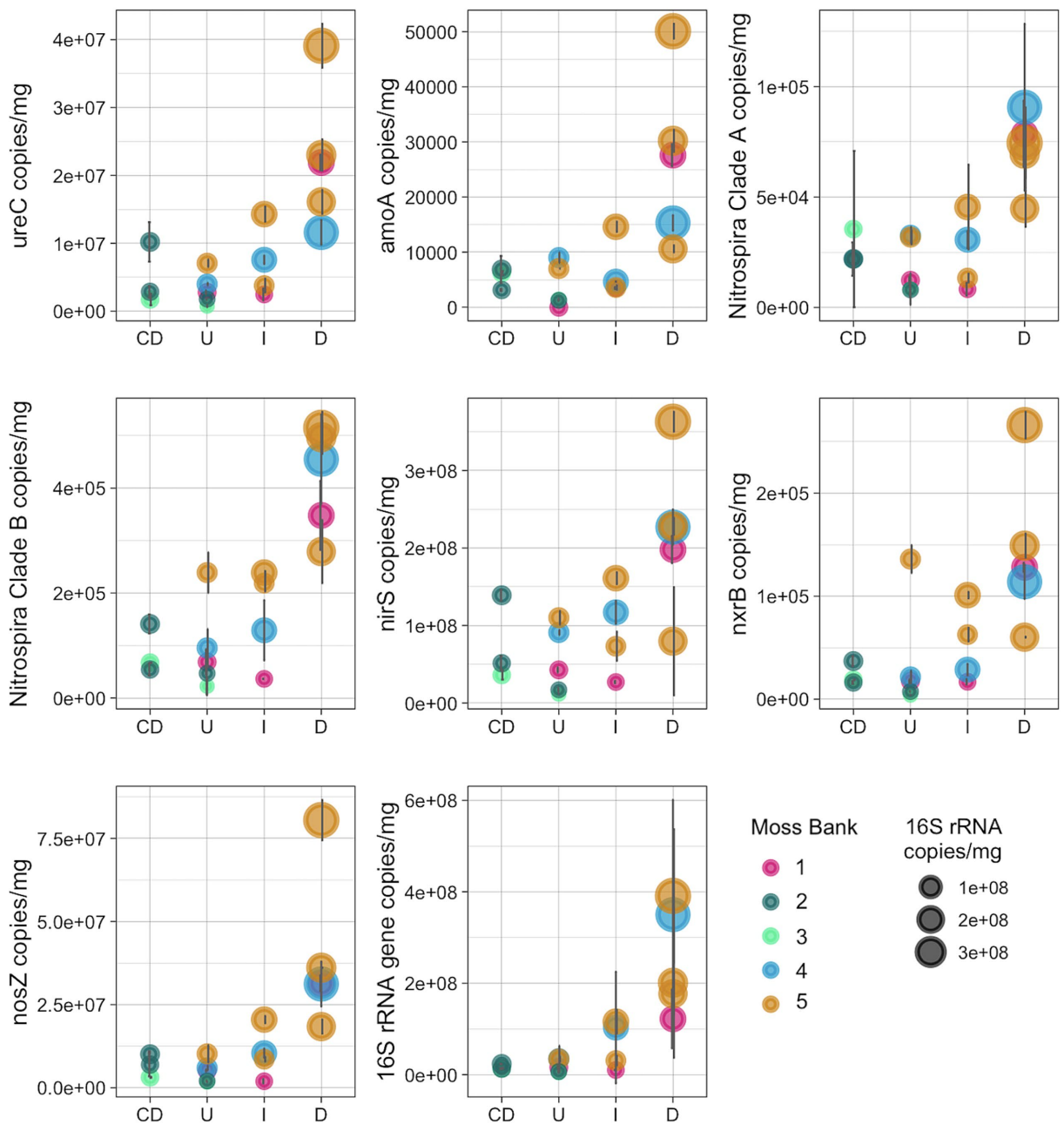

FIGURE 7
Number of copies of the nitrogen-cycle and 16S rRNA genes per mg of peat (wet weight): U, Unaffected; I, Impacted; D, Desolated; CD, Control dead.

specific taxa could lead to enrichment in genes associated with the nitrogen cycle. Nevertheless, interpreting the results should be cautiously approached, given the challenge of distinguishing between causation and spurious correlation in this particular case. The comammox *amoA* gene exclusively belongs to *Nitrospira* members. Therefore, any correlation observed between comammox *amoA* of *Nitrospira* clades A and B with *Polaromonas*, *Simplispira*, *Rhodoferax*, or other taxa is more likely to be a coincidence. The other nitrogen cycle genes examined in the study belong to diverse taxonomical groups and may enhance the functional capabilities of various microorganisms.

4 Discussion

This study explores the influence of gentoo penguin colonization as an indirect impact of climate change on alterations in terrestrial ecosystems in the maritime Antarctic, specifically focusing on microbial communities. Our analysis centers on the changes in microbiota within the peat formed by the Tall moss turf subformation, triggered by the rapid establishment of gentoo penguin colonies on Galindez Island (Argentine Islands) and Cape Tuxen on the mainland of Kyiv Peninsula. It encompasses the examination of the chemical composition of the peat, the taxonomic composition of microbiomes,

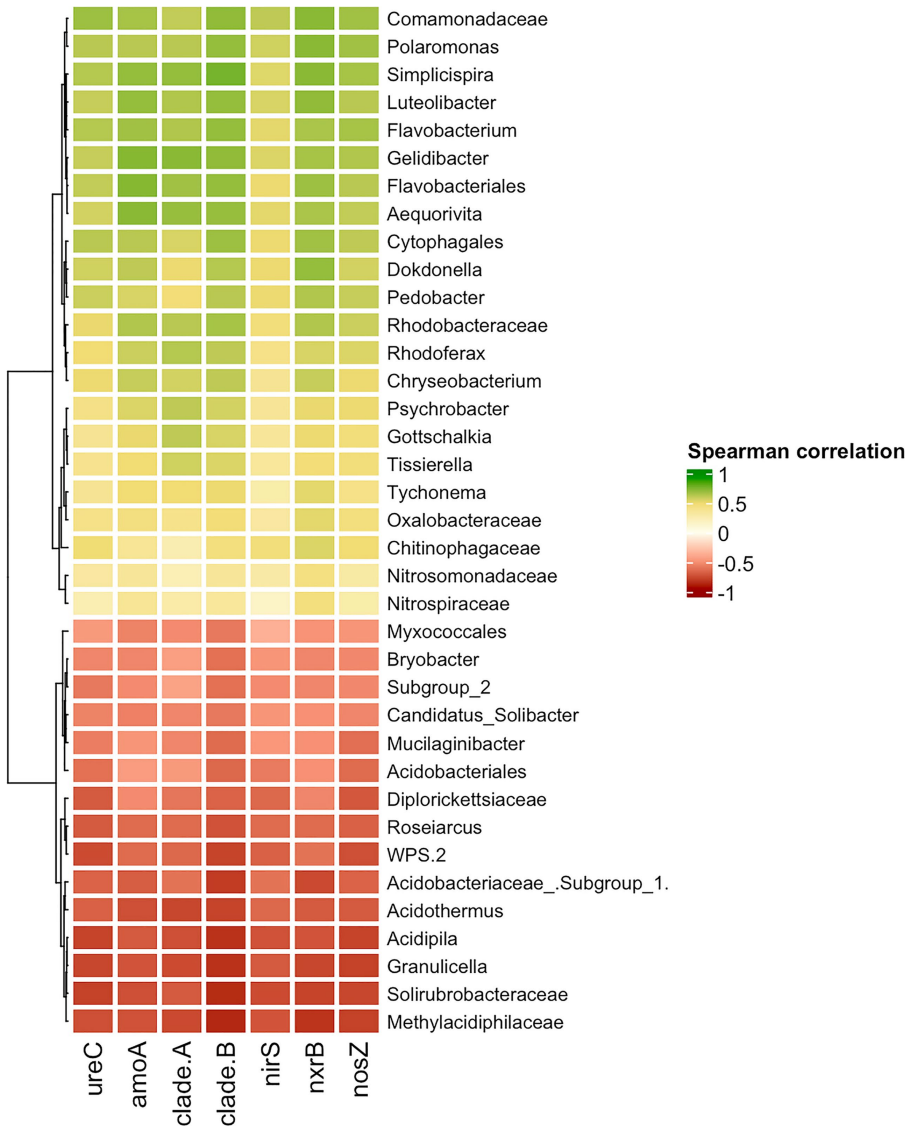

FIGURE 8
Spearman correlation between nitrogen-cycle genes and bacterial taxa. Only moderate (|0.5|) and strong (|0.5–1.0|) correlation is shown.

and the abundance of nitrogen-cycle gene copy numbers in peat samples collected from sites differently affected by penguin presence.

4.1 Chemical composition of the peat

The impact of *P. papua* colonization on moss banks induces alterations in the chemical composition of the peat substrate. Notably, penguin colonization leads to an elevation in peat pH and an increase in the concentration of soluble nitrogen and phosphorous compounds. Our results for Unaffected peat, except for a few points, are consistent with the previous estimates by Parnikoza et al. (2017), in which histozols formed by *Polytrichum strictum* showed low phosphorus content, indicating a low influx of zoogenic materials. Unaffected peat from moss bank 5 had an elevated content of nitrogen compounds. It is possible that, due to the moss bank's location on a steep slope, ornithogenic organics may have leached from the penguin colonies situated above. Alternatively, the volatile ammonium from the penguin rookery could be transported (Lindeboom, 1984). The latter scenario might even promote vegetation growth (Crittenden et al., 2015; Riddick et al., 2016). Thus, the moss bank could be enriched with biogenic compounds without displaying signs of negative eutrophication impact. Similarly, the increased phosphorus content was detected in the Unaffected peat of the moss bank 1. We might speculate that ornithogenic impact in this location occurred earlier, preceding the study, as indicated by the accumulation of biogenic compounds without desolating the moss carpet. Unlike nitrogen compounds, phosphorus does not evaporate from the environment, allowing us to observe its accumulation.

Penguin guano, comprising 15–30% nitrogen and 10% phosphorus (Lorrain et al., 2017), is a key contributor to the changes in the chemical composition of peat. Excess nitrogen and phosphorus originate from the adjacent water regions of the Southern Ocean, where gentoo penguins primarily forage for krill (*Euphausia superba*).

As this specific source of nitrogen and phosphorus becomes predominant in the altered ecosystem of moss banks, it can be speculated that a transformation is occurring in the primary terrestrial polar ecosystem. In this original ecosystem, the atmosphere and bedrock can be assumed as the main nutrient sources. However, the ongoing transformation leads to a new ecosystem that relies on the sea as its primary nutritional source.

The rise in pH from acidic to alkaline is linked to the availability of ammonia in the feces and concurrent biochemical processes within the substrate. The total nitrogen in penguin feces is primarily composed of uric acid, followed by proteins, ammonium, and nitrates (Lindeboom, 1984). Uric acid and proteins undergo degradation into ammonia nitrogen, contributing to substrate alkalization and subsequent ammonia volatilization from the rookery (Lindeboom, 1984). The role of uric acid conversion to ammonium was demonstrated by an increase in the pH of the ornithogenic soil under the penguin colony from 6.7–6.9 in January to 7.1–9.0 in March (Grzesiak et al., 2020).

The elevated pH facilitates ammonia volatilization, thereby explaining the decrease in the concentration of soluble nitrogen compounds in Desolated moss banks compared to Impacted ones. Unlike nitrogen, phosphorus does not evaporate from the rookery, elucidating the gradual accumulation of phosphate (PO_4^-) and inorganic phosphorus (PIN) in Impacted and Desolated peat environments.

4.2 The taxonomic composition of the moss banks differently affected by the penguins' colonization

The initial microbiota of the peat was primarily dominated by *Acidobacteria*, followed by *Actinobacteria* and *Alphaproteobacteria*. In contrast, microbial communities associated with other bryophytes exhibited distinct compositions. For instance, in peat formed by *Sphagnum* mosses, *Proteobacteria* (56.4%) and *Acidobacteria* (8.2%) were dominant (Kolton et al., 2022). On the Keller Peninsula (King George Island), the moss carpet formed by *Saniona* sp. showed *Actinobacteria* (25%), *Proteobacteria* (20%), and *Bacteroidetes* (18%) as the most abundant phyla (Câmara et al., 2021). Unfortunately, we found no available data on the microbial composition of moss banks formed by *P. strictum*. Hence, our findings likely represent the first report on the microbial communities' composition in Unaffected peat formed by Tall moss turf subformation.

The chemical composition of peat and penguin feces is quite contrasting, leading to the elimination and replacement of the indigenous peat microbiota. The increase in pH was a contributing factor to the elimination of initial peat microorganisms, which typically thrive in acidic conditions. In particular, initial microbial taxa found in Unaffected peat, such as *Acidobacteria* members, disappear with increasing intensity of penguin influence. The taxonomic composition of soil microbial communities from Fildes Peninsula, King George Island, with different intensities of penguins' influence, was estimated by Guo et al. (2018). Still, no such variation in the composition of microbial communities was detected. The soil had a higher pH (5.5–6.25) and a different microbial composition of the initial microbial communities, so penguin feces input was less environmentally disruptive.

Colonization of the moss bank by penguins results in the introduction of new microorganisms into the peat. Notably, there was a pronounced increase in the abundance of *Betaproteobacteria* and *Bacteroidota*. Interestingly, the composition of ornithogenic soil on Fildes Island differed from the impacted peat, with *Proteobacteria* (33.4%), *Actinobacteria* (19.9%), and *Gemmatimonadetes* (15.2%) dominating the microbial community (Guo et al., 2018).

The group of bacteria that emerged in the Impacted and Desolated peat and their ability to proliferate and function in the field environment of Antarctica is of particular interest. This group includes taxa associated with birds' gut. *Gottschalkia* is usually found in the intestines and guano of birds. For instance, a high abundance of the *Gottschalkiaceae* family was found in *P. adeliae* guano samples (Grzesiak et al., 2020). *Tissierella* and *Flavobacterium*, identified in the Impacted peat of Galindez Island and Tuxen, were previously detected in the guano of *P. adeliae* (Grzesiak et al., 2020). Members of the *Psychrobacter* genus occur in animal microbiomes, including the respiratory tract of marine mammals (Apprill et al., 2017), the skin of marine mammals (Apprill et al., 2014), the throat and gut of birds (Kämpfer et al., 2015, 2020). *Chryseobacterium* is frequently linked to the intestines of animals, including penguins; proteolytic *Chryseobacterium* sp. was identified in the guano of *P. adeliae* (Grzesiak et al., 2020). *Fusobacteriaceae*, *Moraxellaceae*, *Leuconostocaceae*, *Lachnospiraceae*, *Streptococcaceae*, *Campylobacteriaceae*, *Porphyromonadaceae*, and *Helicobacteriaceae* (Dewar et al., 2013), as well as *Carnobacteriaceae*, *Eurysipelotrichaceae*, *Moraxellaceae*, and *Pseudomonadaceae*, were identified within the penguins' intestinal microbiota. However, they were not detected in the peat in our study.

The environmental conditions in Antarctica markedly differ from those within the penguins' intestines, posing a challenge for the assimilation of such microbiota. The presence of 16S rRNA sequences from these taxa in the metagenome does not necessarily indicate the activity of these microorganisms, as genetic markers can also originate from deceased or dormant organisms. The persistence of genetic markers may be attributed to the continual influx of guano microbiota or the potential adaptation of certain representatives to their new environmental conditions.

In this context, examining moss bank 1 becomes valuable—birds initially colonized it but have since abandoned it, eliminating the fresh influx of guano. Moss bank 1 is an illustrative example of system adaptation and recovery following a significant disturbance. Notably, *Gottschalkia*, *Tissierella*, and *Psychrobacter* were absent in Desolated moss bank 1 despite their presence in other Desolated mosses. In contrast, *Chryseobacterium* persisted in the environment. *Simplicispira*, *Polarobacter*, and *Tychomena*, which were abundant in other Desolated moss bank samples, also exhibited persistence. Notably, some of these, such as *Tychomena*, are not associated with bird gut microbiota; nevertheless, they all benefit from environmental changes.

Previous studies have focused on comparing the microbial composition of abandoned penguin sites and actively colonized soils (Aislabie et al., 2009; Kim et al., 2012). However, our results differ both from these studies. These variations may be attributed to the distinct conditions of the studied sites, including locations in the Ross Sea region, the North and central part of the WAP. In particular, according to Aislabie et al. (2009), formerly penguin-colonized sites at Cape Hallett, around the Ross Sea region of Antarctica, contained

Actinobacteria and *Xanthomonas*. In actively penguin-colonized soils, the dominant taxa included *Firmicutes* and *Psychrobacter. Ferruginibacter*, *Sulfuritalea*, *Polaromonas*, and *Rhodanobacter* dominated the soil of the abandoned penguin sites on the southern coast of the Barton Peninsula of King George Island (Kim et al., 2012). *Thermohalobacter*, *Tissierella*, *Carnobacteriaceae*, *Desulfonispora, Psychrobacter* and *Pseudomonas* were found in high abundance dominant in actively penguin-colonized soils (Kim et al., 2012).

Santamans et al. (2017) and Grzesiak et al. (2020) have addressed intestinal microbiota survival challenges in Antarctic field conditions. The resilience of such microbiota in the harsh conditions of Antarctic terrestrial biotopes may be attributed to the formation of anaerobic microniches, a result of the accumulation of excessive organic matter, trampling, and the consequent high biological oxygen consumption in the environment (Santamans et al., 2017). Grzesiak et al. (2020) discussed modifying environmental conditions over time and adapting birds' intestinal microbiota to these conditions. The guano microbiome of Adélie penguins, sampled at their nesting sites during the summer season, predominantly consisted of dead or inactive bacteria (Grzesiak et al., 2020). Conversely, guano sampled at the end of the summer season contained ten times more bacterial cells and psychrophilic enzymes. Most bacteria in the latter sample exhibited intact membranes, suggesting their adaptation to environmental conditions. The increased bacterial count in fermented guano indicated proliferation, adaptation, and the formation of new niches.

4.3 Effect of the penguins' colonization on the functioning of peat microbial communities

A peat's chemical and microbial composition shift inevitably impacts microbial communities' functionality. We quantified the copy number of several genes involved in various stages of the nitrogen cycle. These genes collectively regulate urea conversion, the primary component of penguin feces, into ammonia, nitrite oxide, and nitrate oxide. Across all studied genes related to the nitrogen cycle, there was an increase in copy number in Impacted peat, reaching its peak in Desolated peat. The uneven distribution of these genes in the peat, influenced differentially by ornithogenic impact, underscored alterations in the functional activity of microbial communities. An increase in the copy number of nitrogen cycle genes is logically related to the high input of nitrogen compounds into the environment and the enrichment of the microbiome with taxa containing such genes. On the other hand, according to Björck et al. (1991), nitrogen loss through denitrification or leaching from moss banks was insufficient. It's noteworthy that in Desolated moss, the copy number of nitrogen cycle genes was the highest, despite the concentration of soluble nitrogen compounds being lower compared to Impacted moss. This fact might suggest elevated activity among nitrogen cycling bacteria, indicating their adaptation to the continuous impact of nitrogen compounds and change in the environmental conditions.

Polaromonas, *Simplisiprira*, *Dokdonella*, *Pedobacter*, *Psychrobacter*, *Rhodoferax,* etc., revealed a strong significant correlation to *ureC* and *nosZ* gene copy number, indicating their potential involvement in urea decomposition and denitrification processes. A moderate and significant correlation was observed between *Nitrosomonadaceae* abundance and *amoA* copy number, and as well as between *Nitrospiraceae* and *nrxB* gene copy number. While an increase in *amoA* and *nrxB* gene copy numbers due to penguin colonization pressure could be associated with *Nitrosomonadaceae* and *Nitrospiraceae* proliferation, no significant elevation of these bacteria ratio was observed in the Impacted and Desolated peat samples.

According to the literature, certain taxa detected in penguin-affected environments can break down uric acid, a major component of guano, and contribute to denitrification. Specifically, members of *Gottschalkia* have demonstrated the capability to metabolize uric acid as their sole source of carbon and energy (Poehlein et al., 2017). Additionally, some *Psychrobacter* members possess lipolytic properties and the capacity to degrade uric acid (Grzesiak et al., 2020). In a study focusing on microbial communities and genes involved in N_2O emissions in Antarctic soils impacted by marine animals, Ramírez-Fernández et al. (2021) found that the only metagenome-assembled genome (MAG) related to *Nitrosospira lacus* included an ammonia monooxygenase (*amoA*) gene and comprised the complete nitrification pathway. *Rhodoferax* is known to thrive using Fe(III) and NO_3^{2-} as electron acceptors, with organic acids serving as electron donors (Finneran et al., 2003). In guano-enriched peat microbial communities, these bacteria may contribute to nitrate reduction. The genus *Simplicispira* enriched in the Impacted and Desolated peat encompasses aerobic and facultative anaerobic bacteria and has denitrification capabilities (Siddiqi et al., 2020), According to Ramírez-Fernández et al. (2021), only three MAGs found among 100 MAGs obtained from animal-impacted soils included all necessary genes for the complete denitrification pathway (i.e., reductions from NO_3^- to N_2): *Pandoraea thiooxydans*, *Pseudomonas stutzeri* and *Oblitimonas alkaliphila*. On the contrary, most MAGs belonging to diverse bacterial phyla carried an incomplete denitrification pathway (Ramírez-Fernández et al., 2021). That shows that denitrification is a highly abundant process carried out by the diverse microbial taxa in Antarctic animal impacted soils.

5 Conclusion

One of the consequences of climate change indirect effects in the maritime Antarctic region is the alteration of terrestrial vegetation, marked by the elimination of moss banks and the associated acidophilic microbial community. This change is attributed to the expansion of nesting territories by gentoo penguins. The proliferation of microorganisms introduced with penguin guano is a contentious issue requiring further research. Nevertheless, it is evident that conditions conducive to the functioning of a new microbial community, shaped by the chemical and microbial composition of penguin guano, have been established. The functional capacity of this microbial community differed from the initial peat community, as demonstrated in this study with the example of the nitrogen cycle. Likely, functional activities related to carbon will also vary, potentially leading to more intensive

mineralization of organic compounds previously conserved in the form of peat. Addressing this question would require future attention through functional assays.

Data availability statement

The dataset of the16S rRNA amplicon metagenomic sequences generated for this study can be found in National Center for Biotechnology Information (NCBI) database (https://www.ncbi.nlm.nih.gov/) under accession number PRJNA1057234.

Ethics statement

Written informed consent was obtained from the individual(s) for the publication of any potentially identifiable images or data included in this article.

Author contributions

YP-K: Formal analysis, Investigation, Methodology, Visualization, Writing – original draft, Writing – review & editing. IP: Conceptualization, Writing – review & editing. AY: Investigation, Writing – review & editing. OS: Investigation, Writing – review & editing. MP: Visualization, Writing – review & editing. MD: Investigation, Writing – review & editing. OY: Investigation, Writing – review & editing. ED: Project administration, Resources, Writing – review & editing.

Funding

The author(s) declare that financial support was received for the research, authorship, and/or publication of this article. This study was funded by the National Antarctic Scientific Center of Ukraine (State Special-Purpose Research Program in Antarctica for 2011–2025).

Acknowledgments

The authors are thankful to Ukrainian Armed Forces, who are making the research and science in Ukraine possible every day, protecting us from the Russian invasion.

Conflict of interest

The authors declare that the research was conducted in the absence of any commercial or financial relationships that could be construed as a potential conflict of interest.

Publisher's note

All claims expressed in this article are solely those of the authors and do not necessarily represent those of their affiliated organizations, or those of the publisher, the editors and the reviewers. Any product that may be evaluated in this article, or claim that may be made by its manufacturer, is not guaranteed or endorsed by the publisher.

Supplementary material

The Supplementary material for this article can be found online at: https://www.frontiersin.org/articles/10.3389/fmicb.2024.1362975/full#supplementary-material

References

Aislabie, J., Jordan, S., Ayton, J., Klassen, J. L., Barker, G. M., and Turner, S. (2009). Bacterial diversity associated with ornithogenic soil of the Ross Sea region, Antarctica. *Can. J. Microbiol.* 55, 21–36. doi: 10.1139/W08-126

Angnes, G., Nicoloso, R. S., da Silva, M. L. B., de Oliveira, P. A. V., Higarashi, M. M., Mezzari, M. P., et al. (2013). Correlating denitrifying catabolic genes with N2O and N2 emissions from swine slurry composting. *Bioresour. Technol.* 140, 368–375. doi: 10.1016/j.biortech.2013.04.112

Apprill, A., Miller, C. A., Moore, M. J., Durban, J. W., Fearnbach, H., and Barrett-Lennard, L. G. (2017). Extensive Core microbiome in drone-captured whale blow supports a framework for health monitoring. *mSystems* 2:2. doi: 10.1128/mSystems.00119-17

Apprill, A., Robbins, J., Eren, A. M., Pack, A. A., Reveillaud, J., Mattila, D., et al. (2014). Humpback whale populations share a Core skin bacterial community: towards a health index for marine mammals? *PLoS One* 9:e90785. doi: 10.1371/journal.pone.0090785

Atkinson, A., Siegel, V., Pakhomov, E., and Rothery, P. (2004). Long-term decline in krill stock and increase in salps within the Southern Ocean. *Nature* 432, 100–103. doi: 10.1038/nature02996

Benjamini, Y., and Hochberg, Y. (1995). Controlling the false discovery rate: A practical and powerful approach to multiple testing. *J. R. Stat. Soc. Ser. B.* doi: 10.1111/j.2517-6161.1995.tb02031.x

Björck, S., Malmer, N., Hjort, C., Sandgren, P., Ingólfsson, Ó., Wallen, B., et al. (1991). Stratigraphic and paleoclimatic studies of a 5500-year-old Moss Bank on Elephant Island, Antarctica. *Arct. Alp. Res.* 23:361. doi: 10.2307/1551679

Bromwich, D. H., Nicolas, J. P., Monaghan, A. J., Lazzara, M. A., Keller, L. M., Weidner, G. A., et al. (2013). Central West Antarctica among the most rapidly warming regions on earth. *Nat. Geosci.* 6, 139–145. doi: 10.1038/ngeo1671

Câmara, P. E. A. S., Convey, P., Rangel, S. B., Konrath, M., Barreto, C. C., Pinto, O. H. B., et al. (2021). The largest moss carpet transplant in Antarctica and its bryosphere cryptic biodiversity. *Extremophiles* 25, 369–384. doi: 10.1007/s00792-021-01235-y

Caporaso, J. G., Kuczynski, J., Stombaugh, J., Bittinger, K., Bushman, F. D., Costello, E. K., et al. (2010). QIIME allows analysis of high-throughput community sequencing data. *Nat. Methods* 7, 335–336. doi: 10.1038/nmeth.f.303

Crittenden, P. D., Scrimgeour, C. M., Minnullina, G., Sutton, M. A., Tang, Y. S., and Theobald, M. R. (2015). Lichen response to ammonia deposition defines the footprint of a penguin rookery. *Biogeochemistry* 122, 295–311. doi: 10.1007/s10533-014-0042-7

Dewar, M. L., Arnould, J. P. Y., Dann, P., Trathan, P., Groscolas, R., and Smith, S. (2013). Interspecific variations in the gastrointestinal microbiota in penguins. *Microbiology* 2, 195–204. doi: 10.1002/mbo3.66

Edgar, R. C. (2013). UPARSE: highly accurate OTU sequences from microbial amplicon reads. *Nat. Methods* 10, 996–998. doi: 10.1038/nmeth.2604

Edgar, R. C., Haas, B. J., Clemente, J. C., Quince, C., and Knight, R. (2011). UCHIME improves sensitivity and speed of chimera detection. *Bioinformatics* 27, 2194–2200. doi: 10.1093/bioinformatics/btr381

Emmerson, L., and Southwell, C. (2022). Environment-triggered demographic changes cascade and compound to propel a dramatic decline of an Antarctic seabird metapopulation. *Glob. Chang. Biol.* 28, 7234–7249. doi: 10.1111/gcb.16437

Fenton, J. H. C. (1980). The rate of peat accumulation in Antarctic Moss banks. *J. Ecol.* 68, 211–228. doi: 10.2307/2259252

Finneran, K. T., Johnsen, C. V., and Lovley, D. R. (2003). *Rhodoferax ferrireducens* sp. nov., a psychrotolerant, facultatively anaerobic bacterium that oxidizes acetate with the reduction of Fe(III). *Int. J. Syst. Evol. Microbiol.* 53, 669–673. doi: 10.1099/ijs.0.02298-0

Grzesiak, J., Kaczyńska, A., Gawor, J., Żuchniewicz, K., Aleksandrzak-Piekarczyk, T., Gromadka, R., et al. (2020). A smelly business: microbiology of Adélie penguin guano (point Thomas rookery, Antarctica). *Sci. Total Environ.* 714:136714. doi: 10.1016/j.scitotenv.2020.136714

Gu, Z., Eils, R., and Schlesner, M. (2016). Complex heatmaps reveal patterns and correlations in multidimensional genomic data. *Bioinformatics* 32, 2847–2849. doi: 10.1093/bioinformatics/btw313

Guo, Y., Wang, N., Li, G., Rosas, G., Zang, J., Ma, Y., et al. (2018). Direct and indirect effects of penguin Feces on microbiomes in Antarctic Ornithogenic soils. *Front. Microbiol.* 9:552. doi: 10.3389/fmicb.2018.00552

Hellberg, M., Aronson, R., Smith, K., Duhon, M., Ayong, S., Lovrich, G., et al. (2019). Population expansion of an Antarctic king crab? *Front. Biogeogr.* 11:3165. doi: 10.21425/F5FBG43165

Jiang, R., Wang, J.-G., Zhu, T., Zou, B., Wang, D.-Q., Rhee, S.-K., et al. (2020). Use of newly designed primers for quantification of complete ammonia-oxidizing (Comammox) bacterial clades and strict nitrite oxidizers in the genus Nitrospira. *Appl. Environ. Microbiol.* 86:e01775. doi: 10.1128/AEM.01775-20

Kämpfer, P., Glaeser, S. P., Irgang, R., Fernández-Negrete, G., Poblete-Morales, M., Fuentes-Messina, D., et al. (2020). Psychrobacter pygoscelis sp. nov. isolated from the penguin *Pygoscelis papua*. *Int. J. Syst. Evol. Microbiol.* 70, 211–219. doi: 10.1099/ijsem.0.003739

Kämpfer, P., Jerzak, L., Wilharm, G., Golke, J., Busse, H.-J., and Glaeser, S. P. (2015). Psychrobacter ciconiae sp. nov., isolated from white storks (*Ciconia ciconia*). *Int. J. Syst. Evol. Microbiol.* 65, 772–777. doi: 10.1099/ijs.0.000013

Khangembam, C. D., Sharma, J. G., and Chakrabarti, R. (2017). Diversity and abundance of ammonia-oxidizing bacteria and archaea in a freshwater recirculating aquaculture system. *Hayati J. Biosci.* 24, 215–220. doi: 10.1016/j.hjb.2017.11.003

Kim, O.-S., Chae, N., Lim, H. S., Cho, A., Kim, J. H., Hong, S. G., et al. (2012). Bacterial diversity in ornithogenic soils compared to mineral soils on King George Island, Antarctica. *J. Microbiol.* 50, 1081–1085. doi: 10.1007/s12275-012-2655-7

Kolton, M., Weston, D. J., Mayali, X., Weber, P. K., McFarlane, K. J., Pett-Ridge, J., et al. (2022). Defining the Sphagnum Core microbiome across the north American continent reveals a central role for diazotrophic methanotrophs in the nitrogen and carbon cycles of boreal peatland ecosystems. *MBio* 13, e03714–e03721. doi: 10.1128/mbio.03714-21

Korczak-Abshire, M., Hinke, J. T., Milinevsky, G., Juáres, M. A., and Watters, G. M. (2021). Coastal regions of the northern Antarctic peninsula are key for gentoo populations. *Biol. Lett.* 17:20200708. doi: 10.1098/rsbl.2020.0708

LaRue, M. A., Ainley, D. G., Swanson, M., Dugger, K. M., Lyver, P. O., Barton, K., et al. (2013). Climate change winners: receding ice fields facilitate colony expansion and altered dynamics in an Adélie penguin metapopulation. *PLoS One* 8:e60568. doi: 10.1371/journal.pone.0060568

Lindeboom, H. J. (1984). The nitrogen pathway in a penguin rookery. *Ecology* 65, 269–277. doi: 10.2307/1939479

Lorrain, A., Houlbrèque, F., Benzoni, F., Barjon, L., Tremblay-Boyer, L., Menkes, C., et al. (2017). Seabirds supply nitrogen to reef-building corals on remote Pacific islets. *Sci. Rep.* 7:3721. doi: 10.1038/s41598-017-03781-y

Lynch, H. J., Naveen, R., Trathan, P. N., and Fagan, W. F. (2012). Spatially integrated assessment reveals widespread changes in penguin populations on the Antarctic peninsula. *Ecology* 93, 1367–1377. doi: 10.1890/11-1588.1

Magoč, T., and Salzberg, S. L. (2011). FLASH: fast length adjustment of short reads to improve genome assemblies. *Bioinformatics* 27, 2957–2963. doi: 10.1093/bioinformatics/btr507

Oksanen, J., Blanchet, F. G., Kindt, R., Legendre, P., Minchin, P. R., O'Hara, R. B., et al. (2016). Vegan: community ecology package. Available at:https://cran.r-project.org/package=vegan

Oshiki, M., Araki, M., Hirakata, Y., Hatamoto, M., Yamaguchi, T., and Araki, N. (2018). Ureolytic prokaryotes in soil: community abundance and diversity. *Microbes Environ.* 33, 230–233. doi: 10.1264/jsme2.ME17188

Parnikoza, I., Abakumov, E., Korsun, S., Klymenko, I., Netsyk, M., Kudinova, A., et al. (2017). Soils of the Argentine islands, Antarctica: diversity and characteristics. *Polarforschung* 86, 83–96. doi: 10.2312/polarforschung.86.2.83

Parnikoza, I., Berezkina, A., Moiseyenko, Y., Malanchuk, V., and Kunakh, V. (2018). Complex survey of the Argentine islands and Galindez Island (Maritime Antarctic) as a research area for studying the dynamics of terrestrial vegetation. *Ukrainian Antarct. J.*, 73–101. doi: 10.33275/1727-7485.1(17).2018.34

Poehlein, A., Yutin, N., Daniel, R., and Galperin, M. Y. (2017). Proposal for the reclassification of obligately purine-fermenting bacteria Clostridium acidurici (Barker 1938) and Clostridium purinilyticum (Dürre et al. 1981) as Gottschalkia acidurici gen. nov. comb. nov. and Gottschalkiapurinilytica comb. nov. and of Eubacterium angustum (Beuscher and Andreesen 1985) as Andreesenia angusta gen. nov. comb. nov. in the family Gottschalkiaceae fam. nov. *Int. J. Syst. Evol. Microbiol.* 67, 2711–2719. doi: 10.1099/ijsem.0.002008

Quast, C., Pruesse, E., Yilmaz, P., Gerken, J., Schweer, T., Yarza, P., et al. (2013). The SILVA ribosomal RNA gene database project: improved data processing and web-based tools. *Nucleic Acids Res.* 41, D590–D596. doi: 10.1093/nar/gks1219

Ramírez-Fernández, L., Orellana, L. H., Johnston, E. R., Konstantinidis, K. T., and Orlando, J. (2021). Diversity of microbial communities and genes involved in nitrous oxide emissions in Antarctic soils impacted by marine animals as revealed by metagenomics and 100 metagenome-assembled genomes. *Sci. Total Environ.* 788:147693. doi: 10.1016/j.scitotenv.2021.147693

Rice, E. and Bridgewater, L.. (2012). Standard methods for the examination of water and wastewater. Washington, D.C.: American Public Health Association. 1496.

Riddick, S. N., Blackall, T. D., Dragosits, U., Daunt, F., Newell, M., Braban, C. F., et al. (2016). Measurement of ammonia emissions from temperate and sub-polar seabird colonies. *Atmos. Environ.* 134, 40–50. doi: 10.1016/j.atmosenv.2016.03.016

Robinson, M. D., McCarthy, D. J., and Smyth, G. K. (2010). edgeR: a Bioconductor package for differential expression analysis of digital gene expression data. *Bioinformatics* 26, 139–140. doi: 10.1093/bioinformatics/btp616

Santamans, A. C., Boluda, R., Picazo, A., Gil, C., Ramos-Miras, J., Tejedo, P., et al. (2017). Soil features in rookeries of Antarctic penguins reveal sea to land biotransport of chemical pollutants. *PLoS One* 12:e0181901. doi: 10.1371/journal.pone.0181901

Siddiqi, M. Z., Sok, W., Choi, G., Kim, S. Y., Wee, J.-H., and Im, W. T. (2020). Simplicispira hankyongi sp. nov., a novel denitrifying bacterium isolated from sludge. *Antonie Van Leeuwenhoek* 113, 331–338. doi: 10.1007/s10482-019-01341-0

Smith, R. C., Ainley, D., Baker, K., Domack, E., Emslie, S., Fraser, B., et al. (1999). Marine ecosystem sensitivity to climate change: historical observations and paleoecological records reveal ecological transitions in the Antarctic peninsula region. *Bioscience* 49, 393–404. doi: 10.2307/1313632

Teixeira, L. C. R. S., Peixoto, R. S., Cury, J. C., Sul, W. J., Pellizari, V. H., Tiedje, J., et al. (2010). Bacterial diversity in rhizosphere soil from Antarctic vascular plants of Admiralty Bay, maritime Antarctica. *ISME J.* 4, 989–1001. doi: 10.1038/ismej.2010.35

Vaughan, D. G., Marshall, G. J., Connolley, W. M., Parkinson, C., Mulvaney, R., Hodgson, D. A., et al. (2003). Recent rapid regional climate warming on the Antarctic peninsula. *Clim. Chang.* 60, 243–274. doi: 10.1023/A:1026021217991

Wang, N. F., Zhang, T., Zhang, F., Wang, E. T., He, J. F., Ding, H., et al. (2015). Diversity and structure of soil bacterial communities in the Fildes region (maritime Antarctica) as revealed by 454 pyrosequencing. *Front. Microbiol.* 6:1188. doi: 10.3389/fmicb.2015.01188

Wickham, H. (2016). *Ggplot2: Elegant graphics for data analysis. 2nd Edn*. New York: Springer International Publishing.

Wierzgoń, M., Ivanets, V., Prekrasna-Kviatkovska, Y., Plášek, V., and Parnikoza, I. (2023). Moss bank composition on Galindez Island (Argentine islands, maritime Antarctic). *Polar Biol.* 46, 1235–1249. doi: 10.1007/s00300-023-03197-7

Wynn-Williams, D. D. (1996). Antarctic microbial diversity: the basis of polar ecosystem processes. *Biodivers. Conserv.* 5, 1271–1293. doi: 10.1007/BF00051979

Yergeau, E., Bokhorst, S., Kang, S., Zhou, J., Greer, C. W., Aerts, R., et al. (2012). Shifts in soil microorganisms in response to warming are consistent across a range of Antarctic environments. *ISME J.* 6, 692–702. doi: 10.1038/ismej.2011.124

Yergeau, E., and Kowalchuk, G. A. (2008). Responses of Antarctic soil microbial communities and associated functions to temperature and freeze–thaw cycle frequency. *Environ. Microbiol.* 10, 2223–2235. doi: 10.1111/j.1462-2920.2008.01644.x

Younger, J., Emmerson, L., Southwell, C., Lelliott, P., and Miller, K. (2015). Proliferation of East Antarctic Adélie penguins in response to historical deglaciation. *BMC Evol. Biol.* 15:236. doi: 10.1186/s12862-015-0502-2

Yu, Z., Beilman, D. W., and Loisel, J. (2016). Transformations of landscape and peat-forming ecosystems in response to late Holocene climate change in the western Antarctic peninsula. *Geophys. Res. Lett.* 43, 7186–7195. doi: 10.1002/2016GL069380

Zhu, R., Liu, Y., Ma, E., Sun, J., Xu, H., and Sun, L. (2009). Nutrient compositions and potential greenhouse gas production in penguin guano, ornithogenic soils and seal colony soils in coastal Antarctica. *Antarct. Sci.* 21, 427–438. doi: 10.1017/S0954102009990204

frontiers | Frontiers in Microbiology

TYPE Original Research
PUBLISHED 01 May 2024
DOI 10.3389/fmicb.2024.1362678

OPEN ACCESS

EDITED BY
Masahiro Ito,
Toyo University, Japan

REVIEWED BY
Maria Papale,
National Research Council (CNR), Italy
Lucas Ruberto,
CONICET Institute of Nanobiotechnology (NANOBIOTEC), Argentina
Roberta Gorra,
University of Turin, Italy

*CORRESPONDENCE
Shiv Mohan Singh
✉ drshivmohansingh@gmail.com

RECEIVED 28 December 2023
ACCEPTED 01 April 2024
PUBLISHED 01 May 2024

CITATION
Singh P, Singh SM, Segawa T and Singh PK (2024) Bacterial diversity and biopotentials of Hamtah glacier cryoconites, Himalaya. *Front. Microbiol.* 15:1362678. doi: 10.3389/fmicb.2024.1362678

Bacterial diversity and biopotentials of Hamtah glacier cryoconites, Himalaya

Purnima Singh[1], Shiv Mohan Singh[2]*, Takahiro Segawa[3] and Prashant Kumar Singh[4]

[1]Indian Institute of Technology, Banaras Hindu University (IIT-BHU), Varanasi, India, [2]Department of Botany, Banaras Hindu University, Varanasi, India, [3]National Institute of Polar Research, Tachikawa-shi, Tokyo, Japan, [4]Department of Biotechnology, Pachhunga University College, Mizoram University (A Central University), Aizawl, India

Cryoconite is a granular structure present on the glaciers and ice sheets found in polar regions including the Himalayas. It is composed of organic and inorganic matter which absorb solar radiations and reduce ice surface albedo, therefore impacting the melting and retreat of glaciers. Though climate warming has a serious impact on Himalayan glaciers, the biodiversity of sub-glacier ecosystems is poorly understood. Moreover, cryoconite holes are unique habitats for psychrophile biodiversity hotspots in the NW Himalayas, but unfortunately, studies on the microbial diversity of such habitats remain elusive. Therefore, the current study was designed to explore the bacterial diversity of the Hamtah Glacier Himalaya using both culturable and non-culturable approaches. The culturable bacterial count ranged from 2.0×10^3 to 8.8×10^5 colony-forming units (CFUs)/g at the different locations of the glacier. A total of 88 bacterial isolates were isolated using the culturable approach. Based on the 16S ribosomal RNA gene (16S rRNA), the identified species belong to seven genera, namely, *Cryobacterium*, *Duganella*, *Janthinobacterium*, *Pseudomonas*, *Peribacillus, Psychrobacter,* and *Sphingomonas*. In the non-culturable approach, high-throughput sequencing of 16S rRNA genes (using MiSeq) showed unique bacterial community profiles and represented 440 genera belonging to 20 phyla, namely, Proteobacteria, Actinobacteria, Firmicutes, Bacteroidetes, Chloroflexi, Acidobacteria, Planctomycetes, Cyanobacteria, Verrucomicrobia, Spirochaetes, Elusimicrobia, Armatimonadetes, Gemmatimonadetes, Deinococcus-Thermus, Nitrospirae, Chlamydiae, Chlorobi, Deferribacteres, Fusobacteria, Lentisphaerae, and others. High relative abundances of Proteobacteria, Actinobacteria, Firmicutes, and Bacteroidetes were observed in the samples. Phototrophic (Cyanobacteria and Chloroflexi) and nitrifier (Nitrospirae) in bacterial populations indicated sustenance of the micro-ecosystem in the oligotrophic glacier environment. The isolates varied in their phenotypic characteristics, enzyme activities, and antibiotic sensitivity. Furthermore, the fatty acid profiles of bacterial isolates indicate the predominance of branched fatty acids. Iso-, anteiso-, unsaturated and saturated fatty acids together constituted a major proportion of the total fatty acid composition. High cold-adapted enzyme activities such as lipase and cellulase expressed by *Cryobacterium arcticum* (KY783365) and protease and cellulase activities by *Pseudomonas sp.* strains (KY783373, KY783377-79, KY783382) provide evidence of the possible applications of these organisms. Additionally, antibiotic tests indicated that most isolates were sensitive to antibiotics. In conclusion, the present study contributed for the first time to bacterial diversity and biopotentials of cryoconites of Hamtah Glacier, Himalayas. Furthermore, the cold-adapted enzymes and polyunsaturated fatty acids (PUFAs) may provide an opportunity for biotechnology in the Himalayas. Inductively coupled plasma mass spectrometry

(ICPMS) analyses showed the presence of several elements in cryoconites, providing a clue for the accelerating melting and retreating of the Hamtah glacier.

KEYWORDS

cryoconites, glacier, Himalaya, bacterial diversity, culturable approach, metagenomics, enzymes, antibiotics

Introduction

Ice masses store about 70% of freshwater, which sustains billions of people on planet Earth (Cook et al., 2016). Glaciers and ice sheets are the largest reservoirs of freshwater ecosystems, and climate change episodes are rapidly forcing the melting of these glaciers and ice sheets globally (Edwards et al., 2013). Understanding the biogeochemical processes at these places is crucial for predicting future changes, their effects on surrounding habitats, and potential losses of functional biodiversity. Cryoconites are dark-colored quasi-spherical granules found on glaciers and ice sheets across the globes, including the Arctic, Antarctic, and Himalayas (Kohshima et al., 1993; Hodson et al., 2008; Singh et al., 2017). The glacier's mass balance is greatly affected by the quantity and quality of cryoconite in a glacier (Nagatsuka et al., 2014). Cryoconites with a large area on the glacier surface primarily comprise organic and inorganic matter (Gerdel and Drouet, 1960; Hodson et al., 2008; Takeuchi et al., 2010; Singh et al., 2017).

Cryoconites are present on the surface or in quasi-cylindrical mini-depressions where the unique biome inhabits cryoconite holes (Wharton et al., 1985). Mineral dust inputs on glaciers depend on eolian dust deposition and transportation processes near the glaciers (Bøggild et al., 2010; Singh et al., 2013), which serve as nutrient sources for the microbes (Nagatsuka et al., 2014). Ice surface albedo is reduced by mineral dust (Bøggild et al., 2010), aggregation of cryoconite granules (Takeuchi et al., 2001; Hodson et al., 2008; Irvine-Fynn et al., 2012), microbial communities (Yallop et al., 2012; Singh et al., 2014), and meltwater production (Gruell, 2000). Due to the impact of climate change, warmer temperature transforms glacier zones into proglacial zones (Prowse et al., 2006), and subsequently, there is recolonization on glacier-retreated lands (Kaštovaká et al., 2005).

Abbot and Pierrehumbert (2010) opined the role of cryoconites as a potential melt catalyst in albedo-driven deglaciation of "Snowball Earth." This unique habitat is a hotspot for culturable and non-culturable microbial diversity of Antarctica (Christner et al., 2003; Boetius et al., 2015; Webster-Brown et al., 2015; Obbels et al., 2016; Sommers et al., 2018; Poniecka et al., 2020) and Arctic (Edwards et al., 2011; Singh and Singh, 2011; Singh et al., 2014, 2020; Lutz et al., 2016; Uetake et al., 2016). Additionally, the studies on ecological succession (Williams et al., 2013), geochemistry of melt waters (Fountain et al., 2004; Tranter et al., 2004; Hodson et al., 2008; Bagshaw et al., 2013), and nutrient cycling (Stibal et al., 2012) have also been conducted. Sommers et al. (2018) advocated that environmental factors (lithology of the nearby mountains, height, and geographic location) also play a crucial role in regulating the cryoconite bacterial populations. Whole-genome analyses of a cryoconite bacteria showed unique genes for stress tolerance, DNA repair, enzyme activity, PUFA, and PGPR genes from the Arctic (Singh et al., 2015). Though cryoconite holes are very dynamic freshwater micro-ecosystems and are home to a rich biological diversity, studies at the range of spatial scales and a holistic understanding of this unique habitat are still a secret and thrust area of investigation (Cook et al., 2016).

Cryoconite holes have immense significance in understanding the sub-glacier ecosystems in the Himalayas. Himalayas have about 54000 glaciers and cover a vast geographical area (~60,000 square kilometers). Due to climate warming Himalayan glaciers are melting and retreating substantially, and may destabilize domestic, agricultural and industrial resources of people in the future. Very little work has been conducted on Himalayan cryoconites. The albedo-reducing, optical properties and microbial communities of cryoconites have been characterized from Nepali Himalaya (Takeuchi et al., 2001, 2010; Singh et al., 2020). The studies on biology and biogeochemistry of Indian Himalayan cryoconites and their interactions with climate remain elusive and are thrust areas for research. Hamtah Glacier is a well-researched benchmark glacier for mass balance, glacier melt runoff, and glacier meteorological and debris cover studies (GSI, 2009). This glacier is prone to climate change and loses its mass significantly during summer (Shukla et al., 2015; Mandal et al., 2016). Recently, Dhume et al. (2022) characterized fungal communities of Hamtah glacier. Bacterial diversity and biopotentials of Hamtah glacier is a gap area, therefore present study was conducted.

The aim of the current study was first, to investigate culturable and non-culturable bacterial communities present in Hamtah glacier cryoconites. Secondly, to characterize the biopotentials (cold-adapted enzymes, fatty acids, antibiotic resistance, carbon source utilization and physiological features). Furthermore, to know the physical properties of cryoconites, the elemental composition was also analyzed.

Materials and methods

Sampling site

Hamtah Glacier (32.24°N, 77.37°E) is an important glacier extending from south to north between 5000 and 4020 masl and covering an area of ~3 km^2 and is ~6 km long (GSI, 2009). This glacier is located in the Chandra Basin on the northern slopes of the Pir-Panjal range of the Indian Himalayas. The landscape of the Hamtah Glacier and pictures of the sampled hole are shown in Supplementary Figure 1. Cryoconite samples were collected from seven different locations of Hamtah Glacier (Figure 1) using a sterile syringe and ampules. Before sampling, the pH and temperature of cryoconite holes were recorded. The temperature varied from 1.2 to 2.1°C, and pH ranged from 7.5

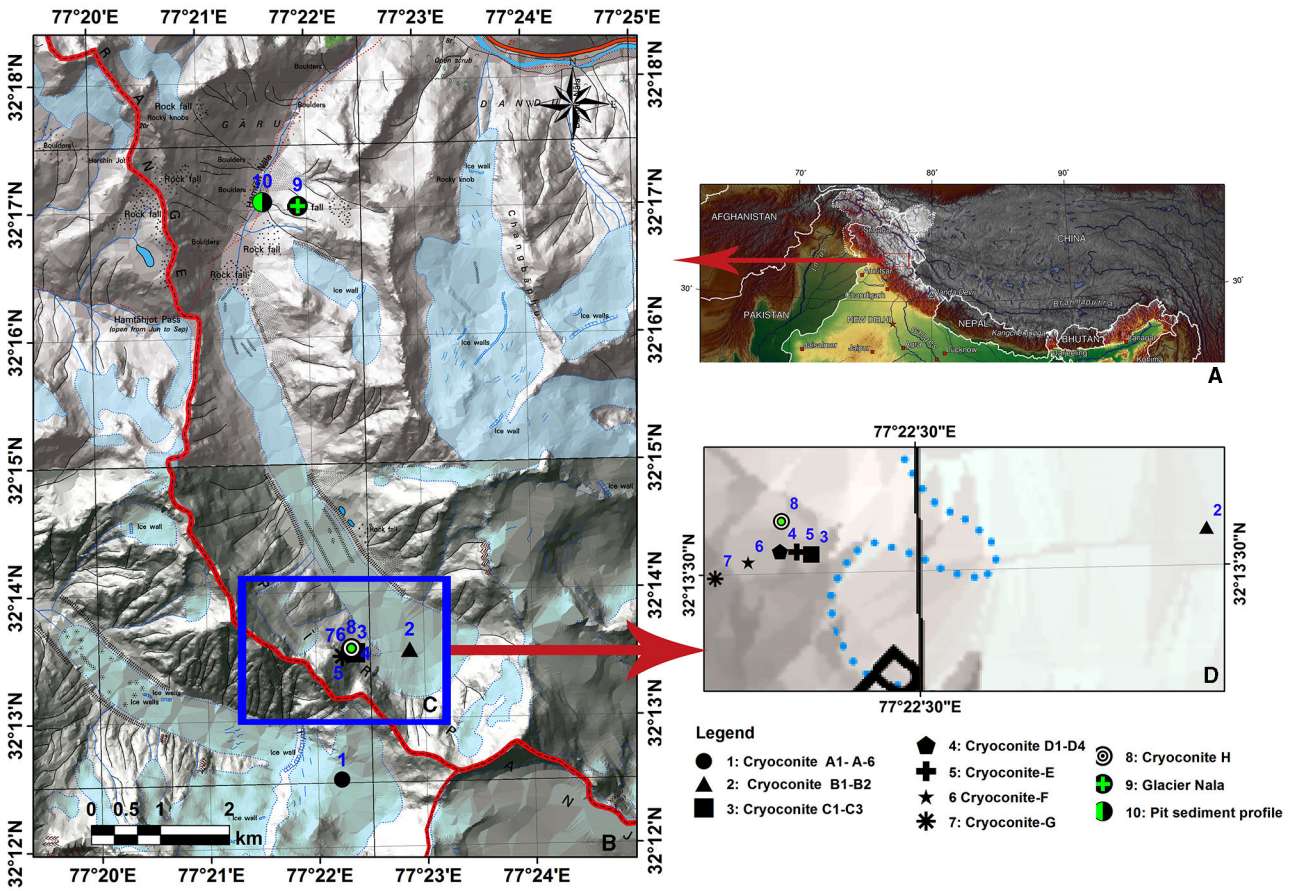

FIGURE 1
(A) Map showing Indian Himalayas, **(B)** Hamtah Glacier, **(C, D)** sampling locations.

to 8.4 at different locations of the glacier. All the samples were stored at sub-zero temperatures and transported to the laboratory for further analysis.

Isolation and culturing of bacteria

One gram of cryoconite was suspended in 9 mL saline solution and diluted serially (10^{-1}, $10^{-2,}$ and 10^{-3}). To maximize the recovery of isolates, several bacteriological media (HiMedia, India) of different strengths (concentrations) were used in the present study. Enumeration of culturable bacteria was done using the spread plate method (0.1 ml) on Nutrient Agar (NA per liter: Beef powder 3 g, Sodium Chloride 8 g, Peptone 5 g and 20g Agar, pH 7.0), 1/10 NA, Marine Broth (MB per liter: Zobell Marine broth 20.25 g and 20 g agar, pH 7.6), 1/10MB, Antarctic Bacterial Medium (ABM per liter: 5 g peptone, 2 g yeast extract, and 15 g agar, pH 7.0), 1/10 ABM and R2Agar (R2Agar-HiMedia 18.12 g, pH 7.2) incubated at two different temperature 4°C and 15°C for 2–4 weeks for optimum growth of psychrophiles (Singh et al., 2016). To observe the emergence of bacterial colonies in a natural environment and compare them with laboratory incubators, the representative samples of each location (a total of 14 cryoconite samples) were also aseptically spread on readymade culture plates and incubated at the natural temperature of the Himalayas itself. The colony-forming units (CFUs) appearing after incubation were counted, and the CFU number per gm soil was calculated. Isolates for further study were picked based on colony morphology (outline, texture, color, etc.) from each plate. The pure bacterial isolates obtained through streaking techniques were preserved in cryovials with glycerol stock (70%) and finally stored at −80°C deep freezer. The unique distinctive cultures were submitted to the Microbial Culture Collection (MCC), Pune, India.

Phenotypic characterization of the bacterial strains

Colony features were observed by a stereo-zoom microscope (Nikon SMZ1500). Carbon utilization tests were carried out using HiCarbo^{TM} kits (KB009, HiMedia, India) and incubated for 2–7 days at 4 and 15°C. ONPG (Ortho-Nitrophenyl-β-D-galactopyranoside) was used to detect β-galactosidase activity. Esculin, citrate, and malonate utilization tests were carried out to detect the capability of bacterial strains to utilize Esculin, citrate and sodium malonate as a sole carbon source. Growth experiments were performed on ABM plates at a range of temperatures (4, 15, 22, and 30°C), pH (3, 5, 7, 9, and 11) and salt concentrations (0, 2, 5, 7, and 15%). The unique bacterial isolates were screened for cold-active enzymes such as amylase, cellulase, lipase, and protease following standard protocol (Singh et al., 2014).

DNA extraction, polymerase chain reaction, sequencing of culturable bacteria and phylogenetic tree construction

Genomic DNA was extracted following the standard method (Sambrook et al., 1989). 16S rRNA universal primers 16F27 (5′-CCA GAG TTT GAT CMT GGC TCA G-3′) and 16R1492 (5′-TAC GGY TAC CTT GTT ACG ACT T-3′) were used for PCR amplification. The amplified 16S rRNA gene PCR product was purified by PEG-NaCl precipitation. DNA sequencing was carried out using an automated DNA sequencer (ABI® 3730XL, Applied Biosystems, Inc., Foster City, CA) at Microbial Culture Collection (MCC), NCCS at Pune, India. Essentially, sequencing was carried out from both ends using additional internal primers so that each position was read at least twice. Assembly was carried out using the Lasergene package followed by an EzTaxon search (Kim et al., 2012) for identification.

The nucleotide sequences of 47 bacterial isolates were deposited in the DNA data bank (NCBI) and assigned accession numbers are KY783365 to KY783401. Nucleotide sequences were subjected to NCBI BLAST search. Sequence alignment of the 16S rRNA region of each isolate was carried out using the Clustal W algorithm, Molecular Evolutionary Genetics Analysis (MEGA) 11.0 software was used for tree construction. The phylogenetic tree was constructed by neighbor-joining (NJ) method with 1000 bootstrap replicates of the phylogeny test, and partial deletion of data sub-set was used with a 95% cut-off setting in the partial deletion method. Red color phylogenetic trees indicate isolates/strains of the present study (sequences) and blue colored for closely related strains of the same species from the database.

Non-culturable bacterial analyses: DNA extraction and high-throughput sequencing of 16s rRNA genes using MiSeq

Genomic DNA was extracted from 14 cryoconite samples (A, A2, A4, A5, A6, B, B2, C, D, D1, D2, D3, EHamtah, G, cryG) and one each from glacier Snout and glacier Nala/stream) using the FastDNA SPIN Kit (Soil DNA Extractionkit:MP Biomedicals, Santa Ana, CA). The bacterial community structure in the cryoconite samples was analyzed by sequencing the 16S rRNA gene using MiSeq sequencer (Illumina, San Diego, CA). Partial 16S rRNA gene sequences including the V3 and V4 regions were amplified. Bakt 341F and Bakt 805R primers with Illumina overhang adaptor sequences attached to their 5′ends were used. PCR amplification of the 16S rRNA gene, reaction clean-up, index PCR and sequencing were performed following Illumina methods for 16S rRNA gene sequencing library preparation, Pyrosequencing, Phylogenetic analyses and Community comparisons were done following standard procedure (Edgar et al., 2011; Segawa et al., 2014; Uetake et al., 2016).

Fatty acid methyl ester analysis

The cultures were grown on a standard media Tryptic Soy Broth Agar (TSBA, Himedia) for FAME analyses, and also on respective isolate-isolation media at two standard psychrophilic temperatures 4^0C and 15^0C for 2 to 3 weeks. Three replicates of individual bacterial isolates were made by streaking on similar media plates and incubating them in similar conditions. The extraction and analysis of cellular fatty acid methyl esters (FAME) was carried out following standard protocol (Buyer, 2008). FAMEs analyses were carried out using a gas chromatograph (Agilent Technologies, CA, USA, Model 7890A), equipped with a flame ionization detector (FID), auto-sampler and capillary column (HP-5 column, 25 m × 0.2 mm × 0.33 μm). Hydrogen was used as carrier gas. The gas chromatography system was calibrated twice with a calibration standard no. 1300AA (MIDI, USA) before analyses of bacterial samples. Additionally, before running the cryoconite bacterial samples, the extraction efficiency of the protocol and authenticity of fatty acid peaks were verified by using a known fatty acid profile of a type strain (*Stenotrophomonas maltophili a* ATCC 13637^T) as a positive control. The individual fatty acid peaks were identified based on the retention time of the standard run. The standard software and database were used (RTSBA6 of MIS, MIDI Inc., Newark, DE, USA) for analysis.

Antibiotic susceptibility

The susceptibility of the bacterial isolates to 45 antibiotics (Supplementary Table 7) was determined by using the impregnated disc method (Bauer et al., 1966). The bacterial isolates were grown at 15°C in nutrient broth up to a turbidity of 0.08–0.13, optical density measured at 620 nm. The bacterial suspensions (100 μl) were spread onto the surface of the Mueller Hinton Agar medium plates, using sterile spreaders. The different antibiotic discs were placed over the individual bacterial lawns, and the plates were incubated at 15°C for 3–4 days. Petri dishes were observed for the formation of a zone of inhibition, if any. The zone formed was measured in millimeters.

Elemental analyses of cryoconites

Cryoconite granules were finely grounded powdered samples were oven-dried at 110°C. An amount of 0.5 g of each sample was acid digested (3 mL of 69% sub-pure HNO_3, 1 mL subpure 30% HCl and 1 mL of 30% H_2O_2) completely in the microwave at 180°C (Ethos 1, Milestone, Italy). The digested samples were analyzed using inductively coupled plasma mass spectrometry (ICP-MS), × Series II, Thermo Fisher Scientific, Bremen, Germany. CertiPUR ICPmulti-element standard (Merck, Darmstadt, Germany) was used for calibration. Elemental concentrations were measured in triplicate and were recorded in mg/kg as described previously (Singh et al., 2017).

Results

Characteristics of the glacier cryoconite samples

The pH and temperature in the cryoconite holes showed varied responses depending upon whether the holes are open or closed

and, their sampling locations on the glacier. The water temperature in the cryoconite holes ranged between 1.2–2.1°C and pH 7.58–8.48. Cryoconites are brownish-black in color, organic carbon ranges from 0.57 to 1.12%, and total phosphorus 0.14 to 0.20 mg/g. The elemental composition showed the presence of 25 elements (Li, Be, Na, Mg, P, K, Ca, V, Cr, Mn, Fe, Co, Ni, Cu, Zn, As, Rb, Sr, Cd, Cs, Ba, Tl, Pb, Bi and U) in all cryoconite samples to varying amount. K, Mg, Mn, Fe, Ca, P and Na were dominant elements in samples (Table 1 and Supplementary Table 1).

Bacterial count and characteristics of the isolated strains

The culturable bacterial count (colony forming units, CFUs) on various bacteriological media ranged from 2.0×10^3 to 8.8×10^5 CFUs per g. Of the numerous CFUs that appeared on the culture media plates, 47 distinct isolates were purified for further studies (Table 1). The culture colonies showed different colors (white, cream, yellow and orange), and morphological features (entire margin, opaque and smooth texture, and convex pulvinate to raised elevation). The shapes of bacterial cells were short to long rods. Most of the isolates showed growth temperature ranges from 4 to 22°C. The optimum temperature for the growth of culturable isolates was 15°C, therefore indicating psychrophilic. The isolates showed salt tolerance at 1 and 7% and optimum growth at pH 6.0 to 7.0. The 16S rRNA gene sequences of 47 bacterial isolates were deposited to GenBank (NCBI) with accession numbers (KY783365 to KY783401, MF467864 to MF467871, and MF467873) (Table 1).

Carbon utilization ability of the isolated strains

Of the 35 carbon sources tested, most of the isolates showed varied responses for carbon utilization tests (Supplementary Table 2). Amongst the isolates tested, *Peribacillus frigoritolerans* E-Cry-4 utilized 25, *Cryobacterium arcticum*-A2–6 utilize 24, *Pseudomonas* simiae-B2–6 utilized 26, *Psychrobacter pulmonis* E-Cry-2 utilize 27, *Sphingomonas glacialis* B2–P7 utilize 17, *Janthinobacterium* svalbardensis B2–8 can utilize as much as 4 (ONPG, esculin, citrate and malonate), of the 35 carbon sources tested. Except isolate E-Cry-2 none of the isolates were capable of utilizing sorbose.

Extracellular enzymatic activities

The 45 bacterial cultures that were screened for enzyme production showed varied responses. Four isolates were positive for amylase, 12 for cellulase, 14 for lipase, and 20 for protease (Supplementary Table 3). Temperature showed a vital role in enzyme production. Cellulase, lipase and protease production decreased with an increase in temperature from 4 to 22°C. In contrast, amylase production increased with an increase in temperature. *Cryobacterium arcticum*-A2–6 was the most promising culture as it has strong cellulase and lipase activity, while 4 other cultures (B2P3, B2P4, B2P6, B2P11) produced three different enzymes: cellulase, lipase and protease. Four cultures (B2–6, HF6, HF8, HF9) indicated strong activity for cellulase and protease. Three cultures (E-cry 4, HF6, HF8) showed amylase activity (Supplementary Table 3).

Phylogenetic analyses/taxonomic analysis of culturable bacteria

The total sequence lengths after alignment, the closest sequence similarities % with the database, and the NCBI sequence deposition numbers are given in Table 1. Sequence alignment was done using clustalW algorithm. The sequence analysis of the 16S rRNA gene domain of isolate *Peribacillus frigoritolerans* Ecry4 (MF467864) indicated their closest relationship to NCBI database species *Bacillus simplex* strain ER20 (99.50%), *Cryobacterium* A2–6 (KY783365) showed closest relationship with species of *Cryobacterium arcticum* strain A52(94.87%). *Duganella* A_4P_6 (KY783370) indicated *their closest relationship with the species of Duganella phyllosphaerae* MILP3 (96.95%). Sequence analysis of 32 bacterial isolates of *Janthinobacterium* (A2(2), A_27, A_45, A_4P1, A_4P_4, A_4P_5, A_4P_7, B_2f, B2(G), B_23, B_28, B_212, B2–14, B_2P_1, B_2P_9, B_2P_{10}, B_2P_{13}, B_2P_{14}, B_2P_{15}, EI_1, EI_2, EI_3, EI_4, EI_5, EI_6, EI_8, EI_9, EI_{10}, EI_{11}, EI_{16}, EI_{17} and Ecry7) indicated their closest relationship to species of *Janthinobacterium svalbardensis* JA-1 (93.01 to 99.79%). Nine bacterial isolates of *Pseudomonas* (B_26, B_2P_3, B_2P_4, B_2P_6, B_2P_{11}, EI_{13}, HF_6, HF_8, HF_9) showed their closest relationship (92.12 to 98.91%) to the species of *Pseudomonas marginalis* strain HCR18v and *Pseudomonas extremaustralis* strain 20BR5VA1. Isolate *Sphingomonas glacialis* B2-P7 (MF467873) indicated their closest relationship with species of *Sphingomonas* sp. 2PM11 (99.39%). Sequence analysis of 2 bacterial isolates of *Psychrobacter pulmonis* Ecry2 (KY783397) and HF_5 (KY783398) indicated their closest relationship with species of *Psychrobacter alimentarius* strain JM48 CECT 5989 (96.82) and *Psychrobacter namhaensis* strain E3 98.11%). The affiliation of the representative isolates of culturable bacteria is shown in a phylogenetic tree (Figures 2A–G).

The bacterial isolates from the cryoconites of different locations in Hamtah glacier belonged to seven different genera, namely, *Cryobacterium*, *Duganella*, *Janthinobacterium*, *Pseudomonas*, *Sphingomonas*, *Peribacillus* and *Psychrobacter* (Table 1). The number of species at each location varied from 2 to 4, while number of isolates varied from 4 to 18. The most predominant species was *Janthinobacterium svalbardensis* followed by *Pseudomonas* simiae. Genera *Cryobacterium*, *Duganella*, *Peribacillus* and *Sphingomonas* were represented the least. Glacier location E showed maximum culturable diversity, representing four different species, while location F of glacier showed minimal diversity, representing only two species.

Analyses of non-culturable bacteria using MiSeq high-throughput sequenced data of 16S rRNA genes

After curation of the MiSeq dataset, 16S rRNA gene sequences representing the non-culturable bacterial populations from the cryoconite samples across Hamtah glacier, Himalaya. The

TABLE 1 Culturable bacteria isolated from Hamtah glacier cryoconites, Himalaya.

Sample name	Sampling location	Isolate no.	Sequence deposition no.	Total sequence length	Closest similarity with NCBI nucleotide database (18.03.2023, ISD)	Nearest match % similarity
Cryoconites A	32 12. 543 N 77 22.210 E Elevation: 4,551 m, Temperature: 1.2, pH:8.48	$A_2$6	KY783365	1,473	*Cryobacterium arcticum* strain A52	94.87
		A2(2)	MF467871	1,396	*Janthinobacterium svalbardensis* strain KCOM 1326	99.79
		$A_2$7	KY783366	1,453	*Janthinobacterium svalbardensis* strain KCOM 1326	97.70
		$A_4$5	KY783367	1,465	*Janthinobacterium* sp. strain M1_12	96.55
		A_4P_1	MF467867	1,373	*Janthinobacterium* sp. strain SNU WT3	99.64
		A_4P_4	KY783369	1,445	*Janthinobacterium svalbardensis* strain 20BR4L12	98.60
		A_4P_5	KY783368	1,470	*Janthinobacterium* sp. Zh1N-4	97.10
		A_4P_6	KY783370	1,468	*Duganella phyllosphaerae* strain MILP3	96.95
		A_4P_7	MF467869	1,363	*Janthinobacterium* sp. RHLS1-2	99.71
Cryoconite B	32 13.541 N 77 22.861 E Elevation: 4,365 m, Temperature:1.4, pH:7.6-7.8	B_2f	KY783371	1,457	*Janthinobacterium* sp. strain xPrg51	98.08
		B_2(G)	MF467863	1,385	*Janthinobacterium* sp. strain BWHT3	99.78
		$B_2$3	KY783372	1,458	*Janthinobacterium* sp. strain BSLA3	97.75
		$B_2$6	KY783373	1,490	*Pseudomonas marginalis* strain HCR18v	92.12
		$B_2$8	KY783374	1,476	*Janthinobacterium svalbardensis* strain 20BR4L12	94.79
		$B_2$12	KY783375	1,445	*Janthinobacterium svalbardensis* strain 20BR4L12	97.66
		B2-14	MF467870	1,320	*Janthinobacterium svalbardensis* strain KCOM 1326	99.54
		B_2P_1	KY783376	1,460	*Janthinobacterium* sp. HLX1	96.97
		B_2P_3	KY783377	1,455	*Pseudomonas* sp. Ln4B.12g	97.33
		B_2P_4	KY783378	1,466	*Pseudomonas* sp.MS-A-S3	97.30
		B_2P_6	KY783379	1,458	*Pseudomonas extremaustralis* strain 20BR4AA9	98.49
		B2-P7	MF467873	1,350	*Sphingomonas* sp. 2PM11	99.39
		B_2P_9	KY783380	1,450	*Janthinobacterium* sp. strain BFS1HT1	97.80
		B_2P_{10}	KY783381	1,568	*Janthinobacterium svalbardensis* strain ACR1p	94.67
		B_2P_{11}	KY783382	1,450	*Pseudomonas extremaustralis* strain 20BR5VA1	97.99

(Continued)

10.3389/fmicb.2024.1362678

TABLE 1 (Continued)

Sample name	Sampling location	Isolate no.	Sequence deposition no.	Total sequence length	Closest similarity with NCBI nucleotide database (18.03.2023, ISD)	Nearest match % similarity
		B_2P_{13}	KY783383	1,453	*Janthinobacterium lividum* strain KOPRI 25648	97.52
		B_2P_{14}	KY783384	1,587	*Janthinobacterium svalbardensis* strain A2(2)	90.73
		B_2P_{15}	KY783385	1,447	*Janthinobacterium lividum* strain MWHB2	97.80
Cryoconite-E	32 13.523 N 77 22.346 E Elevation: 4,365 m, Temperature:2.1, pH:8.04	EI_1	KY783386	1,447	*Janthinobacterium svalbardensis* strain 20BR4R40	97.42
		EI_2	KY783387	1,479	*Janthinobacterium svalbardensis* strain IHBB	95.95
		EI_3	KY783388	1,468	*Janthinobacterium svalbardensis* strain NJ-XFW-1-C	97.62
		EI_4	KY783389	1,465	*Janthinobacterium* sp. sgn 135	97.47
		EI_5	KY783390	1,450	*Janthinobacterium* sp. strain M1_12	98.15
		EI_6	KY783391	1,455	*Janthinobacterium* sp. strain BFS1HT1	97.45
		EI_8	KY783392	1,477	*Janthinobacterium tructae* strain Y2PP14	94.93
		EI_9	KY783393	1„446	*Janthinobacterium lividum* strain KOPRI 25720	97.99
		EI_{10}	KY783394	1,483	*Janthinobacterium* sp.MS-A-S1	95.50
		EI-11	MF467865	609	*Janthinobacterium lividum* strain EIF2	99.02
		EI_{13}	KY783395	1,460	*Pseudomonas* sp. strain S2INA_B3	97.43
		EI-16	MF467866	1,372	*Janthinobacterium svalbardensis* strain A4P1	99.20
		EI_{17}	KY783396	1,448	*Janthinobacterium* sp. strain M1_12	97.70
		Ecry2	KY783397	1,476	*Psychrobacter alimentarius* strain JM48	96.82
		Ecry4	MF467864	1,418	*Bacillus simplex* strain ER20	99.50
		Ecry7	MF467868	1,376	*Janthinobacterium* sp. strain M1_12	99.49
Cryoconite-F	32 13.520 N 77 22.520 E Elevation: 4,550 m, Temperature: 2.1, pH:8.04	HF_5	KY783398	1,447	*Psychrobacter alimentarius* strain JM48	98.11
		HF_6	KY783399	1,478	*Pseudomonas* sp. strain KP-10-2	95.62
		HF_8	KY783400	1,443	*Pseudomonas* sp. strain PCH61	98.91
		HF_9	KY783401	1,467	*Pseudomonas* sp. strain FH1	97.30

10.3389/fmicb.2024.1362678

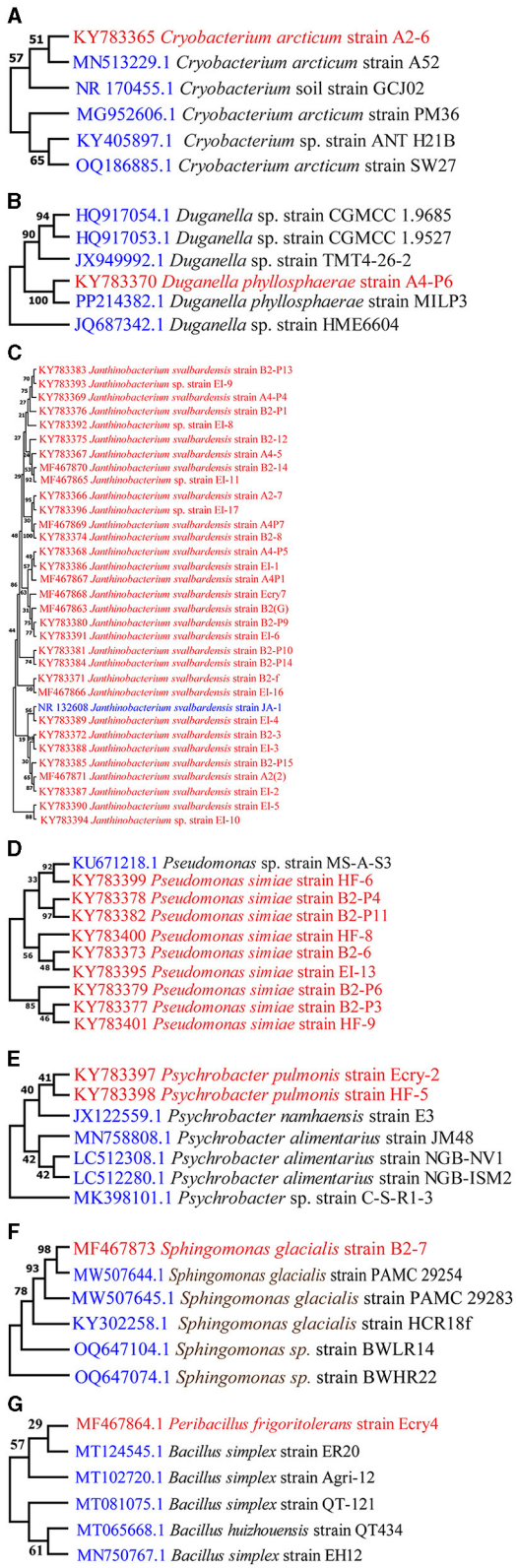

FIGURE 2
Phylogenetic trees of Culturable bacteria: **(A)** *Cryobacterium*, **(B)** *Duganella*, **(C)** *Janthinobacterium*, **(D)** *Pseudomonas*, **(E)** *Psychrobacter*, **(F)** *Sphingomonas*, **(G)** *Peribacillus*.

profiles represent eight major lineages: Proteobacteria was the most dominant (207 genera, 64 families), followed by Actinobacteria (80 genera, 28 families), Firmicutes (52 genera, 19 families), Bacteroidetes (51 genera, 12 families), Cyanobacteria (10 genera, two families) with other member phyla such as Chloroflexi (eight genera and seven families), Acidobacteria (five genera and three families), Planctomycetes (six genera, one family), Verrucomicrobia (five genera, four families) Deinococcus-Thermus (three genera, three families), Chlamydiae (three genera, two families), Spirochaetes (three genera, two families), Armatimonadetes (two families and two genera), The phyla Caldiserica, Deferribacteres, Elusimicrobia, Fusobacteria, Gemmatimonadetes, Lentisphaerae, and Nitrospirae represented least (one family and one genus in each phyla) along with others unknown taxa (Supplementary Table 4). In the present study, Proteobacteria is an important bacterial phylum and represent maximum number of bacteria belonging to five classes such as Betaproteobacteria (77 genera, 11 families), Alphaproteobacteria (54 genera, 19 families), Gammaproteobacteria (47 genera and 15 families), Deltaproteobacteria (23 genera and 16 families) and Epsilonproteobacteria (six genera and three families). Proteobacteria, Actinobacteria, Bacteroidetes and Firmicutes were well represented in all of the sampling sites. Armatimonadetes, Caldiserica, Deferribacteres, Elusimicrobia, Fusobacteria, Gemmatimonadetes, Lentisphaerae and Nitrospirae were present least in samples. The relative abundance (%) of bacterial phyla present at different sampling sites are shown in Figure 3 and Supplementary Table 5. The bacterial profile results indicate that taxa distribution exhibits a specific distribution pattern along the different glacier cryoconites, glacier snouts and glacier streams. The similarity of bacterial community structures between sampling sites is shown in a UniFrac dendrogram (Figure 4).

FAME analysis

Six representative bacterial taxa were characterized for cellular fatty acid composition. *Janthinobacterium svalbardensis* $B_2$8 (KY783374), Gram-negative, and Betaproteobacteria belong to the Oxalobacteraceae family. *Pseudomonas* simiae $B_2$6 (KY783373) Gram-negative, Gammaproteobacteria, belonging to the family Pseudomonadaceae. *Psychrobacter pulmonis* Ecry2 (KY783397) Gram-negative, Gammaproteobacteria, belonging to the family? Moraxellaceae. *Peribacillus frigoritolerans* Ecry4 (MF467864) Gram-positive, Firmicutes, belonging to the family Bacillaceae. *Cryobacterium arcticum* $A_2$6 (KY783365) Gram-positive bacterial strains belong to family Microbacteriaceae. *Sphingomonas glacialis* B_2P-7 (MF467873) Gram-positive, Alphaproteobacteria, belonging to the family Sphingomonadaceae.

In the Hamtah glacier bacterial species, the branched fatty acids varied in composition from a minimum of 0.17% as in *Janthinobacterium svalbardensis* $B_2$8, to a maximum of 96.59% as in *Cryobacterium arcticum* $A_2$6. In *Janthinobacterium svalbardensis* $B_2$8 the low % of branched fatty acids was compensated by a high proportion of unsaturated fatty acids

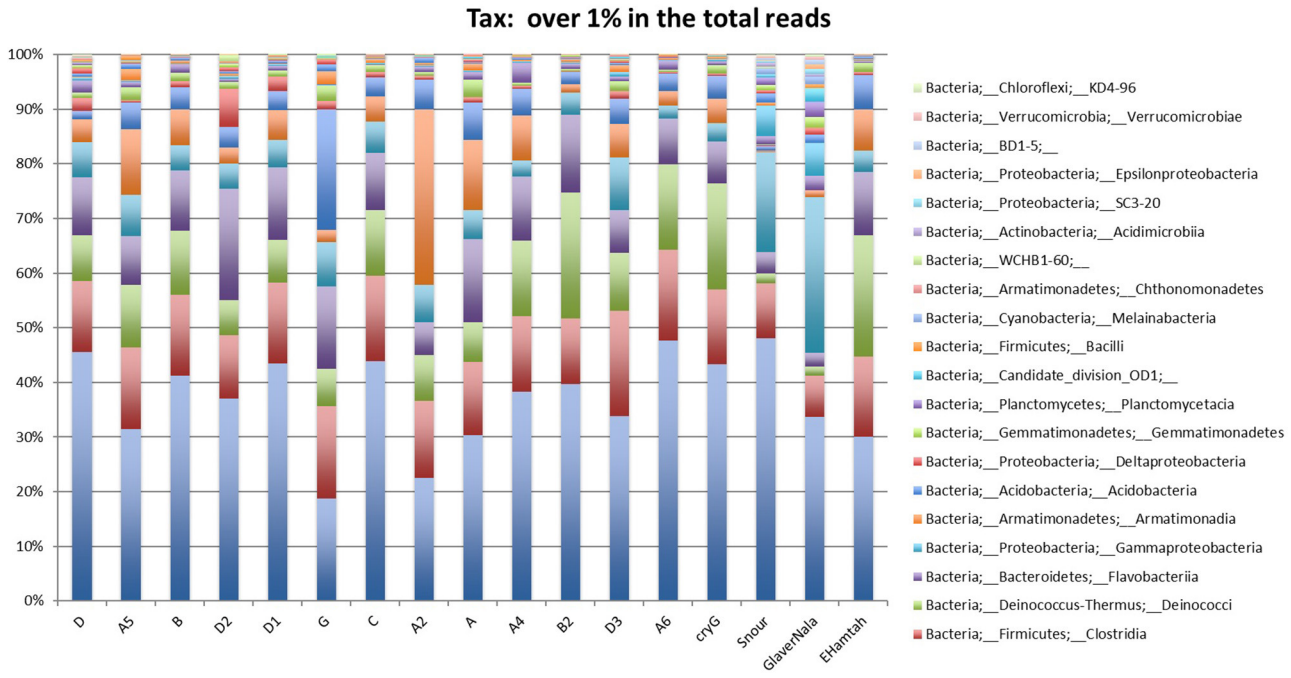

FIGURE 3
Non-culturable Bacteria: showing relative abundance (%) of bacterial phyla in Hamtah glacier cryoconites, snout, and stream (Nala).

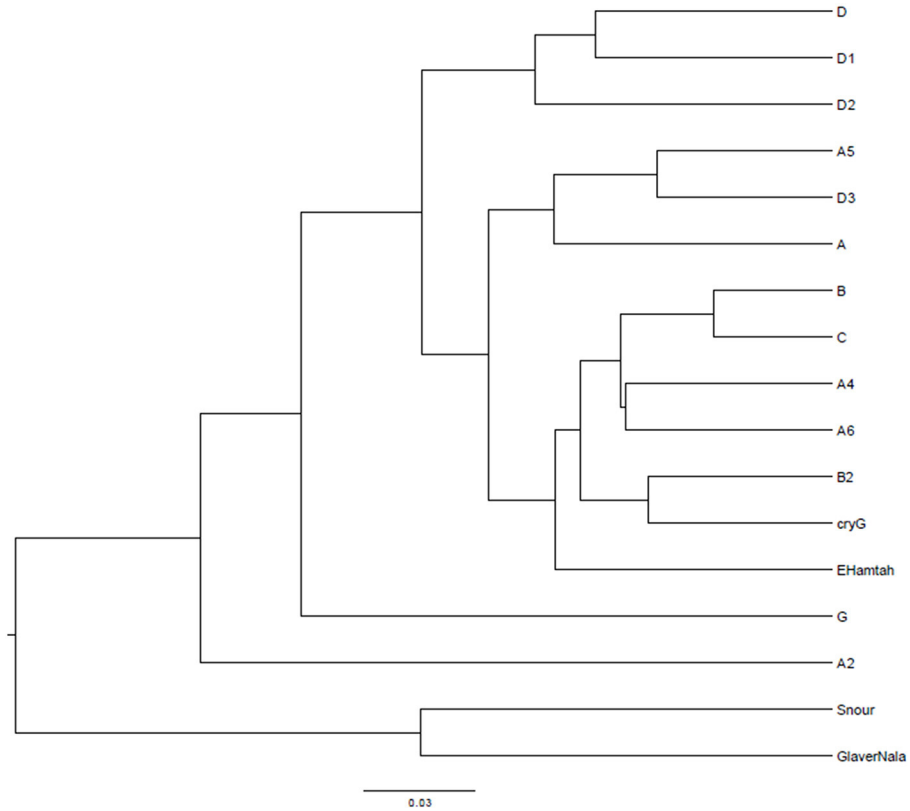

FIGURE 4
UniFrac dendrogram showing the similarity of bacterial community structures between sampling sites.

(63.24%). The unsaturated fatty acid composition in all the bacterial species varied in composition from a minimum of 58.4% as in *Janthinobacterium svalbardensis* $B_2$8, to a maximum of 90.72% as in *Peribacillus frigoritolerans* Ecry4 (Supplementary Table 6). The saturated fatty acid composition in all the bacterial species varied in composition from a minimum of 2.39% as in *Sphingomonas glacialis* B_2P-7, to a maximum of 41.24% as in *Janthinobacterium* svalbardensis $B_2$8 (Supplementary Table 6).

Antibiotic resistance patterns of the isolated strains

Cryoconite bacterial isolates were subjected to 45 antibiotic screening tests. The result showed that most of the isolates were sensitive to antibiotics such as Amikacin, Carbenicillin, Cefoperazone, Ceftazidine, Chloramphenicol, Ciprofloxacin, Doxycycline hydrochloride, Gatifloxacin, Gentamicin, Kanamycin, Levofloxacin, Lomefloxacin, Meropenem, Nalidixic Acid, Netillin, Norfloxacin, Ofloxacin, Rifampicin, Streptomycin, Tetracycline, and Tobramycin (Supplementary Table 7). The sensitivity to other antibiotics tested varied from isolate to isolate. Clidamycin and Methicillin were the least potent antibiotics tested and were sensitive to only two isolates (Ecry-2 and Ecry-4). Of the isolates screened against 45 antibiotics, B2–8 and B2–6 were the most resistant, showing resistance to 19 and 21 antibiotics, respectively. Other isolates showed varied resistance profiles toward the antibiotics.

Discussion

The main aim of the current study was to investigate the bacterial diversity, biopotentials and properties of cryoconites of Hamtah glacier, Himalaya. The pH of the cryoconite holes observed in the present study ranged from 7.5 to 8.4, resembling earlier data pH 5.9–9.6 from Canada glacier Antarctica (Mueller and Pollard, 2004), and pH 7.1–8.6 from Arctic glaciers (Singh et al., 2014). The pH properties of cryoconites holes depends on mineral contents, microbial activities and glacier environment in which it is found (Tranter et al., 2004). The organic carbon content in the present study was low (0.57%−1.12%) confirming the oligotrophic nature of cryoconite habitat. The similar data have also been reported from Arctic (1.07%−2.5%) by Singh et al. (2014), and 5.4%−9.9% from Nepali Himalaya (Takeuchi et al., 2001). Of 25 elements observed in cryoconites of the present study, Mg, Fe, Mn, Ca, P, and Na were dominant, as observed in previous studies (Singh and Singh, 2011; Singh et al., 2017). The accumulation and release of these inorganic material may impact supraglacier and proglacier ecosystems of Himalayas. The elemental content is mainly input from atmospheric, hydrologic and mineral resources, and this finding is further supported by Mueller et al. (2001) and Singh et al. (2017). The bacterial CFUs that emerged on the media plates ranged from 2.0×10^3 to 8.8×10^5 CFUs per g at the different locations of Hamtah glacier studied. The bacterial CFU data similar to the current observation are also reported from Arctic cryoconites (2.7×10^3 to 8.8×10^4 per g, Singh et al., 2014) and from Antarctic cryoconite melt water (8.8×10^4 per ml, Christner et al., 2003).

The bacterial isolates could grow at 4 to 22°C, except for one at 30°C. The optimum temperature of growth was 15°C. The Hamtah glacier isolates profusely grow at 4 and 15°C as compared to 22°C resembles with previous studies from Antarctic and Arctic (Christner et al., 2003; Singh et al., 2014). Although the culturable bacterial diversity in Hamtah cryoconites is limited, but their strains differ widely in their antibiotic sensitivity characteristics. In the present study, the sensitivity of isolates toward antibiotics varied, as recorded in earlier studies from Arctic cryoconites (Singh et al., 2014). The most of the isolates indicated low resistance toward antibiotics in Himalaya similar to Polar regions. Segawa et al. (2012) reported that the Antarctic region has the least antibiotic resistance genes, followed by the Arctic region. The organic carbon sources are important for microbial metabolism but it limited in oligotrophic environment of cryoconite holes. The carbon source utilization tests showed that bacterial isolates from the Himalayan cryoconites prefer monosaccharides similar to Arctic cryoconite (Singh et al., 2014). The limited available organic and inorganic matter in cryoconite holes has also been reported from Antarctica (Foreman et al., 2007). Psychrophilic organisms can produce cold-active enzymes which have immense applications in Agriculture, health and industry (Feller and Gerday, 2003). The 45 bacterial isolates of Hamtah glacier cryoconites showed activities for one or more enzymes (amylase, cellulase, lipase, protease) either at 4°C, 15°C, and (or) 22°C. The ability of these bacterial isolates to produce different enzymes speaks about their biopotentials in sub-glacial environments. Some of the isolates of the present study showed strong cellulase, lipase and protease activity, similar to Arctic cryoconites (Singh et al., 2014). Additionally, there are reports of extracellular enzyme activities by Arctic bacteria (Reddy et al., 2009; Yu et al., 2009) and Himalayan fungi (Dhume et al., 2019).

The taxonomic analyses of bacteria using a culturable approach showed the presence of seven genera *Cryobacterium*, *Duganella*, *Janthinobacterium*, *Pseudomonas*, *Peribacillus*, *Psychrobacter* and *Sphingomonas*. The culturable bacterial genera *Cryobacterium*, *Janthinobacterium*, *Pseudomonas* and *Sphingomonas* of the present study have also been reported from Arctic cryoconites (Svalbard: Singh et al., 2014, Greenland: Perini et al., 2019; Singh et al., 2020). Genera such as *Pseudomonas, Cryobacterium* are of common occurrence in cryoconite habitats and have been previously reported from the Antarctic cryoconites (Christner et al., 2003). *Pseudomonas* has also been documented in the Alpine cryoconites (Lee et al., 2011). The occurrence of related phylotypes in geographically diverse cold environments suggests that they have unique adaptation strategies at low temperatures (Abyzov et al., 1998). These adaptation strategies include the occurrence of pigments, polyunsaturated and branched fatty acids (PUFAa) and or enzymes in the current isolates are active at low temperatures. Fatty acid composition of bacterial isolates of Hamtah glacier indicated presence of unsaturated and branched (including the iso- and anteiso-) fatty acids. Chintalapati et al. (2004) have also described the role of fatty acids in psychrophiles. Nishida and Murata (1996) reported the role of unsaturated and branched fatty acids in maintaining functional membrane fluidity at low temperatures. Thus, psychrophilic and psychrotolerant

bacteria from glacier cryoconite adapt to the cold environment by preferentially synthesizing unsaturated and branched fatty acids. MiSeq high-throughput sequenced data of 16S rRNA genes showed presence of 440 genera of non-culturable bacteria in Hamtah glacier cryoconites (Supplementary Tables 4, 5). The major phyla present in current study are Proteobacteria, Actinobacteria, Bacteroidetes, Firmicutes, followed by Cyanobacteria, Chloroflexi, Acidobacteria, and Armatimonadetes were previously identified from Greenland cryoconites (Uetake et al., 2016). Additionally, the present study also showed seven common phyla such as Proteobacteria, Cyanobacteria, Bacteroidetes, Actinobacteria, Acidobacteria, Chloroflexi and Planctonycetes were also recorded from cryoconites of Svalbard, Arctic (Edwards et al., 2011). Himalayan cryoconites showed dominance of Alpha-, Betaproteobacteria is consistent with earlier studies from Antarctica (Christner et al., 2003). Deltaproteobacteria and Firmicutes were reported from majority of cryoconites holes resembles current observation (Cameron et al., 2012). The presence of eight genera of cyanobacteria (*Chroococcidiopsis, Chamaesiphon, Leptolyngbya, Microcoleus, Phormidesmis, Phormidium, Tychonema, Anabaenopsis, Nostoc, Calothrix*) and non-cyanobacterial photosynthetic bacteria *Rhodobacter* and *Chloroflexi* in current study may have an important role in primary production in Hamtah glacier cryoconites holes. Cyanobacterial taxa have also been identified globally in cryoconites of other cold places (Edwards et al., 2011; Uetake et al., 2016). The chemolithoautotrophic Nitrosomonadales genera *Nitrosomonas* and *Nitrosospira* has ability to oxidize ammonia to nitrite are present in current study were also reported from other cold habitat (Segawa et al., 2012). Besides this other *Nitrosomonadales taxa, Candidatus, Nitrotoga, Ferriphaselus, Gallionella, Sideroxydans* were observed in the present study (Supplementary Table 5). We also identified seven bacterial phyla from Hamtah glacier Snout (Actinobacteria, Bacteroidetes, Chloroflexi, Firmicutes, Proteobacteria, Spirochaetes and Verrucomicrobia), and six phyla from a glacier-stream/Nala (Acidobacteria, Actinobacteria, Bacteroidetes, Cyanobacteria, Firmicutes, Proteobacteria) which are consistent with an earlier report from Himalayan Kafni proglacial soils (Srinivas et al., 2011). Proteobacteria, Actinobacteria, Bacteroidetes and Firmicutes were well represented in all the sampling sites; however, some bacterial groups have shown uneven spatial distribution between sampling sites in the present study, resembling Arctic cryoconite holes (Edwards et al., 2011). Physico-chemical conditions of glaciers, topography, and aerial deposition of dust/propagules are possibly responsible for the spatial distribution pattern of bacteria in Polar cryoconite including the Himalayas. Additionally, Bacterial community composition also depends on bed rock type as reported from Antarctica (Tytgat et al., 2016).

The culturable bacterial community profiles were distinct from those found in the metagenomic community. The non-culturable approach studies document a more enormous assortment of bacteria (440 genera) than the culture-based approach (7 genera) in this study. However, there are some common genera in both approaches, but they are fewer in number. Similar observations have also been recorded from Arctic and Antarctic cryoconites (Christner et al., 2003; Edwards et al., 2011; Uetake et al., 2016). The culture based approach was applied in present study is to determine and compare physiological characteristics/biopotentials of individual species' of-glacier cryoconites. Furthermore, to understand the ecological roles (inter- and intra-species interactions, adaptation strategies etc.) culturable approach is very important (Jiang et al., 2006).

Conclusions

Cryoconite holes are important microcosms on the glacier where cold-adapted microbes flourish. The present study focused on characterizing the bacterial diversity of Himalayan cryoconites holes through culture- and non-culture-based approaches. The culturable bacterial population in cryoconite holes is sizeable (seven genera), whereas the non-culturable population predominates with 440 genera. These are some of the dominant genera known to occur in the colder habitats of the world. Although the culturable bacterial communities in these microhabitats is limited, but strains differ widely in their antibiotic sensitivity characters. Carbon utilization tests showed that the bacterial isolates from cryoconite holes prefer simpler carbon sources. Bacterial isolates produce high amounts of polyunsaturated-branched fatty acids (PUFAs), and various cold active enzymes indicating the prospect of biotechnology in Himalaya. To detect the functions in whole bacterial communities of Himalayan cryoconites there is need of further studies on metatranscriptomics and DNA microarrays.

Data availability statement

The datasets presented in this study can be found in online repositories. The names of the repository/repositories and accession number(s) can be found in the article/Supplementary material.

Author contributions

PS: Writing – original draft, Methodology, Formal analysis. SS: Sampling, Data curation, Funding acquisition, Writing – review & editing. TS: Formal analysis (MiSeq data), Writing – review & editing. PKS: Writing – review & editing.

Funding

The author(s) declare that financial support was received for the research, authorship, and/or publication of this article. Financial support was received for research (sample analyses) from ICAR, India and NIPR Japan.

Acknowledgments

The authors are grateful to National Bureau of Agriculturally Important Microorganisms (NBAIM), India, and Prof. Satoshi Imura, National Institute of Polar Research (NIPR), Japan. SS is thankful to GSI for camping support.

Conflict of interest

The authors declare that the research was conducted in the absence of any commercial or financial relationships that could be construed as a potential conflict of interest.

Publisher's note

All claims expressed in this article are solely those of the authors and do not necessarily represent those of their affiliated organizations, or those of the publisher, the editors and the reviewers. Any product that may be evaluated in this article, or claim that may be made by its manufacturer, is not guaranteed or endorsed by the publisher.

Supplementary material

The Supplementary Material for this article can be found online at: https://www.frontiersin.org/articles/10.3389/fmicb.2024.1362678/full#supplementary-material

SUPPLEMENTARY FIGURE 1
(a, b) Landscape of Hamtah Glacier and **(c1–c4)** Cryoconite holes.

References

Abbot, D. S., and Pierrehumbert, R. T. (2010). Mudball: surface dust and snoball Earth deglaciation. *J. Geophys. Res* 115:D03104. doi: 10.1029/2009JD012007

Abyzov, S., Mitskevich, I., and Poglazova, M. (1998). Microflora of the deep glacier horizons of central Antarctica. *Microbiology* 67, 66–73.

Bagshaw, E. W., Tranter, M., Fountain, A. G., and Welch, K. (2013). Do cryoconite holes have the potential to be significant sources of C,N, and P to downstream depauperate ecosystems of Taylor Valley, Antarctica? *Arct. Antarct. Alp. Res.* 45, 1–15. doi: 10.1657/1938-4246-45.4.440

Bauer, A. W., Kirby, M. M., Sherris, J. C., and Truck, M. (1966). Antibiotic susceptibility testing by a standardized single disk method. *Am. J. Clin. Path.* 45, 493–496. doi: 10.1093/ajcp/45.4_ts.493

Boetius, A., Anesio, A. M., Deming, J. W., Mikucki, J. A., and Rapp, J. Z. (2015). Microbial ecology of the cryosphere: sea ice and glacial habitats. *Nat. Rev. Microbiol.* 13, 677–669. doi: 10.1038/nrmicro3522

Bøggild, C. E., Brandt, R. E., and Brown, K. J. (2010). The ablation zone in northeast Greenland: ice types, albedos and impurities. *J. Glaciol.* 56, 101–113. doi: 10.3189/002214310791190776

Buyer, J. S. (2008). Identification of bacteria from single colonies by fatty acid analysis. *J. Microbiol. Meth.* 48, 259–265. doi: 10.1016/S0167-7012(01)00327-X

Cameron, K. A., Hodson, A. J., and Osborn, A. M. (2012). Structure and diversity of bacterial, eukaryotic and archaeal communities in glacial cryoconite holes from the Arctic and Antarctic. *FEMS Microbial. Ecol.* 82, 254–267. doi: 10.1111/j.1574-6941.2011.01277.x

Chintalapati, S., Kiran, M. D., and Shivaji, S. (2004). Role of membrane lipid fatty acids in cold adaptation. *Cell Mol. Biol.* 50, 631–642.

Christner, B. C., Kvitko, B. H., and Reeve, J. N. (2003). Molecular identification of Bacteria and Eukarya inhabiting an Antarctic cryoconite hole. *Extremophiles* 7, 177–183. doi: 10.1007/s00792-002-0309-0

Cook, J. M., Edwards, A., Takeuchi, N., and Irvin-Fynn, T. (2016). Cryoconite: the dark biological secret of the cryosphere. *Prog. Phys. Geog.* 40, 66–111. doi: 10.1177/0309133315616574

Dhume, G. M., Maharana, A. K., Tsuji, M., Srivastava, A. K., and Singh, S. M. (2019). Cold tolerant endoglucanase producing ability of *Mrakia robertii* A2-3 isolated from cryoconites, Hamtah glacier, Himalaya. *J. Basic Microbiol.* 59, 667–679. doi: 10.1002/jobm.201800300

Dhume, G. M., Tsuji, M., and Singh, S. M. (2022). Identification of fungal communities isolated from Himalayan Glacier Cryoconites. *Sustainability* 14:14814. doi: 10.3390/su142214814

Edgar, R. C., Haas, B. J., Clemente, J. C., Quince, C., and Knight, R. (2011). UCHIME improves the sensitivity and speed of chimera detection. *Bioinformatics* 27, 2194–2200. doi: 10.1093/bioinformatics/btr381

Edwards, A., Anesio, A. M., Rassner, S. M., Sattler, B., Hubbard, B., Perkins, W. T., et al. (2011). Possible interactions between bacterial diversity, microbial activity and supraglacial hydrology of cryoconite holes in Svalbard. *ISME J.* 5, 150–160. doi: 10.1038/ismej.2010.100

Edwards, A., Pachebat, J. A., Swain, M., Hegarty, M., Hodson, A. J., Irvine-Fynn, T. D. L., et al. (2013). A metagenomic snapshot of taxonomic and functional diversity in an alpine glacier cryoconite ecosystem. *Environ. Res. Lett.* 8:035003. doi: 10.1088/1748-9326/8/3/035003

Feller, G., and Gerday, C. (2003). Psychrophilic enzymes: hot topics in cold adaptation. *Nat. Rev. Microbiol.* 11, 200–208. doi: 10.1038/nrmicro773

Foreman, C. M., Sattler, B., Mikuchi, J. A., Porazinska, D. L., and Priscu, J. C. (2007). Metabolic activity and diversity of cryoconites in the Taylor Valley, Antarctica. *J. Geophys. Res.* 112:G04S.32. doi: 10.1029/2006JG000358

Fountain, A. G., Tranter, M., Nylen, T. H., Lewis, K. J., and Mueller, D. R. (2004). Evolution of cryoconite holes and their contribution to meltwater runoff from glaciers in the McMurdo Dry Valleys, Antarctica. *J. Glaciol.* 50, 35–45. doi: 10.3189/172756504781830312

Gerdel, R. W., and Drouet, F. (1960). The cryoconite of the Thule Area, Greenland. *Trans. Am. Microsc. Soc.* 79, 256–272. doi: 10.2307/3223732

Gruell, W. (2000). Melt-water accumulation on the surface of the greenland ice sheet: effect on albedo and mass balance. Geografiska Annaler. *Series A Phys. Geograp.* 82, 489–498. doi: 10.1111/j.0435-3676.2000.00136.x

GSI (2009). Detailed glaciological studies on Hamtah Glacier, Lahaul and Spiti district Himachal Pradesh. *Rec. Geol. Surv.* 8, 136–139.

Hodson, A., Anesio, A. M., Tranter, M., Fountain, A., Osborn, M., et al. (2008). Glacial ecosystems. *Ecol. Monogr.* 78, 41–67. doi: 10.1890/07-0187.1

Irvine-Fynn, T. D. L., Edwards, A., Newton, S., Langford, H., and Rassner, S. M. (2012). Microbial cell budgets of an arctic glacier surface quantified using flow cytometry. *Environ. Microbiol.* 14, 2998–3012. doi: 10.1111/j.1462-2920.2012.02876.x

Jiang, H. L., Tay, S. T. L., Maszenan, A. M., and Tay, J. H. (2006). Physiological traits of bacterial strains isolated from phenol-degrading aerobic granules. *FEMS Microbiol. Ecol.* 57, 182–191. doi: 10.1111/j.1574-6941.2006.00114.x

Kaštovaká, K., Elster, J., Stibal, M., and Šantrůčková, H. (2005). Microbial assemblages in soil microbial succession after glacial retreat in Svalbard (High Arctic). *Microb. Ecol.* 50, 396–407. doi: 10.1007/s00248-005-0246-4

Kim, O. S., Cho, Y. J., Lee, K., Yoon, S. H., Kim, M., Na, H., et al. (2012). Introducing EzTaxon: a prokaryotic 16S rRNA Gene sequence database with phylotypes that represent uncultured species. *Int. J. Syst. Evol. Microbiol.* 62, 716–721. doi: 10.1099/ijs.0.038075-0

Kohshima, S., Seko, K., and Yoshimura, Y. (1993). *Biotic Acceleration of Glacier Melting in Yala Glacier, Langtang region, Nepal Himalaya Snow and Glacier Hydrology (Proc. Kathumandu Symp., Nov.* 1992), Vol. 218. Wallingford: IAHS Pub, 309–316.

Lee, Y. M., Kim, S.-., Y., Jung, J., Kim, E. H., and Cho, K. H. (2011). Cultured bacterial diversity and Human impact on Alpine glacier Cryoconite. *J. Microbiol.* 49, 355–362. doi: 10.1007/s12275-011-0232-0

Lutz, S., Anesio, A. M., Edwards A, and Benning, L. G. (2016). Linking microbial diversity and functionality of arctic glacial surface habitats. *Environ. Microbiol.* doi: 10.1111/1462-2920.13494

Mandal, A., Ramanathan, A., Angchuk, T., Soheb, M., and Singh, V. B. (2016). Unsteady state of glaciers (Chhota Shigri and Hamtah) and climate in Lahaul and Spiti region, western Himalayas: a review of recent mass loss. *Environ. Earth Sci.* 75:1233. doi: 10.1007/s12665-016-6023-5

Mueller, D. R., and Pollard, W. H. (2004). Gradient analysis of cryoconite ecosystems from two polar glaciers. *Polar Biol.* 27, 66–74. doi: 10.1007/s00300-003-0580-2

Mueller, D. R., Vincent, W. F., Pollard, W. H., and Fritsen, C. H. (2001). Glacial cryoconite ecosystems: a bipolar comparison of algal communities and habitats. *Nova Hedwigia Beiheft* 123, 173–197.

Nagatsuka, N., Takeuchi, N., Nakano, T., Shin, K., and Kokado, E. (2014). Geographical variations in Sr and Nd isotopic ratios of cryoconite on Asian glaciers. *Environ. Res. Lett.* 9:045007. doi: 10.1088/1748-9326/9/4/045007

Nishida, I., and Murata, N. (1996). Chilling sensitivity in plants and cyanobacteria: the crucial contribution of membrane lipids. *Annu. Rev. Plant. Physiol. Plant. Mol. Biol.* 47, 541–568. doi: 10.1146/annurev.arplant.47.1.541

Obbels, D., Verleyen, E., Mano, M. J., Namsaraev, Z., Sweetlove, M., et al. (2016). Bacterial and eukaryotic biodiversity patterns in terrestrial and aquatic habitats in the Sør Rondane Mountains, Dronning Maud Land, East Antarctica. *FEMS Microbiol. Ecol.* 92:fiw041. doi: 10.1093/femsec/fiw041

Perini, L., Gostincar, C., Anesio, A. M., Williamson, C., Tranter, M., and Gunde-Cimerman, N. (2019). Darkening of the greenland ice sheet: fungal abundance and diversity are associated with algal bloom. *Front. Microbiol.* 21:557. doi: 10.3389/fmicb.2019.00557

Poniecka, E. A., Bagshaw, E. A., Sass, H., Segar, A., Webster, G., Williamson, C., et al. (2020). Physiological capabilities of cryoconite hole microorganisms. *Front. Microbiol.* 11:1783. doi: 10.3389/fmicb.2020.01783

Prowse, T. D., Wrona, F. J., Reist, J. D., Gibson, J. J., Hobbie, J. E., Lévesque, L. M., et al. (2006). Climate change effects on hydroecology of Arctic freshwater ecosystems. *AMBIO* 35, 347–358. doi: 10.1579/0044-7447(2006)35[347:CCEOHO]2.0.CO;2

Reddy, P. V. V., Rao, S. S. S. N., Pratibha, M. S., Sailaja, B., Kavya, B., Manorama, R. R., et al. (2009). Bacterial diversity and bioprospecting for cold-active enzymes from culturable bacteria associated with sediment from meltwater stream of Midre Lovenbreen glacier, an Arctic glacier. *Res. Microbiol.* 160, 538–546. doi: 10.1016/j.resmic.2009.08.008

Sambrook, J., Fritsch, E. F., and Maniatis, T. (1989). *Molecular Cloning a Laboratory Manual*. New York, NY: Cold Spring Harbor Laboratory Press.

Segawa, T., Ishii, S., Ohte, N., Akiyoshi, A., Yamada, A., Maruyama, F., et al (2014). The nitrogen cycle in cryoconites: naturally occurring nitrification-denitrification granules on a glacier. *Environ. Microbiol.* 16, 3250–3262. doi: 10.1111/1462-2920.12543

Segawa, T., Takeuchi, N., Rivera, A., Yamada, A., Yoshimura, Y., Barcaza, G., et al. (2012). Distribution of antibiotic resistance genes in glacier environments. *Environ. Microbiol. Rep.* 5, 127–134. doi: 10.1111/1758-2229.12011

Shukla, S. P., Mishra, 1. R., and Chitranshi, A. (2015). Dynamics of Hamtah Glacier, Lahaul and Spiti district, Himachal Pradesh. *J. Ind. Geophysic. Union.* 19, 414–421.

Singh, P., Kapse, N., Arora, P., Singh, S. M., and Dhakephalkar, P. (2015). Draft genome of *Cryobacterium* sp. MLB-32, an obligate psychrophile from glacier cryoconite holes of high Arctic. *Mar. Genom.* 21, 25–26. doi: 10.1016/j.margen.2015.01.006

Singh, P., and Singh, S. M. (2011). Characterization of yeast and filamentous fungi isolated from cryoconite holes of Svalbard, Arctic. *Polar Biol.* 35, 575–583. doi: 10.1007/s00300-011-1103-1

Singh, P., Singh, S. M., and Dhakephalkar, P. (2014). Diversity, cold-active enzymes and adaptation strategies of bacteria inhabiting glacier cryoconite holes of High Arctic. *Extremophiles* 18, 229–242. doi: 10.1007/s00792-013-0609-6

Singh, P., Singh, S. M., and Roy, U. (2016). Taxonomic characterization and bio-potentials of bacteria isolated from glacier ice cores in the High Arctic. *J. Basic Microbiol.* 56, 275–285. doi: 10.1002/jobm.201500298

Singh, P., Tsuji, M., Singh, S. M., and Takeuchi, N. (2020). Contrasting pattern of Microbial communities in glacier cryoconites of Nepali Himalaya and Greenland Arctic. *Sustainability* 12:6477. doi: 10.3390/su12166477

Singh, S. M., Kumar, A., Sharma, P., Mulik, R. U., Upadhyay, A. K., Ravindra, R., et al. (2017). Elemental variations in glacier cryoconites of Indian Himalaya and Spitsbergen, Arctic. *Geosci. Front.* 22, 1–15. doi: 10.1016/j.gsf.2017.01.002

Singh, S. M., Sharma, J., Gawas-Sakhalkar, P., and Upadhyay, A. K. (2013). Atmospheric deposition studies of heavy metals in Arctic by comparative analysis of lichens and cryoconite. *Environ. Monit. Assess.* 185, 1367–1376. doi: 10.1007/s10661-012-2638-5

Sommers, P., Darcy, J. L., Gendron, E. M. S., and Stanish, L. F. (2018). Diversity patterns of microbial eukaryotes mirror those of bacteria in Antarctic cryoconite holes. *FEMS Microbiol. Ecol.* 94:fix167. doi: 10.1093/femsec/fix167

Srinivas, T. N. R., Singh, S. M., Pradhan, S., Pratibha, M. S., Kishore, K. H., et al. (2011). Comparision of bacterial diversity in proglacial soil from Kafini glacier, Himalayan Mountain ranges, India, with the bacterial diversity of other glaciers in the world. *Extremophiles*. 49:389. doi: 10.1007/s00792-011-0398-8

Stibal, M., Telling, J., Cook, J., Mak, K. M., Hodson, A., and Anesio, A. M. (2012). Environmental controls on microbial abundance on the Greenland ice sheet: a multivariate analysis approach. *Microbiol. Ecol.* 63, 74–84. doi: 10.1007/s00248-011-9935-3

Takeuchi, N., Kohshima, S., and Seko, K. (2001). Structure, formation, darkening process of albedo reducing material (cryoconite) on a Himalayan glacier: a granular algal mat growing on the glacier. *Arct. Antarct. Alp Res.* 33, 115–122. doi: 10.1080/15230430.2001.12003413

Takeuchi, N., Nishiyama, H., and Li, Z. (2010). Structure and formation process of cryoconite granules on Ürümqi glacier No. 1, Tien Shan, China. *Ann Glaciol* 51, 9–14. doi: 10.3189/172756411795932010

Tranter, M., Fountain, A. G., Fritsen, C. H., Berry Lyons, W., Priscu, J. C., Statham, P. J. et al. (2004). Extreme hydrochemical conditions in natural microcosms entombed within Antarctic ice. *Hydrol. Proc.* 18, 379–387. doi: 10.1002/hyp.5217

Tytgat, B., Verleyen, E., Sweetlove, M., and D'hondt, S. (2016). Bacterial community composition in relation to bedrock type and macrobiota in soils from the Sør Rondane Mountains, East Antarctica. *FEMS Microbiol. Ecol.* 92:fiw126. doi: 10.1093/femsec/fiw126

Uetake, J., Tanaka, S., Segawa, T., Takeuchi, N., Nagatsuka, N., Motoyama, H., et al. (2016). Microbial community variation in cryoconite granules on Qaanaaq Glacier, NW Greenland *FEMS Microbiol. Ecol.* 92:127. doi: 10.1093/femsec/fiw127

Webster-Brown, J. G., Hawes, I., Jungblut, A. D., Wood, S. A., and Christenson, H. K. (2015). The effects of entombment on water chemistry and bacterial assemblages in closed cryoconite holes on Antarctic glaciers. *FEMS Microbiol. Ecol.* 91:fiv144. doi: 10.1093/femsec/fiv144

Wharton, R. A., McKay, C. P., Simmons, G. M., and Parker, B. C. (1985). Cryoconite holes on glaciers. *Bioscience* 35, 499–503. doi: 10.2307/1309818

Williams, L., Singer,G. A., Fasching, C., Battin, T. J., and Besemer, K. (2013). Microbial biodiversity in glacier-fed streams. *ISME J.* 7, 1651–1660. doi: 10.1038/ismej.2013.44

Yallop, M. L., Anesio, A. J., Perkins, R. G., Cook, J., and Telling, J. (2012). Photophysiology and albedo-changing potential of the ice-algal community on the surface of the Greenland ice sheet. *ISME J.* 6, 2302–2313. doi: 10.1038/ismej.2012.107

Yu, Y., Li, H. R., Zeng, Y. X., and Chen, B. (2009). Extracellular enzymes of cold-adapted bacteria from Arctic sea ice, Canada Basin. *Polar Biol.* 32, 1539–1547. doi: 10.1007/s00300-009-0654-x

Frontiers in Microbiology

Explores the habitable world and the potential of microbial life

The largest and most cited microbiology journal which advances our understanding of the role microbes play in addressing global challenges such as healthcare, food security, and climate change.

Discover the latest Research Topics

See more →

Frontiers

Avenue du Tribunal-Fédéral 34
1005 Lausanne, Switzerland
frontiersin.org

Contact us

+41 (0)21 510 17 00
frontiersin.org/about/contact